STEVENS
Institute of Technology

Final Report to the

New Jersey Marine Sciences Consortium

and

New Jersey Department of Transportation
Office of Maritime Resources

MEASUREMENT OF PCB FLUXES TO THE ATMOSPHERE FROM STABILIZED DREDGED MATERIAL

Principal Investigators:
Robert Miskewitz, Richard I. Hires, George P. Korfiatis
Stevens Institute of Technology
Hoboken, NJ 07030

May 12, 2005

TABLE OF CONTENTS

TABLE OF FIGURES

TABLES

APPENDICES

Appendix 1. GC ECD Analytical Methods
Appendix 2. PCB Analysis Results

1.0 INTRODUCTION

This study consisted of a laboratory investigation, during which sediment from New Town Creek, N.Y. was collected and placed in a laminar flow wind tunnel in order to determine PCB fluxes from stabilized dredged material (SDM) to the atmosphere in a controlled laboratory environment. The presently reported work was conducted as Phase II of a study. Phase I was conducted to measure PCB fluxes from SDM in a landfill (Korfiatis et al. 2003). The experiments conducted during this phase of the project, analyzed various environmental and sediment conditions that could not be controlled in the field. These conditions included; the initial concentration of PCBs in the sediment, moisture content of sediment and air, temperature of the sediment and air, wind speed, and percent of cement used to stabilize the sediment. The effects that these conditions have on the flux of PCBs were evaluated to isolate the effect of stabilization on PCB fluxes from sediment.

The presently reported study was conducted in order to; (1) assess the accuracy of these measurements using laboratory PCB flux measurements, and (2) assess the effects of stabilization on the fluxes of PCBs from SDM. This report will present background information, including theory and a review of previously collected flux chamber PCB measurements, and then the laboratory investigation will be discussed. Subsequently, the results and conclusions made from this study will be discussed.

1.1 Theory

1.1.1 Sediment Air Flux Theory

The flux of a substance from sediment to the air is a common process. It was first expressed by Dalton (1802) for the flux of water vapor from the ground into the air.

$$E = C(e_s - e_a) \tag{1}$$

E is the flux of water vapor, C is a mass transfer coefficient for water, and e_a and e_s are moisture contents of the soil and air respectively. This equation can also be used to describe fluxes of contaminants. This flux can be separated into two distinct processes; first the contaminant diffuses to the sediment surface, and second it is transported from the surface into the atmosphere. These two processes can be described by the following equation.

$$F = k_S(C_S - C_A^*) = k_A(C_A^* - C_A^{\infty}) \tag{2}$$

k_S and k_A are the mass transfer coefficients for the sediment and air sides respectively, and C_S, C_A^*, and C_A^{∞} are the sediment-air concentration, surface air concentration, and background air concentrations. Since the flux rate will be constant over both processes they can be combined to yield an expression for the determination of K_T (Schwarzenbach et al 1993).

$$\frac{1}{K_T} = \frac{1}{k_{sed}} + \frac{1}{k_a} \tag{3}$$

It is evident from this equation that the total flux will be limited by the interface with the greatest resistance.

1.1.2 Air Side ResistanceTheory

In laminar flow, particles are forced to move in parallel paths due to viscosity. Laminar flows are, in essence, predictable, given knowledge of the molecular properties of the fluid. Since the flow in the present wind tunnel experiments will be laminar, the only mechanism of transport out of the sediment was diffusion. An equation for the mass transfer coefficient from the surface can be derived using boundary layer theory. The boundary conditions state that the concentration in the sediment is C_o, the concentration in the air away from the surface is zero, and the flux rate at the surface is constant. Thus k_a can be derived for laminar flow of a fluid over a sparingly soluble flat plate using boundary layer theory (Cussler, 1984).

$$\frac{k_a\, x}{D} = 0.323 \left(\frac{\rho\, v^0\, x}{\mu} \right)^{1/2} \left(\frac{\mu}{\rho\, D} \right)^{1/3} \tag{4}$$

k_a	local mass transfer coefficient at position x
x	position along x-axis
D	Molecular diffusion coefficient of species being transferred
ρ	Flowing fluid density
μ	Flowing fluid dynamic viscosity
v^0	Flowing fluid average velocity

The mass transfer coefficient (k_a) is a local mass transfer coefficient since it is a function of the x position along the x-axis. This x dependence, is expected because the hydrodynamic and concentration boundary layer thicknesses vary with x. Since the material balance is applied over the length of the plate, the mass transfer coefficient k_{ma} is different from the local mass transfer coefficient k_a. Here, k_{ma} is a length-averaged mass transfer coefficient defined as:

$$k_{ma} = \frac{1}{L} \int_0^L k_a\, dx \tag{5}$$

where L is the length of the sediment chamber. Substitution into the previous equation yields the following expression for k_a:

$$k_a = \frac{0.646D}{L} \left(\frac{\rho\, v^0\, L}{\mu} \right)^{1/2} \left(\frac{\mu}{\rho\, D} \right)^{1/3} \tag{6}$$

Knowledge of the mass transfer coefficient for the air side of the sediment air interface allows inferences to be made about the rate limiting step in the process of volatilization of PCBs from SDM.

1.1.3 Sediment Side Resistance Theory

The process of release and transport of contaminants from sediment into the air can be thought of as a three part process. First, the contaminant adsorbed to the solid will exist in equilibrium with the concentration of contaminant in the pore water; this is governed by an equilibrium constant, K_D. Second there will also be an equilibrium relationship between the concentration in the pore water and the pore air. This ratio is governed by Henry's Constant. Henry's constant is equal to the concentration of contaminant in the gas phase divided by the concentration in the liquid phase when the two are in equilibrium.

$$H_c = {C_A}/{C_L} \tag{7}$$

And finally, the contaminant will be transported in the vapor phase through the sediment into the atmosphere which will be a function of the diffusivity, D_E.

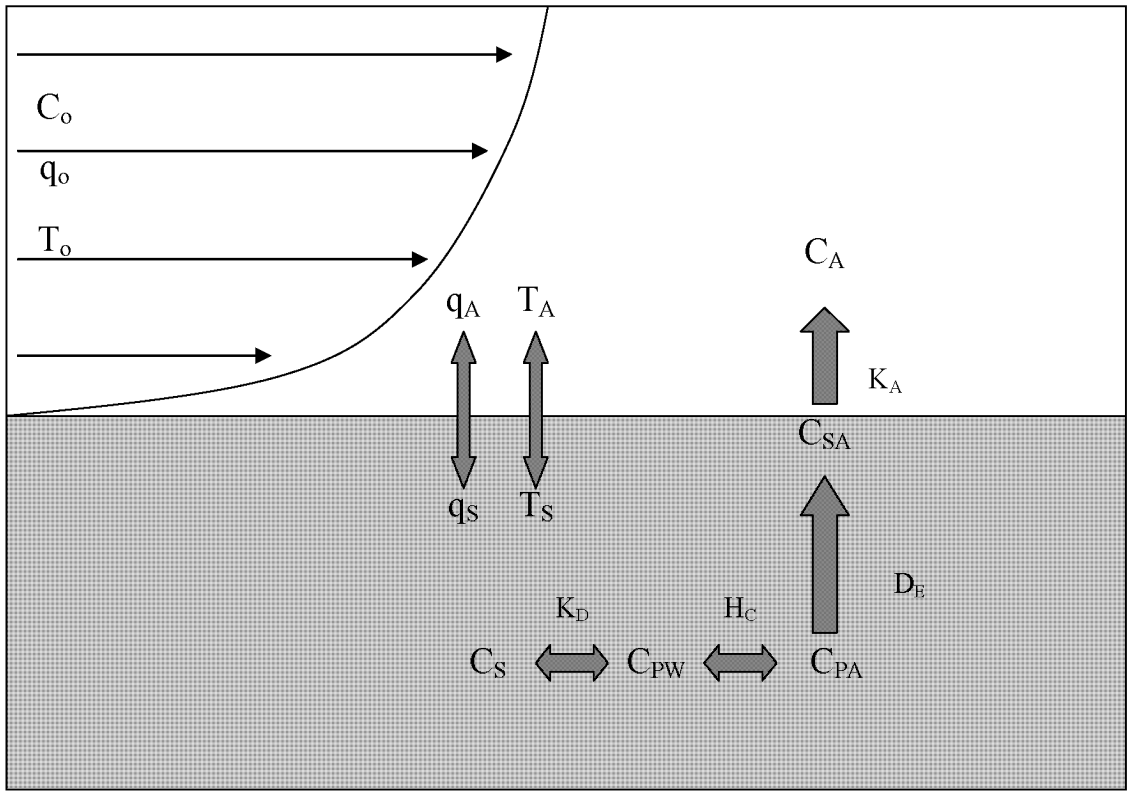

Figure 1. Conceptual Model of PCB Fluxes

The final step in this process is thought to be rate limiting (Dupont 1986). The largest effect on this rate limiting step will result from changing water content of the sediment.

1.1.4 Sediment Flux Models

Various models have been developed to predict the volatilization of substances from soil. Several of these are discussed in the following section.

Hartley Method (Hartley 1969)

The Hartley Method is a model created to predict fluxes of contaminant from soil to air in terms of the heat balance between the contaminant and the air. The flux is expressed as:

$$F = \frac{(\rho_{\max} - \rho_{air})}{\delta} \Bigg/ \left[\frac{1}{D_V} + \frac{\lambda_V^{\,2} \rho_{\max} M}{kRT^2} \right] \tag{8}$$

F = flux of compound
$\rho_{\max}$ = saturated vapor concentration at the temperature of the outer air
ρ_{air} = vapor concentration of the outer air
δ = thickness of viscous sub-layer
D_V = diffusion coefficient of vapor in the air
λ_V = latent heat of vaporization
M = molecular weight
k = thermal conductivity of air
R = gas constant
T = temperature

The denominator in equation 8 is primarily the thermal component of the resistance to volatilization. It is only significant for water or other very volatile compounds. Thus, for less volatile compounds such as PCBs equation 8 becomes:

$$F = \frac{D_V(\rho_{\max} - \rho_{air})}{\delta} \tag{9}$$

This is the film theory equation originally proposed by Nerst (1904). It proposed that the mass transfer coefficient is simply defined as $k=D/\delta$, where D is the molecular diffusion and δ is the width of the film. This model is useful because of its simplicity in determining the flux; however it does not take into account contaminant concentration and moisture content of the soil. It represents a situation where the contaminant is in abundant supply in the soil (unlike PCBs) and is only a function of the diffusivity and height of the viscous sub-layer.

Valsaraj Method (Valsaraj et al 1997)

In order to address the effect of soil moisture content, the model must be adjusted with a term that accounts for the effect that moisture will have on the flux of contaminant. This term is called a retardation factor, it is a function of the porosity, moisture content, Henry's constant, and the 'wet' or 'dry' sediment-air partition coefficient.

$$R_F = \varepsilon_a + \varepsilon_w / H_c + \rho_b K_{dw} \tag{10}$$

ε_a = air filled porosity
ε_w = water filled porosity
H_c = Henry's constant
ρ_b = sediment bulk density
K_{dw} = 'wet' sediment-air partition coefficient

The diffusivity will also be affected by the reduction in air filled pores in the soil. As a result the effective diffusivity must be used. This is determined via the Millington Quirk expression.

$$D_e = D_A \varepsilon_a^{10/3} / \varepsilon_T^{2} \tag{11}$$

D_A = chemical diffusivity in air
ε_T = air filled porosity

The equation used to determine the concentration of a contaminant in a column of soil becomes:

$$\frac{\partial \rho_A}{\partial t} = \frac{D_e}{R_F} \frac{\partial^2 \rho_A}{\partial z^2} \tag{12}$$

ρ_A = the mass concentration of contaminant A in the air in the sediment pore spaces. The boundary conditions are; (1) a lower boundary through which there are no fluxes of contaminant, (2) an upper boundary at which the flux of contaminant through the sediment equals the gradient of concentration between the surface and background air multiplied by an air side mass transfer coefficient, k_a. This mass transfer coefficient will largely be determined by the flow regime over the sediment. The initial condition states that at t=0 the concentration is constant throughout the soil column.

$$\begin{aligned} \frac{\partial \rho_A}{\partial z} &= 0 \text{ at z=0} \\ D_e \frac{\partial \rho_A}{\partial z} + k_a \left(\rho_A - \rho_A^{\infty} \right) &= 0 \text{ at z=H} \\ \rho_A(z,0) &= \rho_A^{0} \text{ at t=0, for all } z \in [0, H] \end{aligned} \tag{13}$$

The resulting flux is:

$$N(t) = 2 D_e \rho_A^{0} \frac{L^2}{H} \sum_{n=1}^{\infty} \frac{e^{-\alpha_n^2 T}}{L(L+1) + \alpha_n^2} \tag{14}$$

The terms L and T are defined by:

$$L = {k_a H}/{D_e} \tag{15}$$

$$T = {D_e t}/{R_{FW} H^2} \tag{16}$$

And α_n are the positive eigan values of:

$$\alpha_n \tan(\alpha_n L) = L \tag{17}$$

This model has the benefit of accounting for the effects of initial moisture content of the sediment. It has been used in several studies to monitor the flux rates of several PAHs from sediment with good results. The moisture content of the sediment is taken into account using the effective diffusivity and the retardation factor. The moisture content of the sediment changes, in order to account for the changing moisture content the authors of this model solved for a 'wet' condition and a 'dry' condition. The changing moisture was then accounted for by changing the ratio area of wet sediment to dry. The assumption is made that the moisture content varied horizontally but is constant vertically in the water column.

In a later study, Valsaraj *et. al.* (1999) proposed a simplified version of this model. The limiting factors were grouped into air-side resistance and sediment-side resistance.

$$\frac{C_A^{\,o}}{N_A} = \frac{1}{k_a} + \sqrt{\frac{\pi t}{D_e R_f}} \tag{18}$$

$C_A^{\,0}$ is the initial concentration of contaminant in the sediment pore air spaces. This equation is the normalized source concentration; the two terms on the right hand side are the air-side and sediment side resistances. The first term, k_a, is the mass transfer coefficient on the air side of the interface. The second term is the sediment side resistance. This term is a function of time, as well as the moisture content of the sediment. This model assumes that the rate limiting step for the flux will be the rate at which the contaminant diffuses to the sediment surface.

Dry sediment will have large D_e and R_f values, thus increasing the resistance from the sediment side. Wet sediment will have large flux values due to lower resistance from the sediment side of the interface. Consequently, the contaminant flux rates are initially the maximum allowable by the air-side mass transfer coefficient. Over time, evaporation occurs, the sediment moisture drops, and the flux becomes limited by the diffusion rate out of the sediment.

1.1.5 Sediment Flux Measurements

PCB fluxes are greatly influenced by the physical characteristics of the sediment. The water content, density, temperature, and organic content have to be taken into account

when attempting to model fluxes from sediment. Chiarenzelli *et al.* (1996) have conducted experiments to measure the effect of water content on the fluxes of PCBs from contaminated dredged sediment. Their study was conducted on PCB contaminated sediment from the St. Lawrence River. The samples were allowed to dry at ambient conditions, and PCB losses from the samples were determined. The sediment samples contained moisture contents ranging from 30%-99%. Filtered air was drawn through the 2 liter experimental chamber at 20 cm^3/sec. Average removal rates of PCBs from the sediment range from 2.1 – 184.2 ng/hr and increase with moisture content. An exponential correlation ($R^2 = 0.932$) was found between the amount of PCBs volatilized and the initial water content. When samples were effectively dry, PCB loss subsided. Analysis of the volatilized PCB congeners and those that remained in the soil, exhibited a great disparity in the amount of chlorination. Four, low molecular weight, ortho-chlorinated congeners represented 54%-76% of the PCBs volatilized. The low molecular weight congeners appeared to have a greater potential to volatilize from the sediment surface.

In another study, Chiarenzelli et al. (1996) dried PCB contaminated sediment samples using air of varied relative humidity. The amount of PCBs lost during drying was monitored. This study determined that PCB fluxes were large during drying of the soil; however, when the soil moisture reached equilibrium with the moisture content of the air, drying no longer occurred and the magnitude of PCB fluxes was greatly reduced. This study also focused on the PCB flux as a function of time. It was found that the fluxes decreased steadily over time, presumably due to the decrease in PCBs available for volatilization.

Thibodeaux et al (1989) conducted PCB volatilization studies in a flux chamber. The sediment was spread out very thin and air flow over it was laminar. Sediment from the New Bedford Harbor, MA superfund site was placed in the chamber and fluxes were monitored. The experiments were run under 'wet' (>4% w/w) and 'dry' (>1% w/w) conditions. During the 'wet' experiments the measured fluxes ranged from 12 to 62 $\mu g/m^2$/hr, and during the 'dry' experiments, the measured values from the sediment were 0.855 ± 0.432 $\mu g/m^2$/hr. The experiments were run using sediment with a concentration of 887 µg/g of Aroclor 1242. This study found a large dependence of the flux on moisture content of the soil, which in turn was the dominant factor in the sediment–air partitioning coefficient. These measured fluxes were compared to a model similar to the 'Valsaraj' method presented in the previous section. The predicted fluxes had a range of 36 to 113 $\mu g/m^2$/hr, The model was found to over predict the fluxes of Aroclor 1242 by 1.4 to 1.8 times.

Valsaraj *et al.* (1997) conducted experiments to measure Poly Aromatic Hydrocarbons (PAH) fluxes in microcosms designed to simulate the drying of sediment, and attempted to model the fluxes using the 'Valsaraj' method. Air was blown over the top of the sediment and sampled for PAHs.

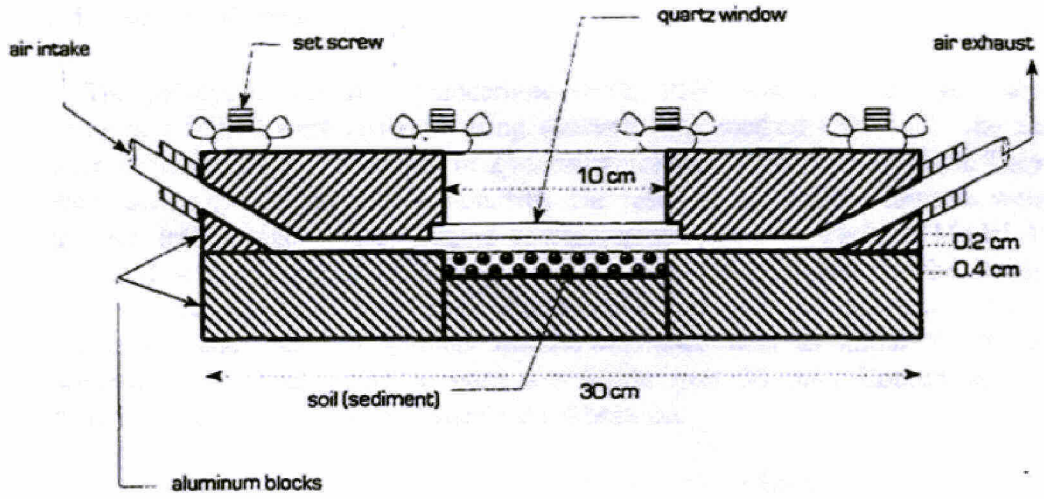

Figure 2. Volatilization Chamber (Valsaraj 1997)

The experimental microcosms had a sediment depth of 4mm and an air space of 2 mm. The exhaust air was pushed through XAD Resin and extracted to determine the PAH flux. This configuration allowed for a measurable moisture front in the sediment, thus they were able to quantify the flux as a sum of the flux from a wet section and a dry section. It was found that the 'wet' section dominated the flux value. This is due to the relatively small size of the sediment – air equilibrium coefficient as compared to Henry's constant. The experimental set-up included the use of sediment from three contaminated dredging sites and sediment spiked with the PAHs in the lab. The contaminant concentration, relative humidity, and soil moisture content were continually monitored.

The model was based on the idea that there are two rate determining resistances to the flux. The resistances were air-side and sediment-side. Depending on the environmental conditions, either may dominate the behavior of the flux. Experimental results from this study support the conclusion that the effect of the air-side mass transfer coefficient, k_a, on the fluxes is only felt during the early stages of the experiment. Beyond this period, emissions are increasingly controlled by the sediment side. Further variations of the experiment included variations in the relative humidity, and remoistening of the soil.

Relative humidity was found to have a great influence on the flux values, by keeping the relative humidity at >99%, the flux rate dropped slowly from an initial rate. Using the same conditions but changing the influent air to 0% relative humidity, the flux rate decreased much more rapidly. When the relative humidity was alternated between >99% and 0%, the flux rates fell to very low values with dry air and increased when the humid air was reintroduced. The response to the change in relative humidity is expected; however the rate at which it occurred may be due to the fact that the experimental microcosm only had a thickness of 4 mm. This experiment shows the large dependence

on the water content of the air on the volatilization of contaminants. "Dry" sediments have a greater affinity for contaminant than do wet sediments because of the competition for space on the sediment with water. As the sediment particles in upper layers of the sediment dry, they not only hold the contaminant absorbed to them tighter, they will also absorb free contaminants that would otherwise diffuse to the surface, thus further increasing the sediment-side resistance. After flux values were determined for sediment, it was blended, and the experiment was rerun. The resulting fluxes were similar in magnitude to the values from the first cycle indicating that the change in the mass of contaminant present in the sediment is very small.

Price et al (1997) conducted a study using experimental microcosm similar to those in the previous studies. They noted the dependence of the flux on the air flow. The flow rates used corresponded to average velocities of 0.28 cm/sec, 2.78 cm/sec, and 27.78 cm/sec. The sediment was contaminated with PAHs. For the first 170 hours of the experiment the air velocity was 0.28 cm/sec. The fluxes were fairly constant and low, indicating that the air side resistance was controlling the flux. When the velocity was increased to 2.78 cm/sec, the flux rate increased approximately 7 times. When the velocity was increased again, no change in flux values was noted, most likely due to the fact that the sediment side resistance had become the rate limiting factor.

Cousins et al. (1997) conducted flux chamber experiments on sediment that was used to amend PCB contaminated sludge. The sludge was applied to the soil. Air with 100% relative humidity was passed over the sludge and through a poly-urethane foam filter. This filter was then extracted to remove the absorbed PCBs which where then analyzed to determine the flux of PCBs from the sludge. Cousins used the 'Jury Model' to predict fluxes, and then compared them to the values from their flux chamber. In addition to fluxes, the model was used to predict the values for the effective diffusion coefficient of individual congeners. The fluxes predicted by the model were relatively close to some of the experimentally determined values of the lighter congeners; however in other cases they varied by as much as an order of magnitude.

2.0 FLUX CHAMBER EXPERIMENT

Phase II of this experiment was conducted using laminar flow wind tunnel to evaluate the fluxes of PCBs from SDM. In order to eliminate the variability of site conditions at the landfill, a chamber was built in which these conditions could be controlled. Fluxes of PCBs from sediment were monitored to evaluate the accuracy of the landfill results and to get a greater understanding of the chemo-dynamics involved in the process. The following sections describe the underlying theory, methods, and the results from these experiments. Finally, the results will be analyzed to get a better understanding of the mechanisms that determine the magnitude of PCB fluxes.

2.1 Experimental Set-up

2.1.1 Wind Tunnel Design

The PCB flux experiments were conducted in a laminar flow wind tunnel designed and constructed at Stevens. The dimensions were 4 meters long, 0.50 meters wide and 0.1 meters deep. The test section is 2 meters long, and has a depth of 20 centimeters. Sediment was placed to a depth of 10 centimeters, and flattened to maintain a smooth channel. In front of the test section is 2 meter section with height of 10 centimeters. This section is for the establishment of a flow regime. The entrance cone of the wind tunnel was designed using a four to one reduction; the curve was designed to have a maximum adverse velocity gradient of 0.025 (Lighthill 1945).

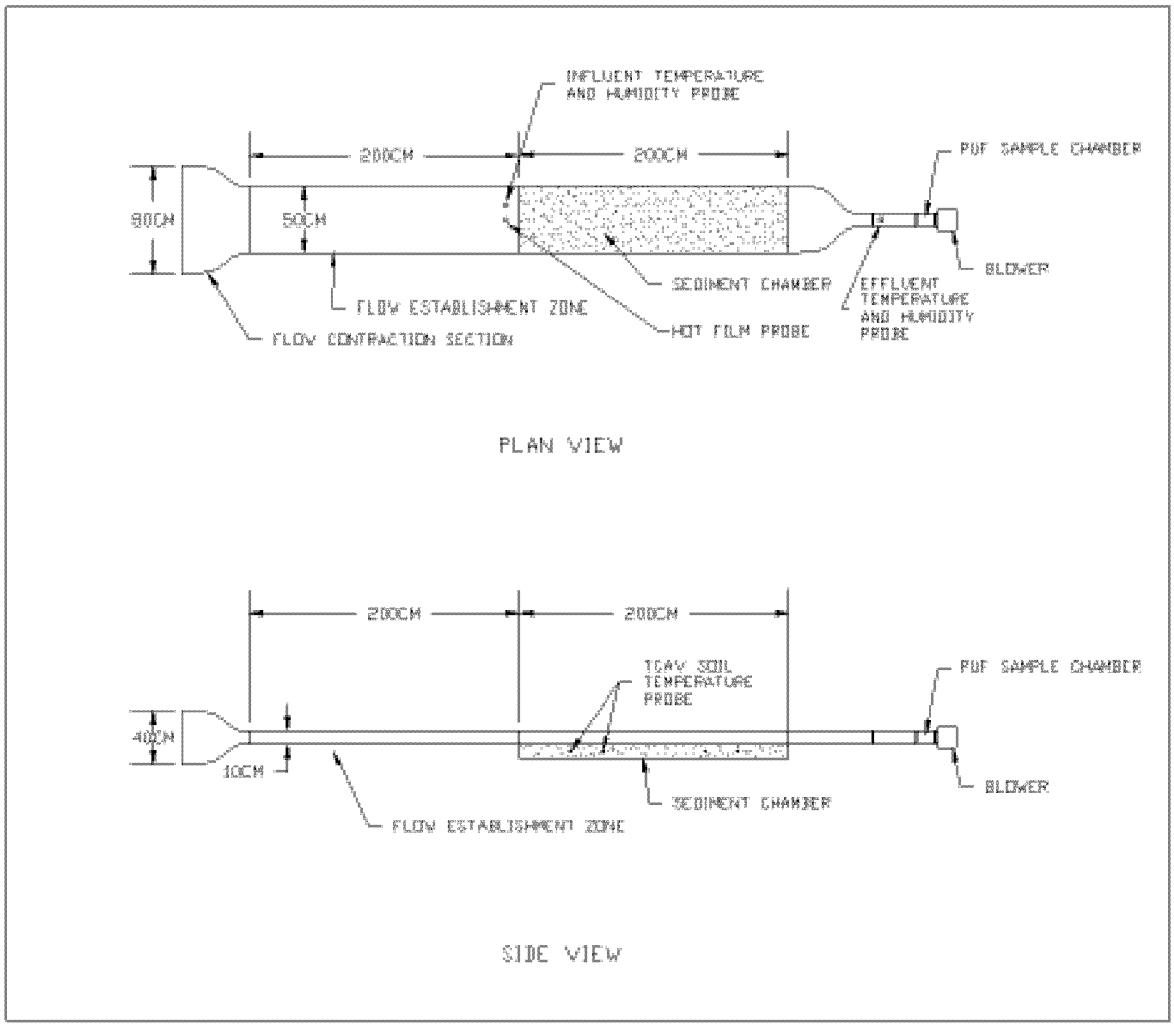

Figure 3. Wind Tunnel Plans

Several instruments were installed in the wind tunnel in order to directly measure various atmospheric and sediment characteristics. These characteristics included inlet and exit air temperature and moisture content, and SDM temperature. The temperatures were measured with chromel-constantan thermocouples with a diameter of 74µm. These thermocouples have a resolution of 0.006°C with 0.1 µV rms noise. The vapor pressures were measured by pumping air through a cooled mirror, dew point hygrometer (Model Dew-10, General Eastern Corp., Watertown, MA). Air was drawn from both inlet and

outlet continuously. The hygrometer was equipped with a solenoid value that switched the air flow through the sensor between the two intakes for two minute intervals. The first minute of the interval was to clear the air from the previous interval, and the measurements were collected in the second. Air was drawn at a flow rate of 0.4 liters/minute with 2 liter mixing chambers to give a 5 minute time constant. The Dew-10 had a resolution of approximately ±0.01 kPa. The spatially averaged SDM temperature was measured with a TCAV (thermocouple averaging) probe. These data were compiled in a Campbell 23X Data logger (Campbell Scientific Inc. Logan, UT).

Sensible and latent heat flux appear to have a large effect on the flux of PCB from the SDM. The sensible heat flux is the amount of energy removed from the sediment through convective heat transport. It was calculated by taking the difference of influent and effluent temperatures, and multiplying this difference by the flow rate, Q, the air density, ρ, and the heat capacity of the air, c_p. The product was then divided by the surface area of the sediment, which was 1 m^2 for the wind tunnel.

$$H = \frac{\rho c_p (T_{out} - T_{in}) Q}{A_{surface}} \tag{19}$$

The units for the sensible heat flux are watts/m^2. The latent heat flux is calculated in much the same way. The difference of influent and effluent air moisture contents were multiplied by the flow rate, and the latent heat of vaporization, λ, then divided by the area of the sediment surface.

$$LE = \frac{\lambda (q_{out} - q_{in}) Q}{A_{surface}} \tag{20}$$

The units for the latent heat flux are also watts/m^2.

The average air flow rate for these experiments was 0.6 m^3/min. This yields an average flow rate of 20 cm/sec. Thus the Reynolds number is 1320. This is below the threshold value of 2000 for laminar flow in pipes. Experiments were conducted to determine the flow profile in the chamber. Precise calibration of the blower was required in order to determine the flow characteristics of the wind tunnel.

2.1.2 Wind Tunnel Calibration

Characterization of the air flow through the wind tunnel was carried out in several steps, first, the blower was calibrated to determine the total air flow, then, a hot film probe was calibrated using the centerline velocity, and finally the vertical flow profile was measured with the hot film probe.

Blower Calibration:

The blower was removed from a Tisch Hi-Vol Sampler and installed at the effluent end of the wind tunnel. Calibrations were carried out using a Tisch Adjustable Orifice Calibrator at five known air flow rates, chosen to bracket field sampling flow rates. The

manometer readings were recorded at these flow rates and corrected for temperature and atmospheric pressure. A linear regression between the flow rate and effluent pressure measurements was used to calculate the flow rate. Regressions run with an $R^2 < 0.98$ were rejected and the calibration was repeated. The sampler's blowers were calibrated prior to and following each sampling run to ensure that flow measurements were accurate. . The effluent pressure readings and corresponding flow rates are shown in table 6.

Table 1. Wind Tunnel Blower Calibration

Reading #	Flow Rate (m^3/min)	Effluent Pressure (Inches of oil)
1	0.53	2.07
2	1.06	8.09
3	0.91	6.20
4	0.73	4.05
5	0.504	1.97
No Flow	0	0

Measurements were corrected for temperature and pressure, and linear regression was performed to create a calibration curve for the blower. The R^2 value for the calibration curve was 0.9996.

Figure 4. Wind Tunnel Blower Calibration Curve

Hot Film Probe Calibration:
A model 1218 Boundary Layer Hot Film Probe from TSI Incorporated (Shoreview, Minnesota) was used to measure the air velocity at various locations in the wind tunnel. The probe was calibrated by correlating the centerline velocity in the wind tunnel to the voltage reading of the probe. The centerline velocity was calculated as 1.75 x's the mean velocity for a rectangular duct with an aspect ratio of 5:1(Spiga and Morini, 1994). The probe was installed in the tunnel and the blower was started. The blower was run at several flow rates. These were recorded along with the voltage readings from the probe. The voltage readings and flow rates were then compared using King's law.

$$E = A + BU^{0.5} \tag{21}$$

E is the bridge voltage, U is the centerline velocity, and A and B are constants. A linear regression was performed to determine A and B. The R^2 value for this regression was 0.987. From this regression, a calibration curve for the Hot Film Probe was created.

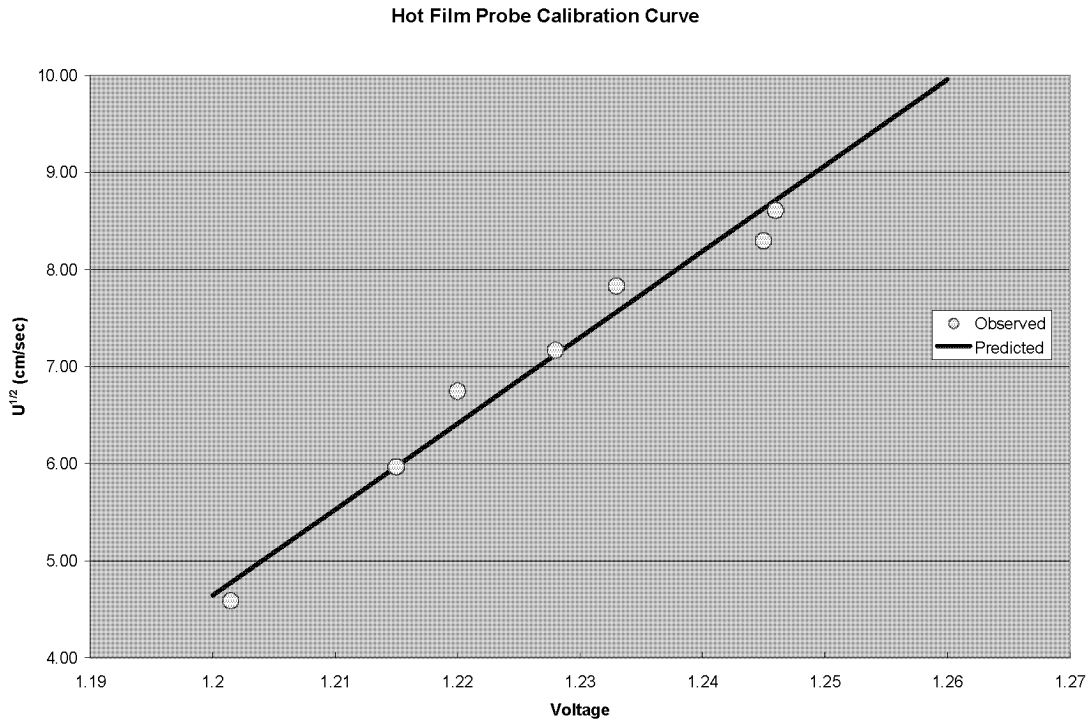

Figure 5. Hot Film Probe Calibration Curve

In order to determine the vertical flow profile in the wind tunnel, the probe was traversed from the center to the lower wall (0.5 cm from the surface) and velocity measurements were collected for each height. The velocity measurements gave a profile that was parabolic. The profile measured agrees well with theoretical values for a laminar flow profile (Spiga and Morini, 1994).

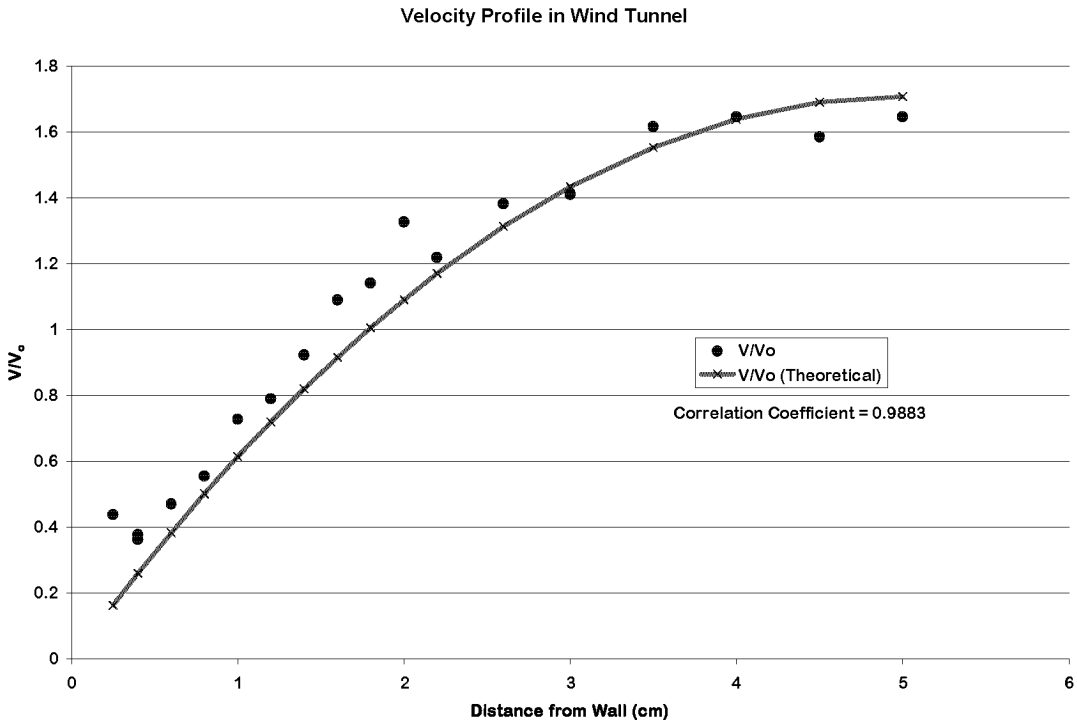

Figure 6. Vertical Velocity Profile

2.2 Methodology

2.2.1 Stabilization of Sediment

The sediment used in this experiment was collected via a clamshell dredge on the US Army Corps of Engineer Vessel, Hayward, from New Town Creek, N.Y.

Figure 7. New Town Creek, N.Y. Sampling Location.

The sediment was collected in three batches; A, B and C. Each of these were homogenized on the deck of the Hayward, then placed into 30-gallon drums and labeled appropriately. The drums were then transported to the Stevens Institute of Technology, Center for Environmental Engineering (CES) and stored in a cold room at 4°C. Each sediment drum was removed from the cold room and transported to the lab prior to the experimental run. Prior the first two experimental runs, the sediment was transported to the lab less than an hour before placement in the wind tunnel. Results from these runs indicated that the sediment was too cold, and should be allowed to equilibrate to the temperature of the laboratory prior to the experimental run. The sediment was brought to the lab two days in advance for the following eight experimental runs.

The sediment was homogenized in the drum using a power drill with a mixer head attachment. The appropriate amount of dry cement, if any, was then weighed out and added to the drum. Experimental, runs were completed with amounts of cement added that were equivalent to 0%, 4%, 6% and 8% of the total by weight. The sediment/cement was then blended until the mix was homogenous. The SDM was then shoveled into the wind tunnel and the surface was smoothed out as flat as possible.

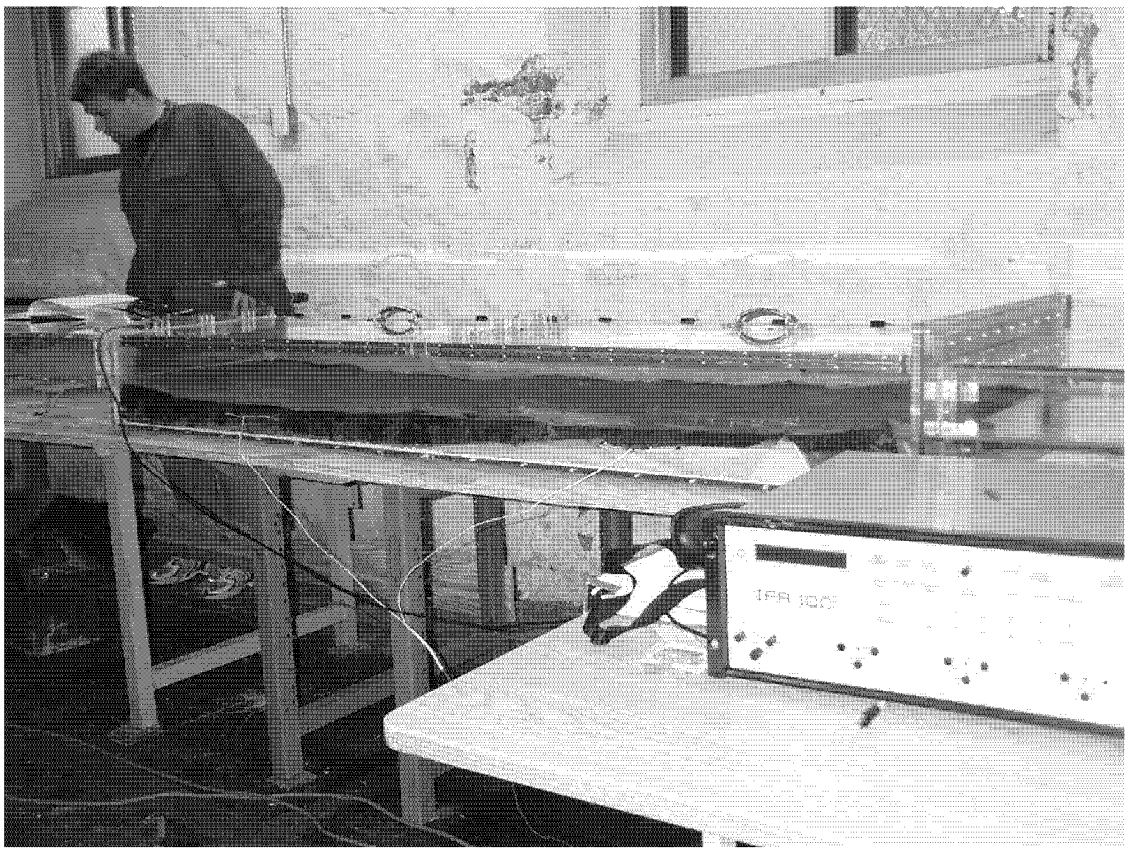

Figure 8. Wind Tunnel filled with Sediment

2.2.2 Wind Tunnel Operation

The wind tunnel was closed and locked down when ready for the start of a sampling run. A PUF sample matrix was installed in the sample chamber of the wind tunnel and the background sampler. The sample chambers were then connected into the two sampling apparatuses. The blowers were turned on, and the start time and flow rates were recorded. The wind tunnel ran for the appropriate length of time. At the end of the sampling interval, the end time and flow rates were recorded. The PCB volatilization flux, $F_{PCB}(t)$ through the chamber was calculated with the total mass of PCB's captured by the PUF sampler in a given time interval using the equation:

$$F_{PCB}(t) = \frac{(C_{EFF} - C_{INF})Q_{AIR}}{A} \quad (21)$$

C_{EFF} = Concentration of PCBs in Effluent air stream

C_{INF} = Concentration of PCBs in Influent air stream (Background)

Q_{AIR} = Flow rate through the wind tunnel

A = Area of the SDM-air interface (m^2)

2.2.3 PCB Analysis

The PUF filters from the experimental runs were extracted using the method described in section 2.1.5 of Korfiatis *et al.* (2003). The sample extracts were analyzed with a Varian 3800 Dual Column Gas Chromatograph with two Electron Capture Detectors at the Center for Environmental Systems at Stevens Institute of Technology (CES). The samples were analyzed for the congeners included in the Supelco PCB Congener Mixes 1 and 2. The methods used for analysis of the samples are included as Appendix 1. These methods include 1) the sample analysis method which includes the injection procedure, temperature program, and detector settings; 2) the recalculation method for quantification of the congeners included in PCB Congener Mix 1; 3) the recalculation method for quantification of the congeners included in PCB Congener Mix 2; and 4) the recalculation method for quantification of the surrogate spikes.

The quality control procedures for PCB analysis included matrix spike, blank spike, laboratory blank, and extraction blank preparation and analysis. The operating procedures were developed in the CES and are based on EPA Method 8082. Prior to initiation of the experiments, an equipment blank was collected in order to determine adsorption to the walls of the enclosure. This was completed by taking advantage of the fact that there are ample PCBs in the ambient air in our region. Two air samples were collected simultaneously; an ambient air sample, and an ambient air sample pulled through the empty flux chamber. The two PCB sample masses collected on the PUFs were then compared to determine if there is a sink of PCBs in the chamber. No significant difference between these samples was found.

2.2.4 Extraction Efficiency

An experiment was conducted to evaluate the efficiency of the extraction procedure. Five clean PUFs were spiked with a mixture of six PCB congeners ranging in chlorination number from 3 to 8 and a pesticide surrogate. The samples were then subjected to the extraction procedure and analyzed. The recovery of the pesticide spike in all samples was used as a reference for the PCB extraction efficiency. The mass of PCB congeners recovered varied by chlorination number. The lower weight congeners had the highest recovery while the high weight congeners exhibited relatively poor recovery. The recoveries were used to create correction factors for the experimental samples. Table 2 shows the percent recovered for each of the samples. These samples were run on two separate days in order to account for temporal variations from the analysis equipment and different calibration runs.

Table 2. Extraction Efficiency Results

	Sample				
	ISR_1	*ISR_2*	*ISR_3*	*ISR_4*	*ISR_5*
Pest. Surrogate (ppb)	**146**	**130**	**123**	**183**	**130**
Percent Recovery	**73.01%**	**65.18%**	**61.58%**	**91.50%**	**65.00%**
Congener Recovery					
14	**96.88%**	**101.34%**	**99.63%**	**100.39%**	**99.49%**
30	**88.65%**	**93.78%**	**88.70%**	**94.57%**	**91.84%**
23	**68.42%**	**72.98%**	**68.10%**	**77.21%**	**63.94%**
65	**52.55%**	**57.46%**	**52.92%**	**59.07%**	**42.79%**
166	**17.82%**	**28.76%**	**15.12%**	**34.80%**	**23.26%**
204	**16.62%**	**26.45%**	**13.17%**	**31.30%**	**20.77%**

The mean recovery efficiency for each congener and the standard deviation are presented in Table 3. The mean recovery efficiencies were then used to correct the PCB concentrations for loss of mass during the extraction procedure.

Table 3. Extraction Efficiency Correction Values

	Percent Recovery	Standard Deviation
14	**99.44%**	**1.61%**
30	**91.40%**	**2.63%**
23	**70.04%**	**4.94%**
65	**52.89%**	**6.27%**
166	**23.91%**	**7.95%**
204	**21.63%**	**7.26%**

The PUF filters collected during sampling runs seven through ten were spiked with 200 µL of a 700 ppb solution containing the six congeners used in the extraction efficiency experiment, as well as the pesticide surrogate spike. The recovery of these congeners was corrected by the recovery of the pesticide spike and the percent recovery was determined. The values for percent PCB congener recovered were very similar to the results presented in table 3.

The extraction efficiencies for the dichlorinated, trichlorinated and tetrachlorinated homologues range from 99.5% to 52.9% with standard deviations that range from 1.3% to 6.2%. The extraction efficiencies found for the heavier homologues are ~22% with a standard deviation of ~7.5%. The lack of extraction efficiency and high standard

deviation are a significant source of error in the concentrations measured for the high molecular weight homologues. As a result, for the presently reported study only the dichlorinated, trichlorinated and tetrachlorinated homologue concentrations will be presented.

2.3 Results

Ten experimental runs were completed for this phase of the project. They included; four runs of unammended dredged sediment, and two each of run stabilized with 4% portland cement, 6% portland cement, and 8% portland cement. The first three runs were completed using sediment from one scoop of the clam shell dredge labeled sample A, the next three were from sample C, and the final four were completed using the four drums that comprised sample B. During each of these runs, PCB concentrations, temperature, and humidity at the influent and effluent were measured. Additionally, the moisture content of the sediment was measured periodically throughout the run. The results from these experimental runs are summarized below. The Chromatograms for each sample are included in Appendix 2.

2.3.1 Run 1

The first experimental run was conducted using unammended dredged sediment from sample A. The experiment was run from December 17, 2003 to December 23, 2003. The initial water content was 77% by weight (weight of water/weight of dry sediment) and fell to 70% after approximately 8 days. The first background sample was collected for the length of the first three wind tunnel samples. The background samples were combined because it was believed that there would not be sufficient mass collected in a background during the relatively short initial sampling intervals. Analysis of the samples revealed that this was not the case, and for the remainder of the study, a background sample was collected for each wind tunnel sample interval.

The temperature of the air and sediment, varied greatly during this experiment. The sediment was spread out in the chamber approximately one hour after being removed from the refrigerated storage room. As a result, the sediment temperature was initially 5°C and rose to 15°C by the end of the first day. The air temperature exhibited a large variance between day and night. There was a slight increase in the temperature of the sediment over the final six days of the experiment.

Measurements of influent and effluent temperature and humidity were used to determine the sensible heat flux and the latent heat flux from the sediment. These values are presented in units of watts/ m^2. The latent heat flux started out negative when the sediment was very cold and became positive as the temperature increased after 24 hours. It became relatively steady for the remainder of the run at approximately 10 watts/m^2. The sensible heat flux was approximately zero with small positive and negative fluctuation occurring throughout the experimental run. These measurements indicate that over this experimental run the relatively cool sediment and influent air combined to create a condition where there was very little convective heating or cooling of the

sediment, and a small but steady moisture flux from the sediment after the initial warming of the sediment.

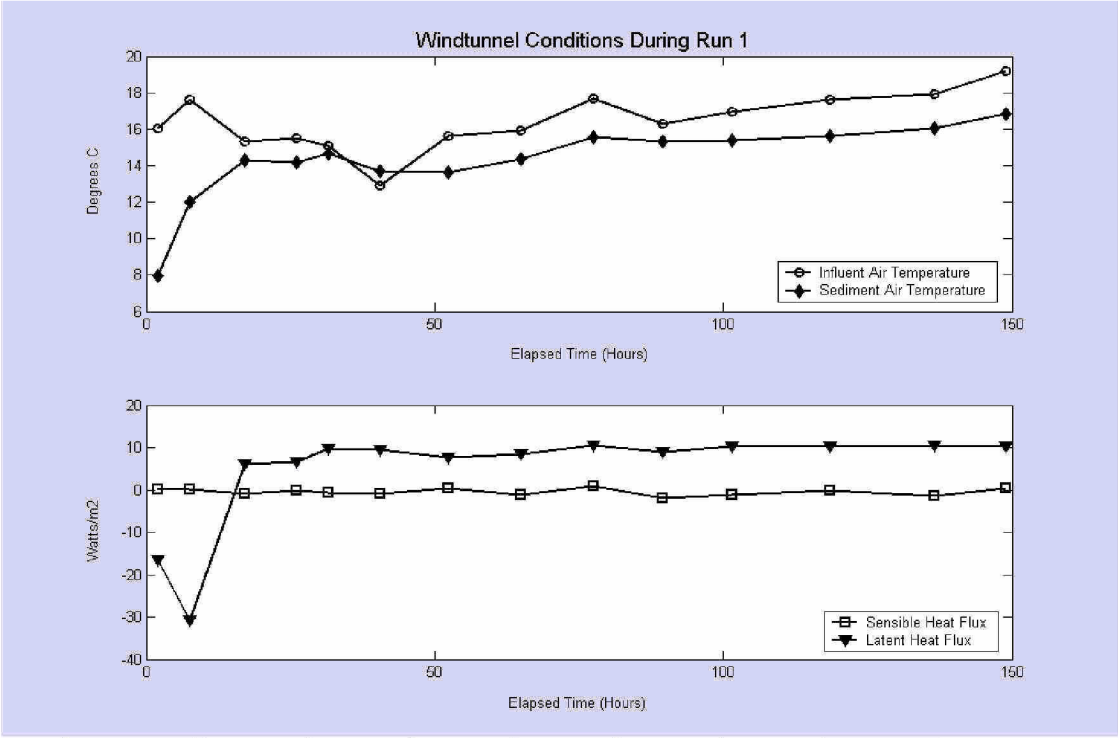

Figure 9. Wind tunnel Conditions During Run 1

The PCB fluxes measured over the first run show a large variance. Reasons for the variance include, the low temperature of the sediment at the time of placement, and the low air temperature in the laboratory. The values for the trichlorinated and tetrachlorinated homologues start off at approximately 80 ng/m^2/hr and decrease over the first 40 hours and reach zero. The fluxes then increase towards the end of the run at 95 hours. This increase corresponds to a large rise in temperature. The dichlorinated homologue is presented on a much larger scale (right axis). The flux measurements increase over the first three intervals then start to decline. There is a strong diurnal variation (>100 ng/m^2/hr), with large fluxes during the day and much smaller during the night. Later in the run there is a large spike in the measured flux at about 85 hours. Despite the high variability in the measure flux values it is observed that both the trichlorinated and tetrachlorinated homologues indicate an elevated initial flux and a decline throughout the run. The dichlorinated homologue has a similar pattern duing the first 60 hours of the run.

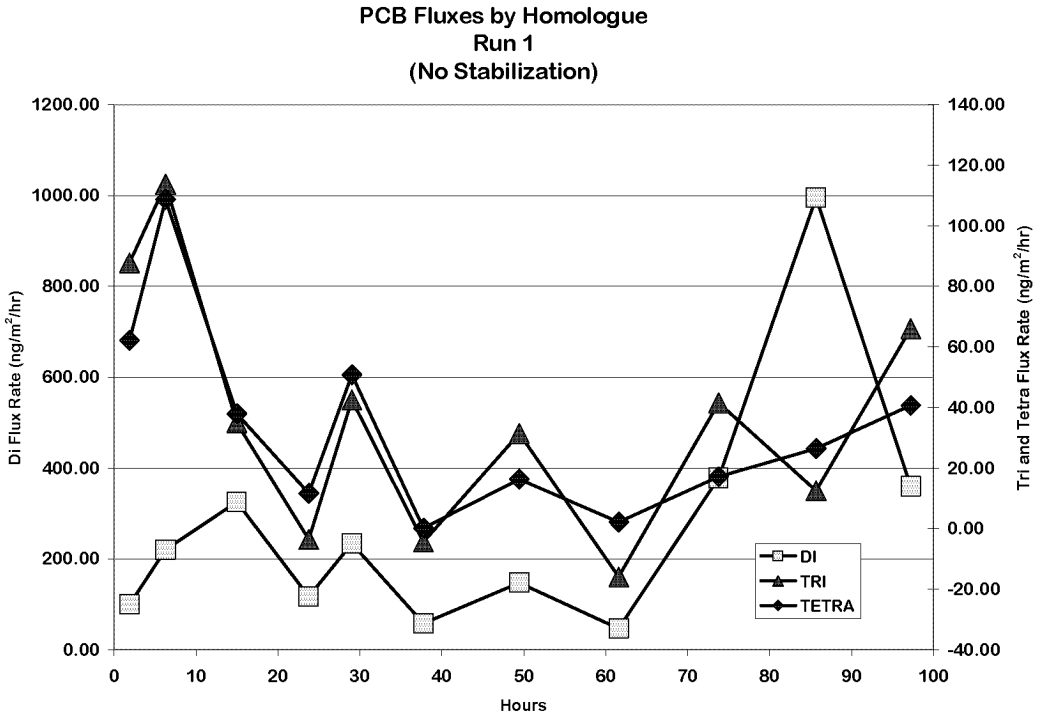

Figure 10. PCB Fluxes by Homologue, Run 1

3.3.2 Run 2

The second experimental run was conducted January 5, 2004 to January 9, 2004. The sediment was stabilized with 8% Portland cement by weight. Prior to stabilization, the moisture content was 75% and after stabilization it was 67%. The moisture content decreased to 45% at the end of the experimental run. Stabilization and placement were completed while the sediment was still cold from storage. The temperature increased from 8 °C to 18 °C within a day. The sediment temperature was then approximately the same as the air temperature. The moisture flux during this experimental run was initially low and then reached a peak that coincided with a peak in the sediment temperature. After this point the moisture flux remained relatively constant. The day/night temperature fluctuations of the air temperature were approximately 3.5° C.

The initial latent heat flux measured was 4 watts/m^2. As the temperature of the sediment increased the latent heat flux also increased. At the same time, the sensible heat flux was very close to zero, and although there is a peak it was very small relative to the latent heat flux. After reaching a peak 25 hours into the experiment, both the latent and sensible heat fluxes decreased slightly. At the end of the run there was a latent heat flux out of the sediment of 11 watts/m^2 and a sensible heat flux into the sediment at approximately -2.5 watts/m^2.

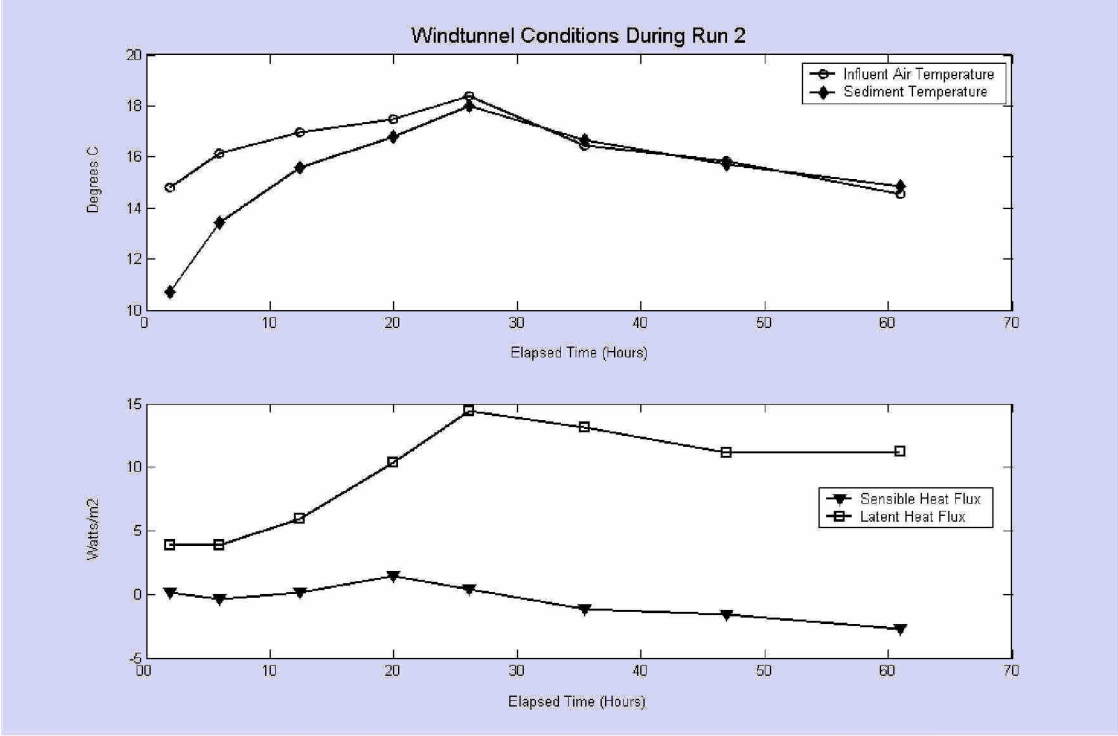

Figure 11. Wind tunnel Conditions During Run 2

PCB fluxes measured during the second experimental run for trichlorinated and tetrachlorinated homologues were high and then decreased rapidly over the subsequent sampling intervals. There was an increase between 11 and 19 hours into the run. This increase occurred in the interval that stretched over midday on the second day when the temperature in the laboratory increased. After this interval the fluxes decreased to approximately zero, until the final measurement. The fluxes measured during this interval were small and directed out of the sediment. This run, like the previous, exhibited a spike in the measured fluxes centered around midday when the temperature was highest. Fluxes of the dichlorinated homologue were very high relative to the other homologues. The initial measured flux was 993 ng/m^2/hr. Twenty hours into the experimental the measured fluxes stabilized at approximately 500 ng/m^2/hr. The measured values exhibit a pattern of elevated initial fluxes that quickly fall off and approach a minimum value. Variations in this pattern arise from the highly variable temperature conditions in the laboratory. During the subsequent experimental runs attempts were made to reduce or eliminate these sources of variance.

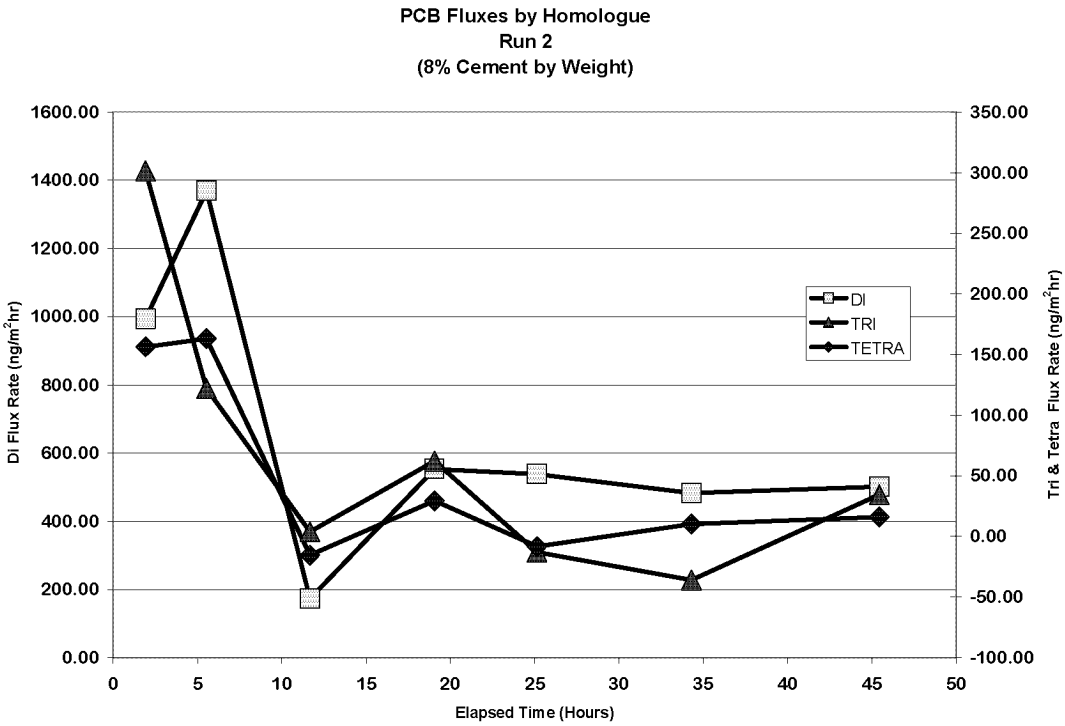

Figure 12. PCB Fluxes by Homologue, Run 2

2.3.3 Run 3

The third run was carried out February 10, 2004 until February 12, 2004. The sediment for the first two runs was placed in the wind tunnel cold, approximately one hour after removing it from the cold storage room. In an attempt to have the sediment at a constant temperature throughout the experimental run, the sediment was removed from cold storage two days prior to the initiation of the experimental run and allowed to equilibrate to the air temperature in the laboratory. The sediment was stabilized with 4% portland cement by weight. Prior to stabilization, the moisture content was 81% and after stabilization it was 75%. By the end of the experiment it was down to 53%. The initial temperature of the sediment was 17°C and rose slightly after being placed. The sediment cooled down over the remainder of the day and into the night, but increased the following day due to warmer influent air. The following night the air and sediment cooled down again.

The latent and sensible heat fluxes behaved much differently during run three than the two previous runs because of the conditions created when the sediment is warmer than the air and vice versa. The variability in the latent heat flux can be seen to correspond very closely to the pattern of sediment temperature versus air temperature. When the sediment was warmer, there was enhanced latent heat flux, and conversely, when the air temperature was greater than the sediment temperature, the latent heat flux appeared to shut down. The sensible heat flux also exhibits a similar pattern; however over the run, the peaks in the latent heat flux appear to reduce while the peaks in the sensible heat flux are increasing. This behavior is presumably due to the drying of the sediment.

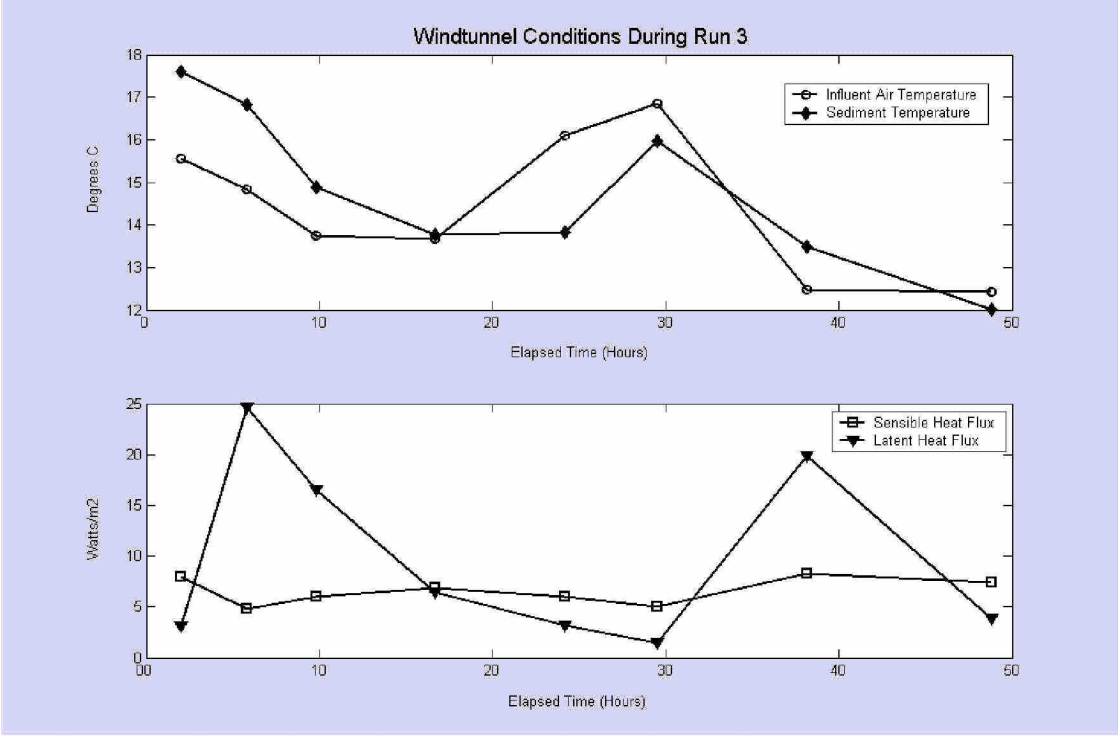

Figure 13. Wind tunnel Conditions During Run 3

PCB fluxes measured during run three for dichlorinated, trichlorinated, and tetrachlorinated chlorinated homologues exhibit large initial fluxes that drop off quickly. There is a slight increase corresponding to the period on the second day when the temperature was elevated; after which the fluxes appear to shut down completely. It is important to notice the scale of the initial measured fluxes compared to the previous experimental run. These are 2.5 times as large for the dichlorinated homologue, and 5 times as large for the tetrachlorinated homologue. The increase results from the high temperature of the sediment at the onset of the run relative to the previous experimental runs. During the rest of the experimental runs, the sediment was allowed to equilibrate with the laboratory temperature.

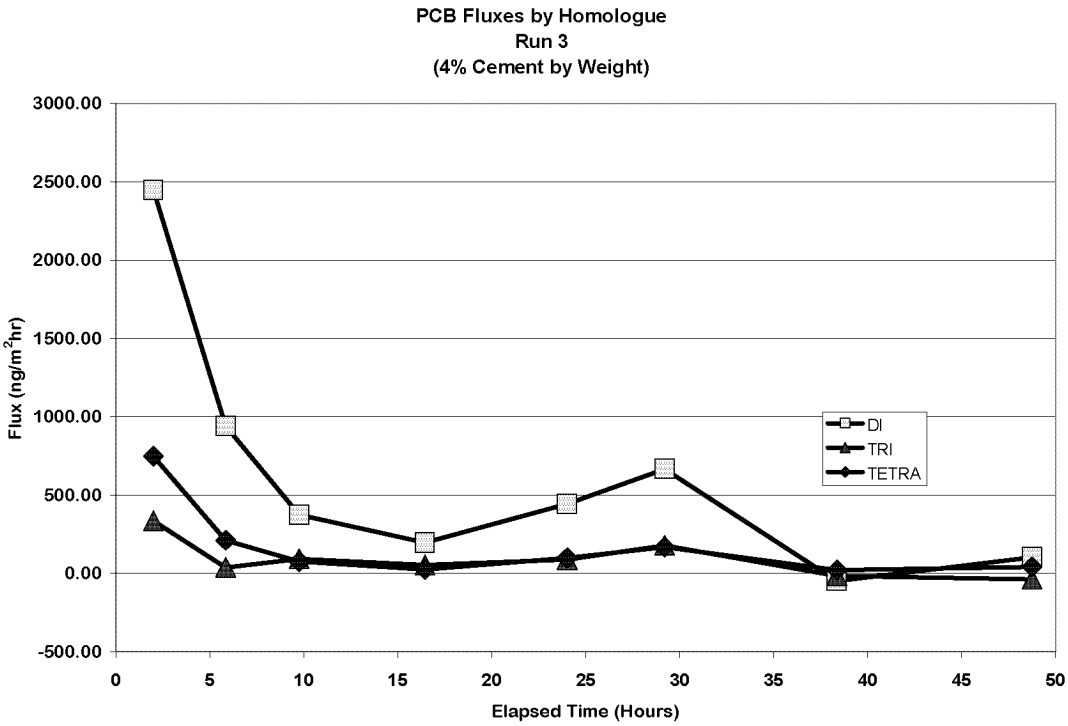

Figure 14. PCB Fluxes by Homologue, Run 3

2.3.4 Run 4

The fourth run was completed March 8, 2004 until March 10, 2004. The sediment used during runs 4, 5, and 6 was from sediment sample C. The sediment had a much higher moisture content than the sediment used in the previous three runs. The sediment was removed from cold storage two days prior to the initiation of the experimental run. In order to regulate the laboratory temperature space heaters with thermostats were used in laboratory and set to 19°C. The sediment was stabilized with 8% Portland cement by weight. Prior to stabilization the moisture content was 184% and after stabilization it was 130%. By the end of the experiment it was down to 117%. The initial temperature of the sediment was 21°C and fell throughout the experimental run to 17.5°C. The influent air temperature remained relatively steady at 19°C with a small increase at midday on the second and third days of the experimental run.

The latent heat flux values measured during this experimental run were relatively small. The initial measurement was zero. The latent heats flux then rose for the first seven hours of the experimental run while the sediment temperature was greater than the influent air temperature. When the air temperature rose to that of the sediment, the latent heat flux decreased until it reached zero, one day into the experimental run. The sensible heat flux was initially 3.5 watts/m^2, then dropped to a minimum at ten hours. It then increased on the second day of the experiment to a peak value at midday equal to the initial value. Following this peak there is a slight decrease overnight and subsequently another increase at midday the following day.

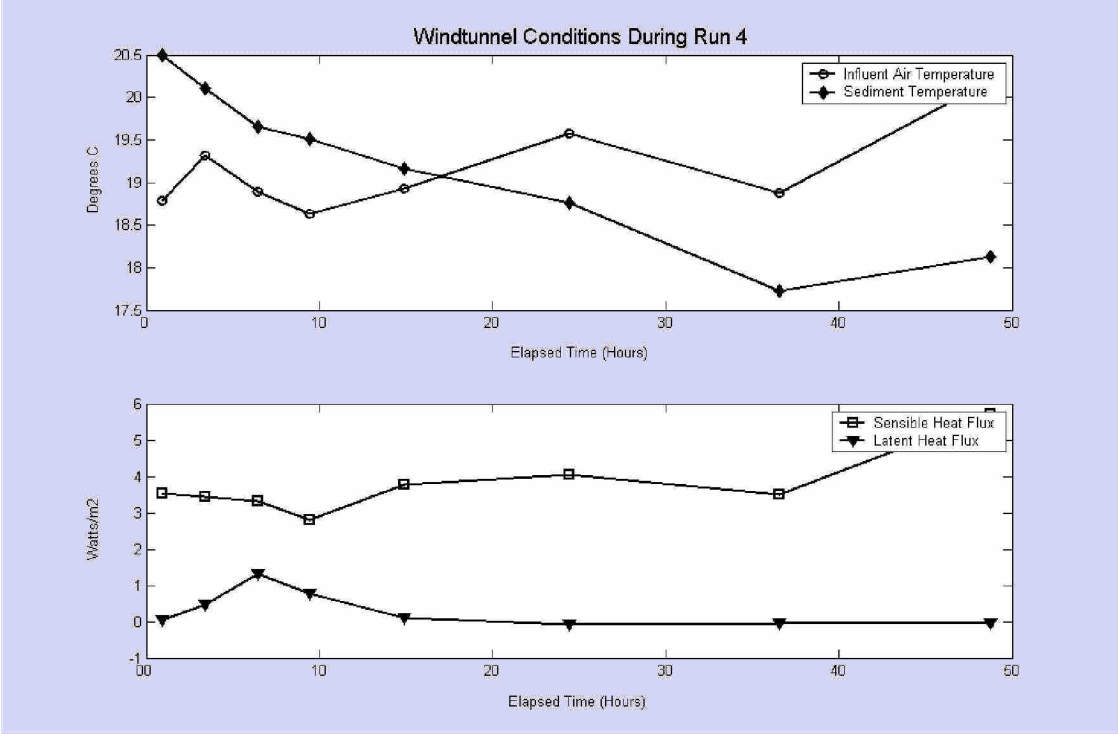

Figure 15. Wind tunnel Conditions During Run 4

PCB fluxes measured during run four of dichlorinated, trichlorinated, and tetrachlorinated homologues exhibited large initial flux measurements that dropped off quickly during the two subsequent sampling intervals. This was followed by a large increase at around 7 hours into the run. Subsequently, the dichlorinated and trichlorinated homologue flux measurements decreased, however the tetrachlorinated homologue flux measurement increased. During the interval centered around 15 hours, the flux measurements for the three homologues decreased significantly, and for the rest of the experimental run they showed a gradual decrease towards zero. The large spike in measured PCB fluxes corresponds directly with a minimum of sensible heat flux and a peak in latent heat flux. The scale of the fluxes was different than for the first three experiments and the distribution of PCB homologues also appeared to be different. The greatest flux was from the tetra-chlorinated homologue group in contrast to the runs conducted with sediment from sample A which had large fluxes from the dichlorinated homologues. The initial flux values for the two runs at 8% stabilization exhibit a five fold increase from sample A to sample C in terms of tetrachlorinated homologues, while the dichlorinated fluxes exhibit a three fold decrease and the trichlorinated homologue fluxes remain relatively constant.

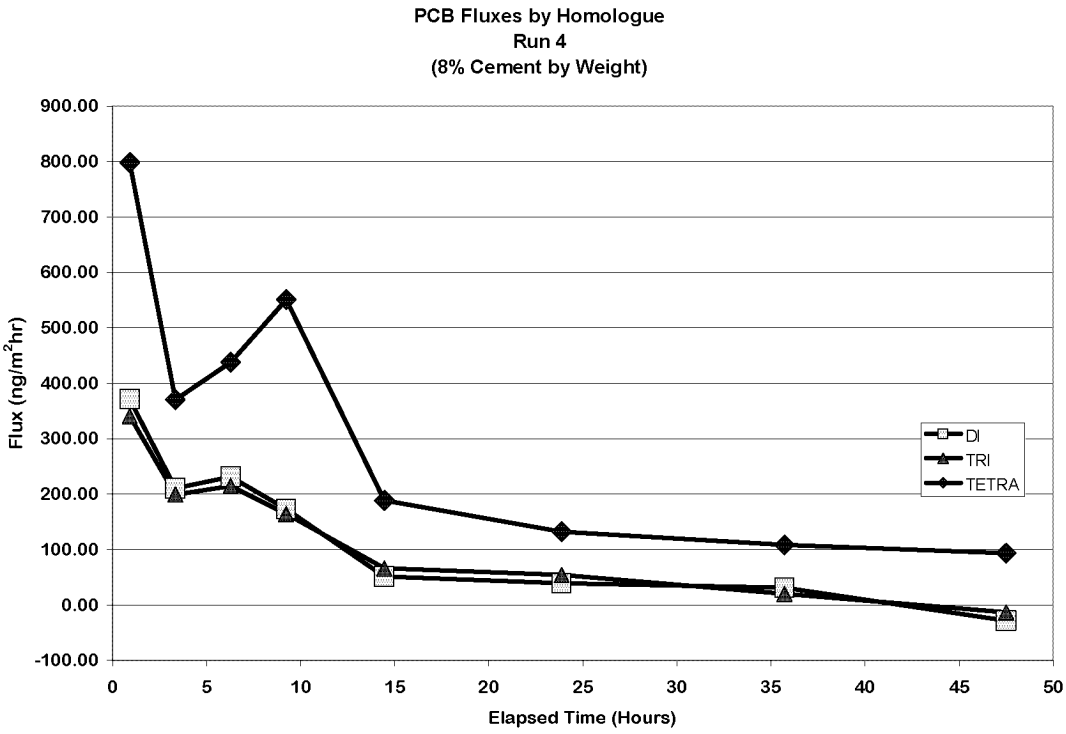

Figure 16. PCB Fluxes by Homologue, Run 4

2.3.5 Run 5

The fifth run was conducted from March 15, 2004 to March 17, 2004. The sediment was stabilized with 4% Portland cement by weight. Prior to stabilization, the moisture content was 184%, and after stabilization it was 147%. At the end of the experimental run it was down to 131%. The initial temperature of the sediment was 19°C and it rose for the first three hours of the experimental run to 20.5°C. During the remainder of the run, it decreased. The influent air temperature followed a similar pattern reaching a peak of 22.2°C at 3 hours. After 20 hours it stabilized at 19.5 °C.

The sensible heat flux during this experimental run reached a peak at approximately 3 hours into the run. This corresponds to the peaks observed in sediment and influent air temperatures. Subsequent to this peak, the sensible heat flux dropped to 4 watts/m^2 and remained steady for the remainder of the experimental run. The latent heat flux was initially 11 watts/m^2 and dropped for the following 20 hours. At 29.8 hours into the run there is a small increase, subsequent to this small peak, the latent heat flux continues to drop to a value close to 2 watts/m^2 at the end of the run (~50 hours).

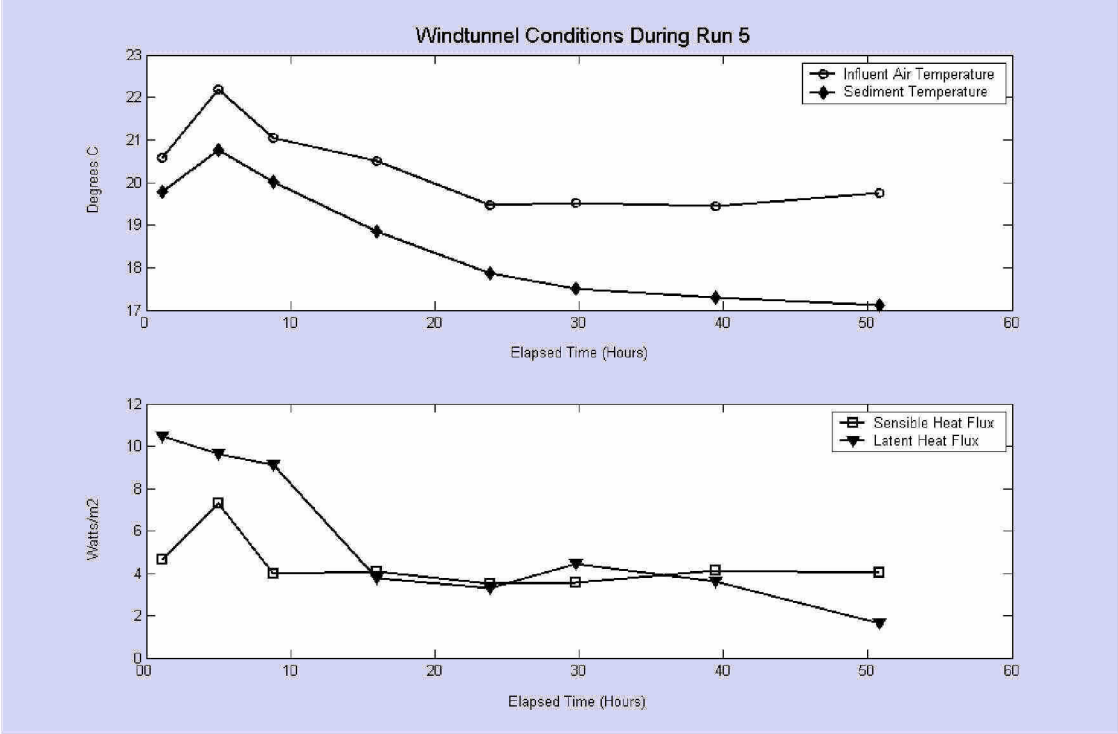

Figure 17. Wind tunnel Conditions During Run 5

The measured PCB fluxes during this experimental run, for dichlorinated, trichlorinated, and tetrachlorinated homologues exhibit an increase from the first interval to the second. The increase in PCB flux measurements coincides with an increase in both the influent air and sediment temperatures. The values for the second interval were similar to the initial flux values measured during the previous run. The measured fluxes then decreased significantly during the following intervals. The dichlorinated homologue exhibits a peak at 23.8 hours and remains elevated during the subsequent sampling interval centered around 29.8 hours. The trichlorinated and tetrachlorinated homologues exhibit a peak at 29.8 hours. These peaks coincide with the small peak in latent heat flux measured at 29.8 hours. These sampling intervals were centered around 9:10 and 15:10 on the second day of the run. The samples were changed at 12:00. Although the temperature of the room varied by less that a degree, there was an increase in humidity and the sun shone through the laboratory's windows directly on the sediment. Presumably, the sunlight warmed the sediment surface, which in turn resulted in an increase in moisture and PCB fluxes. After this peak the flux measurements decreased overnight and appear to have been increasing when the experimental run was ended. It is important to note that the increase in fluxes measured on the second day (~50 hours) are significantly less than those measure on the previous day.

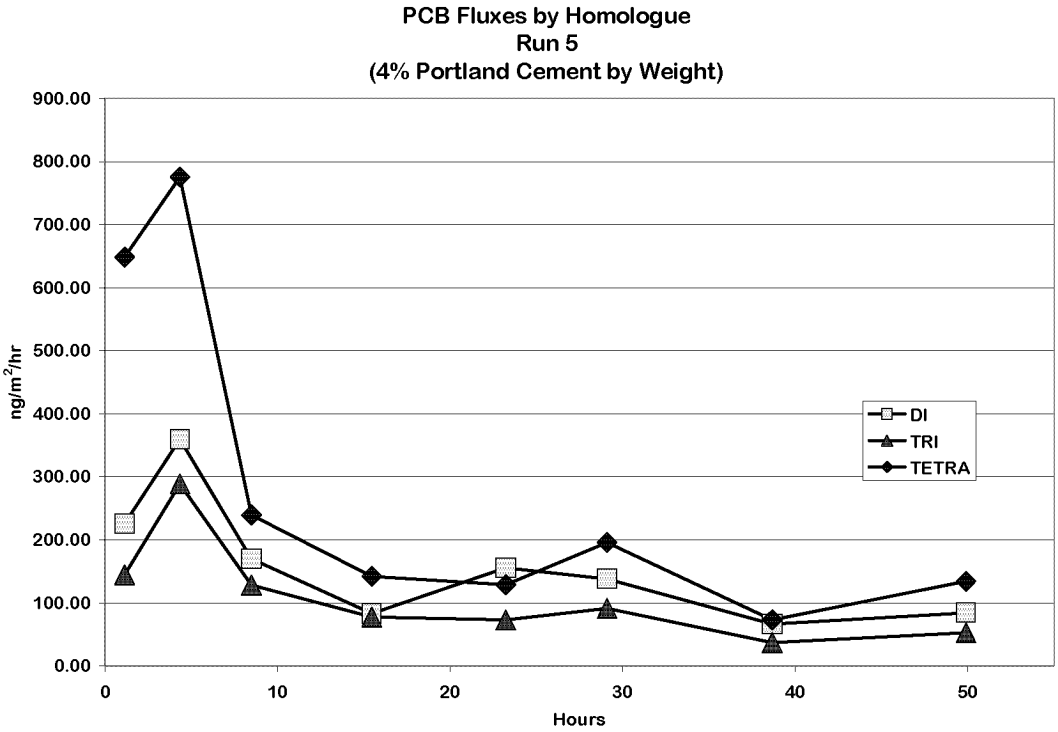

Figure 18. PCB Fluxes by Homologue, Run 5

2.3.6 Run 6

The sixth run was completed March 23, 2004 to March 29, 2004. The sediment was not stabilized. The initial moisture content was 184%. At the end of the experimental run it decreased to 154%. The influent air temperature was initially 20.5°C. It dropped for the next two sampling intervals to a minimum value of 19°C. After reaching the minimum,, there was a steady increase until it reached a peak value of 21.5°C at 28 hours. At the same time there was a sharp increase in the sediment temperature. Following the peak, there was a decline in temperature overnight, which in turn was followed by another increase the following day. The initial temperature of the sediment was 15°C and it increased to approximately 18°C through the experimental run. The sediment temperature increased steadily during the run with the exception two periods of sharper increase. The first was the initial increase from the relatively low temperature of the sediment in the drum, and the second corresponded to the peak in air temperature at 28 hours.

The latent and sensible heat fluxes during this experimental run remained relatively constant. The sensible heat flux was negative, indicating that the sediment was absorbing heat from the air passing over it. This is also indicated by the gradient of temperature between the influent air and sediment temperatures. The latent heat flux, despite a small spike early in the run remained relatively low and constant throughout the run.

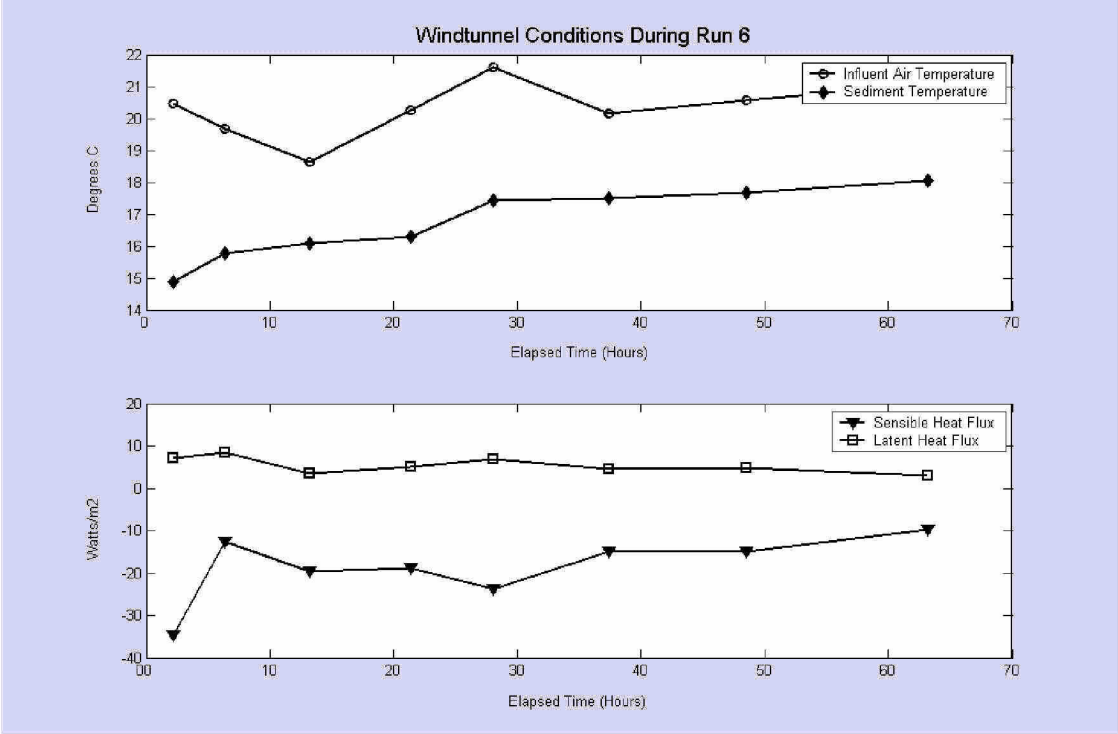

Figure 19. Wind tunnel Conditions During Run 6

The measured PCB fluxes for the dichlorinated, trichlorinated and tetrachlorinated homologues all exhibit similar behavior during this experimental run. They all have relatively high initial values then decrease for the first 12 hours of the run, then increase to a peak one day into the run. This peak is then followed by a decrease for the remainder of the run. The fluctuations observed in this experimental run appear to be directly related to the increase in temperature.

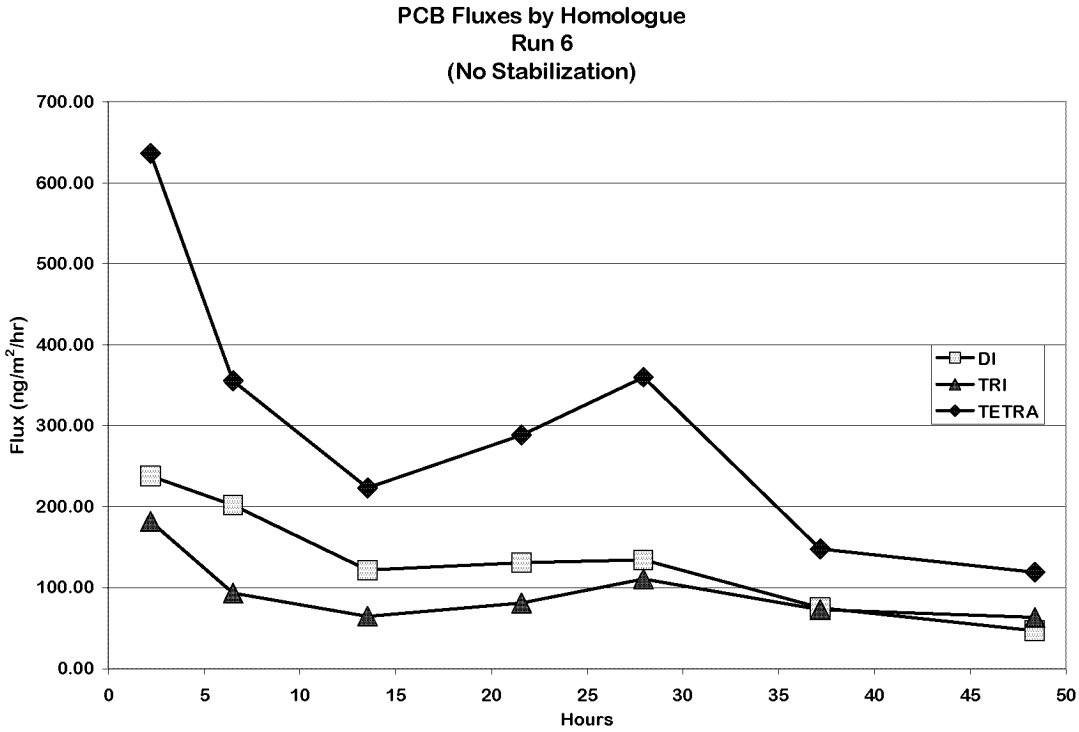

Figure 20. PCB Fluxes by Homologue, Run 6

2.3.7 Run 7

Prior to the final four runs of the experiment, the first six were analyzed. It was determined that the fluctuations in temperature of as little as 3°C were affecting the PCB flux measurements. In order to eliminate the effects of these temperature fluctuations, the equipment was transferred to a laboratory that had greater temperature controls. In order to confirm that the laboratory remained at a relatively constant temperature, the room temperature was recorded for nine days prior to the start of run seven. During these nine days the mean temperature was 23.52 °C with a standard deviation of 0.894 °C.

The final four runs were used to evaluate the effect of varying the airflow rate over the sediment. The four runs consisted of two non-stabilized runs, one at 15 cm/sec mean velocity and one at 20 cm/sec mean velocity (similar to runs 1-6), and two runs with 6% cement at the two speeds.

The seventh run was completed July 12, 2004 to July 14, 2004. The sediment used for this and the following three runs was taken from sediment sample B. The sediment was not stabilized. The mean velocity of the air flowing over the sediment was 15 cm/sec. The initial moisture content of the sediment was 131%. Over the course of the experiment there was no significant decrease in moisture content. The influent air temperature varied very little during this experiment (<2°C). There was a small decrease the second half of the run. The sediment temperature was initially 20.7°C and rose up to a peak 15.8 hours into the experimental run and then decreased slowly for the remainder

of the run. The latent heat flux measurements for this run were positive, however very close to zero, indicating a steady but very small evaporative flux. The sensible heat fluxes were also small, but negative, an indication that the sediment was absorbing a small amount of heat from the air. These measurements decreased as the temperature gradient between the sediment and air decreased during the second half of the run.

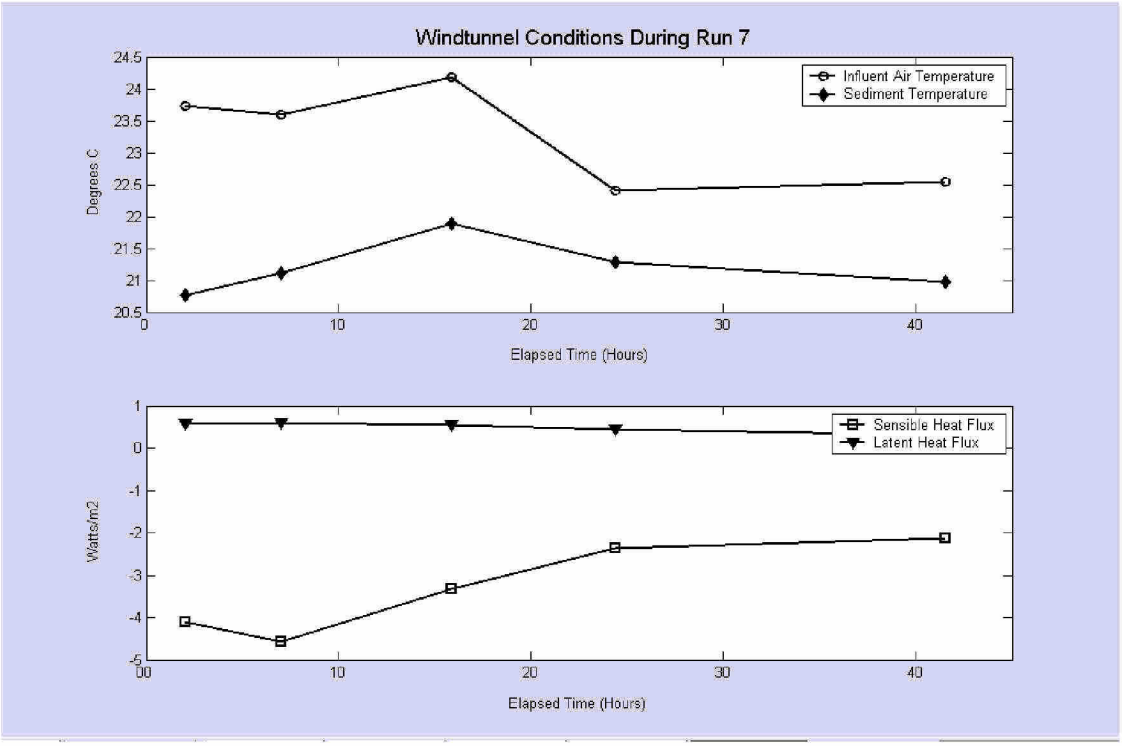

Figure 21. Wind tunnel Conditions During Run 7

The measured PCB fluxes for the dichlorinated, trichlorinated and tetrachlorinated homologues during this experimental run show a gradual decrease over the length of the experiment and do not appear to have any fluctuations due to temperature. The tetrachlorinated homologue has the highest flux rates measured during this interval similar to those fluxes measured during the runs carried out for sample C. When compared with run 6, (also not stabilized) the initial fluxes are similar. At the end of this experimental run (~40 hours), the dichlorinated and trichlorinated homologue flux measurements are very similar and the tetrachlorinated homologue flux measurement is slightly higher.

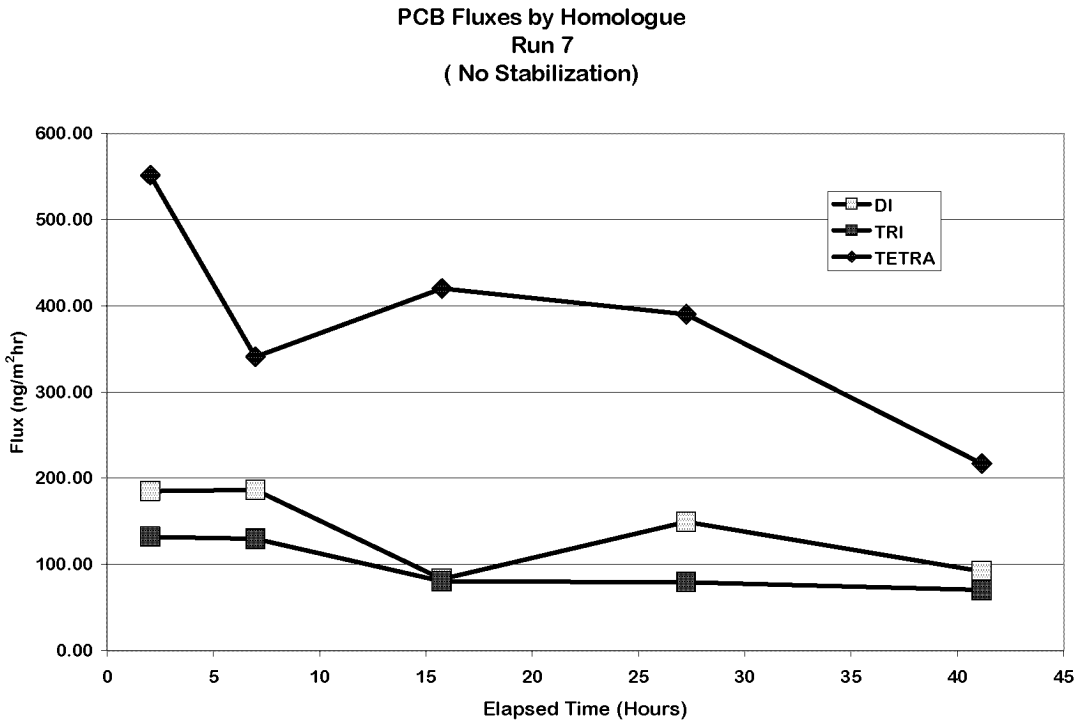

Figure 22. PCB Fluxes by Homologue, Run 7

2.3.8 Run 8

The eighth run was completed July 19, 2004 to July 21, 2004. The sediment was stabilized with 6% Portland cement by weight. The mean velocity of the air flowing over the sediment was 15 cm/sec. The initial moisture content of the sediment was 121%. Over the course of the experiment the moisture content decreased to 106%. The influent air temperature varied very little during this experiment (<1.5°C). Although the fluctuations were very small there appeared to be a pattern of peaks during the day and valleys at night. The sediment temperature did not appear affected by the variation in influent air temperature; instead it rose over the first 12 hours. The latent heat flux measurements, indicate a flux of moisture out of the sediment at 10-20 watt/m^2. The sensible heat flux is very similar to run 7, indicating a small flux of convective heat into the sediment at a fairly constant rate.

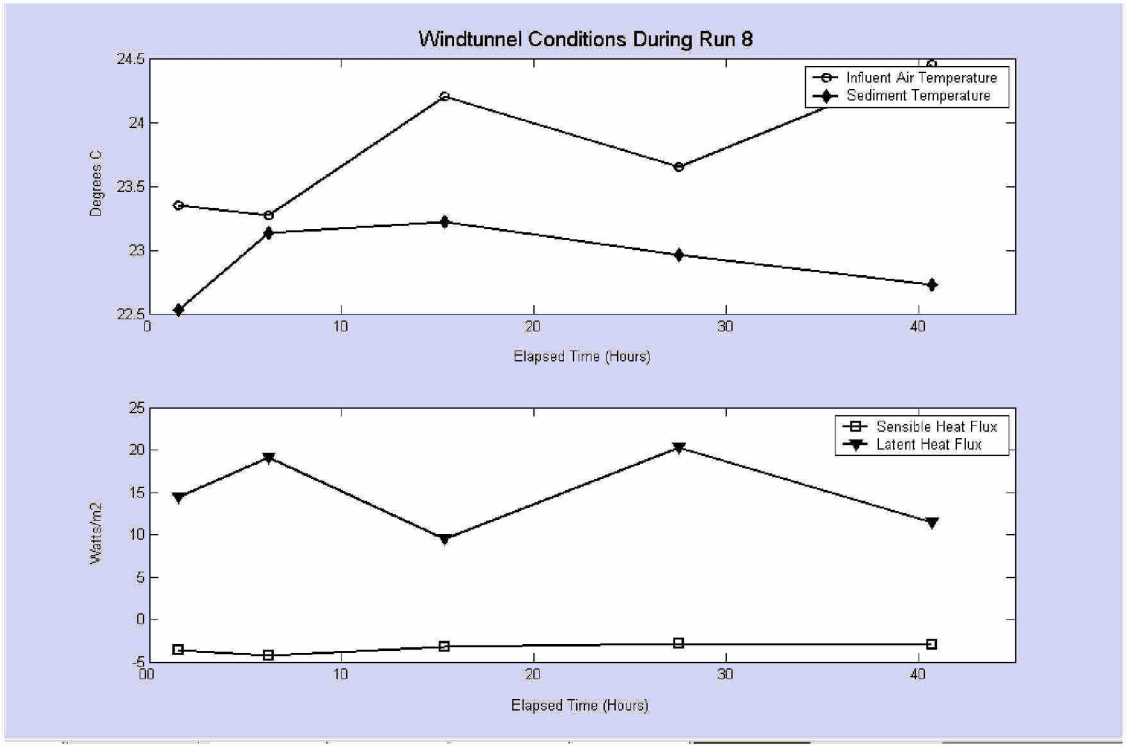

Figure 23. Wind tunnel Conditions During Run 8

The flux measurements for the dichlorinated, trichlorinated, and tetrachlorinated homologues were initially high and fell off rapidly. The initial flux values for the dichlorinated and trichlorinated homologues were approximately two times those measured during the previous run without stabilization, and the tetrachlorinated homologue flux was almost three. The decrease in fluxes was rapid and the final measured values were similar to those measured in the final interval of the previous run.

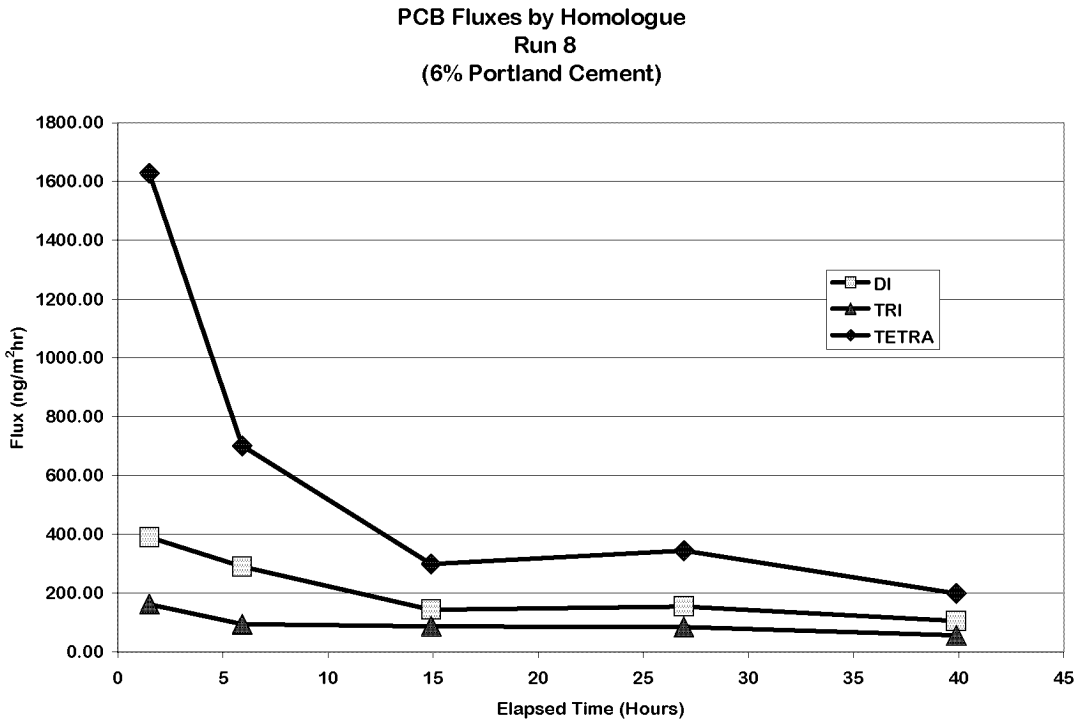

Figure 24. PCB Fluxes by Homologue, Run 8

2.3.9 Run 9

The ninth run was completed July 26, 2004 to July 28, 2004. The sediment was not stabilized. The mean velocity of the air flowing over the sediment was 20 cm/sec. The initial moisture content of the sediment was 150%. Over the course of the experiment the moisture content did not change significantly. The influent air temperature varied very little during this experiment (<1.5°C). Although the fluctuations were very small there appeared to be a pattern of peaks during the daytime and valleys at night. The sediment did not appear affected by the variation in influent air temperature; instead it rose steadily for the extent of this experimental run due to the warmer air blowing over it. The latent heat fluxes measured were close to zero, indicating little or no moisture flux from the sediment. The sensible heat was similar to the two previous runs indicating a small flux of convective heat into the sediment at a fairly constant rate.

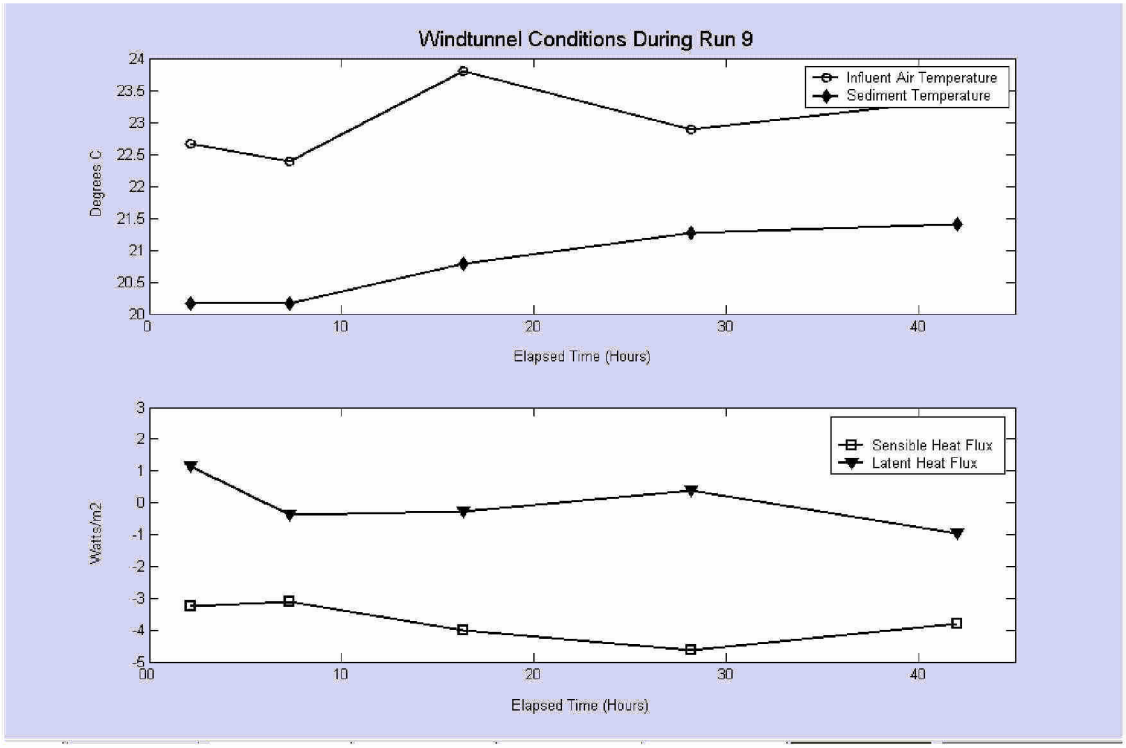

Figure 25. Wind tunnel Conditions During Run 9

Measurements for the third sampling interval in this run were not included because the PUF filter located in the effluent of the wind tunnel folded during the interval and a channel formed allowing the air to bypass the filter, thus the resulting concentrations were not accurate. The PCB fluxes measured in this experimental run were very similar to those measured during run 7. The increased speed compared to run 7 did not appear to have any effect on the measured fluxes.

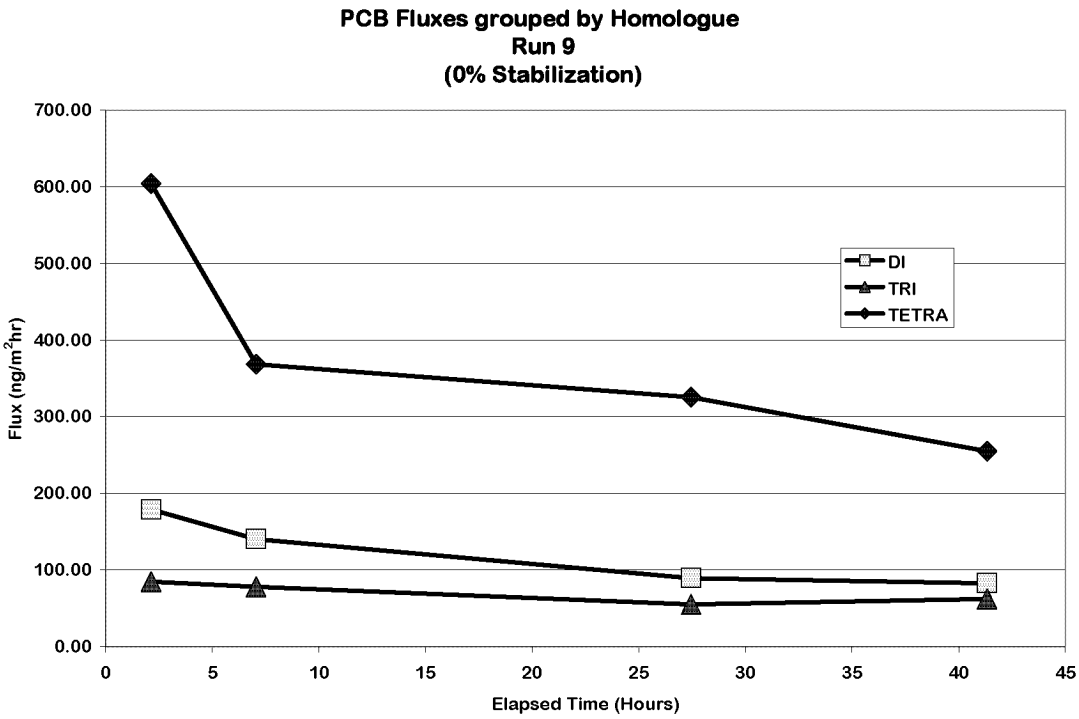

Figure 26. PCB Fluxes by Homologue, Run 9

2.3.10 Run 10

The tenth run was completed July 31, 2004 until August 2, 2004. The sediment was stabilized with 6% portland cement by weight. The mean velocity of the air flowing over the sediment was 20 cm/sec. The initial moisture content of the sediment was 121%. Over the course of the experiment the moisture content decreased to 106%. The influent air temperature during this run increased due to the building's air conditioning shutting down during the second day of this run. The temperature reached as high as 27°C. As a result of the very high air temperature the sediment also got extremely warm. The increase continued until it reached a peak six hours into the final sampling interval. The air conditioning in the room was restarted and the air temperature in the building dropped 2°C. Since the values on the plot are averages, the final interval appears to have a lower temperature than the interval before it even though it was when the peak temperature occurred. The sediment followed the same pattern. The latent heat measurements indicate a flux of moisture out of the sediment at 10-20 watt/m^2, with the highest measurement occurring at the initial measurement when the sediment was warmer than the air. The sensible heat flux is very similar to the previous three runs, indicating a small flux of convective heat into the sediment at a fairly constant rate.

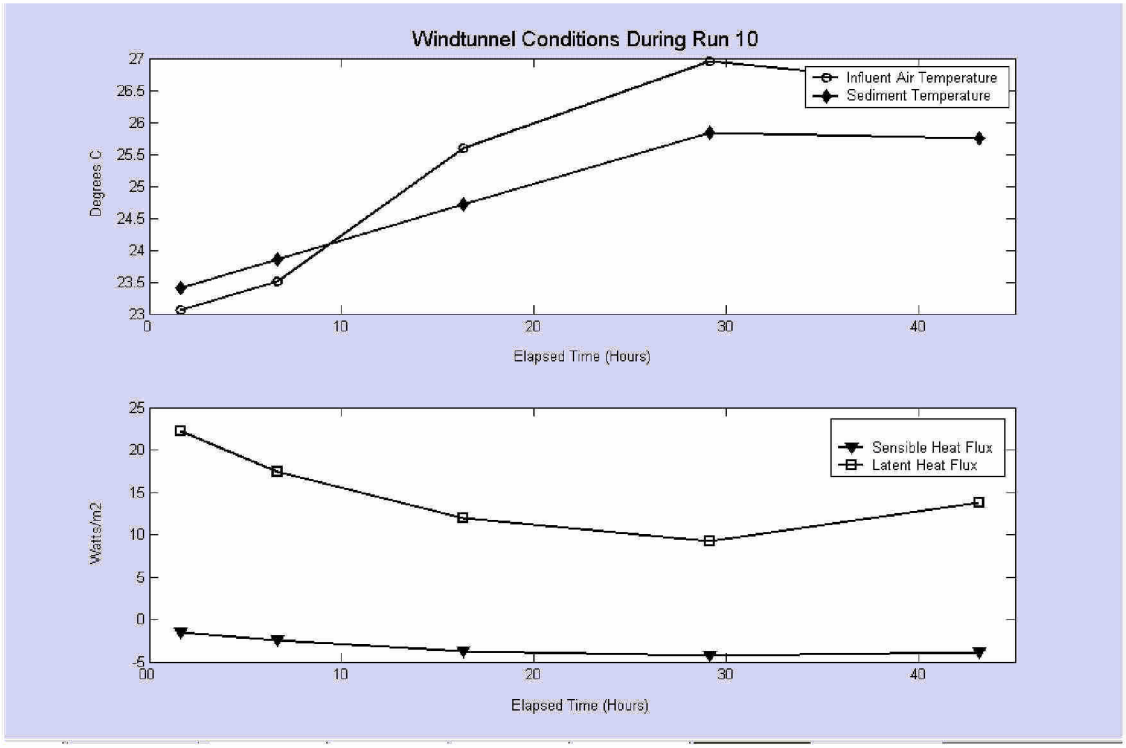

Figure 27. Wind tunnel Conditions During Run 10

The flux measurements for the dichlorinated, trichlorinated, and tetrachlorinated homologues indicate a high initial flux, that drops off quickly. The measure fluxes during this run exhibit a similar pattern to those collected during run 8, however the fluxes measured during run eight are much larger. The increase in temperature at the end of this run appears to have resulted in a small increase in the measured fluxes for the final sampling interval.

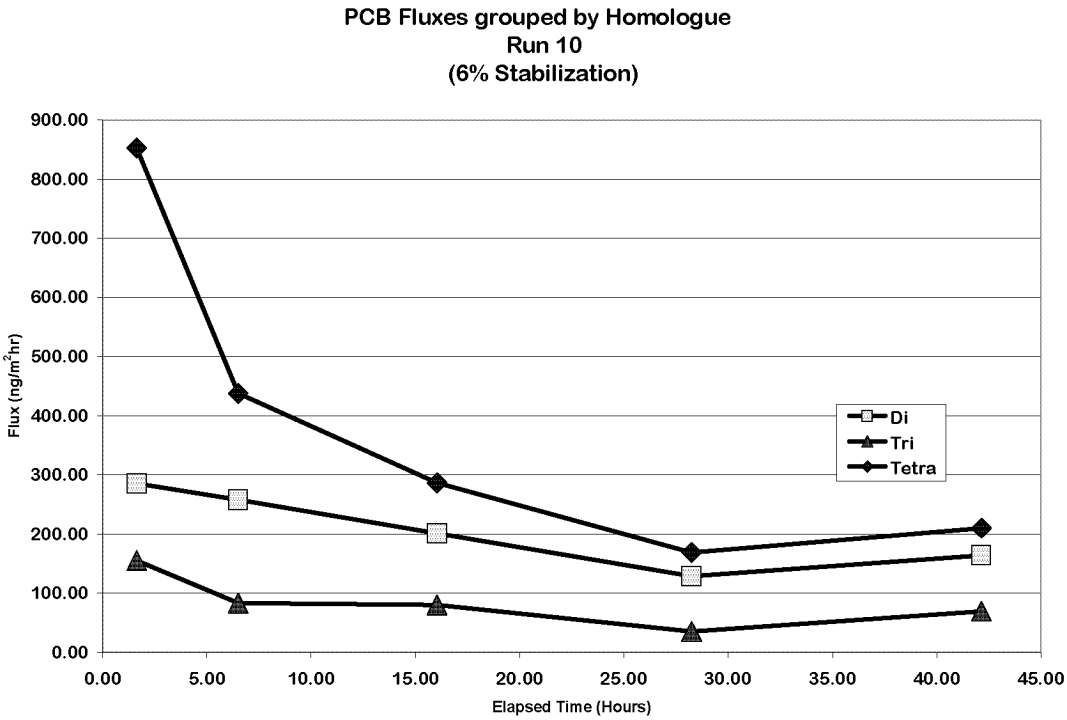

Figure 28. PCB Fluxes by Homologue, Run 10

2.3.11 Sediment Samples

Sediment concentrations of PCBs were analyzed for the various samples. Two samples were analyzed for sediment samples A and C which were composited and analyzed. On the other hand, sediment from sample B was analyzed for each drum in the sample group. The results of these analyses show that there is a somewhat consistent distribution of PCBs in the various homologue groups although sediment analysis has a very high variance. The concentrations measured in sample A reveal that tetrachlorinated homologue is present in the highest concentrations in both A and C, and the value in C is about 1.5 time that found in A. The dichlorinated homologue is higher in A than C. These analyses are consistent with the flux measurements from sample A and C. Fluxes measured from A were dominated by the dichlorinated homologue and those measured from C were dominated by the tetrachlorinated homologue. .

Table 4. Sediment Sample Results: Samples A and C

	Sediment Sample A (ppb)		***Sediment Sample C (ppb)***
	1A	**2A**	**2C**
DI	*445.1*	*202.2*	*181.8*
TRI	*149.2*	*970.8*	*156.7*
TETRA	*908.4*	*802.2*	*1208.9*

The measured concentrations for the samples C and B have a large range, but in general exhibit higher concentrations for the tetrachlorinated homologue. This is expected because the tetrachlorinated homologue dominates the fluxes measured from sediment samples B and C.

Table 5. Sediment Sample Results: Sample B

	Sediment Sample B (ppb)							
	7A	7B	8A	8B	9A	9B	10A	10B
DI	*832.0*	*62.5*	*289.5*	*67.6*	*838.4*	*313.1*	*237.0*	*221.7*
TRI	*48.9*	*190.3*	*128.1*	*238.2*	*86.3*	*88.4*	*20.4*	*43.2*
TETRA	*993.1*	*338.8*	*286.0*	*386.2*	*688.3*	*1151.3*	*587.1*	*424.8*

3.0 DISCUSSION

3.1 Time Dependence of PCB Fluxes

The evolution of the PCB flux after placement of SDM is a great concern, as are the effects of stabilization on that evolution. Each of the experimental runs conducted in the wind tunnel were carried out for at least forty eight hours. Several samples were collected during each run, in order to characterize the behavior of PCB fluxes as the sediment ages and the stabilizing agent cures. The pattern of fluxes with respect to time measured in both the field and laboratory investigations were analyzed to determine how the behavior of the fluxes was affected by the stabilization process. The PCB fluxes indicated a distinct pattern over time. The initial flux was high and it declined rapidly over the next 48 hours.

The fluxes measured for unammended dredged sediment show a similar pattern for samples B and C. Sample A (unammended) was run in the laboratory when it was very cold and the flux values were very low. There were two sampling runs completed on unammended sediment from sample B. These runs were conduced at two air velocities (~15 cm/s, and ~20 cm/sec) to investigate the effect of changing the velocity on the PCB flux. The fluxes measured during the two runs were very similar. The initial flux measurements of the dichlorinated homologue collected for samples B and C (at ~2 hours) were 182 ± 5.6 ng/m^{2}hr and 243 ng/m^{2}hr respectively. These fluxes gradually declined over the sampling run to 88 ± 7.2 ng/m^{2}hr at ~41 hours for sample B, and 85 ng/m^{2}hr at ~37 hours for sample C. These measurements indicate a flux decrease of 52% and 65% for samples B and C with respect to dichlorinated homologues. The tetrachlorinated homologue exhibited similar behavior. The initial flux measurements for samples B and C (at ~2 hours) were 581 ± 35.5 ng/m^{2}hr and 656 ng/m^{2}hr respectively. These fluxes gradually declined over the sampling run to 248 ± 8.4 ng/m^{2}hr at ~41 hours for sample B, and 198 ng/m^{2}hr at ~37 hours for sample C. These measurements indicate a decrease of 57% and 70% respectively for samples B and C with respect to tetrachlorinated homologues. The fluxes measured at approximately 37 hours for sample

C are slightly lower than those measured for sample B at a similar time; this is due to differences in the temperature. The temperature remained relatively stable during the two runs completed with sample B. Conversely, the temperature fluctuated greatly during the run completed with sample C. The sample was collected overnight and the temperature was lower than the samples before and after.

Several runs were completed with varying degrees of stabilization. Experimental runs with sediment samples A and C were conducted with 4% and 8% portland cement by weight. Two runs were completed with sediment sample B and stabilized with 6% portland cement. The sediment collected in sample A varied greatly in its amount and distribution of PCB congeners, as a result comparisons with the other samples are somewhat difficult.

The initial flux measurements for the fifth run in this experiment (sample C, 4% portland cement) were collected in the interval centered around1.14 hours. The fluxes measured during this interval appear to be extremely low. This may be due to the low initial sediment temperature or air by passing the PUF filter. As a result the second sampling interval will be analyzed for both 4% runs. This interval is centered around 4.35 hours for sample C and 5.85 hours for sample A. The dichlorinated homologue measurements collected during the experimental runs sediment stabilized with 4% portland cement for samples A and C (at ~2 hours) were 941 ng/m^{2}hr and 369 ng/m^{2}hr respectively. These fluxes declined sharply to values of 198 ng/m^{2}hr, at ~16.47 hours for sample A, and 83 ng/m^{2}hr at ~15.8 hours for sample C. These represent a decrease of 77% and 82% for fluxes from samples A and C. The tetrachlorinated homologue measurements were 212 ng/m^{2}hr and 649 ng/m^{2}hr respectively. These fluxes declined sharply to values of 25 ng/m^{2}hr, at ~16.47 hours for sample A, and 142 ng/m^{2}hr at ~15.8 hours for sample C. These represent decrease of 79% and 88% for fluxes from samples A and C. The decrease in the flux rate from the sediment is larger in magnitude and shorter duration when the sediment is stabilized.

Two runs were completed with sediment that had been stabilized with 6% portland cement. These were run at two mean air velocities over the sediment (~15 cm/s, and ~20 cm/sec). Run eight was completed with an average air velocity of 15 cm/sec. The initial flux measurement of the dichlorinated homologue (at ~1.5 hours) was 390 ng/m^{2}hr. This flux declined to 143 ng/m^{2}hr at ~15 hours and then decreased to 108 ng/m^{2}hr at ~40 hrs. The initial flux measurement of the tetrachlorinated homologue (at ~1.5 hours) was 1629 ng/m^{2}hr. This flux declined to 299 ng/m^{2}hr at ~15 hours and then decreased to 198 ng/m^{2}hr at ~40 hrs. Run 10 was completed with an average air velocity of 20 cm/sec. The initial flux measurement of the dichlorinated homologue (at ~1.5 hours) was 285 ng/m^{2}hr. This flux declined to 201 ng/m^{2}hr at ~15 hours and then decreased to 164 ng/m^{2}hr at ~40 hrs. The initial flux measurement of the tetrachlorinated homologue (at ~1.5 hours) was 853 ng/m^{2}hr. This flux declined to 286 ng/m^{2}hr at ~15 hours and then decreased to 209 ng/m^{2}hr at ~40 hrs. The fluxes measured during the low velocity run were much higher those for the high velocity run; however they decreased quickly to values that were very similar.

Run 10 was completed at the same velocity as the remainder of the runs in order to compare the effect of varying amounts of stabilization. The initial fluxes were similar for both the dichlorinated and tetrachlorinated homologues, and they both decreased rapidly, however run 10 had an average sediment temperature of 24.7°C and run 5 had an average sediment temperature of 18.7°C. This discrepancy could explain why the fluxes at the end of the runs are much larger for run 10 even though more cement was used.

Two runs were completed using 8% portland cement by weight. The initial flux measured during run 4 was similar to that measured 4.35 hours into run 5 (sample C, %4 portland cement). The difference between the two runs can most easily be seen in the measurements of latent heat flux. In run five there is a positive moisture gradient out of the sediment. In run four however, there is no latent heat flux indicating that the sediment is essentially dry. The relatively low initial flux is most likely due to the loss of the PCBs during the stabilization process. Evidence for this loss of PCBs during stabilization is the background concentration during the initial sampling intervals.

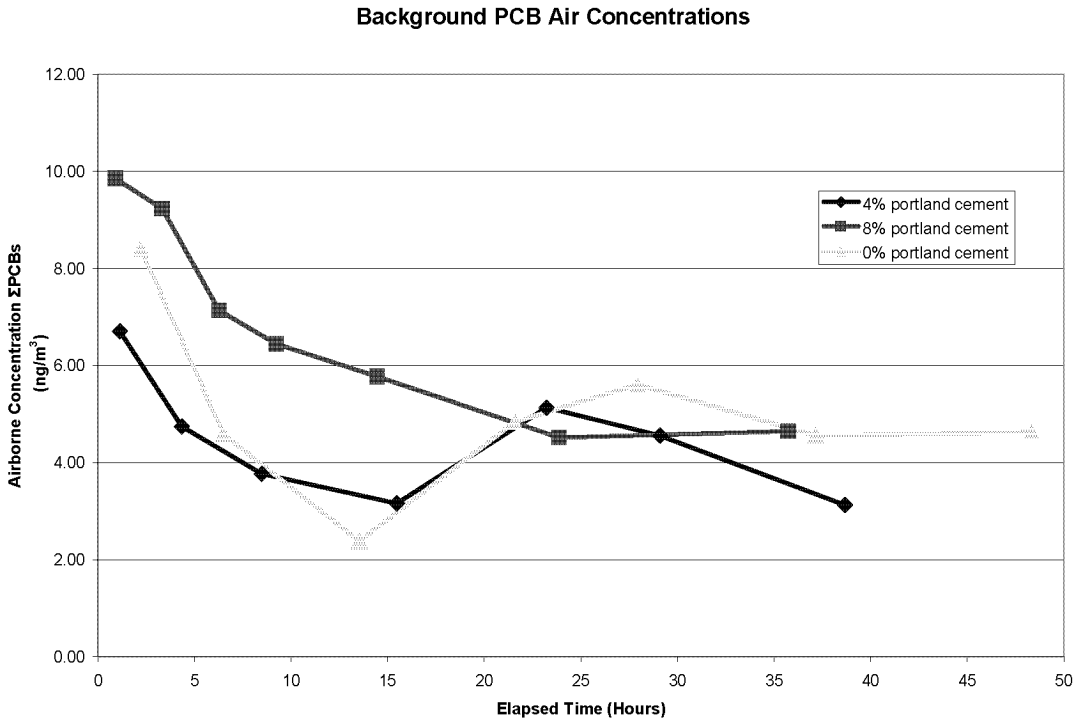

Figure 29. Background Laboratory PCB Air Concentrations

The run completed with 8% cement has a high background concentration which remains high through the first night when the concentrations typically decrease. After the first day the background concentrations return to normal for the laboratory.

The flux rate for the 8% stabilized sediments decreases very steadily over the final four sampling intervals in both. Over the same period the fluxes measured from the 4% stabilized sediments fluctuate along with the air temperature. In addition, fluxes from

non-stabilized sediments have even larger fluctuation due to temperature. Thus it is apparent that temperature has a lesser affect on the fluxes from more highly stabilized sediment.

3.2 Temperature Dependence of PCB Fluxes

The effects of temperature fluctuations can be seen in some of the experimental runs. The two runs affected most by the fluctuations in temperature were runs 3 and 6.

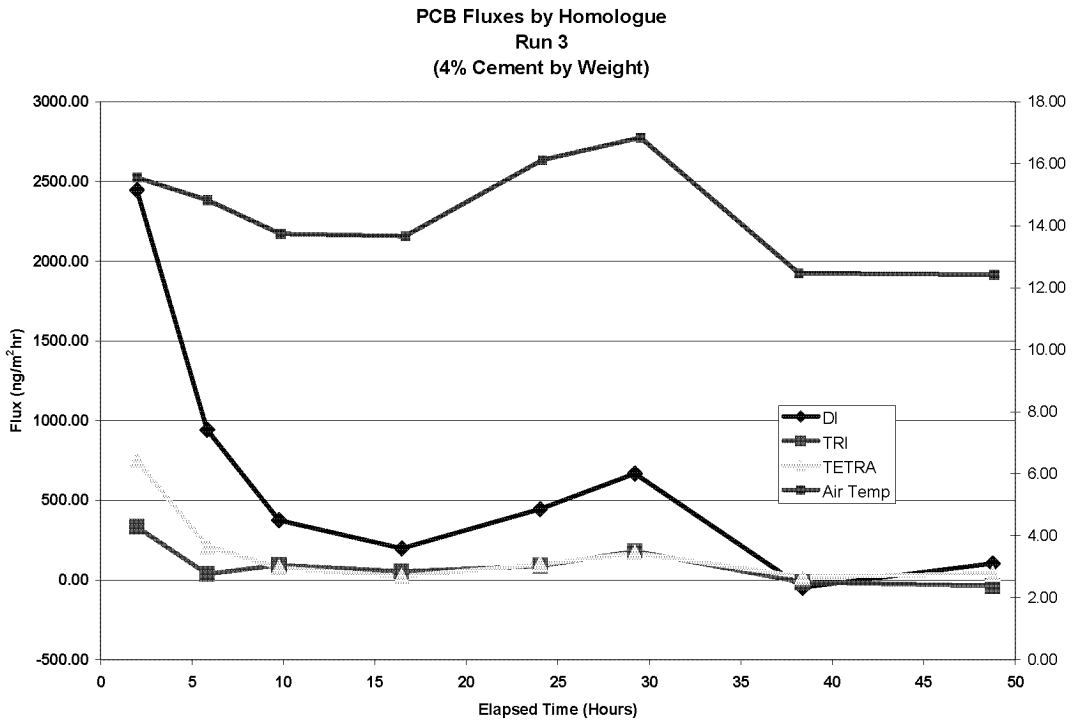

Figure 30. PCB Homologue Fluxes and Air Temperature, Run 3

It can be seen from this figure that spike in temperature that occurred between 24 and 30 hours induced a spike in the PCB fluxes.

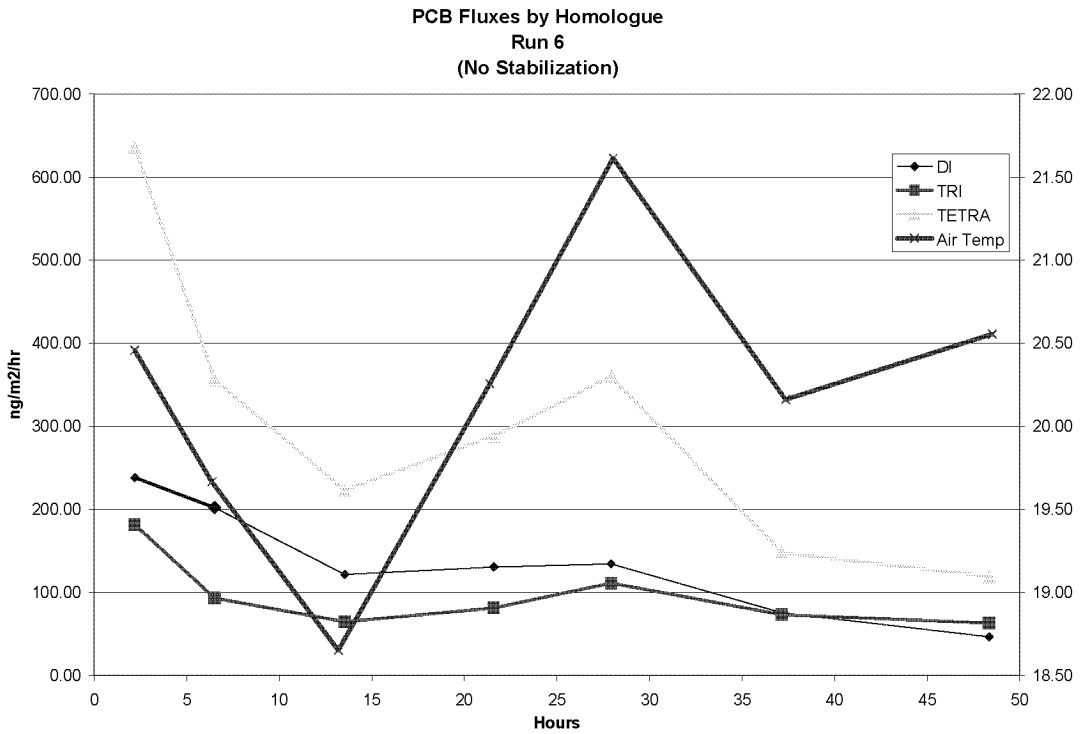

Figure 31. PCB Homologue Fluxes and Air Temperature, Run 6

This plot of run six also shows the influence that temperature fluctuations had on the PCB fluxes. This plot shows that as well as increasing the flux on a temperature peak, there is also a depression in the PCB flux measurements during colder conditions.

The relationship between temperature and the concentrations of PCBs measured in the laboratory background air as well as in the wind tunnel was investigated using a least squares regression of the natural log of the PCB concentration to the reciprocal of the temperature, (1/°K), to yield a Clausisus Clapyeron-like equation. The background PCB concentrations were highly variable. The R^2 values for these relationships are relatively low. Temperature fluctuations in the laboratory account for approximately 40-50% of the variance in PCB concentrations. The background measurements of PCB concentration vary a great deal.

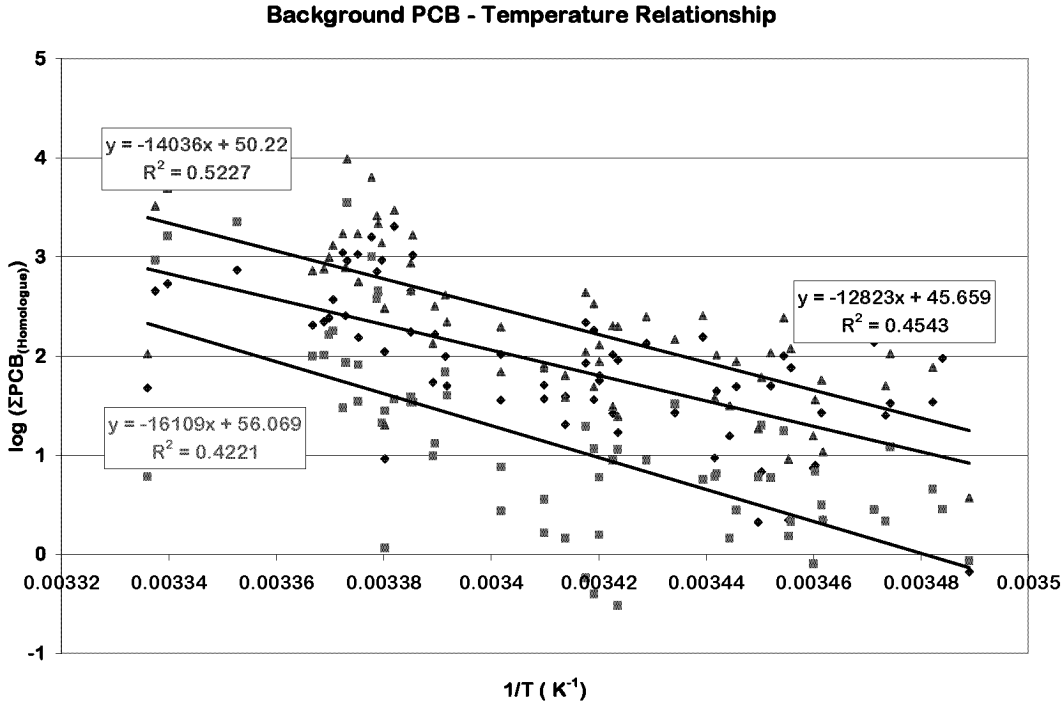

Figure 32. Laboratory Temperature versus PCB Concentration

The relationship shown in the figure above was determined over all of the experimental runs. As a result there is a large amount of variance due to stabilization, initial PCB concentration of the sediment, and initial moisture content. In order to eliminate these variables, each run was investigated separately. The temperature – PCB concentration relationships were then used to correct the measured concentrations in the wind tunnel and background air. Only regressions with an R^2 value greater than 0.5 were used. In addition, the first measurement of PCB concentration was not used due to a consistent large flux observed during the initial sampling interval for each experimental run. Predicted concentrations based solely on temperature were calculated for each time interval. PCB fluxes were calculated using the difference of the predicted concentrations, the flow rate, and the surface area of the dredged material. After the predicted fluxes were calculated, the mean was determined and subtracted out. The remaining values represented the fluctuations in PCB fluxes due to temperature. These were then subtracted from the measured fluxes, the resulting 'corrected' flux values represented the fluxes from the sediment over the length of the experimental run ,with the temperature held constant at the mean temperature measured during the run. This procedure was completed for runs three and six because of the strong influence of temperature. The equations of the regression lines and fit statistics are presented in Table 11.

Table 6. Temperature - PCB Concentration Relationships

		Equation	R^2
Run 3	Wind Tunnel	$\ln (C_{di}) = -20486 \times (1/T) + 73.143$	0.59
		$\ln (C_{tri}) = -31863 \times (1/T) + 111.22$	0.53
		$\ln (C_{tetra}) = -30968 \times (1/T) + 108.03$	0.86
	Background	Background concentrations exhibit $r^2 < 0.5$ when regressed versus temperature, as a result the measured background concentrations were used.	
Run 6	Wind Tunnel	$\ln (C_{di}) = -17523 \times (1/T) + 61.077$	0.68
		$\ln (C_{tri}) = -29705 \times (1/T) + 102.41$	0.82
		$\ln (C_{tetra}) = -27136 \times (1/T) + 94.271$	0.74
	Background	$\ln (C_{di}) = -18447 \times (1/T) + 63.274$	0.62
		$\ln (C_{tri}) = -32755 \times (1/T) + 111.61$	0.64
		$\ln (C_{tetra}) = -24889 \times (1/T) + 85.228$	0.56

Figures 33 and 34 are plots of the measured, predicted, and 'corrected' tetrachlorinated PCB fluxes for runs 3 and 6.

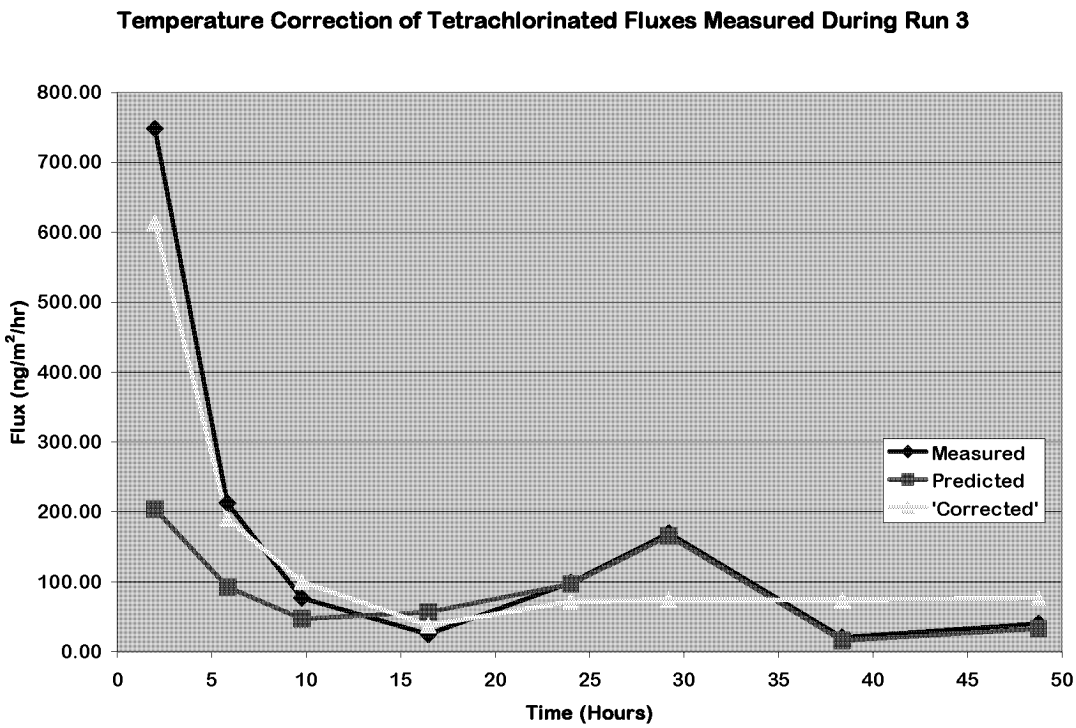

Figure 33. Temperature 'Corrected' PCB Fluxes, Run 3

Run 3 was stabilized with 4% portland cement. This reaction creates heat; as a result the 'corrected' flux is lower than the measured. For the rest of the run fluctuations due to temperature are removed and the tetrachlorinated PCB flux remains steady at ~75 ng/m^2/hr.

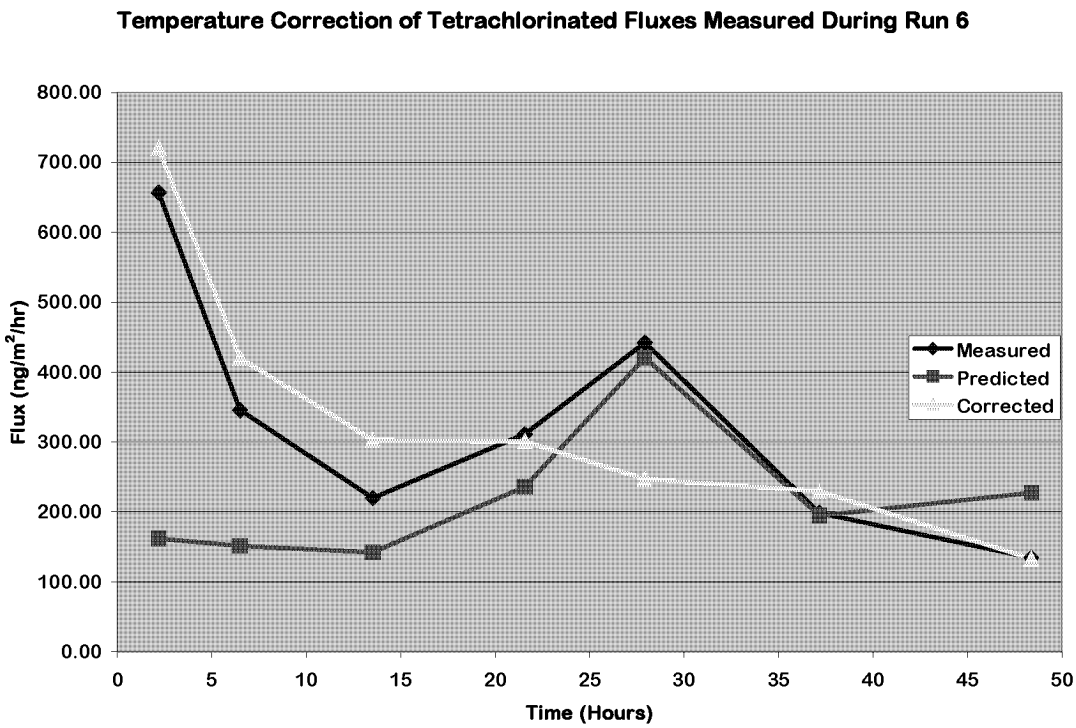

Figure 34. Temperature 'Corrected' PCB Fluxes, Run 6

The sediment used during run 6 was not stabilized. As a result the initial flux occurs at a relatively low temperature and when corrected, increases. The fluxes steadily decrease from the initial value and the peak in temperature on the second day is successfully removed.

3.3 Modeling of PCB Flux Measurements

Several models described in a previous section were evaluated in order to simulate the laboratory measurements. Though several were promising the main confounding variable was the vertical moisture profile. It was determined that a bulk approach would be the most effective method of modeling the data. This approach assumes that the concentration of PCB available to volatilize in the sediment follows a first order 'kinetic'. The initial equation is:

$$\frac{\partial C}{\partial t} = -\alpha C \tag{22}$$

$\frac{\partial C}{\partial t}$ is the change in concentration over time, α, is a pseudo-first order volatilization rate constant, and C, is the concentration of PCBs in the sediment. When this is integrated with and initial condition that C=C° (the initial concentration in the sediment) at t=0, the result is:

$$C = C^{\circ} e^{-\alpha t} \tag{23}$$

This equation can then be substituted into the Nerst equation presented earlier in the description of the Hartley model. It represents the flux as the concentration gradient between the pore air and the free stream concentration of the air, C^{∞}, multiplied by the overall mass transfer coefficient, k.

$$F = k\left(C - C^{\infty}\right) \tag{24}$$

Since PCBs are in extremely low concentrations in the atmosphere, for modeling purposes it can normally be assumed that C^{∞} is equal to zero, ($C^{\infty} = 0$), the resulting equation is

$$F = kC^{\circ} e^{-\alpha t} \tag{25}$$

Thus the flux of contaminant is the product of the mass transfer coefficient, the sediment concentration, and the volatilization rate. Taking the natural log of both sides of this equation and plotting them yields a linear relationship between ln(F) and α. The intercept is the natural log of the product of the mass transfer coefficient at t=0 and the initial sediment concentration. The overall mass transfer coefficient at t=0 is approximately equivalent to the air side mass transfer coefficient because when freshly placed the sediment is moist, and resistances to PCB fluxes are not yet present in the sediment. As time passes, the resistances in the sediment will build up and the flux will be increasingly sediment-side controlled. Since the intercept in the model represents the flux at t=0 the air side mass transfer coefficient can be substituted for the overall mass transfer coefficient. This model was applied to the PCB flux measurements made during this study. The results are presented in Table 7.

Model Results

		Dichlorinated Homologue			Trichlorinated Homologue			Tetrachlorinated Homologue		
		slope	***Intercept***	***R^2***	***slope***	***Intercept***	***R^2***	***slope***	***Intercept***	***R^2***
Unammended	***Run_1***	NA	NA	NA	-0.0256	4.2465	0.4281	-0.0317	4.2347	0.458
	Run_6	-0.0384	5.3604	0.7534	-0.0099	5.118	0.1144	-0.0238	6.034	0.434
	Run_7	-0.0152	5.374	0.3903	-0.0114	5.0638	0.5922	-0.016	6.185	0.6259
	Run_9	-0.0211	5.0393	0.9265	-0.0114	4.0063	0.6985	-0.0167	6.0242	0.7598
4%	***Run_3***	-0.0478	7.0855	0.5562	NA	NA	NA	-0.0472	5.5207	0.4086
	Run_5	-0.0382	5.3008	0.5847	-0.0459	5.5221	0.8047	-0.0455	5.9867	0.6117
6%	***Run_8***	-0.0316	5.977	0.8385	-0.0224	4.9206	0.7347	-0.0428	6.9732	0.7626
	Run_10*	-0.0301	5.7849	0.9875	-0.0488	4.9952	0.898	-0.0565	6.6441	0.9364
8%	***Run_2***	-0.0219	7.0018	0.7145	-0.0428	5.3151	0.8203	-0.0635	5.0758	0.8423
	Run_4	-0.1562	5.7157	0.8685	-0.1247	6.0095	0.9586	-0.0547	6.2314	0.8857
	May-02	-0.0481	7.1973	0.7537	-0.0465	7.3381	0.6495	-0.039	6.9107	0.6727

** Measurement at 42 hours removed due to large temperature spike*

NA = R^2 value >0.05

Table 7. Temperature versus PCB Concentration Relationships

The dichlorinated homologue fluxes exhibit a trend of slopes that are increasingly negative with respect to the amount of portland cement added. The exception to this trend is the 6% stabilized measurements. It is believed that the relatively high temperatures result in slightly increased fluxes even when the sediment is essentially dry, thus reducing the rate of decay of the flux. The intercepts, which are the initial concentrations multiplied by the air side mass transfer coefficients, appear to increase with the amount of cement added. The unammended sediment runs for samples B and C have lower intercepts than those measured for runs with the same samples that have been stabilized. This is presumably due to the increased temperature resulting from the exothermic reaction between the moisture in the sediment and the portland cement. The measurements collected during landfill study of dichlorinated homologue fluxes are very similar to the measurements for Run 3 (4% cement).

The measurements collected for the trichlorinated fluxes exhibit a pattern similar to the dichlorinated fluxes. The field event data has a very large intercept value compared to those measured during the laboratory studies. The model results for the tetrachlorinated results show the most consistent pattern of increasing decay of fluxes with increased cement added. The field data appears similar to the measurement made with sediment stabilized with 4% cement by weight.

The slopes of the various regression lines are dependent on the amount of cement used for stabilization and the chlorination of the various PCB homologues. It can be seen that increasing the amount of Portland cement used to stabilize the sediment will increase the rate at which the fluxes decay from an initial value.

Runs 4, 5, and 6, were completed under similar atmospheric and sediment conditions. These runs represent unammended, 4% , and 8% stabilization. The flux values have been normalized by the initial flux rate in order to eliminate the effects of varied concentration. The May 2003 field measurements were also included to compare the field measurements to the laboratory study. The value found at night during the field event was not included due to the high stability during that interval. The dichlorinated homologue fluxes appear to show a distinct pattern with the 8% Portland cement mix showing the steepest slope. The 4% and 0% appear to have the same slope as each other while the field event has a slope that is slightly more negative than the 4%.

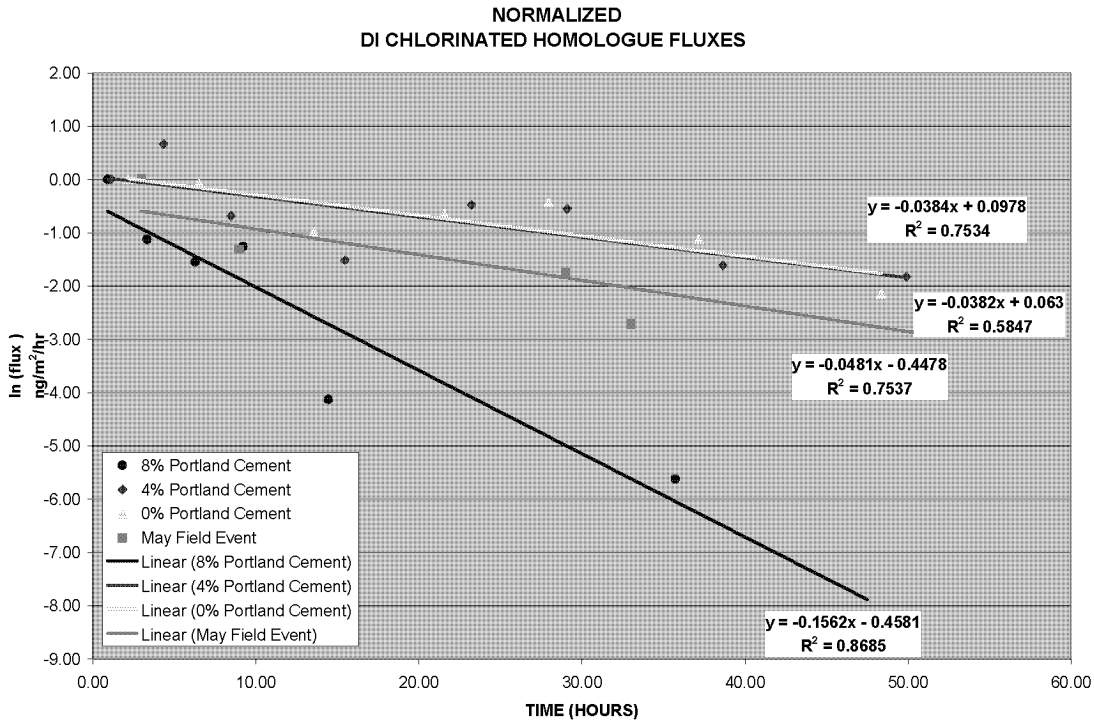

Figure 35. Di-Chlorinated PCB Fluxes

A similar pattern is observed in the trichlorinated homologues. The 4% has a steeper slope than the 0%, and the field event has a slightly more negative slope than the 4%. The 8% is still very steep compared to the less stabilized experimental runs and the field event.

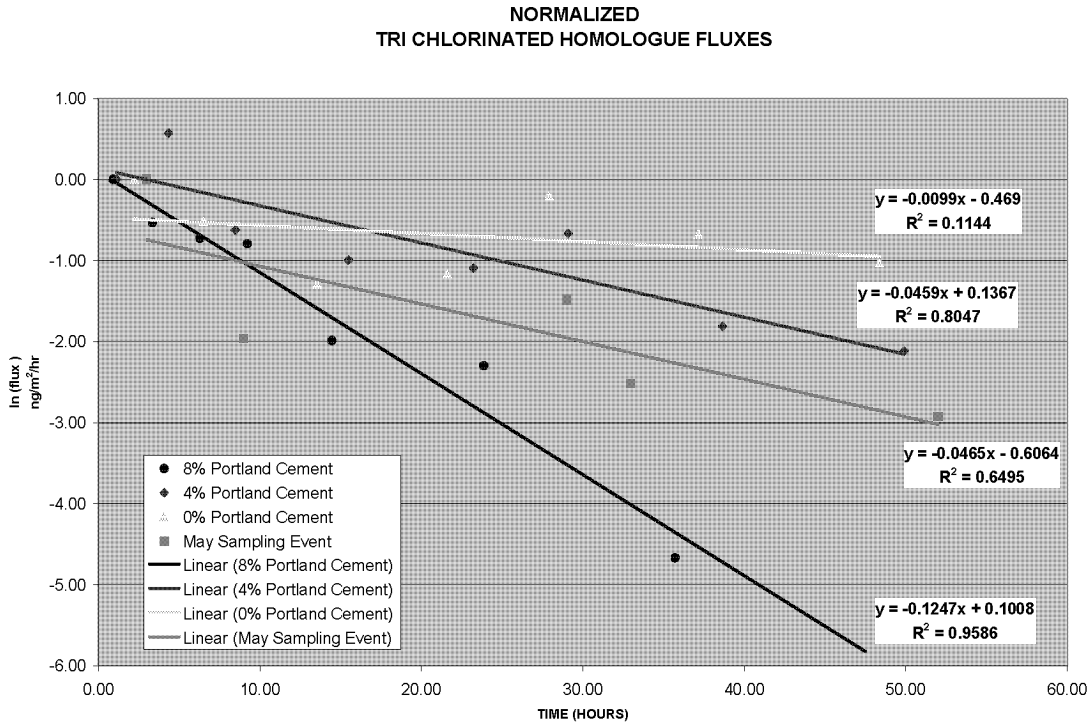

Figure 36. Tri-Chlorinated PCB Fluxes

The tetrachlorinated homologues also exhibited similar behavior. The slopes of all the trend lines are steeper than for the trichlorinated homologues. The 4% and field event are very similar to the 8% stabilized sediment.

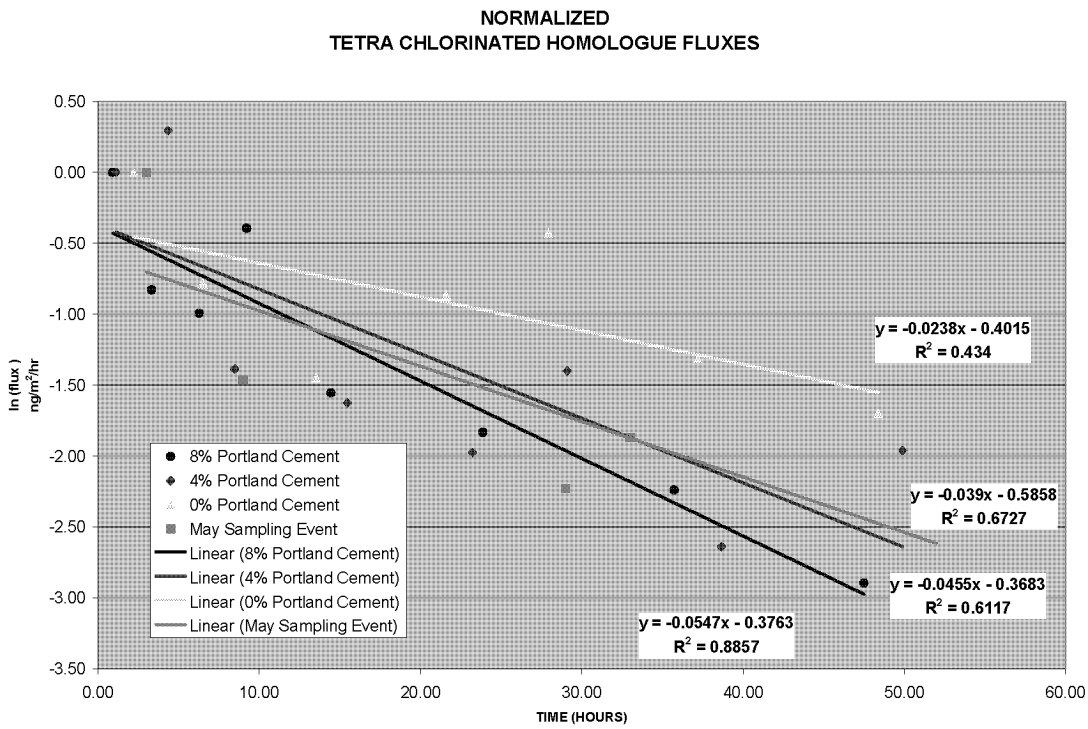

Figure 37. Tetra-Chlorinated PCB Fluxes

It is also apparent that the rate of decay of the fluxes is dependent on the molecular weight of the PCB. The decay is greatest for the tetrachlorinated and least for the dichlorinated homologue. Another apparent effect is that stabilization will affect the homologues differently. The 4% mix appears to have little effect on the decay rate while 8% has a large effect on the dichlorinated homologue. In contrast to this, for the trichlorinated homologue the 4% mix exhibits a slope approximately halfway between the 0% and 8% mixes. And finally for the tetrachlorinated homologue the decay rate for the 4% mix approached the 8% mix.

During the May 2000 field sampling interval, the sediment was stabilized with approximately 12% cement. When compared with the measurements collected for this study it matches closer to the behavior of sediment stabilized with 4% cement. The difference may be due to the sediment sampling method, physical properties of the sediment or meteorological factors (sunlight, wind, etc.).

4.0 CONCLUSIONS

Comparisons between the data collected from the field study at the Bayonne Landfill and the laboratory wind tunnel study were made to determine if the measurements from the laboratory study were a good representation of the field. In addition, these data were also compared to studies conducted by other researchers. In order to make these comparisons it must be noted that there were differences in initial PCB concentration, PCB congeners that were analyzed, and scaling differences. The average of the total PCB flux measured during the laboratory experiment was 577 ng m^{-2} hr^{-1} and they ranged in value from -155 to 4465 ng m^{-2} hr^{-1}. These are well with the range of values measured during the field sampling experiments: 72 to 15,000 ng m^{-2} hr^{-1} with a mean value of 2050 ng m^{-2} hr^{-1} (Korfiatis et al., 2003). These values represent a sum of PCBs, although the sampling set is not the same they all have several of the same congeners represented.

Fluxes of PCBs from stabilized sediment are initially high and decrease rapidly as the sediment dries. Thus the high fluxes measured in the first few hours after placement may appear to represent the largest source of PCBs to the atmosphere. In reality the low magnitude, long term fluxes represent a more significant source. The fluxes measured during runs four and six are a good example of this. The sediment used for run four was stabilized with 8% portland cement. After placement, the initial flux of tetrachlorinated PCB congeners was 798 ng/m^2/hr, this was elevated due to an increase in temperature caused by the reaction of the cement and the water in the sediment. The sediment used in run six was not stabilized. The initial flux rate was 636 ng/m^2/hr. The sediment used for both of these samples was homogenized when it was collected so the initial concentrations in the sediment during both experimental runs were approximately the same. Although the initial flux rate increases with the addition of cement, the flux rate declines much faster over time due to the much lower moisture content of the sediment. When integrated over the length of the experimental run it was found that the non-stabilized sediment released 15 µg of tetrachlorinated PCB congeners to the atmosphere from one square meter of sediment while the stabilized sediment released only 11 µg. Thus it is apparent that stabilization will reduce the total amount of PCB released to the atmosphere.

Table 8. ΣPCBs Volatilized during Experimental runs

Sediment Sample	Experimental Run	Stabilization	ΣPCBs Volatilized (µg) (per m^2 of sediment surface)		
			Di	Tri	Tetra
	Run 1	***0%***	*12.2*	*2.4*	*2.8*
A	***Run 3***	***4%***	*22.9*	*3.2*	*6.4*
	Run 2	***8%***	*29.1*	*1.9*	*1.6*
	Run 6	***0%***	*6.4*	*7.4*	*15.2*
C	***Run 5***	***4%***	*7.3*	*5.2*	*12.4*
	Run 4	***8%***	*3.5*	*3.6*	*11.1*
	Run 7	***0%***	*6.3*	*4.7*	*17.5*
B	***Run 9***	***0%***	*4.7*	*2.1*	*13.7*
	Run 8	***6%***	*10.0*	*5.1*	*24.3*
	Run 10	***6%***	*3.7*	*0.9*	*12.6*

This table shows that in general, the total mass of PCBs volatilizing from the sediment decreases with the amount of stabilization. Notable exceptions to this trend are Run 8 and Run 1. Run 8 exhibited extremely high measured fluxes while having the same pattern of decrease in the flux values as run 10. This could be the result of a higher concentration of PCBs in the sediment. Run 1 was completed with extremely cold sediment, the low temperature acted to restrict the flux of PCB. In both cases, if the experimental runs were extended it is believed that the ΣPCBs volatilized would fit into the pattern. When the fluxes for runs 7 and 8 are calculated using the models proposed in the previous section, the ΣPCBs volatilized from the non-stabilized sediment is equal to the 6% stabilized sediment from run eight, 108 hours after placement, and is larger as time passes.

The first order bulk transport model presented in the previous section can be used to predict PCB fluxes from sediment. The flux will be a function of the initial sediment concentration of PCBs, the decay rate and time.

$$F = C^{\circ} k_a e^{-\alpha t} \tag{26}$$

α is the volatilization rate, k_a is the air-side mass transfer coefficient, and C° is the initial sediment concentration of PCBs. The volatilization rate was determined using the measured flux rates from the wind tunnel study. The reciprocal of the volatilization rate will be in units of hours, as a result it can be used as a time constant for the decrease in flux rate by one factor of e. It was found to be largely a function of the amount of portland cement used for stabilization of the sediment. The time constant for the decrease in the flux rate of PCBs is shown to decrease by more than 50% by the addition of 8% portland cement as compared to addition of none for the di, tri, and tetrachlorinated homologues.

Table 9. Time Constant in Hours (1/α) versus Stabilization

	% Stabilization			
Homologue	**0**	**4**	**6**	**8**
Di	**53.2**	**27.8**	**22.4**	**18.8**
Tri	**74.6**	**25.6**	**19.3**	**15.5**
Tetra	**43.5**	**23.9**	**19.5**	**16.5**

The values for C° can be predicted using the bulk sediment concentration, $C_{sediment}$, and the temperature of the sediment. To predict this value, the ratio of C° and $C_{sediment}$ were compared to the reciprocal of the temperature of the sediment.

$$\ln\left(\frac{C^{\circ}}{C_{sediment}}\right) = a\left(\frac{1}{T}\right) + b \tag{27}$$

Where a and b are regression coefficients and T, is the sediment temperature in °K. The regression coefficients can then used in the model to predict the value for C° for each experimental run.

Table 10. Temperature – Concentration Regression

Homologue	*Equation*	*Correlation*
Di	*y = -8978.4 (1/°K) + 31.771*	*R2 = 0.4496*
Tri	*y = -10085 (1/°K) + 34.733*	*R2 = 0.5351*
Tetra	*y = -15624 (1/°K) + 53.499*	*R2 = 0.7241*

Using these expressions it is possible to predict fluxes of PCB for each homologue based upon the bulk sediment concentration, the temperature, the mass transfer coefficient, and the time of exposure.

$$F = C_{sediment}\left[e^{a/T+b}\right]k_a e^{-\alpha t} \tag{28}$$

This expression was evaluated for all of the experimental flux measurements collected in the wind tunnel.

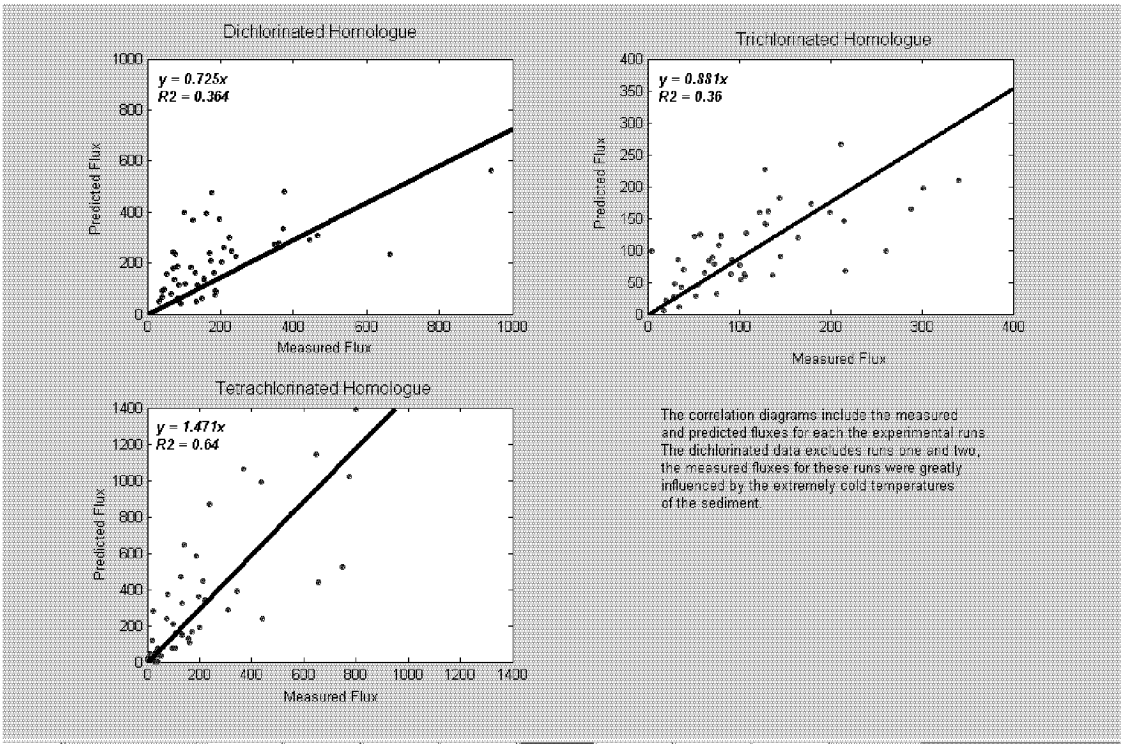

Figure 38. Model Correlation Results

The proposed model was found to under predict the dichlorinated and trichlorinated fluxes by 27.5% and 11.9% and over predict the tetrachlorinated fluxes by 47.1%. The correlation of predicted fluxes to measured fluxes is r^2=0.36 for both dichlorinated and trichlorinated homologue fluxes and r^2=0.64 for the tetrachlorinated homologue fluxes. The model was found to predict fluxes within a factor of 3 for over seventy percent of the fluxes measured in the wind tunnel. Divergences of the predictions from the measured fluxes are a result of variations in temperature over the length of an experimental run, and the equipment error inherent in the measurement of PCB concentrations from the air and sediment samples. This model was created with laminar flows, in a turbulent flow regime; the initial fluxes would be greater due to an increase in the value of k_a. In addition the values for α would also increase due to enhanced water loss from the sediment.

The presented studies were conducted in order to 1) create a viable, repeatable method for the field measurement of PCB fluxes from dredged sediment, 2) verify the field measurements with a bench scale experiment, and 3) produce a predictive model that can be used to assess the fluxes of PCB from dredged sediment. The field measurement technique described in the first section was used in four sampling intensive and yielded consistent results. The PCB fluxes measured using this technique were found to be comparable to fluxes measured in the laminar flow wind tunnel used in the bench scale laboratory experiments. These experiments yielded measurements that were then used to calibrate a model for the determination of fluxes of PCB from dredged sediment.

REFERENCES

Bamford, H., Poster, D., and Baker, J, (2000) Henry's Law Constant of Polychlorinated Biphenyl Congeners and Their Variation With Temperature, Journal of Chemical Engineering Data, Vol 45, 1069-1074.

Chiarenzelli, J., Scrudato, R., Arnold, G. Wunderlich, M., and Rafferty, D., (1996) Volatilization of Polychlorinated Biphenyls from Sediment During Drying at Ambient Conditions, Chemosphere, Vol 33 No. 11, 899-911.

Chiarenzelli, J.R., Scrudato, R.J., Wunderlich, M.L., Oenga, G.N., Lashko, O.P., (1996) PCB Volatile Loss and the Moisture Content of Sediment during Drying, Chemosphere, Vol 34 No. 11, 2429-2436.

Cousins, I. T., Hartlieb, N., Teichmann, C., Jones, K.C. (1997) Measured and Predicted PCB Volatilisation Fluxes from Sludge-Amended Soils. Environmental Pollution 97, no. 3 pp. 229-238.

Cussler, E. L. (1984) Diffusion: Mass Transfer in Fluid Systems. Cambridge University Press, Cambridge

Dalton, J., (1802) Experimental essays on the Constitution of mixed gases, Mem. Manchester Lit. and Phil. Soc. Vol 5, p. 535-602,

Dupont, R.R. (1986) Evaluation of Air Emission Release Rate Model Prediction of Hazardous Organics from Land Treatment Facilities, Environmental Progress Vol. 5, No. 3 pp.197.

Hamaker, J.W. (1972) Diffusion and Volatilization Chapter 5 in Organic Chemicals in the Soil Environment, Vol. 1 ed. By C.A.I. Goring amd J.W. Hamaker, Marcel Dekker, New York

Hartley, G.S., (1969) Evaporation of Pesticides Chapter II in Pesticidal Formulations Research, Physical and Colloidal Chemical Aspects," Advances in Chemistry Series, 86 American Chemical Society, Washington, D.C.

Haugen, J.-E., Wania, F. and Lei, Y.D., 1997. Polychlorinated biphenyls in the atmosphere of southern Norway. Environmental Science and Technology **33**, pp. 2340–2345.

Hoff, R.M., Strachan, W.M.J., Sweet, C.W., Chan, C.H., Shackleton, M., Bidleman, T.F., Brice, K.A., Burniston, D.A., Cussion, S., Gatz, D.F., Harlin, K. and Schroeder, W.H., 1998. Atmospheric deposition of toxic chemicals to the Great Lakes: a review of data through 1994. Atmospheric Environment **30**, pp. 3503–3527.

Jury, W.A., W.F. Spencer, and W.J. Farmer. (1983) Behavior Assessment Model for Trace Organics in Soil: I Model Description. J. Environ. Qual. 12:558-564

Korfiatis, G., Hires, R., Reinfelder, J., Totten, L., and Eisenreich, S., (2003) Monitoring of PCB and Hg Air Emissions in Sites Receiving Stabilized Harbor Sediment, Final Report to the New Jersey Marine Sciences Consortium and New Jersey Department of Transportation Office of Maritime Resources

Lighthill, M.J. (1945) A New Method of Two Dimensional Aerodynamic Design, Reports and Memoranda No. 2112, National Physical Laboratory.

Liss, P. S., and Slater, P.G., Nature (1974), Vol. 247, 181

Mayer, R., J. Letey, and W.J. Farmer (1980) Models for Predicting Volatilization of Soil Incorporated Pesticides, Soil Sci. Soc. Am. J., 44, 445-450

Monin, A.O., Obukov, A.M. (1954) Basic laws of turbulent mixing in the ground layer of the atmosphere. Akad. Nauk. SSSR Geofiz. Inst. Tr. 151:163-187.

Nerst, W (1904) Zeitschrift fur Physikalische Chemie, 47, 52

Price,C. Brannon, J., Myers, T., Valsaraj, K. Thibodeaux, L., and Reible, D. (1997). "Development of laboratory procedures to predict volatile losses from contaminated sediments," Environmental Effects of Dredging Technical Notes Collection (TN EEDP-0223), U.S. Army Engineer Research and Development Center, Vicksburg, MS .www.wes.army.mil/el/dots/eedptn

Schwarzenbach, R. P., Gschwend, P. M., and Imbodn (1993) D. I., Environmental Organic Chemistry, John Wiley and Sons, New York, Chapter 10.

Spiga, M. and Morini, G., (1994) A Symmetric Solution for Velocity Profile in Laminar Flow through Rectangular Ducts, International Communications in Heat and Mass Transfer. Vol.21, no. 4 pp 469-475.

Thibodeaux, L. J. (1989) Theoretical Models for Evaluation of Volatile Emissions to Air During Dredged Material Disposal with Applications to New Bedford Harbor, Massachusetts, Miscellaneous Paper EL-89-3, U.S. Army Engineer Waterways Experiment Station, Vicksburg, MS.

USEPA, EPA Home ,Prevention, Pesticides & Toxic Substances ,Pollution, Prevention & Toxics, PCBs , Oct. 2003, http://www.epa.gov/opptintr/pcb/

USEPA, Region 2 Superfund, Hudson River PCBs, Background and Site Information, Feb. 2004, http://www.epa.gov/hudson/background.htm

Valsaraj, K.T., Choy, B., Ravikrishna, R., Reible, D.D., Thibodeaux, L.J., Price, C.B., Brannon, J.M., Myers, T.E. (1997) Air Emissions from Exposed Contaminated

Sediments and Dredged Materials 1. Experimental Data in laboratory microcosms and mathematical modeling. Journal of Hazardous Materials. 54:65-87.

Valsaraj, K.T., Ravikrishna, R., Choy, B., Reible, D.D., Thibodeaux, L.J., Price, C.B., Yost, S., Brannon, J.M., Myers, T.E. (1999) Air Emissions from Exposed Contaminated Sediments and Dredged Material. Environ. Sci. Technol. 33:142-149.

Wanninkhof, R., Ledwell, J., and Crusius, J. (1991) In Air-Water Mass Transfer, Wilhelm, S., Gulliver, J. Eds, American Society of Civil Engineer, New York , p. 441-458.

THE STATE UNIVERSITY OF NEW JERSEY
RUTGERS

Final Report to the

New Jersey Marine Sciences Consortium

and

New Jersey Department of Transportation
Office of Maritime Resources

EMISSIONS AND ATMOSPHERIC TRANSPORT OF PCBs AND Hg FROM STABILIZED HARBOR SEDIMENTS

Principal Investigators:
John R. Reinfelder, Gera Stenchikov, Lisa A. Totten
Department of Environmental Sciences, Rutgers University
14 College Farm Road, New Brunswick, NJ 08901

June 30, 2006

Emissions and Atmospheric Transport of PCBs and Hg from Stabilized Harbor Sediments
Final Report

Executive Summary

Project Goals, Objectives, and Approach

Previously, vertical fluxes and horizontal gradients of polychlorinated biphenyls (PCBs) and mercury (Hg) were measured by investigators from Rutgers University and Stevens Institute of Technology at a land application site for cement-stabilized dredged material (SDM) from New York Harbor located in Bayonne, New Jersey (Korfiatis et al., 2003). The results of that project pointed to gaps in our understanding of the phase partitioning of PCBs emitted from SDM, the relative importance of SDM PCB emissions to the local atmosphere compared with other sources in the New York/New Jersey metropolitan area, and the sediment side controls of PCB and Hg volatilization. The dynamics of PCB volatilization fluxes that occur as SDM cures were examined at Stevens and the results are described in a separate report (Miskewitz et al., 2005). At Rutgers, PCB sample analyses, modeling, and laboratory experiments were carried out to determine the gas-aerosol partitioning of PCBs in the Bayonne atmosphere, develop an atmospheric transport model of PCBs in the Bayonne peninsula, and further evaluate the environmental controls of Hg volatilization from SDM. The specific objectives of the Rutgers projects were to:

1. Quantify the fraction of PCBs adsorbed to airborne particles in samples previously collected at the stabilized dredged material land application site and at the NJDEP trailer site in Bayonne, NJ in order to determine if the gas-particle system is at equilibrium and assess the importance of aerosol sorption of gas-phase PCBs emitted from the stabilized sediment.
2. Utilize a RAMS/HYPACT model with measured PCB concentrations to characterize air circulation patterns and estimate the transport of PCBs from the SDM application site in Bayonne, NJ during our previous field sampling campaigns.
3. Examine in laboratory flux chamber experiments the sediment side controls of Hg volatilization from SDM.

Gas/Particle Partitioning of PCBs Near a Stabilized Dredge Material Application Site

Particle-phase PCB concentrations were determined in samples collected upwind and downwind of the SDM application site (OENJ Bayonne, see Fig. 1). Particle-phase PCB concentrations at the landfill were significantly elevated on a mass per unit volume of air basis (pg m^{-3}; 1 pg = 10^{-12} g) compared with measurements at a NJDEP air monitoring trailer in Bayonne and at Jersey City, but when these concentrations were normalized to the amount of total suspended particles (TSP) in the air, the levels were comparable between the three locations. There is no evidence in this data of consistent increases in particle-phase PCB concentrations downwind of the SDM. This is true whether the particle-phase PCB concentrations are expressed as pg m^{-3} of air or as pg μg^{-1} TSP. An evaluation of PCB gas/particle partitioning constants and vapor pressures indicates that emissions of either gas- and particle-phase PCBs from the Bayonne SDM landfill are not large enough to significantly alter the gas/particle partitioning of PCBs in this region. This occurs primarily because of the high

background concentrations of PCBs in both the gas and particle phases in Bayonne due to its location within the NYC metropolitan area. These same emissions could be significant, however, if the SDM were placed in a more remote location where the background PCB signal is lower.

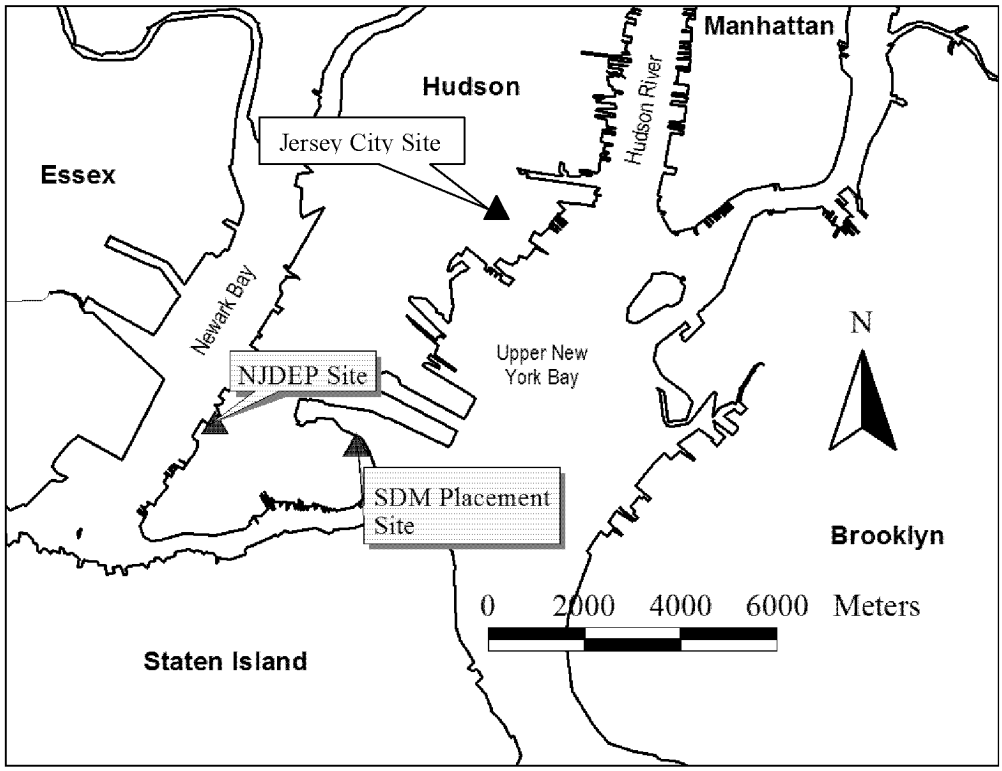

Figure 1. Aerial view of Bayonne peninsula showing the OENJ SDM application site and the NJDEP trailer.

Measurement and Modeling of Urban Atmospheric PCB Concentrations on a Small (8 Km) Spatial Scale

In order to evaluate the SDM placement site in Bayonne as a source of PCB emissions to the New York City-northern New Jersey urban atmosphere and to improve our understanding of urban sources of atmospheric PCBs generally, gas-phase PCBs were analyzed at two monitoring locations near the SDM application site (Bayonne trailer and Jersey City) for the period of December 1999 to November 2000. In addition, in order to assess the PCB emissions required to produce the measured concentrations, PCB transport was modeled using the Hybrid Particle And Concentration Transport model (HYPACT) with local meteorology generated by the Regional Atmospheric Model System (RAMS). The concentrations, congener patterns, and temporal patterns of PCBs differ dramatically at the two monitoring sites which are ~8 km apart and spikes in gas-phase PCB concentration observed at the Bayonne trailer site are not observed at

Jersey City. These results suggest that an important source of atmospheric PCBs exists within 8 km of the SDM application site.

Modeling results show that the magnitude of PCB emissions at the SDM placement site needed to produce the observed gas-phase concentrations at the SDM site (400 pg m^{-2} s^{-1}) is in good agreement with micrometeorological estimates of PCB emission fluxes based on measurements made at the SDM site during placement (570 pg m^{-2} s^{-1}; Korfiatis et al., 2003). The transport of PCB emissions of this magnitude from the SDM placement site could produce concentration spikes of only 100-200 pg m^{-3}, well below those observed at the Bayonne trailer site (400-2000 pg m^{-3}) indicating that PCB emissions from the SDM placement site have a small effect on the overall levels of PCBs measured at the Bayonne trailer and that the emissions source which produced the PCB spikes at the Bayonne trailer is either much greater than the 3 kg y^{-1} produced by the SDM placement site or much closer to the Bayonne trailer than 8 km.

The emissions of ΣPCBs needed to produce observed concentrations at the Bayonne trailer monitoring site is estimated to be on the order of 100 g d^{-1}. Extrapolation of this source magnitude to the area of New York City suggests that this urban area emits at least 300 kg of ΣPCBs to the regional atmosphere each year, an amount similar in magnitude to the flux of ΣPCBs from the Upper Hudson River into the New York/New Jersey Harbor estuary. Unfortunately, there is no way at this time to determine either the identity or exact location of this source.

Hg flux chamber experiments

The volatilization of mercury from estuarine sediments does not decrease with time as was observed for PCBs (Miskewitz et al., 2005), but is primarily controlled by light. Photochemically driven reactions at the sediment-air surface apparently lead to the reduction of Hg(II) and 20 to 40-fold increases in gaseous mercury volatilization fluxes. Cement stabilization appears to accelerate volatilization of Hg in the light perhaps by exposing photoreactive solids directly to light or increasing the surface area of the sediment through drying. The dominant role of light in controlling Hg volatilization from sediments in the laboratory flux chamber is consistent with in situ sediment-air Hg flux observations at the SDM placement site in Bayonne, NJ which were significantly correlated ($r^2 = 0.81$) with solar radiation (Goodrow et al., 2005; 2006). Decreasing the time of exposure of SDM to light during cement stabilization and placement would reduce Hg emissions to the atmosphere from this source. The photochemically-driven Hg volatilization from periodically air exposed freshwater or estuarine wetland sediments has not been directly evaluated and could be a significant flux in the atmospheric Hg cycle.

Recommendations for further study

1. Additional observational and local transport modeling studies are needed to identify and locate the major emission sources of PCBs to the New York/New Jersey metropolitan atmosphere.

2. Particle scavenging needs to be better quantified as a loss mechanism of PCBs from the major emission sources to the New York/New Jersey urban atmosphere.

3. Further examination of the effects of the intensity and wavelength of light and sediment properties (organic matter content) on Hg volatilization from sediments across a range of Hg contamination levels is needed.

4. Studies of the photoreactive/volatile forms of Hg in estuarine sediments are needed to understand the mechanism of photochemically-driven Hg volatilization and to better define the risks that unremediated Hg contaminated sediments pose to human and environmental health in NY/NJ Harbor.

5. In situ studies of sediment-air fluxes of Hg above tidally exposed and vegetated freshwater and estuarine wetlands sediments are needed to quantify this potentially important component of the Hg cycle.

Acknowledgements

This project was supported by the New Jersey Marine Sciences Consortium and the New Jersey Department of Transportation, Office of Maritime Resources. We wish to thank Michael Weinstein (NJMSC) and Scott Douglas (NJDOT) for their guidance and support. This work was made possible by the efforts of Steven J. Eisenreich, Cari L. Gigliotti, Nilesh Lahoti, Andy Sandy, and Lora Smith.

TABLE OF CONTENTS

I. Gas/Particle Partitioning of PCBs Near a Stabilized Dredge Material Land Application Site

NJ Marine Sciences Consortium (NJMSC) and NJ Department of Transportation, Office of Maritime Resources (NJDOT/OMR) recently provided funding to our research group for a study entitled: *Monitoring of PCB and Hg Air Emissions in Sites Receiving Stabilized Harbor Sediment* (Korfiatis et al., 2003). This project was designed to assess the rate and magnitude of volatilization of PCBs from a site in New Jersey where stabilized dredged material (SDM) from the NY/NJ Harbor region is applied to land (Fig. 1).

We have determined the background ambient gas-phase PCB concentrations in the air at the trailer site in Bayonne, NJ prior to and after land application of cement-stabilized sediment. The main goal of this research was to determine the extent to which the land application of these stabilized harbor sediments affects the ambient PCB concentrations in the air in Bayonne. Results from this study demonstrate that net volatilization of PCBs from the stabilized sediment is occurring. Figure 2 compares the concentrations of gas-phase ΣPCBs measured at the NJDEP trailer site (blue) with those measured at the sediment application site (red). Average concentrations at the sediment application site were found to be 1.5-2X higher than those measured at the Bayonne trailer site. Average ΣPCB concentrations during the July 2001 sampling campaign were 7128 pg m^{-3} and 3945 pg/m^3 at the sediment application site and the Bayonne trailer site, respectively. For the October 2001 sampling campaign, average ΣPCB concentrations were 2857 and 1284 pg m^{-3}, respectively. The high ambient PCB levels measured at the sediment application site relative to the local background suggest that volatilization from the sediment is a net source of atmospheric PCBs. In addition, small-scale spatial gradients in PCB concentrations demonstrate that PCBs are higher downwind of the applied sediment relative to levels measured at upwind samplers. In the worst case, gas-phase PCB concentrations downwind were 4 times upwind levels.

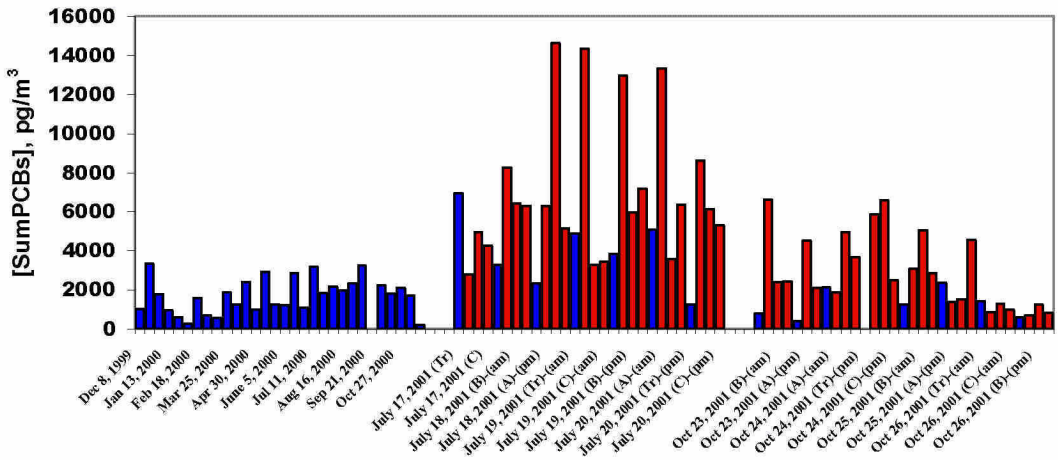

Figure 2. Concentrations of gas phase PCBs measured at the trailer site (blue) and at the sediment application site (red).

In addition to upwind and downwind measurements of PCB concentrations, a research team of scientists from Stevens Institute of Technology performed vertical PCB flux monitoring at the sediment placement site. Their data indicate that substantial amounts of PCBs are volatilized from the sediments (Korfiatis et al., 2003).

Despite the evidence that net volatilization of PCBs from stabilized sediments is occurring, it is not clear to what extent these emissions contribute to the levels of atmospheric PCBs in Bayonne and surrounding communities. During three sampling intervals, winds blew toward the northeast, in the direction of the NJDEP trailer site. On July 18, 2001 in the afternoon, gas phase ΣPCBs were 8700 pg m^{-3} at the sediment application site, but just 2300 pg m^{-3} downwind at the trailer site (Fig. 2). Similarly, on July 20, 2001, ΣPCBs were 6700 pg m^{-3} at the application site and 1300 pg m^{-3} at the trailer. During the October 2001 campaign, east/southeast wind occurred on October 23, in the morning. Concentrations at the sediment application site were 6619 pg m^{-3} downwind of the applied sediment. The ΣPCB concentration across town at the NJDEP trailer was 791 pg m^{-3}, almost a factor of 8 lower. The concentrations of PCBs measured at the trailer site under these wind conditions are low not only relative to those measured at the sediment application site, but also relative to concentrations measured at the trailer site in the year before sediment application began (Fig. 2). Thus high concentrations at the sediment application site do not directly lead to elevated PCB concentrations in the city of Bayonne, and a better understanding of the transport of PCBs from the sediment placement site is needed.

We hypothesized that the transport of gas-phase PCBs in the Bayonne area was influenced by the partitioning of PCBs onto aerosols. Gas/particle partitioning may remove a significant amount of PCBs from the gas phase during transport across the city of Bayonne. PCBs are volatilized from the stabilized sediment into the gas phase. This volatilization is likely enhanced by the elevated temperature of the sediments, which are heated by the exothermic curing of the cement additives and by solar radiation. The air directly above the sediments is also heated, but as the air masses rise, they cool, potentially inducing the PCBs in the air to condense onto airborne particles. Under light winds, air movement across the peninsula will take an hour or more, allowing time for gas/particle partitioning. Thus, in order to more accurately assess the impact of emissions of PCBs from applied sediments, it is necessary to understand the influences of gas/particle partitioning. To further this understanding, we quantified the PCBs in the atmospheric particle phase at the sediment placement and trailer sites, and examined the data for trends in gas/particle partitioning parameters in order to detect the influence of PCB emissions from the SDM on the local atmospheric PCB burden.

Sampling Methods

Details of sample collection were described in Korfiatis et al. (2003). Sample preparation, extraction and analysis procedures can be found elsewhere (Lohman et al., 2000; Gigliotti et al., 2000; Brunciak et al., 2001; Gigliotti et al., 2001; Totten et al., 2001) and will be summarized here. Air samples were collected using a modified high volume air sampler (Tisch Environmental, Village of Cleves, OH, USA) with a calibrated airflow of ~0.5 m^3 min^{-1}. Quartz fiber filters (QFFs; Whatman) were used to capture the particulate phase and polyurethane foam plugs (PUFs) were used to capture the gaseous phase. QFFs were weighed before and after sampling to determine total suspended particles (TSP).

Analytical Procedures

Samples were injected with surrogate standards before extraction. For PCBs the surrogates were 3,5 dichlorobiphenyl (PCB#14), 2,3,5-trichorobiphenyl (PCB#23), 2,3,5,6 tetrachlorobiphenyl (PCB#65), 2,3,4,4',5,6 hexachlorobiphenyl (PCB#166). Samples were extracted in Soxhlet apparati for 24 hours in dichloromethane. These extracts were then reduced in volume by rotary evaporation and subsequently concentrated via N_2 evaporation. The samples were then fractionated on a column of 3% water-deactivated alumina. The PCB fraction was eluted with hexane, concentrated under a gentle stream of nitrogen gas, and injected with internal standard containing PCB #30 (2,4,6-trichlorobiphenyl) and #204 (2,2',3,4,4',5,6,6'-biphenyl) prior to analysis by gas chromatography (GC). PCBs were analyzed on an HP 6890 gas chromatograph equipped with a ^{63}Ni electron capture detector using a 60-m 0.25 mm i.d. DB-5 (5% diphenyl-dimethyl polysiloxane) capillary column with a film thickness of 0.25 μm (Brunciak et al., 2001). Sixty peaks representing 93 congeners were quantified.

Quality Assurance

Recovery of surrogate standards, which were typically better than 71 %, was used to correct individual compound concentrations for surrogate recoveries. Field blanks and matrix spikes were used for quality control purposes. The method detection limit (MDL) for each congener was determined from field blanks by taking the mean of the mass detected in all field blanks plus three times the standard deviation about the mean. The MDL for ΣPCBs on QFF was 8.44 ng.

Results and Discussion

Table 1 summarizes the particle phase ΣPCB (n = 93 congeners) concentrations in samples collected at the SDM landfill and at the NJDEP trailer. Congener-specific data for all particle phase samples is given in Appendix 1. Particle-phase PCB concentrations varied seasonally. Highest concentrations were measured in November and lowest in May. Average ΣPCB concentrations during the July 2001 campaign were 317 and 91 pg m^{-3} at the sediment application sites and Bayonne trailer, respectively. These particle phase concentrations represented 4.4% and 2.3%, respectively, of the total atmospheric PCB burden (gas + particle). In May 2002, average ΣPCB concentrations were 108 (6% of total concentration) and 0.75 pg m^{-3} (0.08 % of total concentration), at the sediment application site and the trailer, respectively. In November 2002, average ΣPCB concentrations were 149 (9% of total concentration) and 1.5 pg m^{-3} (0.17% of final concentration), respectively. Thus the fraction of PCBs in the particle phase was generally higher at the sediment application site than at the trailer.

During virtually all sampling intervals, particle phase ΣPCB concentrations were higher at the landfill than at the trailer, in some cases by more than an order of magnitude. The concentrations at the landfill were usually higher than typical concentrations in Jersey City, NJ that are in the range of 9 to 44 pg m^{-3} (Totten et al., 2004). Particle-phase ΣPCB concentrations at the trailer averaged 25 pg m^{-3} during the intensive sampling periods, similar to the concentrations routinely observed at Jersey City. The differences in particulate phase ΣPCB concentration between the trailer and landfill were eliminated when the PCB concentrations were normalized to TSP. Such normalization results in average (± sd) particle-phase

Table 1. Summary of ΣPCB particulate phase concentration during the Bayonne 2001-2002 sampling campaigns. Samples taken upwind of the SDM are in blue, downwind samples in red.

ΣPCB concentration, pg m^{-3}	Bayonne Trailer	Sediment Site A	Sediment Site B	Sediment Site C
07/17/2001 (all day)			134	
07/18/2001 (morning	33	**91**	**111**	**47**
07/18/2001 (afternoon)	143		**842**	**56**
07/19/2001 (morning)		**449**	**498**	
07/19/2001 (afternoon)	151	**455**	**516**	**151**
07/20/2001 (morning)		**816**		**218**
07/20/2001 (afternoon)	76	**134**	**233**	
05/07/2002 (morning)	0.46	144	291	65
05/07/2002 (afternoon)	0.92		150	85
05/08/2002 (morning)	1.1	**208**	177	76
05/08/2002 (afternoon)	2.0	254		
05/09/2002 (morning)	1.0	60		**48**
05/09/2002 (afternoon)	0.55	171		**33**
05/10/2002 (morning)	0.47		66	34
05/10/2002 (afternoon)	0.44		68	42
11/12/2002 (morning)	0.69	**1237**	**147**	234
11/12/2002 (afternoon)	1.1	**106**	**128**	130
11/13/2002 (morning)	0.27	**58**	79	**54**
11/13/2002 (afternoon)			66	**78**
11/14/2002 (morning)	2.0	66	197	100
11/14/2002 (afternoon)	5.2	0.07	90	71

ΣPCB concentrations at the landfill and trailer of 0.79 (± 0.70) and 0.89 (± 0.64) pg ug^{-1}, respectively. TSP concentrations at the trailer averaged 42 ug m^{-3}, similar to observations at Jersey City (Totten et al., 2004). At the landfill, two TSP measurements were greater than 30,000 μg m^{-3}. Without these two outliers, TSP concentrations at the landfill averaged 375 μg m^{-3}. Thus increased particle-phase PCB concentrations at the landfill are a result of greater numbers of particles there. In general, the SDM does not appear to be responsible for these higher particle densities. Only three sampling intervals (7/19 afternoon, 7/20 morning, and 7/20 afternoon) display significantly elevated particle densities downwind of the SDM. Particle-phase ΣPCB concentrations normalized to TSP during these three intervals were lower downwind of the SDM than upwind. Thus for these three intervals, the SDM may be emitting significant amounts of particles, but they have a lower PCB concentration than the ambient airborne particles. The other high particle-phase PCB concentrations are due to off-site emissions of particles as well as secondary atmospheric aerosol formation.

There is no evidence in this data of consistent increases in particle-phase PCB concentrations downwind of the SDM. This is true whether the particle-phase PCB concentrations are expressed as pg per cubic meter of air or as pg per μg TSP. This suggests that gas-phase emissions of PCBs from the SDM are not large enough to significantly impact the particle-phase PCB concentrations downwind of the SDM. Closer examination of the particle-

phase PCB concentrations is therefore necessary to discern whether PCB emissions from the SDM are significant.

Flux studies have demonstrated that PCBs are emitted into the gas phase from the SDM, but it is unclear how important these emissions are to the prevailing PCB burden in the atmosphere around Bayonne. In the original study of the site we concluded that, despite relatively high gas-phase PCB concentration at the SDM site, the SDM landfill is a relatively weak source of PCBs to the City of Bayonne. The purpose of this study was to examine the gas/particle partitioning of PCBs in the vicinity of Bayonne in order to gain further insight into the relative importance of PCB emissions from the SDM landfill.

The distribution of semi-volatile compounds between the gas and particle-bound phases is the most important factor determining the removal mechanisms and residence time in atmosphere (Junge, 1977; Eisenreich et al., 1981; Cousins & Mackay, 2001; Pankow, 1987). In gas-particle partitioning, the equilibrium partitioning coefficient (K_p) describes the ratio between the particle phase concentration (C_p, pg m^{-3}) and the gas phase concentration (C_g, pg m^{-3}) of the SOC, normalized by the TSP concentration in ug/m^3 (Pankow, 1987; Pankow, 1994; Harner & Bidleman, 1998):

$$K_p = \frac{C_p}{C_g \cdot TSP} \qquad (1)$$

In theory, a plot of log K_p ($m^3/\mu g$) vs. log vapor pressure (log p_l from Falconer and Bidleman, 1994) for individual PCB congeners should yield a slope of ~ -1 when gas/particle partitioning is at equilibrium (Pankow, 1987). In this study we postulated that gas/particle partitioning will be at equilibrium for PCBs being transported in from offsite (upwind of the SDM), but will be far from equilibrium just downwind for the SDM due to gas-phase PCB emissions from the SDM. The congeners volatilized from the SDM appear to be relatively low in molecular weight (Korfiatis et al., 2003), containing 2 to 5 chlorines, and therefore have relatively high vapor pressures, putting them to the right in the lop K_p vs. lop p_l plots (see Figure 3 for an example). Increased gas-phase concentrations of these congeners would decrease their K_p value (equation 1), causing the right side of the regression line to be "dragged" downward, resulting in a slope steeper than the equilibrium value of -1. Particle phase emissions would also disturb the gas/particle partitioning of PCBs, although it is not clear how this disruption would manifest itself in terms of the log K_p vs. log p_l curve.

A summary of log K_p vs. log p_l slopes is given in Table 2. Slopes were significantly shallower than -1 in 13 of 17 intensive samples collected at the trailer site, with an average (± sd) of –0.59 (± 0.17). In previous work, we hypothesized that a significant source of atmospheric PCBs exists within about 6 km of the Bayonne trailer. If these PCBs are emitted primarily into the gas phase, their influence could explain the frequent lack of gas/particle partitioning equilibrium observed at the trailer. The average (± sd) slope at the landfill was -0.69 (± 0.15). Six of 48 samples at the trailer yielded slopes equal to –1. From this data we can conclude either that gas/particle partitioning of PCBs is usually not at equilibrium in the Bayonne area, or that slopes significantly different from –1 can still be indicative of equilibrium, as was argued by Simcik et al. (1998).

Perturbations in the gas/particle partitioning of PCBs upwind and downwind of the SDM can still be instructive even if we cannot establish that partitioning is at equilibrium at either location. We need only look for significant differences in the log K_p vs. log p_l slopes between upwind and downwind sites. In only one sampling interval (7/18/2001 afternoon) are significant differences in slopes observed upwind and downwind of the SDM (Fig. 3). During this interval,

the slope (± 95% confidence interval) was -0.72 (± 0.12) upwind and -0.40 (± 0.12) downwind. The slope at the trailer was -0.45 (± 0.13). For this sampling period, winds came from the SE, with both sites A and C acting as upwind sites and site B as the downwind site. Concentrations upwind (site C = 5153 pg m^{-3}, site A = 6298 pg m^{-3}) were as much as 2.5 times lower than downwind (14647 pg m^{-3}), suggesting that the dredge material contributed to the atmospheric burden of PCBs onsite. The particle-phase ΣPCB concentrations were 15 times higher downwind than upwind. Flux measurements were not taken during this interval, but the difference in upwind/downwind gas-phase PCB concentrations suggests that the flux was substantial. This episode appears to indicate that gas-phase emissions of PCBs from the SDM can have a significant impact on the gas/particle partitioning of PCBs, and that they do cause the slope to become more shallow, as hypothesized.

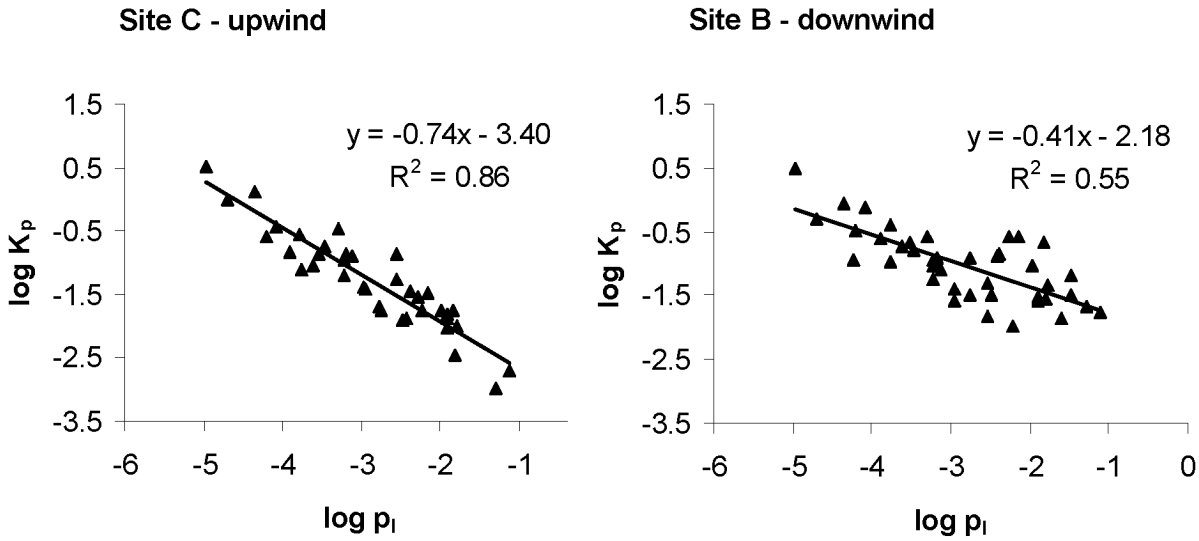

Figure 3. Gas/particle partitioning plots for PCBs at two sites near the SDM on the afternoon of 7/18/01.

Of the 21 sampling intervals listed in Table 2, only 6 coincided with flux measurements above the SDM. During the 5/7/02 (morning and afternoon) and 5/8/02 (morning) events, the ΣPCB flux was large and positive, ranging from 1987 to 2877 ng m^{-2} hr^{-1}. On 5/7/02 the wind was from the W, such that all three landfill sites were upwind. On the morning of 5/8/02, winds were from the NE, such that sample A was downwind of the SDM. There is no difference between the slopes in samples A and C. For the November intensive, fluxes were small but positive, ranging from 76 to 491 ng m^{-2} hr^{-1}. Again there are no observable differences in the slopes between upwind and downwind sites. These results may indicate that fluxes in excess of 3000 ng m^{-2} hr^{-1} are necessary to significantly affect the gas/particle partitioning of PCBs in this region due to the high background of atmospheric PCBs being transported into Bayonne from off site.

Table 2. Summary of gas/particle partitioning results during Bayonne 2001-2002 sampling campaign. Slopes, 95% confidence intervals, and R^2 values for regressions of log K_p vs. lop p_l are shown. Sites in red were downwind of the SDM, sites in blue were upwind.

	Bayonne Trailer			Site A			Site B			Site C		
Dates	**slope**	**95% CL**	**r^2**	**slope**	**95% CL**	**r^2**	**slope**	**95% CL**	**r^2**	**slope**	**95% CL**	**r^2**
7/17/2001 (all day)							-0.63	0.13	0.71			
7/18/2001 (morning)	-0.65	0.30	0.51	**-0.82**	**0.10**	**0.88**	**-0.69**	**0.12**	**0.79**	**-1.00**	**0.25**	**0.73**
7/18/2001 (afternoon)	-0.45	0.13	0.60				**-0.40**	**0.12**	**0.51**	**-0.72**	**0.12**	**0.82**
7/19/2001 (morning)				**-0.61**	**0.09**	**0.83**	**-0.40**	**0.14**	**0.45**			
7/19/2001 (afternoon)	-0.70	0.15	0.76	**-0.58**	**0.08**	**0.86**	**-0.63**	**0.09**	**0.85**	**-0.80**	**0.11**	**0.85**
7/20/2001 (morning)				**-0.57**	**0.08**	**0.83**				**-0.71**	**0.09**	**0.86**
7/20/2001 (afternoon)	-0.36	0.15	0.41	**-0.77**	**0.08**	**0.91**	**-0.72**	**0.09**	**0.88**			
05/07/2002 (morning)	-0.40	0.18	0.41	-0.35	0.11	0.53	-0.58	0.17	0.56	-0.67	0.22	0.56
5/7/2002 (afternoon)	-0.42	0.16	0.70				-0.62	0.15	0.67	-0.36	0.16	0.38
5/8/2002 (morning)	-0.54	0.13	0.67	**-0.63**	**0.09**	**0.82**				-0.62	0.18	0.60
5/8/2002 (afternoon)	-0.63	0.11	0.77	-0.52	0.17	0.49						
5/9/2002 (morning)	-0.43	0.28	0.31	-0.67	0.24	0.52				**-0.69**	**0.21**	**0.62**
5/9/2002 (afternoon)	-0.60	0.18	0.69	-0.78	0.16	0.77				**-0.88**	**0.22**	**0.68**
5/10/2002 (morning)	-0.64	0.21	0.64				-0.75	0.12	0.83	-0.76	0.20	0.64
5/10/2002 (afternoon)	-0.71	0.22	0.60				-0.72	0.11	0.84	-0.61	0.17	0.61
11/12/2002 (morning)	-0.50	0.54	0.46	**-1.00**	**0.17**	**0.81**	**-1.00**	**0.16**	**0.78**	-1.00	0.16	0.83
11/12/2002 (afternoon)	-0.81	0.23	0.64	**-0.96**	**0.17**	**0.79**	**-0.71**	**0.20**	**0.65**	-0.76	0.23	0.65
11/13/2002 (morning)	-0.76	0.46	0.73	**-0.70**	**0.15**	**0.72**	-0.63	0.15	0.69	**-0.76**	**0.16**	**0.77**
11/13/2002 (afternoon)							-0.68	0.14	0.73	**-0.68**	**0.14**	**0.71**
11/14/2002 (morning)	-0.50	0.16	0.59	-0.78	0.15	0.76	-0.63	0.15	0.68	-0.52	0.20	0.58
11/14/2002 (afternoon)	-1.00	0.20	0.83	-0.74	0.17	0.69	-0.61	0.15	0.67	-0.70	0.13	0.76

Conclusions

These results suggest that the emissions of both gas- and particle-phase PCBs from the Bayonne SDM landfill are not large enough to alter the gas/particle partitioning of PCBs in this region. This occurs primarily because of the high background concentrations of PCBs in both the gas and particle phases that occur in Bayonne due to its location within the NYC metropolitan area. These same emissions could be significant if the SDM were placed in a more remote location where the background PCB signal is lower. For example, in large portions of New Jersey, the background gas-phase PCB concentration averages 150-220 pg m^{-3}, nearly an order of magnitude lower than levels prevailing near the Bayonne landfill. The fact that perturbations in the gas/particle partitioning of PCBs downwind of the SDM are not detected does not necessarily imply that this partitioning process is unimportant. Partitioning of gas-phase PCB emissions to particles probably does have an important role to play in removing the emissions from the atmosphere, but this effect is masked by the high background levels of PCB prevailing in the atmosphere of Bayonne.

II. Measurement and Modeling of Urban Atmospheric PCB Concentrations on a Small (8 km) Spatial Scale

Measurement of atmospheric PCB concentrations has been conducted in the east coast of the US and the Great Lakes primarily for the purpose of estimating atmospheric inputs to coastal waters (Baker et al. 1997; Buehler et al. 2001; Totten et al. 2004). The New Jersey Atmospheric Deposition Network (NJADN) was established for this reason and data from this project has been used to estimate atmospheric deposition fluxes to the NY/NJ Harbor Estuary and the tidal Delaware River. NJADN as well as the Integrated Atmospheric Deposition Network (IADN), the Chesapeake Bay Atmospheric Deposition Study (CBADS), and other studies have demonstrated that atmospheric deposition can be an important and sometimes dominant source of PCBs to coastal waters, and that atmospheric PCB concentrations are generally greater in urban areas than in rural or suburban areas (Baker et al. 1997; Buehler et al. 2001; Totten et al. 2004). This observation suggests that urban emissions of PCBs support the regional background concentrations observed in rural areas and control the atmospheric deposition of these compounds. Thus it is important to understand the sources of urban PCBs so that they can be effectively controlled (Gingrich and Diamond 2001, Harner et al. 2004).

A further impetus for understanding urban PCB sources comes from the requirement for Total Maximum Daily Loads (TMDLs) in many aquatic systems in the US. For example, the Delaware River TMDL model, using NJADN data, estimates that the atmospheric load of ΣPCBs is ~4,000 g day^{-1} (Fikslin and Suk, 2003), exceeding the TMDL by an order of magnitude.

The cost and logistics of maintaining atmospheric deposition networks such as NJADN and IADN typically limit the scope of the project to a small number of monitoring sites, mostly located at regional sites and tens to hundreds of km apart. For example, the IADN was originally designed to have one remote site for each of the Great Lakes and was later expanded to include two urban sites in Chicago at the Illinois Institute of Technology (IIT) and the University of Illinois at Chicago (UIC). Concentrations of PCBs at UIC were found to be about twice those at IIT, although congener patterns at the two sites were virtually identical (Basu et al. 2004). The NJADN included at various times 13 monitoring locations in New Jersey, eastern Pennsylvania, and Delaware. Even so, the NJADN spaced monitoring locations as far apart as possible. When only one monitoring station is placed in each city, the tacit assumption is made that this single station accurately characterizes the atmospheric concentrations of PCBs for the whole city.

From December 1999 to November 2000, atmospheric PCBs were measured at two monitoring locations about 8 km apart within the New York City metropolitan area: Jersey City and Bayonne. The Bayonne monitoring site was established to determine the background atmospheric concentrations of PCBs in Bayonne prior to land application of stabilized dredged material from the NY/NJ Harbor at a landfill in Bayonne, NJ (Korfiatis et al. 2003). Here we examine the similarities and differences in PCB concentrations and patterns at these two sites in order to improve our understanding of urban sources of atmospheric PCBs. In order to assess the emissions required to produce the measured concentrations, the Regional Atmospheric Model System (RAMS) was used to generate local meteorology simulations, and the Hybrid Particle And Concentration Transport model (HYPACT) was used to model transport of the emitted PCBs. This represents the first report of the use of the RAMS/HYPACT model system to examine atmospheric concentrations of persistent organic pollutants (POPs).

Experimental Section

Bayonne and Jersey City lie on a peninsula separating Newark Bay from the Upper New York Bay and Hudson River (Fig. 1). The Jersey City site was operated on the grounds of the Liberty Science Center, in a grassy area less than ~30 m from the Hudson River. The Bayonne site was located on top of an air monitoring trailer operated by the NJ Department of Environmental Protection, parked at the edge of the football stadium of Bayonne High School, within ~30 m of Newark Bay.

The entire peninsula is heavily urbanized and industrialized (Fig. 1). Due west lies the city of Newark, home to Port Newark, Newark Airport, and a major incinerator. Just north of Newark lies the New Jersey Meadowlands, home to more than 10 current or former landfill areas. Newark Bay represents the confluence of the Passaic and Hackensack Rivers and receives effluent from at least four paper mills. Newark Bay and the Hudson River are hydraulically linked and tidally mixed. The waters surrounding the peninsula contain about 10-20 ng L^{-1} ΣPCBs (dissolved plus particulate) (Litten, 2003) and are therefore potential sources of atmospheric PCBs (Totten et al. 2001). The rivers feeding this area (the Hudson, Passaic, and Hackensack Rivers) all contain similar levels of PCBs.

Details of sample collection, preparation, extraction and analysis can be found elsewhere (Totten et al. 2001 and 2004; Brunciak et al. 2001) and will be summarized here. Air samples (24 hours) were collected at 12 day frequencies using a modified high volume air sampler (Tisch Environmental, Village of Cleves, OH, USA) with a calibrated airflow of ~0.5 m^3 min^{-1}. Quartz fiber filters (QFFs; Whatman) were used to capture the particulate phase and polyurethane foam plugs (PUFs) were used to capture the gaseous phase. Particle-phase PCBs were not quantified at Bayonne because it was assumed that any PCBs emitted from the stabilized sediment would be emitted into the gas phase, and because the particle phase typically contains <10% of the atmospheric PCB burden. The samples were extracted using a Soxhlet apparatus, cleaned up using 3% deactivated alumina, and analyzed for PCBs by electron capture detection (ECD). Three surrogates were used to quantify the recovery of PCBs: PCBs 23, 65, and 166. Surrogate recoveries were used to correct PCB concentrations, averaged better than 80%, and were never below 50% at both sites.

Results and Discussion

The results from several years of measurements at the Jersey City site are presented in Totten et al. (2004). During the year of simultaneous sampling, average (± standard deviation) gas-phase ΣPCB concentrations were 1600 ± 880 pg m^{-3} at Bayonne and 930 ± 460 pg m^{-3} at Jersey City. These concentrations are typical of those measured over a longer time period at Jersey City (averaging 1260 pg m^{-3} from October 1998 to January 2001). They are significantly higher than the concentrations measured at more remote regions of New Jersey, where gas-phase ΣPCBs typically average 150-220 pg m^{-3} (Totten et al. 2004). ΣPCB concentrations were more variable at Bayonne (Fig. 4). At Bayonne, the ΣPCB concentrations are similar (the ratio of the Bayonne to the Jersey City concentration is between 0.5 and 2) on 15 of the 25 simultaneous sampling days, and dissimilar (Bayonne/Jersey City >2) on 10 days. These periodic spikes in concentration raise the PCB levels at Bayonne on average by about 1500 pg m^{-3}.
Congener patterns at the two sites were usually similar with an R^2 greater than 0.7 for 20 of the 25 paired samples. The days with the most dissimilar congener patterns occurred on days when the relative percent differences in the ΣPCB concentrations ranged from 130% to 11%,

suggesting that differences in congener patterns do not necessarily lead to differences in ΣPCB concentrations. There was no clear correlation between low correlation coefficients or spikes in concentration at Bayonne (Table 3) and any natural phenomena, including wind directions, back trajectory endpoints (NOAA HYSPLIT), precipitation patterns, or tidal cycles (neap vs. spring tides). The only meteorological variable to display a significant ($R^2 = 0.19$, $p = 0.028$) correlation with the Bayonne/Jersey City PCB ratio was the average wind speed, with the ratio being higher when wind speeds were greater. The absolute concentrations at Bayonne were not correlated with wind speed, although at Jersey City, ΣPCB concentrations decreased when wind speeds increased ($R^2 = 0.24$, $p = 0.01$), possibly due to dilution.

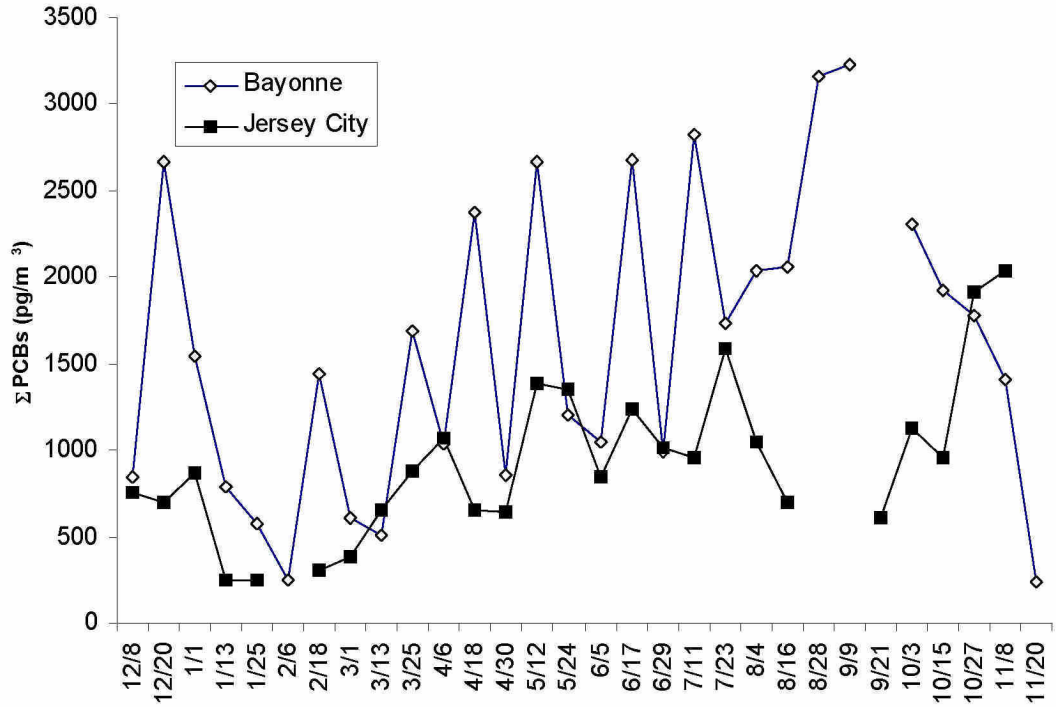

Figure 4. Gas-phase ΣPCB concentrations at the Bayonne trailer and Jersey City from December 1999 to November 2000.

The temperature (T in Kelvin) dependence of the gas-phase PCB partial pressures (p in atm) was investigated by application of the Clausius-Clapeyron equation:

$$\ln p = \frac{a}{T} + b \qquad (1)$$

where a and b are a constants. This approach has been used by many researchers, with steeper slopes thought to indicate closer sources (see Wania et al. 1998 and Carlson and Hites, 2005 for reviews). Carlson and Hites (2005) suggest that the ~25 data points used here are insufficient to

accurately determine the temperature dependence of PCBs over the long term at these sites. The goal of this analysis, however, is not to determine long-term differences in PCB dynamics, but to assess short-term differences in PCB behavior. For this purpose, 25 data points are sufficient to reveal significant differences in PCB dynamics.

Table 3. ΣPCB concentration, ratio of these concentrations at Bayonne to Jersey City, wind direction and speed, and correlation coefficient (R^2) for the congener patterns at Bayonne and Jersey City.

	ΣPCBs (pg m^{-3})		BA/JC	Wind Direction	Average Wind Speed	Congener Pattern
Date	**Bayonne**	**Jersey City**	**ratio**	**(degrees)**	**(m s^{-1})**	**R^2**
12/8/99	845	750	1.1	240	4.8	0.76
2/20/99	2672	702	3.8	190	9.0	0.92
1/1/00	1545	868	1.8	200	3.8	0.74
1/13/00	793	250	3.2	320	16	0.94
1/25/00	573	250	2.3	310	16	0.34
2/6/00	247			250	12	
2/18/00	1444	308	4.7	45	8.8	0.64
3/1/00	605	378	1.6	170	5.5	0.85
3/13/00	501	657	0.8	250	7.1	0.62
3/25/00	1685	873	1.9	220	6.6	0.88
4/6/00	1031	1071	1.0	300	12	0.96
4/18/00	2370	657	3.6	40	15	0.16
4/30/00	861	639	1.3	330	13	0.74
5/12/00	2669	1387	1.9	50	7.8	0.74
5/24/00	1205	1351	0.9	270	9.2	0.56
6/5/00	1052	850	1.2	80	11	0.85
6/17/00	2674	1242	2.2	265	9.1	0.71
6/29/00	991	1008	1.0	210	5.7	0.71
7/11/00	2821	954	3.0	310	10	0.78
7/23/00	1728	1582	1.1	225	5.8	0.74
8/4/00	2032	1047	1.9	270	7.5	0.80
8/16/00	2065	695	3.0	320	10	0.76
8/28/00	3165			80	8.7	
9/9/00	3225			40	5.6	
9/21/00		609		280	11	
10/3/00	2307	1121	2.1	280	7.1	0.84
10/15/00	1928	952	2.0	80	6.5	0.83
10/27/00	1777	1911	0.9	70	6.0	0.92
11/8/00	1403	2034	0.7	40	3.5	0.86
11/20/00	242			250	10	

At Jersey City, the Clausius-Clapeyron regressions were significant ($p < 0.05$) for all PCB congeners and co-eluting congener groups, with R^2 values ranging from 0.30 to 0.89. The slopes (a) values derived displayed a stronger correlation ($p < 10^{-5}$; $R^2 = 0.35$) with the log of the hypothetical subcooled liquid vapor pressure ($\log p_L$ from Falconer and Bidleman 1994) than the slopes at Bayonne. In contrast, the Clausius-Clapeyron regressions were not significant ($p > 0.05$) for 4 congener groups at Bayonne, and the R^2 values, even for the regressions that were significant, were generally weaker than at Jersey City and weakest for congeners with log vapor pressures ranging from –2.2 to –3.5 Pa (i.e. PCBs eluted between and including PCBs 66+95 and PCB 185 and containing 3-6 chlorines). Data from Bayonne for days with no observed PCB spike displayed higher Clausius-Clapeyron correlation coefficients for the congeners between 66+95 and 185 than the "spike" days. This indicates that the "background" PCB concentrations are primarily driven by processes that are correlated with temperature, such as passive volatilization from contaminated land, vegetation, or water surfaces, but the process that is driving the PCB spikes at Bayonne is not driven by temperature. Days with PCB spikes at Bayonne generally did not display positive residuals for the Clausius-Clapeyron regressions at Jersey City, indicating that the spike at Bayonne did not elevate the concentration at Jersey City significantly above the concentration that would be predicted by temperature.

A chemical mass balance model was applied to the PCB concentration data to elucidate the Aroclor pattern of the atmospheric PCBs and to determine whether the PCB spikes were due to emissions of an identifiable Aroclor. The congener compositions from Frame et al. (1996) of the 4 Aroclors produced in highest volumes (Brown, 1994) were multiplied by their sub-colled liquid vapor pressures (Falconer and Bidleman, 1994) to convert them to the congener profile expected in the atmosphere, and then expressed as a percent of the total composition. Aroclor 1016 was not used in this model because it represents a distillation of Aroclor 1242. These congener patterns were then fit via a least-squares regression to the congener pattern of each sample (again expressed as a percent of total), with the constraint that the coefficients a, b, c, and d must be greater than or equal to zero:

$$C_i = a \cdot C_{1242} + b \cdot C_{1248} + c \cdot C_{1254} + d \cdot C_{1260} \qquad (2)$$

Where C_i is the normalized concentration of congener i in the atmospheric sample, and C_{12xx} is the normalized concentration of congener i in Aroclor number 12xx. Aroclors patterns 1248b and 1254b (Frame et al. 1996) were used in the analysis because they consistently gave better fits to the data that the alternative samples of the same Aroclor. Aroclor 1242 was usually present, and the other Aroclors were always present in the samples. The average Aroclor profiles of the two sites were similar, with the percentages of Aroclors 1242, 1248, 1254, and 1260 respectively being 10%, 44%, 21%, and 14% at Jersey City and 14%, 28%, 26%, and 15% at Bayonne. The residual (that part of the congener pattern not described by the Aroclors) averaged 10% at Jersey City and 17% at Bayonne. There were no obvious differences in Aroclor composition between the days with PCBs spikes at Bayonne and the days without, nor between the Bayonne Aroclor composition and the Jersey City composition on the days with spikes. This suggests that the source of the PCBs spikes at Bayonne does not consist of a single Aroclor, but is a mixture of several Aroclors.

This analysis has suggested that one or more active sources of PCBs existed near the Bayonne site during 1999-2000 and may still exist. It also provides some information as to the type and location of the source. The source is probably within ~8 km of the Bayonne monitoring

site, since 8 km away at Jersey City, the signal from this source is not measurable. In addition, it is logical to assume that the source is closer to the Bayonne site than the Jersey City site. Because there is no correlation between PCB spikes at Bayonne and any natural phenomenon (temperature, tides, precipitation), the PCB spikes are thought to arise from anthropogenic activities that could include periodic disposal or trans-shipment of PCB-contaminated waste, and illegal disposal of PCB-containing materials. Finally, the analysis of congener patterns suggests that the source contains a mixture of PCBs, as opposed to being comprised of a single Aroclor. Unfortunately the area around Bayonne contains dozens of sites fitting this description, and additional data collection would be needed to determine which of the many suspects is responsible for the PCB spikes at Bayonne.

The dredging of NY/NJ Harbor to maintain, and in some cases deepen, the shipping channels is of enormous economic importance to the region, but is environmentally problematic due to the relatively high levels of PCBs and other contaminants in the surficial sediments of the Harbor (Adams et al. 1998) . During the period of sample collection, the confined aquatic disposal facility in Newark Bay (NBCDF) was the only disposal option for this dredge material. For this reason, dredging and disposal records provided by NJDOT Office of Maritime Resources were examined to determine whether the NBCDF could be a source of atmospheric PCBs to Bayonne. The records indicate that neither dredging nor disposal occurred in this region during the first half of 2000, suggesting that the NBCDF is not the source of the PCB spikes observed at Bayonne.

How large must the emissions of PCBs be to support the atmospheric concentrations of PCBs observed at Bayonne? To answer this question, a modeling exercise was conducted in which three possible locations for the source of PCBs were examined, the CDF site in Newark Bay, New York City (NYC) and the landfill where sediment dredge material (SDM) from the Harbor was applied to land. The model utilized the Regional Atmospheric Model System (RAMS) and the Hybrid Particle and Concentration Transport model (HYPACT). These models were recently applied by the authors to an investigation of the fate of the plume of contamination emanating from the World Trade Center in lower Manhattan resulting from the terrorist attacks of September 11, 2001 (Stenchikov et al., submitted).

RAMS version 4.3 was used to downscale the Eta Weather Prediction Model forecast (Mesinger et al. 1988; Rogers et al. 1996) conducted with spatial resolution of about 32 km. The downscaled meteorological fields were used in the HYPACT model for fine grid transport and deposition calculations. To account for a multiscale structure of the transport here we conducted calculations in three nested domains centered on the Bayonne peninsula (Fig. 5). The large parent domain is necessary to accommodate mesoscale structures to be downscaled in two smaller nested domains centered at the same central point covering areas of 54 km × 54 km and 10.5 km × 10.5 km, respectively (Fig. 5). The spatial resolution of Grids 1, 2, and 3 is, respectively, 4 km × 4 km, 1 km × 1 km, and 0.25 km × 0.25 km and number of grid points are 75 × 75, 54 × 54, and 42 × 42. The vertical grid is nonuniform, contains 39 levels starting from 10 m surface layer and reaching 1700 m at the top of the domain at the altitude of 16 km.

The original RAMS land elevation and vegetation cover data sets are of 1-km resolution that is sufficient for calculations of mesoscale circulation but is not enough for our application. To conduct finer-resolution simulations in the metropolitan area we adopted high-resolution National Land Cover Dataset (NLCD) and National Elevation Data (NED) from the United States Geological Survey (USGS) (http://edcwww.cr.usgs.gov/doc/edchome/ndcdb/ndcdb.html). NED has a resolution of 1 arc-second or about 30 m for conterminous United States.

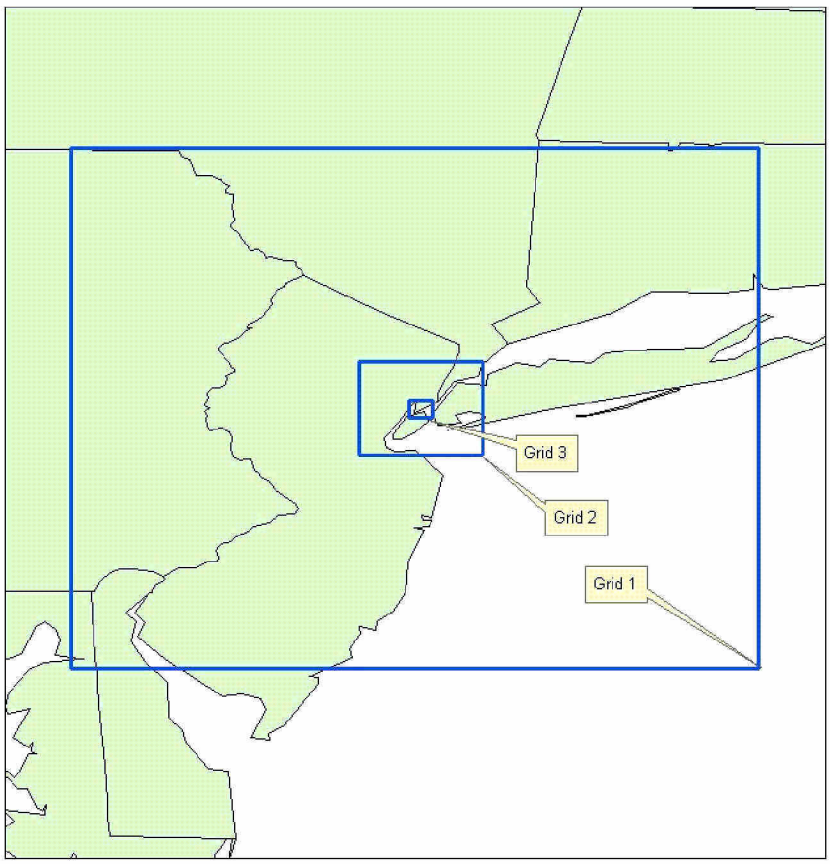

Figure 5. Model domains for the RAMS/HYPACT simulations used in the Bayonne PCB transport model.

NLCD is a multilayer and multi-source database that contains 30-m resolution 21-class land classification for territory of the Unites States in the form of visual images. The Visual Basic script was used to read pixel values and to produce a digital data file. Further we converted the NLCD classes to Olson type classes (http://edcdaac.usgs.gov/glcc/globdoc1_2.html) and then produced a LEAF2 database for RAMS.

The original RAMS Sea Surface Temperature (SST) is based on climatologically averaged monthly mean $1° \times 1°$ resolution data set of Reynolds et al. (2002). However, fine-scale transport of pollutants in this area is almost certainly affected by sea breezes initiated by the actual land/sea temperature contrast. Therefore in our simulations we have used real-time SST with better spatial resolution. For this purpose we acquired 1 km resolution multi-channel Advanced Very High Resolution Radiometer satellite retrievals (Bernstein 1982) from the Marine Remote Sensing Laboratory of the Rutgers Institute for Marine and Coastal Sciences.

These data were processed to remove the effect of clouds seen in the instantaneous retrievals and produce the 3-day SST composites.

The meteorology simulations are driven by the initial and boundary conditions that we developed using the objective analysis package belonging to RAMS. These objectively analyzed fields are calculated using 3-hourly Eta model operational analysis (Mesinger et al. 1988; Rogers et al. 1996) . The Eta Model data were provided by the National Center for Environmental Prediction (NCEP) in gridded binary (GRIB) format on a horizontal grid with the spatial resolution of 32 km. The objectively analyzed 3-hourly fields are used to constrain the flow near the boundaries of the grid 1 domain using nudging type Davies (1976) boundary conditions with the nudging time of 30 minutes at the 5-grid-cell boundary belt. In addition, to keep the flow close to observation during the entire period of simulations we nudged horizontal velocity, potential temperature, and Exner function in the interior of the domain with much larger nudging time of 12 hours to let small-scale high-frequency disturbances to develop. The RAMS simulations were conducted using radiative scheme of Harrington (1997), turbulent closure of Mellor and Yamada (1982), and driving fields calculated using Eta fields. The meteorological fields were saved every 30 minutes.

In an attempt to identify possible sources of the PCB concentrations observed at the Bayonne trailer, we modeled the transport of pollutants from three hypothetical sources, the Bayonne landfill, the NBCDF site, and New York City. Pollutant transport was calculated off-line using the Lagrangian model HYPACT version 1.2 and meteorological output from RAMS. Three unit PCB sources emitting in the 1-m surface layer were included in calculations of PCBs at the Bayonne landfill, the NBCDF, and New York City. The NBCDF location was chosen because it possessed the characteristics attributed to the PCB source: it is within 8 km of the Bayonne trailer and is closer to the Bayonne site than the Jersey City site. The NYC site was chosen because it is reasonable to assume that NYC emits significant quantities of gas-phase PCBs. To distinguish the effects of all these three sources their emissions were treated as different tracers. PCBs at the Bayonne landfill and the NBCDF were assumed to be emitted from a square area of 500 m $\times$ 500 m. The hypothetical source in NYC was assumed to have a rectangular shape of 4 $\times$ 10 km covering the lower part of Manhattan. The actual magnitude of these sources is not known, therefore we conducted calculations with unit sources of 1g s^{-1} and later scaled the emission to fit the observed concentrations, assuming a linear relationship between emission and measured concentration. For this initial modeling effort, PCBs were assumed to exist in the gas phase only and were not subjected to hydroxyl radical reactions. This assumption is reasonable since at equilibrium only about 10% of the total atmospheric burden of PCBs is typically in the particle phase. This assumption is further justifiable considering the short distances involved, which imply travel times of a few hours at most. Also, these assumptions provide the highest, or worst-case scenario, estimates of atmospheric PCB concentrations.

HYPACT simulations were conducted for six periods during which intensive sampling of atmospheric PCBs was conducted at three locations within the landfill and at the NJDEP trailer during placement of SDM at the landfill in Bayonne (Korfiatis et al. 2003). For purposes of calculating the emissions necessary to produce the observed concentrations at the Bayonne trailer, we used results obtained for October 23-26, 2001 which are representative of the typical airflow patterns in this region.

Observed wind series measured by Automated Surface Observation Stations (ASOS) at the JFK and Newark airports available from National Climate Data Center (NCDC)

(http://www4.ncdc.noaa.gov/cgi-win/wwcgi.dll?wwdi~ASOSPhotos) were compared with RAMS output to assess model accuracy (Fig. 6). The simulations captured time variations of wind directions and magnitude fairly accurately at both locations.

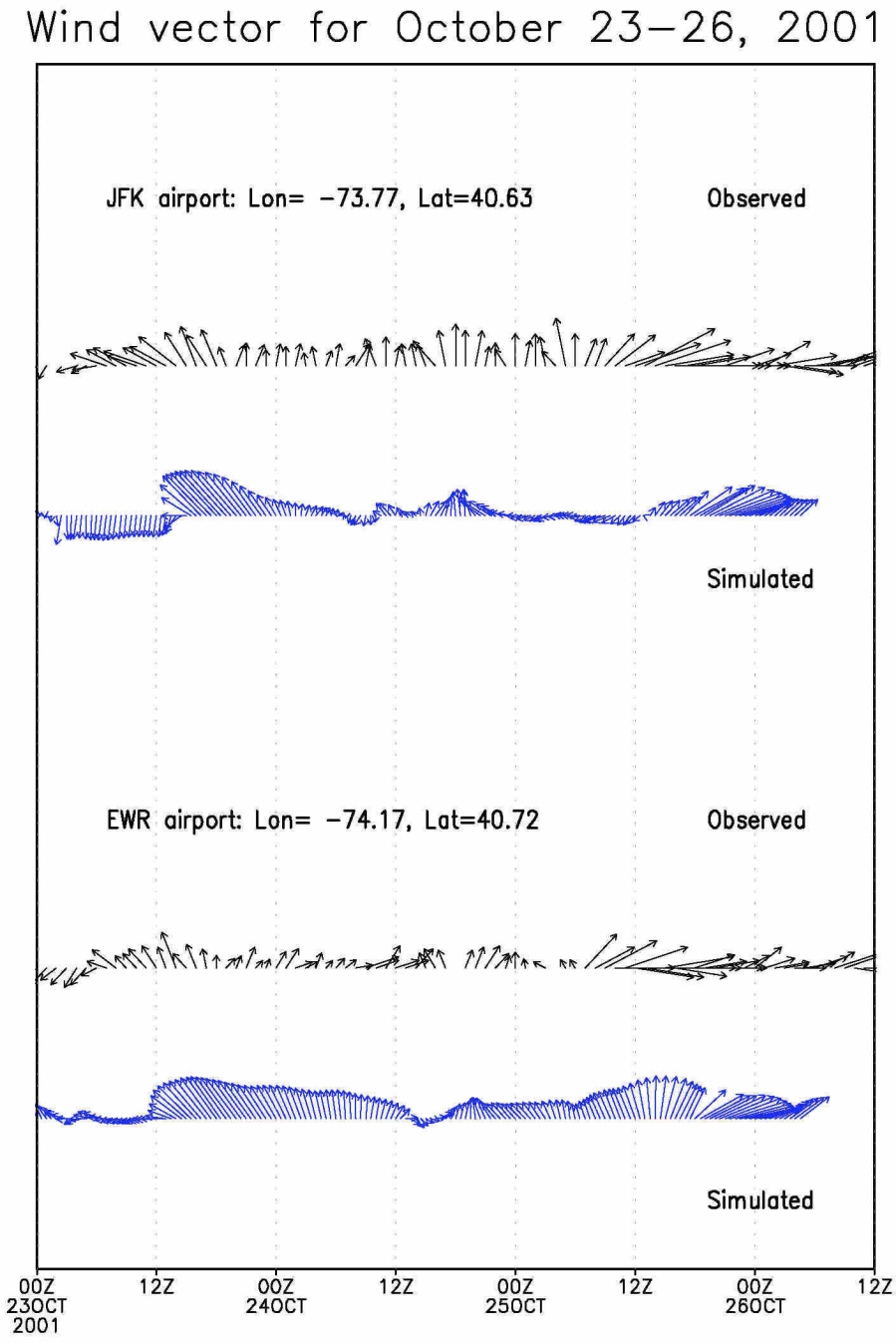

Figure 6. Observed winds (black) at JFK and Newark Airports and simulated (blue) winds at the same locations from the RAMS model at an altitude of 5 m.

Figure 7 depicts observed and simulated PCB concentrations at the SDM and trailer sites for the October, 2001 model period. In interpreting this figure it is important to remember that the measured concentrations represent integrated 4-hour measurements, while the lines are instantaneous predicted concentrations. PCB concentrations predicted at two locations (SMD landfill and trailer) are shown as they are produced by 3 different sources located at SDM landfill, NBCDF, and NYC, as was discussed above. The magnitude of each source needed to produce concentrations of the same magnitude as observed at a particular location was estimated. To our knowledge, this is the first time RAMS/HYPACT or similar atmospheric model has been used to examine emissions of Persistent Organic Pollutants on a local scale, and the results provide powerful insights into the magnitude of emissions necessary to produce the PCB levels

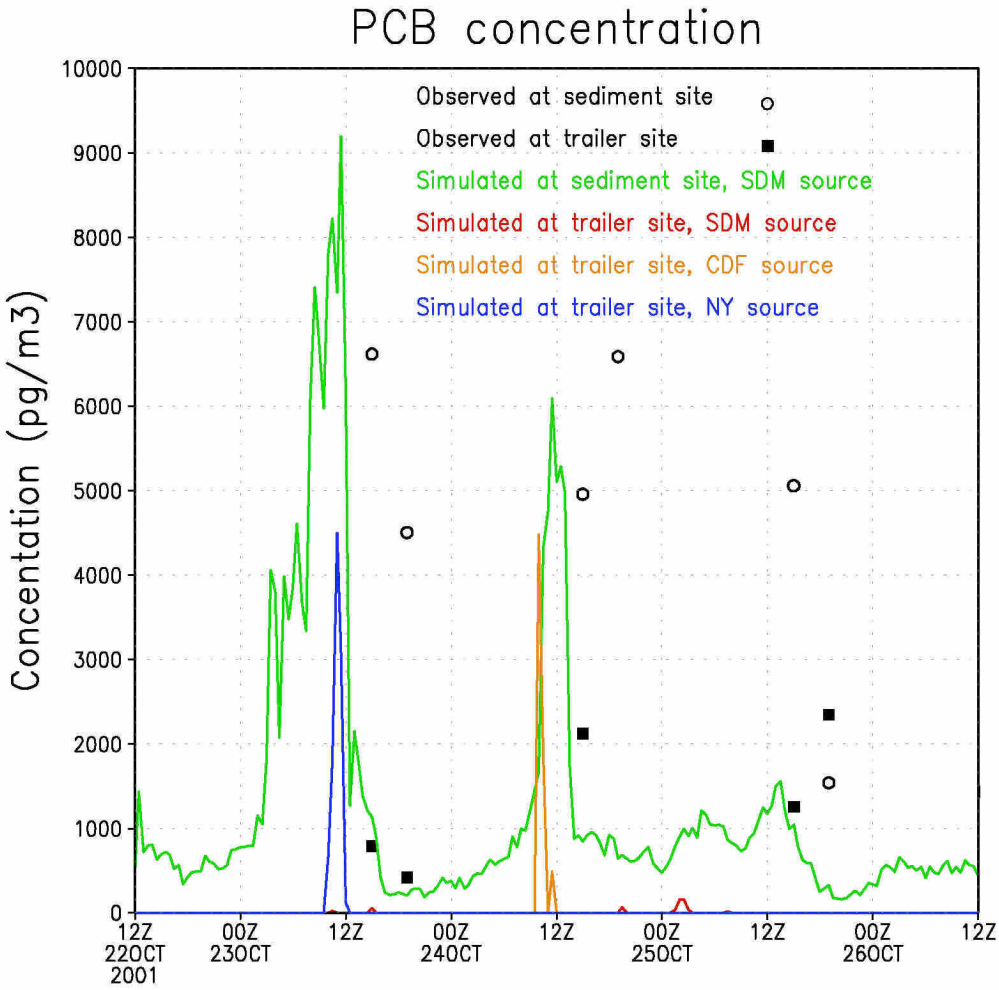

routinely measured in urban areas.

Figure 7. Solid lines depict HYPACT predicted gas-phase ΣPCB concentrations at the landfill (green) or trailer (all other colors) sites, assuming a source at the SDM placement site (Bayonne Landfill) (green and red), Newark Bay CDF (orange), or New York City (blue). The emissions rates used to generate these lines are 10^{-4} g s^{-1} at the SDM landfill (green and red lines), 10^{-3} g s^{-1} at the NBCDF (orange) and 10^{-3} g s^{-1} at NYC (blue). Measured gas-phase ΣPCB concentrations

are shown for the trailer (filled squares) and SDM placement site (open circles).

At the sediment site we have shown only concentrations transported from the local SDM site (green curve). The magnitude of PCB emissions at the SDM site that produces concentrations of 4000-7000 pg m^{-3} as was observed at the landfill (open circles; see Korfiatis et al. 2003) is 10^{-4} g s^{-1} or about 3 kg y^{-1}. Dividing this emission rate by the surface area over which sediment was spread on that particular day yields a surface flux equal to 400 pg m^{-2} s^{-1}. This value is in good agreement with the PCB volatilization flux (570 pg m^{-2} s^{-1}) estimated from micrometeorological measurements at the SDM site (Korifatis et al. 2003). The transport of PCB emissions of this magnitude from the SDM source could produce concentration spikes of 100-200 pg m^{-3} at the Bayonne trailer (red curve). These instantaneous levels are well below observed 4-hour integrated concentrations at this site that range from 400-2000 pg m^{-3} (closed squares), suggesting that the emissions from SDM placement activities at the Bayonne landfill have a small effect on the overall levels of PCBs measured at the Bayonne trailer. That a source of 3 kg of PCBs per year produces a minimal PCB signal 8 km away suggests that the levels of PCBs routinely measured in urban areas are produced by emissions that are orders of magnitude greater. It also suggests that the emissions which produced the PCB spikes at Bayonne are either much greater than 3 kg y^{-1} or that the source is much closer than 8 km.

It is useful to examine the impact that emissions from NYC have on the PCB levels measured at Bayonne, because although we do not know the magnitude of emissions from NYC, it is safe to assume that such emissions do exist. Of course, NYC cannot be the source of the PCB spikes measured at Bayonne because, due to its location, its emissions would have a greater impact at the Jersey City site than at the Bayonne site. Nevertheless, Figure 7 indicates that PCB emissions from NYC on the order of 32 kg y^{-1} are not observable at the Bayonne site most of the time. Only on the relatively rare occasions when the winds blow directly from NYC to Bayonne (for example, Oct 23 at noon) can this level of emissions produce a measurable PCB concentration at Bayonne.

Could emissions from the NBCDF explain the PCB spikes measured at the trailer? PCB concentrations resulting at the trailer site from the NBCDF (orange curve) are also shown in Figure 7. The magnitude of the source needed to produce short-term spikes in PCB concentrations that are similar in magnitude to those observed at the trailer is about 10^{-3} g s^{-1}. Are these emissions plausible? For the NBCDF, the emissions represent some fraction of the total mass of PCBs deposited into the facility during the measurement period. During the second half of 2000, approximately 160,000 cubic yards of dredge material were placed into the CDF. If the density of this material is assumed to be 500 kg m^{-3} and the PCB concentration is assumed to equal that of Newark Bay surface sediments (~750 ppb, Adams et al. 1998), then about 45 kg of PCBs were placed into the NBCDF during this 6-month period. At 10^{-3} g s^{-1}, about 16 kg of PCBs would have volatilized out of the NBCDF during this period, or one-third of the total PCB inventory in the sediments placed in the NBCDF. Given the long residence times of PCBs in sediments, this rate of volatilization seems unreasonably high. This calculation supports the conclusion that the NBCDF cannot be the source of the PCB spikes observed at Bayonne.

In addition to horizontal concentrations, it is useful to examine the vertical distribution of PCBs (Fig. 8). Vertical concentration profiles of unreactive contaminants are determined by three factors: the height of the emissions, the distance from the source, and the structure of the boundary layer. For PCBs, we assume that all emissions occur at ground level. The relatively low temperatures during the period of the modeling (October) will tend to create stable boundary conditions, trapping the ground level emissions below the boundary layer. During hotter months

when the boundary layer is less stable or during front passage or convective events, greater

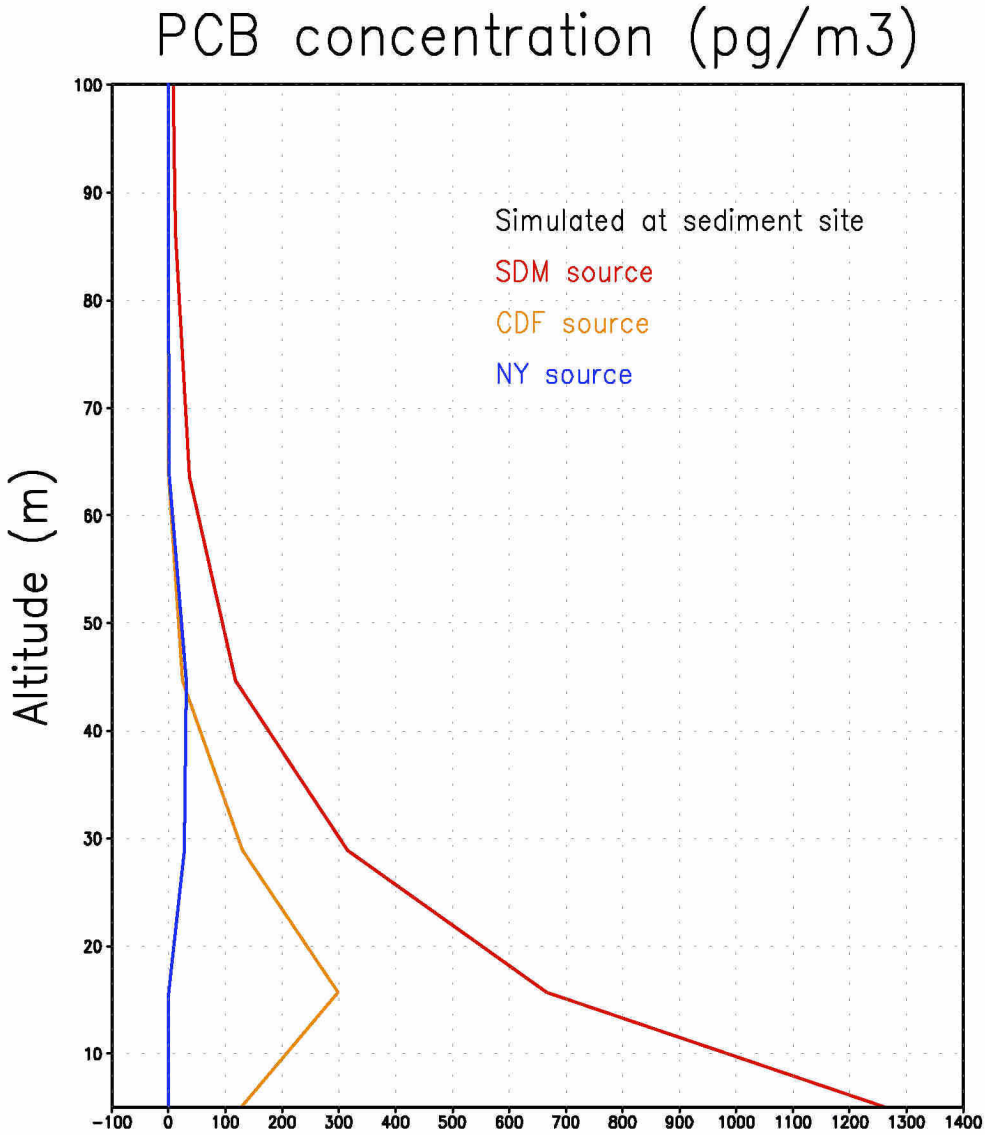

Figure 8. Vertical distribution of PCBs predicted by the RAMS/HYPACT model at the SDM landfill during October 23-26, 2001 assuming emissions at the SDM (red), NYC (blue), and CDF (orange).

turbulent mixing will facilitate the transport of PCBs above the boundary layer, where they will have greater potential for long-range transport (Stenchikov et al. 2005) . Maximum PCB concentrations occur at ground level only when the receptor (monitoring site) is directly above the emission point (in our scenario, at the SDM). When the receptor is removed from the source by a few km (NYC or NBCDF), the PCB concentrations reach a maximum 15-45 km above ground level. Farrar et al. (2005) measured the vertical distribution of PCBs in the urban

atmosphere of Toronto up to 360 meters. These researchers noted a profile characteristic of ground level emissions and a stable boundary layer (concentrations are highest at ground level and decrease with height) for some PCB congeners, but ΣPCBs were generally well mixed up to 360 m. These observations are in good agreement with our model results, which indicate that PCB concentrations do not necessarily display obvious vertical gradients below the urban boundary layer, which is generally above 400 m, unless the receptor is immediately above the emissions source.

Our modeling indicates that PCB concentrations drop to zero at ~100 m, whereas Farrar et al. (2005) measured significant PCB levels at 360 m. This discrepancy results from at least two factors: the stability of the October boundary layer, and the small number and relatively low intensity of the PCB sources in the model. Instability in the boundary layer would lead to a concentration profile that is relatively constant with height. Additional sources added to the RAMS/HYPACT model, especially sources located farther from the receptor, would increase PCB concentrations at heights above 100 m. This fact, coupled with the observations of Farrar et al. (2005), suggest that urban areas such as NYC and Toronto probably emit far more PCBs to the atmosphere than the ~70 kg y^{-1} used in our model.

How high might the urban emissions of PCBs be? The model results can be used to calculate the minimum total PCB emissions necessary to maintain the concentrations measured at the Bayonne trailer and at the nearby Jersey City NJADN site. The modeled urban source flux of 10^{-3} g s^{-1} represents a load of about 32 kg y^{-1} to the atmosphere of the region, and is barely observable 8 km away. Thus a source of this magnitude is sufficient to contaminate the air in only about a 6 km radius, or about 100 km^2. If a source of this magnitude is located within every 100 km^2 block of New York City (785 km^2), combined they would generate a relatively constant gas-phase PCB concentration of about 1000 pg m^{-3} at ground level throughout the City, similar to the levels observed at the Bayonne trailer and the Jersey City NJADN site. This PCB concentration is reasonable given that it is similar to the average gas-phase PCB concentrations measured in urban areas such as Camden, NJ (Totten et al. 2004) and Chicago, IL (Basu et al. 2004). This corresponds to PCB emissions on the order of ~800 g d^{-1}, or ~300 kg y^{-1}. For comparison, the largest single source of PCBs to the water column, the Hudson River, is estimated to contribute about 300 kg y^{-1} to the NY/NJ Harbor (Farley et al. 1999). This represents a minimum estimate because it does not consider the removal of PCBs from the lower atmosphere due to dry deposition and hydroxyl radical reactions.

III. Mercury Flux Chamber Studies

Natural and anthropogenic sources contribute gaseous elemental mercury (Hg°) to the regional and global atmosphere. Although mercury emissions from point sources can be identified and potentially controlled, emissions from contaminated ecosystems and terrestrial surfaces are widely distributed and largely unquantified. Recent attention has been drawn to the importance of Hg volatilization from soils and terrestrial vegetation (Lindberg et al., 1998; Gustin, 2003). In particular, the volatilization of Hg from naturally enriched or industrially contaminated soils and sediments is seen as an important pathway in the redistribution of mercury on watershed to global scales (Ferrara et al., 1998; Gustin et al., 2000). This redistribution of mercury pollution may increase the exposure of aquatic ecosystems to reactive Hg which can be methylated (Compeau and Bartha, 1985; Gilmour et al., 1992), enriched in aquatic and terrestrial food chains (Mason et al., 1996; Burger and Gochfeld, 1997; Watras et al., 1998; Gnamus et al., 2000) and act as a potent neurotoxicant in birds and mammals (Clarkson, 2002). In addition, the re-emission of Hg previously accumulated in soils and sediments via atmospheric deposition is an important aspect of the mercury cycle in non-point source impacted areas that needs to be accounted for in order to accurately quantify net atmospheric inputs of mercury to watersheds and the aquatic ecosystems they supply (Gustin, 2003). Global mercury budgets indicate that 50% of deposited mercury is re-emitted to the atmosphere (Bergan et al., 1999; Mason and Sheu, 2002), but only order-of-magnitude estimates of terrestrial emissions are available (Schroeder and Munthe, 1998; Scholtz et al., 2003).

The global average natural emission rate of mercury from land surfaces has been estimated to be approximately 1 ng m^{-2} h^{-1} (Fitzgerald and Mason, 1996), but field studies have shown that naturally enriched and anthropogenically contaminated soils and waters emit mercury vapor at much higher rates (Lindberg et al., 1979, 1995a,b; Carpi and Lindberg, 1997, 1998; Gustin, 1998; Gustin et al., 1996, 2000). For example, measured Hg fluxes range from 8 to 45 ng m^{-2} h^{-1} for natural soils (Poissant and Casmir, 1998; Carpi and Lindberg, 1998; Engle et al., 2001) and from 10 to 1500 ng m^{-2} h^{-1} for contaminated soils (Lindberg et al., 1995b; Carpi and Lindberg, 1997; Ferrara et al., 1998). Since mercury volatilization from land is dominated by the flux of elemental Hg (Kim and Lindberg, 1995), environments that favor the reduction of Hg(II), such as highly productive wetlands, are likely to support even higher Hg° emissions. Indeed, with few exceptions (Lee et al., 2000), relatively high evasive fluxes of Hg have been measured in natural wetland ecosystems (30-3000 ng m^{-2} h^{-1}, Kozuchowski and Johnson, 1978; Leonard et al., 1998; Lindberg et al., 2002).

Upland placement of dredged materials from navigation channels in the New York/New Jersey Harbor is currently being used to manage sediments deemed inappropriate for open water disposal. Although upland placement sites are equipped with engineering controls (leachate collection and/or barrier walls), little is known of the potential impacts of this approach to air quality. Sediment-air fluxes of Hg at the SDM placement site estimated by the micrometeorological technique (–13 to 1040 ng m^{-2} h^{-1}; sediment to air fluxes being positive) were similar to those for anthropogenically-enriched surfaces and were significantly correlated ($r^2 = 0.81$) with solar radiation (Goodrow et al., 2005). The goal of this project was to determine the sediment side control of Hg volatilization from cement-stabilized sediments in controlled laboratory flux chambers.

Initial experiments

The fluxes of Hg from Newtown Creek sediments were monitored along with those of PCBs under controlled laboratory conditions using a large wind tunnel flux chamber constructed at Stevens Institute of Technology (Fig. 9). The Stevens wind tunnel permitted chemical flux measurements from 1 m^2 of sediment under laminar or turbulent flow conditions. The intake of the wind tunnel was a 6.4:1 (area basis) contraction section designed to ensure parallel flow in the test section. After passing through the contraction section the air passed through a two meter long section in which the flow profile is allowed to develop. The air then passed over the sediment in a 2 m long by 0.5 m wide by 10 cm high section. The air was then pulled through another contraction to the sampling section. In the sampling section, a small sample of air was drawn off for semi-continuous gaseous Hg and water vapor analysis.

Figure 9. **W**ind tunnel used to determine sediment-air fluxes of PCBs and Hg from SDM.

Total gaseous mercury (TGM) concentrations in the laboratory where the flux chamber was initially set up were well above background outdoor concentrations. Concentrations of mercury in this lab ranged from 7 to 40 ng m^{-3} (Figs. 10 and 12) whereas background mercury concentrations in Bayonne, NJ are about 2 ng m^{-3} (Korfiatis et al., 2003). Elevated mercury concentrations in the inflow air of the Stevens flux chamber obscured or reversed mercury volatilization and generally low sediment-air mercury fluxes (<25 ng m^{-2} h^{-1}) or absorption of Hg by the sediment (negative fluxes) were observed measured in all experiments (Table 4).

The volatilization of Hg from Newtown Creek sediment was dependent on temperature. Thus the highest fluxes of Hg out of the sediments were observed over the course of a high temperature excursion during the February 2004 experiment (Fig. 11). Mercury volatilization may also depend on the concentration of mercury in the sediment, but over the relatively small

range of mercury concentrations in the two batches of Newtown Creek sediments used in the six Stevens flux chamber experiments (4.2 and 7.2 μg g^{-1}), no relationship between Hg volatilization and sediment Hg content was observed (Table 4). Another factor controlling the difference in mercury concentration between in and outside of the flux chamber experiment is the air flow rate which, if too high relative to the volatilization rate, could dilute any volatilized mercury below detection by difference with the concentration of Hg in the inflow air. Turning off the flow of air through the chamber and, as a result, stopping the movement of air into the flux chamber laboratory from adjacent rooms, resulted in significantly higher concentrations of gaseous mercury inside the flux chamber with respect to outside the chamber (Fig. 12). This result suggests that mercury volatilization occurred at a relatively slow rate in the Stevens flux chamber.

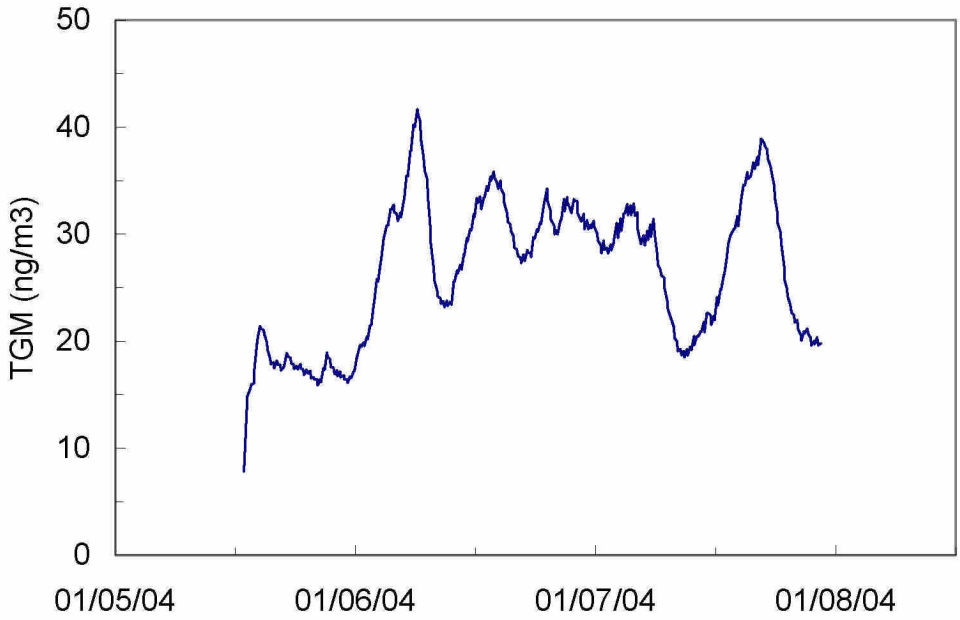

Figure 10. Gaseous mercury concentrations in the flux chamber laboratory, January 2004.

Table 4. Gaseous mercury fluxes from Newtown Creek sediment measured at Stevens Institute. Positive fluxes are from sediment to air.

Date	Cement (%)	Sediment Hg (μg g^{-1} dry wt)	Temp (°C)	heat flux (W m^{-2})	Hg fluxes (ng m^{-2} h^{-1})
Dec-03	0	4.2	12 to 19	low or <0	-150 to +100
Jan-04	8	4.2	14 to 18	low or <0	-130
Feb-04	4	4.2	13 to 17	9 to 15	-75 to +150
March 8-04	8	7.3	19	6 to 10	-200 to 0
March 15-04	4	7.3	20	10	-150 to 0
March 23-04	0	7.3	19	-20 to -40	-300 to 0

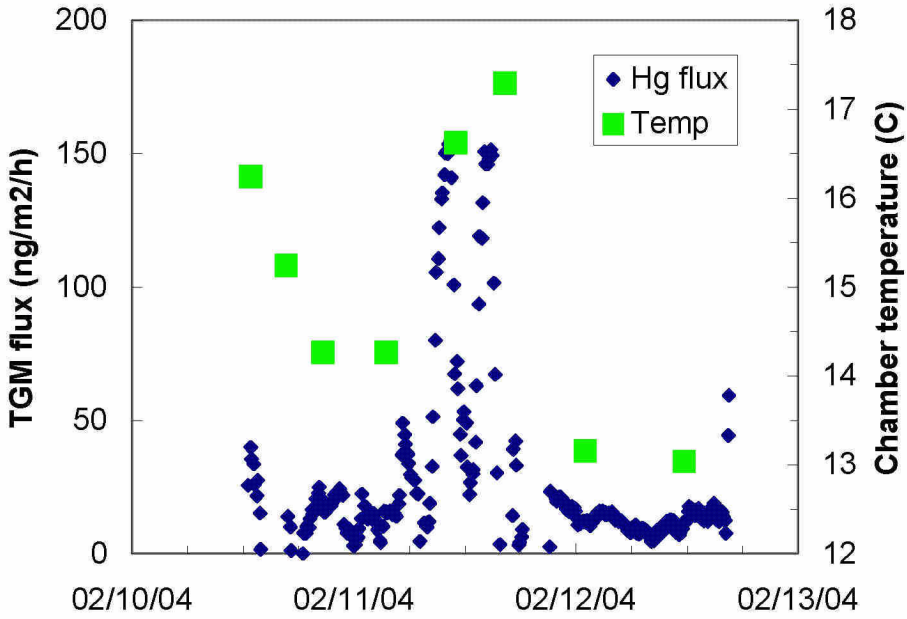

Figure 11. Estimated total gaseous mercury (TGM) fluxes from the first batch of Newtown Creek sediment treated with 4% Portland cement, February 2004.

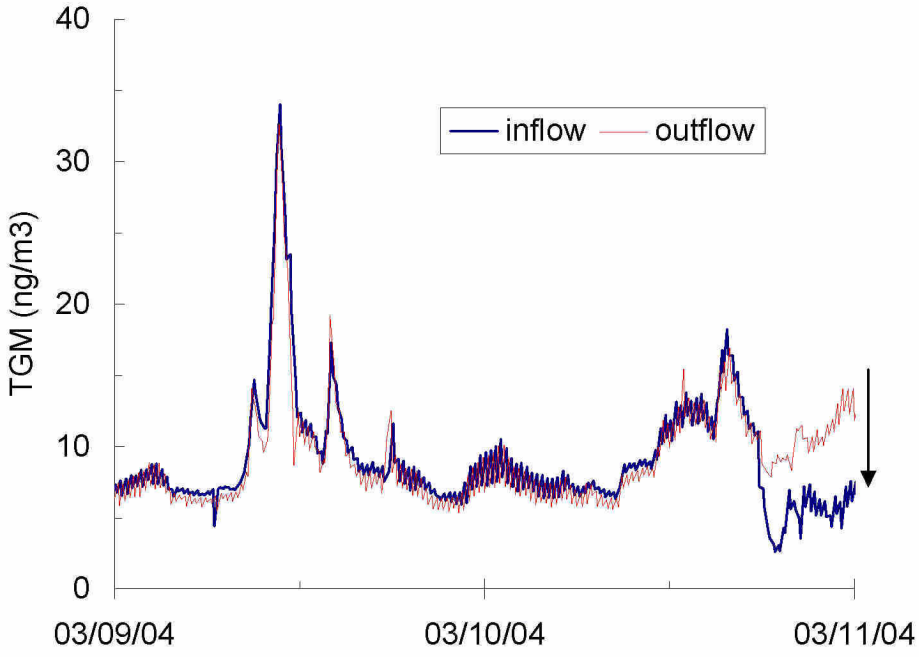

Figure 12. Total gaseous mercury (TGM) concentrations in the inflow and outflow air of the flux chamber during the March 9, 2004 experiment with the second batch of sediment. Air flow

through the chamber (and as a result, into the chamber laboratory from other rooms in the building) was stopped in the afternoon of March 10 (arrow).

In June 2004, the Stevens flux chamber was moved to a laboratory in a different building, but TGM levels were even higher (25 to 50 ng m^{-3}) than in the first location. Consequently, TGM fluxes were not measured during sediment flux chamber experiments in the summer of 2004 and it was decided that a smaller flux chamber in which mercury-free air could be used as the inflow air would be constructed for use at Rutgers.

Experiments with the new flux chamber

The new sediment flux chamber (Fig. 13) was constructed of transparent acrylic and included a 100 cm long, 10 cm wide, and 5 cm deep sediment drawer (sediment surface area = 0.1 m^2) that fits into a 120 cm long sealed chamber with 10 cm flow establishment sections at both ends and a 1 cm headspace above the sediment surface. Mercury-free inflow air supplied by a Tekran zero air generator flows first through the 10 cm flow establishment section, then over 1 m of sediment, and finally through the second 10 cm flow establishment section. All of the exit air is drawn directly into a Tekran continuous gaseous mercury analyzer at a sampling rate of 1.5 L min^{-1}. With a cross-sectional area of 10 cm^2 for the headspace above the sediment and an air velocity of 2.5 cm s^{-1}, the chamber will accommodate laminar air flow with an estimated Reynolds number of 1.7.

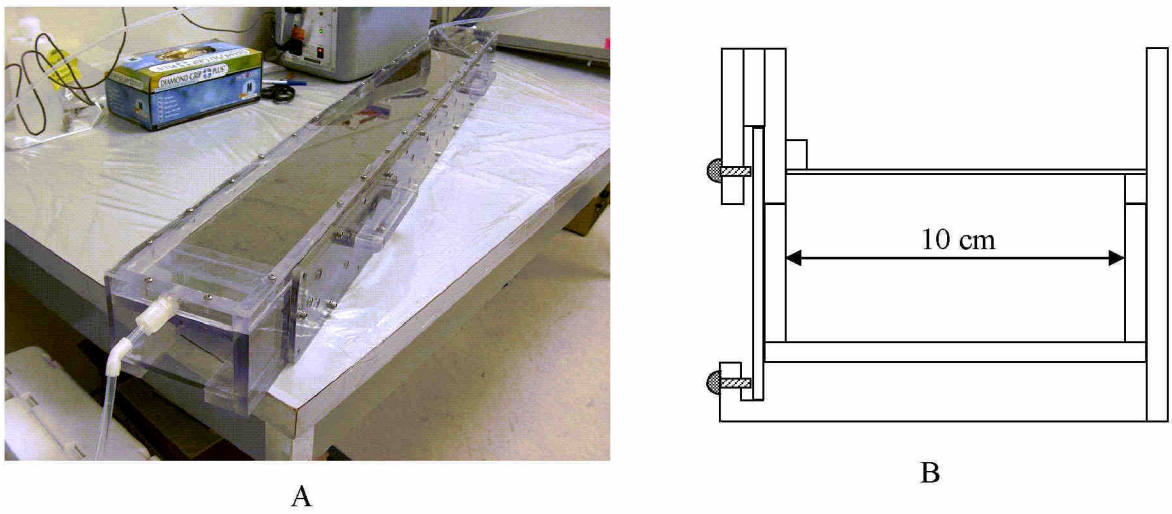

A B

Figure 13. Sediment flux chamber with sediment inside viewed from the mercury-free air inlet end (A) and a schematic cross-section (B).

Sediment flux experiments were carried out over 24 to 72 h by monitoring the concentration of gaseous mercury in air leaving the sediment-filled chamber under laminar flow conditions. Five to 30-minute gaseous mercury concentrations (ng m^{-3}) were converted to mercury fluxes (ng m^{-2} h^{-1}). During initial tests of the sealed flux chamber without sediment, mercury concentrations in the chamber were below detection demonstrating that no mercury leaked into the chamber from the laboratory under normal operating conditions.

Flux chamber experiments were conducted with both unstabilized sediments and cement-stabilized sediment with up to 6% cement by weight. Additional experiments were carried out to assess the role of light on mercury volatilization. Sediment used in these experiments was collected in October 2004 from air-exposed (low tide) mudflats in the Berry's Creek canal at a location where sediment mercury concentrations range from 20 to 40 $\mu g\ g^{-1}$ (Cardona et al., in prep.) and stored at 4°C until use. Approximately 5.5 L of homogenized sediment was placed in the sealed sediment flux chamber and brought to experimental temperature (17.5±1°C) in a controlled temperature room. Once equilibrated to the experimental temperature, the flux chamber was supplied with mercury-free air (≤ 0.5 psi above atmospheric pressure, ambient humidity) under laminar flow conditions and TGM concentrations were measured in the outflow air. Two 40 watt fluorescent bulbs provided 80 $\mu mol\ m^{-2}\ s^{-1}$ visible light and 0.8 $\mu mol\ m^{-2}\ s^{-1}$ UV-A to the chamber and were turned on and off over one hour and 12 h intervals. TGM measurements, accuracy and reproducibility are described in Goodrow et al., 2005.

Results with unstabilized Berry's Creek sediments indicate that photochemical reactions are important to the volatilization of mercury from sediments (Fig. 14). In the dark, TGM in the sediment flux chamber built up to 0.57 ± 0.14 $ng\ m^{-3}$, significantly lower than the "urban background" concentration measured in Bayonne, NJ (2.2 $ng\ m^{-3}$; Korfiatis et al, 2003; Goodrow et al., 2005) and that measured in the controlled temperature room outside the flux chamber (2.8 ± 0.2 $ng\ m^{-3}$). In the light, however, the concentration of TGM in the flux chamber built up to 12 ± 1.0 $ng\ m^{-3}$, about 20 times higher than that in the dark. Sediment temperatures were the same in the light and the dark indicating that the increase of TGM observed in the light was dependent on photochemical reactions. Light had no effect on TGM concentrations in the controlled temperature room outside the flux chamber or within the empty flux chamber.

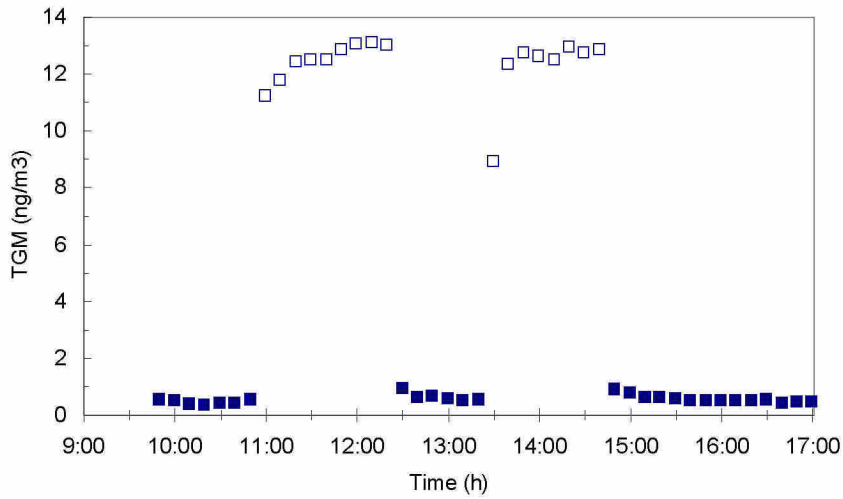

Figure 14. Effects of light on Hg emissions from unstabilized Berry's Creek sediment at 17.5 °C. TGM concentrations were measured in air passing over of a 10 cm x 100 cm sediment surface in a sealed flux chamber provided with Hg-free air in the dark (solid squares) or light (open squares).

Mercury volatilization results for Berry's Creek sediment stabilized with 6% Portland cement (dry cement weight to wet sediment weight) also show that light plays a critical role (Fig. 15). TGM concentrations in the flux chamber with cement-stabilized sediment increased in the light from 2.5 to 7.5 ng m^{-3} over the first 24 h and continued to rise to more than 20 ng m^{-3} during the next four days (Fig. 15). The surface of the cement-stabilized sediment became visually dry after four days in the flux chamber. Throughout short-term (hourly) or longer term (12 h) light-dark cycles, TGM concentrations dropped to < 0.5 ng m^{-3} in the absence of light.

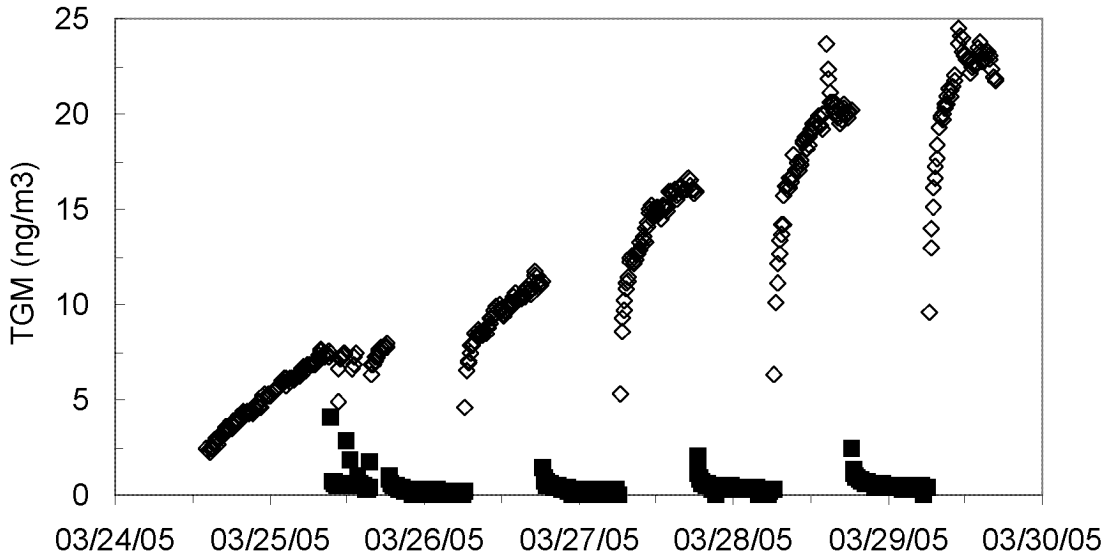

Figure 15. Effects of light on Hg emissions from cement stabilized (6% Portland cement by wet weight) Berry's Creek sediment at 17.5 °C. TGM concentrations were measured in the dark (solid squares) and light (open diamonds).

The near surface (1 cm) TGM concentrations measured in the flux chamber can be used to estimate the expected range of in situ daytime fluxes from this sediment with the modified Thornthwaite-Holtzman equation (Majewski et al., 1993).

$$F_{Hg} = \frac{u_* \kappa (Hg_1 - Hg_2)}{\ln\left(z_2 / z_1\right)\phi} \qquad (1)$$

where F_{Hg} is the land-air Hg flux (ng m^{-2} h^{-1}), u_* is the friction velocity, Hg_1 and Hg_2 are the gaseous Hg concentrations (ng m^{-3}) at heights z_1 and z_2 above the ground, ϕ is the atmospheric stability correction factor, and κ is the Von Karman constant. Using the range of daytime friction velocities we measured previously at a site in Bayonne, NJ (Korfiatis et al. 2003) and assuming that background atmospheric TGM is measured at a height of 3 m and a neutral atmosphere (ϕ = 1), the estimated ranges of in situ daytime sediment-air Hg fluxes are 30-110 ng

m^{-2} h^{-1} and 620-2200 ng m^{-2} h^{-1} for unstabilized sediment in the dark (shaded) and light, respectively, and 30-90 ng m^{-2} h^{-1} and 1200-4200 ng m^{-2} h^{-1} for cement-stabilized sediment in the dark and light, respectively. The estimated fluxes of Hg from cement-stabilized Berry's Creek sediment in the light are four to ten times higher than those from SDM observed during the day at the Bayonne placement site (300-1000 ng m^{-2} h^{-1}). This is likely due to the higher concentration of Hg in Berry's Creek sediment (23 to 35 μg Hg g^{-1} dry wt) than that used in Bayonne (1.3 to 2.6 μg Hg g^{-1} dry wt). However, highly Hg enriched sediment may yield even higher Hg fluxes than those estimated in these laboratory flux chamber experiments since actual daytime irradiances at an outdoor SDM placement site are typically much higher than 80 μmol m^{-2} s^{-1} and the atmospheric stability term (ϕ) is typically less than 1 during the day due to turbulent mixing. Nonetheless, these data clearly show that light has a major effect on Hg fluxes from air-exposed sediments and suggest that further examination of the effects of the intensity and wavelength of light and sediment properties (organic matter content) on Hg volatilization from sediments across a range of Hg contamination levels is needed. These results also show that cement stabilization increases the light-driven volatilization of Hg from sediment, possibly through the greater exposure of Hg photoreactant directly to light and air through enhanced drying.

IV. References

Adams, D. A., O'Connor, J. S. and Weisberg, S. B. 1998. Sediment Quality of the NY/NJ Harbor System, US EPA.

Baker, J. E., Poster, D. L., Clark, C. A., Church, T. M., Scudlark, J. R., Ondov, J. M., Dickhut, R. M. and Cutter, G., 1997. Loadings of atmospheric trace elements and organic contaminants to the Chesapeake Bay. In: Baker, J. E., Ed. Atmospheric Deposition of Contaminants in the Great Lakes and Coastal Waters. SETAC Press, Pensacola, FL. pp.171-194.

Basu, I., Hafner, W. D., Mills, W. J. and Hites, R. A. 2004. Differences in Atmsopheric Persistent Organic Pollutant Concentrations at Two Locations in Chicago. *J. Great Lakes Res.* 30: 310-315.

Bergan, T., Gallardo, L., and Rodhe, H. 1999. Mercury in the global troposphere: a three-dimensional model study. *Atmos. Environ.* 33: 1575-1585.

Bernstein, R. L. 1982. Sea surface temperature estimation using the NOAA-6 advanced very high resolution radiometer. *J. Geophys. Res.* 87 , 9455- 9465.

Brown, J. F. 1994. Determination of PCB metabolic, excretion, and accumulation rates for use as indicators of biological response and relative risk. *Environ. Sci. Technol.* 28 (13), 2295-2305.

Brunciak, P. C., Dachs, J., Gigliotti, C. L., Nelson, E. D. and Eisenreich, S. J. 2001. Atmospheric polychlorinated biphenyl concentrations and apparent degradation in coastal New Jersey. *Atm. Env. 35*, 3325-3339.

Buehler, S. S., Basu, I. and Hites, R. A. 2001. A Comparison of PAH, PCB, and Pesticide Concentrations in Air at Two Rural Sites on Lake Superior. *Environ. Sci. Technol.* 35: 2417 -2422.

Burger, J. and Gochfeld, M. 1997. Risk, mercury levels, and birds - relating adverse laboratory effects to field biomonitoring. *Environ. Res.* 75: 160-172.

Carlson, D. L. and Hites, R.A. 2005. Temperature Dependence of Atmospheric PCB Concentrations. *Environ. Sci. Technol.* 39 , 740-747.

Cardona, T., Schaefer, J.K., Ellickson, K.M., Barkay, T., and Reinfelder, J.R. (in prep) The cycling, reduction, and volatilization of mercury in highly contaminated estuarine surface waters.

Carpi, A., Lindberg, S.E. 1997. Sunlight-mediated emission of elemental mercury from soil amended with municipal sewage sludge. *Environ. Sci. Technol.* 31:2085-2091.

Carpi, A., Lindberg, S.E. 1998. Application of a Teflon (TM) dynamic flux chamber for quantifying soil mercury flux: Tests and results over background soil. *Atmos. Environ.* 32: 873-882.

Clarkson, T.W. 2002. The three modern faces of mercury. *Environ. Health Persp.* 110(Suppl.): 11-23.

Compeau, G.C. and Bartha R. 1985. Sulfate-reducing bacteria: principal methylators of mercury in anoxic estuarine sediment. *Appl. Environ. Microbiol.* 50: 498.

Cousins, I.T., Mackay, D. 2001. Gas-Particle Partitioning of Organic Compounds and Its Interpretation Using Relative Solubilities. *Environ. Sci. Technol.* 35: 643-647.

Davies, H.C. 1976. A lateral boundary formulation for multi-level prediction models. *Quart. J. Roy. Meteor. Soc.* 102: 405-418.

Eisenreich, S.J., Looney, B.B., and Thornton, J.D. 1981. Airborne organic contaminants in the Great Lakes ecosystem. *Environ. Sci. Technol.* 15: 30-38.

Engle, M.A., Gustin, M.S., Zhang H. 2001. Quantifying natural source mercury emissions from the Ivanhoe Mining District, north-central Nevada, USA. *Atmos. Environ.* 35: 3987-3997.

Falconer, R. L. and Bidleman, T. F. 1994. Vapor pressures and predicted particle/gas distributions of polychlorinated biphenyl congeners as a function of temperature and ortho-chlorine substitution. *Atmos. Env.* 28: 547-554.

Farley, K. J., Thomann, R. V., Cooney, T. F. I., Damiani, D. R. and Wands, J. R. 1999. An Integrated Model of Organic Chemical Fate and Bioaccumulation in the Hudson River Estuary. Riverdale, NY, The Hudson River Foundation: 170.

Farrar, N. J., Harner, T., Shoeib, M., Sweetman, A. and Jones, K. C. 2005. Field deployment of thin film passive air samplers for persistent organic pollutants: A study in the urban atmospheric boundary layer. *Environ. Sci. Technol.* 39: 42-48.

Ferrara, R., Maserti, B.E., Andersson, M., Edner, H., Ragnarson, P., Svanberg, S., Hernandez, A. 1998. Atmospheric mercury concentrations and fluxes in the Almaden District (Spain). *Atmos. Environ.* 32: 3897-3904.

Fikslin, T. J. and Suk, N. 2003. Total Maximum Daily Loads For Polychlorinated Biphenyls (PCBs) For Zones 2 - 5 Of The Tidal Delaware River., Report to the USEPA regions II and III.

Fitzgerald, W. and Mason, R. 1996. The global mercury cycle: oceanic and anthropogenic aspects, in W. Baeyens, et al (eds.), *Global and Regional Mercury Cycles: Sources, Fluxes and Mass Balances*, 85-108, Kluwer Academic Publishers, Netherlands.

Frame, G. M., Cochran, J. W. and Boewadt, S. S. 1996. Complete PCB congener distributions for 17 Aroclor mixtures determined by 3 HRGC systems optimized for comprehensive, quantitative, congener-specific analysis. *J. High Resol. Chromatogr.* 19: 657-668.

Gigliotti, C. L., Dachs, J., Nelson, E. D., Brunciak, P. A., Eisenreich, S. J. Polycyclic Aromatic Hydrocarbons in the New Jersey Coastal Atmosphere. *Environ. Sci. Technol.* **2000**, *34*, 3547-3554.

Gigliotti, C.L., Brunciak, P.A., Dachs, J., IV, G.T.R., Nelson, E.D., Totten, L.A., Eisenreich, S.J. 2001. Air-Water Exchange of Polycyclic Aromatic Hydrocarbons in the NY-NJ Harbor Estuary. *Environ. Toxicol. Chem.* 21: 235-244.

Gilmour, C.C., Henry, E.A. and Mitchell, R. 1992. Sulfate stimulation of mercury methylation in freshwater sediments. *Environ. Sci. Technol.* 26: 2281.

Gingrich, S. E. and Diamond, M. L. 2001. Atmospherically derived organic surface films along an urban-rural gradient. *Environ. Sci. Technol.* 35: 4031-4037.

Gnamus, A., Byrne, A.R., Horvat, M. 2000. Mercury in the soil-plant-deer-predator food chain of a temperate forest in Slovenia. *Environ. Sci. Technol.* 34: 3337-3345.

Goodrow, S.M., R. Miskewitz, R.I. Hires, S.J. Eisenreich, W.S. Douglas, J.R. Reinfelder. 2005. Mercury emissions from cement-stabilized dredged material. *Environ. Sci. Technol.* 39: 8185-8190.

Goodrow S.M., R. Miskewitz, R.I. Hires, S.J. Eisenreich, W.S. Douglas, J.R. Reinfelder. 2006. *Correction to* Mercury emissions from cement-stabilized dredged material. Environ. *Sci. Technol.* 40: 409.

Gustin, M.S. 1998. NvMEP : Nevada Mercury Emissions Project-Mercury flux measurements: An intercomparison and assessment, Published Electric Power Research Institute Report, TR-111346.

Gustin. M.S. 2003. Are mercury emissions from geologic sources significant? A status report. *Sci. Total Environ.* 304: 153-167.

Gustin, M.S., G.E. Taylor, T.L. Leonard and T.E. Keislar. 1996. Atmospheric mercury concentrations associated with geologically and anthropogenically enriched sites in central western Nevada. *Environ. Sci. Technol.* 30: 2572-2579.

Gustin, M.S., S.E. Lindberg, K. Austin, M. Coolbaugh, A. Vette, and H. Zhang. 2000. Assessing the contribution of natural sources to regional atmospheric mercury budgets. *Sci. Total Environ.* 259: 61-72.

Harner, T., Bidleman, T.F. 1998. Octanol-Air Partition Coefficient for Describing Particle/Gas Partitioning of Aromatic Compounds in Urban Air. *Environ. Sci. Technol.* 32: 1494-1502.

Harner, T., Shoeib, M., Diamond, M., Stern, G. and Rosenberg, B. 2004. Using passive air samplers to assess urban - Rural trends for persistent organic pollutants. 1. Polychlorinated biphenyls and organochlorine pesticides. Environ. Sci. Technol. 38: 4474-4483.

Harrington, J. Y. (1997) The effects of radiative and microphysical processes on simulated warm and transition season Arctic stratus. Ph.D., Colorado State University.

Junge, C. E. In *Fate of Pollutants in Air and Water Environments (Part I)*, Suffett, I. H., Ed., Wiley: New York, NY, 1977.

Korfiatis, G.P., R.I. Hires, J.R. Reinfelder, L.A. Totten, and S.J. Eisenreich. 2003. Monitoring of PCB and Hg Air Emissions in Sites Receiving Stabilized Harbor Sediment. Report to the New Jersey Marine Sciences Consortium and New Jersey Department of Transportation Office of Maritime Resources.

Kozuchowski, I. and D.L. Johnson. 1978. Gaseous emissions of mercury from an aquatic vascular plant. *Nature* 274:468-469.

Lee X., Benoit G., and Hu X. Z. 2000. Total gaseous mercury concentration and flux over a coastal saltmarsh vegetation in Connecticut, USA. *Atmo. Environ.* 34: 4205-4213.

Leonard T.L., Taylor G.E., Gustin M.S., and Fernandez G.C.J. 1998. Mercury and plants in contaminated soils: 2. Environmental and physiological factors governing mercury flux to the atmosphere. *Environ. Toxicol. Chem.* 17: 2072-2079.

Lindberg, S.E., R.C. Harriss, R.R. Turner, D.S. Shriner, and D.D. Huff. 1979. Mechanisms and rates of atmospheric deposition of trace elements and sulfate to a deciduous forest canopy. ORNL/TM-6674. Oak Ridge National Laboratory, Oak Ridge, Tennessee. 510 pp.

Lindberg, S.E., Meyers, T.P., and J. Munthe. 1995a. Evasion of mercury vapor from the surface of a recently limed acid forest lake in Sweden. *Water, Air, Soil, Pollut.* 85: 725-730.

Lindberg, S.E., Kim, K.H., Meyers, T.P., and Owens, J.G. 1995b. Micrometeorological gradient approach for quantifying air-surface exchange of mercury-vapor - tests over contaminated soils. *Environ. Sci. Technol.* 29: 126-135.

Lindberg S.E., Hanson P.J., Meyers T.P., and Kim K.H. 1998. Air/surface exchange of mercury vapor over forests - The need for a reassessment of continental biogenic emissions. *Atmos. Environ.* 32: 895-908.

Lindberg, S.E., W. Dong, T. Meyers. 2002. Transpiration of gaseous elemental mercury through vegetation in a sub-tropical wetland in Florida. *Atmo. Environ.* 36: 5207-5219.

Litten, S. 2003. Contaminant Assessment and Reduction Project: Water. New York, New York State Department of Environmental Conservation: 158.

Lohmann, R., Nelson, E., Eisenreich, S.J., Jones, K.C. 2000. Evidence for Dynamic Air-Water Exchange of PCDD/Fs: A Study in the Raritan Bay/Hudson River Estuary. *Environ. Sci. Technol.* 34: 3086-3093.

Majewski, M., Desjardins, R., Rochette, P., Pattey, E., Seiber, J., Glotfelty, D. 1993. Field comparison of an eddy accumulation and an aerodynamic-gradient system for measuring pesticide volatilization fluxes. *Environ. Sci. Technol.* 27: 121-128.

Mason, R.P., Reinfelder, J.R., and Morel, F.M.M. 1996. Uptake, toxicity, and trophic transfer of mercury in a coastal diatom. *Environ. Sci. Technol.* 30: 1835-1845.

Mason, R.P. and Sheu, G.R. 2002. Role of the ocean in the global mercury cycle *Global Biogeochem. Cycles* 16: Art. No. 1093.

Mellor, G.L. and Yamada, T. 1982. Development of a turbulence closure model for geophysical fluid problems. Rev. Geophys. Space Phys 20 , 851-875.

Mesinger, F., Janjic, Z. I., Nickovic, S., Gavrilov, D. and Deaven, D. G. 1988. The step-mountain coordinate: Model description and performance for cases of Alpine lee cyclogenesis and for a case of Appalachian redevelopment. *Mon. Wea. Rev.* 116: 1493-1518.

Miskewitz, R., R. Hires, and G. Korfiatis. 2005. Measurement of PCB Fluxes to the Atmosphere from Stabilized Dredged Material. Report to the New Jersey Marine Sciences Consortium and New Jersey Department of Transportation Office of Maritime Resources.

Pankow, J.F. 1987. Review And Comparative Analysis Of The Theories On Partitioning Between The Gas And Aerosol Particulate Phases In The Atmosphere. *Atmos. Env.* 21: 2275.

Pankow, J.F. 1994. An absorption model of gas/particle partitioning of organic compounds in the atmosphere. *Atmos. Env.* 28: 185-188.

Poissant, L., Casimir, A. 1998. Water-air and soil-air exchange rate of total gaseous mercury measured at background sites. *Atmo. Environ.* 32: 883-893.

Rogers, E., T., Black, L., Deaven, D.G. and DiMego, G.J. 1996. Changes to the operational "Early" Eta analysis/forecast system at the national Center for Environmental Prediction. *Wea. Forecasting* 11: 391-413.

Scholtz, M.T., B.J. Van Heyst, W.H. Schroeder. 2003. Modelling of mercury emissions from background soils. *Sci. Total Environ.* 304: 185-207.

Schroeder, W.H. and Munthe, J. 1998. Atmospheric mercury—an overview. *Atmos. Environ.* 32: 809 –822.

Simcik, M.F., Franz, T.P., Zhang, H.X., Eisenreich, S.J. 1998. Gas-particle partitioning of PCBs and PAHs in the Chicago urban and adjacent coastal atmosphere: States of equilibrium. *Environ. Sci. Technol.* 32: 251-257

Stenchikov, G., Lahoti, N., Lioy, P., Georgopoulos, P., Diner, D. and Kahn, R. (submitted). Micrometeorological Pollutant Transport from the Collapse of the World Trade Center on September 11, 2001. *J. Env. Fluid Dynamics*.

Stenchikov, G., Pickering, K., DeCaria, A., Tao, W.K., Scala, J., Ott, L., Bartels, D. and Matejka, T. 2005. Simulation of the fine structure of the 12 July 1996 Stratosphere-Troposphere Experiment: Radiation, Aerosols and Ozone (STERAO-A) storm accounting for effects of terrain and interaction with mesoscale flow. *J Geophys. Res. – Atmos.* 110 (Art. No. D14304).

Totten, L.A., 2005. Present-Day Sources and Sinks for Polychlorinated Biphenyls (PCBs) in the Lower Hudson River Estuary. In: Panero, M., Boehme, S. and Muñoz, G., Eds.,

Pollution Prevention And Management Strategies For Polychlorinated Biphenyls In The New York/New Jersey Harbor. New York Academy of Sciences, New York. p.18.

Totten, L.A., Brunciak, P.A., Gigliotti, C.L., Dachs, J., IV, G.T.R., Nelson, E.D. and Eisenreich, S.J. 2001. Dynamic Air-Water Exchange of Polychlorinated Biphenyls in the NY-NJ Harbor Estuary. *Environ. Sci. Technol.* 35: 3834-3840.

Totten, L.A., Gigliotti, C.L., VanRy, D.A., Offenberg, J.H., Nelson, E.D., Dachs, J., Reinfelder, J.R. and Eisenreich, S.J. 2004. Atmospheric Concentrations and Deposition of PCBs to the Hudson River Estuary. *Environ. Sci. Technol.* 38: 2568-2573.

Wania, F., Haugen, J.-E., Lei, Y.D. and Mackay, D. 1998. Temperature dependence of atmospheric concentrations of semivolatile organic compounds. *Environ. Sci. Technol.* 32: 1013-1021.

Watras, C.J., Back, R.C., Halvorsen, S., Hudson, R.J.M., Morrison, K.A., and Wente, S.P. 1998. Bioaccumulation of mercury in pelagic freshwater food webs. *Sci. Total Environ.* 219: 183-208.

PCB	BAF071801AF1 surr. corrected concentration (pg/m3)	BAF071801M surr. corrected concentration (pg/m3)	BAF071901AF1 surr. corrected concentration (pg/m3)	BAF072001A surr. corrected concentration (pg/m3)	BAF072001MF1 surr. corrected concentration (pg/m3)	BAF111202A surr. corrected concentration (pg/m3)
8+5	28	0	0	13	ıo surrogate adde	0.13
18	3.6	0	2.2	0	(lab error)	0
17+15	1.6	0	1.8	0		0
16+32	2.1	0	0	8.0		0.040
31	3.0	0	0	1.8		0
28	2.0	0	0	0.75		0
21+33+53	2.5	0	0	0.61		0.0078
22	0	3.3	0	0.78		0.070
45	0	0.10	0	0		0.0025
46	0	0	0	0		0
52+43	2.3	0	2.1	1.2		0.022
49	0	0	1.4	0		0.0089
47+48	3.6	0	1.7	7.0		0.0095
44	8.7	1.8	7.2	6.7		0.020
37+42	3.2	0	4.3	1.2		0.0043
41+71	7.1	0	2.3	1.9		0
64	1.2	0	0.78	0.29		0.0045
40	0	0	0	0.89		0
74	2.4	0	3.6	0.80		0
70+76	1.5	0.80	8.4	0		0
66+95	9.3	5.1	11	3.4		0.18
91	0	0	0.56	0.47		0
56+60+89	2.2	0	3.1	1.1		0.025
92+84	3.5	0.61	3.7	1.3		0.040
101	1.6	0.37	2.5	0.92		0.029
99	1.6	5.7	0.56	3.0		0.0032
87+81	1.1	0	2.9	0.50		0.013
85+136	2.5	0.74	3.9	0.87		0.014
110+77	2.5	0.98	6.2	1.9		0.037
82	0	0	0	0.33		0.016
151	0	0	0	0.20		0
135+144+147+124	0	0	0	0.27		0
149+123+107	4.7	0.89	3.1	1.4		0.014
118	4.1	0	2.9	1.2		0.014
146	5.0	0	2.9	2.0		0.045
153+132	9.1	0	12	3.4		0.076
105	0	0	0	0		0
141+179	0.97	0	0.91	0.39		0.0081
137+176+130	0	0	1.8	0.11		0
163+138	0.72	0.042	0.54	0.22		0.00034
158	0.38	0.19	0	0.23		0.0043
187+182	2.0	1.4	5.9	0.67		0.058
183	5.3	0	1.2	0.32		0
185	0	0	0	0.078		0
174	0.50	0.31	1.2	0.37		0.0075
177	1.1	0.70	1.4	0.48		0.029
202+171+156	2.1	0	2.8	1.1		0.0031
180	1.8	1.0	1.6	0.92		0.023
199	0	0	0	0		0
170+190	0.99	0.55	1.8	0.87		0.0084
201	1.2	0.67	8.3	0.60		0.013
203+196	1.5	2.7	6.9	0.98		0.043
195+208	0.78	2.3	7.9	0.29		0.040
194	2.5	1.6	2.5	1.3		0.0088

206	1.1	1.2	15	0.34	0
surrogate recoveries *(%)*					
14	41%	0%	54%	68%	31%
23	63%	88%	64%	62%	100%
65	66%	80%	64%	63%	89%
166	77%	95%	79%	78%	98%

BAF111202M surr. corrected concentration (pg/m3)	BAF111302M surr. corrected concentration (pg/m3)	BAF111402A surr. corrected concentration (pg/m3)	BAF111402M surr. corrected concentration (pg/m3)	BAF050702A surr. corrected concentration (pg/m3)	BAF050802A surr. corrected concentration (pg/m3)	BAF050802MF1 surr. corrected concentration (pg/m3)
0.30	*0*	0.71	0.70	0.28	0.19	0.14
0	0	0.066	0	0	0.022	0.011
0	0	0	0	0	0.011	0.020
0	0	0.15	0.14	0	0.017	0
0	0	0.029	0.046	0	0.034	0.016
0	0	0.013	0.025	0	0.013	0.011
0	0	0	0.013	0	0.0039	0.010
0	0	0.10	0.28	0	0.12	0.016
0	0	0.0052	0.022	0	0.0037	0.0029
0	0	0	0.0058	0	0.0071	0
0	0	0.020	0.032	0	0.035	0.014
0	0	0	0	0	0.0072	0.010
0.11	0	0	0	0	0.017	0.0094
0	0.058	0.090	0.066	0.10	0.042	0.033
0	0.0074	0	0.012	0.0082	0.0069	0.013
0	0.043	0	0.041	0	0.031	0.013
0	0.0068	0	0.0034	0	0.0089	0.0036
0	0.0060	0	0.0066	0	0.0037	0.0034
0	0.025	0	0.047	0	0.049	0.013
0	0.053	0	0.098	0	0.085	0.038
0	0.048	0.39	0.15	0.29	0.18	0.071
0	0	0	0	0	0.0044	0.0071
0	0	0	0.026	0	0.048	0.026
0	0	0.031	0.019	0.022	0.026	0.026
0	0	0.015	0.014	0.020	0.029	0.020
0	0	0.011	0.011	0.013	0.0059	0.017
0	0	0.018	0.013	0	0.017	0.017
0	0	0.011	0.0052	0	0.014	0.013
0.051	0	0.031	0.022	0.040	0.061	0.030
0	0	0	0.0015	0	0.0068	0.0045
0	0	0.040	0.0039	0	0.018	0.0064
0	0	0.078	0	0	0.013	0.0043
0	0	0.17	0.020	0.025	0.064	0.021
0	0	0.13	0.011	0	0.061	0.018
0	0	0	0	0	0.042	0.020
0	0	0.61	0.049	0.030	0.17	0.21
0	0	0	0	0	0	0
0	0	0	0	0	0.024	0.0080
0	0	0	0	0	0.0036	0
0.011	0	0.023	0	0	0	0.0019
0.013	0	0.058	0.0036	0.0053	0.015	0.0050
0.071	0	0	0.0046	0	0.045	0.035
0	0	0	0	0	0.030	0.012
0	0	0	0	0	0.0030	0
0	0	0.093	0.0090	0	0.039	0.0082
0	0	0.18	0.0098	0	0.026	0.0087
0	0	0.084	0.0092	0	0.013	0.013
0.052	0.019	0.24	0.023	0.026	0.099	0.016
0.013	0	0	0	0	0.0021	0
0	0	0.14	0.012	0.0079	0.071	0.014
0	0	0.31	0.012	0.014	0.044	0.0092
0	0	0.64	0.016	0.018	0.057	0.017
0	0	0.34	0.0056	0.0072	0.033	0.0071
0.068	0	0.14	0.0035	0.0055	0.026	0.0094

0	0	0.23	0.0061	0	0.027	0.0066
62%	23%	50%	38%	19%	17%	66%
69%	75%	78%	83%	74%	87%	68%
64%	67%	74%	72%	80%	84%	69%
75%	85%	10%	92%	101%	110%	80%

BAF050902A surr. corrected concentration (pg/m3)	BAF050902M surr. corrected concentration (pg/m3)	BAF051002A surr. corrected concentration (pg/m3)	BAF051002M surr. corrected concentration (pg/m3)
0.067	0.16	0.037	0
0.013	0	0	0
0.015	0	0	0
0	0	0.0048	0.0091
0.020	0	0	0
0.015	0	0.0078	0
0	0	0	0
0.049	0	0.022	0
0.025	0	0	0
0	0	0	0
0.0037	0	0.0070	0
0	0	0.0015	0
0.030	0.23	0.0032	0
0.020	0.064	0.026	0.023
0	0	0.0014	0.0025
0	0.017	0	0
0.011	0.0072	0.0016	0.0025
0	0	0	0
0.0087	0.024	0	0
0	0.11	0	0
0.042	0.070	0.14	0.21
0	0	0	0
0.022	0.014	0.017	0
0.023	0.023	0.0086	0.0083
0.019	0.021	0.0043	0.010
0.036	0.011	0.0030	0.0014
0	0.012	0.0027	0.0092
0	0	0	0
0.025	0.026	0.016	0.021
0	0	0.0061	0
0	0	0	0.0025
0	0	0	0.010
0.016	0.012	0.0068	0
0	0.011	0.0053	0
0	0.032	0.0025	0.0093
0	0.037	0.024	0.035
0	0	0	0
0	0	0.0015	0.010
0	0	0	0
0.0060	0.0058	0.00059	0
0.0042	0.0047	0.0022	0
0.044	0.042	0.024	0.020
0	0	0.0011	0
0	0	0	0
0	0.0032	0.0021	0.0031
0	0.0043	0.010	0.021
0	0.0037	0	0
0.014	0.012	0.0068	0.0076
0.0072	0	0	0
0	0.027	0.0046	0.0052
0.0082	0.0076	0.0037	0.0049
0.014	0.012	0.017	0.0025
0	0	0.016	0.024
0	0	0.0039	0.0079

0	0	0.0039	0.0024
61%	36%	35%	48%
74%	64%	82%	82%
74%	67%	79%	88%
77%	107%	84%	94%

PCB	SAF071701B surr. corrected concentration (pg/m3)	SAF071801AM surr. corrected concentration (pg/m3)	SAF071801BA surr. corrected concentration (pg/m3)	SAF071801BM surr. corrected concentration (pg/m3)	SAF071801CA surr. corrected concentration (pg/m3)
8+5	5.0	6.5	24	0	0
18	1.6	1.3	13	0	0.80
17+15	0.90	0.85	15	0	0.55
16+32	2.8	1.7	19	2.8	0.38
31	3.2	2.4	56	2.5	0
28	4.5	0.85	16	1.1	0
21+33+53	1.9	1.3	5.0	1.7	0.45
22	2.5	4.8	3.4	4.6	0
45	0.082	0.092	2.8	0.077	0
46	0.24	0	41	0.55	0
52+43	2.5	1.5	36	4.7	0.90
49	2.3	1.2	35	3.9	1.4
47+48	1.9	0.79	161	4.1	1.7
44	2.0	3.0	16	3.3	2.9
37+42	1.5	0.38	7.7	0.55	1.4
41+71	3.1	2.8	47	2.9	2.4
64	1.0	0.91	4.0	0.60	0.53
40	0.31	0.29	11	0.45	0.55
74	3.0	1.9	28	0.75	1.9
70+76	29	2.6	61	3.9	2.7
66+95	9.2	8.7	9.6	25	4.9
91	0.27	0.50	23	0.53	0.33
56+60+89	3.4	2.6	28	3.0	2.4
92+84	6.6	1.6	50	2.0	1.8
101	1.2	1.5	11	2.4	1.1
99	2.7	0.31	2.2	0.58	1.8
87+81	0.77	1.0	9.6	0.59	0.62
85+136	0.16	0.85	16	2.3	1.8
110+77	2.9	4.4	41	6.3	1.7
82	0.33	0.18	1.2	0.58	1.2
151	0.52	0.32	1.1	0	0.27
135+144+147+124	0	0.51	0.94	0.39	0.55
149+123+107	2.3	2.4	4.0	2.6	1.5
118	5.5	2.8	4.2	4.4	1.4
146	2.4	1.6	2.2	1.3	1.8
153+132	5.8	5.4	12	5.6	5.1
105	0	0	0	0	0
141+179	0.61	0.63	1.0	0.55	0.55
137+176+130	0.021	0	0.29	0	0
163+138	0.17	0	1.9	0.28	0.35
158	0.67	0.63	0.88	0.62	0.32
187+182	0.95	2.0	2.3	2.6	0.52
183	0.71	0.51	1.4	0	0.73
185	0.13	0.12	0.27	0	0.14
174	1.1	0.73	1.3	0.73	0.53
177	5.0	2.7	1.0	0.56	0.29
202+171+156	0	0	1.8	0	1.1

180	2.6	2.2	2.9	1.7	0.90
199	0.039	0.046	0.073	0	0
170+190	2.4	3.0	2.9	1.6	0.63
201	1.4	1.2	1.3	0.82	0.64
203+196	1.9	3.1	1.7	2.2	0.74
195+208	1.4	2.6	1.3	2.1	0.76
194	0.89	0.68	1.1	0.61	0.33
206	1.6	1.3	1.8	0.65	0.66

surrogate recoveries *(%)*					
14	46206%	53%	99%	187%	44%
23	100%	77%	70%	74%	48%
65	99%	74%	14%	66%	48%
166	97%	79%	87%	72%	58%

SAF071801CM surr. corrected concentration (pg/m3)	SAF071901AA surr. corrected concentration (pg/m3)	SAF071901AM surr. corrected concentration (pg/m3)	SAF071901BA surr. corrected concentration (pg/m3)	SAF071901BM surr. corrected concentration (pg/m3)	SAF071901CA surr. corrected concentration (pg/m3)	SAF072001AA surr. corrected concentration (pg/m3)
0	0	0	19	35	5.4	12
0	16	18	8.8	13	2.2	3.1
0	8.1	12	6.5	8.0	1.3	1.9
0	21	17	14	18	2.3	3.2
0	46	37	16	40	4.6	2.7
0	33	34	18	28	4.4	4.2
0	29	16	14	22	2.8	2.9
0	0	26	11	43	0.24	0
0	1.5	1.5	1.6	1.9	0.20	0
0	0.94	1.5	0	5.9	0	0
0	13	17	19	16	3.4	3.1
0	10	13	15	11	2.2	2.0
0	9.8	11	14	12	1.2	1.7
1.9	14	15	18	14	3.5	5.3
0	3.8	2.7	6.6	7.1	0.75	2.2
0	13	12	16	17	3.0	5.5
0.21	5.8	7.5	5.9	7.7	1.3	1.5
0.18	2.4	1.1	3.5	2.2	0.63	0.61
0	8.2	7.2	6.7	7.6	1.5	2.3
0	24	16	22	21	5.9	5.0
8.9	31	22	38	26	11	9.1
0	1.9	0.60	3.1	0.71	0.74	0.95
1.0	19	14	19	19	4.9	4.9
1.7	7.1	4.6	10	5.7	3.5	2.6
0.87	7.0	7.7	14	8.5	3.4	2.6
0.27	12	2.5	6.4	3.8	1.4	0.98
0.26	3.7	5.4	6.7	3.2	2.0	1.1
1.7	1.4	5.7	11	0.70	6.0	1.1
3.4	13	16	22	15	6.2	5.1
0	2.0	1.0	2.5	1.3	1.8	0.98
0.27	1.5	1.9	3.1	2.1	0.82	0.78
0.098	1.4	1.0	2.2	1.4	0.82	0.47
2.0	5.8	6.9	11	6.1	3.6	3.1
1.1	9.6	16	12	17	4.0	3.8
0.80	7.8	9.9	7.6	7.1	3.0	2.8
5.0	16	16	32	14	22	9.8
0	0	0	0	0	0	0
0.48	1.8	1.6	2.8	0.65	1.0	1.1
0	1.6	0	0	0	0.40	0
0.042	12	2.4	4.3	0.12	0.75	1.3
0.52	1.8	1.8	2.8	1.4	0.87	0.51
1.5	3.4	6.6	7.2	3.5	2.5	1.8
0.49	1.7	1.5	3.1	1.5	1.1	1.4
0.057	0.57	0.18	0	0.15	0.41	0
0.78	2.0	2.1	3.7	1.3	1.2	1.1
0.65	1.5	2.0	2.5	1.8	0.91	1.2
0	4.1	0.78	0	0.80	1.3	1.7

2.3	6.2	6.2	9.2	3.7	3.5	2.8
0	0.23	0.19	0	0.12	0.13	0
2.1	5.3	5.4	8.2	2.6	3.1	2.5
1.0	3.7	3.7	6.6	3.2	1.7	1.8
2.5	4.1	5.8	7.1	5.0	2.1	2.5
2.0	1.4	3.6	2.1	4.5	2.4	1.0
1.8	1.9	2.8	5.0	2.7	2.9	1.7
0.76	4.5	6.1	15	3.4	1.9	3.1

809%	205%	374%	69%	464%	73%	66%
102%	69%	62%	59%	70%	64%	61%
91%	67%	64%	58%	69%	60%	61%
98%	80%	72%	72%	75%	71%	75%

SAF072001AM surr. corrected concentration (pg/m3)	SAF072001BA surr. corrected concentration (pg/m3)	SAF072001BA surr. corrected concentration (pg/m3)	SAF072001CM surr. corrected concentration (pg/m3)	SAF111202AA surr. corrected concentration (pg/m3)	SAF111202AM surr. corrected concentration (pg/m3)	SAF111202BA surr. corrected concentration (pg/m3)
89	9.6	0	15	0	9.4	31
28	3.7	9.6	4.1	0	3.0	0
14	2.9	5.1	2.1	0	1.7	0
34	5.6	16	5.1	0	5.3	5.3
71	5.8	21	9.7	0	10	0
58	6.6	16	4.7	0	3.5	0
48	5.9	13	8.4	1.2	4.8	4.6
33	2.3	2.3	6.4	6.7	11	2.1
2.7	0.45	1.7	1.1	0	1.7	0.30
1.9	0.88	1.6	0	0	46	0
20	7.8	15	5.2	1.5	11	2.3
17	6.8	8.1	3.5	0.86	2.4	7.1
18	5.7	6.4	2.4	0	6.2	0.83
24	7.6	13	5.1	2.1	18	1.8
7.8	2.1	4.7	1.0	0.30	1.2	0.48
25	8.4	11	5.1	0	10	0
11	2.3	4.7	1.4	0.51	3.0	0.31
5.4	1.2	2.3	0	0.28	0.83	0
13	2.4	4.7	4.7	0.42	34	0.93
35	9.4	19	14	2.1	57	0.64
45	18	37	20	12	1.3	36
2.6	1.3	4.0	1.5	0.043	11	0
30	5.1	16	5.4	2.3	18	0
10	5.1	9.7	2.7	2.8	16	0
9.2	6.4	15	4.1	2.3	0	0
9.2	2.4	16	1.1	1.5	18	0
4.2	2.0	5.9	1.6	0.77	6.2	0.41
3.8	1.9	7.7	0.75	1.7	13	0
17	10	27	8.4	5.7	27	0
3.2	1.6	3.1	0.20	0.17	4.5	0
1.9	1.4	2.9	0.77	0.60	7.8	0
1.8	1.1	2.6	1.1	0.62	22	0
7.0	5.6	11	5.6	4.4	14	1.4
12	6.8	14	11	2.5	0	0
10	4.6	8.3	1.2	10	0	2.1
21	16	31	13	12	68	5.3
0	0	0	0	0	0	0
2.3	1.6	3.3	1.6	1.3	8.1	0.21
0.95	0.47	0	0	0	0	0
14	2.0	2.7	0	0.63	132	0.30
2.2	1.5	2.9	1.4	0.96	8.1	0.61
4.3	3.4	6.9	3.4	4.5	396	3.6
2.5	1.6	2.9	2.6	1.2	56	0.41
0.52	0.30	0.69	2.5	0.049	1.5	0.060
3.0	2.0	3.2	0	1.5	14	0.83
2.1	1.4	2.2	1.7	1.6	0	1.9
5.5	2.0	5.3	0.92	0	11	0.30

8.2	5.8	8.3	7.4	3.9	40	3.0
0.20	0.14	0.30	0	0.041	0.60	0.037
7.0	4.7	6.1	5.0	2.5	33	1.1
4.5	3.5	5.9	4.0	2.0	20	2.5
5.4	3.9	5.9	4.8	5.1	19	5.5
1.9	4.3	1.7	1.5	2.8	12	3.0
2.3	1.8	2.7	1.6	0.87	9.1	1.7
4.2	6.0	13	3.0	0.83	9.5	0.71

840%	139%	403%	18%	62%	87%	49%
78%	80%	69%	81%	88%	65%	91%
77%	78%	67%	75%	74%	61%	79%
95%	96%	79%	104%	81%	61%	94%

SAF111202BM surr. corrected concentration (pg/m3)	SAF111202CA surr. corrected concentration (pg/m3)	SAF111202CM surr. corrected concentration (pg/m3)	SAF111302AM surr. corrected concentration (pg/m3)	SAF111302BA surr. corrected concentration (pg/m3)	SAF111302BM surr. corrected concentration (pg/m3)	SAF111302CA surr. corrected concentration (pg/m3)
12	11	5.7	7.1	17	7.1	8.5
1.7	0	2.4	2.7	0	0	3.8
0.56	0	0.89	1.2	0	0	1.2
1.4	0	0.81	0.22	0	0.69	0.54
3.6	0	2.7	0	0	0	6.4
0	0	1.6	0	0	0	0.64
0	0	1.3	0	0	0	0.70
7.8	0	0	0	0	0	0.87
0.098	0	0	0	0	0	0.19
0.38	0	0	0	0.58	0	0.41
2.9	0	1.2	0.53	1.0	3.5	0.85
2.4	0	3.0	1.1	0.76	1.3	0.72
0.083	0	4.4	5.0	0	11	0.45
3.5	6.7	9.8	3.0	3.0	2.8	3.3
0.51	0	0.30	0.38	0.79	1.2	0.51
0	0	3.2	1.5	1.2	2.4	2.3
1.4	0	0.64	0.44	0.43	0.57	0.41
0.38	0	0.61	0	0.36	3.5	0.34
1.5	6.7	0	1.6	2.6	2.1	2.8
4.9	14	3.9	1.9	3.0	4.1	12
17	15	8.1	2.3	4.0	5.5	3.3
0.10	1.3	0.62	0	0.44	0	0.18
3.8	5.5	6.4	1.4	1.6	2.3	1.6
2.3	2.5	3.9	1.9	2.0	2.2	1.7
2.4	2.3	2.5	1.0	1.0	1.1	1.0
0.47	0.93	12	4.1	1.3	2.1	2.6
0.94	1.0	1.6	0.45	1.1	0.72	0.64
0.93	0	0	0.76	2.8	0.80	1.5
7.1	5.1	6.3	1.4	2.0	1.4	1.9
0.50	0	0.95	0.17	0.38	0	0.27
0.95	0.45	1.8	0.29	0.43	0	0.35
0.83	0	5.1	0.48	0.23	0	0.25
3.9	2.9	0	1.0	1.1	1.1	0.99
6.5	13	4.4	1.2	0.91	0.87	1.2
8.0	8.1	0	4.1	3.1	3.5	1.6
11	6.2	6.0	3.0	3.1	4.1	3.5
0	0	0	0	0	0	0
1.2	0.78	1.1	0.42	0.44	0.38	0.32
0	0	0	0	0	0	0
0.12	0.64	1.6	0.33	1.0	0.87	0.20
1.1	0.77	1.2	0.24	0.24	0.22	0.22
4.0	5.6	103	1.4	0.88	1.1	1.9
0.98	0	0	0.36	0.46	0.30	0.34
0.11	0	0	0	0	0	0
1.5	1.3	1.6	0.47	0.39	0.50	0.46
2.4	2.3	0	0.49	0.54	0.37	0.34
0.66	4.6	0	0.36	0.74	2.6	0.52

4.5	2.9	4.5	0.89	0.90	0.66	0.87
0.11	0	0	0	0.065	0	0
3.6	2.5	3.4	0.49	0.61	0.74	1.1
3.6	2.0	5.0	0.50	0.87	0.79	0.61
5.9	2.1	3.2	0.81	0.64	0.83	0.75
2.9	0	0	0.26	0.19	2.3	0.33
1.6	0.57	5.2	0.20	0.47	1.1	0.64
1.4	1.7	3.3	0.23	0.46	0.51	0.29

51%	60%	69%	75%	73%	74%	78%
87%	66%	63%	77%	74%	76%	71%
82%	67%	57%	75%	66%	74%	64%
88%	74%	57%	95%	72%	98%	76%

SAF111302CM surr. corrected concentration (pg/m3)	SAF111402AA surr. corrected concentration (pg/m3)	SAF111402AM surr. corrected concentration (pg/m3)	SAF111402BA surr. corrected concentration (pg/m3)	SAF111402BM surr. corrected concentration (pg/m3)	SAF111402CA surr. corrected concentration (pg/m3)	SAF111402CM surr. corrected concentration (pg/m3)
16	0.015	26	25	67	17	47
0	0	3.5	6.5	2.0	8.0	1.2
0	0	0.45	0.35	4.5	4.0	2.6
1.2	0.00070	2.0	4.0	7.8	0.82	6.0
0	0.0018	1.5	1.9	4.2	0	0
0	0.0011	0.56	0	0	0	0
1.3	0.00089	0	0	0.95	0.85	0
0	0.0024	0.54	0	16	0	11
0	0.000045	0	0	1.2	0	0
0	0	0	0	0.62	0	0
1.3	0.0012	0.55	1.6	3.2	1.4	2.7
0.61	0.00039	0.60	0.92	3.1	0.46	0
1.3	0.0013	0	0.82	0	0.49	0
2.5	0.0010	1.1	2.1	5.7	1.4	0
0.52	0.00031	0.26	0.94	0.91	0.47	0
3.1	0	2.8	2.2	1.4	0.95	0
0.42	0.00024	0.29	0.54	0.37	0.39	0
0	0	0	0.32	0.23	0.27	0
0	0.00034	0.54	1.1	3.8	0.73	0
0	0.0063	0.75	2.9	13	1.5	0
6.9	0.0029	1.6	4.2	12	3.5	6.3
0	0	0	0.57	0.39	0.23	0
0.85	0.00032	0.58	1.9	2.6	0.98	1.4
0.98	0.0016	1.2	2.5	1.8	1.4	1.7
1.0	0.00085	0.58	1.6	2.1	0.88	1.1
0.38	0.00091	0.35	0.52	1.0	0.43	0
0.41	0.00030	0.60	0.68	1.4	1.1	0
0	0.00017	0.19	0.61	0.38	1.2	0
1.3	0.0023	1.6	2.9	5.4	1.8	1.6
0.14	0	0.20	0.46	0.33	0.32	0
0.31	0.00020	0.32	0.54	0.98	0.38	0
0.36	0.00019	0	0.36	0	0.29	1.2
1.2	0.0012	1.2	2.0	3.4	1.4	0
0	0.0011	1.2	1.5	6.6	1.1	0
0.29	0.0028	0	2.2	1.8	1.6	0
4.3	0.0046	3.6	5.5	8.7	4.3	5.7
0	0	0	0	0	0	0
0.71	0.00049	0.37	0.53	1.1	0.41	0
0	0	0	0	0.16	0.16	0
0	0.00011	0.33	0.46	0	0.23	0
0.37	0.00043	0.32	0.41	0.76	0.28	0.43
0.26	0.0015	0.93	0.93	0.63	1.5	0.65
0.47	0.00035	0.59	0.67	0.97	0.45	0.59
0	0.000057	0.11	0.089	0.18	0.079	0
0.57	0.00083	0.34	0.60	0	0.58	0.97
0.47	0.00092	0.054	0.51	1.0	0.47	1.4
0.36	0.00020	0.54	0.61	0.65	0.54	0

1.4	0.0016	1.7	1.4	2.9	1.2	1.9
0	0.000022	0	0	0.11	0	0
0.27	0.0014	1.1	1.1	0	1.1	0.48
0.57	0.00086	0.96	0.75	1.2	0.76	1.4
0.97	0.0018	1.2	1.2	1.6	1.1	1.8
0	0.0019	0.34	0.39	0.54	1.0	0.16
0.65	0.00049	1.6	1.2	0.43	0.52	0.33
0	0.00077	0.41	0	0.41	0.49	0.97

48%	4747%	105%	82%	41%	73%	16%
74%	91%	78%	73%	80%	78%	59%
77%	85%	66%	67%	72%	74%	62%
94%	91%	81%	79%	92%	78%	73%

SAF050702AM surr. corrected concentration (pg/m3)	SAF050702BA surr. corrected concentration (pg/m3)	SAF050702BM surr. corrected concentration (pg/m3)	SAF050702CA surr. corrected concentration (pg/m3)	SAF050702CM surr. corrected concentration (pg/m3)	SAF050802AA surr. corrected concentration (pg/m3)	SAF050802AM surr. corrected concentration (pg/m3)
14	3.6	6.8	12	14	11	9.2
4.1	1.1	4.7	0.74	0	2.8	3.6
3.1	0.63	0	0.43	0	1.4	2.3
2.1	1.2	4.0	0.37	5.3	1.8	4.2
9.0	3.2	7.6	0	0	8.4	8.3
5.6	0	6.7	0	0	8.5	9.5
0	1.0	2.5	0	0.92	2.5	2.5
5.7	4.9	9.7	0	3.1	0	1.7
0.92	0.14	0.36	0	0	0	0.17
0	0.41	0.36	0.46	0.24	0.081	0.60
3.2	2.6	5.9	0.63	0.82	6.6	4.9
1.1	0.98	3.2	0.39	0.21	4.5	3.8
2.2	1.8	2.9	1.8	0.50	13	2.9
4.0	3.1	5.7	6.0	2.0	7.5	6.1
0.60	0.55	1.1	1.4	0.19	1.0	1.7
4.0	1.6	5.6	2.2	0	7.3	5.0
1.0	0.77	1.8	0.50	0.20	2.8	2.2
0.47	0.43	0.61	0.38	0.15	0.68	1.2
0.67	3.2	6.4	1.5	0	4.2	3.3
6.3	4.4	14	1.3	0	11	9.5
9.3	9.6	28	4.6	7.7	15	16
0.48	0.54	1.5	0	0	2.7	1.3
5.0	3.3	9.1	1.9	0.92	11	8.5
2.2	1.9	4.2	1.5	0.91	7.3	5.3
2.4	2.5	5.4	1.2	0.74	6.8	4.8
1.4	0.56	2.1	0.44	0.16	9.0	2.1
0.91	1.0	2.1	2.9	0.53	4.8	2.4
0.34	0.40	0.73	4.9	0.48	1.6	9.3
4.8	5.4	12	2.0	1.9	14	8.9
0.57	0.52	0.97	0.50	0	0.75	1.2
1.1	1.5	2.2	1.0	0.37	1.6	1.3
0.60	1.3	1.9	0.46	0.25	0.19	1.0
3.4	5.4	8.3	2.1	1.4	4.8	5.2
5.3	4.9	14	1.1	0.91	6.0	5.3
1.2	2.2	4.9	1.1	0.68	7.2	3.8
9.4	13	20	10	3.8	14	15
0	0	0	0	0	0	0
1.3	1.8	3.2	0.60	0.45	1.5	1.5
0	0.22	0.14	0	0	0.092	0
0	0	0.033	0.28	0.020	3.9	0.44
0.81	1.2	2.0	0.40	0.29	1.3	1.2
1.3	4.2	4.9	3.5	1.7	8.2	4.0
1.2	2.1	3.1	0.54	0.25	1.7	1.7
0.28	0.46	0.83	0	0	0.28	0.25
1.8	2.9	3.8	0.87	0.61	2.3	2.0
1.2	1.8	2.4	1.7	2.1	2.1	1.3
0.87	1.4	2.1	0	0	0.41	2.6

5.2	7.5	10	2.0	1.7	6.4	4.7
0.11	0.19	0.25	0	0	0.096	0.21
3.4	5.0	7.1	2.9	1.6	5.6	3.8
2.8	5.9	7.6	1.5	1.1	3.5	2.9
3.4	5.7	7.7	2.0	2.7	4.4	3.2
1.1	1.4	2.0	0.78	1.9	4.0	0.99
1.3	1.9	2.8	0.92	1.4	2.3	1.2
2.4	17	22	0.87	1.0	4.5	2.7

25%	24%	49%	50%	0%	0%	51%
86%	72%	91%	55%	103%	51%	55%
81%	73%	83%	53%	85%	53%	52%
104%	100%	112%	50%	95%	89%	67%

SAF050802BA surr. corrected concentration (pg/m3)	SAF050802BM surr. corrected concentration (pg/m3)	SAF050802CM surr. corrected concentration (pg/m3)	SAF050902AA surr. corrected concentration (pg/m3)	SAF050902AM surr. corrected concentration (pg/m3)	SAF050902CA surr. corrected concentration (pg/m3)	SAF050902CM surr. corrected concentration (pg/m3)
	12	21	2.6	6.9	9.3	3.8
	2.3	0	0.61	0	0	0
	1.2	0	0.52	0	0	0
	2.1	6.4	0	1.7	0.17	0.42
	6.6	0	0	0	0	0
	4.0	0	0	0	0	0
	1.0	3.4	0	0.95	0	0
	7.1	4.1	0	2.2	1.0	0
	0.78	0.44	0	0	0	0
	0	0	0	0	0	0
	2.4	1.9	1.6	0.53	0.26	0.93
	1.2	0.27	0.87	0.42	0.10	0.70
	5.6	0	16	0	0	2.0
	8.4	2.0	0	1.5	0.52	2.3
	0.98	0.25	0	0.19	0.12	0
	2.8	0	0	0	0	0
	0.62	0.21	0	0.20	0.14	0.83
	0.67	0.18	0	0	0	0
	7.1	0.48	4.3	0	0	0
	10	0.40	5.9	0	0.17	0.83
	12	5.5	11	8.7	4.1	3.6
	1.2	0	0	0	0	0
	6.4	1.0	5.6	0.71	0.13	1.3
	2.3	1.5	3.8	1.1	0.52	1.2
	2.7	0.97	4.0	1.2	0.42	1.1
	1.4	0.45	11	1.2	0.11	0.75
	1.7	0.49	2.5	0.47	0.36	0.47
	1.1	0.29	0	0.28	0.088	0.44
	7.1	2.3	12	3.0	1.6	2.3
	0.72	0.46	1.6	0	0.11	0.40
	1.0	0	1.5	0.20	0.26	0.54
	0	0.13	1.2	0	0.11	0.22
	3.2	1.4	3.9	1.5	0	1.3
	11	1.1	20	2.3	0	0.93
	2.0	0.45	12	8.7	1.5	2.6
	10	3.8	17	4.7	2.9	4.5
	0	0	0	0	0	0
	1.3	0	1.6	0.54	0.14	0
	0	0	0	0	0	0
	1.0	0.097	3.9	0.045	0.017	0.53
	1.3	0.46	2.3	0.49	0.27	0.37
	0	1.5	2.0	2.0	1.7	0.90
	0	0.49	1.1	0.28	0.14	0.11
	0	0	0.19	0	0	0.086
	1.7	0.58	1.6	0.38	0.27	0
	2.8	0.92	1.3	1.3	1.1	0.32
	4.6	0	0.78	0.14	0.12	0

4.4	1.7	4.4	1.1	0.73	1.4
0	0.39	0	0	0	0
3.8	1.3	4.4	0.50	0.60	1.0
3.2	1.2	1.5	0.50	0.31	0.56
3.6	2.6	1.6	2.2	1.8	0.60
2.3	1.7	1.6	1.6	1.4	0.17
0.94	0.75	2.3	0.33	0.41	8.3
4.4	1.1	1.5	0.12	0.089	0.070

62%	55%	79%	43%	0%	54%
74%	93%	71%	80%	63%	70%
71%	81%	75%	75%	74%	65%
71%	101%	88%	84%	96%	76%

SAF051002BA surr. corrected concentration (pg/m3)	SAF051002BM surr. corrected concentration (pg/m3)	SAF051002CA surr. corrected concentration (pg/m3)	SAF051002CM surr. corrected concentration (pg/m3)
4.6	5.7	0	3.1
0	0	0	0
0	0	0	0
0.79	1.1	0.83	0.42
0	1.7	2.5	0.93
0	0.44	0	0.13
0	1.3	0.076	0.25
0	4.1	3.1	2.6
0	0.18	0	0.073
0	0.28	0	0
0.81	1.6	0.67	0.23
0.32	0.35	0.22	0
0.68	0.47	0.26	0
2.7	2.3	3.5	0.67
0.48	0.72	0.20	0.18
1.4	0	0	0
0.36	0.18	0.11	0.11
0	0.11	0	0
0	0	0.50	0
0.70	0	1.8	0
16	11	6.8	4.5
0.087	0	0	0
0.95	1.3	0.64	0.65
0.92	0.96	0.63	0.81
1.2	0.90	0.49	0.47
0.38	0.32	0.35	0.11
0.31	0.67	0.27	0.42
0.24	0.61	0.23	0.44
2.2	2.8	1.5	1.6
0	0.17	0.10	0.12
0.23	0.40	0.25	0.29
0.30	0.37	0.18	0.26
1.9	1.6	0.93	0.90
1.1	1.5	0.66	0.88
1.0	1.0	0.36	1.0
4.9	4.3	2.9	2.5
0	0	0	0
0.56	0.49	0.29	0.23
0	0	0.039	0
0	0	0.052	0.025
0.44	0.37	0.20	0.23
2.6	1.8	1.8	1.6
0.61	0.37	0.31	0.19
0.095	0.077	0.054	0
0.76	0.65	0.49	0.26
1.2	2.1	1.3	1.3
0.51	0.32	0	0.066

2.1	1.7	1.0	0.71
0.068	0.044	0	0.035
1.5	1.3	0.91	0.74
1.6	1.0	0.49	0.39
3.3	2.9	1.9	1.6
3.3	2.5	1.6	1.6
0.78	0.81	0.72	0.92
4.0	2.0	0.34	0

48%	18%	58%	22%
72%	90%	81%	76%
75%	77%	80%	78%
89%	83%	87%	84%

	LAB BLANK	LAB BLANK	LAB BLANK	LAB BLANK	LAB BLANK	LAB BLANK
	LBF071604F1	LBF010405F1	LBF010605F1	LB033005	LB042105	LB042905
PCB	surr. corrected mass (pg)	surr. corrected mass (pg)	surr. corrected mass (pg)	surr. corrected mass (pg)	surr. corrected mass (pg)	surr. corrected mass (pg)
8+5	0	0	0	264	0	0
18	0	0	0	0	0	0
17+15	0	0	0	0	0	0
16+32	0	0	0	0	0	0
31	0	0	0	0	0	0
28	0	0	0	0	0	0
21+33+53	0	0	0	0	0	0
22	0	0	0	0	0	0
45	0	0	0	0	0	0
46	0	0	0	0	0	0
52+43	0	0	0	0	0	0
49	0	0	0	0	0	0
47+48	0	0	0	5800	0	0
44	0	0	0	0	0	0
37+42	0	0	0	0	0	0
41+71	0	0	0	0	0	0
64	0	0	0	0	0	0
40	0	0	0	0	0	0
74	0	0	0	0	0	0
70+76	0	0	0	0	0	0
66+95	0	0	0	0	0	0
91	0	0	0	0	0	0
56+60+89	0	0	0	0	0	0
92+84	0	0	0	0	0	0
101	0	0	0	0	0	0
99	0	0	0	0	0	0
87+81	0	0	0	0	0	0
85+136	0	0	0	0	0	0
110+77	0	0	0	0	0	0
82	0	0	0	0	0	0
151	0	0	0	0	0	0
135+144+147+124	0	0	0	0	0	0
149+123+107	0	0	0	0	0	0
118	0	0	0	0	0	0
146	0	0	0	0	0	0
153+132	0	0	0	0	0	0
105	0	0	0	0	0	0
141+179	0	0	0	0	0	0
137+176+130	0	0	0	0	0	0
163+138	0	0	0	0	0	0
158	0	0	0	0	0	0
187+182	0	0	0	0	0	0
183	0	0	0	0	0	0
185	0	0	0	0	0	0
174	0	0	0	0	0	0
177	0	0	0	0	0	0
202+171+156	0	0	0	0	0	0
180	0	0	0	0	0	0
199	0	0	0	0	0	0
170+190	0	0	0	0	0	0
201	0	0	0	0	0	0
203+196	0	0	0	0	0	0
195+208	0	0	0	0	0	0
194	0	0	0	0	0	0
206	0	0	0	0	0	0

surrogate recoveries (%)						
14	58%	56%	0%	80%	0%	0%
23	58%	65%	37%	60%	63%	66%
65	65%	68%	49%	67%	78%	79%
166	71%	76%	60%	62%	76%	91%

LAB BLANK	LAB BLANK	LAB BLANK	LAB BLANK	FIELD BLANK	FIELD BLANK
LB051805	LB052305	LB052505	LB052805	BAF071801FB	BAF050602FBF1
surr. corrected mass (pg)	surr. corrected mass (pg)	surr. corrected mass (pg)	surr. corrected mass (pg)	surr. corrected mass (pg)	surr. corrected mass (pg)
0	0	0	0	0	0
0	0	0	0	0	109
0	0	0	0	0	57
0	0	0	0	0	0
0	0	0	0	0	0
0	0	0	0	0	0
0	0	0	0	0	0
0	0	0	0	0	0
0	0	0	0	0	0
0	0	0	0	0	0
0	0	0	0	0	153
0	0	0	0	0	0
0	0	0	0	0	92
0	0	0	0	0	467
0	0	0	0	0	185
0	0	0	0	0	0
0	0	0	0	0	0
0	0	0	0	0	0
0	0	0	0	0	561
0	0	0	0	0	0
1186	1301	877	838	798	271
0	0	0	0	0	0
0	0	0	0	0	0
0	0	0	0	0	0
0	0	0	0	0	0
0	0	0	0	0	0
0	0	0	0	0	0
0	0	0	0	0	0
0	0	0	0	0	0
0	0	0	0	0	0
0	0	0	0	0	0
0	0	0	0	0	0
0	0	0	0	0	0
0	0	0	0	0	0
0	0	0	0	0	0
0	0	0	0	0	0
0	0	0	0	0	0
0	0	0	0	0	0
0	0	0	0	0	0
0	0	0	0	0	0
0	0	0	0	0	0
0	629	0	478	0	0
0	0	0	0	0	0
0	0	0	0	0	0
0	0	0	0	0	0
225	229	163	192	0	199
0	0	0	0	0	0
0	0	0	0	0	0
0	0	0	0	0	0
0	0	0	0	0	0
0	0	0	0	0	0
429	447	316	315	0	346
334	340	243	262	0	263
0	0	0	0	0	0
0	0	0	0	0	0

0%	0%	0%	0%	64%	0%
47%	49%	80%	80%	68%	90%
64%	79%	100%	93%	65%	72%
72%	72%	92%	83%	76%	87%

FIELD BLANK	FIELD BLANK	FIELD BLANK	FIELD BLANK	FIELD BLANK	FIELD BLANK	FIELD BLANK
BAF050802FB	BAF050902FB	BAF111202FB	BAF111302FB	BAF111402FBF1	SAF050602FBF1	SAF050802FB
surr. corrected mass (pg)	surr. corrected mass (pg)	surr. corrected mass (pg)	surr. corrected mass (pg)	surr. corrected mass (pg)	surr. corrected mass (pg)	surr. corrected mass (pg)
0	647	0	425	0	0	0
0	0	0	0	0	0	0
0	0	0	0	0	0	0
0	0	0	0	0	0	0
0	0	0	0	0	0	1020
0	0	0	0	0	0	283
0	0	0	0	0	0	1276
0	0	0	0	0	0	0
0	0	0	0	0	0	0
0	0	0	0	0	0	0
0	0	0	0	0	0	0
0	0	0	0	0	0	0
0	2913	0	0	0	0	0
0	1314	0	0	0	0	153
0	0	0	0	0	0	0
0	0	0	0	0	0	0
0	0	0	0	0	0	0
0	0	0	0	0	0	0
0	0	0	0	0	0	0
0	0	0	0	0	0	0
0	0	736	0	0	0	0
0	0	0	0	0	0	0
0	0	0	0	0	0	0
0	0	0	0	0	0	0
0	0	0	0	0	0	0
0	0	0	0	0	0	0
0	0	0	0	0	0	0
0	0	0	0	0	0	0
0	0	0	0	0	0	0
0	0	0	0	0	0	0
0	0	0	0	0	0	0
0	0	0	0	0	0	0
0	0	0	0	0	0	0
0	0	0	0	0	0	0
0	0	0	0	0	0	0
0	0	0	0	0	0	0
0	0	0	0	0	0	0
0	0	0	0	0	0	0
0	0	0	0	0	0	0
0	0	0	0	0	0	0
4673	485	0	0	0	2756	0
0	0	0	0	0	0	0
0	0	0	0	0	0	0
0	0	0	0	0	0	0
0	219	0	0	0	0	0
0	0	0	0	0	0	0
0	0	0	0	0	0	0
0	0	0	0	0	0	0
0	0	0	0	0	0	0
0	0	0	0	0	0	0
0	409	0	0	0	0	0
0	299	0	0	0	0	0
0	0	0	0	0	0	0
0	0	0	0	0	0	0

59%	0%	0%	0%	55%	73%	51%
55%	71%	64%	58%	67%	60%	67%
58%	75%	60%	62%	66%	62%	70%
1511%	76%	75%	74%	85%	151%	75%

FIELD BLANK	FIELD BLANK	FIELD BLANK	FIELD BLANK	MATRIX SPIKE	MATRIX SPIKE
SAF050902FB	SAF051002FB	SAF111202FB	SAF111402FB	MSF071604F1	MSF010605F1
surr. corrected mass (pg)	surr. corrected mass (pg)	surr. corrected mass (pg)	surr. corrected mass (pg)	surr. corrected mass (pg)	surr. corrected mass (pg)
392	0	4635	0	5739	4244
0	0	0	0	1462	1404
0	0	0	0	890	826
0	0	0	0	1402	1405
0	0	0	0	2041	1263
0	0	0	0	1992	2016
0	0	0	0	2046	1528
0	0	0	0	1295	622
0	0	513	0	314	200
0	0	0	0	182	199
0	0	0	0	1471	1591
0	0	0	0	1026	1040
8280	0	0	0	969	934
0	0	288	0	2021	1820
0	0	0	0	752	674
0	0	0	0	1792	1095
0	0	0	0	963	777
0	0	0	0	493	315
0	0	0	0	1154	582
0	0	0	0	2740	1450
0	0	0	7280	3328	1934
0	0	0	0	185	156
0	0	0	0	2234	1640
0	0	0	0	581	775
0	0	0	0	574	629
0	0	0	0	349	256
0	0	0	0	326	176
0	0	0	0	594	760
0	0	0	0	964	771
0	0	0	0	223	146
0	0	0	0	772	662
0	0	0	0	370	273
0	0	0	0	1660	1480
0	0	0	0	369	412
0	0	0	0	223	135
0	0	0	0	3096	3000
0	0	0	0	0	0
0	0	0	0	791	620
0	0	0	0	322	318
0	0	0	0	618	408
0	0	0	0	156	130
0	0	0	0	2315	2025
0	0	0	0	1160	937
0	0	0	0	249	308
206	0	0	0	1662	1387
0	0	0	0	921	692
0	0	0	0	497	441
0	0	0	0	3536	2493
0	0	0	0	148	114
0	0	0	0	1819	1328
0	0	0	0	2317	1770
378	0	0	0	2659	2002
302	0	0	0	1261	931
199	0	0	0	1078	874
0	323	0	0	924	626

0%	0%	8%	8%		104%	1743%
70%	70%	82%	82%		67%	61%
79%	68%	71%	71%		72%	75%
80%	84%	86%	86%		57%	79%

MATRIX SPIKE	MATRIX SPIKE	MATRIX SPIKE	MATRIX SPIKE	MATRIX SPIKE
MS030305	MS042105	MS042905	MS052305	MS052805
surr. corrected mass (pg)	surr. corrected mass (pg)	surr. corrected mass (pg)	surr. corrected mass (pg)	surr. corrected mass (pg)
6936	0	6489	0	0
1902	2098	2458	1886	2084
1010	1168	1382	1090	1093
1691	1885	2404	2348	2418
3580	1348	0	16828	0
2374	0	0	0	2980
3012	0	497	2183	1392
2283	0	0	1674	0
370	302	341	260	251
2406	236	204	0	0
2423	2515	2361	2282	2154
1252	1719	1607	1516	1582
3500	1747	1619	1610	1606
2816	2878	2797	2577	2476
615	696	664	676	563
2117	1675	1893	0	0
1025	1189	1233	1313	1451
502	405	594	0	485
6542	1565	1381	1852	0
4783	2452	3447	5312	2395
4630	3064	5152	13495	3995
0	243	318	0	0
3483	1916	1830	3332	5110
707	755	954	628	0
759	869	771	857	870
205	334	403	475	0
629	189	247	445	467
1996	154	352	566	557
1541	1137	1179	1384	1277
43	254	205	259	0
146	1077	1095	1089	1157
322	434	477	504	446
0	2387	2214	2243	2111
93	452	0	516	0
0	216	432	131	153
526	3992	4050	3966	3930
0	0	0	0	0
145	1126	0	1094	987
0	347	378	290	0
62	0	15	0	181
32	220	209	237	224
5732	2888	2741	2595	2429
1225	1707	1588	1646	1552
44	493	383	391	426
294	2405	2232	2151	2078
216	1182	1117	1145	1124
136	804	751	602	679
667	5018	4474	4929	4309
26	220	203	197	189
341	2140	2024	2348	2289
433	3216	2825	3044	2820
498	3442	3070	3430	3231
240	1580	1441	1573	1577
209	1226	1104	1476	1320
148	955	646	961	834

64%	0%	0%	0%	0%
66%	51%	63%	77%	73%
72%	68%	73%	90%	80%
438%	81%	91%	85%	81%

Mercury Emissions from Cement-Stabilized Dredged Material

SANDRA M. GOODROW,[†]
ROBERT MISKEWITZ,[‡]
RICHARD I. HIRES,[‡]
STEVEN J. EISENREICH,[†,§]
W. SCOTT DOUGLAS,[||] AND
JOHN R. REINFELDER*,[†]

Department of Environmental Sciences, Rutgers University, 14 College Farm Road, New Brunswick, New Jersey 08901, Center for Environmental Systems, Stevens Institute of Technology, Castle Point on Hudson, Hoboken, New Jersey 07030, Institute for Environment and Sustainability, European Commission, Joint Research Centre, TP 290, Ispra, Italy 21020, and Office of Maritime Resources, New Jersey Department of Transportation, 1035 Parkway Avenue, Ewing, New Jersey 08628

Upland placement of dredged materials from navigation channels in the New York/New Jersey Harbor is currently being used to manage sediments deemed inappropriate for open water disposal. Although upland placement sites are equipped with engineering controls (leachate collection and/or barrier walls), little is known of the potential impacts of this approach to air quality. The aim of this study was to estimate the flux of mercury to the atmosphere from New York/New Jersey Harbor stabilized dredged material (SDM) that was used for land reclamation at a site in northeastern New Jersey. Total gaseous mercury (TGM) was measured at a site receiving SDM in August and October 2001 and May and November 2002. TGM was also monitored at an urban reference site 3.5 km west of the SDM site in September 2001 and from February 2002 to July 2002 and from October 2002 to February 2003. The concentration of TGM at the urban reference site averaged 2.2 ± 1.1 ng m^{-3}, indicating some local contribution to the Northern Hemisphere background. TGM concentrations exhibited seasonality with the highest values in summer (3.3 ± 2.1 ng m^{-3} in June 2002) and the lowest in winter (1.7 ± 0.6 ng m^{-3} in January 2003). TGM concentrations at the SDM placement site ranged from 2 to 7 ng m^{-3} and were significantly higher ($p < 0.001$) than those at the urban reference site. Sediment−air fluxes of Hg at the SDM placement site estimated by the micrometeorological technique ranged from −13 to 1040 ng m^{-2} h^{-1} (sediment to air fluxes being positive) and were significantly correlated to solar radiation ($r^2 = 0.81$). The estimated contribution of Hg emissions from land-applied SDM to local TGM concentrations was found to be negligible (<4%). However, the estimated annual volatilization rate of TGM at the SDM site (130 kg y^{-1}) was comparable to those of other industrial sources in New Jersey (140−450 kg y^{-1}).

* Corresponding author phone: (732) 932-8013; fax: (732) 932-8644; e-mail: reinfelder@envsci.rutgers.edu.
[†] Rutgers University.
[‡] Stevens Institute of Technology.
[§] European Commission.
[||] New Jersey Department of Transportation.

Introduction

In the New York/New Jersey Harbor, maintenance dredging produces an annual volume of about 3×10^6 m^3 of dredged material and the annual maintenance dredging of all ports in the United States yields over 3×10^8 m^3 of dredged material (*1*). Sediment dredged from navigation channels of urban/industrial harbors is often contaminated with various chemicals that may be released to the atmosphere and surface waters following disposal or beneficial use on land or in coastal waters. The prohibition against ocean disposal of contaminated dredged material has led to the development of alternatives including the stabilization of dredged materials with cement or lime for use as fill or capping material at construction sites, remediation sites, or abandoned coal mines. The cost of this alternative ranges widely from $30 to $90 per cubic yard (approximately 5−20 times higher than open water disposal), depending on the method of stabilization, size of the dredging job, and placement site location (*1*).

As regulations on open water disposal of dredged sediments become increasingly more stringent, upland management is viewed as a favorable alternative, but the processing and placement of dredged material may lead to the release of volatile contaminants, including Hg, to the atmosphere. Since the stabilization process generates heat and exposes sediments to light, it could enhance the photoreduction and volatility of mercury. In regions such as the greater New York metropolitan region that already experience significant Hg contamination, any increase in either ambient air concentration or overall Hg loading is a serious concern for regulatory agencies.

Land−atmosphere exchange of mercury has been measured over a variety of uncontaminated (*2*−*5*), naturally enriched (*6*, *7*), and contaminated (*7*−*10*) soils and wetlands (*11*−*14*), but not from land-applied stabilized dredged material (SDM). Thus, the goal of this study was to estimate the land-atmosphere fluxes of mercury from land-applied SDM at a typical placement site in the New York/New Jersey Harbor estuary.

Experimental Section

Emissions of total gaseous mercury (TGM) from SDM were measured at a 50 ha site (Figure 1) on the eastern side of Bayonne, NJ, adjacent to the Hudson River estuary (40° 39.77′ N, 74° 5.65′ W), where dredged materials were stabilized with Portland cement and spread across the land surface as part of an overall remediation strategy for an abandoned industrial site (35 ha) that adjoins a former municipal landfill (15 ha). Prior to the beginning of SDM application at this site, all buildings were removed and approximately 1−3 m of capping material (construction debris, crushed glass, and soil) were applied to the land, resulting in a barren, low-lying (4−8 m above sea level) landscape. As dredged sediments became available, they were brought to the site by barge and mixed with portland cement (8% by wet weight) in two on-site pug mills to produce SDM. Since dredged material was not continuously available, 2 million cubic yards of SDM was applied to the site intermittently from July 2001 to July 2003, during which time less than 20% of the site area was covered with SDM at any given time. Capping material was applied to different areas of the site continuously during this entire period, but not to SDM areas of the site during Hg emissions measurements.

Freshly mixed SDM, which had the consistency of a heavy ooze, was distributed to different areas of the site by dump

10.1021/es050506n CCC: $30.25
Published on Web 00/00/0000

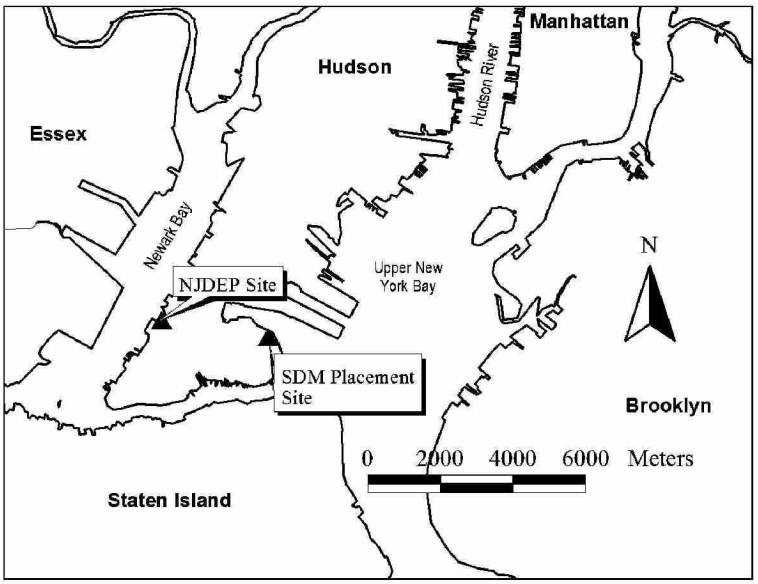

FIGURE 1. Map of the New York/New Jersey harbor estuary showing the locations of the stabilized dredged material (SDM) placement site and the urban reference total gaseous mercury monitoring (NJDEP) site in Bayonne, NJ.

TABLE 1. Site Conditions at the SDM Land Application Site in Bayonne, NJ, during Sampling Events[a]

date	local time	wind speed ($m\ s^{-1}$)	air temp (°C)	RH (%)	PAR ($\mu mol\ m^{-2}\ s^{-1}$)	SDM temp (°C)
8/30/01	13:10−14:36	3.6	25	42	1239	ND
10/23/01	11:00−12:00	3.9	19	65	836	ND
10/24/01	12:35−15:55	2.6	29	42	840	ND
10/25/01	10:50−12:45	7.4	26	48	988	ND
	13:25−15:20	7.6	26	40	884	ND
5/07/02	10:45−12:00	1.9	21	59	2314	19.7
	12:05−14:55	3.6	24	52	1744	23.3
	20:30−23:05	1.3	24	58	0	20.6
5/08/02	9:55−12:10	4.6	20	45	2619	19.3
	13:30−16:00	5.1	19	59	1788	23.4
11/14/02	10:00−11:50	3.8	11	69	465	ND
	12:10−16:35	3.1	13	50	469	ND
11/15/02	9:20−11:50	3.8	13	65	305	ND
	12:10−14:00	3.8	15	45	704	ND

[a] RH, relative humidity; PAR, photosynthetically active radiation; ND, not determined.

trucks. SDM was deposited into 2-m-deep prepared depressions of approximately 1−2 ha in area. Field sampling was coordinated to occur shortly after (1−2 d) the filling of a reasonably large depression with SDM and when safe access to a location with a more than 100 m fetch over SDM was possible. Sampling events were undertaken on August 30, 2001; October 23−25, 2001; May 7−8 2002; and November 14−15, 2002 (Table 1). In October 2001, May 2002, and November 2002, SDM had been produced and applied to the land 1−2 d prior to TGM measurements. In August 2001, SDM had been produced 3 weeks before field measurements, but was dug up and spread out over the 2 days prior to sampling. New York/New Jersey Harbor sediments used for land application at the Bayonne SDM site contained 8% organic matter and were composed of 66% silt, 14% clay, and 16% sand-sized particles (*15*). The Hg content of these sediments varied from 1.3 to 2.6 ppm (*16*). The Hg content of portland cement is typically (more than 75% of samples measured) below detection (0.001 ppm) but can be as high as 0.04 ppm (*17*).

To compare TGM concentrations measured above SDM with those that would occur otherwise in this urban/industrial setting, TGM was also monitored at an urban reference site 3.5 km west of the SDM site in Bayonne adjacent to Newark Bay (40° 40.23′ N, 74° 7.63′ W). TGM was sampled from the roof of the New Jersey Department of Environmental Protection air monitoring trailer at a height of 3.6 m. Being in the heart of industrial New Jersey, with Brooklyn and New York to the east and ports Newark and Elizabeth to the west, dozens of industrial and municipal Hg emissions sources at all points of the compass have the potential to contribute to the TGM signal at this reference site, which is subject to prevailing west winds as well as an episodic sea breeze from the east. TGM was monitored at the reference site on September 17, 2001 and from February 2002 to July 2002 and from October 2002 to February 2003.

Vertical fluxes of Hg from SDM were estimated using measured vertical concentration gradients of TGM and the vertical wind speed profile in a modified form of the Thornthwaite−Holzmann equation

$$F_{Hg} = \frac{u^* \kappa (Hg_1 - Hg_2)}{\ln(z_2/z_1)\phi_W} \quad (1)$$

where F_{Hg} is the land−air Hg flux (ng m^{-2} h^{-1}), u^* is the friction velocity, Hg_1 and Hg_2 are the gaseous Hg concentrations (ng m^{-3}) at heights z_1 and z_2 above the ground, ϕ_W is the atmospheric stability correction factor for water vapor, and κ is the Von Karman constant (*18, 19*). The friction velocity was measured directly using an eddy correlation system (see below), and the stability correction factor for water vapor (ϕ_W), which was used here to represent that of Hg^0, was derived from the measured water vapor flux. Vertical fluxes were calculated every 10 or 30 min. and averaged within morning, afternoon, and evening sampling intervals.

Physical atmospheric parameters were measured using two micrometeorological systems. The first, an aerodynamic gradient system (Campbell Scientific, Logan, UT), was used to simultaneously measure temperature, water vapor pressure, and wind speed at two heights above the ground surface. Temperature was measured with 74 μm diameter Chromel−Constantan thermocouples. These thermocouples have a resolution of 0.006 °C with 0.1 μV root-mean-square noise. Water vapor pressure was measured by pumping air through a cooled mirror, dew point hygrometer (Dew-10, General Eastern Corp., Watertown, MA). Air was drawn from both heights continuously through downward pointing Teflon filters (1 μm) to remove dust and liquid water and delivered

TABLE 2. Average Vertical Concentration Gradients of Total Gaseous Mercury (TGM), Friction Velocities (u^*), Atmospheric Stability Correction Factors for Water Vapor (ϕ_W), and Sediment–Air Hg Fluxes for Each Sampling Period at the SDM Placement Site in Bayonne, NJ[a]

date	local time	u^*	ϕ_W	TGM gradient (ng m^{-3})	flux (ng m^{-2} h^{-1})
8/30/01	13:10–14:36	0.49 ± 0.05	1.19 ± 0.01	0.42 ± 0.06	187 ± 34
10/23/01	11:00–12:00	0.21 ± 0.02	1.00 ± 0.00	0.23 ± 0.05	30 ± 8
10/24/01	12:35–15:55	0.22 ± 0.07	0.91 ± 0.21	0.78 ± 0.07	156 ± 64
10/25/01	10:50–12:45	0.32 ± 0.10	1.00 ± 0.00	1.68 ± 0.08	446 ± 140
	13:25–15:20	0.45 ± 0.03	1.00 ± 0.00	1.12 ± 0.13	412 ± 57
5/07/02	10:45–12:00	0.19 ± 0.02	0.18 ± 0.02	0.91 ± 0.07	1043 ± 184
	12:05–14:55	0.29 ± 0.06	0.33 ± 0.07	0.32 ± 0.06	314 ± 115
	20:30–23:05	0.10 ± 0.05	1.73 ± 0.62	0.29 ± 0.06	19 ± 12
5/08/02	9:55–12:10	0.67 ± 0.08	0.34 ± 0.08	0.45 ± 0.06	966 ± 289
	13:30–16:00	0.69 ± 0.22	0.36 ± 0.05	0.26 ± 0.06	552 ± 235
11/14/02	10:00–11:50	0.18 ± 0.05	0.30 ± 0.15	0.05 ± 0.04	34 ± 40
	12:10–16:35	0.23 ± 0.04	0.41 ± 0.14	0.03 ± 0.03	17 ± 19
11/15/02	9:20–11:50	0.24 ± 0.03	0.73 ± 0.29	−0.04 ± 0.05	−13 ± 12
	12:10–14:00	0.26 ± 0.02	0.81 ± 0.20	0.11 ± 0.05	41 ± 22

[a] Values are means ± propagated error for TGM gradients and fluxes and means ± SD for u^* and ϕ_W.

to the hygrometer via a solenoid valve that switches the air flow between the two intakes every 2 min. The Dew-10 has a resolution of approximately ±0.01 kPa. Horizontal wind speeds were measured using cup anemometers (R. M. Young 03001–5 Wind Sentries) with a range of 0–50 m s^{-1} and a threshold value of 0.5 m s^{-1}. All measurements taken with the aerodynamic gradient system were averaged over 20-min intervals.

The second micrometeorological system, an eddy correlation system, includes quick response instruments capable of measurements at 10 Hz in order to resolve the turbulent fluctuations in vertical velocity, horizontal velocity, temperature, and specific humidity, in the near surface atmosphere. These measurements were processed to give 20-min average friction velocities (u^*) and sensible heat and water vapor (latent heat) fluxes. Vertical and horizontal wind speeds were measured using a three-dimensional sonic anemometer (CSAT3, Campbell Scientific) sampling at 60 Hz and with 1 mm s^{-1} of noise in the horizontal and 0.5 mm s^{-1} in the vertical. Fluctuations in moisture content of the air were measured using an ultraviolet krypton hygrometer (KH2O, Campbell Scientific). High precision (±0.002 °C) temperature measurements were made using 12.7-μm fine wire thermocouples (FW05, Campbell Scientific). Measured water vapor concentration gradients from the aerodynamic gradient system plus water vapor fluxes and friction velocities from the eddy correlation system were used to determine the atmospheric stability correction factor for water vapor (ϕ_W). Solar radiation data were obtained from the Hudson River NERR meteorology site (42° 01.09′ N, 73° 55.02′ W; *34*).

Total gaseous mercury (TGM), which is primarily elemental Hg (*2*), was measured at the SDM and reference sites using a single Tekran Model 2357A Mercury Vapor Analyzer (Tekran Inc., Toronto, Canada) at an air flow rate of 1.5 L min^{-1} and a sampling period of 5 min (*20*). Air was collected through $^1/_4$ in. Teflon tubing at two heights (0.8 and 3 m) above the SDM approximately 1 m downwind of the micrometeorological sensors using an instrument-controlled solenoid valve to switch between the two heights. The height switching period was 10 min, except on October 25, 2001, when the period was 30 min. Teflon tubing was cleaned with 1 N HCl and rinsed with ultrapure water prior to and between sampling events. Instrument calibrations were performed every day while working at the SDM site and every week while monitoring TGM at the NJDEP air monitoring reference site. Calibrations were accomplished using the Tekran's internal permeation source and external injections of gaseous elemental mercury standards. The two methods of calibration gave instrument response factors that agreed to within 3–9% of each other. Field blank measurements were made by connecting the sampling lines to a source of Hg-free air and always gave zero peak areas and TGM concentrations. Vertical concentration gradients in TGM (Table 2) were evaluated as the difference in paired TGM values measured at 0.8 and 3 m. The significance of vertical concentration gradients was evaluated using the percent gradient method in which the relative difference between upper and lower TGM concentrations is compared with the analytical uncertainty (*21*). The percent gradient was evaluated according to the following equation:

$$\%\ \text{gradient} = \frac{|\text{TGM}_{\text{lower}} - \text{TGM}_{\text{upper}}|}{\text{TGM}_{\text{lower}}} \times 100 \qquad (2)$$

Analytical uncertainty was evaluated as the coefficient of variation (standard deviation divided by mean × 100) of replicate measurements over a 30-min period at the NJDEP site ($n = 6$) and was found to be 1.3%. Vertical concentration gradients with percent gradients greater than twice the analytical uncertainty (2 × 1.3% or 2.6%) were considered significant and used to estimate positive or negative fluxes. Percent gradients for paired measurements at the SDM placement site ranged from 0.3% to 32%. With an analytical uncertainty of 2.6%, 86% (96 out of 112) of all vertical gradients were significant and indicative of net (positive or negative) sediment–air Hg fluxes. Gradients whose percent gradients were less than the analytical uncertainty were assigned vertical fluxes of zero.

Results and Discussion

Total Gaseous Hg Concentrations in Bayonne, NJ, and at the SDM Placement Site. The average concentration of TGM at the urban reference site in Bayonne, NJ, for the sampling periods from September 2001 to February 2003 (2.2 ± 1.1 ng m^{-3}) was somewhat higher than continental background values (1.6–2.0 ng m^{-3}) for the Northern Hemisphere (*22, 23*). Reference site TGM concentrations ranged from 1.7 ± 0.6 ng m^{-3} in January 2003 to 3.3 ± 2.1 ng m^{-3} in June 2002 and were generally lower and less variable in winter than in the summer (Figure 2). In addition, TGM concentrations at the urban reference site were not normally distributed. For example, the distribution of reference site TGM concentrations in June 2002 (mean = 3.3 ng m^{-3}, median = 2.9 ng m^{-3}, $n = 5017$) had a shoulder of elevated concentrations from 3.5 to 6.0 ng m^{-3}, which accounted for 44% of the difference

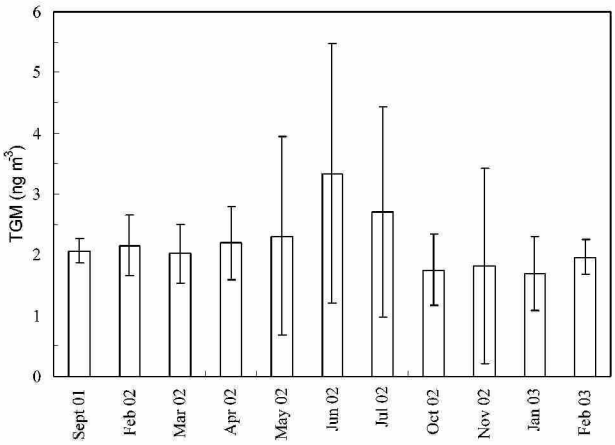

FIGURE 2. Monthly average total gaseous mercury (TGM) concentrations at the NJDEP air monitoring site in Bayonne, NJ, for the periods February 2002–July 2002 and October 2002–February 2003 and on September 17, 2001. Error bars are ±1 standard deviation.

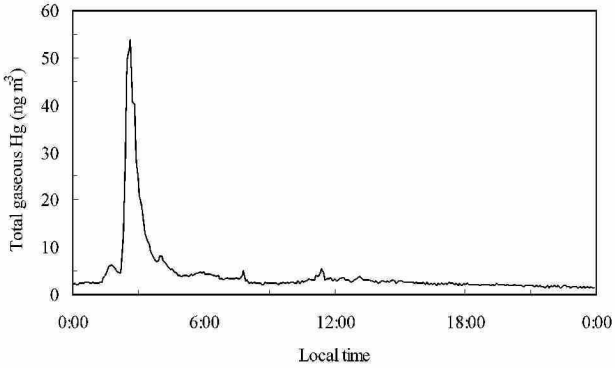

FIGURE 3. Total gaseous mercury concentrations at the urban reference site in Bayonne, NJ, June 30, 2002.

between June and January concentrations. When this shoulder was removed from the June 2002 data, the subset had a normal distribution (mean = median = 2.6 ng m^{-3}, n = 3499). Distributions of TGM concentrations in winter months had less pronounced shoulders of lower concentrations.

Throughout the monitoring period, "spikes" of elevated TGM (>6 ng m^{-3} up to 54 ng m^{-3}) were observed at the NJDEP site lasting from 15 min to a few hours and occurring primarily between midnight and 5 a.m. The highest concentration among these spikes (54 ng m^{-3}) was recorded on June 30, 2002 (Figure 3). No relationship between the occurrence of these spikes and meteorological conditions has been found, and they are likely related to local, episodic industrial activities. Similar spikes observed in New York City were also attributed to local anthropogenic sources (*24*). Since these spikes were of short duration and represented less than 2% of the total number of measurements, their effect on monthly or annual average TGM concentrations was small (<10%). For example, after removing TGM values >6 ng m^{-3}, the mean TGM concentration for June 2002 decreased from 3.3 to 3.1 ng m^{-3}.

TGM concentrations measured at the SDM placement site were consistently higher than those measured at the urban reference site (Figure 4). Thus the average TGM concentration measured at the SDM site's upper elevation (3.2 ± 0.63 ng m^{-3}) was significantly higher (Mann–Whitney U-test, $p < 0.001$) than the average TGM concentration at the urban reference site measured on days that bracketed sampling events (1.8 ± 0.18 ng m^{-3}).

Sediment–Air Fluxes of Hg from SDM. Average vertical concentration gradients of TGM at the SDM placement site ranged from −0.04 to 1.7 ng m^{-3} (Table 2), but only 11% (12 of 112) of all paired gradients and only 6% (6 of 106) of the daytime gradients were less than zero. As a result, average TGM gradients and estimated land–air fluxes were positive during 13 of 14 sampling periods (Table 2). Large TGM gradients were observed in August and October 2001 and May 2002, while very low or negative TGM gradients were measured in November 2002. On and offsite sources other than SDM such as capping materials, vehicles, or local industry may have contributed to the TGM measured at the SDM site, but with more than 100 m of SDM surface between these sources and the TGM sampling site, vertical TGM gradients and fluxes were primarily influenced by SDM. Estimated daytime sediment–air Hg fluxes ranged from 30 to 1040 ng m^{-2} h^{-1} in August, October, and May, but only −13 to 41 ng m^{-2} h^{-1} in November (Table 2). The nighttime Hg flux estimate for May 7, 2002 was less than 3% of the average daytime fluxes observed during the May 2002 campaign.

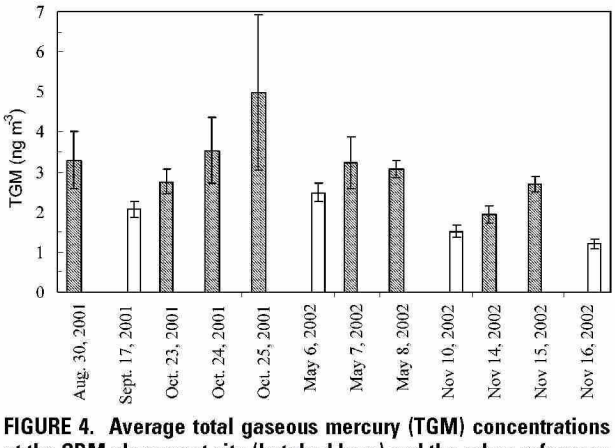

FIGURE 4. Average total gaseous mercury (TGM) concentrations at the SDM placement site (hatched bars) and the urban reference site (open bars) during field sampling events. Error bars are ±1 standard deviation.

Estimates of the global mercury cycle indicate that the average terrestrial emission rate is approximately 1 Mt y^{-1} or 0.8 ng m^{-2} h^{-1} (*25*) and that this rate has changed little since preindustrial times (*26*). Since this value is the average for all land surface types, it underestimates the emissions of Hg from more enriched soils and sediments. Estimates of soil–air Hg fluxes for uncontaminated or naturally enriched soils range from −2.2 to 45 ng m^{-2} h^{-1} (*2*–*6*). Emissions from Hg mining waste (*7*, *10*), contaminated soil (*8*), or soil amended with municipal sewage sludge (*9*) are much higher and range from 10 to 3900 ng m^{-2} h^{-1}. The range of daytime Hg fluxes from SDM observed in this study (Table 2) is similar to that for anthropogenically enriched surfaces.

Mercury volatilization from land is dominated by the flux of elemental Hg (*2*). Thus, environments that favor the reduction of Hg(II) to Hg^0 are likely to support higher TGM emissions. Sunlight can drive the reduction of Hg(II) in soil (*9*) and Hg fluxes are often correlated with incident radiation (*4*). The fluxes of TGM from SDM observed in May 2002 closely followed diurnal changes in solar radiation (Figure 5). The highest Hg and solar radiation fluxes were observed on the mornings of May 7 and 8, with lower fluxes in the afternoons and very low Hg fluxes at night in the absence of light even though the vertical TGM gradient had only dropped from 0.32 to 0.29 ng m^{-3} (Table 2). Although increased atmospheric stability ($\phi_W = 1.7$) also contributed to the low nighttime TGM flux, wind speed was not generally a dominant factor controlling the flux of Hg from SDM, as no significant correlation between wind speed and Hg flux was observed ($r^2 = 0.24$, $p > 0.05$). Indeed, TGM fluxes for the SDM site were highly correlated ($r^2 = 0.81$) with solar radiation (Figure 6), a correlation which may be used to predict Hg volatilization

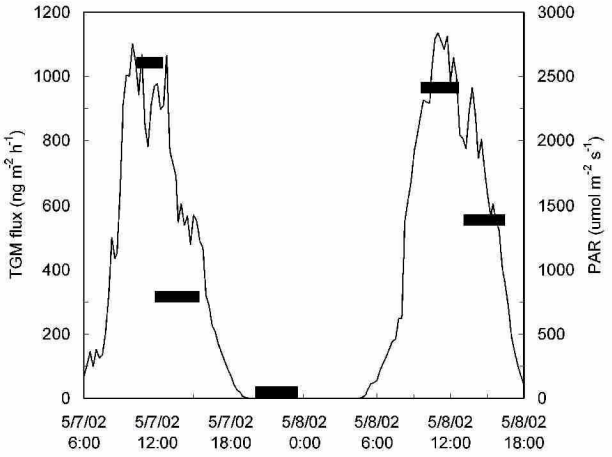

FIGURE 5. Time course of TGM fluxes and photosynthetically active radiation (PAR) at the SDM application site during the May 2002 field experiment. PAR data are from the Hudson River NERR meteorology station (*34*).

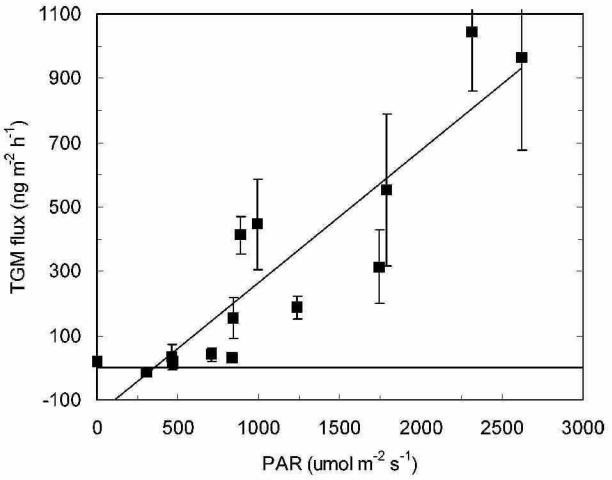

FIGURE 6. Relationship between TGM fluxes and photosynthetically active radiation (PAR) at the SDM placement site. TGM values are means ± propagated error from Table 2. PAR data are from the Hudson River NERR meteorology station (*34*). The regression line is TGM flux = 0.41 × PAR − 146 (r^2 = 0.81).

from land applied SDM or tidally exposed native sediments and to select appropriate times of the day or of the year to apply SDM in order to reduce Hg volatilization.

Other factors including soil temperature and Hg and water content can also affect the volatilization of Hg from soils. TGM concentrations were generally correlated with air temperature at the urban reference site (r^2 of 0.57, $p < 0.05$) consistent with other studies showing significant correlations between media (soil, water) temperatures and atmospheric Hg (*27*). During the October 2001 sampling event, the vertical TGM flux increased from 30 ng m^{-2} h^{-1} on October 23 to 160 ng m^{-2} h^{-1} on October 24 (Table 2) as the air temperature rose from 19 to 29 °C and other parameters including solar radiation were unchanged (Table 1), indicating a warming-driven increase in Hg flux. Low temperatures (11−15 °C) may have contributed to low volatilization fluxes of Hg from SDM in November 2002, when low TGM gradients and fluxes were observed despite wind speeds and atmospheric stabilities that were similar to those measured during other sampling periods (Tables 1 and 2). In contrast to the above, TGM flux was negatively correlated with SDM temperature in May 2002 (Tables 1 and 2), when solar radiation fluxes were high.

The concentration of Hg in the dredged material used at the Bayonne SDM site during this study ranged from 1.3 to 2.6 ppm (*16*), well above the preindustrial concentration of 0.3−0.4 ppm for the Hudson River drainage basin (*28*). The short-term, daytime fluxes of Hg from SDM observed in this study were similar to those estimated for naturally enriched Nevada soil (*29*) or sewage-sludge-amended soil (*9*) with similar Hg concentrations, but these latter rates were estimated using flux chambers, which generally give lower fluxes than micrometeorological methods. Lindberg et al. (*8*) used a micrometeorological approach to estimate Hg fluxes from an impacted site in East Fork Poplar Creek in Oak Ridge, TN, where the concentration of mercury in the soil ranged from 5 to 50 ppm and the corresponding flux ranged from 10 to 200 ng m^{-2} h^{-1}, but Hg fluxes at this site may have been limited by low solar radiation fluxes to soils below a forest canopy. The relatively narrow range in Hg sediment concentrations at the SDM site compared with the nearly 100-fold range in Hg volatilization fluxes suggests that Hg concentration does not play a dominant role in Hg emissions from SDM.

Water can affect the evaporative flux of soil-bound contaminants by the displacement of chemicals from the soil surface (*30*), and Hg fluxes from soils can increase following rain events (*31*). In the case of land-applied SDM, which is initially saturated with water, displacement by rain cannot occur. As SDM dries over days to weeks, the loss of moisture may expose more SDM surfaces directly to the atmosphere and thereby enhance Hg volatilization, but drying may also cause contaminants to become sequestered within the cemented SDM matrix, producing a declining flux over time. Hg fluxes did not decline as SDM aged from May 7 to May 8 (Table 2), suggesting that short-term stabilization did not have an effect on Hg volatilization. To accurately evaluate the specific effects of environmental factors on Hg volatilization from untreated and cement-stabilized dredged materials requires laboratory studies under controlled light, temperature, and air flow conditions.

SDM as a Source of Hg to the Local and Regional Atmosphere. The concentrations of TGM observed at the urban reference site in Bayonne, NJ, indicate that, in addition to regional sources upwind of New Jersey, current and historic industrial activities in the New York/New Jersey metropolitan area contribute Hg to the atmosphere of the lower Hudson River estuary (*32*). Despite significant enrichment, TGM concentrations in this highly urbanized area, as well as those at the Bayonne SDM site during active placement, never approached the human chronic effects limit for total gaseous mercury (200 ng m^{-3}) established by the Agency for Toxic Substances and Disease Registry. However, emissions of Hg to the atmosphere are of environmental concern primarily because of the long residence time of Hg in the atmosphere (*26*) and the deposition of Hg in proximate or remote water bodies where it may be transformed and bioaccumulated (*25*). Maximum seasonal and annual Hg emissions from the SDM placement site were estimated using the solar radiation−Hg flux relationship of Figure 6 and diurnal sunlight patterns for winter and summer months and assuming continuous 20% coverage of the SDM site. These fluxes show that the SDM site contributed less than 4% per day of the ambient concentration of TGM to the local atmosphere. They also show that the site's annual Hg emission rate (130 kg y^{-1}) could be comparable to some of New Jersey's major industrial sources (Table 3) and approximately 30% of New Jersey's atmospheric deposition flux (*33*). Since 1997, more than 7 million cubic yards of SDM from the New York/New Jersey Harbor have been placed at sites in New York, New Jersey, and Pennsylvania, but the intermittent nature of the exposure of SDM to the atmosphere at these sites makes their contribution to regional Hg emissions difficult to evaluate. In addition, the emissions of Hg from native (unstabilized), tidally exposed estuarine sediments, which constitute a vastly

TABLE 3. Annual Emissions of Hg to the Atmosphere from New Jersey Industrial Sources and the SDM Application Site

source category	emissions rate (kg y^{-1})
steel and iron manufacturing[a]	450
aluminum scrap processing[a]	450
coal combustion[a]	320
MSW incineration[a]	150
product volatilization[a]	140
SDM application site	130

[a] Reference *33*.

larger area than SDM sites and are continuously present in the environment, need to be quantified as a potentially important part of the Hg cycle in coastal areas.

Acknowledgments

This paper was greatly improved by the comments of four anonymous reviewers. This project was supported by the New Jersey Marine Sciences Consortium (NJMSC) and the New Jersey Department of Transportation (NJDOT), Office of Maritime Resources through a grant from the Port Authority of New York and New Jersey and a Hatch/McIntyre-Stennis grant through the New Jersey Agricultural Experiment Station.

Literature Cited

(1) Douglas, W. S.; Baier, L. J.; Gimello, R. J.; Lodge, J. A comprehensive strategy for managing contaminated dredged material in the Port of NY and NJ. *J. Dredging Eng.* **2003**, *5*, 1−12.

(2) Kim, K. H.; Lindberg, S. E. Design and initial tests of a dynamic enclosure chamber for measurements of vapor-phase mercury fluxes over soils. *Water Air Soil Pollut.* **1995**, *80*, 1059−1068.

(3) Carpi, A.; Lindberg, S. E. Application of a Teflon (TM) dynamic flux chamber for quantifying soil mercury flux: Tests and results over background soil. *Atmos. Environ.* **1998**, *32*, 873−882.

(4) Poissant, L.; Casimir, A. Water−air and soil-air exchange rate of total gaseous mercury measured at background sites. *Atmos. Environ.* **1998**, *32*, 883−893.

(5) Engle, M. A.; Gustin, M. S.; Zhang H. Quantifying natural source mercury emissions from the Ivanhoe Mining District, north-central Nevada, USA. *Atmos. Environ.* **2001**, *35*, 3987−3997.

(6) Zehner, R. E.; Gustin, M. S. Estimation of mercury vapor flux from natural substrate in Nevada. *Environ. Sci. Technol.* **2002**, *36*, 4039−4045.

(7) Nacht, D. M.; Gustin, M. S.; Engle, M. A.; Zehner, R. E.; Giglini, A. D. Atmospheric Mercury Emissions and Speciation at the Sulphur Bank Mercury Mine Superfund Site, Northern California. *Environ. Sci. Technol.* **2004**, *38*, 1977−1983.

(8) Lindberg, S. E.; Kim, K. H.; Meyers, T. P.; Owens, J. G. Micrometeorological gradient approach for quantifying air−surface exchange of mercury-vapor—Tests over contaminated soils. *Environ. Sci. Technol.* **1995**, *29*, 126−135.

(9) Carpi, A.; Lindberg, S. E. Sunlight-mediated emission of elemental mercury from soil amended with municipal sewage sludge. *Environ. Sci. Technol.* **1997**, *31*, 2085−2091.

(10) Ferrara, R.; Maserti, B. E.; Andersson, M.; Edner, H.; Ragnarson, P.; Svanberg, S.; Hernandez, A. Atmospheric mercury concentrations and fluxes in the Almaden District (Spain). *Atmos. Environ.* **1998**, *32*, 3897−3904.

(11) Kozuchowski, I.; Johnson, D. L. Gaseous emissions of mercury from an aquatic vascular plant. *Nature* **1978**, *274*, 468−469.

(12) Leonard, T. L.; Taylor, G. E.; Gustin, M. S.; Fernandez, G. C. J. Mercury and plants in contaminated soils: 2. Environmental and physiological factors governing mercury flux to the atmosphere. *Environ. Toxicol. Chem.* **1998**, *17*, 2072−2079.

(13) Lee, X.; Benoit, G.; Hu, X. Z. Total gaseous mercury concentration and flux over a coastal saltmarsh vegetation in Connecticut, USA. *Atmos. Environ.* **2000**, *34*, 4205−4213.

(14) Lindberg, S. E.; Dong, W.; Meyers, T. Transpiration of gaseous elemental mercury through vegetation in a sub-tropical wetland in Florida. *Atmos. Environ.* **2002**, *36*, 5207−5219.

(15) Maher, A.; Bennert, T.; Jafari, F.; Douglas, W. S.; Gucunski, N. Geotechnical properties of stabilized dredged material from New York-New Jersey Harbor. *Transport. Res. Rec.* **2004**, *1874*, 86−96.

(16) ETL. Elizabeth Channel Composite Sediments. Report to the New Jersey Department of Environmental Protection, 2001.

(17) Johansen, V. C.; Hawkins, G. J. *Mercury Speciation in Cement Kilns: A Literature Review*; R&D Serial No. 2567; Portland Cement Association: Skokie, IL, 2003, 16 p.

(18) Thornthwaite, C.; Holzman, B. The determination of evaporation from land and water surfaces. *Month. Weath. Rev.* **1938**, *Jan.*, 4−11.

(19) Majewski, M.; Desjardins, R.; Rochette, P.; Pattey, E.; Seiber, J.; Glotfelty, D. Field comparison of an eddy accumulation and an aerodynamic-gradient system for measuring pesticide volatilization fluxes. *Environ. Sci. Technol.* **1993**, *27*, 121−128.

(20) Schroeder, W. H.; Keeler, G.; Kock, H. H.; Roussel, P.; Schneeberger, D.; Schaedlich, F. International field intercomparison of atmospheric mercury measurement methods. *Water Air Soil Pollut.* **1995**, *80*, 611−620.

(21) Kim, K.-H.; Kim, M.-Y. The exchange of gaseous mercury across soil-air surface interface in a residential area of Seoul, Korea. *Atmos. Environ.* **1999**, *33*, 3153−3165.

(22) Slemr, F.; Langer, E. Increase in global atmospheric concentrations of mercury inferred from measurements over the Atlantic Ocean. *Nature* **1992**, *355*, 434−437.

(23) Temme, C.; Slemr, F.; Ebinghaus, R.; Einax, J. W. Distribution of mercury over the Atlantic Ocean in 1996 and 1999−2001. *Atmos. Environ.* **2003**, *37*, 1889−1897.

(24) Carpi, A.; Chen, Y.-F. Gaseous elemental mercury fluxes in New York City. *Water Air Soil Pollut.* **2002**, 140, 371−379.

(25) Lindqvist, O.; Johansson, K.; Astrup, M.; Anderson, A.; Bringmark, L.; Hovsenius, G.; Hakanson, L.; Iverfeldt, A.; Meili, M.; Timm, B. Mercury in the Swedish environment: Recent research on causes consequences and corrective methods. *Water Air Soil Pollut.* **1991**, *55*, 23−32.

(26) Mason, R. P.; Fitzgerald W. F.; Morel, F. M. M. The biogiochemical cycling of elemental mercury: Anthropogenic influences. *Geochim. Cosmochim. Acta* **1994**, *58*, 3191−3198.

(27) Gillis, A. A.; Miller, D. R. Some local environmental effects on mercury emission and absorption at a soil surface. *Sci. Total Environ.* **2000**, *260*, 191−200.

(28) Wakeman, T. H.; Themelis, N. A basin-wide approach to dredged material management in New York/New Jersey Harbor. *J. Hazard. Mater.* **2001**, *85*, 1−13.

(29) Gustin, M. S.; Lindberg, S. E.; Austin, K.; Coolbaugh, M.; Vette, A.; Zhang, H. Assessing the contribution of natural sources to regional atmospheric mercury budgets. *Sci. Total Environ.* **2000**, *259*, 61−71.

(30) Spencer, W. F.; Cliath, M. M.; Farmer, W. J. Vapor density of soil-applied dieldrin as related to soil−water content, temperature and dieldrin concentration. *Soil Sci. Soc. Am. Proc.* **1969**, *33*, 509−511.

(31) Wallschlager, D.; Kock, H. H.; Schroeder, W.; Lindberg, S. E.; Ebinghaus, R.; Wilken, R. Mechanism and significance of mercury volatilization from contaminated flood plains of the German river Elbe. *Atmos. Environ.* **2000**, *34*, 3745−3755.

(32) de Cerreño, A. L. C.; Panero, M.; Boehme, S. Pollution prevention and management strategies for mercury in the New York/New Jersey Harbor. New York Academy of Sciences, 2002.

(33) New Jersey Mercury Task Force: Report to the New Jersey Department of Environmental Protection, 2001.

(34) NOAA, Office of Ocean and Coastal Resource Management, National Estuarine Research Reserve System-wide Monitoring Program. Centralized Data Management Office, Baruch Marine Field Lab, University of South Carolina, 2004. http://cdmo.baruch.sc.edu.

Received for review March 15, 2005. Revised manuscript received July 24, 2005. Accepted August 28, 2005.

ES050506N

EMISSIONS OF PCBS AND MERCURY FROM STABILIZED HARBOR SEDIMENTS

Final Project Summary

A Report to the

New Jersey Marine Sciences Consortium and New Jersey Department of Transportation
Office of Maritime Resources

Principal Investigators:
John R. Reinfelder, Gera Stenchikov, Lisa A. Totten
Department of Environmental Sciences, Rutgers University
14 College Farm Road, New Brunswick, NJ 08901

Robert Miskewitz, Richard I. Hires, George P. Korfiatis
Stevens Institute of Technology
Hoboken, NJ 07030

THE STATE UNIVERSITY OF NEW JERSEY
RUTGERS

STEVENS
Institute of Technology

June 30, 2006

Emissions of PCBs and Mercury from Stabilized Harbor Sediments

Final Project Summary

Introduction

The Port of New York and New Jersey is the largest container and petroleum port on the East Coast of the United States. Natural depth of New York Harbor is only 6 meters, necessitating construction of over 400 km of engineered waterways that require nearly continuous improvement and maintenance. Between 3 and 5 million cubic meters of sediment are dredged annually, with actual volumes depending on construction and maintenance schedules. Historically, dredged material management relied almost exclusively on in-water disposal, despite the fact that much of the material dredged is fine grained and tends to contain varying levels of anthropogenic chemicals and trace metals. In the early 1990s, increasing environmental awareness resulted in a regional shift away from disposal toward upland beneficial use (McDonough et al., 1999).

The primary beneficial use strategy has been to use stabilized dredged material (SDM) as a capping and/or filling material for landfills, industrial sites, and abandoned mines (Douglas *et al.*, 2003). Stabilized dredged material, or SDM, is fine grained dredged material that has been mixed with a pozzolanic additive such as Type II Portland Cement, coal fly ash or incinerator ash to achieve a product with soil-like engineering properties. The strategy has multiple positive environmental benefits including reduction of runoff and leachate from contaminated sites, reduction of use of greenfields for industrial development, and providing affordable reliable locations to place dredged material. Since 1997, over 7 million cubic meters of contaminated dredged material have been successfully utilized upland in the States of New Jersey, New York and Pennsylvania (USACE 2006).

The success of the upland beneficial use strategy necessitates a firm understanding of the environmental risks and benefits. Since the beginning of the program, the State of New Jersey has had a policy that limits the placement of contaminated sediments to those sites that are already contaminated with similar substances in similar or higher amounts. The SDM is used specifically to implement a remedial action on the site consistent with a reduction or elimination of loss of contaminants into surrounding water bodies, groundwater or into the food chain. Rigorous monitoring of these sites confirms that not only are the remedial actions successful at ensuring that contaminants in SDM are not mobilized, but also those contaminants that were present on the site initially are no longer posing an ongoing threat (Douglas et al. 2005). Polychlorinated biphenyls (PCBs) and mercury (Hg) are two contaminants of particular concern with regard to the land application of SDM since they may volatilize to the atmosphere. Once in the atmosphere, these contaminants can deposit in proximate or remote ecosystems and become enriched in aquatic and terrestrial animals including humans where they may have toxic effects (Stern et al., 1996; Burger and Gochfeld, 1997; Watras et al., 1998; Gnamus et al., 2000; Berglund et al., 2001; Borga et al., 2004). Thus the atmospheric cycles of PCBs and Hg are critical to understanding and managing their environmental impact. An evaluation of the potential for SDM or the SDM manufacturing process to release PCBs and Hg into the atmosphere was initiated in 2001. This study included an evaluation of the air quality surrounding processing equipment and a placement site in northern New Jersey, as well as

controlled laboratory evaluations of contaminant flux. The results of these studies are presented in this report.

Project Scope and Rationale

The goals of this project were to assess the volatilization of polychlorinated biphenyls (PCBs) and mercury (Hg) from land-applied, stabilized dredge material (SDM), the effects of cement stabilization on the release of these contaminants, and potential impacts of land-applied SDM to the ambient air quality of placement sites and adjacent areas. Thus the first phase of this project (see Korfiatis et al., 2003) included in situ measurements of PCB and Hg concentrations and land-air fluxes at a site in Bayonne, New Jersey where SDM from the NY/NJ Harbor was placed. The results of that project demonstrated that PCBs and Hg were emitted from SDM, but pointed to gaps in our understanding of the sediment side controls of PCB and Hg volatilization, the aerosol partitioning of PCBs emitted from SDM, and the relative importance of SDM PCB emissions to the local atmosphere compared with other sources in the New York/New Jersey metropolitan area. The second phase of this project therefore included laboratory flux chamber measurements of PCB volatilization from cement-stabilized Newtown Creek sediment (see Miskewitz et al., 2005), and evaluations of the gas phase-aerosol partitioning of PCBs at the Bayonne site, the development of a local atmospheric transport model of PCBs in the harbor atmosphere, and flux chamber studies of Hg volatilization from cement-stabilized Berry's Creek sediment (see Reinfelder et al., 2006). The major findings of these studies and their implications for the land-application of SDM, where appropriate, are summarized below.

Assessment of PCB emissions from land-applied SDM

PCB concentrations and volatilization fluxes at the Bayonne SDM placement site

At the Bayonne SDM site, gaseous air concentrations of ΣPCBs measured directly above SDM (3 – 14 ng m^{-3}) as it cured were relatively high compared to regional background values (1 – 3 ng m^{-3}), but they were two orders of magnitude below the NIOSH recommended exposure limit of 1 μg m^{-3} and five orders of magnitude lower than the OSHA permissible exposure limits of 0.5 to 1.0 mg m^{-3} (Korfiatis et al., 2003). Average ΣPCB concentrations at the SDM application site were approximately two times higher than those at an urban reference site 3.5 km west of the SDM site, but approximately 20% of the time, PCB concentrations at the urban reference site were greater than those at the SDM application site (Korfiatis et al., 2003). Upwind /downwind concentration gradients of PCBs were rare (5 of 29 cases) at the SDM landfill site. This suggests that SDM is not the only or dominant source of PCBs to the air above the landfill and that other offsite sources may be important.

Estimated vertical fluxes of PCBs from SDM at the Bayonne site ranged from 72 to 15,000 ng m^{-2} h^{-1} and averaged 2050 ng m^{-2} h^{-1}. Modeling results show that the transport of PCB emissions of this magnitude from the SDM placement site could produce concentration spikes of only $1/4^{th}$ to $1/10^{th}$ of those observed at the urban reference site indicating that PCB emissions from the SDM placement site have a small effect on the overall levels of PCBs measured within 3.5 km of its perimeter. Due to the high background concentrations of PCBs in both the gas and particle phases in the NYC metropolitan area, emissions of either gas- or particle-phase PCBs from the Bayonne SDM site are not large enough to alter the gas/particle partitioning of PCBs in this region. These emissions could, however, be important if SDM were placed in a more remote location where the background PCB signal is lower.

Effect of cement stabilization on the volatilization of PCBs from SDM

In the Bayonne field study, PCB fluxes from recently placed SDM were initially high, but decreased quickly as the SDM dried (Korfiatis et al., 2003). This was also observed in the laboratory flux chamber study where the rate at which the PCB flux decreased was found to be highly dependent on the degree of cement stabilization (Miskewitz et al., 2005). The average time constant for the decrease of PCB fluxes from unstabilized sediments was 61 h, while that for sediment stabilized with 8% portland cement was 15 h. Thus the addition of cement acts to decrease PCB fluxes from dredged sediment. The stabilization process will dry the sediment and thus reduce the amount of PCB volatilized (see *Effects of site and atmospheric conditions* section below).

What fraction of the sediment PCBs is lost to the atmosphere?

The fraction of ΣPCBs in New York/New Jersey Harbor dredged material that escapes to the atmosphere during land-application can be estimated from the average sediment PCB concentration and the average time dependent area PCB volatilization rate for SDM at the Bayonne site. The average PCB concentration in New York/New Jersey Harbor sediments exceeds 400 ng g^{-1} dry wt (Ho et al., 2000). Using a dry sediment mass density of 500 kg m^{-3} and a sediment PCB concentration of 400 ng g^{-1} dry wt yields a total sediment PCB concentration of 0.2 g m^{-3}. PCB area loads to the atmosphere from unstabilized and 8% cement-stabilized sediments were estimated by integrating the maximum initial PCB flux observed at the Bayonne SDM site (15,000 ng m^{-2} h^{-1}; Korfiatis et al., 2003) over periods of 215 and 54 h, respectively, (i.e. five half-lives of the logarithmic decreases observed in the laboratory flux chamber experiments, final flux = 3% of initial flux, see by Miskewitz et al., 2005). The resulting PCB loads to the atmosphere are 900 and 200 μg m^{-2}, for unstabilized and 8% cement-stabilized sediments, respectively. With an average SDM depth of 2 m, this is equivalent to losses of 450 and 100 μg m^{-3}. Thus without stabilization, an average of about 0.2% of the ΣPCBs in land applied sediments would be lost to the atmosphere, but only 0.05% of the ΣPCBs in land applied sediments stabilized with 8% cement would be lost to the atmosphere.

Effects of site and atmospheric conditions on the volatilization of PCBs from SDM

Estimated PCB flux rates exhibited a large dependence on the atmospheric and site conditions. Since the atmosphere tends to be stable at night, nighttime PCB fluxes were low. Very low PCB fluxes also occurred during daytime intervals when it was cloudy and cool, such as on the morning. The moisture content of the dredged material may also have an effect on PCB volatilization. Dry sediments have a greater affinity for volatile contaminants than wet sediments because of the competition for adsorption or absorption space with water (Valsaraj et al., 1997). As the sediment particles in upper layers of the sediment dry they not only hold the contaminant absorbed to them tighter, they will also absorb free contaminants that would otherwise diffuse to the surface, thus further increasing the sediment-side resistance to contaminant flux to the atmosphere. In the Bayonne field study, the sensible heat flux from dry SDM exceeded the latent heat flux indicating restricted transport of water vapor out of the SDM and estimated PCB fluxes above dry SDM were zero or directed into the ground (Korfiatis et al., 2003). In the laboratory flux chamber experiments, temperature was also found to exert a large influence on the magnitude of PCB fluxes from SDM (Miskewitz et al., 2005). Thus sediment that is stabilized and applied to the land during warmer summer months will release more PCBs to the atmosphere.

Assessment of Hg emissions from land-applied SDM

Hg concentrations and volatilization fluxes at the Bayonne SDM placement site

Total gaseous mercury (TGM) concentrations at the Bayonne SDM site ranged from 2 to 7 ng m^{-3}, compared with 1.7 to 3.3 ng m^{-3} at an urban reference site 3.5 km west of the SDM site. Daily average concentrations of TGM at the Bayonne SDM site during active placement were <5 ng m^{-3}, and much lower than the human chronic effects limit for total gaseous mercury (200 ng m^{-3}) established by the Agency for Toxic Substances and Disease Registry. Thus there is no direct human impact of Hg emissions from the placement of SDM as carried out at the Bayonne site.

The emissions of Hg to the atmosphere are primarily of environmental concern because of the long residence time of Hg in the atmosphere (Mason et al., 1994) and the deposition of Hg in proximate or remote water bodies where it may be transformed and bioaccumulated (Lindqvist et al., 1991). Maximum seasonal and annual Hg emissions from the SDM placement site were estimated using the solar radiation-Hg flux relationship of Goodrow et al., 2005 and diurnal sunlight patterns for winter and summer months and assuming continuous 20% coverage of the SDM site. These estimates show that the average Hg volatilization flux from the SDM placement site in Bayonne, NJ was 130 g y^{-1} or 0.36 g d^{-1} (Goodrow et al., 2006), much lower than major industrial sources of Hg to the atmosphere in New Jersey (140 to 450 kg y^{-1}) and approximately 0.03% of New Jersey's atmospheric deposition flux. Given the transient nature of SDM placement sites which are eventually capped, effectively reducing Hg emissions to those from background soils, Hg emissions from the placement of SDM as carried out at the Bayonne site is expected to present only a minor emissions source of Hg to the atmosphere.

Effects of cement stabilization on Hg volatilization from SDM

Cement stabilization did not reduce Hg fluxes over the course of two days at the SDM site (Korfiatis et al., 2003). This was also observed in the laboratory experiments where the volatilization fluxes of Hg from cement stabilized sediments were twice as high as those from unstabilized sediments (Reinfelder et al., 2005). We conclude that cement stabilization does not reduce Hg volatilization from land-applied SDM over the course of a few days.

What fraction of the sediment Hg is lost to the atmosphere?

The fraction of total mercury in dredged material that escapes to the atmosphere during land-application can be estimated from the average sediment Hg concentration and the average area Hg volatilization rate for SDM at the Bayonne site. Using a dry sediment mass density of 500 kg m^{-3} and a sediment Hg concentration of 2 μg g^{-1} dry wt yields a total sediment mercury concentration of 1 g m^{-3}. Over the two year active lifetime of the Bayonne SDM site, the average area volatilization rate of Hg was 500 μg m^2. With an average SDM depth of 2 m, this is equivalent to a loss rate of 250 μg m^{-3}. Thus ¼ of one one-thousandth or 0.025% of the total Hg content of dredged sediment was lost to the atmosphere.

Hg volatilization fluxes expected from SDM with higher Hg concentrations

For soils, Hg volatilization fluxes generally increase with Hg soil concentration according to a log-linear relationship (Gustin et al., 2000; Nacht et al., 2004). This is also likely the case for sediments and indeed the estimated fluxes of Hg from cement-stabilized Berry's Creek sediment which contained 20 to 40 μg Hg g^{-1} dry wt (Reinfelder et al., 2005) are four to ten times higher than those observed at the Bayonne SDM placement site which contained 1 to 3 μg

Hg g^{-1} dry wt. Assuming that the land application of SDM with a Hg concentration of 40 μg g^{-1} at a site similar to that in Bayonne will result in a ten-fold higher Hg volatilization flux, the average Hg volatilization flux would be about 1.3 kg y^{-1} or 3.6 g d^{-1}. Thus the land application of SDM with a Hg concentration of up to 40 μg g^{-1} is unlikely to present a major source of Hg to the atmosphere. The impact on the environment of the land application of SDM with a Hg concentration significantly greater than 40 μg g^{-1} requires further evaluation.

Effects of light on Hg volatilization from SDM

The volatilization of mercury from estuarine sediments does not decrease with time as was observed for PCBs (Miskewitz et al., 2005), but is primarily controlled by light. The dominant role of light in controlling Hg volatilization from sediments in the laboratory flux chamber is consistent with in situ sediment-air Hg flux observations at the SDM placement site in Bayonne, NJ which were significantly correlated ($r^2 = 0.81$) with solar radiation (Goodrow et al., 2005). Decreasing the time of exposure of SDM to light during cement stabilization and placement would reduce Hg emissions to the atmosphere from this source.

Summary Conclusions

The field and laboratory results from this project allow us to evaluate the land application of cement-stabilized dredge materials from the perspective of its possible impact on the emissions of contaminants to the atmosphere. Perhaps one of the most important findings is that although emissions of PCBs and Hg to the atmosphere will occur during the land application of SDM, these represent very small fractions (<0.05%) of the total contaminant loads contained in the sediments. For the contaminant concentrations in the sediments used at the Bayonne site, these emissions therefore represent minor contributions to the local or region atmosphere. Interestingly, cement stabilization appears to have opposite effects on the volatilization of PCBs (retards) and Hg (enhances), but emissions of both are transient decreasing rapidly in only a few days in the case of PCBs and stopping altogether when covered. Based on these findings, we conclude that the land application of SDM represents a very minor impact on atmospheric levels and cycling of PCBs and Hg.

References

Berglund, O., Larsson, P., Ewald, G., and Okla, L. 2001. The effect of lake trophy on lipid content and PCB concentrations in planktonic food webs. *Ecology* 82:1078-1088.

Borga, K., Fisk, A.T., Hoekstra, P.F., and D.C.G. Muir. 2004. Biological and chemical factors of importance in the bioaccumulation and trophic transfer of persistent organochlorine contaminants in arctic marine food webs. *Environ. Toxicol. Chem.* 23: 2367–2385.

Burger, J. and Gochfeld, M. 1997. Risk, mercury levels, and birds - relating adverse laboratory effects to field biomonitoring. Environ. Res. 75: 160-172.

Douglas, W.S., Baier, L.J., Gimello, R.J., and Lodge, J. (2003). A comprehensive strategy for managing contaminated dredged material in the Port of NY and NJ. *J. Dredging Eng.* 5(3):1-12.

Douglas, W.S., Maher A, Jafari F. 2005. An analysis of the environmental effects of the use of stabilized dredged material from the New York/New Jersey harbor in the construction of roadway embankments. *Integrated Environ. Assess. Mgmt.* 1(4):1-10.

Gnamus, A., Byrne, A.R., and Horvat, M. 2000. Mercury in the soil-plant-deer-predator food chain of a temperate forest in Slovenia *Environ. Sci. Technol.* 34: 3337-3345.

Goodrow, S.M., R. Miskewitz, R.I. Hires, S.J. Eisenreich, W.S. Douglas, and J.R. Reinfelder. 2005. Mercury emissions from cement-stabilized dredged material. *Environ. Sci. Technol.* 39: 8185-8190.

Goodrow S.M., R. Miskewitz, R.I. Hires, S.J. Eisenreich, W.S. Douglas, and J.R. Reinfelder. 2006. *Correction to* Mercury emissions from cement-stabilized dredged material. *Environ. Sci. Technol.* 40: 409.

Gustin, M.S., Lindberg, S.E., Austin, K., Coolbaugh, M., Vette, A., and Zhang, H. 2000. Assessing the contribution of natural sources to regional atmospheric mercury budgets. *Sci. Total Environ.* 259: 61-71.

Ho, K., R. Burgess, M. Pelletier, J. Serbst, S. Ryba, M. Cantwell, A. Kuhn, and P. Raczelowski. 2000. An Overview of Toxicant Identification in Sediments and Dredged Materials. Conference on Dredge Material Management: Options and Environmental Considerations, Massachusetts Institute of Technology, Cambridge Massachusetts, USA.

Korfiatis, G.P., R.I. Hires, J.R. Reinfelder, L.A. Totten, and S.J. Eisenreich. 2003. Monitoring of PCB and Hg Air Emissions in Sites Receiving Stabilized Harbor Sediment. Report to the New Jersey Marine Sciences Consortium and New Jersey Department of Transportation Office of Maritime Resources.

Lindqvist, O., Johansson, K., Astrup, M., Anderson, A., Bringmark, L., Hovsenius, G., Hakanson, L., Iverfeldt, A., Meili, M., Timm, B. 1991. Mercury in the Swedish environment: recent research on causes consequences and corrective methods. *Water Air Soil Pollut.* 55:23-32.

Mason, R.P., Fitzgerald W.F., and Morel, F.M.M. 1994. The biogiochemical cycling of elemental mercury: anthropogenic influences. *Geochim. Cosmochim. Acta* 58: 3191-3198.

McDonough, F.M., Boehm, G.A., Douglas, W.S. (1999). Dredged material management in New Jersey: A multifaceted approach for meeting statewide dredging needs in the 21st century. *Proc., 31st Annual Dredging Seminar.* Western Dredging Association.

Miskewitz, R., R. Hires, and G. Korfiatis. 2005. Measurement of PCB Fluxes to the Atmosphere from Stabilized Dredged Material. Report to the New Jersey Marine Sciences Consortium and New Jersey Department of Transportation Office of Maritime Resources.

Nacht, D.M., Gustin, M.S., Engle, M.A., Zehner, R.E., and Giglini, A.D. 2004. Atmospheric mercury emissions and speciation at the sulphur bank mercury mine superfund site, northern California. *Environ. Sci. Technol.* 38: 1977-1983.

Reinfelder, J.R., G. Stenchikov, and L.A. Totten. 2005. Emissions and Atmospheric Transport of PCBs and Hg from Stabilized Harbor Sediments. Report to the New Jersey Marine Sciences Consortium and New Jersey Department of Transportation Office of Maritime Resources.

Stern, A.H., Korn, L.R. and Ruppel, B.E. 1996. Estimation of fish consumption and methylmercury intake in the New Jersey population. *J Exp. Analysis Environ. Epidem.* 6: 503-525.

U.S. Army Corps of Engineers. (2006). Dredged material management plan for the port of New York and New Jersey: 2005 Update. USACE – NY District, New York, NY.

Valsaraj, K.T., Choy, B., Ravikrishna, R., Reible, D.D., Thibodeaux, L.J., Price, C.B., Brannon, J.M., Myers, T.E. 1997. Air emissions from exposed contaminated sediments and dredged materials 1. Experimental data in laboratory microcosms and mathematical modeling. *J Haz. Mat.* 54:65-87.

Watras, C.J., Back, R.C., Halvorsen, S., Hudson, R.J.M., Morrison, K.A., and Wente, S.P. 1998. Bioaccumulation of mercury in pelagic freshwater food webs. *Sci. Total Environ.* 219: 183-208.

Final Report to the

New Jersey Marine Sciences Consortium
and
New Jersey Department of Transportation
Office of Maritime Resources

Monitoring of PCB and Hg Air Emissions in Sites Receiving Stabilized Harbor Sediment

Principal Investigators:

George P. Korfiatis, Richard I. Hires
Center for Environmental Engineering, Stevens Institute of Technology
Hoboken, NJ 07030

John R. Reinfelder, Lisa A. Totten, Steven J. Eisenreich
Department of Environmental Sciences, Rutgers University
14 College Farm Road, New Brunswick, NJ 08901

August 15, 2003

Center for Environmental Engineering

THE STATE UNIVERSITY OF NEW JERSEY
RUTGERS

NEW JERSEY MARINE SCIENCES CONSORTIUM

STEVENS Institute of Technology

Monitoring of PCB and Hg Air Emissions in Sites Receiving Stabilized Harbor Sediment

Executive Summary

Project Goals, Objectives, and Approach

The goal of this project was to assess the volatilization of gas phase polychlorinated biphenyls (PCBs) and mercury (Hg) from a landfill in Bayonne, New Jersey where stabilized dredged material (SDM) from the NY/NJ Harbor is being placed. This information was used to evaluate the potential impact of land-applied SDM to the ambient air quality of placement sites and adjacent areas. The specific objectives of the project were to determine the background ambient PCB and Hg concentrations in the air in Bayonne, NJ prior to and following the land application of SDM, and to estimate vertical fluxes and horizontal gradients of PCBs and Hg at the SDM landfill. Background concentrations of 59 PCB congeners or congener groups (total of 93 congeners quantified) and total gaseous Hg (TGM) were measured at the NJDEP air-monitoring trailer on the western side of the Bayonne peninsula near Newark Bay. Vertical fluxes of PCBs and Hg were estimated using the micrometeorological method with simultaneous measurements of vertical concentration gradients and atmospheric stability parameters above SDM. Horizontal gradients of PCBs were determined from measurements around the perimeter of the SDM landfill.

Field Sampling Operations

Ambient monitoring of PCBs at the NJDEP air-monitoring trailer on the western side of the Bayonne peninsula began in December 1999 and continued through November 2002. Ambient monitoring of total gaseous mercury (TGM) was carried out at the NJDEP trailer site from September 2001 to February 2003. Vertical fluxes and horizontal gradients of PCBs and Hg at the SDM landfill were estimated during six intensive sampling campaigns of one to three days duration conducted in July, August, and October 2001 and in May and November 2002. Sampling campaigns were divided into morning, afternoon, and occasional night sampling events. During sampling, chemical gradients and micrometeorological parameters were measured within the surface microlayer (approximately 10 m above the ground surface), which is that part of the atmospheric boundary layer over which the vertical fluxes of heat, water, and chemicals are constant with height. Sampling was conducted at the SDM landfill in the presence of recently deposited, un-stabilized dredged material (August 1, 2001), SDM that had been in place for up to three weeks (July 17-20, 2001, August 29-30, 2001), and recently placed SDM (October 23-25, 2001, May 6-8, 2002, November 13-15, 2002). PCB samplers were run for 4 h during each sampling event while TGM was sampled continuously and analyzed automatically on site in five-minute intervals.

Gaseous PCB Concentrations in Bayonne, NJ and at the SDM Landfill

Ambient concentrations of the sum of all measured PCB congeners (ΣPCBs) in the gas phase in Bayonne, NJ as measured at the NJDEP trailer averaged 1.7 ng m^{-3}, which is higher than the North American continental average background concentration (~0.3 ng m^{-3}), but similar to average ΣPCB concentrations measured in Jersey City, NJ and other large urban and industrial areas such as Chicago, IL and Baltimore, MD. Gas phase ΣPCB concentrations at the trailer and sediment application sites

followed a seasonal pattern that is likely due to temperature-dependent land-air exchange processes. Consequently, the average concentrations of ΣPCBs followed the order July (23°C) > Oct (20°C) > Nov (10°C) and May (8°C). The highest concentrations of gaseous ΣPCBs measured at the NJDEP trailer site occurred during NE winds, while the lowest were observed when the winds were out of the west. Thus, potential sources of PCBs to Bayonne from the northeast including Bayonne itself, the Hudson River, and New York City are greater than sources from the west such as Newark Bay. During E/SE winds, when the SDM landfill was upwind of the NJDEP trailer, gas phase PCB concentrations at the trailer were lower than average values.

Gaseous Mercury Concentrations in Bayonne, NJ and at the SDM Landfill

The annual average concentration of TGM in Bayonne (2.2 ng m^{-3}) was slightly higher than the range of average global background levels (1.5 to 2.0 ng m^{-3}; Slemr and Langer, 1992). Monthly averaged TGM concentrations at the NJDEP trailer in Bayonne ranged from 1.8 ng m^{-3} to 3.3 ng m^{-3} and were significantly correlated with air temperature ($r^2 = 0.57$; $p < 0.05$). Thus, TGM concentrations were generally lower and less variable in the winter than in the summer. Throughout the monitoring period, spikes of elevated TGM (>4 ng m^3 up to 54 ng m^{-3}) lasting fifteen minutes to a few hours were observed. These spikes occurred primarily between midnight and 5 am. No relationship between the occurrence of these spikes and meteorological conditions has been found. These spikes are not addressed in this report, but have been used to calculate average TGM concentrations at in Bayonne. Because these spikes were of short duration (≤1 h) and represented less than 2% of the total number of measurements, their effect on monthly or annual average TGM concentrations was negligible.

TGM concentrations measured at the Bayonne landfill were consistently higher than those measured at the background site on the Western shore of Bayonne (Table 2). The average TGM concentration measured at the SDM landfill (3.2 ng m^{-3}, sampled 3 m above the surface), was significantly higher ($p < 0.05$) than the average background concentration measured at the NJDEP trailer or in New Brunswick, NJ on days that bracketed the SDM landfill sampling campaigns (1.8 ng m^{-3}).

Sediment – Air Fluxes of PCBs from SDM

The estimation of sediment-air PCB fluxes from SDM by the micrometeorological approach requires the measurement of concentration gradients within the surface microlayer. The results of this project demonstrate that gas phase PCB gradients can be measured within 3.5 m above the surface of SDM. Positive vertical fluxes (sediment-to-air) of ΣPCBs were observed during 16 of 20 sampling periods. These fluxes ranged from 72 to 15,000 ng m^{-2} h^{-1} and averaged 2050 ng m^{-2} h^{-1}. Nighttime PCB fluxes were an order of magnitude lower than daytime fluxes. Lower molecular weight di-, tri- and tetra-chlorinated PCBs dominated the vertical flux from SDM. Thus the volatilization of PCBs was dominated by the flux of higher vapor pressure, lower K_{ow}, less bioaccumulative and toxic PCB congeners. Temperature and atmospheric stability had significant effects on vertical PCB fluxes. Fluxes were positively related to temperature and thus highest in August and October and lowest in November and May. At night, the surface microlayer became increasingly stable resulting in decreases in both water vapor and PCB fluxes. During the day, as near-ground wind speeds and vertical convective air movement increased, PCB fluxes increased. The vertical flux of ΣPCBs decreased significantly as SDM aged over 5 d. Thus, emissions of PCBs from SDM are expected to be highest during the placement of fresh SDM and to decrease within a day or two thereafter.

Sediment – Air Fluxes of Hg from SDM

Among paired measurements of TGM at two heights above the surface at the SDM landfill, 86% (97 out of 113) of all gradients recorded were significant and indicative of net (positive or negative) sediment-air Hg fluxes. Positive sediment – air fluxes of TGM were observed in 14 out of 15 sampling periods. Sediment-air fluxes of Hg fluxes ranged from 17 to 1043 ng m^{-2} h^{-1} and averaged 312 ng m^{-2} h^{-1}. A single nighttime Hg flux estimate for May 7, 2002 was less than 3% of the average daytime fluxes observed in during the May 2002 campaign. Sediment – air Hg fluxes measured at the SDM landfill often exceeded those expected based on a reported relationship between soil Hg content and Hg flux. Thus the predicted flux for SDM with a Hg content of 3 ug g^{-1} (80 ng m^{-2} h^{-1}) was exceeded during 60% of the sampling events.

Summary of Findings and Conclusions

Gas phase concentrations of PCBs and Hg in Bayonne and at the SDM landfill were typical of urban environments, but orders of magnitude lower than regulatory safety limits. Vertical gas-phase concentration gradients of PCBs and Hg measured at the SDM landfill were consistent with net sediment to air volatilization fluxes. Net land-air fluxes of PCBs and Hg were quantified at the sediment application site and found to be generally positive during the day, but low to negative at night. These flux rates are highly variable and dependent on atmospheric conditions as well as the condition of the SDM. The gross contribution of SDM to the masses of PCBs and Hg in the air above the SDM landfill and to the atmosphere of Bayonne and adjacent environs is estimated to be minimal.

Our findings suggest that the SDM landfill is a relatively weak source of PCBs, that PCBs volatilized from the SDM landfill are rapidly scavenged by aerosols or deposited as they are carried west, that wind vectors alone cannot accurately account for the local atmospheric dynamics in this region, or that some combination of these and other factors are operating locally. Regardless of the mechanism, the present results demonstrate that the city of Bayonne, NJ, as represented by the NJDEP trailer air monitoring station, is impacted to a greater extent by PCB sources from areas other than the SDM site and suggest that the SDM landfill is not the primary source of PCBs to the city of Bayonne.

The average concentration of ΣPCBs at the SDM landfill was nearly twice as high as that at the NJDEP trailer, but there were sampling periods (6 of 29) when the concentrations at the trailer were greater than each of the three perimeter concentrations measured at the sediment application site. Higher downwind than upwind concentrations of ΣPCBs around the perimeter of the SDM landfill site were observed in only 5 out of 29 cases which suggests that SDM is not the only or dominant source of PCBs to the air above the landfill and that other offsite sources may be important. The PCB air concentrations measured directly above the SDM (3 – 14 ng m^{-3}) as it cures are relatively high compared to background values measured in the region (1 – 3 ng m^{-3}), but they are two orders of magnitude below the NIOSH recommended exposure limit of 1 μg m^{-3} and five orders of magnitude lower than the OSHA permissible exposure limits of 0.5 to 1.0 mg m^{-3}.

Similarly, by using Hg flux estimates from the SDM landfill and background Hg concentrations measured at the NJDEP trailer, the contribution of Hg from the placement of SDM to the air in Bayonne was estimated. This analysis showed that the contribution of Hg emissions from the SDM

landfill was only about 5% and 0.4% of the total TGM in the boundary layer of Bayonne in the summer and winter, respectively. Moreover, all TGM concentrations measured at the SDM landfill and the NJDEP trailer during this project were well below chronic effects limits for total gaseous mercury (200 ng m^{-3}, Agency for Toxic Substances and Disease Registry-CDC; 300 ng m^{-3}, EPA).

In conclusion:

- PCB concentrations measured in the city of Bayonne are similar to those in other large urban and industrial areas in the U.S.
- PCB and Hg concentrations were elevated in the air above the SDM landfill relative to background concentrations in Bayonne, but are *orders of magnitude* below potentially adverse human exposure limits.
- Significant positive vertical concentration gradients of gas-phase PCBs and Hg were observed during most sampling events at the SDM landfill.
- Net sediment-air fluxes of PCBs and Hg at the sediment application site were found to be generally positive during the day, but low to negative at night.
- Vertical fluxes of PCBs and Hg were highly variable and dependent on atmospheric conditions as well as the age and condition of the SDM.
- The city of Bayonne is impacted to a greater extent by PCB sources from areas other than the SDM site.
- The emissions of Hg from SDM are estimated to contribute <5% of this contaminant to the air of Bayonne and adjacent areas.

Recommendations for Further Study

1. Controlled laboratory studies of the volatilization of Hg and PCBs from SDM are needed to understand the variability of contaminant fluxes observed in the field and to study the importance of SDM properties such as water and cement content, grain size, and temperature on the sediment side resistance to volatilization.

2. An analysis of aerosol phase PCBs and Hg is needed to understand the phase transitions, transport, and deposition fate of these contaminants.

3. Fine scale modeling of the local atmosphere is needed to predict the transport and impact of contaminants emitted from SDM landfills and, with back trajectory dispersion models, to determine the source(s) of high background concentrations of PCBs and Hg in the NY/NJ metro area including the large spikes of TGM observed at the NJDEP trailer.

4. Laboratory and field studies of the emissions of Hg and PCBs from native (untreated), tidally exposed estuarine sediments are needed to quantify this potentially important part of the cycles of these contaminants.

Acknowledgements

This project was supported by the New Jersey Marine Sciences Consortium and the New Jersey Department of Transportation, Office of Maritime Resources. We wish to thank Michael P. Weinstein (NJMSC) and Scott Douglas (NJDOT) for their guidance and support. This work was made possible by the efforts of Robert Miskewitz at Stevens Institute and Cari Giggliotti and Sandra Goodrow at Rutgers University. This is contribution no. NJSG_____ of the New Jersey Sea Grant College Program.

TABLE OF CONTENTS

LIST OF FIGURES

LIST OF TABLES

1.0 INTRODUCTION

The disposal of sediments that have been removed from navigation channels by maintenance dredging has become a significant problem for many ports and harbors. In New York Harbor maintenance dredging produces an annual volume of about $3x10^6$ m^3 of dredged material (Weinstein and Douglas, 2002). The annual maintenance dredging of all ports in the United States yields over $3x10^8$ m^3 of dredged material. Much of this material is contaminated and in recent years has been ruled unsuitable for ocean disposal. One alternative to ocean disposal is to use dredged materials, stabilized with cement or lime, as fill at construction or coastal restoration sites. The present study was conducted on a 50 ha site in Bayonne, New Jersey, USA (Fig. 1) where the use of stabilized dredged material (SDM) as a semi-impervious cap was permitted. This site, which is operated by the OENJ Cherokee Corporation, was a former town landfill and brownfield that was closed to dumping in 1983. It is estimated that this site will be able to accept 4.5 million cubic yards of SDM as structural fill at $29 per cubic yard.

Figure 1. Regional Map of the New York/New Jersey Harbor Estuary.

The dredged material at the Bayonne site comes from maintenance dredging operations in New York Harbor, primarily from the channels and berthing areas for container ships such as those in Newark Bay. These dredged sediments contain many types of contaminants including metals, polycyclic aromatic hydrocarbons, and polychlorinated biphenyls (PCBs). An evaluation of the emissions of volatile pollutants, specifically PCBs and mercury (Hg) is included in the dredge disposal permit at the Bayonne landfill site. The average PCB concentration in the sediments of New York Harbor exceeds 40 ppb on a dry weight basis (Ho et al., 2000). This value exceeds the concentration for toxic effects of PCBs in marine organisms. Among large East Coast urban estuaries, the lower NY/NJ Harbor Estuary has some of the highest concentrations of Hg in surface sediments (EPA, 1997).

At the OENJ Bayonne landfill site, dredged sediments are mixed with cement prior to placement and the resulting SDM contains 12% cement by weight. This processing of harbor sediments and their

subsequent placement on land could lead to the volatilization of gas phase PCBs and Hg. Enhanced gaseous PCB and Hg release from dredged sediments may occur during stabilization, drying, and compaction due to heat build up, or the chemical production of volatile forms of inorganic mercury including Hg° and $HgCl_{2(g)}$. The primary form of Hg in estuarine sediments is oxidized Hg(II) bound in sulfide solids or adsorbed to organic-rich mineral phases, with monomethylmercury (CH_3Hg) accounting for < 2% of the total (Mason and Lawrence, 1999). Sediment-bound Hg may become volatile upon exposure to sunlight as a result of the photochemical reduction of Hg(II) to Hg°. Quantifying the emissions of PCBs and Hg from native, processed, and land-applied sediments is an important part of the evaluation of the environmental impacts of various uses of dredge materials and our understanding of PCB and Hg cycles in urban harbors.

The objectives of this project were to determine background ambient gas phase PCB and Hg concentrations in Bayonne, NJ prior to and following the land application of SDM and to estimate vertical fluxes and horizontal gradients of PCBs and Hg at the SDM landfill. Vertical PCB and Hg fluxes above SDM were estimated using a micrometeorological approach that combined the Aerodynamic Gradient Method, previously used to measure land-air pesticide fluxes (Majewski et al., 1991) and the Eddy Correlation Method to provide turbulent correction parameters. Mean wind speed, temperature, water vapor, and PCB and Hg concentrations were measured at two elevations above the ground as required by the Aerodynamic Gradient Method. Simultaneous measurements of the vertical turbulent flux of momentum, sensible heat, and latent heat at an intermediate height were also collected to provide realistic turbulent correction parameters by the Eddy Correlation approach. The vertical fluxes of PCBs and Hg were calculated using the Thornthwaite-Holtzmann equation (Thornthwaite et al., 1939) modified to account for non-adiabatic conditions. The underlying theory for these methods is provided in the next section. This is followed by results, discussion and conclusions.

2.0 ESTIMATION OF VERTICAL ENERGY AND MASS FLUXES

2.1 Aerodynamic Gradient and Eddy Correlation Theory

Most natural flows are turbulent as opposed to laminar. In laminar flow, agitation of fluid particles is of a molecular nature and, hence, at submicroscopic scales. On the macroscopic, observational scales laminar flow appears to be one in which particles are constrained to move in parallel paths due to viscosity. Laminar flows are, in essence, predictable given knowledge of the molecular properties of the fluid. In contrast, turbulent flows are characterized by random fluctuations in particle velocities, and contain a random field of embedded vortices or eddies. Exchange processes in turbulent flows are substantially enhanced relative to laminar flows. In particular, the flux of momentum, characterized by the stress in the fluid is of concern. The momentum per unit mass in the horizontal, x, direction is simply the fluid velocity component in the x direction, u. The flux of x-component momentum in an orthogonal direction, say in the vertical, z, direction is the shear stress, τ. In laminar flows the shear stress τ is given by:

$$\tau = \mu \frac{\partial u}{\partial z}$$

where μ is the coefficient of dynamic viscosity and is solely a property of the fluid. For turbulent flow, an early study by Boussinesq (1877) proposed that this shear stress would be:

$$\tau = \varepsilon \frac{\partial u}{\partial z} \tag{1}$$

where $\partial u / \partial z$ is the vertical gradient in mean velocity and ε is an eddy viscosity several orders of magnitude greater than μ and except very close to boundaries it is a function of the flow and not of the fluid properties.

The modern approach to turbulent flow began with the investigations of Reynolds (1895) who introduced the idea of decomposing the instantaneous velocity into a deterministic mean part and a randomly fluctuation, i.e.,

$$u = \bar{u} + u' \tag{2}$$

where $\bar{u}$ is the average velocity and u' is the fluctuation. Reynolds' work showed that the sear stress, τ, can be written as:

$$\tau = -\rho \overline{u'_x u'_z} \tag{3}$$

where ρ is the fluid density, and $\overline{u'_x u'_z}$ is the time average covariance of the turbulent fluctuations in horizontal and vertical velocities. Taylor (1921) demonstrated that there is a diffusive action in the lower atmosphere that is clearly stronger than could be attributed to molecular diffusion. He proceeded to derive an "eddy diffusivity" which was independent of the item that was being diffused. Independently of Taylor, Prandtl (1926) related the turbulent fluctuations to the general flow by suggesting that small fluid parcels are transported by turbulence a mean distance, l, from regions of one velocity to regions of another and in doing so suffer changes in their general velocities of motion. The distance l, was termed the mixing length, and Prandtl stated that the change in velocity over the length l is proportional to the velocities in each direction:

$$\tau = -\rho \overline{u'_x u'_z} = \rho l^2 \left(\frac{du}{dz} \right)^2 \tag{4}$$

This expression can then be combined with equation (1) to get an expression for ε, the eddy viscosity:

$$\varepsilon = \rho l^2 \left(\frac{du}{dz} \right) \tag{5}$$

von Karmen (1921) related the results of Prandtl to the actual flow profile near a wall using the relation l = κz. In this expression l is Prandtl's mixing length, z is the height, and κ is a constant. This constant was found experimentally to have a value of 0.4, and is known as von Karmen's constant. Using the previous relation and substituting into Prandtl's equation for shear stress, an expression for the logarithmic distribution of wind speed can be reached:

$$\frac{\partial u}{\partial z} = \frac{\sqrt{\tau/\rho}}{\kappa z} \tag{6}$$

Instead of shear stress it is convenient to introduce u_*, the friction velocity, where $u_* = \sqrt{\tau/\rho}$. The mixing length and eddy viscosity concepts were developed in the study of turbulent shear stress. These concepts may be readily extended to predictions for evaporative and sensible heat loss. Thornthwaite and Holzmann (1938) were the first to explore the application of these ideas to evaporative flux from land. Following Schmidt (1925) the vapor flux in the turbulent boundary layer is expressed as:

$$E = -A\left(dq/dh\right) \tag{7}$$

where A is the Austausch (mixing) coefficient developed by Schmidt, and dq/dh is the vapor concentration gradient. The research of Prandtl and von Karman led to an expression for the Austausch coefficient using the concepts of mixing length and shear stress. This led to the following equation for the evaporative flux:

$$E = \frac{\kappa \rho u_* (q_1 - q_2)}{\ln \frac{z_2}{z_1}} \tag{8}$$

where q_1, and q_2 are specific humidity values at the heights z_1 and z_2 respectively with z_2 above z_1. The friction velocity in this expression may be replaced by integrating the velocity profile equation between h_1 and h_2 to get:

$$u_2 - u_1 = \frac{u_*}{\kappa} \ln\left(z_2/z_1\right) \tag{9}$$

Substituting for u_* yields

$$E = \frac{\kappa^2 \rho (q_1 - q_2)(u_1 - u_2)}{\left[\ln\left(z_2/z_1\right)\right]^2} \tag{10}$$

This is the Thornthwaite Holzmann equation and it can be used provided there are adiabatic conditions in the atmosphere. An exactly analogous approach can be undertaken to obtain the flux of sensible heat, H, from observations at two elevations of the temperature and velocity, i.e.

$$H = \frac{\kappa^2 \rho C_p (T_1 - T_2)(u_1 - u_2)}{\left[\ln\left(h_2 / h_1\right)\right]^2} \tag{11}$$

where C_p is the specific heat of the fluid at constant pressure.

When there is stable vertical density stratification, such as at night, or unstable vertical density stratification such as hot days with low wind the atmosphere cannot be modeled with these equations. The first evidence of departure from adiabatic profiles was given by Pasquill (1945, 1948). He conducted a large scale experiment and collected data that clearly demonstrated that under certain conditions, the profiles of wind speed, heat, and water vapor were stretched or contracted depending on the atmospheric stability. Richardson (1920) proposed a method for classifying the atmosphere as a compressible environment.

$$Ri = \frac{g}{T} \frac{\partial\theta / \partial z}{\left(\partial u / \partial z\right)^2} \tag{12}$$

where g is the acceleration due to gravity, T is the absolute temperature, and θ is the potential temperature. Three cases are given for this classification scheme; (1) if Ri < 0 stratification is unstable and the energy of turbulence is increased, (2) if Ri > 0 stratification is stable thus hindering the development of turbulence, and (3) Ri = 0 stratification is neutral and does not affect the formation of turbulence. Another measure of stability is L, the Monin Obukov length scale, given by (Obukov, 1946).

$$L = \frac{\rho C_p u_*^{\,3} \theta}{\kappa g H} \tag{13}$$

where H is the directly measured value of the sensible heat flux. This can be modified to account for the effects of water vapor by replacing H with (H+0.07Le). The term z/L can then be used a classification scheme similar to that for the Richardson Number. Monin and Obukov (1954) used similarity theory to derive expressions for the profiles of wind speed, temperature, and moisture content of the air and take into account the possibility of non-adiabatic conditions. These equations are as follows:

$$\frac{\partial u}{\partial z} = \frac{u_*}{\kappa z} \phi_M \tag{14a}$$

$$\frac{\partial \theta}{\partial z} = \frac{H}{\rho C_p \kappa u_* z} \phi_H \tag{14b}$$

$$\frac{\partial \rho_e}{\partial z} = \frac{Le}{\lambda \kappa u_* z} \phi_W \tag{14c}$$

where u_* is the friction velocity, κ is von Karman's constant, ρ is the air density, C_p is the specific heat of the air at constant pressure, H is the sensible heat flux, Le is the Latent heat flux, ρ_e is the vapor density, and λ is the latent heat of vaporization. The values ϕ_M, ϕ_H, and ϕ_W represent atmospheric

stability correction factors for momentum, heat, and water vapor, they represent the departure of the atmosphere from adiabatic conditions. For unstable vertical density stratification the values for ϕ become less than one while for stable stratification they become greater than one. These values can be solved for directly, or estimated empirically as either a function of Ri or z/L.

Values of the atmospheric stability correction factors can be determined using measurements from an aerodynamic gradient system that measures wind speed, temperature, and water vapor concentration at two heights, and an eddy correlation system that directly measures u_*, and the sensible and latent heat fluxes. These data can then be used to estimate the atmospheric stability correction factors via two methods: (1) assume that the value of the correction factor is constant over the measurement interval, or (2) take an average value of the factor over the interval.

The first case assumes that the atmospheric stability correction factor is constant over the measured interval. The benefit of this assumption is that the mathematics involved are simple and the error involved in making this assumption is relatively small. The main drawback to this assumption is that the factors are a function of either Ri or z/L, both of which are a function of height. The following equations are used to determine the values for ϕ_M, ϕ_H, and ϕ_W:

$$\phi_M = \frac{(u_2 - u_1)}{\kappa u_* \ln(z_2/z_1)} \tag{15a}$$

$$\phi_H = \frac{\rho C_p \kappa u_* (\theta_2 - \theta_1)}{H \ln(z_2/z_1)} \tag{15a}$$

$$\phi_W = \frac{\lambda \kappa u_* (\rho_{e2} - \rho_{e1})}{Le \ln(z_2/z_1)} \tag{15a}$$

These values make the assumption that ϕ_M, ϕ_H, and ϕ_W are not a function of the height of measurement. Otherwise integration of the equations presented in the previous section would yield very different results.

The second case takes an average value of atmospheric stability correction factor by comparing the measured profile to a theoretical profile over the interval from the two measurement heights. This method is based on two assumptions: (1) There is a logarithmic distribution of velocity, temperature, and moisture content over the distance between the ground and the highest point of measurement, and (2) that u*, H, and Le are all constant over the same distance. The second assumption is commonly made for the turbulent boundary layer of the atmosphere. The equation for the logarithmic boundary layer under adiabatic conditions is:

$$\frac{\partial u}{\partial z} = \frac{u_{*_A}}{\kappa z} \tag{16}$$

Where the u_{*A} is the frictional velocity under adiabatic conditions. This equation can be modified to account for non-adiabatic conditions.

$$\frac{\partial u}{\partial z} = \frac{u_{*N}}{\kappa z}\phi_M \tag{17}$$

Where the u_{*N} is the frictional velocity under non-adiabatic conditions. The wind speed gradients in both equations are equal because the represent a value measured in the field. When the second equation is divided into the first a relation between the u_* values is determined.

$$\phi_M = \frac{u_{*A}}{u_{*N}} \tag{18}$$

This quantity can readily be determined using the eddy correlation system to directly measure the value of u_{*N}, and the aerodynamic gradient measurements entered into the equation for the logarithmic boundary layer under adiabatic conditions to determine the value of u_{*A}. The value determined for ϕ_M will be the mean value over the distance between the two sensor arms of the aerodynamic gradient system. Using this method it is also possible to determine the values for ϕ_H and ϕ_W, although both include the term ϕ_M.

$$\phi_H = \frac{H_A}{H_N \phi_M} \tag{19}$$

$$\phi_W = \frac{\rho_{eA}}{\rho_{eN} \phi_M} \tag{20}$$

Much research has been performed to generate values for the atmospheric stability coefficients. The stability coefficients have to be determined for both stable and unstable conditions, many researchers have done so, and in the two following tables their results are summarized.

Table 1. Empirical values for ϕ 's under unstable conditions.

Authors	Comments	Heat	Water Vapor	Momentum
Swinbank (1968)	Using κ=0.4, u* observed from drag coefficient -0.1>z/L>-2	$\phi_H = 0.227\left(-z/L\right)^{-0.44}$		$\phi_M = 0.613\left(-z/L\right)^{-0.20}$
Webb (1970)	Profiles only, no direct flux measurement z/L>-0.03	$\phi_H = 1+4.5\left(z/L\right)$	$\phi_W = 1+4.5\left(z/L\right)$	$\phi_M = 1+4.5\left(z/L\right)$
Dyer and Hicks (1970)	Using κ=0.41, Comparison of direct eddy fluxes and profiles 0>z/L>-1	$\phi_H = \left(1-16\left(z/L\right)\right)^{-1/2}$	$\phi_W = \left(1-16\left(z/L\right)\right)^{-1/2}$	$\phi_M = \left(1-16\left(z/L\right)\right)^{-1/4}$
Businger *et al.* (1971)	Using κ=0.41, Comparison of direct eddy fluxes and profiles z/L>-2	$\phi_H = 0.74\left(1-9\left(z/L\right)\right)^{-1/}$		$\phi_M = \left(1-15\left(z/L\right)\right)^{-1/4}$
Pruitt *et al.* (1973)	Using κ=0.42, Richardson Number used for stability measure		$\phi_W = 0.885\left(1-22Ri\right)^{-0.4}$	$\phi_M = \left(1-16\left(Ri\right)\right)^{-1/3}$

Table 2. Empirical values for ϕ 's under stable conditions.

Authors	Comments	Heat	Water Vapor	Momentum
Webb (1970)	Profiles only, no direct flux measurement z/L>-0.03	$\phi_H = 1 + 5.2(z/L)$	$\phi_W = 1 + 5.2(z/L)$	$\phi_M = 1 + 5.2(z/L)$
Businger *et al.* (1971)	Using κ=0.41, Comparison of direct eddy fluxes and profiles z/L>-2	$\phi_H = 0.74 + 4.7(z/L)$		$\phi_M = 0.74 + 4.7(z/L)$
Pruitt *et al.* (1973)	Using κ=0.42, Richardson Number used for stability measure		$\phi_W = 0.885(1 + 34Ri)^{0.40}$	$\phi_M = (1 + 16(Ri))^{1/3}$

2.2 Chemical Contaminant Flux Estimation

The methods used for estimating the flux of contaminants from atmospheric measurements require knowledge of the gradient of contaminant concentrations in the measurement area as well as the atmospheric conditions. In order to use the atmospheric stability correction factors presented in the previous section to calculate contaminant flux estimates an assumption must be made. This assumption requires that the atmospheric stability function for contaminants, ϕ_C, is equal to ϕ_W. An equation for the profile of contaminants can be created in a manner similar to that for momentum, sensible, and latent heat.

$$\frac{\partial C}{\partial z} = \frac{F_c}{\kappa u_* z}\phi_C \tag{21}$$

If the first method for calculating atmospheric stability correction factors is used for the calculation of fluxes, the profile equation for contaminants can be integrated between heights z_2 and z_1 to yield:

$$C_1 - C_2 = \left[\frac{F_c}{\kappa u_*}\ln\left(z_2/z_1\right)\right]\phi_C \tag{22}$$

If we use the equation for (u_2-u_1) to eliminate the quantity ku_* in this second equation for concentration differences then it can be found that:

$$F_C = \frac{(u_2 - u_1)(C_1 - C_2)\kappa^2}{\left[\ln\left(z_2/z_1\right)\right]^2 \phi_C \phi_M} \tag{23}$$

This is the Thornthwaite-Holzmann Equation.

Substituting the velocity profile (Eq. 9) into Eq. 23 yields and alternative expression for the chemical flux:

$$F_C = \frac{u_* \kappa (C_1 - C_2)}{\ln\left(z_2/z_1\right)\phi_C} \tag{24}$$

Since, in the present observation, the friction velocity is directly measured this last equation may be used directly to find F_C.

The second method for calculating atmospheric stability correction factors will use the same initial equation while assuming that $\phi_C = 1$, thus adiabatic conditions are present. From this equation a value for the adiabatic flux, F_{CA}, is determined. Since values for ϕ_M and ϕ_C have been previously determined it is possible to estimate the flux of contaminants with the following equation:

$$F_{CN} = \frac{F_{CA}}{\phi_M \phi_C} \tag{25}$$

These two methods have been used in the determination of fluxes for the present study.

3.0 INSTRUMENTATION AND METHODS

3.1 Micrometeorological Systems

Micrometeorological data were collected in order to determine the vertical flux of PCBs. This was carried out using two micrometeorological systems purchased from Campbell Scientific of Logan, Utah, USA (www.campbellsci.com). The first, the Aerodynamic Gradient system, simultaneously measured temperature, vapor pressure, and wind speed at two heights, approximately one and three meters above the ground surface. The temperatures were measured with chromel-constantan thermocouples with a diameter of 74 μm. These thermocouples have a resolution of 0.006°C with 0.1 μV rms noise. The vapor pressures were measured by pumping air through a cooled mirror, dew point hygrometer (Model Dew-10, General Eastern Corp., Watertown, MA). Air is drawn from both heights continuously through inverted Teflon filters (Pore size 1 μm). The filters remove any dust or liquid water from the air stream. The hygrometer is equipped with a solenoid value that switches the air flow through the sensor between the two intakes for two minute intervals. The first minute of the interval is used to clear the air from the previous interval, while the second is used to collect the actual readings. The air is drawn at a flow rate of 0.4 l min^{-1} with 2 l mixing chambers to give a 5 min time constant. The Dew-10 has a resolution of approximately ±0.01 kPa. Wind speeds were measured using

R. M. Young 03001-5 Wind Sentries. These included a cup anemometer and a directional wind vane. The anemometer has a range of 0 to 50 m sec^{-1} with a threshold value of 0.5 m sec^{-1}. All measurements taken with the Aerodynamic Gradient system were averaged over twenty min intervals. The Aerodynamic Gradient system (Figure 2), as well as the PCB air samplers, are described in further detail in section 3.3 of this report.

Figure 2. Aerodynamic Gradient System.

The second system, the Eddy Correlation system (Figure 3), included quick response instruments capable of measurements at 10 hertz in order to resolve the turbulent fluctuations in vertical velocity, w', horizontal velocity, u', temperature, θ', and specific humidity, q', in the near surface atmosphere. These measurements were processed and averaged to give 5-min averages of friction velocity and latent and sensible heat fluxes. The Eddy Covariance system consists of three sensors, the CSAT3 is a 3-D Sonic Anemometer that can sample at 60 Hertz, with noise in the horizontal directions of 1 mm sec^{-1}, 0.5 mm sec^{-1} in the vertical, and at 0.002 ^{o}C for the sonic temperature measurement. The range of wind speed measurement is ±65.535 m sec^{-1}. The fluctuations in the moisture content of the air are measured using a KH2O Ultraviolet Krypton Hygrometer capable of measuring at rates up to 100 Hertz. The system also includes a FW05 fine wire thermocouple (0.0013 cm) that measures very accurately at high sampling rates and is not affected by solar radiation.

3.2 Meteorological Station

A standard 10 m high meteorological tower (UT30 Weather Station) was employed to measure atmospheric conditions. These included temperature, wind speed and direction, pressure, humidity, and rainfall. The temperature and relative humidity were measured using a HMP45C Temperature and Relative Humidity Probe with a Platinum Resistance Temperature Detector and a Vaisala HUMICAP

180 capacitive relative humidity sensor. The temperature sensor is accurate to within ±0.4°C over the operating range of the sensor (-40°C to +60°C). The relative humidity sensor is accurate to within ±3%. The wind speed and direction were measured with a Young 05103 Wind Monitor. Wind speed from 0 to 60 m sec^{-1} can be measured with an accuracy of ±0.3 m sec^{-1} with a threshold value of 1 m sec^{-1}. The wind direction is measured accurately to within ±3°. The barometric pressure was measured with a CS105 Barometric Pressure Sensor which measures barometric pressure over 600 to 1060 mBar range with an accuracy of ±0.5 mBar @ +20°C. Finally the rainfall was measured using a TE525WS Tipping Bucket Rain Gage. The bucket Tips at 0.03 mm increments and is accurate to ±1% at rate of up to 2.5 cm h^{-1}.

Figure 3. Eddy Correlation System.

3.2 Gas Phase PCB Sampling

Gas-phase PCB samples were collected using high-volume air samplers (Tisch Environmental, Village of Cleves, OH) operated at a calibrated airflow rate of ~800 l min^{-1}. Gaseous PCB samples were collected over four hour sampling periods on solvent-cleaned polyurethane foam plugs (PUF) from air that had passed through pre-combusted quartz fiber filters (QFF). The two high-volume samplers used to measure vertical PCB concentration gradients above SDM were modified to sample air at the two heights of the micrometeorological sensors. This was accomplished using flexible aluminum duct. The high-volume samplers consist of a vacuum pump and a manometer to measure the air flow rate through the sampler. The sampler's manometers were calibrated prior to and following each sampling event to ensure that flow measurements were accurate. Manometer calibration was carried out using a Tisch Adjustable Orifice Calibrator at five known air flow rates that were chosen to bracket field sampling flow rates. A linear regression was then used to determine the actual flow rate in the field. Calibrations run with an $r^2 < 0.98$ were rejected and the calibration was repeated.

3.4 Total Gaseous Hg Sampling

Total gaseous mercury was measured continuously in ambient air using a Tekran Model 2357A Mercury Vapor Analyzer (Tekran Inc., Toronto, Canada). Air was sampled at a flow rate of 1.5 l min^{-1} for a period of five-min during which time total gaseous mercury is concentrated by amalgamation onto one of two gold traps. At the Bayonne landfill, vertical TGM concentration gradients were determined from two five-min air samples collected at each of two heights above the SDM using the Synchronized Two-Port Sampler (Tekran, Model 1110) thereby reducing the potential for cartridge bias.

3.5 Field Work

Background ambient monitoring of atmospheric PCBs commenced on 8 December 1999 at the NJDEP air-sampling trailer located in Bayonne, NJ adjacent to Newark Bay (Figure 4). Twenty-four hour integrated air samples were collected at this site every 12 days for a total of 30 air samples.

Intensive sampling campaigns at the SDM landfill in Bayonne, NJ were carried out during four days in July 2001, three days in August 2001, three days in October 2001, three days in May 2002, and three days in November 2002. During these intensive sampling campaigns, air samples were collected at the NJDEP trailer on the west side of the Bayonne Peninsula for background PCB and Hg concentrations and above recently placed stabilized sediment and the SDM application site in Bayonne for the assessment of vertical fluxes (Figure 4). Additional PCB samples were collected at sites on the perimeter of the SDM application site in Bayonne to assess horizontal gradients. At the start of each

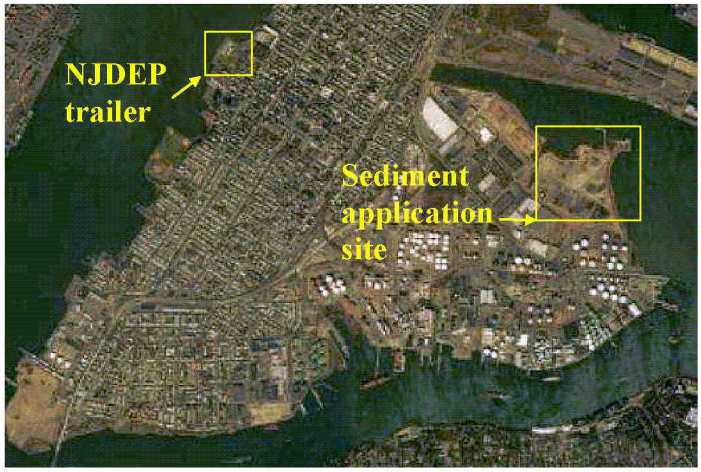

Figure 4. Aerial view of the Bayonne peninsula showing the sediment application site and the NJDEP air monitoring trailer where background concentrations of PCBs and Hg were measured.

sampling campaign, OENJ personnel were consulted to identify an appropriate site for the vertical flux measurements and every effort was made to place the sampling apparatus on top of recently placed SDM. Sampling was conducted over SDM under three conditions: On 1 August 2001, a sample was taken over recently laid, un-treated dredged material; on 29-30 August 2001, samples were taken over SDM that had been in place for three weeks; and on 23-25 October 2001, 6-8 May 2002, and 13-15

November, 2002, samples were taken over recently placed SDM. Weather conditions as well as forecasts for the following days were also taken into account in order to ensure that air would pass over freshly placed dredge prior to contact with sampling equipment. The micrometeorological systems were assembled and run on DC power from 12 volt batteries and once started, were allowed to collect data continuously for the length of the sampling campaign, unless there was a rain event.

For the vertical gradient measurements, air sample intakes for PCB and Hg samplers were placed downwind of the micrometeorological systems and the intakes attached to the upper and lower sampling bars. The samplers were powered by 1 kW portable generators, placed approximately 15 m downwind of the sampling location. PUF sampling media was brought to the site at the start of each day. Prior to being brought to the site, all PUFs were placed in glass sleeves in the lab and wrapped in aluminum foil. In this manner, they were easily placed in the sampler and the amount of time they were exposed was reduced. PCB samplers were run for 4 h during each sampling event; the flow rate was recorded at the beginning of the 4 h periods and periodically during each interval. At the conclusion of the 4 h interval, the samples were removed and labeled and the elapsed time was recorded to determine the total flow. Sampling campaigns were 3 to 4 days and encompassed day and night-time sampling. At the end of each day the samples were brought back to the laboratory, where they were removed from the sample holders and placed in extraction cells.

3.6 Chemical Analyses

Gas phase PCBs

The vertical gradient PUF samples were extracted using a Dionex ASE 300 Accelerated Solvent Extractor using dichloromethane. The extractions were done at 100 °C and at 1500 psi. The samples were then concentrated using a Rotary Evaporator. The concentrated extract requires a clean-up step prior to analysis. This was done using Supelclean LC-Florisil SPE Tubes. The samples were passed though the Florisil, which is then rinsed with hexane to ensure that none of the sample is retained in the Florisil. The elution is then concentrated with nitrogen.

Perimeter and background (NJDEP trailer) PUF samples were spiked with a surrogate standard and extracted in Soxhlet apparatus for 24 h in petroleum ether. The sample extracts were concentrated using rotary evaporation (Büchi Model RotoEvaporator111) to ~2 ml and the solvent switched to hexane. The extracts were transferred to 12 ml amber vials and blown-down with a nitrogen-evaporator (Organomation Associates 111) under a steady stream of purified N_2 gas to ~0.5 ml.

The samples were then fractionated on a 3% water deactivated alumina column (Brockman neutral activity 1- mesh size: 60-325). The first elution using 12ml of hexane was captured in centrifuge vials which were then concentrated by a gentle stream of purified N_2 gas and transferred to 2ml vials. Copper granules were 'activated' with a 1 N solution of HCl and placed into the sample vials prior to injection into the gas chromatograph-electron capture detector (GC-ECD) to remove any sulfur chromatographic interferences resulting from the high sulfur content of the sediment.

Congener-specific quantification of PCBs was performed by GC-ECD using a 60 m, 5% diphenyl-dimethylpolysiloxane column (DB-5: 60m, 0.32 mm ID, 0.25 mm film thickness). Hydrogen was used as the carrier gas and a P5 mixture (5%-CH_4, 95% Ar) was used as the make-up gas.

Quality assurance and quality control were determined using laboratory blanks and field blanks. Laboratory blanks are used to assess the potential for contamination of samples in the laboratory during handling and processing. PCB masses in the laboratory blanks (n = 19 laboratory blanks) were low relative to the masses in the samples accounting for from 0.1 to 3 % of the total PCB mass in PUF samples. Therefore, a correction for laboratory contamination was unwarranted. Field blanks, used to determine PCB detection limits, consisted of PUFs placed into the samplers with no air flow. The method detection limits, defined as the mass plus three times the standard deviation of the mass in the site-specific field blank ranged from 9.1 pg (PCB congeners 137+176+130) to 1030 pg (congeners 8+5) and from 8.3 (PCB congeners 137+176+130) to 1080 pg (PCB congeners 81+87) for gas phase PUFs at the NJDEP trailer site and the sediment application site, respectively. Average PUF field blank masses accounted for 1.5 % and 2.9 % of the total sample masses for the NJDEP trailer site and the sediment application site, respectively. Average PUF field blank masses accounted for from 0.3 to 7% of the total sample masses.

Total gaseous Hg

Trapped Hg collected with the Tekran 2537A was automatically quantified in the field by cold vapor atomic fluorescence spectrometry (CV-AFS) following thermal desorption (Schroeder et al., 1995). Alternating sample collection and analysis on the Tekran's two gold traps allowed for continuous sample analysis. The significance of the vertical TGM concentration gradients was evaluated using the percent gradient (PG) method (Kim and Kim, 1999). In this method, the percent difference of the vertical concentration gradient (percent gradient) is compared with the analytical uncertainty. Analytical uncertainty was evaluated as the coefficient of variation (standard deviation divided by mean x 100) of replicate measurements over a 30 min period at the NJDEP trailer site (n = 6) and was found to be 1.3 %. Vertical gradients whose percent difference values were greater than twice the analytical uncertainty (2 x 1.3 % or 2.6 %) were considered significant and used to estimate positive or negative fluxes. Gradients whose percent difference values were less than the analytical uncertainty were assigned vertical fluxes of zero. The percent gradient was evaluated according to the following equation:

$$\text{Percent gradient} = \frac{|TGM_{lower} - TGM_{upper}|}{TGM_{lower}} \times 100 \qquad (26)$$

5.0 RESULTS

5.1 Gas Phase PCB Concentrations in Bayonne, NJ and at the SDM Landfill

For the period of December 1999 – November 2000, background gas phase ΣPCB concentrations measured at the NJDEP trailer in Bayonne ranged from 0.27 to 3.7 ng m^{-3} and averaged 1.8 ng m^{-3} (Figure 5). Gas phase PCB concentrations varied seasonally with the highest concentrations occurring in the summer and fall and the lowest in the winter and spring. Although concentrations differed seasonally, the relative PCB congener profiles were statistically similar among all four months (winter vs. spring: r^2=0.88, $p<0.001$; winter vs. summer: r^2=0.80, $p<0.001$; winter vs. fall: r^2=0.85, $p<0.001$; spring vs. summer: r^2=0.83, $p<0.001$; spring vs. fall: r^2=0.73, $p<0.001$; summer vs. fall: r^2=0.92,

p<0.001). The highest individual ΣPCBs concentrations occurred under predominantly northeast winds from over the city of Bayonne and the lowest ΣPCB concentrations occurred when winds were out of the west across Newark Bay.

Average PCB concentrations measured around the perimeter of the sediment application site were 1.5 to 2-fold higher than Bayonne background concentrations measured at the NJDEP trailer site (Figure 6). Average ΣPCB concentrations during the July 2001 campaign were 7128 pg m^{-3} and 3945 pg m^{-3} at the perimeter of the sediment application site and the Bayonne trailer site, respectively. For the October 2001 campaign, average ΣPCB concentrations were 2857 and 1284 pg m^{-3}, respectively. For the May 2002 campaign, average ΣPCB concentrations were 1604 and 947 pg m^{-3}, respectively. For the November 2002 campaign, average ΣPCB concentrations were 1644 and 881 pg m^{-3}, respectively.

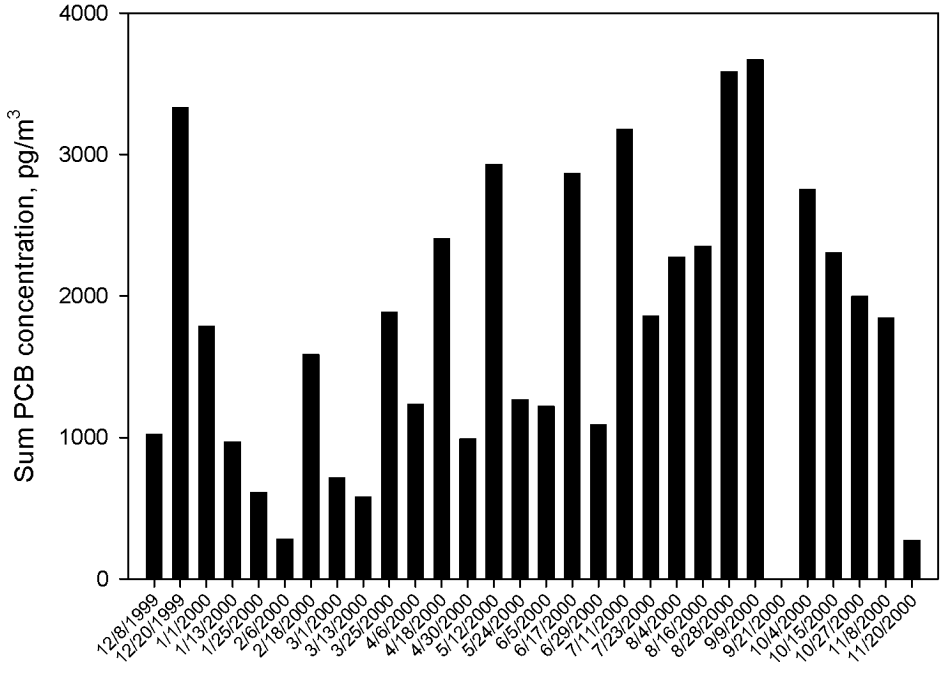

Figure 5. Gas phase ΣPCB concentrations measured at the NJDEP Bayonne trailer site for the year of Dec 1999 – Nov 2000.

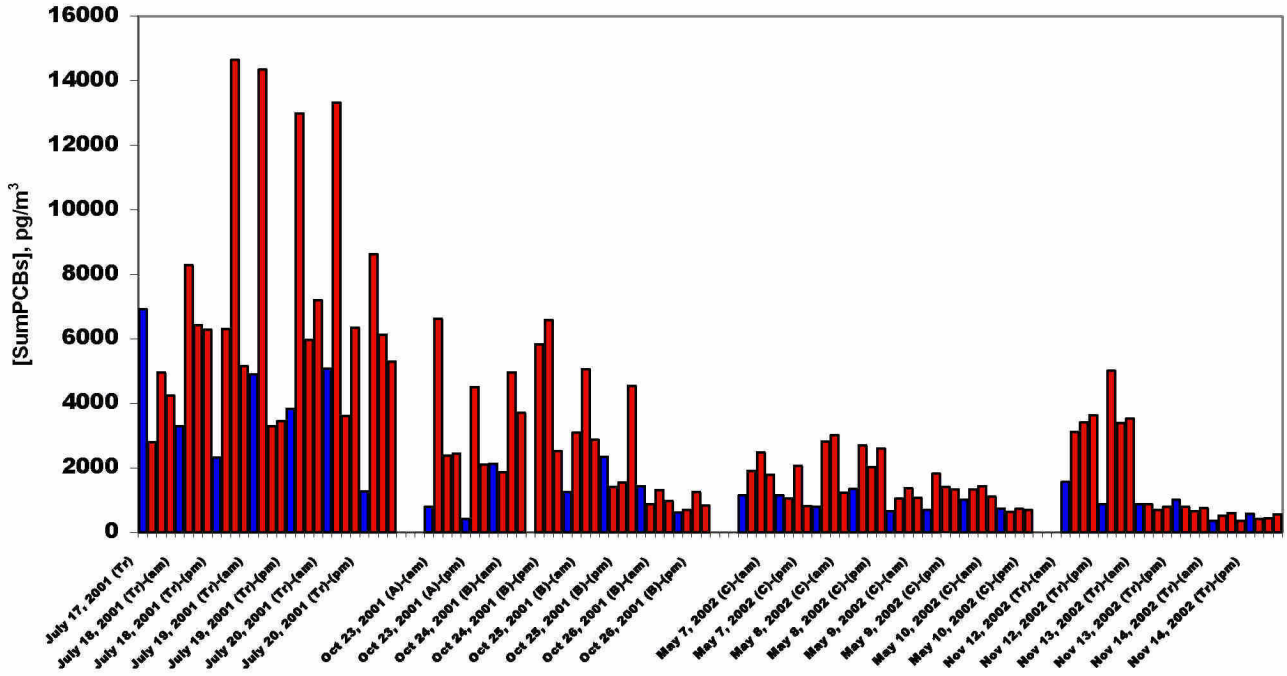

Figure 6. Concentrations of gas phase PCBs measured at the trailer site (blue) and at the perimeter of the sediment application site (red).

5.2 Total Gaseous Hg Concentrations in Bayonne, NJ and at the SDM Landfill

The average concentration of total gaseous mercury (TGM) measured at the NJDEP trailer in Bayonne, NJ for the period of September 2001 to February 2003 was 2.2 ng m^{-3}, a value consistent with background levels for the Northern Hemisphere (Slemr and Langer, 1992). Average monthly Hg vapor concentrations ranged from 1.69 ng m^{-3} (January 2003) to 3.34 ng m^{-3} (June 2002) and the range and variability of TGM concentrations was generally lower in the winter than in the summer (Table 3; Figure 7). However, throughout the monitoring period, "spikes" of elevated Hg that lasted for fifteen minutes to a few hours and occurred primarily between the hours of midnight and 0500 were observed at the NJDEP trailer. The highest concentration among these spikes (54 ng m^{-3}) was recorded on 30 June 2002 (Figure 8). No relationship between the occurrence of these spikes and meteorological conditions has been found. Average total gaseous Hg concentrations were significantly higher ($p < 0.01$) at the sediment application site than at either the Bayonne or New Brunswick background sites (Figure 9). The average background TGM concentration for samples collected on the days before and after intensive field campaigns at the SDM landfill was 1.8 ng m^{-3} compared with an average of 3.2 ng m^{-3} measured at the landfill.

Table 3. Monthly average total gaseous mercury (TGM) concentrations at the NJDEP trailer site in Bayonne, NJ.

	TGM (ng m^{-3})			
Month	**Average**	**Min**	**Max**	**n**
February 2002	2.15	1.38	5.89	0
March 2002	2.02	1.46	18.62	4804
April 2002	2.19	1.62	11.82	1858
May 2002	2.31	1.15	34.62	2344
June 2002	3.34	1.28	53.86	5017
July 2002	2.70	1.46	21.67	2699
October 2002	1.75	0.51	20.74	6604
November 2002	1.82	0.53	27.93	3147
January 2003	1.69	0.98	18.01	3279
February 2003	1.96	1.55	6.47	969

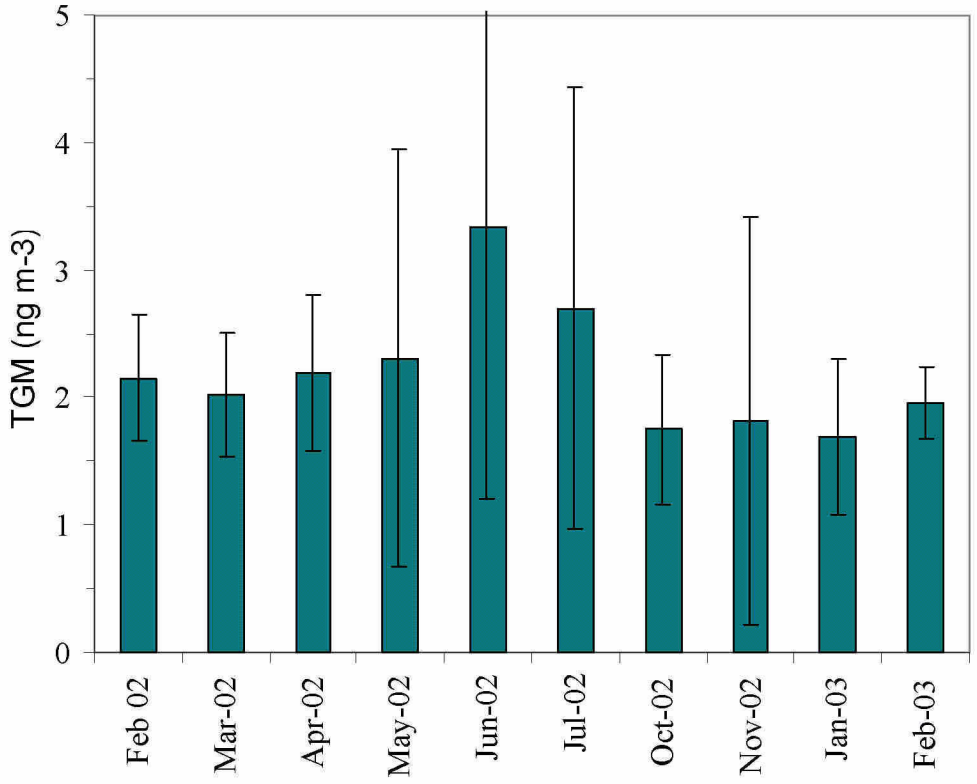

Figure 7. Monthly average total gaseous mercury concentrations at the NJDEP trailer site in Bayonne, NJ for the period February 2002 – February 2003.

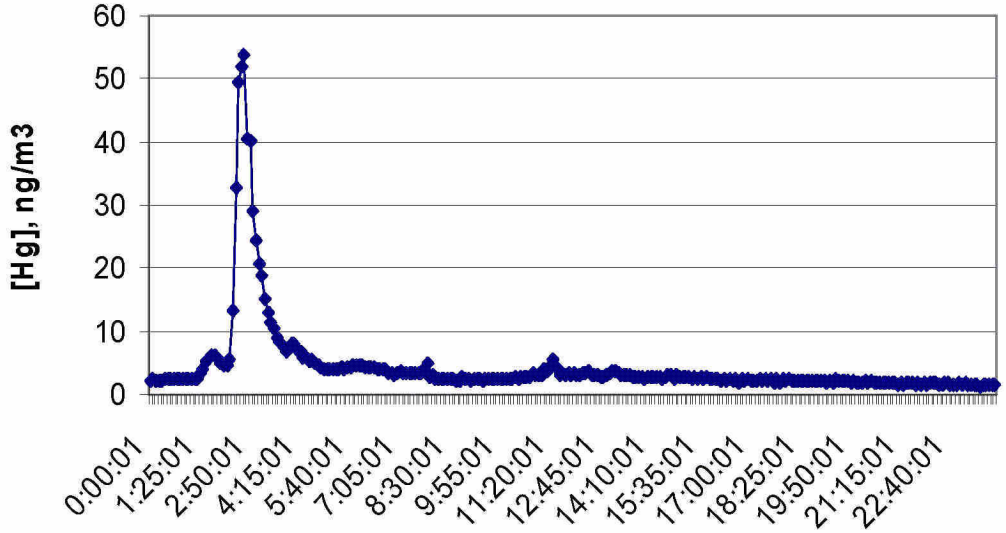

Figure 8. Total gaseous mercury concentrations at the NJDEP trailer site in Bayonne, NJ on 30 June 2002.

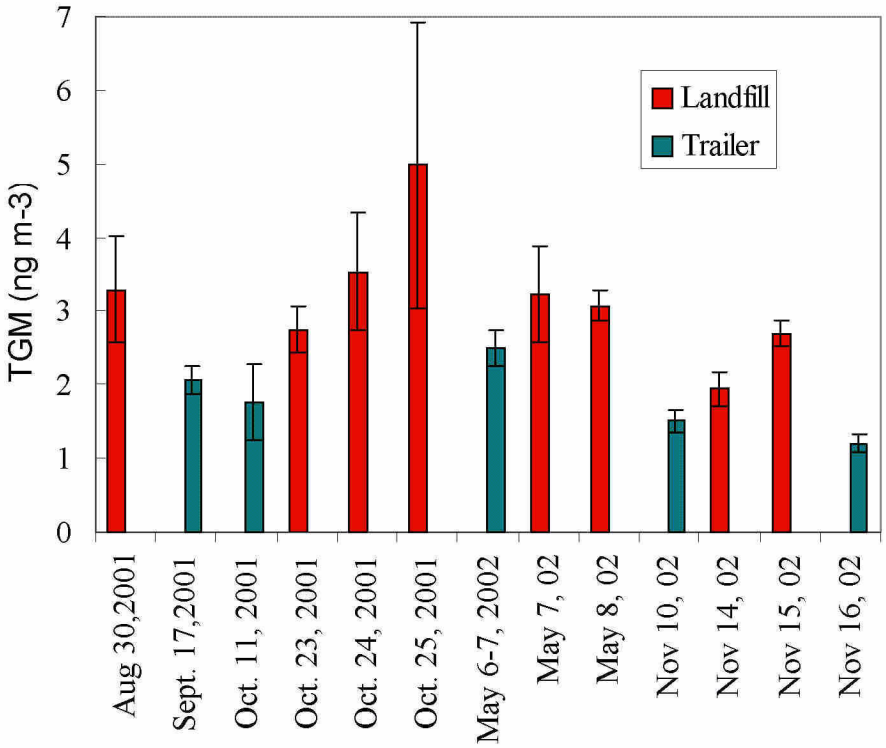

Figure 9. Average total gaseous mercury (TGM) concentrations at the SDM landfill and the NJDEP trailer during intensive field campaign.

5.3 Summary of Vertical Fluxes of PCBs and Hg at the SDM landfill

Micrometeorological estimates of sediment-air fluxes of gas phase PCBs and Hg from SDM are summarized in Tables 4 and 5. Positive vertical fluxes (sediment-to-air) were observed during 16 of 20 sampling periods for ΣPCBs and in 14 of 15 sampling periods for Hg. Negative fluxes do not necessarily indicate net absorption of the contaminants by SDM; they may be the result of variable atmospheric conditions during those sampling periods that resulted in inverted concentration gradients (lower near the SDM surface). Vertical PCB fluxes ranged from 72 to 15,000 ng m^{-2} h^{-1} and were highest in during the May 2002 campaign (Table 4). Nighttime PCB fluxes were an order of magnitude lower than daytime fluxes. Sediment-air fluxes of Hg fluxes ranged from 17 to 1043 ng m^{-2} h^{-1} and, like the PCB fluxes, were highest in May 2002 (Table 4). The percent difference in vertical TGM gradients measured at the SDM landfill site ranged from 0.3% to 32.3% (Appendix 6). With an analytical uncertainty of 2.6% in the difference between paired measurements, 86% (97 out of 113) of all gradients recorded were significant and indicative of net (positive or negative) sediment-air Hg fluxes. The single nighttime Hg flux estimate for 7 May 2002 was less than 3% of the average daytime fluxes observed in during the May 2002 campaign.

Table 4. Sediment-air fluxes of gas phase PCBs and meteorological parameters at the SDM landfill in Bayonne.

Date	Local Time	Wind speed ($m\ s^{-1}$)	Temp (^0C)	Vertical gradient (ng m^{-3})	Flux (ng m^{-2} h^{-1})
08/01/01	1030-1245	2.0	28	0.62	201
	1245-1441	3.0	29	0.62	134
08/29/01	2225-0210	2.2	21	-0.49	-47
08/30/01	1030-1430	4.7	29	-5.07	-1944
10/23/01	1020-1400	4.3	32	-0.42	-106
	1430-1807	6.7	27	3.51	1276
10/24/01	1020-1419	2.2	26	8.53	2205
	2010-2330	3.7	22	1.56	326
10/25/01	0800-1200	3.3	28	3.72	1366
05/06/02	1230-1530	3.4	24	6.38	14871
	1530-1830	4.2	21	2.12	4207
05/07/02	0930-1230	2.4	23	1.82	1987
	1300-1600	3.4	26	2.37	2332
	2000-2315	0.9	21	1.05	72
05/08/02	0930-1230	4.3	19	0.97	2877
11/13/02	1537-1930	5.6	9	0.24	76
11/14/02	0815-1130	3.3	7	0.71	492
	1200-1500	2.7	13	0.48	260
	1630-1945	3.7	12	-0.08	-17
11/15/02	0830-1130	4.2	11	0.24	74

Table 5. Sediment-air fluxes of gas phase Hg and meteorological parameters at the SDM landfill in Bayonne.

Date	Local Time	Wind speed ($m\ s^{-1}$)	Temp (^0C)	Average vertical gradient ($ng\ m^{-3}$)	Flux ($ng\ m^{-2}\ h^{-1}$)
8/30/01	1310 - 1436	3.6	25	0.42	187
10/23/01	1100 - 1200	3.9	19	0.23	30
	1320 - 1330	4.3	19	0.46	139
10/24/01	1235 - 1555	2.6	29	0.78	156
10/25/01	1110 - 1120	7.6	26	2.11	559
	1445 - 1455	8.0	26	0.84	310
5/07/02	1045 - 1200	1.9	21	0.91	1043
	1205 - 1455	3.6	24	0.32	314
	2030 - 2305	1.3	24	0.29	19
5/08/02	0955 - 1210	4.6	20	0.45	966
	1330 - 1600	5.1	19	0.26	552
11/14/02	1000 - 1150	3.8	11	0.05	34
	1210 - 1635	3.1	13	0.03	17
11/15/02	0920 - 1150	3.8	13	-0.04	-13
	1210 - 1400	3.8	15	0.11	41

5.4 17-20 July 2001 Sampling Campaign

Background and Perimeter Gas-Phase PCBs

In July 2001, samples for gas-phase PCBs were taken simultaneously around the perimeter of the SDM landfill and the NJDEP trailer site. The three high-volume air samplers were labelled A, B and C. Station A was located adjacent to the front entrance security gate, station B was located about 9 m from the meteorological tower, and station C was located near the pug mill on the Hudson River side of the site (see Figure 20 below). A total of 34 (28 samples plus 6 field blanks) air samples were taken during this campaign. Samples were taken in the morning (0900 – 1300) and in the afternoon (1300 – 1700) on each day at both sites. ΣPCB (n= 93 congeners) concentrations ranged from ~1200 to 7000 pg m^{-3} at the trailer site and ~3000 to 15000 pg m^{-3} at the SDM landfill perimeter sites during the July sampling campaign (Figure 6). Vertical PCB and Hg concentration gradients were not measured during this campaign.

5.5 1 August 2001 Sampling Campaign

SDM landfill site conditions

During the 1 August 2001 sampling campaign, vertical PCB fluxes were measured on an access road leading from the pug mill along the waterfront on the eastern side of the SDM landfill site (Figure 10). The wind was from the southwest. Directly adjacent to the experimental set-up and up-wind was a lagoon of one-day old un-stabilized dredged material. The weather conditions at the site are summarized in Figure 11. The sampling interval was from 1040 to 1440 PM. During the first three hours of sampling, the wind was blowing across the dredged material. In final hour the wind direction changed such that it was blowing off the water and there was a pronounced change in the observations.

Figure 10. Bayonne landfill site conditions, 1 August 2001.

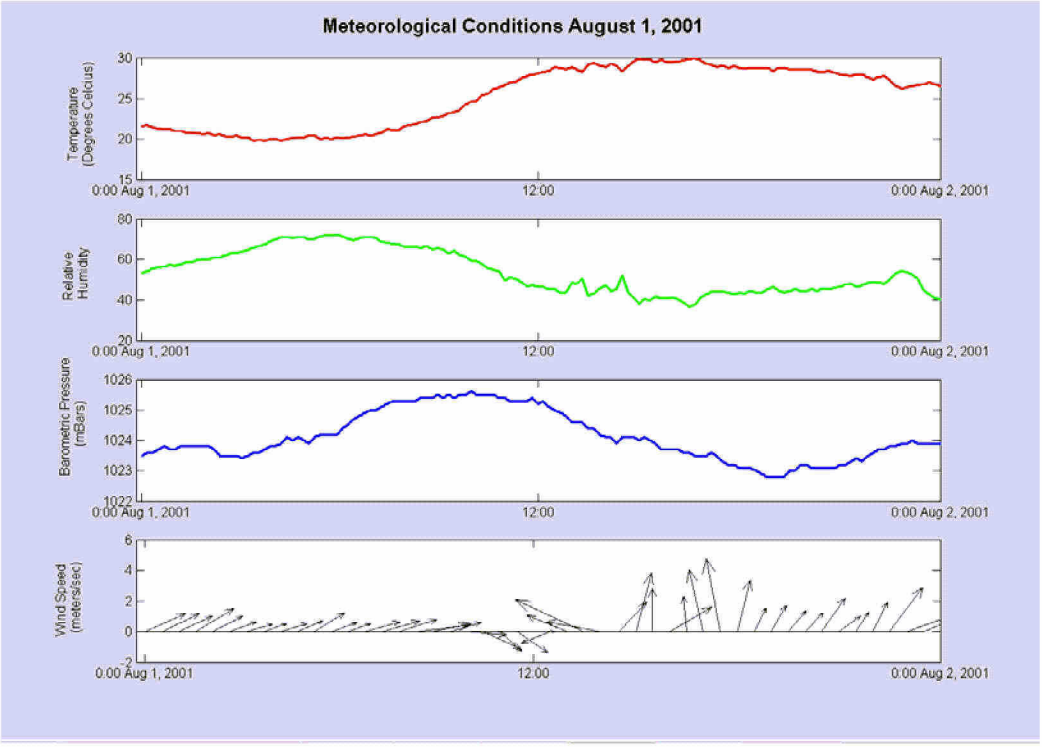

Figure 11. Meteorological conditions at the Bayonne landfill site, 1 August 2001.

The change in conditions also had an impact on the micrometeorological observations. The wind speed gradient in the last two hours dropped from 0.3 to 0.1 m s^{-1} over the two meter elevation difference, while the u_* values were only slightly changed. The temperature gradient in the last two hours decreased from > 1 ^{0}C to < 0.2 ^{0}C over the 2 m elevation difference, while the Latent Heat Flux increased from 250 to 500 watts m^{-2}. The Sensible Heat Flux remained nearly constant through out the sampling interval with values ranging from 100 to 160 watts m^{-2} (Figure 12). These changes indicate a shift from stable conditions to unstable conditions that would facilitate the flux of PCB from the drying sediment. Vapor pressure data obtained on this date were found to be incorrect due to a calibration problem. Subsequent discussion with the manufacturer uncovered the problem, which was corrected for the remainder of the sampling campaign. Average values of ϕ_M and ϕ_H were found to be 0.704 and 0.974 respectively. Due to the aforementioned problem with the vapor pressure data, the ϕ_H value was used in place of ϕ_W in the calculation of PCB flux. It has been shown in studies by Pruitt et al. (1973), that for slight departures of atmospheric stability from a neutral condition, that ϕ_W has approximately the same value as ϕ_H.

Vertical PCB Fluxes

The ΣPCB concentrations at 1.03 m and 3.04 m above the surface were 13.2 ng m^{-3} and 12.5 ng m^{-3}, respectively. The congener distribution on August 1 was greatly skewed toward the lower molecular weight PCBs (Appendix 8, Figure 1). This pattern was repeated for most of the samples taken at the site during this project.

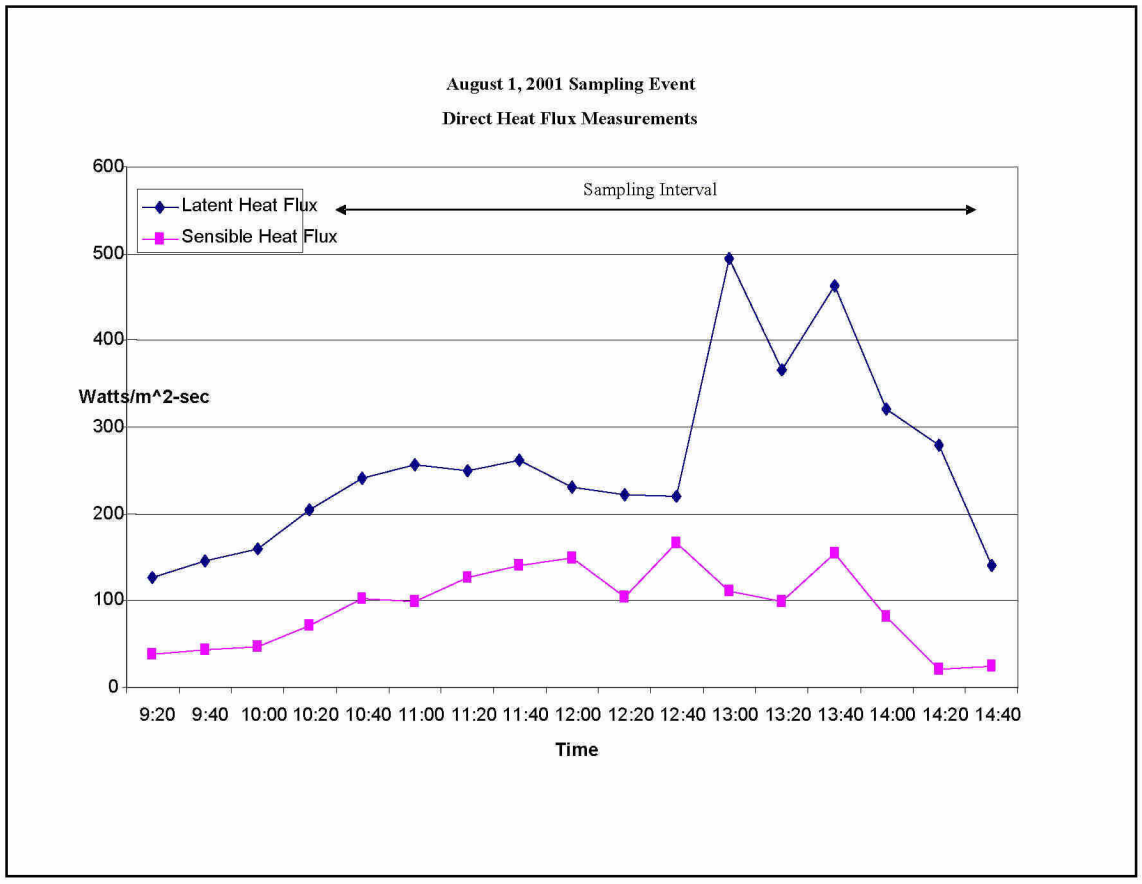

Figure 12. Latent and sensible heat fluxes at the Bayonne landfill sampling site, 1 August 2001.

Although the gradient of ΣPCB concentrations at the two heights would appear to denote a flux into the ground, if the various PCB homologues are evaluated separately a different picture emerges. For example, since only the lower molecular weight congeners will volatilize, then it seems reasonable to assume that some subset of the lighter PCB congeners will dominate the sediment-air flux. Estimates of the vertical fluxes for each PCB homologue group are presented for the August and October 2001 sampling campaigns in Figure 13.

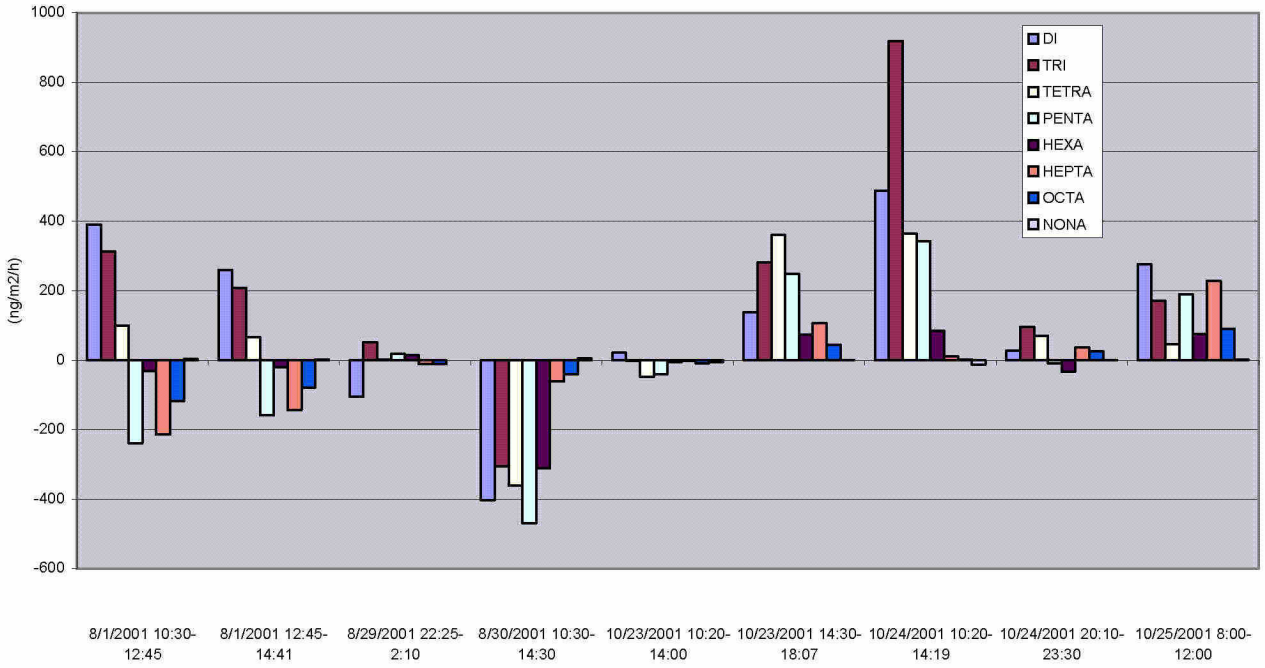

Figure 13. PCB homologue flux rates at the Bayonne landfill, 1 August 2001.

5.6 29-30 August 2001 Sampling Campaign

SDM Landfill Site Conditions

Although dredge material was not being delivered on site during sampling, the experimental set up was erected on recently spread stabilized dredge material. The material had been stabilized three weeks prior, however it was dug back up and spread in the two days prior to sampling. The wind was from the Northwest. The Eddy Correlation System, Bowen Ratio System, and air samplers were set up and run for approximately four hours at three separate time intervals. Sampling occurred during the day on the 29th and 30th, and overnight on the 29th. Due to equipment failure, PCB concentrations were not determined during the daytime on August 29th. The site conditions for the two sampling intervals are shown in Figures 14 and 15. The weather conditions are summarized in Figure 16.

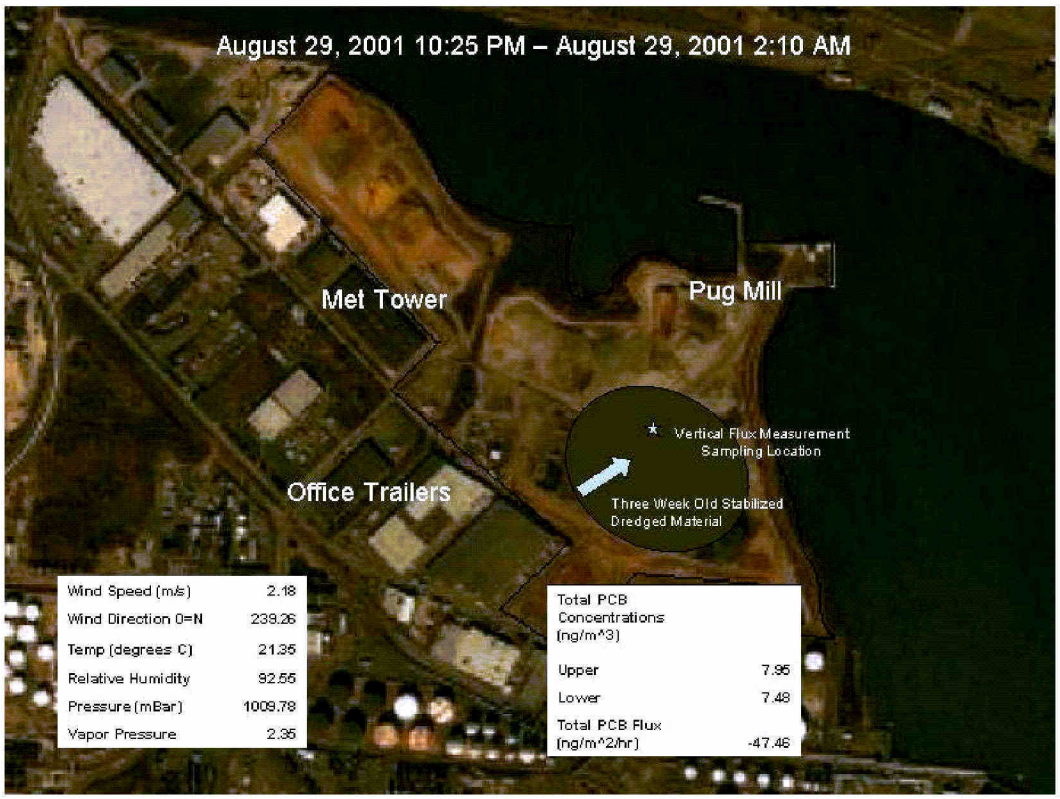

Figure 14. Bayonne landfill site conditions, 29-30 August 2001.

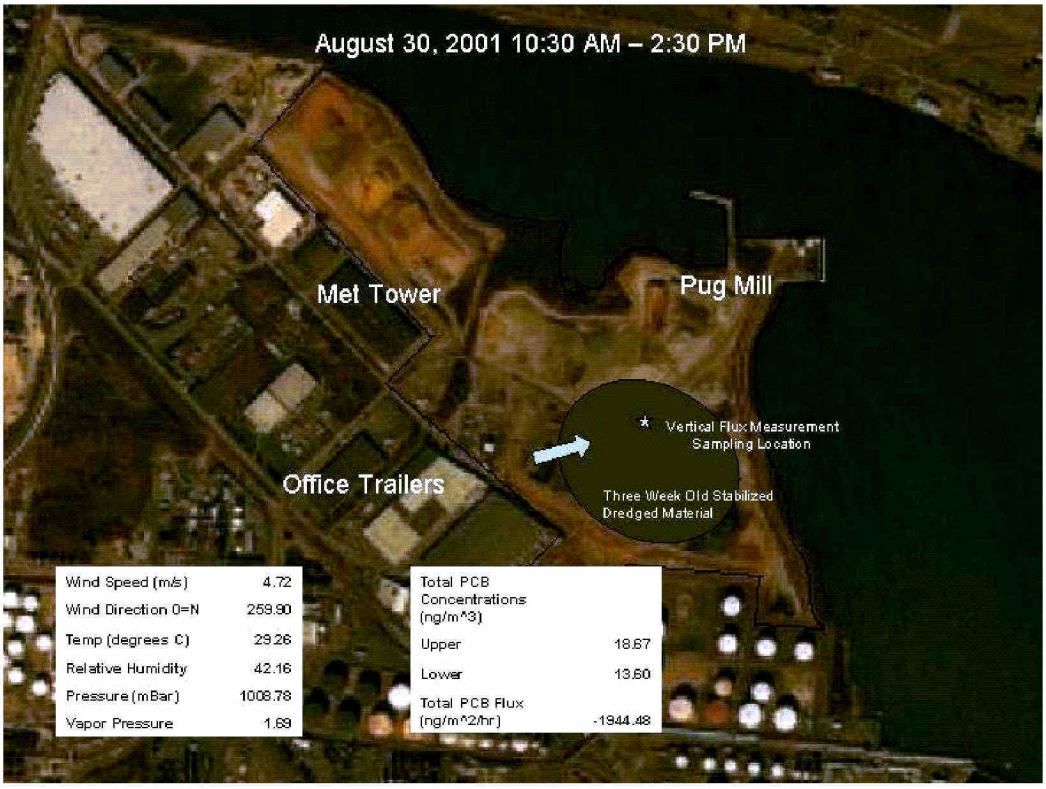

Figure 15. Bayonne landfill site conditions, 30 August 2001.

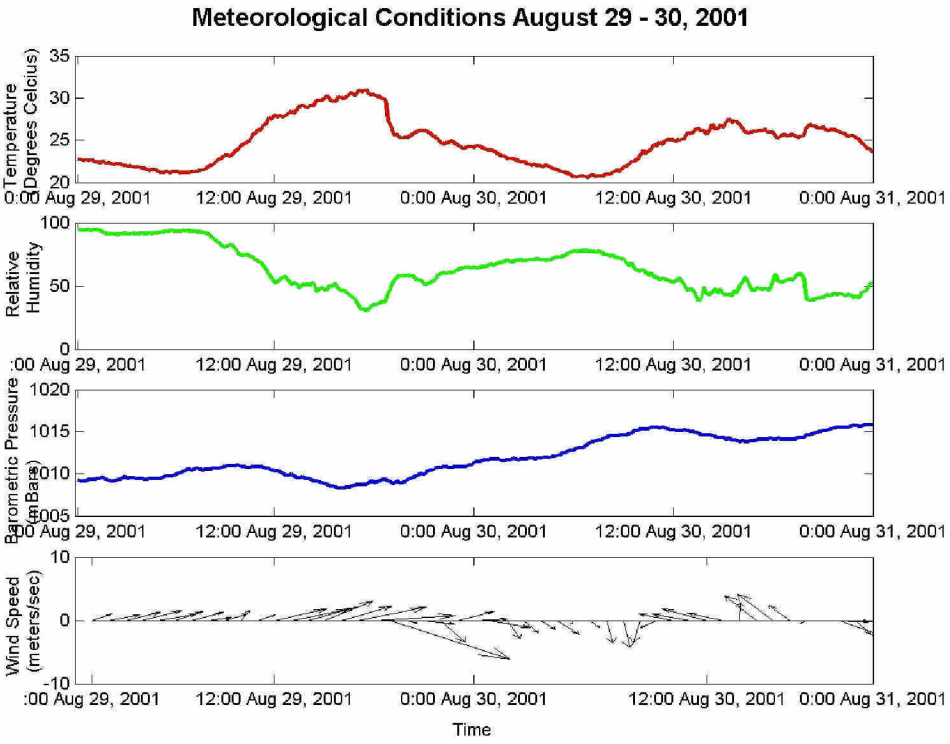

Figure 16. Meteorological conditions at the Bayonne landfill site, 29-30 August 2001.

All system worked well during this deployment including the vapor pressure measurements at two heights. After extensive consultation with personnel at Campbell Scientific the problems with the calibration procedure for the cooled mirror hygrometer in the Bowen Ratio System were completely resolved. During this deployment there were no apparent problems with the vapor pressure measurements.

Measurements of sensible heat flux were made for the three sampling intervals. On 29 August, these revealed a positive heat flux during the day of the order of 130 watts m^{-2}, while during the night sampling a negative heat flux (into the ground) of the order of –10 watts m^{-2} was found. During August 29th, a positive heat flux of the order of 120 watts m^{-2} was found. During these same consecutive sampling times the latent heat flux values were 200 watts m^{-2}, 34 watts m^{-2} and 100 watts m^{-2} respectively. The heat flux measurements for the nighttime sampling interval are shown in Figure 17.

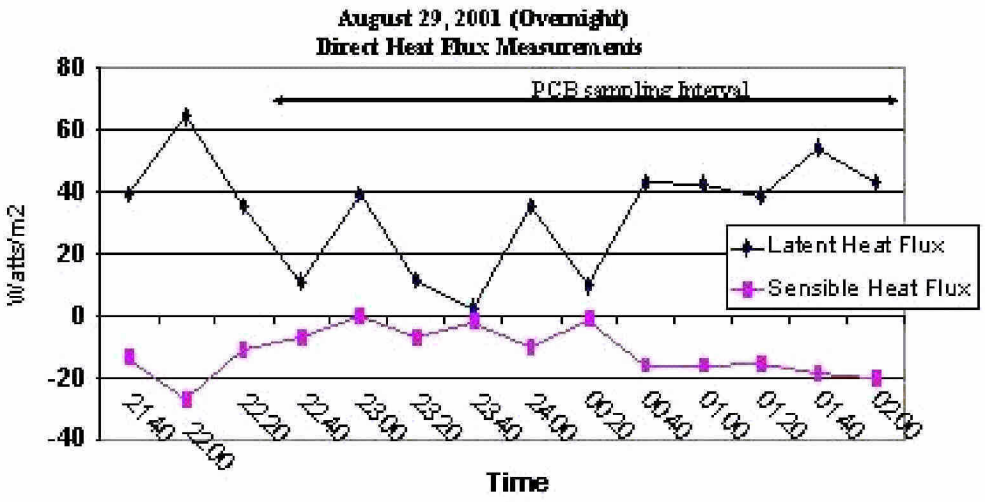

Figure 17. Nighttime latent and sensible heat flux measurements at the Bayonne landfill site, 29 August 2001.

The decrease in daytime latent heat flux in combination with the high sensible heat flux relative to the latent heat flux from 29-30 August may be attributed to the drying of the amended dredge material. This drying was apparent from the white crust observed during day two forming on the surface. Figure 18 is a plot of the heat flux measurements during 30 August.

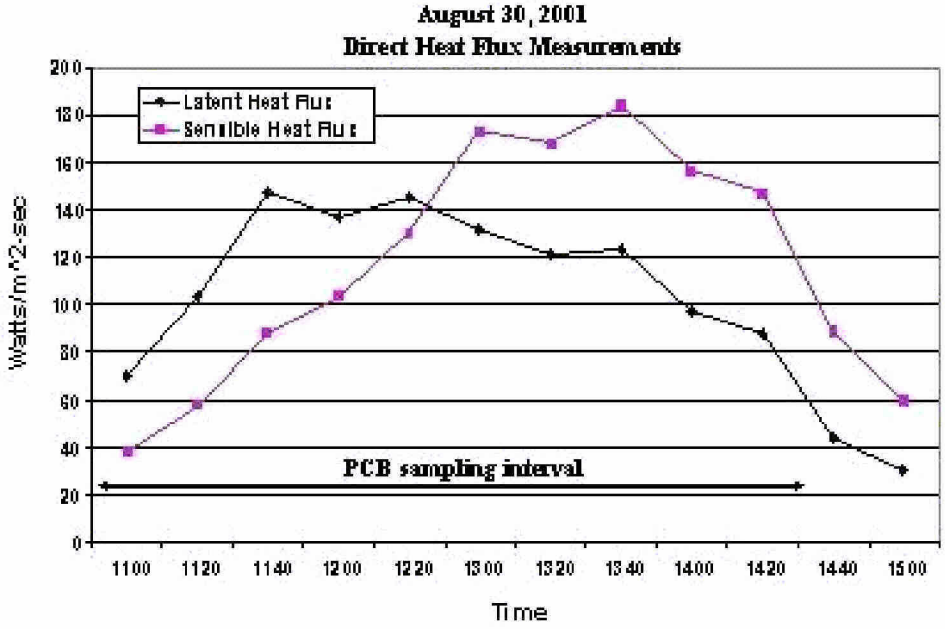

Figure 18. Latent and sensible heat flux measurements at the Bayonne landfill site, 30 August 2001.

Atmospheric stability coefficients were determined using our flux-gradient equations. The daytime value for ϕ_M was 0.54 and the value for ϕ_W was 1.19. This indicates conditions where the atmosphere is slightly stable with respect to the latent heat, but is very unstable with respect to momentum. This could be a result of the drying of the SDM. During the overnight interval the atmosphere was stable with values for ϕ_M and ϕ_W of 1.34 and 1.91 respectively.

Vertical PCB Fluxes

PCB concentrations measured above three-week old SDM during the overnight sampling interval on 29 August were very similar at the two heights with values of 7.95 and 7.46 ng m^{-3} for the upper and lower heights, respectively. The congener distribution of PCBs in these samples (Appendix 8, Figure 2) shows that the vast majority of the airborne PCBs have low molecular weight. It also shows a gradient out of the ground for those low molecular weight PCB congeners; however the opposite is true for the higher weight congeners. The small gradients in both directions, along with a relatively stable nighttime atmosphere led to small flux estimates. The total flux was estimated to be -47 ng m^{-2} h^{-1}, however, there were concentration gradients both into and out of the ground and fluxes in both directions depending on the molecular weight.

On 30 August, very high PCB concentrations were measured and there was a large gradient from the upper intake to the lower intake (19 and 14 ng m^{-3} for the upper and lower intakes, respectively). This gradient is found to be consistent over homologues (Appendix 8, Figure 3). The large gradient of PCB concentrations into the ground results in a PCB flux estimate of -1944 ng m^{-2} h^{-1}. The elevated PCB concentrations observed on this day may have been the result of the advection of PCBs to the site from an upwind source. SDM may not necessarily have been absorbing PCBs, but this is strong evidence that PCBs were not volatilizing from the site on 30 August.

Total Gaseous Mercury Fluxes

Positive vertical gradients in TGM concentrations were observed above the SDM on 30 August with average TGM concentrations of 4.1 ng m^{-3} and 3.3 ng m^{-3} for the lower (0.8 m) and upper heights (3 m), respectively. Paired measurements used in flux estimates had an average gradient of 0.42 ng m^{-3} and yielded an average net flux of Hg out of the SDM of 187 ng m^{-2} h^{-1} (Table 5).

5.7 23-25 October 2001 Sampling Campaign

Background and Perimeter Gas-Phase PCBs

Samples were taken in the morning (0900 – 1300 hours) and in the afternoon (1300 – 1700 hours) on each day at the perimeter of the sediment application and the trailer site for a total of 34 air samples (30 samples plus 4 field blanks). ΣPCB (n= 93 congeners) concentrations ranged from ~400 to 2000 pg m^{-3} at the trailer site and ~700 to 7000 pg m^{-3} at the perimeter of the sediment application site over the October sampling campaign.

During the first sampling interval (23 October 2001, 1020 – 1400 hours) the wind was blowing over a SDM lagoon that was just starting to be filled during this time period. The perimeter PCB concentration measurements for this interval show that there were greater concentrations measured

near the Office Trailers which were downwind of the large SDM lagoon in the center of the site than near the Pug Mill, which was upwind of the site. The conditions during the second sampling interval on 23 October 2001 (1430 – 1807 hours) were similar to those of the earlier sampling interval in that wind blew from the ocean and it was overcast and cool. Neither of the perimeter samples was representative of air blowing over the SDM. On 24 October 2001, the wind was directly over the fresh dredge, and much slower than the previous day. PCB concentrations collected during this interval on the perimeter show an increase in the concentrations leaving the site. The samples collected on the evening of 24 October 2001 were taken while the wind was blowing in off the ocean. It was blowing over both SDM lagoons for part of this interval. Perimeter samples were not taken during this time interval. The wind during 25 October was blowing in off the ocean. The perimeter samples show greater PCB concentrations in air that has traveled over the site than in air that has not.

SDM Landfill Site Conditions

Vertical gradients in PCB and Hg concentrations were collected over five sampling events during this campaign. The micrometeorological systems and air samplers were setup on the eastern side of the site between two lagoons where SDM was being dumped continuously during the campaign. The sampling location can be seen in Figures 19 – 23; these show the site conditions during each of the five sampling intervals as well as perimeter PCB concentrations during four of the five intervals. During the three-day interval, meteorological conditions at the site varied. This included wind direction which varied from over the two different SDM lagoons and areas of the site with no SDM. The resulting flux estimates reflect the variability of the meteorological conditions.

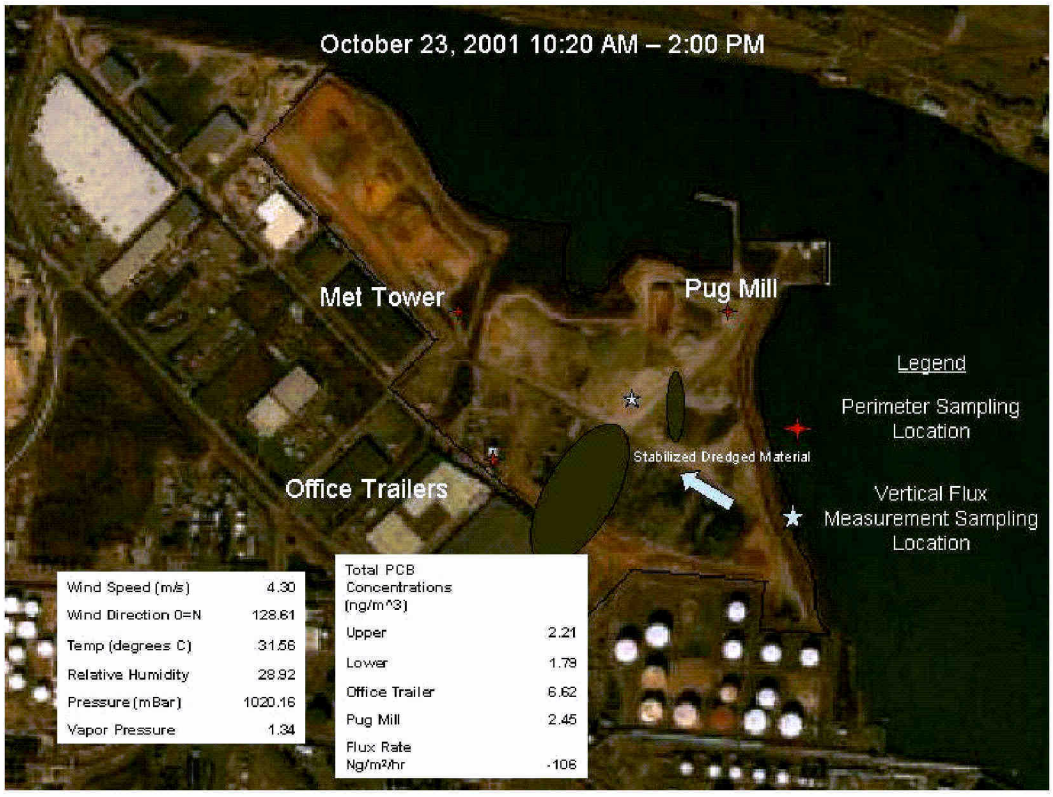

Figure 19. Bayonne landfill site conditions, 23 October 23 2001, 1020 – 1400 hours.

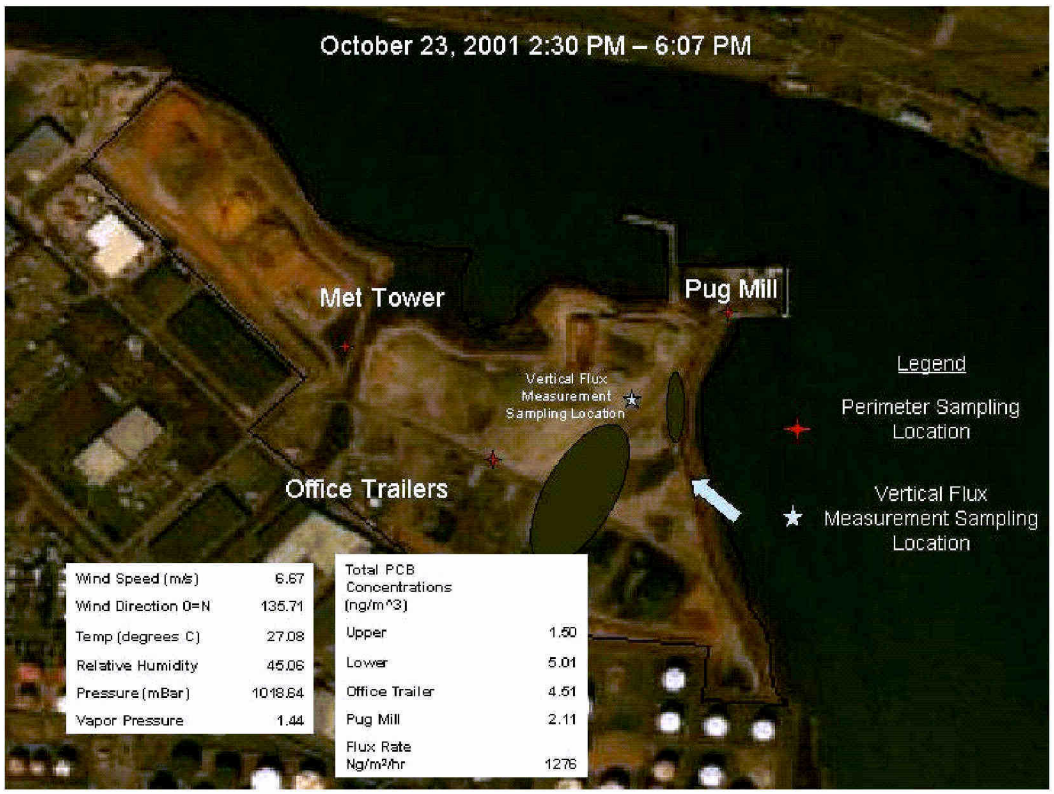

Figure 20. Bayonne landfill site conditions, 23 October 2001, 1430 – 1807 hours.

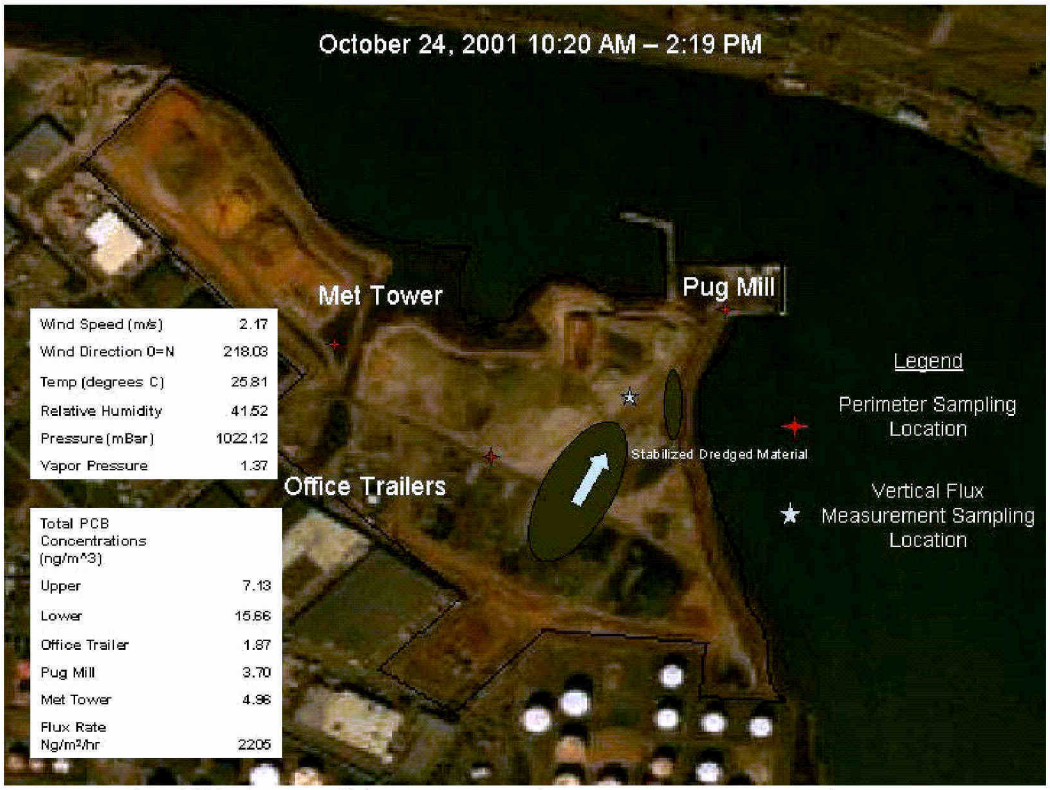

Figure 21. Bayonne landfill site conditions, 24 October 2001, 1020 - 1419 hours.

Figure 22. Bayonne landfill site conditions, 24 October 2001, 0810 – 1130 hours.

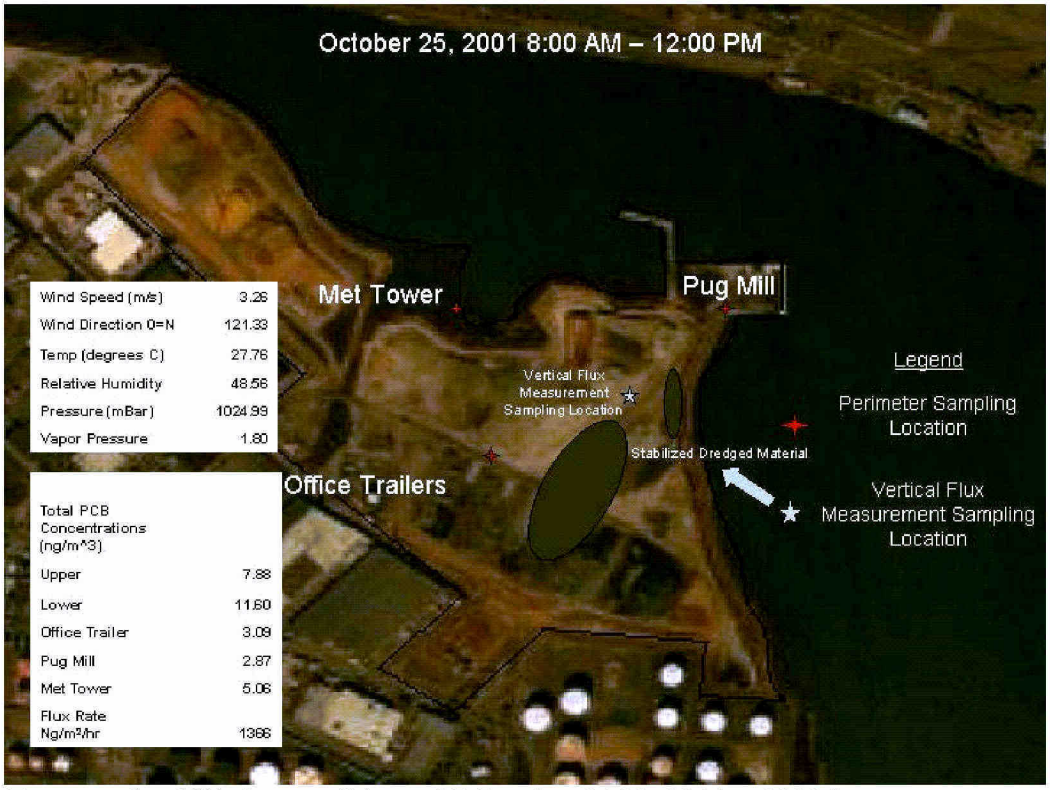

Figure 23. Bayonne landfill site conditions, 25 October 2001, 0800 – 1200 hours.

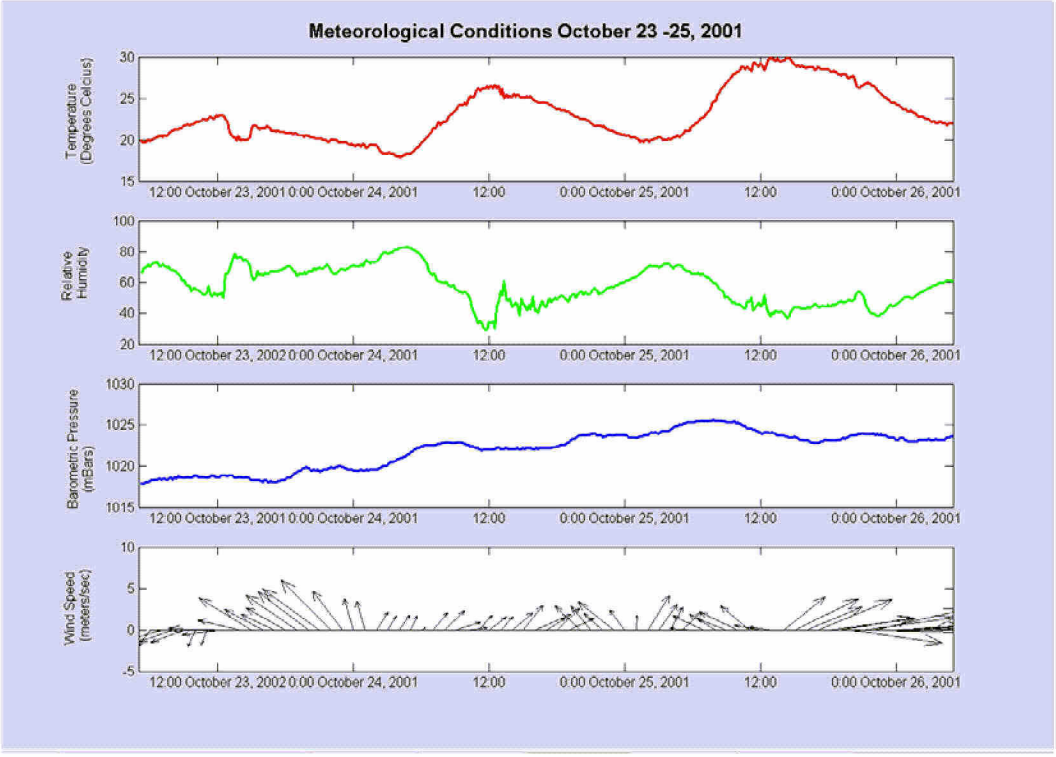

Figure 24. Bayonne landfill meteorological conditions, 23 -25 October 2001.

The meteorological conditions for the sampling interval are presented in Figure 24. The weather during the October sampling campaign changed over the three days. It began on a cool overcast day. High pressure moved in as time went on and the cloud cover cleared and the temperature rose.

Vertical PCB Fluxes

The observed PCB fluxes are closely linked to the latent and sensible heat flux values in magnitude and direction. However, the latent heat flux appears to have a greater effect (Figure 25). It is observed that there are relatively high latent and sensible heat flux values during the day and very small or negative values at night; this is due to the solar radiation heating up the ground surface.

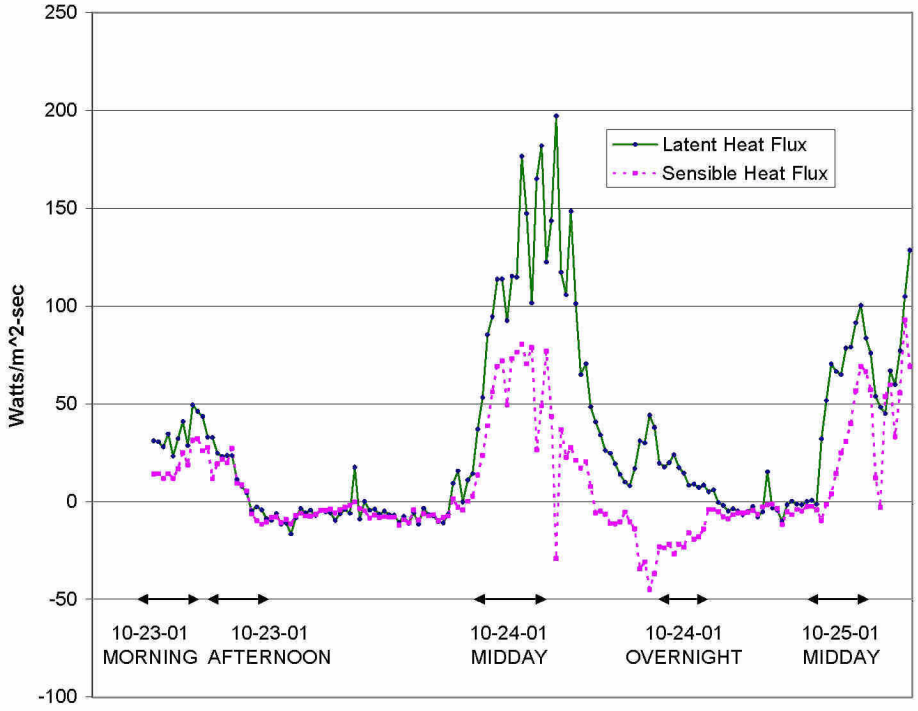

Figure 25. Observed fluxes of sensible and latent heat during the October sampling campaign.

On 23 October 2001 it was overcast and the wind was off the water from the southeast. As a result of the presence of cooler, humid air and little sunlight, the sensible heat flux on this day was very small. These conditions combined to yield nearly neutral stability. The values for ϕ_M were 0.99 and 0.94, and the values for ϕ_W were 1.00 and 1.00 for the two sampling periods on 23 October, respectively. The ϕ_W value for the second sampling interval is 1.00 because a range of stabilities was observed as indicated by Richardson numbers of –0.03 to 0.01. During this sampling interval, the sun set, sensible and latent heat fluxes declined, and ϕ_W values varied from less than one to greater than one. The following two days the wind changed to southwest, the skies cleared, and relative humidity was lower, and as a result the atmosphere became unstable. The daytime sample on 24 October 2001 exhibited a less stable atmosphere, but the gradient in the moisture content was below the resolution of the cooled mirror hygrometer. As a result the value for ϕ_W used was that for the ϕ_H. For slight departures of atmospheric stability from a neutral condition, ϕ_W has approximately the same value as ϕ_H (Pruitt et al., 1973). The final two intervals included a nighttime sample and a sample on 25 October 2001. The nighttime sampling interval was atypical in that the temperature inversion eroded as the winds changed from southwest to southeast (from over the bay). In Figure 25, there is a small spike of latent heat flux during the sampling campaign, indicating a certain amount of instability with respect to the moisture content. Because measured values could not be determined during the nighttime sampling event, fluxes were estimated using ϕ values of 1.0.

PCB concentrations were measured during the five intervals and in each case, except the morning sample on 23 October, exhibited a gradient out of the ground. The samples for the morning sampling interval on 23 October, exhibited a gradient out of the ground only for the lowest molecular weight

congeners. The congener distributions for the five sampling intervals are presented in Appendix 8, Figures 4 through 8.

The concentrations measured during this interval were very low in comparison to those measured later in the campaign. As a result, this interval had the lowest flux estimate for the sampling campaign. Although the concentrations were small there was a pronounced gradient from the lower sampling intake to the upper intake. The gradient was present for all the congeners regardless of molecular weight. This distribution still showed that the highest concentrations observed were for the lowest molecular weight congener, but there were relatively high concentrations of congeners with chlorination numbers of three and four.

The PCB concentrations collected during this sampling interval were much higher than the previous day's. There was a distinct gradient in the magnitude of concentrations from the lower intake to the upper intake. The congener distribution showed much higher concentrations for the low molecular weight congeners.

The nighttime samples collected on 24 October 2001 are very similar in magnitude; however a small gradient can be seen between the lower intake and the upper intake. The congener distribution shows higher concentrations for the low molecular weight congeners. There was a spike that represents three co-eluting peaks 56+60+89, this was at first assumed to be an analytical error, however it was also present in the subsequent sampling interval.

The final sampling event of the campaign resulted in the highest flux rates and there was a consistent gradient in the PCB concentrations collected at the site. The large peak for congener 56+60+89 was present again, and there was also a spike in the area of the heaviest congeners corresponding to PCB congener 180.

Total Gaseous Mercury Fluxes

During the October sampling campaign, the average TGM concentration measured at the lower height rose from 3.1 ng m^{-3} on the morning of 23 October 2001 to 7.3 ng m^{-3} on the afternoon of 25 October 2001. Over the three day campaign, the observed vertical TGM concentration gradient increased from 0.23 ng m^{-3} on 23 October, to 0.78 ng m^{-3} on the 24th, and 2.1 ng m^{-3} on the morning of 25 October (Table 5). Following the change in wind direction, the vertical gradient in TGM concentration dropped to 0.84 ng m^{-3} in the afternoon of 25 October. The vertical flux of TGM from SDM was 30 ng m^{-2} h^{-1} on the morning of 23 October and increased to 139 and 156 ng m^{-2} h^{-1} on the afternoons of 23 and 24 October, respectively (Table 5). On 25 October, the vertical TGM flux increased to 559 ng m^{-2} h^{-1}in the morning and 310 ng m^{-2} h^{-1} in the afternoon.

5.8 6-8 May 2002 Sampling Campaign

Background and Perimeter Gas-Phase PCBs

PCB samples were also collected in the morning (0900 – 1300 hours) and in the afternoon (1300 – 1700 hours) on each day at the perimeter of the sediment application site and at the trailer for a total of 39 air samples (32 samples plus 7 field blanks). The 3 high-volume air samplers were labeled A, B

and C. Station A was located west of the SDM along the western perimeter of the landfill, station B was located about 30 feet from the meteorological tower, and station C was located NW of the SDM near the perimeter of the landfill (see Fig. 26). ΣPCB (n= 93 congeners) concentrations ranged from ~600 to 1300 pg m^{-3} at the trailer site and ~600 to 3000 pg m^{-3} at the perimeter of the sediment application site over the sampling campaign.

SDM Landfill Site Conditions

The May 2002 sampling campaign was conducted directly on top of freshly placed SDM. The SDM had developed a solid surface layer and was strong enough to support sampling equipment, however at one foot below the surface, the sediment had apparently not yet cured. The sampling equipment was placed downwind of approximately 100 m of exposed, freshly laid SDM. Placement of SDM in the area of study ceased on the first day of the sampling campaign. During the campaign, the SDM dried and developed a white crust. Sampling took place on the western side of the site and the wind blew over the SDM for the duration of the sampling campaign with the exception of the final interval when the wind changed and blew from the northeast. At that time, the sampling equipment was moved as far as possible to the southwest. After moving the equipment, it was downwind of approximately 25 m of SDM.

Figure 26 shows the site conditions during the early afternoon sampling interval on 6 May when the highest estimated PCB fluxes were observed. During this sampling interval the wind was blowing from the southwest directly over SDM placed just prior to the sampling interval.

Site conditions during the late afternoon/evening sampling interval on 6 May are shown in Figure 27. The weather conditions were similar to the early afternoon, except that the there was a slight temperature drop toward evening.

On the second day of sampling the wind was variable, and it was hot and sunny. The wind was blowing directly over the SDM. Figures 28 and 29 show the conditions at the site on 7 May 2002.

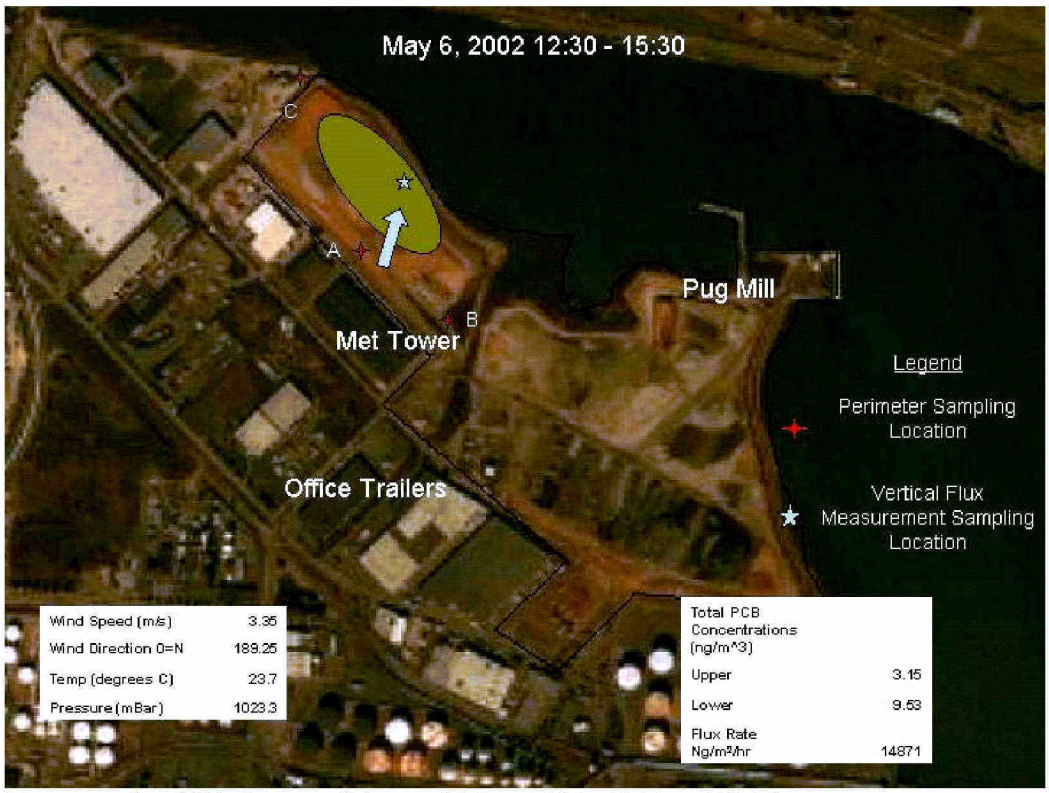

Figure 26. Bayonne landfill site conditions, 6 May 2002, 1230 – 1530 hours.

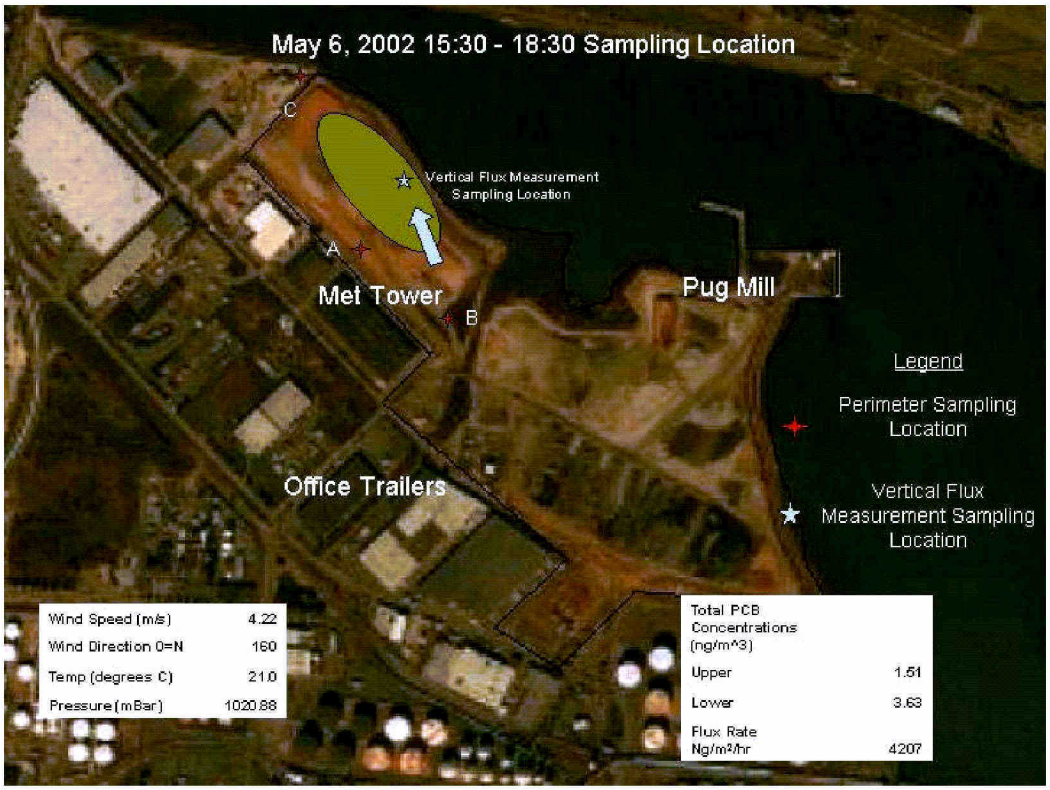

Figure 27. Bayonne landfill site conditions, 6 May 2002, 1530 – 1830 hours.

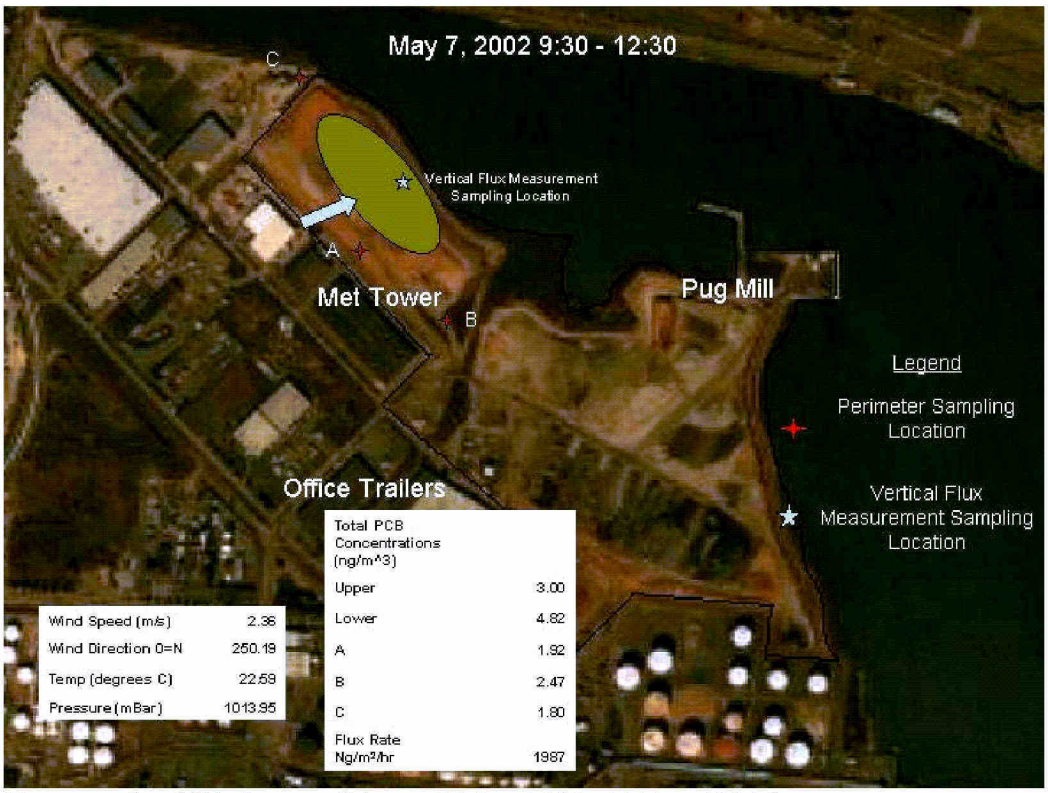

Figure 28. Bayonne landfill site conditions, 7 May 2002, 0930 – 1230 hours.

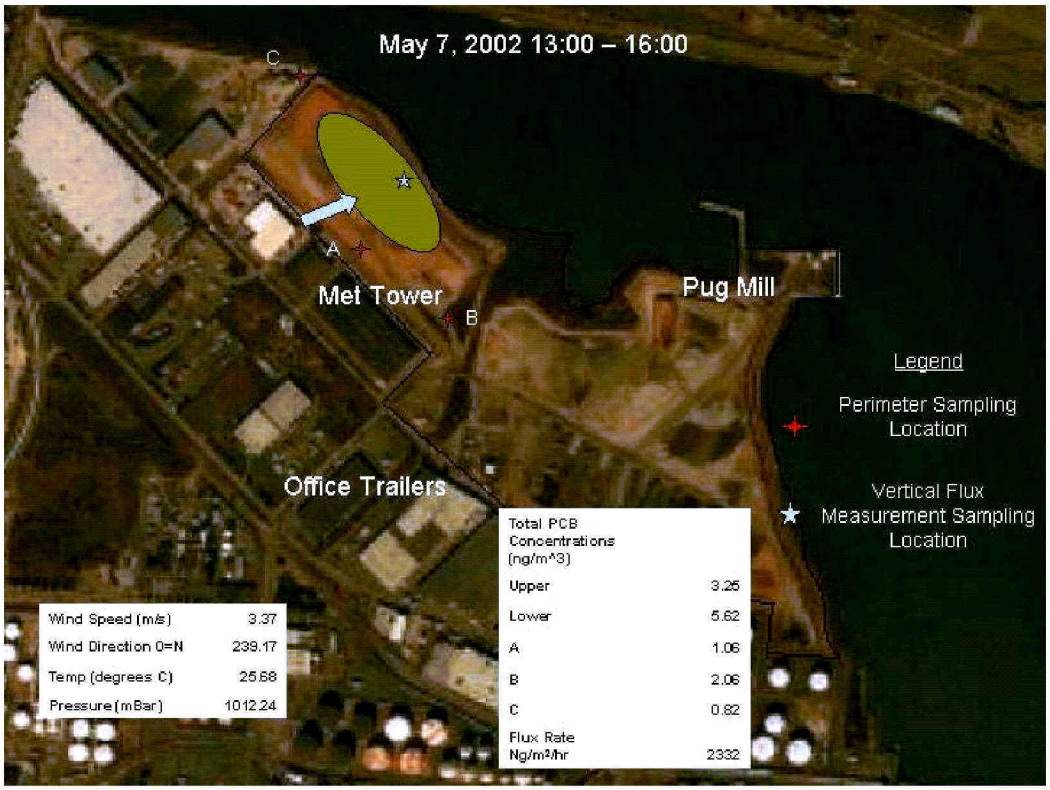

Figure 29. Bayonne landfill site conditions, 7 May 2002, 1300 – 1600 hours.

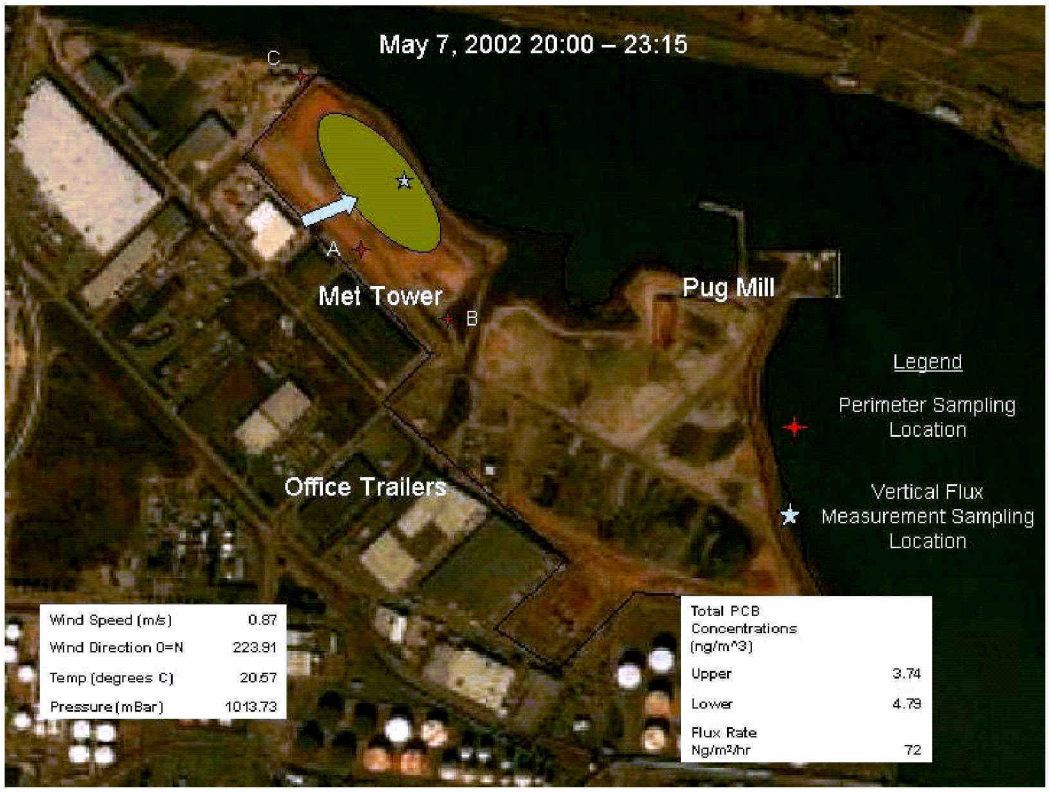

Figure 30. Bayonne landfill site conditions, 7 May 2002, 2000 – 2315 hours.

During the overnight sampling on 7 May 2002 the wind died down and it was cool. The condition atop the SDM differed greatly from the surrounding area. The air over the SDM was extremely humid and warm, while the air about 30 m to the north the air was cooler and drier. Figure 30 shows the conditions at the site during the nighttime sampling interval on 7 May 2002.

On the final day of the sampling campaign the wind changed and blew out of the northeast. The sampling equipment was moved to increase the amount of SDM over which the wind was blowing. The Site conditions are shown in Figure 31.

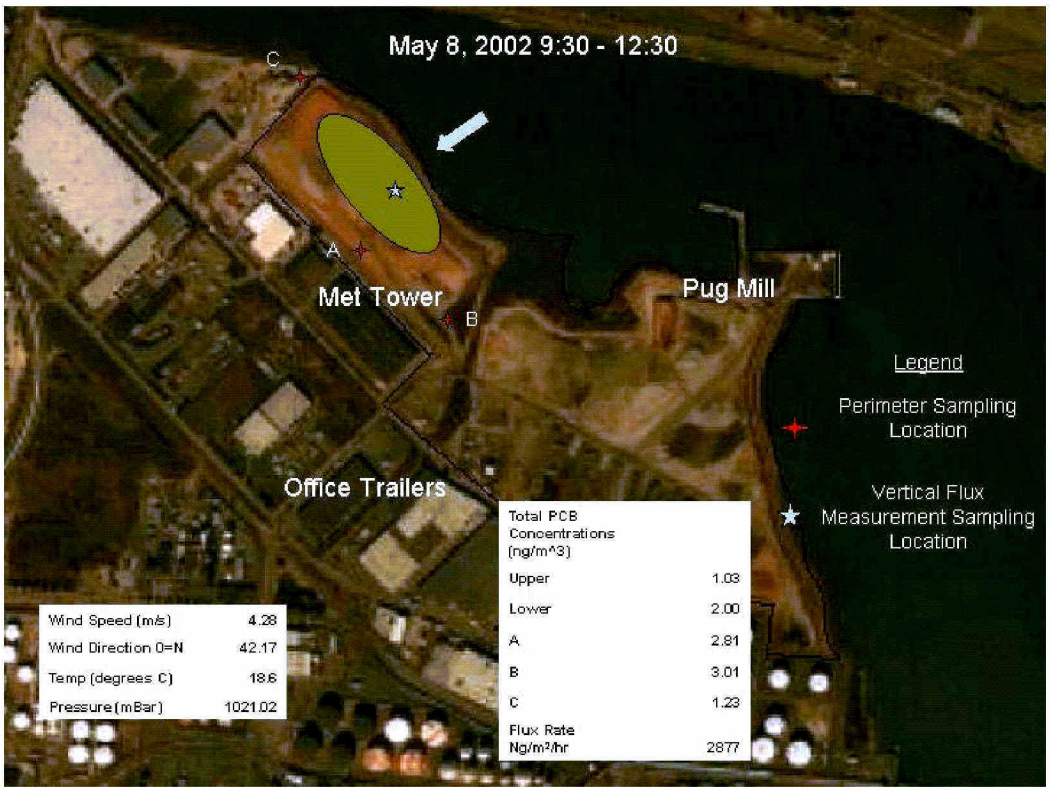

Figure 31. Bayonne landfill site conditions, 8 May 2002, 0930 – 1230 hours.

The meteorological data collected during the May sampling campaign is presented in Figure 32. Due to a malfunction with the on-site meteorological tower, weather data for the site was lost. However, meteorological data was retrieved from the National Oceanic and Atmospheric Administration (NOAA) site located at Bergen Point, NY (see Appendix 9). This site is on Staten Island and located approximately 3.2 km (2 miles) southwest of the site. The site identification information can be accesses at: http://co-ops.nos.noaa.gov/data_res.html.

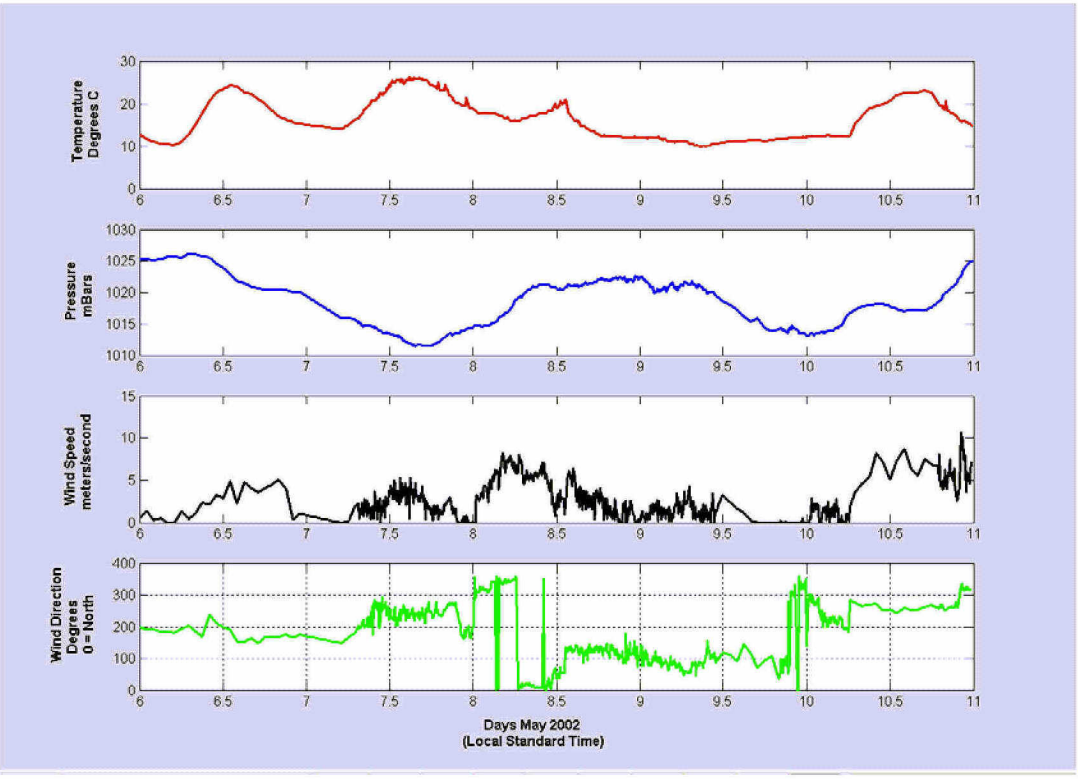

Figure 32. Bayonne landfill meteorological conditions, 6-10 May 2002.

Figure 33 shows the observed heat fluxes during May 2002 sampling campaign. It can be seen that during the first sampling interval there is a very large latent heat flux corresponding to the drying of the SDM. During the sampling interval on 8 May there were large heat fluxes observed however by this point the surface of the SDM had dried, this can be seen by the fact that the sensible and latent heat fluxes had very similar values. The atmospheric stability coefficients for these intervals were similar for all of the intervals with the exception of the overnight sample. The daytime values for ϕ_M averaged 1.04 with a standard deviation of 0.22 and the values for ϕ_W averaged 0.25 with a standard deviation of 0.04. This denotes conditions where the atmosphere is relatively neutral with respect to the momentum, but is very unstable with respect to latent heat. During the overnight interval, the atmosphere became very stable and measured values of ϕ_M and ϕ_W were both much greater than those that inhibit fluxes of momentum and latent heat.

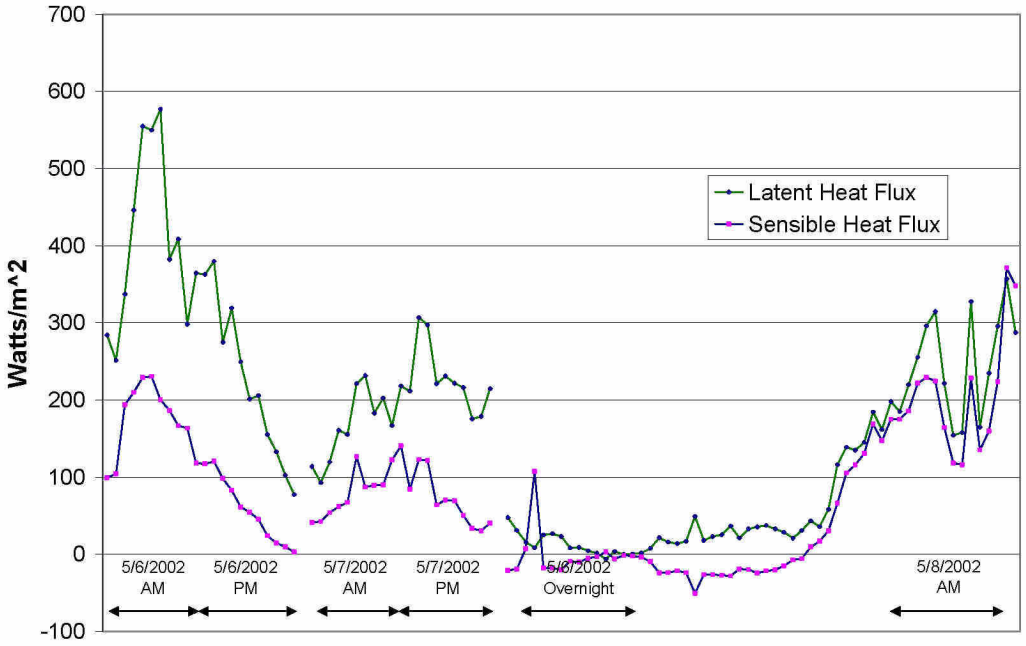

Figure 33. Observed fluxes of sensible and latent heat during the May sampling campaign.

Vertical PCB Fluxes

PCB concentrations were measured during all six sampling intervals and they all yielded positive vertical gradients out of the ground. ΣPCB concentrations ranged from 1 to 9.5 ng m^{-3} and the distribution of PCB congeners in each sample followed the same pattern presented earlier in which low molecular weight PCBs were present in much higher concentrations than high molecular weight congeners (Appendix 8, Figs. 9-14). As a result, the vertical fluxes of PCBs were dominated by the di-, tri-, and tetrachlorinated PCBs during the May campaign (Fig. 34).

SDM samples for moisture content and PCB analysis were collected during the May sampling campaign. The SDM was found to have high moisture content and very high PCB concentrations. The samples were taken from the fresh dredged material about 15 cm below the surface. Total PCB concentrations were 21 and 31 ppb. The distribution of PCB congeners in the SDM differed greatly from the PCB air concentrations (Appendix 8, Fig. 15). The PCB congeners present in the highest abundance in the SDM were in the middle of the molecular weight range for PCBs corresponding to chlorination numbers of three, four, and five.

The PCB flux estimates decreased over time during the May 2002 campaign. During this three-day period, the flux of ΣPCBs decreased from approximately 15,000 ng m^{-2} h^{-1} to approximately 2900 ng m^{-2} h^{-1} (Table 4) following a decreasing trend in PCB concentrations above the SDM. Atmospheric conditions also changed, thus influencing the PCB flux estimates. Most notably during the 7 May overnight sampling interval the PCB flux appears to approach zero, this is due to a stable atmosphere that restricted vertical fluxes.

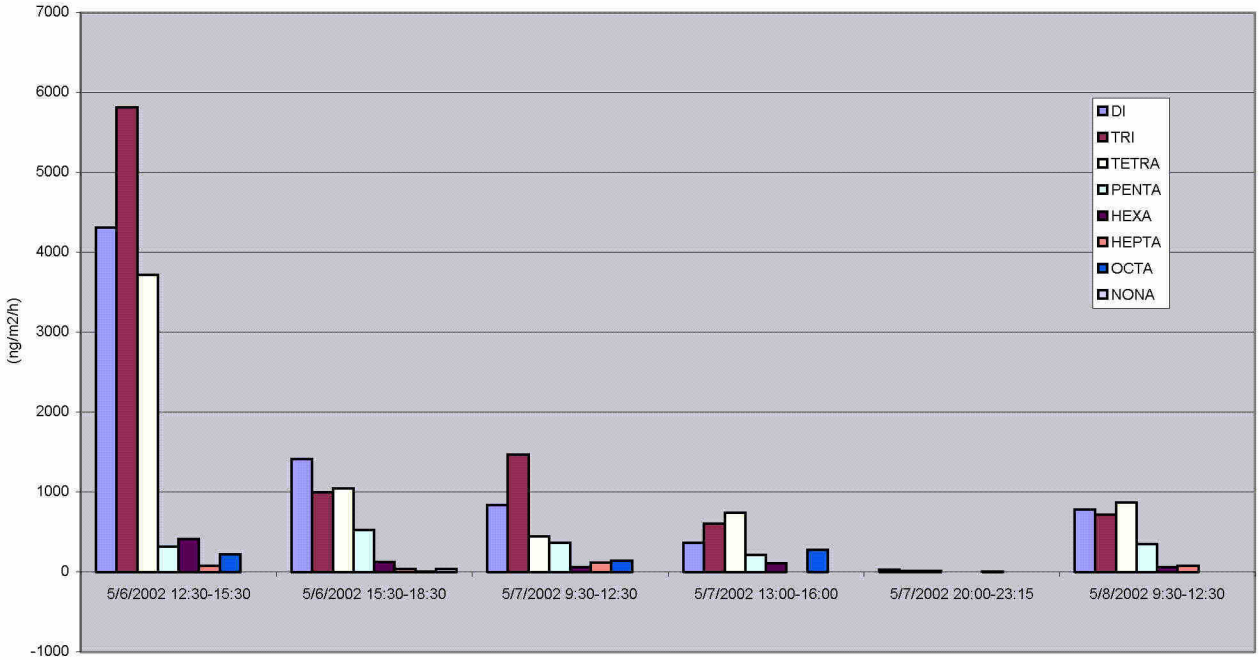

Figure 34. Estimated PCB flux values for the May 2002 sampling campaign (grouped by homologue).

Total Gaseous Mercury Fluxes

In May 2002, average TGM concentrations measured at the lower height ranged from 3.3 to 4.4 ng m^{-3} and at the upper height ranged from 3.1 to 3.5 ng m^{-3}. The vertical TGM concentration gradient was greatest on the morning of 7 May (0.91 ng m^{-3}) and decreased to 0.32 ng m^{-3} during the day (Table 5). On 7 May, the sediment-air flux was estimated to be 1043 ng m^{-2} h^{-1} during the morning and 314 ng m^{-2} h^{-1} in the afternoon. During the nighttime sampling period of 7 May (2030 and 2300 hours), a large decrease in the sediment-air TGM flux was observed. Along with a large increase in atmospheric stability, the vertical TGM flux decreased to 19 ng m^{-2} h^{-1} even though the average vertical gradient was still 0.29 ng m^{-3}. The following day brought higher wind speeds and vertical fluxes of 966 and 552 ng m^{-2} h^{-1} in the morning and afternoon, respectively (Table 5).

5.9 13-15 November 2002 Sampling Campaign

Background and Perimeter Gas-Phase PCBs

Samples were collected in the morning (0900 – 1300 hours) and in the afternoon (1300 – 1700 hours) on each day at the perimeter of the sediment application site and the Bayonne trailer for a total of 28 air samples (24 air samples plus 4 field blanks). The 3 high-volume air samplers were labeled A, B and C. Station A was located about 30 feet from the meteorological tower, station B was located SW of the SDM along the western perimeter of the landfill, and station C was located SE of the SDM near the oil tank field (see Figure 35). ΣPCB (n= 93 congeners) concentrations ranged from ~400 to 1600

pg m^{-3} at the trailer site and ~400 to 5000 pg m^{-3} at the sediment application site over the sampling campaign.

SDM Landfill Site conditions

Sampling occurred for three days in November 2002 (Figures 35 to 39). During the sampling campaign, observations over 4 h were made during five intervals: the afternoon of the 13th, the morning, the afternoon, and the evening of the 14th and the morning of the 15th. The sampling

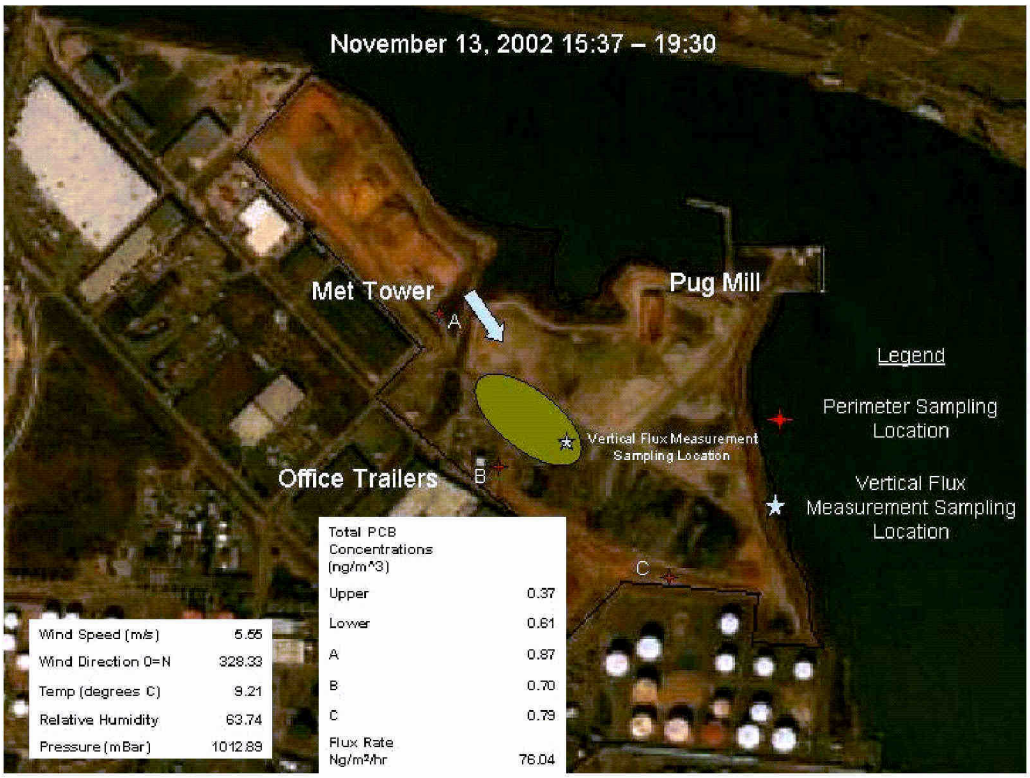

Figure 35. Bayonne landfill site conditions, 13 November 2002, 1537 – 1930 hours.

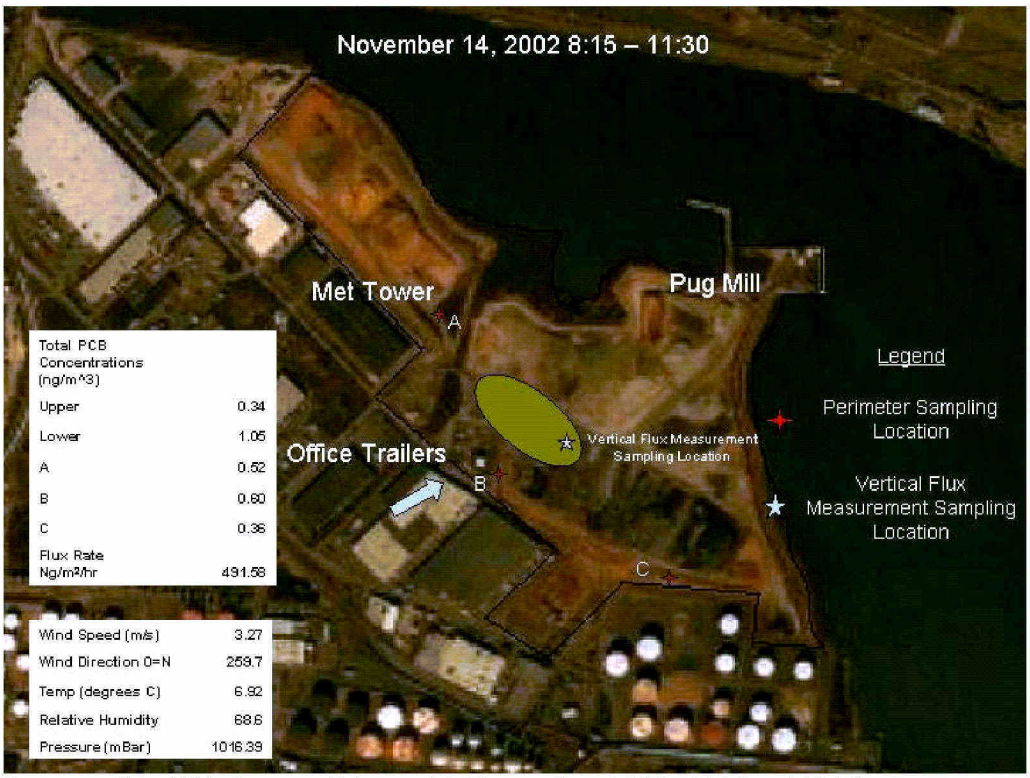

Figure 36. Bayonne landfill site conditions, 14 November 2002, 0815 – 1130 hours.

Figure 37. Bayonne landfill site conditions, 14 November 2002, 1200 – 1500 hours.

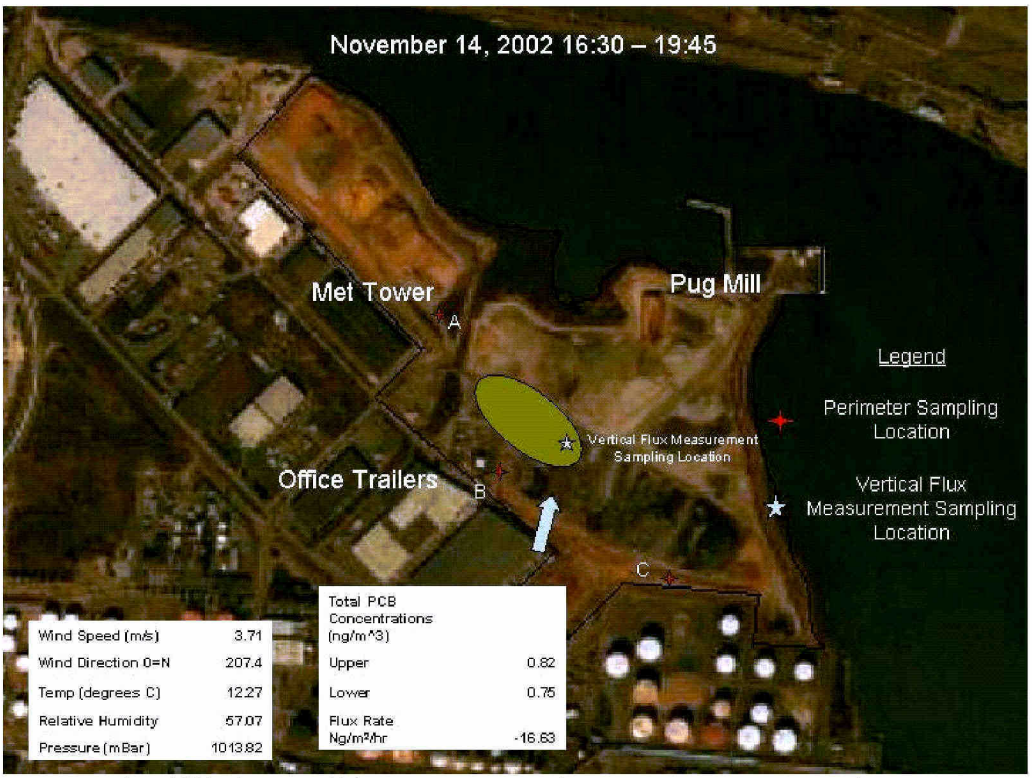

Figure 38. Bayonne landfill site conditions, 14 November 2002, 1630 – 1945 hours.

Figure 39. Bayonne landfill site conditions, 15 November 2002, 0830 – 1130 hours.

equipment was set up on the south end of the site directly on top of recently placed SDM. During the campaign, SDM was continuously placed to the west of the sampling site. Initially the wind was from the northwest directly over a large expanse of SDM, however the wind changed to the southwest and reduced the distance over SDM that the wind was blowing to approximately 30 m.

The weather during the sampling campaign was cold, rainy, and overcast. The heat fluxes monitored during the sampling campaign are small relative to previous sampling campaigns. This is due to the colder temperatures and lack of sunlight. During our sampling campaigns we have made every effort to remain either down wind or directly on top of the SDM, however wind speed and direction are variable. During this time period the wind was initially blowing from the north and then turned to the southwest during the last day of the sampling campaign. Figure 40 shows the meteorological conditions at the site during the November 2002 sampling campaign.

Vertical PCB Fluxes

Daytime vertical PCB fluxes at the SDM landfill ranged from 74 to 492 ng m^{-2} h^{-1} during the November campaign (Table 4). A negative PCB concentration gradient was observed during the evening of 14 November (Table 4), indicating that the PCB flux had shut down overnight.

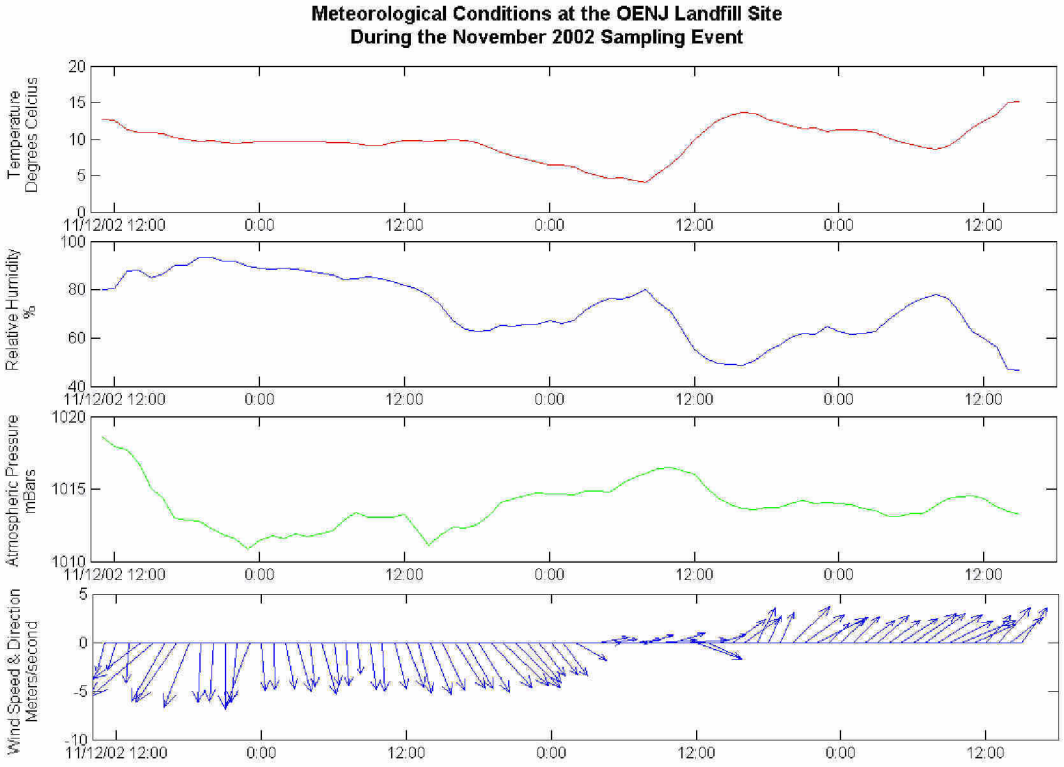

Figure 40. Bayonne landfill meteorological conditions, November 2002.

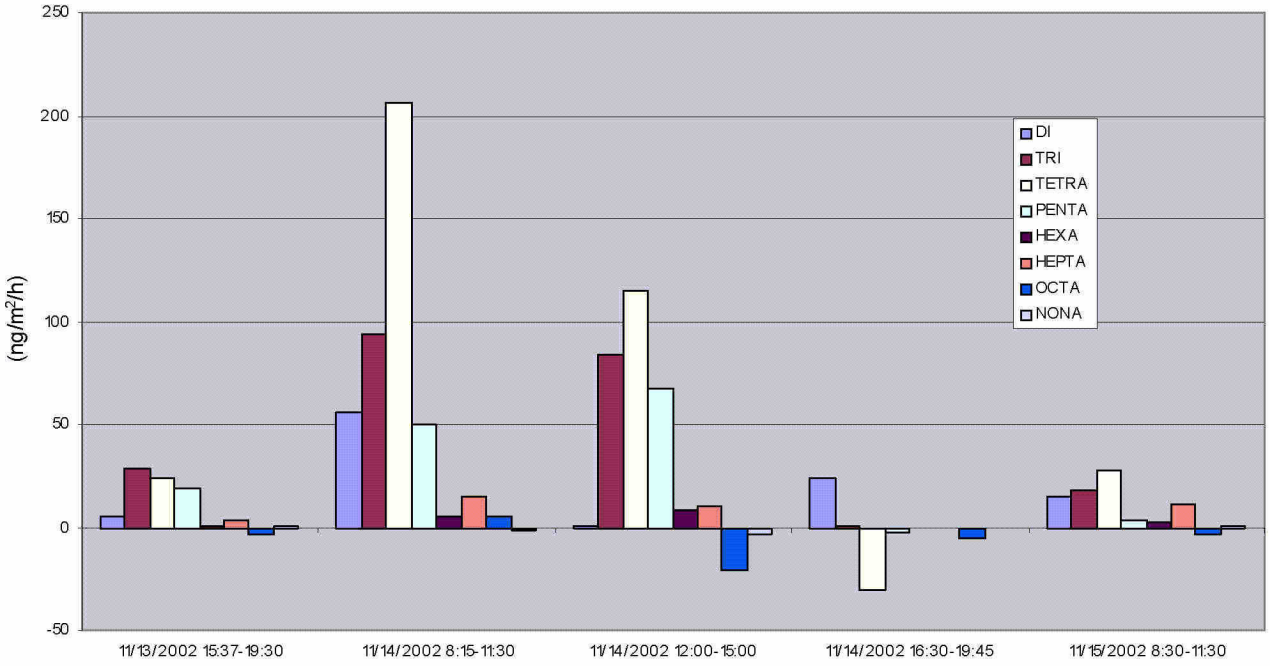

Figure 41. Estimated vertical fluxes of PCBs at the SDM landfill during the November 2002 sampling campaign (grouped by homologue).

Total Gaseous Mercury Fluxes

Vertical TGM concentration gradients ranged from -0.04 to 0.11 ng m^{-3} during the November 2002 sampling campaign (Table 5). Small chemical gradients and a nearly neutral surface microlayer resulted in low Hg fluxes during this campaign. On 14 November, very small vertical concentration gradients were detected (0.05 and 0.03 ng m^{-3}) resulting in estimated average vertical fluxes of 34 and 17 ng m^{-2} h^{-1} in the morning and afternoon, respectively (Table 5). On the morning of 15 November, a small negative concentration gradient was observed (-0.04 ng m^{-3}). In the afternoon of 15 November, a small net flux of Hg out of the sediment (41 ng m^{-2} h^{-1}) was estimated based on the observed positive vertical gradient of 0.11 ng m^{-3} (Table 5).

6.0 DISCUSSION

6.1 Micrometeorology

Stability correction factors for momentum (ϕ_M), heat (ϕ_H), and water (ϕ_W) were determined from *in situ* measurements in two ways. These two methods led to nearly identical values for the stability factors. As a consequence, all reported stability correction factors were determined using what will be referred to as the approximate integration method. For this method, the profile equations are integrated between the two measurement levels z_1 and z_2 in the following manner:

$$\int_{z_1}^{z_2}\frac{\partial u}{\partial z}dx = u(z_2)-u(z_1)=\int_{z_1}^{z_2}\frac{u_*}{\kappa z}\phi_M(z)dz=\phi_{Mest}\frac{u_*}{\kappa z}\ln\left(z_2/z_1\right) \tag{27}$$

$$\int_{z_1}^{z_2}\frac{\partial \theta}{\partial z}dx = \theta(z_2)-\theta(z_1)=\int_{z_1}^{z_2}\frac{H}{\kappa u_*\rho C_p}\phi_H(z)dz=\phi_{Hest}\frac{H}{\kappa u_*\rho C_p}\ln\left(z_2/z_1\right) \tag{28}$$

$$\int_{z_1}^{z_2}\frac{\partial \rho_e}{\partial z}dx = \rho_e(z_2)-\rho_e(z_1)=\int_{z_1}^{z_2}\frac{Le}{\kappa u_*\lambda}\phi_W(z)dz=\phi_{West}\frac{Le}{\kappa u_*\lambda}\ln\left(z_2/z_1\right) \tag{29}$$

The values for $\phi_{M\,est}$, $\phi_{H\,est}$, and $\phi_{W\,est}$, are found from these integrated equations. Focusing on just momentum, the stability factor $\phi_{M\,est}$ is obtained from

$$\phi_{M\,est}=\frac{u(z_2)-u(z_1)}{\left(u_*/\kappa\right)\ln\left(z_2/z_1\right)} \tag{30}$$

which can be evaluated from observations of $u(z_2)$, $u(z_1)$, and the frictional velocity u_*. The quantity $\phi_{M\,est}$ was considered to be the average stability factor over the interval from z_2 to z_1. The other stability correction factors are found in a similar manner.

It is useful to determine the nature of the error in estimating the stability factors using this approximate integration method. To do this, the theoretical formulation for ϕ_M, as a function of z/L (see Section 2.1, Eq. 13) developed by Dyer and Hicks (1970) for unstable stratification and the theoretical formulation of Webb (1970) for stable stratification will be used. The approach will be to assume that the theoretical models are correct and then determine the difference between the actual average stability factor and that estimated from equation (4). The Dyer and Hicks (1970) model for unstable stratification is

$$\phi_M\left(z/L\right)=\left[1-16\left(z/L\right)\right]^{-1/4} \tag{31}$$

This formulation for ϕ_M can be simplified by expanding in a Taylor series about z/L = 0; i.e.

$$\phi_M\left(z/L\right)=\phi_M(z=0)+\left.\frac{\partial\phi}{\partial z}\right|_{z=0}\left(z/L\right)+\text{ higher order terms} \tag{32}$$

Substituting equation (5) into equation (6) the following approximation for ϕ_M is obtained:

$$\phi_M\left(z/L\right)=1+4\left(z/L\right)+\text{ higher order terms} \tag{33}$$

Retaining just the first two terms allows for the integration of the profile equation between z_2, and z_1 to obtain the "log + linear" profile equation for velocity:

$$u(z_2) - u(z_1) = \frac{u_*}{\kappa} \ln\left(z_2 / z_1\right) + \frac{4}{L}\frac{u_*}{\kappa}(z_2 - z_1) \tag{34}$$

The average value of ϕ_M over the interval from z_2 to z_1 is found as follows:

$$\phi_{Mavg} = \frac{1}{z_2 - z_1}\int_{z_1}^{z_2} \phi_M\left(z/L\right) dz \tag{35a}$$

$$\phi_{Mavg} = \frac{1}{z_2 - z_1}\int_{z_1}^{z_2} \left[1 + 4\left(z/L\right)\right] dz \tag{35b}$$

$$\phi_{Mavg} = 1 + \frac{4}{2L}\frac{\left(z_2^{\,2} - z_1^{\,2}\right)}{z_2 - z_1} \tag{35c}$$

$$\phi_{Mavg} = 1 + \left(4/L\right) z_{avg} \tag{35d}$$

Combining equation (8) with equation (4) yield the following expression for ϕ_{Mest} i.e.,

$$\phi_{Mest} = \frac{\ln\left(z_2/z_1\right) + 4/L\,(z_2 - z_1)}{\ln\left(z_2/z_1\right)} \tag{36}$$

$$\phi_{Mest} = 1 + \frac{4/L\,(z_2 - z_1)}{\ln\left(z_2/z_1\right)} \tag{37}$$

Equations (9d) and (11) may be used to evaluate the assumed true value of ϕ_{Mavg} and to compare it with the values for ϕ_{Mest}. For the measurements at the landfill typical values for z_1, z_2 and u_* were 1 m, 3 m, and 2 m respectively. For values of L ranging from –10 to –100 the values for ϕ_{Mest} are given in Table 6.

Table 6. Stability correction factors for momentum.

L (m)	Z_{avg}/L	ϕ_{Mavg}	ϕ_{Mest}
-10	-0.200	0.20	0.27
-20	-0.100	0.60	0.54
-40	-0.050	0.80	0.82
-60	-0.033	0.87	0.88
-80	-0.025	0.90	0.91
-100	-0.020	0.92	0.93
-200	-0.010	0.96	0.96

For values of the magnitude of z/L less than 0.1. The error in the approximate integration method is less than 10% and for magnitudes less than 0.05 it is less than 3%.

The results are much the same using Webb's (1970) formulation for ϕ_M for stable stratification. This formulation is

$$\phi_M = 1 + 5.2\, z/L \quad \text{for L>0} \tag{38}$$

The use of this expression yields an average value of ϕ_M over the interval z_2 to z_1.

$$\phi_{Mavg} = 1 + \frac{5.2}{L} z_{avg} \tag{39}$$

The equation for calculating ϕ_{Mest} becomes

$$\phi_{Mest} = 1 + \frac{5.2/L\,(z_2 - z_1)}{\ln\left(z_2/z_1\right)} \tag{40}$$

For z_1= 1 m, z_2= 3 m, z_{avg}= 2 m, and for L= +40 m, the true coverage value of the stability factor is ϕ_{Mavg} = 1.26 and the value estimated from the approximate integration is ϕ_{Mest} = 1.24. Thus, for stable stratifications similar results are obtained for reasonably small values of z/L.

6.2 Background and Perimeter SDM Landfill PCB Concentrations

Background Concentrations of PCBs at the NJDEP Trailer in Bayonne

The sources of PCBs to Bayonne may include the city of Bayonne itself, adjacent Newark Bay, and surrounding urban/industrial areas. On the day of highest PCB concentration in Bayonne (9 September 2000), winds were coming primarily from the northeast, directly over the city of Bayonne toward the sampling station. The second highest ΣPCB concentration occurred on 28 August 2000, when winds came from the east, also from over the city of Bayonne. On the date of the lowest ΣPCB concentration (20 November 2000) winds were coming from the west over Newark Bay. The second lowest PCB concentration occurred on 6 February 2000 and again the winds were from the west. This simple analysis suggests that Newark Bay, which has been subject to historical PCB contamination and is located due west of the NJDEP trailer in Bayonne, is not the largest source of PCBs to the city of Bayonne. If Bayonne is under the influence of one dominant source-type for PCBs, then the PCB congener distributions should be similar regardless of the total PCB concentration. Regression of the congener profiles from 9 September 2000 and 20 November 2000 yielded an r^2 of 0.90 ($p < 0.001$) indicating that the two profiles were not statistically different from one another. Thus despite differences in PCB concentrations and wind directions between these samples, the PCB fingerprints indicate that they are influenced by the same source type or source process.

In order to gain perspective regarding the magnitude of the PCB concentrations measured at the NJDEP trailer in Bayonne, we have compared the concentrations of PCB congeners from Bayonne with those measured elsewhere in North America (Table 7). The average concentrations of PCB congeners were higher in Bayonne than at three New Jersey Atmospheric Deposition Network stations located in or near urban/industrial areas (Jersey City, New Brunswick, Sandy Hook). Most PCB congeners had higher concentrations at Bayonne than all of the other North American sites with the exception of Chicago, IL (Table 7). PCB concentrations measured at Bayonne show a striking contrast to those measured near the Arctic at Alert, Canada demonstrating the extent of PCB contamination in the NY/NJ metropolitan area.

A more detailed comparison of PCB concentrations is possible for Bayonne and Jersey City since on four occasions in December 1999 and January 2000 simultaneous samples were collected at these two sites (Figure 42). The Jersey City site at the Liberty Science Center is located 8 km northeast of the NJDEP trailer in Bayonne. On 8 December 1999, gas phase, congener-specific PCB concentrations at the two sites were virtually identical. However, for the next three sampling periods the concentrations differed by as much as a factor of 4 (Figure 42).

Table 7. Average gas phase concentrations of PCB congeners (pg m^{-3}) at the NJDEP trailer in Bayonne and at other sites in the United States and Canada.

PCB Concentration (pg m^{-3})	Bayonne, NJ (gas)	Jersey City, NJ (gas)	New Brunswick, NJ (gas)	Sandy Hook, NJ (gas)	Chesapeake Bay (gas)	Chicago, IL (gas)	Alert, Cananda (may-sept) (gas)	Egbert, Ontario Cananda (gas)
datasource	this study	a	a	a	b	c	d	e
18	109	76	39	34	20	191	5.1	6.6
16+32	106	84	46	30	25	204	0.80	8.8
28	82	58	28	20	63*	432*	1.3	16
52+43	102	56	31	31	16	96	1.8	16
41+71	33	22	9.1	9.6	19	111	0.30	2.3
66+95	105	75	43	38	33	303	1.6	6.5
101	52	27	16	14	6.8	51	0.89	6.4
87+81	27	13	8.1	6.6	3.7	29	0.27	2.0
110+77	51	25	17	14	7.9	91	0.65	4.0
149+123+107	22	10	5.9	5.2	7.1	29	0.90	2.8
153+132	22	10	5.4	5.2	10	71	0.77	3.2
163+138	26	9.9	6.0	5.0	4.4	43	0.47	2.8
187+182	3.5	2.6	2.0	2.1	2.3	7.8	0.39	1.7
174	2.7	1.7	0.90	0.70	1.8	4.9	0.14	0.92
180	3.3	2.1	1.2	1.0		44	0.55	1.1

a: Brunciak et al, 2000; b: Nelson et al, 1998; c: Simcik et al, 1998; d: Stern et al, 1997; e: Hoff et al, 1992; * includes PCB #31

To further quantify differences in congener profiles at the two sites, PCB congener concentrations at Bayonne and Jersey City were regressed against each other for each simultaneous sample (Fig. 43). The slope of the line relating PCB congener concentrations at the two sites for the December 8, 1999 samples is 0.92 indicating a nearly 1:1 relationship (Fig. 43). The regression of the December 8 data gives an r^2 of 0.77 ($p<0.01$), but if the two outlying congeners (out of 93) are removed, the r^2 improves to 0.94 ($p<0.01$). Regressions of PCB congener concentrations at the two sites for the other three simultaneous samples have slopes that deviate significantly from the 1:1 line (12/20/99 slope=0.24; 01/01/00 slope=0.70; 01/13/00 slope=0.34) reflecting higher PCB concentrations at Bayonne than in Jersey City. The congener-specific profiles for 20 December 1999 and 13 January 2000 are statistically similar (r^2=0.92, $p<0.01$ and r^2=0.94, $p<0.01$, respectively), indicating that although different concentrations of PCBs were measured at Bayonne and Jersey City on these days, the sources may be related.

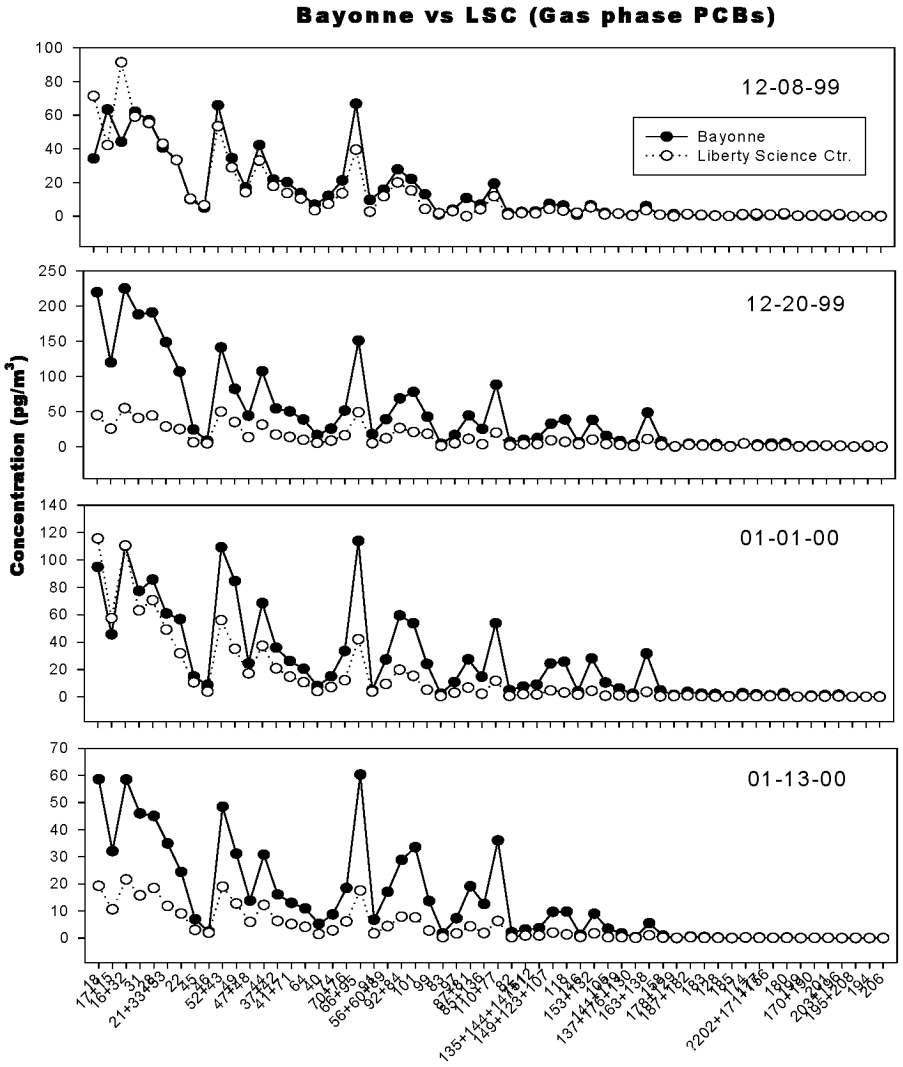

Figure 42. Comparison of congener-specific PCB concentrations for four simultaneous air samples collected in December 1999 and January 2000 at the NJDEP trailer in Bayonne and at the Liberty Science Center in Jersey City.

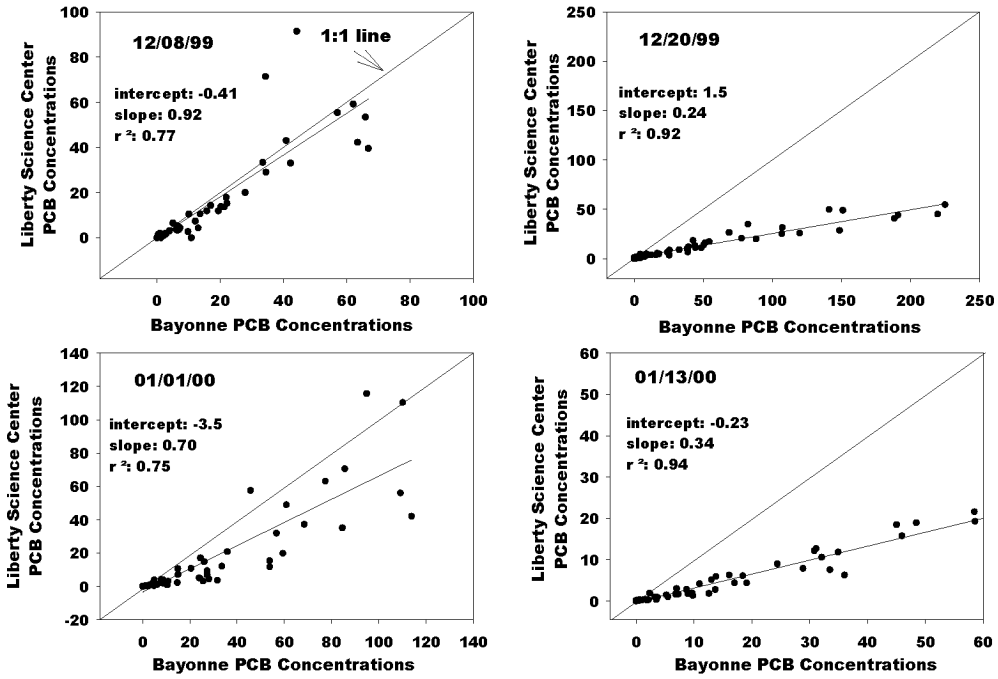

Figure 43. Correlations between gas phase PCB congener concentrations measured at the NJDEP trailer in Bayonne and at the Liberty Science Center in Jersey City for four simultaneous samples collected in December 1999 and January 2000.

The highest gas phase concentrations in Bayonne were measured in the summer when warm temperatures can lead to increased volatilization via air-surface exchange. In order to look more closely at the relationship between PCB concentrations and temperature, we employed an equilibrium model (Eq. 41) to predict how much of the variation in concentration can be explained by temperature alone:

$$\log[PCB]_{gasphase} = a + \frac{m}{T} \qquad (41)$$

In this case, we have divided the individual PCB congeners into their respective homologue groups. That is, we have summed all of the di-chlorinated biphenyls together, the tri-chlorinated together, etc. The PCB homologue groups with the strongest temperature-dependencies are the octa-chlorinated biphenyls (with T explaining 65% of the variability) and the tri-chlorinated biphenyls (with T explaining 58% of the variability) (Figure 44). If the r^2 values were all near 1, then air-surface exchange would be the only process controlling PCB concentrations in this area. This plot clearly demonstrates that other factors in addition to temperature affect gas phase PCB concentrations in Bayonne.

Figure 44. Clausius-Clapeyron-type plot of the log of the concentration of PCB homologue groups versus inverse temperature.

PCB Concentrations at the SDM landfill Before and after SDM Application, May 2001

A comparison of gas phase, congener-specific PCB concentrations in samples collected at the SDM landfill in Bayonne before and after the placement of SDM indicates that gas phase ΣPCB concentrations were found to be lower (1.5X) after the sediment was applied to the site at the end of May compared to the beginning of May (Figure 45). A regression between the relative congener profiles of the two samples gave an r^2 value of 0.55, indicating that the profiles are not statistically identical at the 95% confidence level and that these two samples were influenced by different PCB sources. Therefore, there appears to be a source of PCBs at the SDM landfill (possibly the SDM itself) on May 31st which is not seen at the site prior to SDM application or at the NJDEP trailer. The wind direction was not the same on the two sampling days in May at the sediment application site. On 1 May 2001 (pre-sediment application), winds came out of the SW at an average wind speed of 4.5 m s^{-1}; whereas on 31 May 2001 (post-sediment application) winds came from the NW at an average wind speed of 7.0 m s^{-1}. Wind direction does not explain the difference in ΣPCB concentrations on these two days since at the DEP trailer site, the lowest concentrations were measured under southwesterly winds. Wind speed may play a role with high winds resulting in greater dilution on 31 May. Thus although the volatilization of PCBs from SDM may add to observed concentrations at the SDM landfill, this signal will be affected by wind direction and speed and neighboring sources.

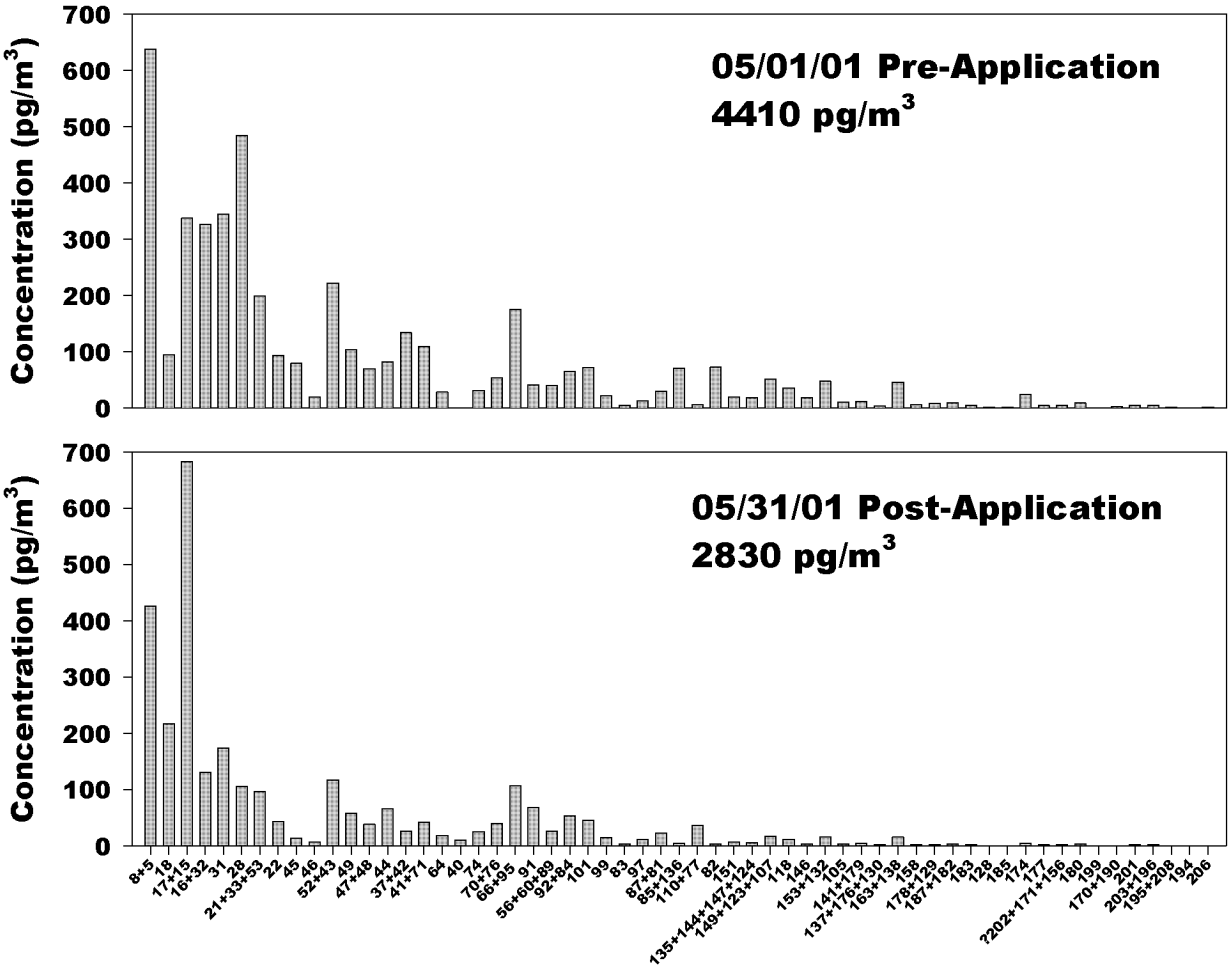

Figure 45. Congener-specific, gas phase PCB concentrations at the SDM landfill in Bayonne before (1 May 2001) and after (31 May 2001) SDM was applied.

The gas phase ΣPCB concentrations measured at the SDM landfill in May 2001 can be compared with those collected from December 1999 to November 2000 at the NJDEP trailer in Bayonne. The two samples taken at the sediment application site in May 2001 were both higher than the average concentration at the trailer and the concentration at the SDM landfill on 1 May was higher than the highest value observed at the trailer during the period prior to SDM application (see Figure 5).

Horizontal Gradients of PCBs at the SDM Landfill in Bayonne

July 2001 Campaign

An important aspect of this study involves interrogating the horizontal concentration gradients seen at the sediment application site under different wind regimes. During the July 2001 campaign, three high volume air samplers were deployed near the perimeters of the SDM application areas in the eastern

part of the site. The triangulation of the samplers allows for an assessment of upwind/downwind gradients under appropriate wind direction regimes (Table 8).

Table 8. Summary table of gas phase ΣPCB concentrations (pg m^{-3}) at the NJDEP trailer and the SDM landfill in Bayonne during the July 2001 intensive sampling campaign.

Σ PCB Concentration pg m^{-3} (Gas Phase) July 2001	**Bayonne Trailer**	**Sediment Site A**	**Sediment Site B**	**Sediment Site C**
17 July (All Day)	6925	2804	4958	4248
18 July (Morning)	3288	8278	6434	6289
18 July (Afternoon)	2322	6298	14647	5153
19 July (Morning)	4983	14350	3285	3445
19 July (Afternoon)	3838	12993	5971	7202
20 July (Morning)	5085	13326	3604	6354
20 July (Afternoon)	1265	8625	6132	5298

17 July 2001 all day: On this day, there were two dominant wind directions NE, and W,SW. The variability in wind direction does not allow for an assessment of upwind/ downwind gradients. As it appeared that wind direction at the site shifted from morning to afternoon, the decision was made to sample two times per day for all remaining samples for the study.

18 July 2001 morning: For this sampling period, winds were primarily from the E, such that site "C" (in grid H16) represented upwind conditions and sites "A" and "B" were downwind of the applied dredge material. ΣPCB concentration at the upwind site C was 6289 pg m^{-3} and the downwind concentrations were 6434 pg m^{-3} (site B) and 8278 pg m^{-3} (site A). The increase in ΣPCB concentrations was not greater than the 20% inherent uncertainty associated with the PCB measurements between sites C and B. There was, however, a significant increase in PCB concentrations from site C to site A.

18 July 2001 afternoon: For this sampling period, winds came from the SE, with both sites A and C acting as upwind sites and site B as the downwind site. Concentrations upwind (site C = 5153 pg m^{-3}, site A = 6298 pg m^{-3}) were as much as 2.5X lower than downwind (14647 pg m^{-3}), suggesting that the dredge material contributed to the atmospheric burden of PCBs onsite.

19 July 2001 morning: On the morning of July 19, 2001, strong winds were coming out of the NE. Site C "saw" PCB concentrations from off-site (3445 pg m^{-3}); whereas, site A saw concentrations coming from over the sediment application area (14647 pg m^{-3}). Site B also saw concentrations that arrived from off-site (3285 pg m^{-3}). This provided clear insight into the impact of PCB emissions on-site versus off-site showing that PCB volatilization on-site can be a significant contributor to atmospheric PCB concentrations.

19 July 2001 afternoon: For this sampling period, winds were still out of the NE, and concentrations at the two upwind sites, B (5971 pg m^{-3}) and C (7208 pg m^{-3}) were significantly lower than those measured downwind of the dredge material at site A (14350 pg m^{-3}). The perimeter sampling again supported the conclusion that the dredge material contributes to the air burden on-site.

20 July 2001 morning: Morning winds were out of the NE, and once again, the upwind sites had lower ΣPCB concentrations than sites downwind of the dredge material by at least a factor of 2. ΣPCB concentrations upwind at site C and site B were 6354 and 3604 pg m^{-3}, respectively. The ΣPCB concentration at the downwind site was 12993 pg m^{-3}.

20 July 2001 afternoon: For this sampling period, the winds shifted to the SE, thus sites C and A were upwind of the dredge material and site B was downwind. However, ΣPCB concentrations at the upwind site A (8625 pg m^{-3}) were higher than downwind at site B (6132 pg m^{-3}), suggesting that the dredge material was not the dominant source of PCBs to the air above the sediment application site. Off-site sources contributed more strongly to the burden during this sampling period.

Samples were also collected at the Bayonne trailer site, located across town to the northwest of the sediment application site (see Figure 4). This allowed us to investigate whether the Bayonne trailer site can "feel" the influence of the sediment application site. In order for the Bayonne trailer site to feel the direct influence of the sediment application site, there must be strong winds from the E/SE. Two sampling periods during the July 2001 intensive met this condition, 18 July in the afternoon and 20 July in the afternoon.

If the Bayonne NJDEP trailer site "feels" the influence of the sediment application site, then it would be expected that concentrations would be elevated at the trailer. Under E/SE winds on those two days, the trailer site had the lowest concentrations measured during the entire July 2001 campaign. The average ΣPCB concentration at the trailer site was 3945 pg m^{-3} during the July 2001 campaign and on the two E/SE wind regime days concentrations were 2322 and 1265 pg m^{-3}, thus the sediment application site is not the dominant source of PCBs to the city of Bayonne, NJ.

October 2001 Campaign

The sampler locations for the October 2001 campaign were the same as in the July 2001 campaign. A summary of the gas phase ΣPCB concentrations from the October 2001 intensive campaign are presented in Table 9.

October 23, 2001 (morning): Winds were consistently out of the SE, thus all the sites were downwind of the applied dredge material. The ΣPCB concentration at site A (6619 pg m^{-3}) was greater than that at site C (2446 pg m^{-3}). This observation was consistent with the fact that the primary area with the largest amount of dredge applied was SE of site A. Dredge was also applied SE of site C, though in a considerably smaller quantity. Because of sampling problems, an assessment using site B cannot be performed.

October 23, 2001 (afternoon): Winds were again out of the SE during this sampling period. The ΣPCB concentration at site A (4506 pg m^{-3}) was greater than that at site C (2113 pg m^{-3}), thus, as was

the case for the morning, the dredge material was a source of PCBs to the air on-site. Because of sampling problems, an assessment using site B cannot be performed.

October 24, 2001 (morning): The winds were predominantly out of the SW. Therefore, sites A and B were upwind of the applied dredge material and site C was downwind. The ΣPCB concentration was higher downwind at site C (3704 pg m^{-3}) than upwind at site A (1869 pg m^{-3}) consistent with the dredge acting as a source of PCBs to the site. However, site B, upwind of the applied dredge material, had the highest ΣPCB concentrations on-site (4959 pg m^{-3}) suggesting that PCB sources other than the dredge material are affecting concentrations on-site.

Table 9. Summary table of gas phase ΣPCB concentrations (pg m^{-3}) at the NJDEP trailer and the SDM landfill in Bayonne during the October 2001 sampling campaign. (Note: Only one full day sample was taken at Site B on 23 October).

Σ PCB Concentration pg m^{-3} (Gas Phase) October 2001	**Bayonne Trailer**	**Sediment Site A**	**Sediment Site B**	**Sediment Site C**
23 October (Morning)	791	6619	3278	2446
23 October (Afternoon)	418	4506	-	2113
24 October (Morning)	2125	1869	4959	3704
24 October (Afternoon)	-	5839	6591	2517
25 October (Morning)	1260	3091	5058	2875
25 October (Afternoon)	2344	1414	1542	-
26 October (Morning)	1436	872	1318	975
26 October (Afternoon)	614	704	1244	834

24 October 2001 (afternoon): For this sampling period, winds were out of the SE, as was the case on 23 October. The ΣPCB concentrations at sites A (5839 pg m^{-3}) and B (6591 pg m^{-3}) are not statistically different from one another, because they are within the 20% uncertainty bounds about the concentrations, although site A was closer than site B to the area where dredge was applied. Once again, site C had a lower ΣPCB concentration (2517 pg m^{-3}) than sites B and A.

25-26 October 2001 (morning and afternoon): The winds came out of the W for these 4 sampling periods, from over the city of Bayonne toward the sediment application site. Therefore, both sites A and B were upwind. However, site C was not directly downwind of the dredge material, not allowing for an upwind/downwind spatial assessment. Interestingly, ΣPCB concentrations at the site on 25 October in the afternoon through the end of the afternoon on 26 October, were the lowest measured during the campaign, ranging from ~700 to 1500 pg m^{-3}. This can likely be attributed to a dilution factor, because wind speeds were ~3X the average from the earlier sampling periods in the campaign. During the October 2001 campaign, E/SE wind occurred on 23 October, in the morning. Concentrations at the sediment application site were 6619 pg m^{-3} downwind of the applied sediment. The ΣPCB concentration across town at the NJDEP trailer was 791 pg m^{-3}, nearly 8X lower. It is apparent that although concentrations at the sediment application site are high, the concentrations are lower only a short distance downwind from the site.

May 2002 Campaign

The sampler locations for the May 2002 campaign were not the same as in the July and October 2001 campaigns (see Figure 26). A summary of the gas phase ΣPCB concentrations from the May 2002 intensive campaign is presented in Table 10.

Table 10. Summary table of gas phase ΣPCB concentrations (pg m^{-3}) at the NJDEP trailer and the SDM landfill in Bayonne during the May 2002 sampling campaign.

Σ PCB Concentration pg m^{-3} (Gas Phase) May 2001	**Bayonne Trailer**	**Sediment Site A**	**Sediment Site B**	**Sediment Site C**
7 May (Morning)	1147	1915	2473	1797
7 May (Afternoon)	1162	1056	1992	821
8 May (Morning)	796	2809	3013	1230
8 May (Afternoon)	1349	2691	2033	2602
9 May (Morning)	658	1048	1363	1074
9 May (Afternoon)	696	1826	1418	1339
10 May (Morning)	1023	1328	1436	1114
10 May (Afternoon)	744	638	728	695

7 May 2002 (morning): Winds were out of the W/SW such that all sites A, B, and C represented upwind concentrations or concentrations coming from off-site. Concentrations at sites A (1915 pg m^{-3}) and C (1797 pg m^{-3}) were not statistically different from one another (assuming an inherent 20% uncertainty around the PCB measurements). However, the ΣPCB concentration at site B was statistically higher (2473 pg m^{-3}).

7 May 2002 (afternoon): Under W winds, all sites were once again upwind of the applied dredge material. Similarly, site B, located adjacent to the Stevens Institute meteorological tower, had a higher ΣPCB concentration (1992 pg m^{-3}) than sites A (1056 pg m^{-3}) and site C (821 pg m^{-3}).

8 May 2002 (morning): During this sampling period, the winds came out of the NE. There was no statistical difference between concentrations at site B (3013 pg m^{-3}) and site A (2809 pg m^{-3}), although site A (and not site B) was downwind of the applied dredge material. Site C displayed a significantly lower ΣPCB concentration (1230 pg m^{-3}).

8 May 2002 (afternoon): Under SE winds, site B was located upwind of the dredge material and site C was downwind. However, concentrations were statistically similar at the upwind site B (2033 pg m^{-3}) and the downwind site C (2602 pg m^{-3}), indicating that the dredge material was contributing a negligible portion to the overall air burden above the sediment site.

9 May 2002 (morning): Once again, the site was affected by SE wind conditions. Identical to the conclusion drawn for May 8th (afternoon), concentrations were statistically similar at the upwind site B

(1363 pg m^{-3}) and the downwind site C (1074 pg m^{-3}), indicating that the dredge material was contributing minimally to the overall air burden above the sediment site.

9 May 2002 (afternoon): During this sampling period, there were once again SE winds. Thus, the same conclusion can be drawn for this sampling event as well. The dredge material was not contributing significantly to the air burden on-site. This conclusion was drawn, because the concentration at the upwind site B (1418 pg m^{-3}) was similar to that at the downwind site C (1339 pg m^{-3}).

10 May 2002 (morning): On this sampling period, winds shifted and came out of the W leaving all sites upwind of the applied dredge material. All sites had similar ΣPCB concentrations: site A (1328 pg m^{-3}), site B (1436 pg m^{-3}), and site C (1114 pg m^{-3}).

10 May 2002 (afternoon): Winds were out of the W and concentrations were statistically similar among the three sites: site A (638 pg m^{-3}), site B (728 pg m^{-3}), and site C (695 pg m^{-3}).

Under three sampling periods, conditions were ideal such that an assessment could be made regarding whether the NJDEP trailer site can "feel" the influence of the sediment application site: May 8 (afternoon), May 9 (morning), and May 9 (afternoon). The concentrations measured at the NJDEP trailer site on May 9 in the morning (658 pg m^{-3}) and in the afternoon (696 pg m^{-3}) were the two lowest ΣPCB concentrations measured at the site during the May campaign, indicating that the sediment site is not the dominant source of PCBs to the air near the NJDEP Bayonne trailer. However, for the May 8 afternoon sampling event, gas phase ΣPCB concentrations were the highest measured during the May campaign at the trailer (1349 pg m^{-3}).

November 2002 Campaign

The sampler locations for the November 2002 campaign were not the same as in any of the previous campaigns (see Fig. 35). A summary of the gas phase ΣPCB concentrations from the November 2002 intensive campaign is presented in Table 11.

Table 11. Summary table of gas phase ΣPCB concentrations (pg m^{-3}) at the NJDEP trailer and the SDM landfill in Bayonne during the November 2002 sampling campaign.

Σ PCB Concentration pg m^{-3} (Gas Phase) November 2002	**Bayonne Trailer**	**Sediment Site A**	**Sediment Site B**	**Sediment Site C**
12 November (Morning)	1568	3118	3411	3638
12 November (Afternoon)	883	5009	3395	3530
13 November (Morning)	878	869	697	793
13 November (Afternoon)	1010	797	656	753
14 November (Morning)	362	517	600	361
14 November (Afternoon)	586	421	461	564

12 November 2002 (morning): During this sampling period, winds came out of the NE. The upwind Site A saw PCBs from off-site; whereas, site B was downwind of the dredge sediment. ΣPCB concentrations were similar at all three sites: A (3118 pg m^{-3}), B (3411 pg m^{-3}), and C (3638 pg m^{-3}), indicating that the application of dredge sediment was not the controlling factor in PCB concentrations on-site.

12 November 2002 (afternoon): During this sampling period, winds came out of the NE. The upwind Site A saw PCBs from off-site; whereas, site B was downwind of the dredge sediment. However, ΣPCB concentrations were similar at these two sites: B (3398 pg m^{-3}), and C (3530 pg m^{-3}). Site A, the site upwind of the applied sediment, had a significantly larger gas phase ΣPCB concentration (5009 pg m^{-3}).

13 November 2002 (morning): Winds were derived from the N/NW over this sampling event. Site A would therefore represent the upwind site, and site C the downwind site. However, the ΣPCB concentrations at all three sites were statistically similar (within the 20% uncertainty surrounding the PCB measurements): Site A (869 pg m^{-3}), Site B (697 pg m^{-3}), and Site C (793 pg m^{-3}). Thus, there was no apparent upwind/downwind gradient and the applied sediment did not contribute significantly to the over-site air.

13 November 2002 (afternoon): Winds were once again from the N/NW over this sampling period. Site A would therefore represent the upwind site, and sites C the downwind site. However, the ΣPCB concentrations at all three sites were again statistically similar (within the 20% uncertainty surrounding the PCB measurements): Site A (797 pg m^{-3}), Site B (656 pg m^{-3}), and Site C (753 pg m^{-3}). Thus, there was no apparent upwind/downwind gradient and the applied sediment did not contribute significantly to the over-site air.

14 November 2002 (morning): On this sampling period, the winds came from the W and all sites were therefore upwind of the dredge material. ΣPCB concentrations were similar at sites A (517 pg/m^3) and B (600 pg/m^3), but lower at site C (361 pg/m^3).

14 November 2002 (afternoon): Under SW winds, all three sites were also upwind of the dredge material. Sites A (421 pg m^{-3}) and B (461 pg m^{-3}) were similar in magnitude, but site C displayed a higher ΣPCB concentration (564 pg m^{-3}).

Unfortunately, during the November intensive campaign, there were no SE wind conditions that would allow for an assessment of the impact of the dredge sediments on atmospheric PCB concentrations at the NJDEP trailer site.

Summary

Average concentrations at the sediment application site were found to be ~1.5-2X higher than those measured at the Bayonne trailer (Figure 6). Average ΣPCB concentrations during the July 2001 campaign were 7128 pg m^{-3} and 3945 pg m^{-3} at the sediment application site and the Bayonne trailer site, respectively. For the October 2001 campaign, average ΣPCB concentrations were 2857 and 1284 pg m^{-3} at the two sites, respectively. Average ΣPCB concentrations for the May 2002 campaign were 1604 at the SDM landfill and 947 pg m^{-3} at the NJDEP trailer. For the November 2002 campaign,

average ΣPCB concentrations were 1644 and 881 pg m^{-3}, at the SDM landfill and trailer sites, respectively. Average ΣPCB concentrations during the intensive field campaigns were highest during the warmest seasonal campaigns, July 2001 (average temperature: 23°C) and October 2001 (average temperature 20°C). ΣPCB concentrations were lowest during the two coolest seasonal campaigns, May 2002 (average temperature: 8°C) and November 2002 (average temperature: 10°C).

Average ambient PCB concentrations in the city of Bayonne can be compared before and after the application of SDM. The average annual concentration of ΣPCB at the Bayonne trailer for the year prior to the application of SDM (December 1999 – November 2000) was 1711 pg m^{-3}. This value is similar to the average annual concentration of ΣPCB (1764 pg m^{-3}) for the period over which SDM was being applied. This value was estimated as the average of the ΣPCB concentrations measured at the trailer during the intensive campaigns, which include all four seasons.

In Figure 46, ΣPCB concentrations at the trailer site and SDM application site are compared with data from other studies. ΣPCB concentrations at the Bayonne trailer and the SDM application site are of similar magnitude to those from other urban/industrial sites such as Baltimore, MD, Chicago, IL, and Jersey City, NJ. Concentrations at both the trailer site and the sediment application site are significantly higher than those measured at "rural" sites which are near continental background concentrations of ~300 pg m^{-3}.

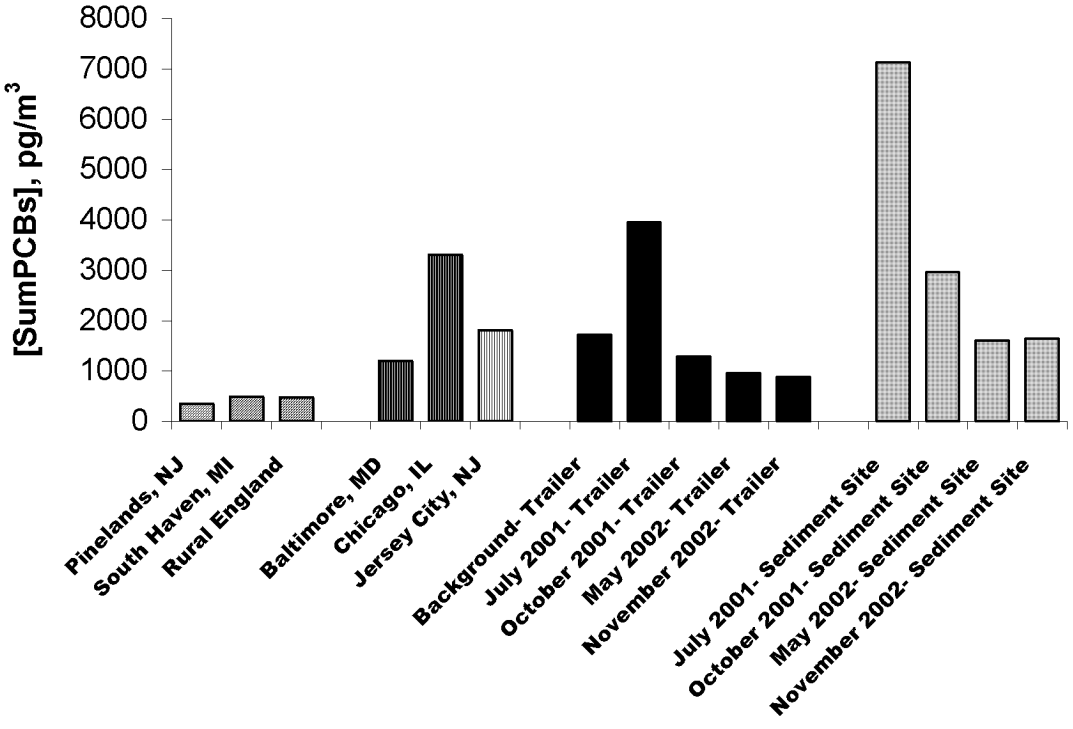

Figure 46. Comparison of gas phase ΣPCB concentrations (pg m^{-3}) from this study to other studies:

Pinelands: NJADN data (Van Ry et al, *ES&T,* 2002), Jersey City: NJADN data (Totten et al., *ES&T*, in review), South Haven/Chicago: (Simcik et al, *ES&T*, 1997), Baltimore: (Offenberg et al, *J.AWMA*, 1999), Rural England: (Lee and Jones, *ES&T*, 1999).

6.3 Vertical PCB Fluxes at the SDM Landfill

The determination of the flux of PCB's has been based on theoretical considerations of exchange processes in a turbulent boundary layer. A fundamental assumption underlying the theory is that the flow is in steady state or nearly so. During intervals of changing wind conditions the vertical distributions of velocity, temperature and water vapor will undergo an adjustment toward a new equilibrium. During such intervals of change it is entirely possible that one measure of stability, say the Richardson Number, Ri, may indicate unstable conditions (temperature decreasing with height above the ground) while another measure such as z/L simultaneously indicates a stable stratification because the heat flux is negative on/into the ground. For the 19 PCB vertical gradient measurement intervals just three cases occurred where the sampling interval average values of Ri and z/L had opposite signs - August 1, 2001, last 2 hours; October 24, 2001 evening and October 25, 2001 morning. In each of these cases, the wind had shifted during the sampling interval significantly in direction leading to a lack of equilibrium conditions in the lower atmosphere. Thus, the estimates for the vertical flux of PCB's for these three intervals must be considered with caution.

One measure of the reasonableness of the observations at the landfill is to compare the values of the stability correction factors for momentum exchange, ϕ_M, calculated from the present measurements with values obtained in other studies. In Figure 47, the presently calculated values for ϕ_M are plotted against values of z/L. Also shown on this figure are the empirically-based equations for this dependence developed in five other studies. The results from the presently reported observations were taken from selected intervals in which the wind conditions were reasonably steady. There is considerable scatter in the data similar to most micrometeorological observational studies, but there is substantial agreement with the theoretical dependence of ϕ_M on z/L.

For a few sampling intervals the values of the stability factors were in marked disagreement with expectations. For example, for the late afternoon sampling on November 14, 2002, the atmosphere was unquestionably stable with Ri and z/L both greater than zero. The stability factor for momentum was, surprisingly, significantly <1 while the factor for sensible heat was >1 as expected. The reasons for this are obscure but there was a significant shift in wind direction during this interval.

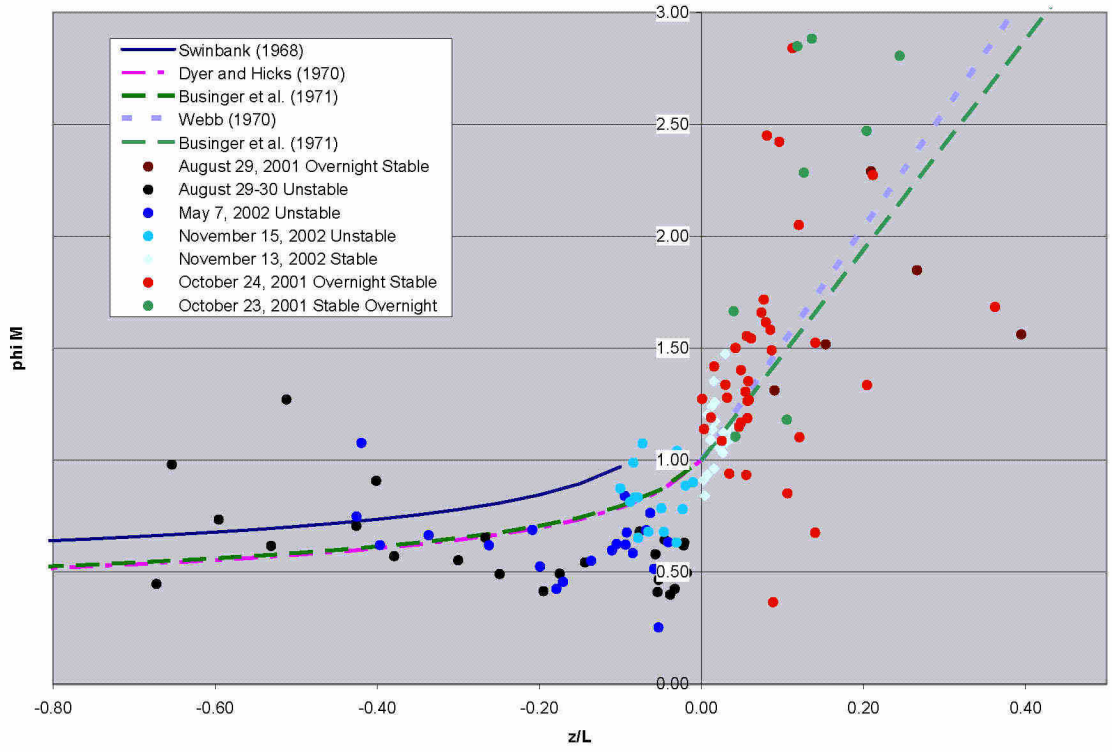

Figure 47. Relationship between calculated stability correction factors for momentum exchange (ϕ_M) and z/L.

The flux of PCB's depends on the properties of the treated dredged material and on the atmospheric conditions. In this study, only some gross aspects of the dependence of the flux on the properties of the dredged material can be inferred. During the May 2002 sampling campaign amended dredged material was placed upwind of the instrumentation site just hours prior to the first sampling interval. The calculated flux for this interval of the order of 15,000 ng m^{-2} s^{-1} was the highest found during this study, exceeding the next highest value by a factor of three. The pattern of fluxes calculated for the first four sampling intervals in May 2002 would indicate that there is a marked decrease in flux with age of the placed materials over the first few hours, which becomes more gradual as the age increases to a day or more.

The effect of atmospheric conditions on the flux of PCB's is a direct dependence on the friction velocity and a less obvious dependence on atmospheric stability. The directly measured values of the friction velocity, u_*, in the individual sampling intervals, varied from 0.10 to 0.59 m s^{-1}. Thus, by itself, this range in the value of u_* would produce a factor of 6 variation in PCB flux. The stability factor, estimated from either Φ_W or Φ_H exhibited a range of values from 0.3 to 1.8 which again provides for a factor of 6 variation in PCB flux.

A difficulty arose for several sampling intervals in the determination of the stability correction factor for evaporation. The resolution of the measurement of the average vapor pressure at the two fixed elevations was 0.01 mb. On several occasions the vertical gradient was less than this instrumental resolution. In contrast, the temperature gradient was always measurable and the stability correction

factor for sensible heat flux could be reliably measured. In cases where the factor for evaporative flux could not be found, the factor for sensible heat flux was used as a surrogate for the stability correction factor for the flux of PCB's. It has been argued in the literature; see, for example, Dyer and Hicks (1970) that the factors for heat and vapor behave similarly with identical numerical values with variation in atmospheric stability.

An estimate of the magnitude of horizontal gradients expected at the landfill can be made using the following assumptions:

Typically the lagoon of freshly placed dredged material had a horizontal dimension of the order of 100 m. The expected height of the concentration boundary layer for PCB's at the downwind edge of this lagoon for wind speeds of about 2 m s^{-1} would be of the order of 10 m or less. If the vertical flux is of the order of 1000 ng m^{-2} h^{-1}, then the increase in concentration, ΔC, between an upwind and downwind perimeter station can be found for a simple box model; the excess flux per unit width of PCB's through a vertical section with height, h = 10 m, and average velocity u = 2 m s^{-1} must equal the vertical flux of 0.3 ng m^{-2} s^{-1} over a patch length of 100 m.

The result is an expected difference in PCB concentration of the order of 1.5 ng m^{-3}. This is in reasonable agreement with observations on those occasions when there were perimeter measurements upwind and downwind of the recently placed dredge material. On October 24 for example, the wind was blowing from the office trailer toward the pug mill and directly over the site where the vertical flux measurements were being made. The measured concentration at the office trailer was 1.9 ng m^{-3} and at the pug mill it was 3.7 ng m^{-3}. Hence in this instance ΔC= 1.8 mg m^{-3}.

The ΣPCB flux rates measured in this study may be compared to previously determined PCB flux rates over large bodies of water including New York Harbor and Raritan Bay, NJ (Totten et al., 2001) Chesapeake Bay, MD (Nelson et al., 1998), and Green Bay, WI (Achman et al., 1993). The flux rates, determined using thin film theory, were significantly lower than the values calculated in this study. In New York Harbor and Raritan Bay the average flux rates were 1900 and 840 ng m^{-2} d^{-1} respectively with a range of 310 to 2700 ng m^{-2} d^{-1} over a three day period in July 1998. In Chesapeake Bay, the annual mean flux rate was 96 ng m^{-2} d^{-1} with a range of -63 to 800 ng m^{-2} d^{-1}. The annual flux rate found in the Green Bay study was 81 ng m^{-2} d^{-1} with a range of 13 to 1300 ng m^{-2} d^{-1}. Assuming that active volatilization of PCBs occurred only during the daytime (Table 4), the ΣPCB fluxes estimated at the SDM landfill ranged from 870 – 1.8 x 10^5 ng m^{-2} d^{-1}. As found in the air-water exchange studies, the lesser chlorinated PCBs corresponding to lower molecular weight congeners tended to have higher sediment-air fluxes.

The flux rates of PCBs have exhibited a large dependence on the atmospheric and site conditions. Since latent and sensible heat fluxes stop or greatly decline at night, lower PCB flux rates were measured at night. Very low PCB fluxes also occurred during daytime intervals, when it was cloudy and cool, such as on the morning of 23 October 2001 when there were lower heat flux rates. The moisture content of the dredged material may also have an effect on PCB volatilization. The 29-30 August 2001 sampling campaign exhibited vastly different behavior from that found for recently laid SDM. During this campaign, the SDM was dry and a white crust had formed on it. During this time the sensible heat flux was greater than the latent heat flux, suggesting that the transport of water vapor out of the SDM had been restricted. The estimated PCB fluxes during 29-30 August 2001 were

directed into the ground. In a study conducted using a laboratory flux chamber it was concluded that "dry" sediments have a greater affinity for contaminants than wet sediments because of the competition for adsorption or absorption space with water (Valsaraj et al., 1997). As the sediment particles in upper layers of the sediment dry they not only hold the contaminant absorbed to them tighter, they will also absorb free contaminants that would otherwise diffuse to the surface, thus further increasing the sediment-side resistance to contaminant flux to the atmosphere. In another laboratory study conducted with contaminated St. Lawrence River sediment, Chiarenzelli et al. found a very high correlation between the evaporation rate of water and the amount of PCBs volatilized in the first 24 hours of drying (Chiarenzelli et al., 1996).

6.4 Vertical Hg Fluxes at the SDM Landfill

This study presents the first measurements of the emissions of Hg from stabilized or unstabilized freshwater or marine sediments. However, the emissions of Hg from stabilized sediments measured here can be compared with the fluxes of Hg from soils. Modeling studies of the mercury cycle indicate that the average terrestrial emission rate is approximately 1 Mt y^{-1} or 0.8 ng m^{-2} h^{-1} (Lindqvist et al., 1991) and that this rate has changed little since pre-industrial times (Mason et al, 1994). Since this value is the average for all land surface types, it greatly underestimates the emission from more reactive pools in the terrestrial environment including soils. Estimates of soil-air Hg fluxes for uncontaminated natural soils range from –2.2 to 45 ng m^{-2} h^{-1} (Kim and Lindberg, 1995; Carpi and Lindberg, 1998; Poissant and Casmir, 1998; Engle et al., 2001). An assessment of the emissions of Hg from geologically enriched soils such as those in Nevada suggests that the Hg flux in these areas ranges from 3.5 to 13 ng m^{-2} h^{-1}, depending on hydrothermal alteration (Zehner and Gustin, 2002). Contaminated soils such as those near Hg mining activities can have much higher Hg emission rates that range from 10 to 1500 ng m^{-2} h^{-1}(Lindberg et al., 1995; Carpi and Lindberg, 1997; Ferrara et al., 1998). The range of vertical Hg fluxes estimated in this study of SDM (17 to 1043 ng m^{-2} h^{-1}) is certainly within the upper range of soil-air fluxes.

Many estimates of soil-air Hg fluxes were made using flux chambers (Engle et al., 2001; Carpi and Lindberg, 1998; Ferrara et al., 1998). The benefit of using flux chambers is that environmental parameters are well controlled and their effect on Hg volatilization can be assessed. Micrometeorological methods, such as those used in this study, however, are thought to provide more accurate measures of *in situ* vertical fluxes (Gustin et al., 1999). Comparisons show that micrometeorological methods consistently yield fluxes that are nearly three times higher than those determined with flux chambers (Gustin et al., 1999).

The age, temperature and water content of the stabilized sediment are expected to affect sediment-air fluxes of TGM. As the sediment proceeds through the cementation reaction, it is expected that the contaminants will become secure within a matrix, thereby producing a declining flux over the curing time, thus older stabilized sediments should have lowering fluxes. The intensity of incident radiation is also expected to play a significant role in the degree to which mercury is volatilized from land applied sediments.

In addition to meteorological and site conditions, the mercury concentration in the sediments being processed, has a large effect on the observed fluxes. The dredged material is heterogeneous as to its mercury content, but is estimated to range between 1.3 ppm (Con Edison analytical evaluation of the

dredge applied during October 2001) and 2.6 ppm (ETL, 2001), well above the pre-industrial concentration of 0.3 to 0.4 ppm of the Hudson drainage basin (Wakeman and Themelis, 2001). TGM fluxes can be compared with the mercury content of the substrate; e.g., Lindberg et al.(1995), evaluated an impacted site in East Fork Poplar Creek in Oak Ridge, Tennessee, where soils were contaminated by weapons manufacturing activities in the 1950's. The concentration of mercury in the soil ranged from 5 to 50 ug per gram soil and the related flux ranged from 10 to 200 ng m^{-2} h^{-1}. In a study done by Carpi and Lindberg, 1997, the flux of mercury was measured from soils amended with sewage sludge. The average sludge mercury concentration averaged 7.3 ug g^{-1} soil, and the flux was approximately 100 ng m^{-2} h^{-1} above the background flux. [Note: EPA monthly average, maximum allowable pollutant concentration for unrestricted land application is 17 ug g^{-1} sludge (EPA, 1993].

In an extensive study of the flux of mercury from naturally enriched substrates in Nevada, Gustin et al., (2000), proposed a scale in which the soil concentration of mercury is related to the flux out of the soil. For example, the scale projects a flux of approximately 80 ng m^{-2} h^{-1} with a soil concentration of 3 ug g^{-1}. Flux estimates for the SDM landfill in Bayonne, for which sediment concentrations are in the range of 1.3 to 2.6 ug g^{-1}, were higher in August 2001, October 2001, and May 2002 than this relationship would predict (Table 5). Higher than expected fluxes of Hg above SDM (in relation to sediment concentration) may be the result of greater reactivity (thermal or photochemical) of sediment-bound Hg than Hg in soils. Since the temperature of SDM is moderated by the large water content, temperature may play less of a role in Hg emissions from SDM than from soils. A modest, but significant correlation was found between Hg concentrations measured at the NJDEP trailer in Bayonne and air temperature (r^2 of 0.57, $p < 0.05$). This correlation likely reflects temperature driven volatilization of Hg from soils and surface waters in the region and is consistent with other studies showing significant correlations between soil temperature and Hg concentrations in the atmosphere (Gillis and Miller, 2000). Incident radiation has also been found to facilitate the volatilization of Hg from soils. Sunlight has been implicated in the reduction of oxidized mercury to its more volatile elemental state, Hg^0 (Carpi and Lindberg, 1997). This reduction occurs in the shallow layer of surface soil (<0.5 cm) where the penetration of light is possible (Carpi and Lindberg, 1997). This mechanism may play a significant role in the amount of volatilized species observed above land-applied sediments. It has been found that light-enhanced emissions of Hg from natural soils are 1.5 to 116 times emissions in the dark (Gustin, et al., 2002). Poissant and Casmir (1998) found that the Hg flux was correlated to incident radiation with an r^2 of 0.92, whereas the correlation with temperature had an r^2 of 0.38. This information may be used in selecting appropriate times of year to apply stabilized dredged sediments in order to reduce the extent of the potential flux. Wind speed can also drive the vertical flux of volatile contaminants, but in this study, no significant correlation between wind speed and the magnitude of the Hg flux at the SDM landfill in Bayonne was observed (r^2=0.24, $p > 0.05$).

The water content of soil can have an effect on the evaporative flux of the soil bound contaminant so it has been theorized that increased flux of volatile contaminants from moist soil is due to the increase in vapor pressure caused by the displacement of the chemical from the soil surface by the water (Spencer et al., 1969). For example, Hg fluxes from soils have been observed to increase following rain events (Wallschlager et al., 2000). At the SDM landfill, sediments are applied to the land saturated with water, so displacement by rain cannot occur. As SDM dries over days to weeks, the loss of moisture may slow down the volatilization of Hg and other contaminants.

6.5 Contribution of the SDM Landfill to Hg in Bayonne Air

The annual average concentration of gaseous Hg in Bayonne, NJ in 2002-03 (2.19 ng m^{-3}) was slightly higher than the reported range of global average background levels (1.5 to 2.0 ng m^{-3}; Slemr, 1992). In addition to upwind sources such as coal burning power plants and other industry to the west of New Jersey, current and historic industry in the NY/NJ metropolitan area contribute Hg to the air in Bayonne, NJ. As such the potential contribution of Hg from the land application of SDM needs to be assessed in the context of the total steady-state pool of TGM in Bayonne. In order to predict the relative potential contribution of TGM from the SDM landfill to the Bayonne area, a simple box model integrating our measured background TGM concentrations and estimated Hg flux parameters and has been formulated.

The Bayonne landfill covers an area of approximately 5 x 10^5 m^2. In our model, approximately 20% of the total area of the landfill was assumed to be receiving SDM at any given time. A vertical flux of 600 ng m^{-2} h^{-1} was assumed to be representative of the summer (rounded average of daytime fluxes estimated for August 2001 and May 2002) and a flux of 30 ng m^{-2} h^{-1} was used for the winter months (rounded average of positive fluxes estimated for November 2002). Since it has been shown here and elsewhere that soil-air fluxes of mercury are significantly reduced at night, fluxes were estimated over a 12 h day.

During the summer months, the contribution of mercury to the atmosphere from the application of the stabilized dredge sediments is estimated to be 720 mg d^{-1}. Assuming a vertical mixing height of 500 m, which is characteristic of coastal regions (Garrat, 1992), and an average summertime concentration of Hg of 3 ng m^{-3}, the air over the city of Bayonne (10 km^2) contains 15 g of gaseous Hg. Therefore, Hg emissions from the SDM landfill would contribute approximately 5% d^{-1} of the ambient concentration of the total gas phase Hg during the summer. In the winter, the SDM landfill is estimated to emit 36 mg Hg d^{-1}. Assuming an average Hg concentration of 2 ng m^{-3} in the winter, the atmosphere above Bayonne contains a total of 10 g of gas phase Hg. The SDM landfill would then add approximately 0.4% d^{-1} of the ambient concentration of gas phase Hg in the winter.

7.0 CONCLUSIONS

The results of this project show that PCB concentrations measured at the Bayonne trailer site are of similar magnitude to average concentrations measured in other large urban and industrial areas (Chicago, Illinois; Baltimore, Maryland; Jersey City, New Jersey). The highest ΣPCB concentrations at the NJDEP trailer site occurred under NE winds and not W winds, as would be the case if Newark Bay was the dominant source of PCBs to western Bayonne. Potential sources located to the NE of the trailer site include the city of Bayonne, the Hudson River, and New York City. In addition to wind direction, there is a seasonality to the dataset: gas phase PCB concentrations followed the order of July 2001 > October 2001 > November 2002, May 2002, likely due to enhanced air-surface exchange processes under warmer temperatures.

Average ΣPCB concentrations at the sediment application site were approximately 2X higher than those at the background trailer site and as much as 50X higher than the global continental background (~300 pg/m^3). However, there were sampling periods (6 of 29) when the concentrations at the trailer were greater than each of the three concentrations at the sediment application site. Upwind /downwind

concentration gradients of PCBs were rare (5 of 29 cases) at the SDM landfill site. This suggests that SDM is not the only or dominant source of PCBs to the air above the landfill and that other offsite sources may be important.

Gas phase PCB and Hg concentrations were elevated in the air above the SDM landfill in Bayonne, NJ relative to background concentrations in Bayonne, but are orders of magnitude below exposure limits. Thus PCB air concentrations measured directly above SDM (3 – 14 ng m^{-3}) as it cures were relatively high compared to background values measured in the region (1 – 3 ng m^{-3}), but they were two orders of magnitude below the NIOSH recommended exposure limit of 1μg m^{-3} and five orders of magnitude lower than the OSHA permissible exposure limits of 0.5 to 1.0 mg m^{-3}. The average gaseous Hg concentration measured at the SDM landfill (3.2 ng m^{-3}) was significantly higher ($p < 0.05$) than the average background concentration measured at the NJDEP trailer or in New Brunswick, NJ on days that bracketed the SDM landfill sampling campaigns (1.8 ng m^{-3}), all TGM concentrations measured during this project were well below chronic effects limits for total gaseous mercury (200 ng m^{-3}, Agency for Toxic Substances and Disease Registry-CDC; 300 ng m^{-3}, EPA).

It has been shown through this study that it is possible to quantify vertical gradients in PCB and Hg air concentrations in the surface microlayer of the atmosphere. Using these concentration gradients and a combination of the Aerodynamic Gradient and Eddy Correlation methods, net sediment-air fluxes of PCBs and Hg at the sediment application site were estimated. Vertical fluxes of PCBs and Hg were generally positive during the day and low to negative at night, but they were highly variable and dependent on atmospheric conditions as well as the age and condition of the SDM. Estimated vertical fluxes of PCBs from SDM at the Bayonne landfill ranged from 72 to 15,000 ng m^{-2} h^{-1} and averaged 2050 ng m^{-2} h^{-1}. It appears from this study that although the flux of PCBs from recently treated and placed SDM may be high, it decreases quickly as the SDM dries. Although PCB concentrations are much lower than the limits for Industrial Standards, the contribution of SDM sites to regional PCB air concentrations should be investigated further. Sediment-air Hg fluxes for the Bayonne SDM landfill ranged from 17 to 1043 ng m^{-2} h^{-1}, averaged 312 ng m^{-2} h^{-1}, and were similar to those measured from contaminated soils (Lindberg et al., 1995; Ferrara et al, 1998).

One of the concerns regarding the land application of SDM in populated areas is the potential impact of volatile contaminants to the local atmosphere. The present results demonstrate that the city of Bayonne, NJ, as represented by the NJDEP trailer air monitoring station, is impacted to a greater extent by PCB sources from areas other than the SDM site. This suggests that the SDM landfill is not the primary source of PCBs to the city of Bayonne. A simple box model shows that the contribution of Hg emissions from the SDM landfill to total gas phase Hg in the boundary layer of the city of Bayonne is minimal (<5%).

8.0 REFERENCES

Achman, D.R., Hornbuckle, K.C., Eisenreich, S.J. (1993) Volatilization of polychlorinated biphenyls from Green Bay, Lake Michigan. *Environ. Sci. Technol.* 27: 75-87.

Boussinesq, J. (1877) Essay on the Theory of Flowing Water. French Academy of Sciences.

Brunciak, P.A., Dachs, J., Gigliotti, C.L., Nelson, E.D., Eisenreich, S.J. (2001) *Atmos. Environ.* 35, 3325-3339.

Businger, Wyngaard, Izumi, and Bradley (1971) Flux profile relationships in the atmospheric surface layer. *J Atmo. Sci.* 28:181-189.

Carpi, A., Lindberg, S.E. (1997) Sunlight-mediated emission of elemental mercury from soil amended with municipal sewage sludge, *Environ. Sci. Technol.* 31:2085-2091.

Carpi, A., Lindberg, S.E. (1998) Application of a Teflon (TM) dynamic flux chamber for quantifying soil mercury flux: Tests and results over background soil. *Atmos. Environ.* 32: 873-882.

Chiarenzelli, J., Serudato, R., Arnold, G., Wunderlich, M., Rafferty, D. (1996) Volatilization of polychlorinated biphenyls from sediment during drying at ambient conditions. *Chemosphere* 33: 899-911.

Dyer, A.J., Hicks, B.B. (1970) Flux gradient relationships in the constant flux layer. Quart. *J. Royal Met. Soc.* 96:715-721.

Engle, M.A., Gustin, M.S., Zhang H. (2001) Quantifying natural source mercury emissions from the Ivanhoe Mining District, north-central Nevada, USA. *Atmos. Environ.* 35: 3987-3997.

EPA (1993) 40 C.F.R. Part 503, *Fed. Regist.* 58(Feb 19), 32.

ETL Report (2001) Elizabeth Channel Composite Sediments. NJDEP.

Ferrara, R., Maserti, B.E., Andersson, M., Edner, H., Ragnarson, P., Svanberg, S., Hernandez, A. (1998) Atmospheric mercury concentrations and fluxes in the Almaden District (Spain). *Atmos. Environ.* 32: 3897-3904.

Garratt, J.R., The Atmospheric Boundary Layer, Cambridge University Press, Cambridge, 1992.

Gillis, A.A., Miller, D.R. (2000) Some local environmental effects on mercury emission and absorption at a soil surface. *Sci. Total Environ.* 260: 191-200.

Gustin, M.S., Lindberg, S., Marsik, F., Casimir, A., Ebinghaus, R., Edwards, G., Hubble-Fitzgerald, C., Kemp, R., Kock, H., Leonard, T., London, J., Majewski, M., Montecinos, C., Owens, J., Pilote, M., Poissant, L., Rasmussen, P., Schaedlich, F., Schneeberger, D., Schroeder, W., Sommar, J., Turner, R., Vette, A., Wallschlaeger, D., Xiao, Z., Zhang, H. (1999) Nevada STORMS project: Measurement of mercury emissions from naturally enriched surfaces. *J. Geophys. Res. Atmo.* 104:21831-21844.

Gustin, M.S., Lindberg, S.E., Austin, K., Coolbaugh, M., Vette, A., Zhang, H. (2000) Assessing the contribution of natural sources to regional atmospheric mercury budgets. *Sci. Total Environ.* 259:61-71.

Gustin, M.S., Biester, H., Kim, C.S. (2002) Investigation of the light-enhanced emission of mercury from naturally enriched substrates. *Atmo. Environ.* 36:3241-3254.

Hoff, R.M., Muir, D.C.G., Grift, N.P. (1992) *Environ. Sci. Technol.* 26, 266-275.

Kim K.H., Lindberg S.E. (1995) Design and initial tests of a dynamic enclosure chamber for measurements of vapor-phase mercury fluxes over soils. *Water Air Soil Pollut.* 80:1059-1068.

Kim, K.-H., Kim, M.-Y. (1999) The exchange of gaseous mercury across soil-air surface interface in a residential area of Seoul, Korea. *Atmo. Environ.* 33:3153-3165.

Lee, R.M.G., Jones, K.C. (1999) *Environ. Sci. Technol.* 33, 705-712.

Lindberg, S.E., Kim, K.H., Meyers, T.P., Owens, J.G. (1995) Micrometeorological gradient approach for quantifying air-surface exchange of mercury-vapor - tests over contaminated soils. *Environ. Sci. Technol.* 29: 126-135.

Lindqvist, O., Johansson, K., AAstrup M. et al. (1991) Mercury in the Swedish environment: recent research on causes consequences and corrective methods. *Water Air Soil Pollut.* 55: 23-32.

Mason, R., Fitzgerald W., Morel F. (1994) The biogiochemical cycling of elemental mercury: anthropogenic influences. *Geochim. Cosmochim. Acta* 58:3191-3198.

Monin, A.O., Obukov, A.M. (1954) Basic laws of turbulent mixing in the ground layer of the atmosphere. Akad. Nauk. SSSR Geofiz. Inst. Tr. 151:163-187.

Nelson, E.D., McConnell, L.L., Baker, J.E. (1998) Diffusive exchange of gaseous polycyclic aromatic hydrocarbons and polychlorinated biphenyls across the air-water interlace of the Chesapeake Bay. *Environ. Sci. Technol.* 32: 912-919.

Obukov, A.M. (1946) Turbulence in an atmosphere with inhomogeneous temperature. Tr. Inst. Teor. Geofiz. Akad. Nauk. SSSR 1:95-115.

Offenberg, J.H., Baker, J.E. (1999) *J. Air Waste Mngmt Assoc.* 49, 959-965.

Pasquill, F. (1949) Some estimates of the amount and diurnal variation of evaporation from a clayland pasture in fair spring weather. *Quart. J. Royal Met. Soc.* 75:249-256.

Pasquill, F. (1948) Eddy Diffusion of Water Vapour and Heat Near the Ground, Meteorological Office, London and School of Agriculture, University of Cambridge.

Poissant, L., Casimir, A. (1998) Water-air and soil-air exchange rate of total gaseous mercury measured at background sites. *Atmo. Environ.* 32: 883-893.

Prandtl, L. (1926) Ueber die ausgebbildete Turbulenz. Proc. 2nd Intern. Congr, *Applied Mech.* Zurich, p. 62.

Pruitt, W.O., Morgan, D.L., and Lourence, F.J. (1973) Momentum and mass transfer in the surface boundary layer. *Quart. J. Met. Soc.* 99: 370-386.

Reynolds, O. (1895) On the dynamical theory of incompressible viscous fluids and the determination of the criterion. Phil. *Trans. Roy. Soc.*, A1, 186: 123.

Richardson, L.F. (1920) The supply of energy from and to atmospheric eddies. *Proc. Royal Soc.* A 97: 354-373.

Schmidt, W. (1925) Der massenaustausch in frier luft und verwandte erscheinungen, Hamberg.

Schroeder, W. H., Keeler, G., Kock, H.H., Roussel, P., Schneeberger, D. and Schaedlich, F. (1995) International field intercomparison of atmospheric mercury measurement methods. *Water Air Soil Pollut.* 80: 611-620.

Simcik, M.F., Ph.D. Thesis, Rutgers University, 1998.

Simcik, M.F., Zhang, H., Eisenreich, S.J., Franz, T.P. (1997) *Environ. Sci. Technol.* 31, 2141-2147.

Slemr, F, Langer, E. (1992) Increase in global atmospheric concentrations of mercury inferred from measurements over the Atlantic Ocean. *Nature* 355: 434-437.

Spencer, W.F., Cliath, M.M., Farmer, W.J. (1969) Vapor density of soil-applied dieldrin as related to soil-water content, temperature and dieldrin concentration. *Soil Sci. Soc. Am. Proc.* 33: 509-511.

Stern, G.A., Halsall, C.J., Barrie, L.A., Muir, D.C.G., Fellin, P., Rosenberg, B., Rovinsky, F.Ya., Kononov, E.Ya., Pastuhov, B. (1997) *Environ. Sci. Technol.* 31, 3619-3628.

Swinbank, W.C. (1968) A comparison between predictions of dimensional analysis for the constant flux layer and observations in unstable conditions. *Quart. J. Royal Met. Soc.* 94: 460-467.

Taylor, G. I. (1921) Diffusion by continuous movements. *Proc. London Math. Soc.* Ser. A20: 196-211.

Thornthwaite, C., Holzman, B. (1938) The determination of evaporation from land and water surfaces, *Monthly Weath. Rev.* January, pp 4-11.

Totten, L.A., Brunciak, P.A., Gigliotti, C.L., Dachs, J., Glenn, T.R., Nelson, E.D., Eisenreich, S.J. (2001) Dynamic air-water exchange of polychlorinated biphenyls in the New York - New Jersey Harbor Estuary. *Environ. Sci. Technol.* 35: 3834-3840.

Totten, L.A.; Gigliotti, C.L.; Van Ry, D.A.; Offenberg J.H.; Nelson, E.D.; Dachs, J.; Reinfelder, J.R.; Eisenreich, S.J. (in review) *Environ. Sci. Technol.*

Valsaraj, K.T., Choy, B., Ravikrishna, R., Reible, D.D., Thibodeaux, L.J., Price, C.B., Brannon, J.M., Myers, T.E. (1997) Air emissions from exposed, contaminated sediments and dredged materials .1. Experimental data in laboratory microcosms and mathematical modeling. *J. Haz. Mat. 54*: 65-87.

Van Ry, D.A., Gigliotti, C.L., Glenn IV, T.R., Nelson, E.D., Totten, L.A., Eisenreich, S.J. (2002) *Environ. Sci. Technol.* 36, 3201-3209.

von Karmen, T., (1921) Zeits. Fur angew. *Math. U. Mech.* 1: 233-252.

Wakeman, T.H., Themelis, N. (2001) A basin-wide approach to dredged material management in New York/ New Jersey Harbor. *J. Haz. Mat.* 85: 1-13.

Wallschlager, D., Kock, H.H., Schroeder, W., Lindberg, SE, Ebinghaus, R., and Wilken, R. (2000) Mechanism and significance of mercury volatilization from contaminated floodplains of the German river Elbe. *Atmo. Environ.* 34: 3745-3755.

Webb, E.K. (1970) Profile relationships: the log linear range, and extension to strong stability. Quart. *J. Royal Met. Soc.* 96: 67-90.

Weinstein, M.P., Douglas, S. (2002) Sediment toxicity risk assessment: Where are we and where should we be going? *Proc. MIT Dredge Conference*, December 3-6, 2000. NJSG-02-482.

Zehner, R.E., Gustin, M.S. (2002) Estimation of mercury vapor flux from natural substrate in Nevada. *Environ. Sci. Technol.* 36: 4039-4045.

Date	Time of Day	Wind Direction	Wind Speed (m/s)	Temperature (°C)
12/8/1999	all day	NW	4.8	5.8
12/20/1999	all day	NE/ S	3.5	8.0
1/1/2000	all day	SW	1.8	5.2
1/13/2000	all day	N	8.1	-4.6
1/25/2000	all day	N	9.3	-3.0
2/6/2000	all day	W	6.4	-0.2
2/18/2000	all day	NE	4.9	2.4
3/1/2000	all day	NW/SE	2.7	6.5
3/13/2000	all day	variable- mostly NW	3.3	10
3/25/2000	all day	variable	3.6	14
4/6/2000	all day	N/ W,SW	5.8	16
4/18/2000	all day	NE	8.0	7.0
4/30/2000	all day	N,NW	6.7	14
5/12/2000	all day	NE/SE	4.1	16
5/24/2000	all day	W	4.5	19
6/5/2000	all day	E	5.8	17
6/17/2000	all day	variable	4.8	25
6/29/2000	all day	variable	3.0	21
7/11/2000	all day	N	5.1	25
7/23/2000	all day	variable- mostly W,SW	3.0	23
8/4/2000	all day	N	3.8	23
8/16/2000	all day	NW	5.4	23
8/28/2000	all day	E, NE	4.3	23
9/9/2000	all day	variable- mostly NE		24
9/21/2000	all day	----------(no data)----------		
10/4/2000	all day	variable- mostly NE	4.3	19
10/15/2000	all day	N	3.5	21
10/27/2000	all day	variable	2.2	17
11/8/2000	all day	variable	2.0	13
11/20/2000	all day	W	5.5	3
7/17/2001	all day	W/SW then NW	3	25.4
7/18/2001	am	E	2.5	23.5
7/18/2001	pm	SE	5.2	23.9
7/19/2001	am	NE	6.4	20.5
7/19/2001	pm	NE	5.4	23.1
7/20/2001	am	NE	4.5	22.9
7/20/2001	pm	SE	3.5	25
10/23/2001	am	SE	3.7	17.4
10/23/2001	pm	SE	3.4	18.6
10/24/2001	am	SW	3.8	24.0
10/24/2001	pm	SE	3.3	24.3
10/25/2001	am	W	9.0	24.9
10/25/2001	pm	W	8.5	21.6
10/26/2001	am	W	10.2	13.8
10/26/2001	pm	W	8.5	10.3
5/7/2002	am	W,SW	4.4	14.0

5/7/2002 pm	W	5	14.0
5/8/2002 am	NE	5.6	7.3
5/8/2002 pm	SE	4.4	7.9
5/9/2002 am	SE	3.5	6.9
5/9/2002 pm	SE	3.3	8.1
5/10/2002 am	W	9.1	7.7
5/10/2002 pm	W	8.9	3.1
11/12/2002 am	NE	5.7	11.5
11/12/2002 pm	NE	8.1	10.2
11/13/2002 am	N,NW	6.2	10.0
11/13/2002 pm	N,NW	6.1	9.0
11/14/2002 am	W	2.8	10.6
11/14/2002 pm	SW	4.5	12.2

Detection Limits (pg)
(defined as avg mass plus 3 times stdev of field blanks)

PCB Congeners	BA-trailer site	SA-sediment site
8+5	1032	1034
18	208	234
17+15	285	633
16+32	324	627
31	141	258
28	119	248
21+33+53	242	202
22	232	227
45	78	38
46	58	71
52+43	622	264
49	413	262
47+48	245	177
44	189	315
37+42	241	149
41+71	69	136
64	126	73
40	668	174
74	76	73
70+76	117	141
66+95	253	246
91	101	45
56+60+89	43	56
92+84	151	82
101	74	66
99	55	36
83	53	15
97	358	53
87+81	1000	1081
85+136	128	175
110+77	114	123
82	364	18
151	158	94
135+144+147+124	53	22
149+123+107	132	82
118	329	32
146	103	17
153+132	542	345
105	77	29
141+179	41	21
137+176+130	9.1	8.3
163+138	172	174
158	33	16
178+129	36	19
187+182	303	137
183	29	24
128	34	17
185	228	552
174	180	126
177	110	120
202+171+156	100	65
180	88	40

199	40		14	
170+190	27		13	
201	55		24	
203+196	113		83	
195+208	68		89	
194	61		43	
206	28		14	
	11329		9550	
		9		8
		1032		1081

Gas Phase PCB Masses (pg) - Field BlanksBayonne Trailer Site

PCB Congeners	*BAHAP122099FB*	*BAHAP032400FB*	*BAHAP061600FB*
8+5	813	344	112
18	142	105	124
17+15	126	112	165
16+32	205	119	123
31	80	43	54
28	56	109	44
21+33+53	203	201	109
22	34	141	29
45	3.4	68	10
46	31	17	20
52+43	384	155	38
49	161	235	201
47+48	183	157	120
44	30	56	39
37+42	20	54	42
41+71	12	24	11
64	11	62	29
40	33	87	739
74	46	36	24
70+76	112	32	19
66+95	100	3	115
91	8.2	9	12
56+60+89	7.2	38	9.3
92+84	30	58	11
101	31	65	62
99	9	9.2	42
83	54	28	2.9
97	36	88	8.4
87+81	324	233	372
85+136	34	23	37
110+77	49	89	23
82	34	36	24
151	19	20	10
135+144+147+124	21	33	26
149+123+107	30	31	60
118	33	30	59
146	45	33	45
153+132	29	36	62
105	10	9	84
141+179	11	12	24
137+176+130	2.5	3.5	5.3
163+138	18	31	107
158	6.2	6.5	28
178+129	11	9.7	4.5
187+182	31	55	39
183	2.5	5.5	29
128	5.7	5.5	7.1
185	21	18	25
174	12	22	3.3
177	19	8.3	40
202+171+156	19	19	20
180	9.5	7.3	95

199	13	11	9.0
170+190	7.8	15	6.4
201	9.1	9.3	29
203+196	14	14	8.4
195+208	4.5	9	20
194	9.1	2.4	2.5
206	1.9	13	2.4
Sum PCBs	3821	3311	3623
Surrogate Recoveries(%)			
PCB-23	80	74	67
PCB-65	88	84	51
PCB-166	89	93	82

BAP080300FB	*BAP081700FB*	*BAP071801FB*	*BAP071901FB*	*BAP072001FB*	*BAP102501FB*
240	129	597	524	524	213
168	24	50	78	108	47
165	192	67	68	215	40
143	41	104	197	269	43
135	32	76	81	63	35
60	33	53	62	49	20
26	42	61	67	57	29
48	26	158	42	59	37
21	10	38	5.5	2.8	19
34	21	37	21	31	24
188	87	130	39	147	183
251	254	120	108	63	272
52	23	101	97	75	76
38	59	131	134	94	50
54	56	50	20	19	74
17	25	42	22	16	32
66	72	53	9.1	8.2	27
230	156	265	100	38	21
54	41	44	13	46	23
29	19	50	41	38	26
122	110	158	76	126	84
14	7.7	30	118	9.5	11
14	7.8	24	12	3.9	13
8.3	28	30	18	9.1	64
21	19	33	20	15	15
14	6.4	51	17	14	5.3
2.1	4.6	4.2	1.3	7.2	6.1
20	6.0	46	7.4	14	91
344	3.2	448	496	416	424
17	13	78	38	28	33
15	9.4	63	37	22	36
24	27	24	20	14	92
3.6	16	24	18	23	49
44	4.9	30	26	6.7	8.6
12	10	24	96	19	36
17	29	87	29	70	79
77	8.4	15	8.2	7.2	22
27	35	26	24	21	151
3.1	4.2	5.5	8.9	28	5.9
14	5.5	6.2	4.8	10	13
5	3.2	1.2	1.6	3.0	3.4
14	18	42	7.1	14	37
6.0	11	5.9	2.5	2.3	10
11	10	10	2.4	16	6.5
68	63	27	88	75	56
4.0	12	2.7	3.2	6.3	5.6
6.1	6.1	3.4	4.9	5.4	7.9
19	12	1.4	1.5	3.6	66
33	10	177	25	14	35
47	42	57	5.8	3.8	29
25	21	23	22	20	40
17	11	20	30	20	8.4

14	6.9	3.6	6.8	4.1	11
13	6.3	7.9	3.1	4.0	8.3
6.6	24	12	2.6	4.9	16
9.0	12	36	4.1	7.6	28
22	2.3	33	18	8.9	23
4.2	3.7	54	23	3.6	17
8.5	3.2	8.2	0.8	9.1	6.5
3165	1972	3960	3057	3009	2943

85	88	88	82	81	88
85	89	94	88	88	93
87	92	98	95	97	98

BAP102601FB	*BAP050602FB*	*BAP050702FB*	*BAP050902FB*	*BAP051002FB*
101	114	118	150	99
31	18	35	67	30
32	10	31	49	31
25	32	28	59	21
40	29	45	46	11
15	13	35	39	14
17	14	27	41	16
22	208	32	65	27
10	10	11	9.2	6.8
16	12	26	10	12
104	75	65	69	34
22	226	32	76	27
40	88	43	73	35
30	38	34	24	20
19	31	23	26	20
39	55	33	29	17
8.5	12	6.5	8.0	5.2
18	12	47	21	8.6
15	49	24	19	23
18	27	80	7.9	8.7
102	184	22	114	111
12	28	19	11	11
12	27	18	21	4
27	69	60	18	11
11	22	14	15	14
10	21	4.3	8.5	5.6
21	22	11	6.2	3.8
20	32	420	5.8	1.9
222	696	2.4	427	503
11	121	13	30	13
53	90	57	41	40
9.6	26	3.9	7.1	3.1
140	72	66	51	16
21	18	6.4	5.7	6.9
112	64	66	23	30
87	112	9.4	6.9	5.9
17	10	3.5	4.7	7.6
429	428	219	182	230
39	18	3.3	6.2	3.2
29	28	7.7	5.7	27
8	6.2	1.8	2.0	4.3
57	140	24	16	124
24	10	16	1.8	4.8
33	25	7.6	9.2	11
136	300	17	42	21
19	10	3.5	7.8	10
21	33	8.6	6.0	21
60	16	50	5.8	264
79	100	43	7.4	3.9
58	100	40	5.9	24
101	64	36	33	38
46	13	13	12	11

12	26	3.1	4.6	6.1
17	14	8.7	3.5	5.2
26	30	15	5.0	6.7
70	107	47	7.4	6.2
63	45	21	28	21
33	20	11	8.7	6.4
20	25	3.1	6.3	6.1
2892	4247	2171	2093	2110

89	50	91	85	93
93	40	93	89	94
98	63	96	94	98

BAP111202FB	*BAP111302FB*
658	40
54	49
57	35
82	25
41	31
8.8	4.4
28	32
55	6.6
61	9.0
53	19
643	106
120	19
192	37
150	21
280	22
54	27
109	3.8
7.1	20
43	4.6
5.8	28
157	16
8.1	7.0
15	4.7
141	87
16	17
3.5	4.5
2.1	7.6
6.3	22
784	404
30	79
20	21
434	14
108	4.1
16	8.4
46	15
370	2.9
87	6.8
95	29
12	4.9
3.6	23
4.9	4.2
4.1	16
8.9	17
1.5	2.7
191	9.4
1.9	4.4
1.8	2.4
8.1	1.3
57	61
41	35
46	47
4.5	1.4

SAP071801FB	*SAP071901FB*	*SAP072001FB*
406	593	704
41	69	184
380	500	208
281	275	533
65	73	109
31	58	78
97	68	141
26	22	133
2	4.8	11
25	5.7	28
17	65	215
73	54	121
108	77	139
58	70	259
79	16	44
4.4	20	41
6.0	10	25
160	22	76
31	36	52
57	32	113
129	130	208
6.0	3.9	4.5
9.2	13	13
32	26	36
23	29	37
14	16	27
1.4	2.1	6.1
44	19	32
387	470	519
3.1	44	53
24	38	38
7.7	7.9	5.6
13	17	22
2.8	3.8	17
1.1	11	19
3.8	28	4.5
3.5	3.7	8.1
26	16	18
10	7.4	26
1.2	5.8	16
0.69	1.3	6.6
5.0	23	19
4.6	1.9	4.5
1.3	3	14
3.9	88	10
1.2	1.4	12
2.9	3.1	3.9
1.1	1.1	5.1
13	21	108
58	1.7	104
18	18	35
27	6.7	31

39	1.0	1.7	2.5	8.7
23	1.0	4.0	3.8	7.1
51	2.2	2.3	6.6	3.9
46	31	38	4.6	48
23	21	27	2.4	85
23	37	18	1.7	39
9.5	7.4	2.7	1.4	7.1
6723	1620	2918	3158	4873

81	80	81	84	77
83	83	87	90	84
87	87	94	97	91

SAP102401FB	*SAP102501FB*	*SAP102601FB*	*SAP050802FB*	*SAP050902FB*
220	114	154	106	635
61	32	35	64	164
246	87	108	62	142
177	54	78	50	144
55	30	37	41	243
35	23	21	28	239
54	42	44	37	144
78	78	66	72	70
8.1	8.1	8.4	10	36
17	27	21	16	65
92	49	54	72	180
89	79	82	89	171
67	68	64	57	108
72	32	35	36	200
27	36	38	27	134
27	61	36	77	115
11	6.6	16	63	39
25	42	43	15	35
33	29	27	41	50
32	17	23	25	83
142	111	111	170	194
12	10	13	27	38
13	12	11	24	53
30	25	37	42	74
26	18	23	47	51
13	9.1	10	14	27
6.4	4.5	6.0	13	6.7
14	13	17	16	25
478	539	485	557	599
64	28	53	138	119
48	38	49	102	66
10	9.1	9.4	11	5.5
30	32	31	42	48
10	6.1	8.2	14	8.6
20	23	30	61	41
12	7.6	8.1	13	11
6.4	6.8	8.2	9.8	3.7
51	66	130	256	197
11	6.2	8.3	16	5.6
8.3	9.6	13	7.7	9.1
3.2	2.7	3.5	3.8	1.4
28	38	47	65	164
7.8	6.6	8.1	7.4	5.1
9.4	7.2	7.1	13	8.2
53	33	32	96	29
6.6	6.5	8.9	20	6.7
5.3	8.6	10	10	3.1
116	67	154	527	16
53	27	28	11	5.8
35	20	29	31	42
29	26	35	44	41
13	13	13	15	6.6

5.9	5.6	5.3	6.3	3.5
4.8	4.8	5.3	6.7	3.0
10	8.0	8.4	11	6.7
36	25	32	54	8.2
30	24	23	24	24
14	11	15	7.0	9.8
6.2	5.6	6.2	4.8	7.3
2897	2228	2525	3527	4974

86	93	92	89	93
96	95	96	98	96
99	96	99	99	101

SAP051002FB	*SAP111302FB*	*SAP111402FB*
190	73	26
51	21	20
57	20	15
36	26	13
46	30	16
25	10	3
42	13	6
189	34	13
13	8.7	2.7
27	12	10
45	80	57
203	17	18
82	42	15
42	16	6.6
42	14	18
29	27	19
11	3.2	3.6
12	10	4.9
33	40	4.4
5.3	5.3	4.3
130	142	101
18	5.8	6.5
11	11	3.8
23	39	10
20	17	7.7
10	7.0	4.7
6.2	4.9	2.0
4.7	9.1	5.6
519	858	26
58	37	35
70	15	17
12	16	7.5
78	3.1	6.0
10	4.5	4.6
53	8.0	11
15	6.8	3.6
15	3.5	2.3
171	22	27
8.4	3.0	10
11	2.8	5.9
5.1	1.7	1.4
34	10	11
8.4	14	5.0
7.1	6.9	5.7
31	64	69
12	1.7	6.4
13	0.89	5.7
63	0.97	7.9
56	53	38
7.9	1.9	33
38	1.5	25
13	0.76	6.7

11	4.3	2.8
10	1.0	1.6
20	5.9	16
36	39	53
23	22	16
14	5.6	6.6
11	1.9	6.5
2836	1955	891

92	76	84
100	81	88
100	85	99

Gas Phase PCB Masses (pg) - Field BlanksBayonne Trailer Site

PCB Congeners	*BAHAP122099FB*	*BAHAP032400FB*	*BAHAP061600FB*
8+5	813	344	112
18	142	105	124
17+15	126	112	165
16+32	205	119	123
31	80	43	54
28	56	109	44
21+33+53	203	201	109
22	34	141	29
45	3.4	68	10
46	31	17	20
52+43	384	155	38
49	161	235	201
47+48	183	157	120
44	30	56	39
37+42	20	54	42
41+71	12	24	11
64	11	62	29
40	33	87	739
74	46	36	24
70+76	112	32	19
66+95	100	3	115
91	8.2	9	12
56+60+89	7.2	38	9.3
92+84	30	58	11
101	31	65	62
99	9	9.2	42
83	54	28	2.9
97	36	88	8.4
87+81	324	233	372
85+136	34	23	37
110+77	49	89	23
82	34	36	24
151	19	20	10
135+144+147+124	21	33	26
149+123+107	30	31	60
118	33	30	59
146	45	33	45
153+132	29	36	62
105	10	9	84
141+179	11	12	24
137+176+130	2.5	3.5	5.3
163+138	18	31	107
158	6.2	6.5	28
178+129	11	9.7	4.5
187+182	31	55	39
183	2.5	5.5	29
128	5.7	5.5	7.1
185	21	18	25
174	12	22	3.3
177	19	8.3	40
202+171+156	19	19	20
180	9.5	7.3	95

199	13	11	9.0
170+190	7.8	15	6.4
201	9.1	9.3	29
203+196	14	14	8.4
195+208	4.5	9	20
194	9.1	2.4	2.5
206	1.9	13	2.4
Sum PCBs	3821	3311	3623
Surrogate Recoveries(%)			
PCB-23	80	74	67
PCB-65	88	84	51
PCB-166	89	93	82

BAP080300FB	*BAP081700FB*	*BAP071801FB*	*BAP071901FB*	*BAP072001FB*	*BAP102501FB*
240	129	597	524	524	213
168	24	50	78	108	47
165	192	67	68	215	40
143	41	104	197	269	43
135	32	76	81	63	35
60	33	53	62	49	20
26	42	61	67	57	29
48	26	158	42	59	37
21	10	38	5.5	2.8	19
34	21	37	21	31	24
188	87	130	39	147	183
251	254	120	108	63	272
52	23	101	97	75	76
38	59	131	134	94	50
54	56	50	20	19	74
17	25	42	22	16	32
66	72	53	9.1	8.2	27
230	156	265	100	38	21
54	41	44	13	46	23
29	19	50	41	38	26
122	110	158	76	126	84
14	7.7	30	118	9.5	11
14	7.8	24	12	3.9	13
8.3	28	30	18	9.1	64
21	19	33	20	15	15
14	6.4	51	17	14	5.3
2.1	4.6	4.2	1.3	7.2	6.1
20	6.0	46	7.4	14	91
344	3.2	448	496	416	424
17	13	78	38	28	33
15	9.4	63	37	22	36
24	27	24	20	14	92
3.6	16	24	18	23	49
44	4.9	30	26	6.7	8.6
12	10	24	96	19	36
17	29	87	29	70	79
77	8.4	15	8.2	7.2	22
27	35	26	24	21	151
3.1	4.2	5.5	8.9	28	5.9
14	5.5	6.2	4.8	10	13
5	3.2	1.2	1.6	3.0	3.4
14	18	42	7.1	14	37
6.0	11	5.9	2.5	2.3	10
11	10	10	2.4	16	6.5
68	63	27	88	75	56
4.0	12	2.7	3.2	6.3	5.6
6.1	6.1	3.4	4.9	5.4	7.9
19	12	1.4	1.5	3.6	66
33	10	177	25	14	35
47	42	57	5.8	3.8	29
25	21	23	22	20	40
17	11	20	30	20	8.4

14	6.9	3.6	6.8	4.1	11
13	6.3	7.9	3.1	4.0	8.3
6.6	24	12	2.6	4.9	16
9.0	12	36	4.1	7.6	28
22	2.3	33	18	8.9	23
4.2	3.7	54	23	3.6	17
8.5	3.2	8.2	0.8	9.1	6.5
3165	1972	3960	3057	3009	2943

85	88	88	82	81	88
85	89	94	88	88	93
87	92	98	95	97	98

BAP102601FB	*BAP050602FB*	*BAP050702FB*	*BAP050902FB*	*BAP051002FB*
101	114	118	150	99
31	18	35	67	30
32	10	31	49	31
25	32	28	59	21
40	29	45	46	11
15	13	35	39	14
17	14	27	41	16
22	208	32	65	27
10	10	11	9.2	6.8
16	12	26	10	12
104	75	65	69	34
22	226	32	76	27
40	88	43	73	35
30	38	34	24	20
19	31	23	26	20
39	55	33	29	17
8.5	12	6.5	8.0	5.2
18	12	47	21	8.6
15	49	24	19	23
18	27	80	7.9	8.7
102	184	22	114	111
12	28	19	11	11
12	27	18	21	4
27	69	60	18	11
11	22	14	15	14
10	21	4.3	8.5	5.6
21	22	11	6.2	3.8
20	32	420	5.8	1.9
222	696	2.4	427	503
11	121	13	30	13
53	90	57	41	40
9.6	26	3.9	7.1	3.1
140	72	66	51	16
21	18	6.4	5.7	6.9
112	64	66	23	30
87	112	9.4	6.9	5.9
17	10	3.5	4.7	7.6
429	428	219	182	230
39	18	3.3	6.2	3.2
29	28	7.7	5.7	27
8	6.2	1.8	2.0	4.3
57	140	24	16	124
24	10	16	1.8	4.8
33	25	7.6	9.2	11
136	300	17	42	21
19	10	3.5	7.8	10
21	33	8.6	6.0	21
60	16	50	5.8	264
79	100	43	7.4	3.9
58	100	40	5.9	24
101	64	36	33	38
46	13	13	12	11

12	26	3.1	4.6	6.1
17	14	8.7	3.5	5.2
26	30	15	5.0	6.7
70	107	47	7.4	6.2
63	45	21	28	21
33	20	11	8.7	6.4
20	25	3.1	6.3	6.1
2892	4247	2171	2093	2110

89	50	91	85	93
93	40	93	89	94
98	63	96	94	98

Field Blanks- sediment application site

BAP111202FB	*BAP111302FB*	*SAP071801FB*	*SAP071901FB*	*SAP072001FB*
658	40	406	593	704
54	49	41	69	184
57	35	380	500	2076
82	25	281	275	533
41	31	65	73	109
8.8	4.4	31	58	78
28	32	97	68	141
55	6.6	26	22	133
61	9.0	2	4.8	11
53	19	25	5.7	28
643	106	17	65	215
1203	19	73	54	121
192	37	108	77	139
150	21	58	70	259
280	22	79	16	44
54	27	4.4	20	41
109	3.8	6.0	10	25
7.1	20	160	22	76
43	4.6	31	36	52
5.8	28	57	32	113
157	16	129	130	208
8.1	7.0	6.0	3.9	4.5
15	4.7	9.2	13	13
141	87	32	26	36
16	17	23	29	37
3.5	4.5	14	16	27
2.1	7.6	1.4	2.1	6.1
6.3	22	44	19	32
784	404	387	470	519
30	79	3.1	44	53
20	21	24	38	38
434	14	7.7	7.9	5.6
108	4.1	13	17	22
16	8.4	2.8	3.8	17
46	15	1.1	11	19
370	2.9	3.8	28	4.5
87	6.8	3.5	3.7	8.1
95	29	26	16	18
12	4.9	10	7.4	26
3.6	23	1.2	5.8	16
4.9	4.2	0.69	1.3	6.6
4.1	16	5.0	23	19
8.9	17	4.6	1.9	4.5
1.5	2.7	1.3	3	14
191	9.4	3.9	88	10
1.9	4.4	1.2	1.4	12
1.8	2.4	2.9	3.1	3.9
8.1	1.3	1.1	1.1	5.1
57	61	13	21	108
41	35	58	1.7	104
46	47	18	18	35
4.5	1.4	27	6.7	31

39	1.0	1.7	2.5	8.7
23	1.0	4.0	3.8	7.1
51	2.2	2.3	6.6	3.9
46	31	38	4.6	48
23	21	27	2.4	85
23	37	18	1.7	39
9.5	7.4	2.7	1.4	7.1
6723	1620	2918	3158	6741

81	80	81	84	77
83	83	87	90	84
87	87	94	97	91

SAP102401FB	*SAP102501FB*	*SAP102601FB*	*SAP050802FB*	*SAP050902FB*
220	114	154	106	635
61	32	35	64	164
246	87	108	62	142
177	54	78	50	144
55	30	37	41	243
35	23	21	28	239
54	42	44	37	144
78	78	66	72	70
8.1	8.1	8.4	10	36
17	27	21	16	65
92	49	54	72	180
89	79	82	89	171
67	68	64	57	108
72	32	35	36	200
27	36	38	27	134
27	61	36	77	115
11	6.6	16	63	39
25	42	43	15	35
33	29	27	41	50
32	17	23	25	83
142	111	111	170	194
12	10	13	27	38
13	12	11	24	53
30	25	37	42	74
26	18	23	47	51
13	9.1	10	14	27
6.4	4.5	6.0	13	6.7
14	13	17	16	25
478	539	485	557	599
64	28	53	138	119
48	38	49	102	66
10	9.1	9.4	11	5.5
30	32	31	42	48
10	6.1	8.2	14	8.6
20	23	30	61	41
12	7.6	8.1	13	11
6.4	6.8	8.2	9.8	3.7
51	66	130	256	197
11	6.2	8.3	16	5.6
8.3	9.6	13	7.7	9.1
3.2	2.7	3.5	3.8	1.4
28	38	47	65	164
7.8	6.6	8.1	7.4	5.1
9.4	7.2	7.1	13	8.2
53	33	32	96	29
6.6	6.5	8.9	20	6.7
5.3	8.6	10	10	3.1
116	67	154	527	16
53	27	28	11	5.8
35	20	29	31	42
29	26	35	44	41
13	13	13	15	6.6

5.9	5.6	5.3	6.3	3.5
4.8	4.8	5.3	6.7	3.0
10	8.0	8.4	11	6.7
36	25	32	54	8.2
30	24	23	24	24
14	11	15	7.0	9.8
6.2	5.6	6.2	4.8	7.3
2897	2228	2525	3527	4974

86	93	92	89	93
96	95	96	98	96
99	96	99	99	101

SAP051002FB	*SAP111302FB*	*SAP111402FB*
190	73	26
51	21	20
57	20	15
36	26	13
46	30	16
25	10	3.1
42	13	6.0
189	34	13
13	8.7	2.7
27	12	10
45	80	57
203	17	18
82	42	15
42	16	6.6
42	14	18
29	27	19
11	3.2	3.6
12	10	4.9
33	40	4.4
5.3	5.3	4.3
130	142	101
18	5.8	6.5
11	11	3.8
23	39	10
20	17	7.7
10	7.0	4.7
6.2	4.9	2.0
4.7	9.1	5.6
519	858	26
58	37	35
70	15	17
12	16	7.5
78	3.1	6.0
10	4.5	4.6
53	8.0	11
15	6.8	3.6
15	3.5	2.3
171	22	27
8.4	3.0	10
11	2.8	5.9
5.1	1.7	1.4
34	10	11
8.4	14	5.0
7.1	6.9	5.7
31	64	69
12	1.7	6.4
13	0.89	5.7
63	0.97	7.9
56	53	38
7.9	1.9	33
38	1.5	25
13	0.76	6.7

11	4.3	2.8
10	1.0	1.6
20	5.9	16
36	39	53
23	22	16
14	5.6	6.6
11	1.9	6.5
2836	1955	891

92	76	84
100	81	88
100	85	99

Gas Phase PCB Masses (pg) - Lab Blanks

PCB Congeners	*LBP020600*	*LBP020800*	*LBP050800*	*LBP072400*	*LBP101100*
8+5	52	19	164	193	77
18	86	22	74	51	48
17+15	72	8.8	73	47	128
16+32	265	23	116	15	273
31	57	14	97	51	32
28	120	13	268	8.1	44
21+33+53	491	93	262	15	75
22	20	21	111	23	20
45	7.4	10	28	8.1	19
46	21	35	33	24	42
52+43	262	106	286	0.10	506
49	169	224	578	41	302
47+48	723	15	173	75	95
44	160	61	79	78	68
37+42	194	13	66	19	89
41+71	45	20	91	28	31
64	42	31	49	23	78
40	62	213	278	520	253
74	90	24	35	37	47
70+76	109	7.5	94	20	48
66+95	207	43	171	119	145
91	19	59	22	50	5.8
56+60+89	18	44	55	88	4.3
92+84	47	34	34	18	12
101	51	21	23	37	2.6
99	12	12	14	12	11
83	2.9	16	8	18	3.0
97	34	22	27	88	44
87+81	299	58	396	445	385
85+136	13	19	100	14	98
110+77	47	24	162	17	66
82	3.9	7.3	40	16	36
151	8.4	4.9	29	13	6.3
135+144+147+124	22	16	243	28	8.4
149+123+107	21	23	80	65	27
118	18	42	73	57	42
146	14	35	32	14	7.9
153+132	3.9	104	37	23	41
105	8.9	18	13	10	13
141+179	2.7	3.7	7.4	12	11
137+176+130	2.2	10	6.0	28	1.8
163+138	23	56	18	65	35
158	12	37	21	57	4.0
178+129	29	27	22	12	3.8
187+182	145	47	48	23	53
183	18	23	20	12	3.9
128	19	14	16	7.5	7.9
185	8.2	13	34	7.8	11
174	3.9	3.4	70	12	15
177	3.8	38	39	11	4.4
202+171+156	11	58	54	15	24
180	12	36	36	40	21
199	11	17	12	9.1	3.0

170+190	2.8	21	12	11	7.4
201	6.9	4.3	21	6.2	42
203+196	13	33	19	6.6	44
195+208	23	21	13	9.8	20
194	4.1	1.2	4.9	6.7	3.3
206	1.9	2.7	9.9	1.3	3.4
Sum PCBs	4255	2042	5000	2758	3551
Surrogate Recoveries(%)					
PCB-23	77	65	74	89	82
PCB-65	89	79	86	91	82
PCB-166	88	78	91	94	84

LBP072401a	*LBP072401b*	*LBP072501a*	*LBP072501b*	*LBP120501*	*LBP121101*	*LBP060302*
147	741	583	540	308	418	262
146	96	101	37	85	73	55
104	643	90	203	264	160	468
626	220	437	122	221	102	73
16	115	22	83	64	71	125
15	82	23	39	43	32	59
49	172	68	18	67	37	65
198	540	26	104	138	106	66
59	81	6.3	6.1	31	15	32
38	46	45	14	34	29	20
602	323	292	46	260	108	131
401	222	373	42	271	290	340
101	151	114	64	94	76	80
50	188	69	41	90	63	145
35	60	23	48	61	54	145
319	47	17	11	70	41	62
13	86	6.9	2.9	49	30	94
259	527	2.7	5.7	263	163	516
12	66	39	30	50	40	92
64	112	83	17	52	26	38
154	248	144	112	154	133	119
13	22	9.2	5.5	19	13	22
4.2	24	5.7	2.6	38	35	104
23	58	21	8.0	38	37	62
23	50	22	8.3	30	23	39
7.3	25	3.7	3.5	16	13	27
1.2	10	1.6	1.8	10	8.1	10
33	68	19	1.1	37	13	10
489	417	491	421	458	522	463
59	51	10	8.8	95	40	287
38	71	26	7.8	45	27	42
24	113	15	61	51	46	74
62	43	15	69	37	44	22
20	57	9.2	5.2	235	166	102
43	48	11	10	40	23	55
94	121	80	28	64	30	63
73	72	11	4.7	29	25	23
27	27	4.0	5.6	63	80	103
29	38	9.4	16	21	15	36
8.2	4.2	8.1	3.8	14	21	34
0.66	2.6	0.70	1.0	7.3	4.0	13
5.6	28	21	3.8	72	35	18
3.2	7.3	2.7	0.89	47	19	16
10	2.1	3.4	1.4	26	23	45
75	43	58	64	57	45	77
12	15	2.9	3.2	30	13	35
3.2	3.5	5.0	4.2	16	8.9	44
3.5	10	4.8	0.60	68	87	20
57	104	18	13	216	73	56
73	71	5	5.0	37	36	49
20	26	20	1.7	35	80	111
28	25	18	1.1	38	34	60
12	16	4.7	1.0	16	10	15

1.5	6.7	4.6	0.85	13	6.6	25
4.1	2.7	1.9	1.5	23	17	72
43	44	8.7	4.4	39	18	56
29	36	6.4	29	52	25	37
51	31	18	6.5	23	14	39
3.5	27	3.4	15	49	21	54
4913	6587	3548	2415	4876	3817	5408

84	82	75	85	80	89	71
89	88	84	91	84	89	75
92	99	93	98	90	96	80

LBP060402	*LBP060502*	*LBP091102*	*LBP090902*	*LBP120402*
235	765	225	851	813
72	60	115	121	69
563	105	68	132	270
73	64	51	65	61
95	123	55	107	60
82	33	34	48	11
62	51	28	38	38
62	50	170	153	553
33	17	11	7.7	79
32	17	25	32	76
176	77	50	159	345
400	387	87	1013	1471
86	90	49	179	161
99	74	27	131	167
101	116	18	249	18
19	38	34	83	62
84	86	7.6	58	12
24	534	4.6	37	6.3
75	46	36	52	48
34	37	19	18	2.9
170	107	136	122	145
26	26	8.1	26	13
54	109	23	54	3.1
77	46	29	43	46
49	40	20	27	18
25	25	14	7.0	3.6
23	12	14	9.4	23
24	9	9	7.2	2.1
449	441	526	508	807
223	63	21	25	13
57	31	41	40	26
85	48	46	60	119
60	35	72	345	95
734	546	3.7	6.1	2.9
41	25	32	118	293
54	48	3.7	71	221
25	84	3.1	78	92
80	120	200	585	21
31	26	4	10	24
23	20	13	15	4.3
11	8.2	1.7	6.7	5.5
358	55	45	37	3.3
280	39	4.3	3.8	2.4
124	74	8.2	8.8	2.7
124	52	6.7	35	11
150	16	12	3.2	7.5
50	12	8.0	8.1	3.8
152	17	339	122	11
412	27	56	6.4	71
51	66	29	49	35
23	275	38	38	45
100	121	9.4	10	6.8
58	26	7.4	23	32

44	5	3.6	14	30
48	35	5.4	17	31
108	41	3.5	8.5	58
257	8.9	18	20	22
32	36	2.4	5.3	9.3
45	27	3.8	7.7	15
7143	5572	2935	6117	6696

83	79	95	91	72
86	85	94	95	74
80	87	97	99	77

LBP120902	*LBP121002*
250	211
66	15
159	75
53	13
33	10
11	3.8
21	5.7
66	86
7.3	4.2
56	2.9
108	31
663	25
86	22
80	14
27	17
53	11
3.3	2.9
9.8	8.2
36	19
3.6	5.5
157	78
8.1	5.3
2.9	2.1
66	48
17	10
7	3.1
3.1	2.3
10	2.3
761	407
12	3.9
12	4.8
22	18
8	4.0
40	2.1
6.1	3.1
6.4	6.8
2.7	0.92
9.9	0.83
8.4	7.0
53	2.5
2.0	36
1.5	2.1
1.8	1.0
3.8	7.3
45	14
1.2	1.9
3.7	4.0
10	10
55	27
44	3.5
49	3.3
1.2	2.5
1.1	2.4

10	0.89
20	1.8
2.1	5.9
20	1.0
1.7	1.7
9.0	1.2
3285	1321

85	100
87	100
92	100

Gas Phase PCB Concentrations (pg/m3) - Bayonne Trailer Site

PCB Congeners	*12/8/99*	*12/20/99*	*1/1/00*	*1/13/00*	*1/25/00*	*2/6/00*
8+5	172	652	234	173	36	30
18	34	220	95	59	17	16
17+15	63	120	46	32	10	9.3
16+32	44	225	110	58	18	16
31	62	188	77	46	16	13
28	57	191	86	45	16	15
21+33+53	41	149	61	35	11	11
22	33	107	57	24	7.7	7.7
45	10	24	15	7.0	3.2	2.5
46	5.0	8.7	8.7	2.3	1.6	2.4
52+43	66	141	109	48	34	18
49	34	82	85	31	16	12
47+48	17	44	25	14	7.8	6.2
44	42	107	68	31	21	12
37+42	22	54	36	16	9.2	8.0
41+71	20	50	26	13	8.6	6.4
64	14	39	20	11	6.5	4.0
40	6.8	17	7.9	5.2	3.0	2.5
74	12	26	15	8.7	7.2	3.1
70+76	21	51	34	18	17	5.6
66+95	67	151	114	60	58	17
91	9.8	18	4.9	6.8	5.9	2.8
56+60+89	16	39	27	17	16	4.8
92+84	28	69	59	29	31	9.8
101	22	78	54	34	37	7.5
99	13	43	24	14	14	4.9
83	1.1	4.1	2.4	1.7	1.8	0.49
97	3.9	17	11	7.3	8.4	1.7
87+81	11	44	27	19	22	4.2
85+136	6.9	25	15	13	13	2.4
110+77	19	88	54	36	45	7.3
82	2.0	6.6	5.0	2.1	2.8	0.46
151	2.6	9.7	7.6	3.2	3.4	0.96
135+144+147+124	2.9	12	8.9	3.7	4.7	0.93
149+123+107	7.2	33	24	9.7	13	2.3
118	6.4	39	26	9.8	16	2.2
146	0.87	6.1	3.9	1.3	2.4	0.29
153+132	6.4	38	28	9.0	16	2.5
105	2.0	16	11	3.5	6.6	0.73
141+179	1.6	8.2	6.1	1.7	3.0	0.84
137+176+130	0.64	3.4	2.3	0.39	1.0	0.86
163+138	6.0	49	32	5.5	16	2.2
158	0.83	7.4	4.8	0.92	2.5	0.37
178+129	1.2	0	1.5	0	1.7	0
187+182	1.1	4.2	3.6	0.61	0.81	0.33
183	0.46	3.1	2.3	0.43	0.89	0.59
128	0.42	3.8	2.1	0.23	0.99	0.20
185	0.16	0.75	0.54	0.064	0.11	0
174	0.74	4.3	2.6	0.17	0.56	0.14
177	0.38	3.3	1.9	0.21	0.45	0.12
202+171+156	0.72	4.5	1.1	0.14	0.47	0.14
180	0.91	5.0	2.6	0.26	0.57	0.27
199	0.10	0.81	0	0	0	0

170+190	0.33	1.7	0.87	0.064	0	0.041
201	0.38	1.4	1.3	0.045	0	0
203+196	0.50	1.4	1.7	0.0	0	0
195+208	0	0.12	0	0	0	0
194	0.054	0.13	0.10	0	0	0
206	0.21	0.24	0.25	0	0	0
Sum PCBs	*1023*	*3333*	*1788*	*968*	*610*	*279*
Surrogate Recoveries(%)						
PCB-23	88.3	92.3	83.4	90.9	90.3	94.5
PCB-65	88.9	91.3	78.0	90.8	88.3	94.0
PCB-166	90.1	83.0	84.5	86.1	90.8	91.4

2/18/00	*3/1/00*	*3/13/00*	*3/25/00*	*4/6/00*	*4/18/00*	*4/30/00*	*5/12/00*	*5/24/00*	*6/5/00*
138	106	76	195	196	31	123	252	57	162
55	54	36	132	100	23	61	138	60	75
30	29	22	72	52	14	33	155	30	102
60	58	36	154	105	28	67	94	41	71
58	43	29	113	84	32	57	125	88	55
43	38	26	107	70	32	46	100	62	56
42	30	22	79	53	25	37	80	40	43
30	24	17	64	41	21	28	33	22	34
6.5	9.1	4.1	15	14	7	14	20	29	14
3.5	3.6	2.7	7.2	5.0	4.2	5.5	7.1	4.1	4.8
92	40	34	104	63	145	60	225	95	62
38	31	22	64	46	49	36	81	88	35
18	13	8.8	30	22	22	18	41	28	17
58	24	21	73	44	85	35	105	72	43
24	14	11	39	25	27	13	30	19	19
23	13	8.9	41	25	40	20	38	27	17
17	7.8	7.0	22	13	22	11	23	12	13
7.8	5.2	4.5	9.2	6.6	11	6.5	0	2.9	4.4
16	5.8	5.2	15	9.2	28	10	31	13	10
44	11	11	33	17	82	20	75	27	21
150	32	36	104	53	290	34	253	79	70
15	3.2	2.9	7.1	4.6	28	5.0	20	8.4	6.9
39	11	9.3	28	15	71	18	50	15	18
88	21	20	57	31	163	33	88	37	36
88	15	17	45	21	185	29	166	35	35
30	6.9	11	25	11	60	17	49	12	12
3.0	0.63	0.80	1.7	1.0	6.6	1.8	6.5	1.6	2.2
19	3.1	3.7	9.8	4.4	39	5.9	29	6.8	7.7
52	8.3	11	26	12	108	17	68	20	18
29	4.5	6.4	14	7.2	54	5.7	38	70	26
98	13	17	48	20	215	33	104	28	33
6.5	1.1	1.5	4.2	1.7	15	2.9	5.0	2.3	2.1
8.6	1.8	2.0	6.3	2.9	17	3.8	20	7.0	4.7
11	2.0	2.1	6.6	2.8	25	4.7	24	6.7	5.4
33	5.1	5.8	22	8.0	72	12	60	16	12
29	4.8	5.6	20	7.0	72	12	63	14	12
4.8	2.8	2.8	4.8	3.2	12	3.9	13	2.8	6.4
30	6.0	5.8	25	9.0	78	14	55	17	13
8.4	2.2	2.0	8.9	3.0	29	5.5	14	3.5	5.2
5.1	1.2	1.3	5.1	2.1	14	2.9	18	4.9	3.7
1.2	0.3	0.3	1.5	1	4.5	1.0	4.4	2.3	0.66
20	5.2	5.1	25	8.7	79	14	71	22	14
2.6	0.52	0.59	2.9	1	10	1.2	10	2.7	2.2
0	0	0.77	0	1.5	0	0	1.2	4.0	0.80
1.3	0.73	0.66	3.9	2.1	4.3	1.9	8.3	4.8	2.6
1.1	0.43	0.40	2.2	1.11	3.1	1.1	5.8	2.3	1.3
1.1	0.49	0.39	1.9	0.61	7.0	1.6	2.5	1.3	0.87
0.24	0.20	0.046	0.24	0.17	0.27	0	0.81	0.37	0.19
1.0	0.65	0.52	2.5	1.3	3.5	1.3	7.6	3.0	2.4
0.66	0.42	0.28	1.8	0.89	2.3	0.83	6.0	2.2	1.0
0.32	0.29	0.41	1.5	1.2	3.1	0.74	1.1	3.9	0.64
0.39	0.42	0.35	3.4	1.7	2.9	1.5	7.5	4.4	2.0
0.17	0.12	0.043	0.25	0.17	0.60	0	0	0.36	0.33

0.19	0.056	0.057	1.0	0.44	1.4	0.33	2.5	1.2	0.55
0.19	0	0.080	1.8	1.4	0.93	0	2.7	2.8	1.1
0.23	0	0.097	1.0	1.4	1.0	0	2.8	3.3	1.1
0	0	0.028	0.22	0.20	0.14	0	0.22	0.62	0.20
0	0.064	0	0	0.064	0	0	0.14	0.52	0.15
0.081	0	0.020	0	0.046	0	0	0.23	0.27	0.15
1586	*715*	*580*	*1887*	*1232*	*2405*	*989*	*2928*	*1266*	*1219*

93.0	94.7	97.3	80.7	87.4	98.5	90.9	97.7	78.5	96.2
92.5	94.5	96.7	79.6	83.9	97.3	89.7	91.2	84.8	99.7
93.3	91.2	93.8	85.4	87.4	94.1	91.9	83.2	83.5	98.0

6/17/00	*6/29/00*	*7/11/00*	*7/23/00*	*8/4/00*	*8/16/00*	*8/28/00*	*9/9/00*	*9/21/00*
177	97	347	122	239	277	405	428	no
148	72	185	105	142	161	257	260	data
122	106	270	190	262	178	413	368	
157	44	169	98	126	155	249	257	
144	60	164	96	150	218	301	268	
140	42	153	87	91	115	175	136	
90	28	111	63	79	106	183	147	
82	17	66	35	42	60	114	104	
44	19	22	30	12	16	25	19	
13	3.5	9.0	6.9	4.8	8.6	14	15	
184	61	192	131	123	137	175	182	
127	41	96	81	70	98	80	102	
52	17	48	34	35	44	47	47	
146	29	134	91	82	102	103	124	
60	16	45	26	27	34	41	45	
61	52	0	31	48	53	60	65	
36	0	0	19	17	22	25	27	
11	0	8.6	4.6	2.5	2.7	1.2	2.3	
26	8.5	28	19	19	20	24	23	
56	18	67	38	38	36	50	52	
193	52	210	120	118	103	147	168	
19	3.9	16	9.2	12	9.6	15	9.4	
55	13	53	27	30	26	37	47	
125	31	101	52	57	57	66	86	
86	26	111	57	53	38	66	72	
28	7.0	35	19	17	11	18	19	
4.1	0.80	7.2	1.8	2.7	2.3	3.2	3.5	
18	4.6	24	13	12	8.6	14	15	
43	15	57	27	26	18	35	34	
76	52	15	10	108	93	123	142	
90	21	109	48	47	33	59	68	
7.8	1.7	6.1	3.4	3.4	2.2	4.6	9.7	
12	6.0	12	9.4	11	5.0	11	16	
12	6.2	16	10	8.2	5.1	12	17	
31	18	42	22	27	16	39	48	
31	15	50	21	25	14	33	37	
13	4.0	8.1	8.2	4.6	3.1	6.6	8.7	
37	16	45	7.4	26	13	32	41	
14	3.7	17	6.4	4.6	5.5	8.5	13	
8.7	4.8	10	7.9	5.8	3.6	9.0	11	
2.4	2.0	4.0	1.7	1.5	1.0	2.6	3.3	
40	22	63	28	31	16	43	51	
5.0	2.6	8.8	3.4	3.5	1.8	5.1	5.6	
0.97	5.9	2.3	1.3	3.9	1.3	2.8	2.9	
6.0	4.3	4.8	6.4	4.5	3.2	7.7	10	
3.6	2.5	3.4	3.9	2.3	1.7	5.7	5.5	
3.3	0.79	3.7	1.9	1.0	0.51	1.5	2.1	
0.60	0.34	0.45	1.2	0.28	0.27	0.53	0.96	
4.5	3.6	5.2	5.3	3.0	2.3	5.2	7.1	
3.0	2.0	2.9	2.6	1.9	1.5	3.2	4.3	
2.0	1.8	4.7	1.7	2.4	1.5	3.7	4.6	
5.5	4.4	6.3	4.6	4.4	3.4	7.9	11	
0.44	0.50	0.48	0.29	0.28	0.29	0.53	1.1	

1.6	1.4	2.3	1.2	1.3	0.98	2.3	3.0	
2.7	2.7	2.1	2.7	2.3	1.4	4.5	6.9	
2.9	2.6	2.2	2.7	2.4	1.6	4.5	6.9	
0.14	0.30	0.39	0.48	0.42	0.29	0.75	1.1	
0.48	0.32	0.28	0.32	0.36	0.25	0.70	0.98	
0.31	0.28	0.17	0.29	0.31	0.17	0.63	0.87	
2864	*1092*	*3178*	*1857*	*2275*	*2350*	*3584*	*3668*	*no data*

92.8	76.4	93.9	87.6	93.8	95.5	91.0	101
102	54.9	92.0	92.0	93.9	88.2	85.7	100
94.2	83.5	93.7	82.6	91.7	84.2	86.1	90.6

10/4/00	*10/15/00*	*10/27/00*	*11/8/00*	*11/20/00*
436	363	213	435	28
177	154	165	158	15
74	399	86	70	9
174	148	160	143	18
303	143	226	149	19
207	74	89	70	12
110	74	104	76	8.6
89	51	81	57	6.9
19	17	17	25	2.2
11	13	6.3	7.1	1.5
122	108	104	89	19
64	57	57	48	11
34	33	34	28	6.5
89	89	68	61	12
45	32	35	32	8.3
49	48	57	38	8.5
25	21	21	16	3.8
13	15	7.4	5.6	2.7
22	13	20	12	2.8
41	24	34	21	4.6
122	75	92	65	15
9.6	10	5.5	5.1	2.1
36	18	23	18	3.8
58	37	41	33	8.9
49	33	30	24	5.7
17	11	9.6	7.9	2.1
2.4	1.8	1.5	1.2	0.3
11	7.3	6.7	5.0	1.1
25	17	13	11	2.4
89	63	48	38	11
54	30	30	22	4.7
4.8	2.3	3.9	2.0	0.35
6.7	5.4	4.3	3.5	0.76
8.3	5.8	5.3	3.7	0.79
23	17	16	10	1.8
24	15	16	9.4	1.8
9.3	5.0	3.4	4.3	0.84
23	16	15	9.9	1.9
11	5.0	6.7	3.6	0.67
5.4	4.2	3.4	2.6	0.47
1.8	1.3	1.1	0.85	0.13
27	18	16	9.5	1.9
3.0	2.1	1.8	1.0	0.23
2.3	2.7	0.94	1.5	0.31
3.6	4.5	2.7	2.3	0.39
2.5	2.3	1.7	1.3	0.27
1.9	0.67	0.91	0.48	0.12
0.38	0.38	0.21	0.31	0.047
3.1	2.7	1.9	1.6	0.32
1.8	1.5	1.1	0.8	0.24
2.6	2.5	0.7	1.0	0.15
4.3	4.0	3.0	2.0	0.39
0.27	0.39	0.20	0.20	0.079

1.3	0.9	0.9	0.4	0.10
1.8	2.6	1.5	1.0	0.19
2.0	2.8	1.6	1.2	0.25
0.38	0.46	0.25	0.28	0.091
0.23	0.33	0.19	0.42	0.067
0.14	0.25	0.082	0.12	0.016
2754	*2304*	*1996*	*1846*	*272*

88.5	84.6	101	87.8	84.9
85.1	94.5	96.9	88.3	85.1
87.4	86.8	83.7	86.4	86.5

Gas Phase PCB Concentrations (pg/m3) - Bayonne Sediment Site

PCB Congeners	*SAP050101*	*SAP053101b*
8+5	596	425
18	97	208
17+15	340	673
16+32	318	119
31	391	173
28	489	103
21+33+53	219	90
22	103	39
45	88	22
46	21	10
52+43	244	121
49	114	74
47+48	77	52
44	90	87
37+42	147	39
41+71	119	44
64	31	28
40	11	16
74	34	39
70+76	59	64
66+95	193	172
91	44	107
56+60+89	43	42
92+84	73	86
101	78	74
99	24	24
83	5.1	5.2
97	14	17
87+81	33	25
85+136	85	14
110+77	54	42
82	3.6	2.9
151	10	6.5
135+144+147+124	9.1	5.4
149+123+107	26	13
118	18	12
146	9.3	3.7
153+132	24	15
105	5.2	3.1
141+179	5.9	4.2
137+176+130	1.8	1.4
163+138	23	15
158	3.1	2.2
178+129	4.1	1.9
187+182	4.8	3.6
183	2.5	2.0
128	0.65	0.37
185	0.56	0.40
174	12	3.9
177	2.2	1.3
202+171+156	2.2	1.8
180	4.4	2.9
199	0.43	0.43

170+190	1.2	0.74
201	2.3	1.5
203+196	2.3	1.5
195+208	0.77	0.77
194	0.39	0.37
206	0.88	0.65
Sum PCBs	4414	3141
Surrogate Recoveries(%)		
PCB-23	85	67
PCB-65	70	66
PCB-166	97	63

Codes:

example:	BAP102301A SAP102301AM

(BA) = **BA**yonne trailer site
(SA) = **S**ediment **A**pplication site

102301 = a date (yes I knew you'd figure that one out on

For BA samples:	there is one letter after the date A = afternoon M = morning
For SA samples:	there are two letters after the date the first letter is (A), (B), or (C indicating the sampler The second letter is (A) or (M) A = afternoon M = morning

Sometimes there is no A or M after a sample: that means it ran all day (9:00am to 5:00pm)

The samples at the trailer site (labelled "background") are all 24-hr samples that ran from 9:
the date on the label/code indicates the "start" date of the sample!

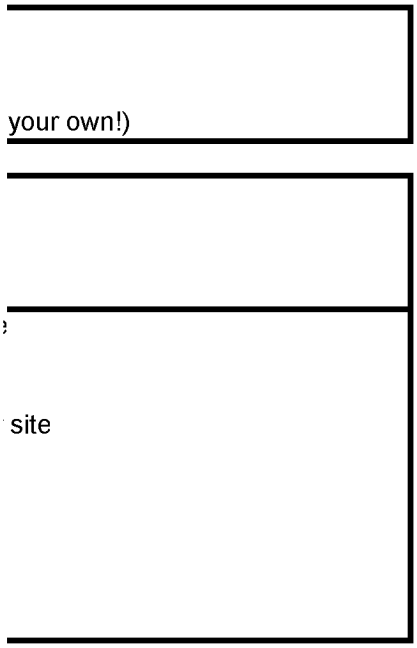

:00am to 9:00am.

Gas Phase PCB Concentrations (pg/m3)

PCB Congeners	BAP071701 (all day)	BAP071801M (morning)	BAP071801A (afternoon)
8+5	1330	812	214
18	172	206	112
17+15	1848	98	62
16+32	668	234	117
31	211	233	143
28	110	106	65
21+33+53	53	119	82
22	114	109	71
45	60	19	15
46	38	14	12
52+43	175	123	108
49	101	56	54
47+48	45	28	26
44	141	90	74
37+42	167	43	49
41+71	69	43	35
64	47	26	25
40	38	14	15
74	28	22	26
70+76	39	42	46
66+95	155	134	136
91	61	5.5	8.9
56+60+89	31	39	41
92+84	159	59	76
101	74	60	66
99	244	19	21
83	22	2.3	5.5
97	14	14	18
87+81	93	36	51
85+136	198	150	191
110+77	72	75	85
82	37	6.3	8.0
151	13	10	10
135+144+147+124	13	11	12
149+123+107	27	30	26
118	29	27	28
146	44	17	31
153+132	24	32	33
105	14	14	16
141+179	8.7	8.7	8.7
137+176+130	6.1	0.67	0.59
163+138	32	32	38
158	2.1	3.0	5.0
178+129	6.4	5.3	3.0
187+182	8.3	7.6	4.8
183	3.3	4.5	3.9
128	1.6	2.5	3.3
185	0.6	1.1	1.2
174	8.5	6.3	6.8
177	12	3.5	3.8
202+171+156	5.7	4.1	4.4
180	9.0	8.9	7.0

199	2.2	1.0	0.69
170+190	1.9	2.4	2.3
201	9.4	6.9	4.5
203+196	9.7	7.1	5.6
195+208	2.3	1.0	1.5
194	13	0.74	0.68
206	1.4	0.74	0.59
Sum PCBs	*6925*	*3288*	*2322*
Surrogate Recoveries(%)			
PCB-23	83	77	81
PCB-65	91	77	86
PCB-166	91	94	93

BAP071901M (morning)	BAP071901A (afternoon)	BAP072001M (morning)	BAP072001A (afternoon)	SAP071701A (all day)
1209	789	1182	134	360
399	277	315	52	197
167	102	126	28	100
373	282	381	75	200
457	327	380	67	223
190	134	246	43	113
213	162	200	43	143
155	104	152	33	82
30	27	24	6.7	48
12	16	16	4.6	14
193	142	312	93	169
84	71	194	68	96
56	61	50	14	76
134	111	161	44	98
81	60	52	18	61
75	67	58	19	61
43	31	43	9.2	27
26	33	35	7.6	12
39	30	30	10	23
68	56	97	35	42
181	159	224	86	130
19	25	4	3	16
46	69	51	10	35
72	67	69	30	69
73	71	63	28	44
28	23	22	9.0	16
4.3	6.6	4.0	1.7	4.7
15	19	17	7.6	10
40	54	76	41	16
105	110	93	54	116
74	83	88	40	44
7.0	7.9	10	4.1	4.9
9.1	10	12	5.9	6.1
11	12	13	6.3	6.7
28	32	40	19	17
29	27	34	15	14
13	17	14	10	11
30	37	40	20	17
13	12	16	8.1	39
10	12	12	5.1	4.2
1.3	1.0	1.0	0.63	1.0
33	37	46	21	16
3.6	4.2	6.6	2.3	1.6
2.0	1.6	3.9	2.0	2.0
6.2	6.1	6.7	4.1	2.0
4.0	4.6	7.8	2.9	2.2
2.4	2.5	4.1	1.6	1.2
1.0	0.77	2.4	0.88	0.71
5.3	6.5	9.6	4.0	3.1
3.9	3.8	9.0	2.4	1.5
3.7	5.5	5.8	2.5	1.7
6.5	9.0	9.7	5.7	2.7

0.75	0.76	0.46	0.40	0.19
1.7	2.1	2.5	1.5	0.73
2.8	8.9	5.7	2.3	1.1
3.4	5.2	5.8	2.7	1.3
0.82	1.9	1.2	0.63	0.33
0.42	1.5	0.9	0.39	0.15
0.41	0.62	0.95	0.45	0.21
4893	*3838*	*5085*	*1265*	*2804*

83	82	96	87	88
85	87	95	87	88
94	100	72	69	93

SAP071701B (all day)	SAP071701C (all day)	SAP071801AM (site A - morning)	SAP071801BM (site B - morning)	SAP071801CM (siteC - morning)
388	404	1371	533	1007
392	231	716	317	450
158	105	279	1519	196
405	279	682	339	478
477	333	806	355	457
283	149	324	207	275
270	182	402	232	257
205	137	245	194	208
41	31	54	49	37
18	11	41	34	24
275	238	425	299	305
145	114	213	168	136
98	75	169	119	93
195	146	283	192	201
108	75	142	115	100
95	92	184	114	137
63	42	78	61	68
27	25	32	71	34
51	37	66	42	47
84	74	116	79	92
237	237	343	283	310
20	11	33	39	36
77	57	94	73	84
89	115	165	121	164
80	88	113	101	124
27	68	37	39	40
5.2	4.0	12	9.5	11
17	20	26	25	30
33	41	40	54	49
144	212	334	244	280
82	107	113	116	132
10	16	11	9.9	15
12	18	15	12	18
12	17	15	14	20
36	57	53	41	62
32	43	45	33	49
17	22	15	20	23
37	55	48	39	59
97	115	17	14	27
9.5	14	11	9.9	14
1.8	4.2	1.0	1.8	3.1
41	56	48	40	59
4.3	4.2	3.8	4.3	4.7
5.2	7.0	2.7	6.6	6.7
7.0	11	7.7	6.7	8.5
4.9	7.0	4.9	4.2	7.0
3.7	5.4	3.6	2.8	5.3
1.0	1.8	1.1	0.91	1.5
6.1	9.7	7.0	7.0	10.3
3.4	5.0	4.0	3.8	4.3
3.9	6.1	3.7	4.1	5.4
10	15	8.3	6.4	9.9

0.59	1.2	0.47	0.31	0.76
2.7	4.0	2.3	1.8	2.9
3.8	4.5	3.2	2.1	3.2
4.0	5.2	3.6	2.2	3.5
0.86	1.3	0.84	0.65	0.88
0.69	1.0	0.92	0.37	0.39
0.44	0.94	0.44	0.21	0.28
4958	*4248*	*8278*	*6434*	*6289*

100	92	93	84	83
89	101	90	81	82
92	99	95	92	93

SAP071801AA (site A - afternoon)	SAP071801BA (site B - afternoon)	SAP071801CA (site C - afternoon)
746	1561	742
488	733	391
183	629	149
523	894	373
577	859	447
307	476	213
316	757	219
248	237	136
123	57	34
38	150	32
310	1223	263
165	736	132
122	746	92
219	543	192
128	301	111
148	512	132
65	129	55
31	70	27
58	104	57
99	230	91
272	889	271
21	87	29
98	200	67
153	380	130
93	360	89
67	149	33
5	29	16
20	70	22
39	112	37
256	425	217
100	329	94
9.8	23	8.7
14	33	13
15	36	14
37	100	37
32	99	31
18	27	14
36	95	36
16	40	13
9.2	18	8.7
1.6	3.0	2.0
38	90	37
3.8	7.9	3.0
2.2	14	5.0
3.3	10	3.7
4.3	9.0	4.0
3.0	8.3	2.7
0.77	1.7	0.80
6.7	12	7.0
3.8	5.3	3.3
3.4	6.7	3.1
8.2	12	6.2

0.75	0.65	0.55
2.2	3.8	1.7
3.0	3.3	2.3
3.6	5.1	2.9
1.4	1.5	0.59
0.65	2.1	0.32
0.47	0.59	0.20
6298	*14647*	*5153*

89	86	83
94	85	85
92	85	93

SAP071901AM (site A - morning)	SAP071901BM (site B - morning)	SAP071901CM (site C - morning)
3461	479	430
1539	294	225
685	123	88
1423	315	223
1432	248	321
669	146	129
785	126	131
489	101	45
87	26	33
51	22	15
517	183	190
274	92	89
233	62	58
380	121	125
200	65	65
216	65	69
123	35	35
55	21	19
82	24	31
130	41	57
342	147	192
44	13	19
101	45	52
121	65	93
106	59	84
42	21	28
10	4	8.3
25	12	20
44	22	38
264	87	170
106	54	91
8.9	5.5	7.5
13	8.4	12
15	8.4	13
38	23	38
39	16	34
14	8.4	11
40	24	37
20	7.6	13
10	5.7	8.7
1.5	1.1	0.94
41	21	39
4.7	1.8	4.6
5.5	3.5	6.1
8.6	2.9	6.4
7.0	3.1	4.5
3.0	1.8	2.4
1.5	0.53	0.95
7.5	3.9	5.4
3.6	2.2	3.3
4.3	2.8	3.5
9.0	4.7	6.7

0.93	0.58	0.67
2.5	0.86	1.6
7.0	3.6	3.6
7.1	4.1	4.1
1.4	1.4	0.8
0.75	0.35	0.35
0.67	0.47	0.20
14350	*3285*	*3445*

87	83	92
85	88	89
90	95	95

SAP071901AA (site A - afternoon)	SAP071901BA (site B - afternoon)	SAP071901CA (site C - afternoon)
2293	705	1263
1245	385	648
509	235	292
1130	451	627
1430	376	726
658	215	276
748	251	308
538	151	233
90	40	40
75	45	50
552	420	340
292	221	162
245	175	110
417	226	226
235	121	127
262	134	130
122	62	72
60	30	39
93	50	56
151	85	95
394	318	278
44	35	48
140	97	78
162	159	125
129	141	102
51	58	38
12	12	8.8
29	30	25
53	54	46
333	207	191
122	138	110
13	10	12
17	16	17
17	20	18
45	47	42
48	40	43
21	16	15
48	47	46
28	24	17
12	11	11
2.3	2.2	1.7
52	47	48
5.8	5.6	5.3
6.5	6.0	3.0
8.6	4.5	4.9
5.5	4.8	6.0
4.4	3.3	3.8
1.3	0.73	1.2
7.9	8.0	7.9
4.7	4.4	5.2
4.4	4.6	5.3
9.8	7.8	9.7

0.68	1.2	0.68
3.2	1.8	2.5
4.6	3.9	3.2
4.9	3.7	3.7
2.4	2.5	1.1
0.72	0.46	0.37
0.73	0.82	0.29
12993	*5971*	*7202*

98	83	79
93	80	79
94	93	94

SAP072001AM (site A - morning)	SAP072001BM (site B - morning)	SAP072001CM (site C - morning)
2671	639	924
1389	245	490
613	148	251
1317	265	513
1386	242	553
633	120	270
778	140	275
537	96	209
93	26	42
43	28	30
484	202	309
243	95	148
187	54	97
406	122	200
257	62	119
239	48	107
126	32	65
77	7.3	35
87	25	56
141	47	96
364	179	288
25	25	27
125	49	87
142	81	126
114	87	128
40	33	48
7.8	6.6	9.1
23	20	28
52	38	56
284	101	199
122	87	132
10	6.2	14
13	13	20
18	14	24
41	35	57
41	27	50
19	13	22
43	38	62
19	12	19
11	8.0	14
1.3	3.0	3.7
46	36	58
5.9	5.4	6.4
6.8	5.3	7.0
4.6	2.5	8.3
5.2	4.2	7.6
2.8	2.3	3.9
1.1	1.2	1.6
6.8	5.6	16
4.0	5.1	7.1
3.8	4.9	7.1
8.3	5.9	11

0.68	0.44	1.8
2.2	1.4	2.7
3.3	2.6	4.2
4.1	3.0	4.6
0.98	1.4	1.1
0.57	0.21	0.55
0.42	0.42	0.45
13326	*3604*	*6354*

94	80	87
78	83	90
97	93	97

SAP072001AA (site A - afternoon)	SAP072001BA (site B - afternoon)	SAP072001CA (site C - afternoon)
971	740	481
752	390	249
341	253	1021
827	445	291
847	447	285
449	223	225
482	274	149
395	139	118
69	33	29
51	34	11
392	417	318
203	226	248
170	181	78
270	213	159
142	109	66
163	181	75
103	55	58
44	53	113
93	66	34
145	110	101
370	358	253
47	51	23
135	77	61
156	123	116
117	138	77
49	48	36
12	7.5	8.4
28	27	22
52	53	70
272	174	136
126	131	89
11	11	12
15	16	17
18	20	21
45	54	40
47	48	35
17	15	18
49	51	36
24	21	10
11	12	9.3
2.0	2.1	1.2
48	47	35
5.3	5.8	4.9
5.2	6.9	3.2
4.4	3.9	8.7
6.5	5.1	5.1
3.9	2.5	2.9
1.1	1.5	1.2
7.1	5.8	13
4.2	3.7	7.1
3.9	3.7	4.4
9.0	7.5	7.2

0.63	0.60	0.14
2.6	1.8	2.4
3.7	2.9	2.4
4.3	3.3	2.2
1.5	1.7	0.07
0.67	0.39	0.92
0.49	0.47	0.22
8625	*6132*	*5298.3*

85	81	85
80	79	89
94	91	88

Gas Phase PCB Concentrations (pg/m3)

PCB Congeners	BAP102301M (morning)	BAP102301A (afternoon)	BAP102401M (morning)
8+5	68	68	233
18	30	16	94
17+15	20	17	59
16+32	35	31	103
31	34	14	101
28	31	14	88
21+33+53	26	7.6	64
22	23	7.6	55
45	7.1	3.0	15
46	2.9	7.3	9.5
52+43	44	19	110
49	21	10	66
47+48	13	7.2	41
44	25	13	76
37+42	20	14	53
41+71	14	6.9	43
64	8.2	4.2	25
40	3.4	1.8	14
74	10	3.8	26
70+76	16	6.8	42
66+95	51	20	135
91	10	2	22
56+60+89	13	5	24
92+84	25	11	20
101	21	9.5	36
99	7.4	3.0	40
83	1.4	0.6	15
97	5.4	2.5	4.2
87+81	26	9.5	13
85+136	55	26	60
110+77	26	11	154
82	1.7	1.0	36
151	4.2	2.3	4.7
135+144+147+124	2.6	1.5	8.8
149+123+107	9.4	4.5	7.1
118	9.4	3.7	26
146	3.1	2.2	10
153+132	24	7.7	4.4
105	5.0	2.0	58
141+179	2.7	1.3	3.8
137+176+130	0.31	0.22	8.4
163+138	12	5	26
158	1.4	0.57	3.1
178+129	0.80	0.58	3.0
187+182	5.9	2.5	18
183	1.2	0.60	5.2
128	0.67	0.27	1.2
185	0.23	0.14	1.0
174	2.7	1.3	6.4
177	1.2	1.0	4.4
202+171+156	1.5	0.76	5.8

180	2.7	1.3	10
199	0.27	0.23	1.5
170+190	1.5	0.27	2.4
201	1.6	0.81	12
203+196	2.2	0.90	13
195+208	0.33	0.35	2.2
194	0.62	0.20	1.2
206	0.20	0.19	0.87
Sum PCBs	*791*	*418*	*2125*
Surrogate Recoveries(%)			
PCB-23	*80*	*71*	*92*
PCB-65	*81*	*71*	*94*
PCB-166	*73*	*62*	*79*

BAP102401A (afternoon)	BAP102501M (morning)	BAP102501A (afternoon)	BAP102601M (morning)	BAP102601A (afternoon)
Sample	141	509	203	110
Lost	64	183	88	42
	40	103	52	25
	70	184	97	45
	63	148	80	31
	63	135	81	33
	42	108	57	24
	40	83	54	21
	12	24	15	6.5
	6.0	10	6.9	2.7
	71	103	81	32
	37	54	48	18
	25	42	34	14
	46	73	57	22
	35	51	46	15
	24	42	35	12
	16	26	21	7.2
	10	15	13	4.0
	13	18	14	4.3
	22	30	22	7.6
	71	81	65	24
	11	11	8.1	2.5
	21	20	17	6.6
	47	38	35	14
	24	29	21	8.2
	9.5	12.9	8.9	3.6
	2.0	2.1	2.4	0.6
	6.1	7.5	4.7	2.0
	20	26	25	13
	85	47	41	16
	29	30	22	8.0
	2.4	2.8	2.1	0.94
	4.3	4.2	3.1	1.3
	2.8	3.2	1.9	0.88
	8.8	9.9	7.3	3.1
	9.1	12	7.4	2.9
	3.5	1.9	2.0	0.30
	17	22	20	12
	5.5	6.3	2.6	0.99
	3.0	2.5	1.9	0.60
	0.94	0.15	0.18	0.10
	11	12	7.7	2.2
	1.3	1.9	1.2	0.37
	1.9	1.7	1.4	0.36
	4.4	5.9	7.0	5.3
	1.8	0.99	1.1	0.36
	0.91	0.73	0.57	0.17
	0.27	0.25	0.10	0.07
	2.0	1.5	1.8	0.88
	1.2	1.4	1.1	0.48
	1.5	0.86	1.2	0.43

2.9	1.6	1.4	0.69
0.25	0.24	0.38	0.13
1.2	0.94	1.2	0.54
1.8	0.86	1.6	0.54
2.2	1.47	2.0	0.95
0.41	0.52	1.7	0.36
0.29	0.10	1.8	0.15
0.19	0.073	1.5	0.28
1260	*2344*	*1436*	*614*
94	*86*	*92*	*90*
95	*88*	*98*	*93*
84	*77*	*80*	*79*

SAP102301AM (site A - morning)	SAP102301BM (site B - morning)	SAP102301CM (siteC - morning)	SAP102301AA (site A - afternoon)
1315	463	309	780
523	165	157	362
331	115	85	203
589	189	171	337
400	148	134	244
421	120	142	321
315	113	97	218
177	51	66	135
48	34	24	50
37	16	13	19
321	141	142	211
225	90	75	149
184	80	57	120
195	72	94	149
129	46	64	86
118	56	51	78
61	20	33	46
31	11	14	24
53	15	24	38
84	27	40	61
245	100	153	183
30	13	20	23
81	27	40	54
223	60	90	156
79	35	51	70
39	18	22	57
10	3.7	4.2	7.2
26	8.7	11	24
42	14	24	30
18	6.1	16	14
77	31	51	60
4.8	2.3	3.4	3.1
12	4.8	13	11
10	5.0	8.6	17
26	13	28	28
21	9.2	14	21
6.0	2.7	4.8	6.1
28	13	26	26
15	6.4	12	14
4.1	1.9	3.9	3.8
2.0	0.47	1.9	0.43
23	11	21	29
2.8	1.4	2.5	3.7
3.9	1.5	2.7	2.4
6.6	2.8	6.3	4.6
2.8	1.5	3.2	2.3
1.6	0.93	1.3	1.2
0.64	0.29	0.50	0.41
4.7	2.2	4.8	4.7
2.1	1.2	2.6	3.2
1.8	1.2	2.0	1.1

4.7	2.3	4.6	5.9
0.37	0.14	0.35	0.64
1.2	0.67	1.3	1.8
2.3	1.1	2.0	3.1
2.3	1.2	2.1	3.4
1.6	0.42	0.42	0.24
0.19	0.14	0.18	0.38
2.0	0.39	0.28	0.93
6619	*2378*	*2446*	*4506*

81	*101*	*93*	*87*
82	*100*	*97*	*94*
83	*98*	*96*	*93*

SAP102301BA (site B - afternoon)	SAP102301CA (site C - afternoon)	SAP102401AM (site A - morning)	SAP102401BM (site B - morning)	SAP102401CM (siteC - morning)
No sample	252	168	927	581
(morning sample went	140	68	303	243
	68	50	226	129
	146	85	351	252
	130	93	293	231
	106	67	252	156
	78	66	243	152
	60	65	130	95
	19	11	42	28
	15	11	43	25
	122	75	267	202
	64	51	164	109
	48	30	141	86
	78	55	153	126
	53	53	97	86
	44	31	114	73
	26	20	48	37
	18	11	27	28
	20	19	40	29
	32	35	64	53
	128	105	206	197
	16	19	26	26
	36	39	65	60
	83	83	128	128
	44	41	79	72
	17	14	92	31
	4.1	5.0	6.7	7.9
	12	13	19	21
	22	24	37	37
	13	245	13	17
	43	49	78	82
	4.3	4.1	7.7	8.6
	13	7	12	15
	11	5.3	13	16
	27	18	33	41
	13	18	31	26
	5.0	15	7.4	7.9
	26	22	39	43
	12	8.7	24	23
	4.1	5.7	6.1	7.0
	2.1	0.75	3.3	3.9
	20	25	38	38
	2.4	2.6	5.1	4.7
	3.1	1.5	2.3	6.0
	5.7	5.7	9.5	9.0
	3.4	2.9	4.7	5.5
	1.6	1.7	3.4	3.8
	0.66	0.55	1.1	0.86
	5.1	3.8	8.6	9.6
	3.0	2.9	3.7	4.7
	2.6	2.7	4.1	5.4

5.7	5.8	14	11
0.33	0.38	0.47	0.53
1.5	1.9	2.3	2.8
1.9	2.2	3.6	4.0
2.2	2.7	4.0	4.2
0.55	0.79	1.9	1.2
0.22	0.45	0.67	0.44
0.64	0.27	1.1	1.1
2113	*1869*	*4959*	*3704*
93	*92*	*95*	*95*
97	*94*	*100*	*97*
89	*84*	*96*	*85*

SAP102401AA (site A - afternoon)	SAP102401BA (site B - afternoon)	SAP102401CA (site C - afternoon)	SAP102501AM (site A - morning)
1062	1002	319	215
473	396	144	111
220	257	87	77
477	443	159	132
422	395	112	142
367	330	148	119
316	325	89	111
234	157	64	88
45	100	26	26
37	48	11	17
245	396	147	138
157	253	73	84
95	228	53	47
165	218	92	96
141	138	57	75
81	168	43	51
52	60	35	30
27	34	13	18
40	49	23	35
82	93	42	61
197	312	162	195
24	40	27	37
63	95	42	56
316	195	97	134
70	128	67	84
21	61	29	25
1.9	11	3.6	9.2
30	26	15	24
47	52	36	50
17	21	23	343
76	125	68	103
6.7	13	3.3	7.7
16	18	14	14
10	20	8.9	11
28	51	30	36
25	46	20	39
7.3	12	4.3	20
34	60	32	43
21	37	17	20
4.2	9.5	4.5	12
1.1	2.1	0.57	1.3
30	58	29	47
3.2	7.4	3.3	5.4
5.5	5.4	2.0	3.9
10	13	8.8	15
2.7	7.9	3.5	6.4
2.4	5.9	1.3	3.4
0.64	1.2	0.71	1.1
7.1	13	5.9	8.1
3.4	6.3	3.0	5.0
2.5	6.7	2.4	6.8

6.9	15	6.9	13
0.58	0.88	0.28	1.3
2.0	4.8	1.6	3.5
2.7	7.5	2.9	12
3.7	7.6	3.0	13
0.23	1.8	0.79	2.3
0.42	1.1	0.37	2.3
0.40	1.6	0.64	2.0
5839	*6591*	*2517*	*3091*

94	*98*	*89*	*90*
90	*94*	*96*	*89*
94	*95*	*99*	*84*

SAP102501BM (site B - morning)	SAP102501CM (siteC - morning)	SAP102501AA (site A - afternoon)	SAP102501BA (site B - afternoon)	SAP102501CA (site C - afternoon)
472	315	127	173	no
228	116	76	69	sample
187	69	46	61	
289	101	84	84	
303	101	79	73	
228	50	69	64	
236	61	64	66	
152	100	56	43	
32	21	11	10	
35	12	7	11	
285	136	72	98	
202	66	41	66	
185	37	31	63	
164	94	46	51	
127	77	35	43	
142	95	27	44	
50	32	17	17	
30	29	11	12	
55	22	18	19	
96	44	29	28	
318	208	85	98	
47	40	13	16	
100	61	27	27	
115	250	49	34	
110	84	31	39	
44	21	12	24	
7.8	5.7	3.0	2.3	
25	21	7.8	7.1	
52	34	17	17	
218	99	83	42	
127	105	38	32	
10	10	2.4	2.2	
18	17	5.1	6.5	
13	9.5	3.8	4.2	
46	42	13	13	
46	34	12	13	
20	28	5.0	5.3	
56	64	14	15	
27	28	5.8	4.2	
13	13	3.7	4.2	
1.6	1.1	0.36	0.34	
55	27	14	14	
5.8	2.9	1.8	1.7	
4.0	2.8	1.0	1.3	
12	15	4.4	5.4	
6.8	6.0	1.5	1.7	
4.1	3.9	0.87	0.64	
1.7	1.4	0.36	0.40	
9.6	3.3	2.2	2.4	
5.5	3.8	1.7	1.6	
5.4	4.9	1.0	1.5	

14	12	2.9	3.3
0.77	0.81	0.23	0.42
4.3	2.7	0.77	1.0
5.7	14	1.3	1.5
6.5	14	1.6	2.2
2.3	2.6	0.41	0.78
1.2	1.3	0.21	0.30
1.4	1.2	0.18	0.31
5058	*2875*	*1414*	*1542*

92	*91*	*88*	*99*
90	*89*	*91*	*100*
83	*89*	*78*	*89*

SAP102601AM (site A - morning)	SAP102601BM (site B - morning)	SAP102601CM (siteC - morning)	SAP102601AA (site A - afternoon)
84	116	271	84
43	63	53	41
28	51	58	27
50	83	36	46
44	68	50	40
40	65	20	33
36	60	13	33
34	26	16	29
5.9	10	7.2	5.2
4.2	8.8	3.0	3.7
50	100	23	40
38	66	13	27
19	57	80	17
28	54	14	25
35	29	26	25
18	35	12	17
10	16	6.4	8.1
5.4	6.0	15	3.9
8.8	14	2.8	6.6
16	23	10	12
49	79	27	35
6.2	11	11	4.8
15	24	8.5	11
26	32	19	18
21	33	18	13
7.5	12	13	4.7
1.5	2.0	2.7	1.5
4.7	8.0	4.7	2.9
13	18	21	10
40	8	22	28
23	27	12	13
1.4	1.7	3.3	1
3.5	5.0	5.8	2
2.4	3.9	2.7	1
8.1	12	5.1	4.8
6.9	11	4.0	4.0
2.6	3.3	5.0	1.3
9.7	15	11	5.5
2.6	7.8	9.9	1.7
2.4	2.1	2.7	1.3
0.33	1.0	0.82	0.11
9.3	14	3.5	4.6
1.0	2.0	1.5	0.61
0.62	1.0	1.9	0.68
4.6	3.4	1.2	3.8
1.1	1.8	2.2	0.67
0.56	1.0	1.2	0.31
0.25	0.36	1.4	0.20
1.9	3.3	2.4	1.1
1.3	1.8	2.9	1.0
0.65	2.0	2.4	0.7

2.2	5.4	2.1	0.9
0.15	0.34	0.89	0.12
0.81	2.2	1.2	0.35
1.0	3.7	3.7	0.42
1.4	4.2	4.0	0.81
0.48	1.7	1.0	0.39
0.40	1.4	1.1	0.27
0.48	3.5	1.3	0.24
872	*1318*	*975*	*704*
96	*89*	*75*	*91*
100	*92*	*76*	*96*
88	*96*	*86*	*83*

SAP102601BA (site B - afternoon)	SAP102601CA (site C - afternoon)
120	108
63	43
54	29
79	46
60	37
55	36
58	32
37	23
12	6.9
11	4.9
88	46
57	25
53	19
47	26
35	16
33	17
16	8.8
7.4	4.3
12	7.6
19	14
71	47
10	7.6
20	11
21	18
26	18
12	6.6
2.3	1.7
4.5	3.8
17	20
34	45
23	22
2	1.7
3	2.9
3	2.5
8.6	8.0
8.6	6.7
2.5	2.4
8.1	9.5
3.2	2.9
2.2	2.2
0.28	0.28
9.0	9.4
1.2	1.1
0.77	1.3
6.4	10.0
1.2	1.7
0.76	0.62
0.24	0.29
2.1	2.7
1.9	2.1
1.6	1.6

3.4	4.2
0.44	0.22
1.4	1.8
2.4	2.3
3.3	3.6
2.1	1.0
0.88	1.0
6.8	1.4
1244	*834*

88	*87*
91	*88*
84	*80*

Gas Phase PCB Concentrations (pg/m3)

PCB Congeners	BAP050702M (morning)	BAP050702A (afternoon)	BAP050802M (morning)
8+5	47	67	63
18	35	52	38
17+15	26	33	24
16+32	37	53	37
31	45	52	35
28	47	60	39
21+33+53	34	36	23
22	17	20	14
45	12	12	7.3
46	4.5	5.1	4.0
52+43	62	72	51
49	47	56	42
47+48	22	26	20
44	47	52	32
37+42	19	24	16
41+71	17	22	15
64	12	14	10
40	5.8	6.2	4.7
74	14	14	9.2
70+76	25	24	16
66+95	72	74	49
91	5.4	6.9	4.6
56+60+89	21	17	12
92+84	43	38	24
101	44	32	23
99	15	13	8.7
83	2.8	2.7	1.4
97	10	8.1	5.3
87+81	20	17	11
85+136	127	78	48
110+77	34	26	15
82	1.5	1.4	1.1
151	5.7	5.4	3.8
135+144+147+124	4.0	5.5	4.7
149+123+107	12	12	8.2
118	10	11	7.1
146	5.7	4.9	3.4
153+132	15	13	8.1
105	5.1	3.9	3.1
141+179	4.4	3.7	1.9
137+176+130	1.6	1.2	0.68
163+138	15	14	7.7
158	2.6	1.8	1.2
178+129	3.2	2.6	0.72
187+182	7.5	5.1	2.5
183	3.3	2.4	1.3
128	0.66	0.58	0.39
185	1.0	0.58	0.19
174	8.4	3.2	0.63
177	23	23	8.9
202+171+156	34	22	20

180	5.3	3.3	1.6
199	1.3	0.76	0.43
170+190	1.2	1.1	0.57
201	4.7	2.2	1.3
203+196	4.3	2.6	1.8
195+208	0.99	1.3	0.80
194	0.68	0.48	0.29
206	0.75	0.29	0.18
Sum PCBs	*1147*	*1162*	*796*
Surrogate Recoveries(%)			
PCB-23	30	81	85
PCB-65	38	89	90
PCB-166	58	83	81

BAP050802A (afternoon)	BAP050902M (morning)	BAP050902A (afternoon)	BAP051002M (morning)	BAP051002A (afternoon)
97	91	83	54	36
62	37	36	35	31
37	21	24	25	21
71	38	35	39	33
73	36	33	60	45
72	35	33	39	31
56	31	29	33	23
27	17	19	23	16
9.6	5.1	8.4	8.4	5.5
5.4	3.5	4.1	4.4	3.1
71	36	34	49	40
37	19	22	34	27
22	12	11	16	14
50	24	29	33	25
21	13	13	25	19
19	11	12	21	18
14	8.6	7.8	11	8.3
12	5.5	3.9	5.5	4.7
16	6.7	7.1	11	9.5
31	12	13	21	15
92	37	38	62	46
8.9	3.0	3.9	8.3	6.2
23	10	10	17	13
40	18	18	30	21
57	16	18	24	15
21	5.8	6.4	9.5	7.7
3.6	1.2	1.0	2.4	1.5
13	4.2	4.7	6.1	4.6
35	11	11	16	9
83	26	27	82	55
44	14	16	43	26
2.0	1.0	0.92	1.3	0.84
6.7	2.3	2.4	12	9.0
7.4	4.2	3.1	2.4	1.7
14	5.3	5.9	23	16
13	4.9	5.8	7.4	5.1
5.0	2.6	3.4	4.2	2.0
15	5.8	6.1	63	43
5.4	2.7	2.9	2.7	2.0
4.4	1.4	1.6	5.2	2.8
1.7	0.40	0.36	0.37	0.28
16	5.4	7.1	36	23
2.5	1.3	1.3	0.57	0.36
2.5	1.3	0.99	1.6	0.96
4.2	1.6	1.6	3.3	2.1
2.3	0.76	0.72	1.0	0.69
0.67	0.35	0.32	0.93	0.43
0.69	0.26	1.3	1.64	0.18
3.0	2.0	3.5	1.85	0.92
2.1	0.88	12	1.33	0.67
3.0	1.1	20	0.99	0.41

3.1	0.70	0.93	1.9	1.1
0.34	0.077	0.17	0.32	0.21
1.1	0.12	0.29	0.59	0.30
1.6	0.37	0.41	1.3	0.56
2.1	0.64	0.55	1.5	0.63
3.7	0.34	0.26	0.39	0.17
0.68	0.11	0.084	0.26	0.089
0.57	0.082	0.070	0.17	0.075
1349	*658*	*696*	*1023*	*744*

22	78	76	50	72
31	88	82	64	85
56	86	77	90	94

SAP050702AM (site A - morning)	SAP050702BM (site B - morning)	SAP050702CM (siteC - morning)	SAP050702AA (site A - afternoon)	SAP050702BA (site B - afternoon)
205	305	134	67	128
95	149	86	41	81
57	93	53	26	56
95	142	87	45	80
82	126	82	40	85
87	134	91	44	79
61	99	61	33	41
43	49	38	25	42
15	22	17	8.0	14
16	16	9.4	6.1	25
107	156	109	57	105
62	88	61	32	58
40	52	39	18	45
75	94	76	36	65
34	40	33	19	29
33	35	32	15	29
21	26	23	12	15
14	4.8	7.4	5.5	71
18	21	23	10	24
30	39	37	19	34
110	139	119	67	103
10	12	11	7.1	8.5
27	27	27	17	31
71	65	65	47	49
53	65	54	34	64
20	21	19	12	22
5.5	4.3	3.9	3.3	6.5
13	15	11	8.5	13
26	31	26	19	27
152	152	159	100	117
47	53	42	30	46
2.0	2.3	1.8	1.7	9.7
8	12	10	6.8	14
13	6.4	4.8	4.8	120
16	26	21	13	29
13	20	16	9.4	22
8.2	5.7	6.8	8.5	12
18	25	20	15	46
5.7	6.2	5.2	5.2	13
5.7	8.1	6.1	4.4	10
0.72	2.5	1.7	0.79	2.3
22	29	21	15	29
2.8	3.9	2.3	2.4	7.8
3.7	4.8	3.3	2.5	10
6.9	7.0	5.8	5.8	13
3.8	3.6	2.4	2.5	8.3
1.2	0.63	0.65	0.70	4.6
1.1	1.1	0.55	0.55	7.1
8.5	9.4	15	9.8	2.7
10	3.3	2.4	6.0	11
8.0	2.8	2.1	23	3.0

7.0	4.5	3.8	4.0	5.9
1.0	0.76	0.34	0.63	2.4
2.1	1.2	1.1	1.4	1.9
3.5	3.0	1.5	2.6	7.6
3.6	2.9	2.1	2.8	1.2
2.5	1.2	1.1	2.3	2.2
3.9	0.18	0.43	0.37	2.9
8.0	6.1	1.6	0.20	0.38
1915	*2473*	*1797*	*1056*	*1992*

21	82	76	82	83
22	85	81	88	83
27	82	88	85	84

SAP050702CA (site C - afternoon)	SAP050802AM (site A - morning)	SAP050802BM (site B - morning)	SAP050802CM (siteC - morning)	SAP050802AA (site A - afternoon)
54	402	518	146	327
36	199	212	73	139
19	114	120	39	80
33	187	211	64	144
33	162	163	60	120
34	188	176	61	130
21	107	132	45	97
16	59	84	27	51
5.8	27	24	9.3	18
5.0	14	18	6.1	11
51	156	165	75	142
24	89	91	41	73
14	65	58	25	54
28	98	102	40	85
14	55	55	21	49
12	49	49	18	41
8.9	32	31	13	28
3.0	11	7.7	4.6	14
8.2	26	23	14	23
16	44	42	24	42
50	142	140	78	143
4.3	21	13	7.9	17
12	35	35	17	37
24	72	76	27	80
28	57	63	41	69
9.1	25	22	14	28
1.8	3.8	4.3	2.4	4.6
6.2	13	14	7.7	15
15	29	29	20	35
60	144	125	51	205
21	43	50	28	60
1.1	2.2	3.6	1.6	2.6
5.7	8.6	9.5	8.1	7.3
5.0	4.7	4.9	4.6	6.6
12	19	22	17	16
8.8	15	17	12	13
4.5	9.5	13	4.0	6.9
12	21	22	16	17
2.8	5.5	7.1	3.5	6.7
3.0	5.3	5.9	4.6	4.4
0.8	1.8	1.2	1.2	1.1
12.5	17	21	17	16
1.8	2.1	3.1	2.3	3.5
1.9	4.0	4.0	3.5	2.5
4.1	5.0	4.4	5.2	5.0
2.0	2.7	2.2	2.3	5.4
0.33	0.59	1.1	0.50	1.5
0.28	0.53	1.0	0.48	41
8.7	2.9	5.5	5.6	73
16	2.1	2.5	7.5	42
28	1.7	1.2	1.9	44

3.3	3.2	2.9	2.9	2.7
0.76	0.38	0.90	0.44	0.34
0.65	0.99	0.75	0.75	1.2
2.2	1.5	1.6	1.0	2.1
4.9	1.7	1.7	1.4	2.8
3.2	0.63	0.57	0.36	0.88
1.7	0.31	0.24	0.25	0.27
6.9	0.42	0.59	0.71	1.6
821	*2809*	*3013*	*1230*	*2691*

85	82	87	88	25
89	90	93	92	30
85	90	90	82	78

SAP050802BA (site B - afternoon)	SAP050802CA (site C - afternoon)	SAP050902AM (site A - morning)	SAP050902BM (site B - morning)
275	321	100	204
114	189	50	76
68	102	31	49
125	166	60	79
95	163	42	111
103	170	52	60
81	110	35	57
53	54	23	42
18	28	9.2	11
11	12	7.2	7.6
112	178	55	68
59	91	28	36
40	73	20	27
74	105	37	48
36	54	18	38
33	57	19	35
24	33	13	14
7.8	11	6.4	9.1
18	29	10	14
33	49	20	24
116	149	65	76
18	15	8.5	17
31	32	19	19
65	50	44	31
54	56	30	24
21	23	13	11
4.0	2.9	2.3	2.3
14	11	8.2	6.0
29	27	18	14
104	73	75	64
52	38	31	28
3.7	2.4	2.7	2.2
8.1	8.5	3.4	2.9
6.3	7.2	2.9	3.3
19	19	9.0	7.9
15	14	10	7.5
8.3	4.5	4.7	4.6
20	16	10	7.5
6.7	3.8	6.9	3.3
4.7	4.8	2.0	1.6
1.8	0.60	0.83	0.51
18	16	10	6.5
2.1	1.8	1.7	0.6
2.9	2.2	0.28	1.0
4.3	4.1	1.9	1.7
2.4	2.1	0.90	0.68
1.1	0.53	0.68	2.7
0.48	0.51	0.19	0.68
5.4	4.7	6.4	0.65
1.9	1.7	6.2	0.72
1.7	1.6	12.8	1.1

2.6	2.3	0.71	0.51
0.42	0.35	0.20	0.13
0.78	0.49	0.22	0.18
1.4	1.5	0.29	0.19
1.7	1.7	0.40	0.44
1.2	0.72	0.23	0.16
0.28	0.22	0.099	0.081
0.24	5.5	0.40	0.071
2033	*2602*	*1048*	*1363*

85	93	89	88
92	99	102	98
91	94	87	98

SAP050902CM (siteC - morning)	SAP050902AA (site A - afternoon)	SAP050902BA (site B - afternoon)	SAP050902CA (site C - afternoon)
85	360	222	142
55	122	90	77
34	70	53	46
64	125	89	83
51	88	75	68
59	92	79	75
39	73	53	53
26	41	29	28
11	16	13	14
6.0	12	6.5	8.9
68	87	76	86
38	42	41	46
25	33	31	34
42	55	49	53
25	35	30	30
23	28	28	30
14	19	16	18
8.0	8.7	9.1	7.0
10	13	11	13
19	26	19	23
70	87	71	84
8.0	11	8.4	10
16	22	16	20
40	54	42	44
29	39	27	34
11	16	11	14
2.0	2.7	2.6	2.7
6.2	11	7.3	7.8
16	23	14	18
51	83	54	56
25	37	24	29
1.9	2.6	1.4	1.8
5.7	4.8	4.1	6.0
5.4	4.8	4.2	4.7
12	13	9.0	14
7.2	13	6.4	8.6
4.7	6.8	2.6	3.9
11	13	7.9	12
2.8	5.4	2.1	2.7
2.6	2.8	1.9	1.2
0.73	1.1	0.62	0.96
9.4	13	8.5	11
1.5	1.8	1.9	1.8
1.7	2.1	1.4	1.7
1.4	1.7	1.8	3.0
1.2	1.0	0.85	1.2
0.37	0.76	0.37	0.45
0.27	0.31	0.12	0.28
2.9	2.8	3.6	3.6
9.8	0.93	21	1.0
14	0.64	33	0.69

0.95	0.97	0.84	1.3
0.26	0.12	0.21	0.15
0.35	0.26	0.28	0.43
0.43	0.32	0.48	0.49
0.54	0.48	0.58	0.76
0.58	0.36	0.30	0.24
0.095	0.14	0.09	0.10
0.13	0.41	0.21	0.53
1074	*1826*	*1418*	*1339*

80	79	80	81
89	90	90	90
82	78	76	82

SAP051002AM (site A - morning)	SAP051002BM (site B - morning)	SAP051002CM (siteC - morning)	SAP051002AA (site A - afternoon)
140	162	128	47
60	70	53	21
41	42	34	14
65	76	50	22
92	107	71	38
47	54	35	19
52	63	40	19
46	49	39	16
9.7	10	7.3	3.5
8.3	11	6.1	3.1
59	71	51	31
36	37	27	18
23	23	16	9.6
47	54	41	21
36	35	28	14
30	30	22	14
14	15	12	7.1
8.1	8.9	7.6	4.0
13	14	13	7.4
22	27	19	14
76	89	63	45
11	14	9.1	5.3
27	26	7.6	14
35	32	31	19
31	33	27	19
13	14	11	7.6
3.4	2.7	2.3	2.3
8.1	8.2	6.7	4.6
20	21	18	15
95	77	92	59
40	40	33	23
3.6	3.5	3.3	1.7
5.2	5.7	5.1	3.5
5.8	6.2	7.9	3.5
13	14	13	8.1
15	15	12	8.7
12	8.8	12	5.8
15	15	13	9.6
7.8	6.9	5.2	3.5
3.7	3.7	3.7	2.5
0.97	1.2	0.91	0.73
15	14	14	10
1.3	1.3	1.1	0.88
2.6	2.9	2.0	1.6
3.5	3.5	3.2	3.3
1.6	1.6	1.7	1.6
1.1	0.98	1.0	0.81
0.45	1.7	0.61	3.6
2.3	2.5	3.3	2.2
1.5	1.4	1.3	1.2
1.1	1.6	1.6	1.0

2.4	2.2	2.3	2.7
0.37	0.34	0.22	0.29
0.64	0.59	0.65	0.74
1.1	1.3	0.90	1.4
1.1	1.2	1.1	1.4
0.31	0.53	0.25	0.45
0.18	0.17	0.12	0.31
0.17	0.25	0.11	0.20
1328	*1436*	*1114*	*638*

92	89	98	93
93	94	98	99
101	100	100	102

SAP051002BA (site B - afternoon)	SAP051002CA (site C - afternoon)
58	72
32	27
20	18
34	27
64	43
31	21
32	22
25	21
4.7	4.0
5.5	3.5
41	34
22	17
13	8.7
28	26
15	15
13	11
7.4	7.1
3.3	3.3
8.4	7.9
14	13
47	43
5.3	6.1
14	14
17	18
21	19
7.8	9.1
2.6	2.3
4.5	4.6
13	14
35	54
22	23
2.1	2.4
3.1	3.5
3.3	3.9
7.5	8.6
8.0	9.9
4.3	7.8
8.1	11
3.4	5.3
2.2	2.3
0.77	0.60
7.9	11
0.73	1.3
1.0	1.6
2.5	2.6
1.1	1.3
0.72	0.82
0.72	0.93
1.5	2.9
1.0	1.0
1.5	1.4

1.6	2.0
0.19	0.21
0.48	0.63
0.83	0.88
1.0	1.2
0.52	0.40
0.26	0.13
0.69	0.18
728	*695*

64	94
76	96
91	100

Gas Phase PCB Concentrations (pg/m3)

PCB Congeners	BAP111202M (morning)	BAP111202A (afternoon)	BAP111302M (morning)
8+5	226	86	82
18	87	47	52
17+15	53	28	32
16+32	91	39	50
31	98	49	64
28	63	32	44
21+33+53	47	21	30
22	41	24	23
45	9.9	6.4	6.5
46	6.3	5.8	3.5
52+43	87	50	49
49	56	40	32
47+48	24	13	14
44	56	32	34
37+42	42	24	24
41+71	28	18	19
64	17	11	12
40	12	6.2	6.5
74	13	9.4	8.7
70+76	27	19	18
66+95	83	58	52
91	8.7	3.6	5.0
56+60+89	25	16	15
92+84	40	29	26
101	35	24	19
99	13	9.2	7.1
83	3.6	1.7	1.9
97	7.8	5.2	4.5
87+81	30	23	20
85+136	75	52	55
110+77	36	25	20
82	4.7	4.3	1.4
151	6.3	4.1	2.6
135+144+147+124	4.8	3.2	1.9
149+123+107	15	10	6.0
118	23	21	4.7
146	13	5.8	5.0
153+132	15	7.5	6.4
105	4.6	3.1	2.5
141+179	2.3	1.3	0.99
137+176+130	0.39	0.14	0.15
163+138	9.7	5.6	4.6
158	0.94	0.48	0.52
178+129	1.9	0.66	0.67
187+182	9.2	2.9	4.4
183	1.3	0.60	0.60
128	0.97	0.46	0.42
185	1.1	0.26	0.34
174	2.8	1.0	1.4
177	2.3	0.73	0.89
202+171+156	1.4	0.61	0.71

180	1.3	0.50	0.67
199	1.1	0.88	0.14
170+190	1.0	0.30	0.20
201	2.1	0.94	0.42
203+196	1.6	0.13	0.87
195+208	0.74	0.11	0.34
194	0.74	0.10	0.12
206	0.27	0.31	0.086
Sum PCBs	*1568*	*883*	*878*
Surrogate Recoveries(%)			
PCB-23	32	86	35
PCB-65	35	91	44
PCB-166	66	85	52

BAP111302A (afternoon)	BAP111402M (morning)	BAP111402A (afternoon)	SAP111202AM (site A - morning)	SAP111202BM (site B - morning)
147	37	74	587	689
76	23	36	228	252
36	15	22	119	139
67	16	26	214	238
80	25	46	230	268
53	16	27	126	145
40	12	23	131	149
26	7.2	16	95	101
6.5	2.2	4.0	20	24
5.1	2.2	3.1	16	14
55	25	33	124	157
33	16	21	64	86
16	6.6	9.7	30	41
38	13	21	82	110
25	11	18	68	88
20	11	15	43	58
12	5.1	7.8	28	33
6.4	3.1	4.4	12	17
8.8	3.7	6.6	24	26
16	7.6	12	41	46
48	22	32	143	156
4.1	2.2	3.8	16	20
14	4.4	9.1	39	42
24	7.9	15	69	63
17	8.9	13	57	57
6.7	3.2	4.7	20	23
2.0	1.2	1.1	5.8	5.3
4.9	1.9	2.9	12	13
18	8.2	10	38	37
41	20	27	230	120
17	7.5	12	59	65
1.3	0.31	0.93	5.0	5.7
2.5	1.1	1.9	8.3	6.9
2.3	1.1	1.6	9.1	7.4
5.4	2.7	4.3	23	18
3.7	2.3	4.1	24	22
2.9	0.76	1.2	15	10
5.0	2.6	3.9	19	16
1.9	0.82	1.3	7.7	8.6
0.81	0.45	0.75	3.9	3.1
0.23	0.067	0.11	1.8	1.3
3.2	1.9	3.0	13	13
0.39	0.19	0.32	1.3	1.3
0.71	0.26	0.56	1.7	2.2
9.0	1.2	1.7	5.2	4.3
0.37	0.22	0.47	2.4	1.6
0.33	0.10	0.12	0.80	1.0
0.24	0.17	0.19	0.35	0.46
0.44	0.50	0.75	2.8	2.7
1.00	0.32	0.45	1.2	1.2
0.75	0.27	0.64	1.0	1.3

0.28	0.20	0.34	1.1	1.4
0.24	0.058	0.16	0.31	0.56
0.18	0.063	0.093	0.49	0.72
0.26	0.16	0.40	0.68	0.78
0.69	0.29	0.56	0.59	0.84
0.39	0.13	0.19	0.22	0.28
0.41	0.034	0.067	0.24	0.093
0.16	0.030	0.038	0.19	0.13
1010	*362*	*586*	*3118*	*3411*

28	101	97	85	79
36	101	100	94	85
51	101	101	89	76

SAP111202CM (siteC - morning)	SAP111202AA (site A - afternoon)	SAP111202BA (site B - afternoon)	SAP111202CA (site C - afternoon)	SAP111302AM (site A - morning)
904	1321	793	825	119
318	472	288	505	58
170	225	152	192	31
312	414	267	286	54
304	408	248	308	59
154	220	142	165	35
185	229	143	169	32
119	167	95	98	26
18	31	28	19	7.9
12	25	13	16	7.2
114	167	138	105	39
72	88	79	61	21
42	45	37	29	10
97	117	93	80	27
71	93	68	58	25
59	63	63	47	16
29	41	30	26	11
14	23	18	14	3.7
23	32	28	21	10
36	55	44	35	17
114	159	131	99	49
11	15	25	14	6.0
34	50	36	27	14
53	67	55	41	26
40	54	47	36	19
16	21	19	14	7.4
4.2	5.9	3.8	3.1	1.6
9.8	12	11	7.7	4.2
32	38	35	26	19
102	128	82	71	53
49	61	50	38	19
5.5	8.3	8.0	4.5	1.6
5.8	9.1	7.0	5.1	2.4
7.0	10	5.8	4.9	2.5
17	22	19	13	6.0
18	27	31	19	5.4
12	20	8.0	6.5	4.4
13	18	15	11	5.2
7.7	8.9	8.7	6.0	2.6
2.5	3.3	2.4	1.8	0.95
1.5	1.4	0.35	0.25	0.14
10	13	9.7	7.6	3.7
1.2	1.2	0.81	0.69	0.36
1.3	2.9	0.35	0.53	0.19
3.3	5.5	5.1	3.8	1.4
1.5	1.5	1.4	1.0	0.36
1.1	1.0	0.86	0.62	0.27
0.43	0.35	0.33	0.22	0.087
2.6	2.4	1.4	2.1	1.2
1.2	1.3	1.3	0.94	0.55
0.9	0.9	1.1	0.87	0.52

1.4	1.0	0.79	0.66	0.20
0.38	0.41	1.0	0.39	0.053
0.70	0.23	0.45	0.15	0.071
1.8	0.83	1.1	0.60	0.12
1.4	0.77	1.0	0.57	0.32
0.42	0.29	0.46	0.23	0.21
0.11	0.63	1.9	0.34	0.27
0.34	0.075	0.41	0.13	0.018
3638	*5009*	*3395*	*3530*	*869*

76	81	76	80	87
85	88	80	84	94
77	81	77	81	88

SAP111302BM (site B - morning)	SAP111302CM (siteC - morning)	SAP111302AA (site A - afternoon)	SAP111302BA (site B - afternoon)
71	113	105	90
34	48	53	39
21	26	28	24
33	50	43	35
41	55	55	42
24	29	34	23
23	24	31	26
17	19	22	18
5.2	5.7	6.5	5.1
3.5	4.6	4.3	3.8
41	45	42	35
21	25	26	22
9	11	11	8.8
27	28	24	20
20	21	18	16
14	20	14	13
9.1	11	10	7.5
3.8	4.7	4.8	3.9
6.2	6.7	7.2	9.0
13	14	15	13
45	46	46	39
5.9	6.5	6.2	5.1
12	11	13	10
22	19	23	17
20	18	19	13
7.7	7.4	8.3	5.7
1.7	1.4	1.8	1.3
4.5	4.3	4.3	3.3
17	17	16	15
57	42	44	44
20	19	18	15
1.4	1.5	1.4	1.3
2.8	2.3	2.5	2.0
2.5	2.2	2.1	2.0
6.9	6.8	6.0	4.9
5.5	5.5	5.4	4.2
4.6	3.6	3.9	3.7
6.7	5.5	5.3	4.2
2.6	2.0	2.0	1.9
1.4	0.91	1.0	0.74
0.14	0.14	0.17	0.14
4.6	3.6	4.2	2.8
0.48	0.33	0.45	0.27
0.57	0.54	0.93	0.53
2.6	2.8	1.8	1.2
0.43	0.41	0.56	0.31
0.31	0.17	0.28	0.21
0.16	0.081	0.16	0.085
1.2	0.47	0.99	1.1
0.59	0.56	0.61	0.56
0.59	0.48	0.55	0.53

0.24	0.22	0.33	0.085
0.083	0.089	0.093	0.048
0.12	0.092	0.13	0.060
0.15	0.15	0.21	0.078
0.32	0.37	0.36	0.39
0.23	0.20	0.23	0.23
0.30	0.18	0.22	0.26
0.063	0.051	0.077	0.053
697	*793*	*797*	*656*

75	79	70	78
84	83	74	84
90	80	75	84

SAP111302CA (site C - afternoon)	SAP111402AM (site A - morning)	SAP111402BM (site B - morning)	SAP111402CM (siteC - morning)	SAP111402AA (site A - afternoon)
109	69	68	40	50
54	28	32	25	21
28	19	22	14	13
48	25	30	14	17
52	33	33	25	29
31	18	19	14	15
34	18	20	12	19
24	16	14	6.7	10
6.8	3.4	4.5	1.9	2.7
5.0	3.5	3.4	3.0	2.2
41	27	35	23	23
26	14	16	13	10
12	5.9	7.2	4.8	5.1
27	17	22	13	14
25	15	16	14	9.0
21	13	14	8.7	6.5
12	7.3	8.3	4.6	4.7
4.7	4.5	6.3	2.9	1.3
5.3	5.4	5.0	3.1	4.5
10	10	12	6.9	9.5
35	31	41	22	30
3.9	2.8	5.1	2.2	3.3
9.0	10	10	4.0	7.5
19	20	21	7.9	11
13	14	19	10	14
5.2	4.8	7.1	3.5	5.0
1.3	1.1	1.5	1.0	0.98
3.0	2.8	4.4	2.2	4.6
17	10	15	9.3	12
30	28	30	20	20
14	13	21	8.9	15
1.1	0.9	1.5	0.4	1.1
1.8	1.7	2.4	1.5	2.3
1.8	1.4	2.2	1.3	1.9
4.3	3.9	6.2	3.5	5.3
2.7	3.0	6.3	3.1	5.3
2.6	2.9	1.8	0.86	0.85
3.3	3.5	5.9	2.8	4.6
1.2	1.4	2.3	0.89	1.3
0.48	0.64	0.91	0.51	0.79
0.15	0.07	0.09	0.11	0.20
1.9	2.1	4.1	2.0	2.9
0.18	0.22	0.46	0.21	0.32
0.34	0.30	0.50	0.16	0.22
0.88	1.4	1.7	1.0	0.92
0.18	0.29	0.28	0.20	0.27
0.16	0.15	0.22	0.075	0.09
0.041	0.11	0.060	0.060	0.18
1.0	0.30	0.28	0.22	0.45
0.46	0.37	0.42	0.34	0.39
0.51	0.32	0.31	0.28	0.31

0.13	0.10	0.11	0.09	0.12
0.12	0.048	0.048	0.079	0.053
0.058	0.066	0.053	0.056	0.041
0.13	0.093	0.061	0.097	0.099
0.45	0.27	0.25	0.31	0.29
0.27	0.13	0.14	0.15	0.73
0.28	0.27	0.045	0.082	0.054
0.067	0.025	0.029	0.14	0.058
753	*517*	*600*	*361*	*421*

84	95	97	96	92
90	97	97	98	100
88	98	100	100	101

SAP111402BA (site B - afternoon)	SAP111402CA (site C - afternoon)
39	80
16	31
13	24
16	32
28	46
16	23
16	23
8.8	17
4.6	4.2
6.3	4.1
37	31
13	15
8.4	7.0
18	18
15	12
12	12
6.6	6.8
4.6	4.5
3.4	4.3
8.2	7.9
34	27
4.6	4.2
7.4	7.9
13	15
14	13
5.4	4.6
1.0	1.0
3.4	3.0
12	11
22	27
16	17
1.2	1.7
1.8	1.7
1.7	1.6
5.2	4.5
5.5	4.8
4.1	3.0
6.8	4.4
1.4	1.9
0.79	0.73
0.11	0.088
3.8	3.2
0.36	0.30
0.26	0.37
0.96	0.56
0.41	0.44
0.18	0.26
0.23	0.15
0.49	0.51
0.44	0.53
0.36	0.37

0.23	0.20
0.11	0.079
0.077	0.074
0.12	0.13
0.30	0.30
0.52	0.20
0.049	0.11
0.023	0.18
461	*564*

95	99
100	100
100	100

PCB Mass Data (in ng) - Stevens Institute of Technology (SIT)

(PCB data quantified by the Eisenreich Laboratory)

August 1, 2001

PCB Concentration (ng/m^3)	P16080101 (SIT)	P17080101 (SIT)	P3082801 (SIT)
Congeners 8+5	*1.93*	*3.13*	*2.35*
18	*0.48*	*1.08*	*0.34*
17+15	*0.23*	*0.53*	*0.26*
16+32	*1.37*	*1.37*	*0.44*
31	*0.23*	*0.55*	*0.46*
28	*0.41*	*0.27*	*0.25*
21+33+53	*0.25*	*0.31*	*0.18*
22	*0.16*	*0.23*	*0.20*
37+42	*0.48*	*0.23*	*0.27*
45	*0.12*	*0.18*	*0.05*
46	*0.06*	*0.05*	*0.01*
52+43	*0.58*	*0.47*	*0.34*
49	*0.23*	*0.16*	*0.11*
47+48	*0.13*	*0.12*	*0.12*
44	*0.09*	*0.41*	*0.39*
41+71	*0.07*	*0.14*	*0.10*
64	*0.02*	*0.09*	*0.08*
40	*0.05*	*0.07*	*0.07*
74	*0.07*	*0.06*	*0.03*
70+76	*0.09*	*0.11*	*0.06*
66+95	*0.35*	*0.33*	*0.21*
91	*0.11*	*0.05*	*0.01*
56+60+89	*0.10*	*0.12*	*0.00*
92+84	*0.25*	*0.23*	*0.14*
101	*0.18*	*0.14*	*0.11*
99	*0.22*	*0.22*	*0.22*
83	*0.03*	*0.04*	*0.00*
97	*0.02*	*0.03*	*0.03*
87+81	*0.65*	*0.07*	*0.14*
85+136	*0.31*	*0.26*	*0.04*
110+77	*0.22*	*0.14*	*0.18*
82	*0.06*	*0.06*	*0.04*
118	*0.04*	*0.10*	*0.05*
105	*0.03*	*0.24*	*0.02*
151	*0.02*	*0.05*	*0.01*
135+144+147+124	*0.03*	*0.05*	*0.01*
149+123+107	*0.05*	*0.10*	*0.05*
146	*0.45*	*0.05*	*0.04*
153+132	*0.03*	*0.13*	*0.02*
141+179	*0.01*	*0.07*	*0.01*
137+176+130	*0.26*	*0.02*	*0.00*
163+138	*0.01*	*0.10*	*0.07*
158	*0.01*	*0.01*	*0.00*
128	*0.11*	*0.08*	*0.00*
178+129	*0.40*	*0.24*	*0.01*
187+182	*0.07*	*ND*	*0.00*

183	*0.04*	*0.06*	*0.01*
185	*0.01*	*ND*	*0.01*
174	*0.30*	*0.17*	*0.09*
177	*0.30*	*0.15*	*0.01*
180	*0.25*	*0.07*	*0.12*
170+190	*0.02*	*0.03*	*0.00*
202+171+156	*0.26*	*0.12*	*0.01*
199	*0.10*	*ND*	*0.01*
201	*0.01*	*ND*	*0.05*
203+196	*0.01*	*0.02*	*0.02*
195+208	*0.03*	*0.01*	*0.01*
194	*0.13*	*0.02*	*0.07*
206	*0.01*	*0.02*	*0.00*

August 29-30, 2001

P4082801 (SIT)	P5082801 (SIT)	P6082801 (SIT)
1.26	3.15	2.10
0.31	0.79	0.65
0.84	0.50	1.06
0.34	1.01	0.70
0.36	1.00	1.19
0.20	0.58	0.67
0.18	0.65	0.55
0.48	1.65	0.60
0.22	0.52	0.47
0.05	0.48	0.10
0.03	0.32	0.07
0.27	0.89	0.54
0.14	0.29	0.32
0.08	0.37	0.19
0.44	0.48	0.68
0.14	0.28	0.24
0.05	0.13	0.17
0.04	0.09	0.18
0.01	0.16	0.45
0.07	0.24	0.13
0.26	0.72	0.43
0.03	0.08	0.04
0.05	0.27	0.11
0.21	0.35	0.27
0.18	0.34	0.12
0.23	0.28	0.29
0.00	0.02	0.03
0.02	0.06	0.03
0.09	0.20	0.05
0.11	0.35	0.25
0.14	0.40	0.14
0.02	0.07	0.02
0.07	0.18	0.04
0.03	0.11	0.02
0.03	0.10	0.01
0.02	0.11	0.02
0.09	0.25	0.04
0.04	0.08	0.04
0.07	0.17	0.05
0.02	0.08	0.01
0.00	0.01	0.01
0.07	0.11	0.05
0.00	0.05	0.00
0.02	0.04	0.03
0.03	0.04	0.01
0.01	0.05	0.04

0.03	*0.02*	*0.04*
0.01	*0.02*	*0.01*
0.02	*0.08*	*0.06*
0.02	*0.14*	*0.09*
ND	*0.01*	*0.00*
0.02	*0.06*	*0.02*
0.01	*0.04*	*0.05*
0.00	*0.05*	*0.02*
0.02	*0.06*	*0.01*
0.00	*0.04*	*0.03*
0.00	*0.02*	*0.01*
0.01	*0.03*	*0.01*
ND ND		*0.01*

PCB Mass Data (in ng) - Stevens Institute of Technology (SIT)

(PCB data quantified by the Eisenreich Laboratory)

PCB Concentration (ng/m^3)	P1	P3	P5	P6	P7	P8
Congeners 8+5	0.37	0.28	0.24	0.62	0.81	0.94
18	0.08	0.04	0.02	0.10	0.20	0.04
17+15	0.04	0.05	0.02	0.06	0.14	0.19
16+32	0.08	0.23	0.08	0.21	0.23	0.22
31	0.16	0.10	0.05	0.20	0.22	0.38
28	0.11	0.08	0.05	0.13	0.19	0.36
21+33+53	0.06	0.00	0.02	0.09	0.01	0.11
22	0.05	0.06	0.03	0.11	0.09	0.09
37+42	0.03	0.05	0.02	0.17	0.11	0.25
45	0.02	0.00	0.00	0.02	0.12	0.31
46	0.00	0.00	0.00	0.07	0.04	0.11
52+43	0.07	0.21	0.09	0.25	0.32	0.25
49	0.05	0.03	0.03	0.15	0.11	0.11
47+48	0.05	0.16	0.02	0.17	0.06	0.13
44	0.00	0.00	0.00	0.02	0.00	0.04
41+71	0.04	0.06	0.02	0.10	0.06	0.10
64	0.02	0.02	0.01	0.04	0.03	0.03
40	0.02	0.01	0.01	0.04	0.03	0.11
74	0.01	0.00	0.00	0.04	0.02	0.03
70+76	0.02	0.02	0.02	0.09	0.05	0.07
66+95	0.08	0.05	0.09	0.29	0.18	0.07
91	0.01	0.02	0.01	0.07	0.02	0.01
56+60+89	0.02	0.18	0.00	0.11	0.04	0.10
92+84	0.07	0.11	0.07	0.20	0.16	0.25
101	0.02	0.04	0.05	0.11	0.09	0.00
99	0.09	0.06	0.07	0.18	0.14	0.17
83	0.00	0.00	0.00	0.07	0.00	0.00
97	0.00	0.00	0.00	0.04	0.01	0.02
87+81	0.01	0.00	0.03	0.07	0.06	0.03
110+77	0.04	0.03	0.06	0.10	0.13	0.04
82	0.00	0.01	0.00	0.00	0.02	0.01
118	0.02	0.02	0.02	0.07	0.04	0.03
105	0.02	0.05	0.02	0.09	0.03	0.04
85+136	0.00	0.00	0.00	0.00	0.04	0.02
151	0.01	0.00	0.01	0.02	0.06	0.00
135+144+147+124	0.01	0.01	0.01	0.07	0.04	0.00
149+123+107	0.02	0.01	0.03	0.10	0.04	0.01
146	0.00	0.02	0.00	0.03	0.02	0.01
153+132	0.03	0.04	0.04	0.05	0.04	0.04
141+179	0.00	0.03	0.00	0.02	0.00	0.01
137+176+130	0.01	0.01	0.01	0.01	0.01	0.02
163+138	0.01	0.00	0.05	0.05	0.04	0.03
158	0.00	0.00	0.03	0.02	0.01	0.00
128	0.00	0.00	0.00	0.01	0.00	0.02
178+129	0.00	0.00	0.03	0.06	0.01	0.06
187+182	0.01	0.01	0.01	0.00	0.02	0.03
183	0.00	0.00	0.01	0.00	0.01	0.01
185	0.01	0.00	0.01	0.00	0.00	0.00
174	0.01	0.00	0.01	0.03	0.04	0.06
177	0.00	0.00	0.01	0.03	0.01	0.07
180	0.00	0.03	0.01	0.07	0.02	0.07

170+190	*0.00*	*0.00*	*0.01*	*0.21*	*0.00*	*0.00*
202+171+156	*0.00*	*0.01*	*0.01*	*0.01*	*0.01*	*0.02*
199	*0.00*	*0.01*	*0.00*	*nd*	*0.01*	*0.02*
201	*0.00*	*0.00*	*0.00*	*0.08*	*0.02*	*0.08*
203+196	*0.00*	*0.00*	*0.00*	*0.05*	*0.01*	*0.05*
195+208	*0.00*	*0.02*	*0.01*	*0.01*	*0.01*	*0.02*
194	*0.00*	*0.00*	*0.00*	*0.00*	*0.00*	*0.00*
206	*0.00*	*0.03*	*0.02*	*0.02*	*0.01*	*0.01*

P21	P22	P23	P24
2.44	1.69	3.19	1.31
0.57	0.46	0.85	0.33
0.46	0.41	0.63	0.26
1.03	0.60	1.02	0.41
0.67	0.63	1.27	0.70
0.51	0.42	0.66	0.49
0.08	0.35	0.79	0.00
0.12	0.19	0.40	0.20
0.35	0.26	0.48	0.17
0.17	0.19	0.07	0.08
0.02	0.11	0.09	0.08
0.42	0.38	0.70	0.31
0.25	0.19	0.35	0.15
0.27	0.20	0.47	0.14
0.15	0.12	0.20	0.10
0.12	0.13	0.26	0.11
0.07	0.07	0.13	0.05
0.06	0.05	0.08	0.04
0.05	0.04	0.10	0.37
0.10	0.06	0.16	0.06
0.24	0.22	0.48	0.20
0.05	0.03	0.07	0.01
0.18	0.08	0.13	0.03
0.36	0.22	0.39	0.12
0.11	0.06	0.16	0.06
0.24	0.19	0.48	0.15
0.01	0.04	0.48	0.21
0.01	0.01	0.03	0.02
0.15	0.07	0.05	0.02
0.08	0.06	0.20	0.10
0.06	0.00	0.02	0.00
0.07	0.03	0.07	0.03
0.09	0.01	0.03	0.01
0.01	0.00	0.04	0.09
0.02	0.01	0.04	0.00
0.04	0.02	0.04	0.01
0.06	0.02	0.10	0.00
0.01	0.00	0.02	0.01
0.03	0.01	0.07	0.01
0.03	0.00	0.03	0.02
0.04	0.01	0.02	0.00
0.05	0.02	0.10	0.02
0.00	0.01	0.02	0.02
0.03	0.01	0.04	0.01
0.11	0.01	0.09	0.04
0.03	0.01	0.01	0.00
0.00	0.00	0.02	0.03
nd	0.00	0.01	0.01
0.01	0.01	0.05	0.02
0.05	0.02	0.05	0.09
0.49	0.01	0.09	0.08

0.00	*0.01*	*0.03*	*0.04*
0.05	*0.02*	*0.13*	*0.09*
0.07	*0.02*	*0.03*	*0.04*
0.16	*0.02*	*0.04*	*0.00*
0.02	*0.01*	*0.04*	*0.13*
0.02	*0.00*	*0.01*	*0.01*
0.01	*0.01*	*0.04*	*0.01*
0.01	*0.00*	*0.01*	*0.06*

PCB Mass Data (in ng) - Stevens Institute of Technology (SIT)

(PCB data quantified by the Eisenreich Laboratory)

PCB Concentration (ng/m^3)	SIT2	SIT3	SIT4	SIT5	SIT7	SIT8
Congeners 8+5	0.13	0.57	0.52	0.64	1.98	0.85
18	0.02	0.08	0.12	0.12	0.33	0.12
17+15	0.02	0.07	0.08	0.08	0.32	0.09
16+32	0.04	0.12	0.17	0.14	0.85	0.24
31	0.02	0.06	0.10	0.10	0.29	0.11
28	0.02	0.08	0.11	0.11	0.26	0.13
21+33+53	0.01	0.03	0.04	0.06	0.13	0.05
22	0.01	0.08	0.05	0.02	0.18	0.07
37+42	ND	0.04	0.02	ND	0.19	0.06
45	ND	0.05	ND	ND	0.09	0.03
46	0.06	0.18	0.35	0.33	0.74	0.17
52+43	0.02	0.06	0.07	0.07	0.55	0.13
49	0.02	0.04	0.05	0.04	0.43	0.05
47+48	0.02	0.09	0.09	0.15	0.30	0.08
44	0.02	0.09	0.11	0.12	0.19	0.06
41+71	0.01	0.05	0.04	0.03	0.11	0.05
64	0.01	0.03	0.03	0.03	0.07	0.03
40	0.01	0.01	ND	0.01	0.11	0.02
74	0.01	0.02	0.02	0.02	0.17	0.02
70+76	0.01	0.04	0.03	0.02	0.09	0.03
66+95	0.03	0.12	0.08	0.07	0.38	0.11
91	0.01	ND	0.01	0.02	ND	0.02
56+60+89	0.01	ND	0.02	0.02	0.11	0.05
92+84	0.02	0.08	0.07	0.05	0.33	0.08
101	0.01	0.04	0.03	0.03	ND	0.05
99	0.02	0.08	0.07	0.06	ND	0.09
83	ND	0.01	0.01	0.00	ND	0.01
97	0.00	0.02	0.01	0.01	0.02	0.01
87+81	0.00	0.02	0.01	0.01	0.03	0.02
110+77	ND	0.01	0.01	ND	ND	0.01
82	0.01	0.03	0.02	0.03	0.11	0.04
118	ND	0.01	0.00	0.01	0.01	0.01
105	0.00	0.01	0.00	0.01	0.01	0.01
85+136	0.00	0.01	0.00	0.01	0.02	0.01
151	0.01	0.02	0.01	0.02	0.04	0.02
135+144+147+124	0.01	0.02	0.01	0.02	0.05	0.02
149+123+107	0.01	0.02	0.01	0.01	0.03	0.01
146	0.00	0.01	0.01	0.01	0.04	0.00
153+132	ND	ND	ND	ND	ND	ND
141+179	0.00	0.01	0.00	0.01	0.05	0.00
137+176+130	ND	ND	ND	ND	ND	ND
163+138	0.01	0.02	0.01	0.01	0.03	0.01
158	ND	0.00	0.00	0.01	ND	0.00
128	0.00	0.01	0.00	0.01	ND	ND
178+129	0.00	0.00	0.00	0.00	0.01	0.00
187+182	ND	0.00	0.00	0.01	0.00	ND
183	ND	ND	0.00	ND	ND	ND
185	0.00	0.02	0.00	0.02	0.01	0.00
174	ND	0.02	ND	ND	0.02	0.00
177	ND	ND	ND	ND	ND	ND
180	ND	ND	ND	ND	ND	ND

170+190	*ND*	*0.01*	*0.00*	*0.00*	*ND*	*ND*
202+171+156	*ND*	*ND*	*ND*	*ND*	*ND*	*0.00*
199	*ND*	*0.00*	*0.00*	*0.01*	*ND*	*ND*
201	*ND*	*ND*	*ND*	*0.01*	*ND*	*ND*
203+196	*ND*	*ND*	*ND*	*0.00*	*0.06*	*ND*
195+208	*ND*	*ND*	*ND*	*ND*	*0.02*	*0.00*
194	*ND*	*ND*	*ND*	*0.00*	*0.01*	*0.00*
206	*ND*	*0.00*	*ND*	*0.00*	*ND*	*0.00*
	0.61	*2.37*	*2.41*	*2.58*	*8.75*	*2.95*

SIT9	SIT10	SIT11	SIT12	SIT13	SIT14	SIT16	SIT18
0.85	0.34	0.33	0.66	0.36	0.00	0.51	0.40
0.14	0.05	0.09	0.10	0.05	0.00	0.06	0.05
0.25	0.08	0.07	0.09	0.07	0.00	0.05	0.05
ND	0.07	0.07	0.47	0.13	0.00	0.23	0.15
0.10	0.04	0.04	0.10	0.07	0.00	0.08	0.05
0.09	0.03	0.04	0.08	ND	0.00	0.08	0.04
0.02	0.03	0.02	0.06	0.03	0.00	0.04	0.02
0.06	0.03	0.02	0.06	0.04	0.00	0.04	0.03
0.02	0.01	0.02	0.04	0.02	0.00	0.03	ND
ND	0.01	0.03	ND	ND	ND	ND	0.03
0.21	0.08	0.08	0.18	0.11	0.00	0.20	0.13
0.04	0.04	0.02	0.06	0.05	0.00	0.04	0.03
0.08	0.18	0.04	0.12	0.07	0.00	0.11	0.06
0.03	0.02	0.03	0.06	0.04	0.00	0.06	0.04
ND	ND	0.03	0.07	0.04	0.00	0.06	0.04
0.12	0.02	0.01	0.05	0.03	0.00	0.04	0.03
ND	0.01	0.01	0.02	0.01	0.00	0.01	0.02
0.01	0.05	0.02	0.05	0.02	0.00	0.04	0.03
0.03	0.02	0.03	0.06	0.02	0.00	0.08	0.04
0.02	0.03	0.02	0.03	0.02	0.00	0.04	0.04
0.08	0.07	0.04	0.09	0.06	0.00	0.13	0.07
ND	ND	0.02	0.05	0.01	0.00	0.02	0.02
ND	0.03	0.01	0.05	0.03	0.00	0.03	0.03
0.05	ND	0.07	0.23	0.03	0.00	0.07	0.05
0.04	0.04	0.02	0.03	0.02	0.00	0.03	0.01
0.07	0.05	0.03	0.06	0.03	0.00	0.05	0.03
0.02	0.02	ND	0.01	0.01	0.00	0.01	ND
0.02	ND	0.00	0.00	0.01	0.00	0.00	0.00
0.02	0.01	0.00	0.01	0.01	0.00	0.01	0.01
ND	0.00	0.00	0.06	ND	ND	ND	0.01
0.02	0.02	0.01	0.02	0.02	0.00	0.02	0.02
0.04	0.00	0.01	0.00	0.01	0.00	0.02	0.01
0.01	0.01	0.00	0.01	0.01	0.00	0.01	0.01
0.08	0.01	0.01	0.02	0.01	0.00	0.02	0.01
0.00	0.01	0.02	0.02	0.01	0.00	0.03	0.02
0.03	0.02	0.01	0.03	0.01	0.00	0.03	0.02
0.03	0.00	0.01	0.01	0.01	0.00	0.01	0.01
0.01	0.00	0.00	0.01	0.00	0.00	0.01	0.00
ND	ND	ND	ND	ND	ND	ND	ND
0.00	ND	ND	0.02	0.01	0.00	ND	ND
ND	0.02	0.01	ND	0.01	0.00	0.02	ND
ND	0.01	ND	ND	0.01	0.00	0.02	0.03
ND	ND	ND	0.00	ND	ND	0.00	ND
ND	ND	ND	0.08	ND	ND	ND	ND
ND	0.00	ND	0.00	0.00	0.00	0.01	0.01
ND	ND	ND	ND	0.00	0.00	0.00	ND
ND	ND	ND	ND	ND	ND	ND	ND
0.03	0.02	ND	0.01	0.00	0.00	ND	0.01
0.01	ND	0.01	0.00	0.00	0.00	0.02	0.01
ND	ND	ND	ND	ND	0.00	0.00	ND
ND	ND	ND	ND	0.00	ND	ND	ND

ND	*ND*	*ND*	*ND*	*ND*	*ND*	*ND*	*ND*
ND	*ND*	*ND*	*ND*	*ND*	*ND*	*ND*	*0.02*
ND	*ND*	*ND*	*ND*	*ND*	*ND*	*ND*	*ND*
ND	*ND*	*ND*	*0.06*	*0.29*	*0.00*	*0.08*	*ND*
ND	*ND*	*ND*	*ND*	*0.04*	*0.00*	*0.10*	*ND*
ND	*ND*	*ND*	*ND*	*0.00*	*0.00*	*0.00*	*0.02*
ND	*0.01*	*ND*	*0.04*	*0.03*	*0.00*	*0.01*	*0.01*
0.02	*0.00*	*ND*	*0.00*	*0.00*	*0.00*	*0.01*	*0.01*
2.65	*1.51*	*1.28*	*3.29*	*1.85*	*0.02*	*2.59*	*1.72*

PCB Mass Data (in ng) - Stevens Institute of Technology (SIT)

(PCB data quantified by the Eisenreich Laboratory)

PCB Concentration (ng/m^3)	Lower 11-13	Upper 11-13	Lower 11-14 #1	Upper 11-14 #1
8+5	0.14	0.12	0.18	0.10
18.00	0.01	0.02	0.04	0.01
17+15	0.02	0.01	0.01	0.01
16+32	0.03	0.01	0.05	0.02
31.00	0.03	0.01	0.04	0.01
28.00	0.03	0.01	0.02	0.00
21+33+53	0.01	0.00	0.01	0.00
22.00	0.03	0.01	0.05	0.02
45.00	0.01	0.00	0.00	0.00
46.00	0.01	0.00	0.02	0.00
52+43	0.03	0.02	0.04	0.02
49.00	0.02	0.01	0.03	0.01
47+48	0.02	0.01	0.04	0.01
44.00	0.01	0.01	0.02	0.01
37+42	0.02	0.01	0.06	0.01
41+71	0.01	0.01	0.08	0.01
64.00	0.01	0.00	0.01	0.00
40.00	0.01	0.00	0.01	0.00
74.00	0.00	0.00	0.02	0.00
70+76	0.01	0.00	0.03	0.00
66+95	0.01	0.01	0.03	0.01
91.00	0.00	0.00	0.02	0.00
56+60+89	0.01	0.00	0.03	0.00
92+84	0.01	0.01	0.04	0.02
101.00	0.01	0.00	0.02	0.01
99.00	0.01	0.01	0.01	0.02
83.00	0.00	0.00	0.00	0.00
97.00	0.00	0.00	0.00	0.00
87+81	0.01	0.00	0.01	0.00
85+136	0.02	0.00	0.01	0.01
110+77	0.01	0.00	0.02	0.00
82.00	0.00	0.00	0.00	0.00
151.00	0.00	0.00	0.00	0.00
135+144+147+124	0.00	0.00	0.00	0.00
149+123+107	0.01	0.00	0.01	0.01
118.00	0.00	0.00	0.00	0.00
146.00	0.00	0.00	0.00	0.00
153+132	0.01	0.00	0.01	0.00
105.00	0.01	0.00	0.01	0.00
141+179	0.00	0.01	0.00	0.00
137+176+130	0.00	0.00	0.00	0.00
163+138	0.00	0.00	0.00	0.00
158.00	0.00	0.00	0.00	0.00
178+129	0.00	0.01	0.00	0.01
187+182	0.01	0.00	0.01	0.00
183.00	0.00	0.00	0.01	0.00
128.00	0.00	0.00	0.00	0.00
185.00	0.00	0.00	0.02	0.01
174.00	0.00	0.00	0.00	0.00
177.00	0.00	0.00	0.00	0.00
202+171+156	0.00	0.00	0.00	0.00

180.00	*0.01*	*0.00*	*0.01*	*0.00*
199.00	*0.00*	*0.01*	*0.00*	*0.01*
170+190	*0.00*	*0.00*	*0.02*	*0.00*
201.00	*0.00*	*0.00*	*0.00*	*0.01*
203+196	*0.00*	*0.00*	*0.00*	*0.00*
195+208	*0.00*	*0.00*	*0.01*	*0.01*
194.00	*0.00*	*0.00*	*0.00*	*0.00*
206.00	*0.00*	*0.00*	*0.00*	*0.00*

Upper 11-14 #2	Lower 11-14 #2	Upper 11-14 #3	Lower 11-14 #3	Sampler A 11-15 #2
0.12	0.12	0.29	0.40	0.14
0.00	0.02	0.01	0.01	0.02
0.00	0.02	0.01	0.00	0.01
0.02	0.04	0.02	0.02	0.03
0.01	0.04	0.01	0.02	0.03
0.01	0.02	0.01	0.01	0.02
0.00	0.01	0.00	0.00	0.01
0.02	0.06	0.02	0.01	0.03
0.00	0.00	0.00	0.00	0.01
0.00	0.01	0.01	0.00	0.01
0.02	0.05	0.04	0.03	0.04
0.01	0.02	0.02	0.01	0.02
0.01	0.02	0.11	0.02	0.01
0.02	0.02	0.01	0.01	0.03
0.02	0.04	0.01	0.01	0.04
0.02	0.08	0.02	0.01	0.04
0.00	0.01	0.00	0.00	0.01
0.00	0.02	0.00	0.00	0.01
0.01	0.02	0.01	0.00	0.01
0.01	0.03	0.01	0.01	0.02
0.02	0.03	0.03	0.02	0.04
0.01	0.01	0.01	0.00	0.02
0.01	0.00	0.01	0.00	0.02
0.02	0.05	0.01	0.02	0.05
0.01	0.03	0.01	0.01	0.02
0.02	0.03	0.01	0.01	0.03
0.00	0.00	0.00	0.00	0.00
0.00	0.02	0.00	0.00	0.01
0.01	0.01	0.00	0.01	0.01
0.02	0.03	0.06	0.02	0.01
0.01	0.02	0.01	0.01	0.02
0.00	0.01	0.00	0.00	0.00
0.00	0.00	0.00	0.00	0.00
0.00	0.00	0.00	0.00	0.00
0.00	0.01	0.01	0.01	0.00
0.00	0.01	0.00	0.00	0.00
0.01	0.00	0.00	0.00	0.00
0.00	0.00	0.00	0.00	0.00
0.00	0.01	0.00	0.00	0.00
0.00	0.00	0.00	0.00	0.00
0.00	0.00	0.00	0.00	0.00
0.00	0.01	0.00	0.01	0.01
0.00	0.00	0.00	0.00	0.00
0.00	0.00	0.01	0.00	0.01
0.01	0.00	0.01	0.00	0.00
0.00	0.00	0.00	0.00	0.00
0.00	0.00	0.00	0.00	0.00
0.00	0.02	0.01	0.01	0.00
0.00	0.00	0.00	0.01	0.00
0.00	0.01	0.00	0.00	0.00
0.00	0.00	0.00	0.00	0.00

0.01	*0.00*	*0.01*	*0.00*	*0.00*
0.01	*0.00*	*0.01*	*0.00*	*0.00*
0.01	*0.00*	*0.01*	*0.00*	*0.00*
0.01	*0.00*	*0.00*	*0.00*	*0.01*
0.00	*0.00*	*0.00*	*0.00*	*0.00*
0.02	*0.00*	*0.00*	*0.00*	*0.00*
0.01	*0.00*	*0.00*	*0.00*	*0.00*
0.01	*0.01*	*0.00*	*0.00*	*0.00*

Upper 11-15 #1	*Lower 11-15 #1*	*Sampler B 11-15 #2*
0.12	*0.17*	*0.19*
0.01	*0.02*	*0.02*
0.01	*0.01*	*0.01*
0.03	*0.04*	*0.04*
0.02	*0.05*	*0.04*
0.01	*0.02*	*0.02*
0.01	*0.01*	*0.02*
0.03	*0.04*	*0.03*
0.02	*0.00*	*0.01*
0.00	*0.00*	*0.00*
0.03	*0.04*	*0.04*
0.01	*0.03*	*0.03*
0.02	*0.03*	*0.04*
0.02	*0.02*	*0.04*
0.02	*0.02*	*0.05*
0.01	*0.04*	*0.03*
0.00	*0.01*	*0.01*
0.00	*0.01*	*0.01*
0.01	*0.02*	*0.02*
0.01	*0.02*	*0.02*
0.03	*0.03*	*0.04*
0.01	*0.01*	*0.01*
0.01	*0.01*	*0.02*
0.04	*0.04*	*0.07*
0.01	*0.02*	*0.01*
0.02	*0.02*	*0.02*
0.00	*0.00*	*0.00*
0.00	*0.00*	*0.00*
0.00	*0.04*	*0.10*
0.07	*0.02*	*0.04*
0.01	*0.04*	*0.02*
0.00	*0.00*	*0.00*
0.00	*0.00*	*0.00*
0.00	*0.00*	*0.00*
0.01	*0.01*	*0.01*
0.00	*0.01*	*0.00*
0.00	*0.00*	*0.01*
0.00	*0.00*	*0.00*
0.01	*0.01*	*0.01*
0.00	*0.00*	*0.00*
0.00	*0.01*	*0.00*
0.00	*0.01*	*0.00*
0.00	*0.00*	*0.00*
0.00	*0.00*	*0.01*
0.00	*0.01*	*0.01*
0.00	*0.00*	*0.00*
0.00	*0.00*	*0.00*
0.00	*0.00*	*0.00*
0.00	*0.00*	*0.00*
0.00	*0.00*	*0.00*
0.00	*0.00*	*0.01*

0.00	*0.02*	*0.01*
0.01	*0.00*	*0.01*
0.01	*0.01*	*0.02*
0.01	*0.00*	*0.01*
0.00	*0.00*	*0.00*
0.00	*0.00*	*0.02*
0.01	*0.00*	*0.01*
0.00	*0.01*	*0.01*

Sampling Interval	Time	Wind Speed (m/s)	Temperature (°C)	Ri	z/L	Phi M	Phi H	Phi W	u_star	Upper Arm Total PCB Conc. (ng/m^3)	Lower Arm Total PCB Conc. (ng/m^3)	PCB Flux ($ng/m^2/h$)
08/01/01	10:30-12:45	2.0	27.6	-0.82	-0.54	0.62	0.75	ND	0.18	12.5	13.2	201
08/01/01	12:45-14:41	3.0	28.9	1.11	-0.97	0.58	ND	ND	0.16	12.5	13.2	134
08/29/01	22:25-2:10	2.2	21.4	0.09	0.20	1.26	0.80	1.32	0.11	7.95	7.46	-47
08/30/01	10:30-14:30	4.7	29.3	-0.23	-0.30	0.54	0.36	1.00	0.33	18.7	13.6	-1944
10/23/01	10:20-14:00	4.3	31.6	-0.08	-0.04	0.99	2.69	1.00	0.23	2.21	1.79	-106
10/23/01	14:30-18:07	6.7	27.1	-0.03	-0.01	0.94	3.39	1.00	0.33	1.50	5.01	1276
10/24/01	10:20-14:19	2.2	25.8	-0.35	-0.18	0.64	0.98	ND	0.23	7.13	15.7	2205
10/24/01	20:10-23:30	3.7	21.6	-0.03	0.13	1.85	ND	ND	0.19	4.26	5.82	326
10/25/01	8:00-12:00	3.3	27.8	0.05	-0.02	1.83	ND	0.72	0.24	7.88	11.6	1366
05/06/02	12:30-15:30	3.4	23.7	-0.04	-0.02	0.47	0.47	0.30	0.59	3.15	9.53	14871
05/06/02	15:30-18:30	4.2	21.0	0.00	-0.01	0.66	0.22	0.33	0.55	1.51	3.63	4207
05/07/02	9:30-12:30	2.4	22.6	-0.18	-0.25	0.61	0.35	0.24	0.22	3.00	4.82	1987
05/07/02	13:00-16:00	3.4	25.7	-0.04	-0.09	0.66	0.27	0.34	0.28	3.25	5.62	2332
05/07/02	20:00-23:15	0.9	20.6	0.27	0.23	1.39	1.73	ND	0.10	3.74	4.79	72
05/08/02	9:30-12:30	4.3	18.6	-0.01	-0.04	0.93	0.32	0.25	0.63	1.03	2.00	2877
11/13/02	15:37-19:30	5.6	9.2	0.01	0.01	1.00	1.12	ND	0.32	0.366	0.605	76
11/14/02	8:15-11:30	3.3	6.9	-0.02	-0.19	1.25	0.29	ND	0.18	0.343	1.049	492
11/14/02	12:00-15:00	2.7	12.8	-0.09	-0.19	0.77	0.41	ND	0.20	0.554	1.035	260
11/14/02	16:30-19:45	3.7	12.3	0.16	0.06	0.56	1.06	ND	0.21	0.821	0.745	-17
11/15/02	8:30-11:30	4.2	11.3	-0.02	-0.04	0.94	0.85	ND	0.24	0.713	0.949	74

The value of phi W was assumed to be 1 due to varying conditions and gradients in moisture vapor below the resolution of the sampling apparatus

ND — The value could not be calculated due to technical or atmospheric problems

Date	Time	AVG (ng/m3)	Time	Station Type	Maintenance indicator
2/20/2002	14:50	2.18	1451	AO21	-
2/20/2002	15:50	2.34	1551	AO21	-
2/20/2002	16:50	2.40	1651	AO21	-
2/20/2002	17:50	2.27	1751	AO21	-
2/20/2002	18:50	2.19	1851	AO21	-
2/20/2002	19:50	2.05	1951	AO21	-
2/20/2002	20:50	2.01	2051	AO22	-
2/20/2002	21:50	1.98	2151	AO22	-
2/20/2002	22:50	1.98	2251	AO22	-
2/20/2002	23:50	2.07	2304	AO22	-
2/21/2002	0:50	2.35	51	AO20	-
2/21/2002	1:50	2.20	151	AO20	-
2/21/2002	2:50	2.20	251	AO20	-
2/21/2002	3:50	2.68	351	AO20	-
2/21/2002	4:50	3.04	451	AO20	-
2/21/2002	5:50	2.85	551	AO20	-
2/21/2002	6:50	3.12	651	AO20	-
2/21/2002	7:50	3.22	751	AO20	-
2/21/2002	8:50	4.39	851	AO20	-
2/21/2002	9:50	4.24	951	AO20	-
2/21/2002	10:50	2.75	1051	AO21	-
2/21/2002	11:50	2.35	1151	AO21	-
2/21/2002	12:50	2.09	1251	AO21	-
2/21/2002	13:50	2.04	1351	AO21	-
2/21/2002	14:50	1.99	1451	AO21	-
2/21/2002	15:50	1.93	1551	AO21	-
2/21/2002	16:50	1.91	1651	AO21	-
2/21/2002	17:50	1.87	1751	AO21	-
2/21/2002	18:50	1.92	1851	AO21	-
2/21/2002	19:50	1.99	1951	AO21	-
2/21/2002	20:50	2.17	2051	AO22	-
2/21/2002	21:50	2.07	2151	AO22	-
2/21/2002	22:50	2.09	2251	AO22	-
2/21/2002	23:50	2.06	2351	AO22	-
2/22/2002	0:50	2.06	51	AO20	-
2/22/2002	1:50	1.95	151	AO20	-
2/22/2002	2:50	2.04	251	AO20	-
2/22/2002	3:50	2.08	351	AO20	-
2/22/2002	4:50	2.05	451	AO20	-
2/22/2002	5:50	2.99	551	AO20	-
2/22/2002	6:50	3.28	651	AO20	-
2/22/2002	7:50	2.09	751	AO20	-
2/22/2002	8:50	2.05	851	AO20	-
2/22/2002	9:50	1.93	951	AO20	-
2/22/2002	10:50	1.89	1051	AO21	-
2/22/2002	11:50	1.91	1151	AO21	-
2/22/2002	12:50	1.89	1251	AO21	-
2/22/2002	13:50	1.90	1351	AO21	-
2/22/2002	14:50	1.90	1451	AO21	-
2/22/2002	15:50	1.95	1551	AO21	-

2/22/2002	16:50	1.86	1651	AO21	-
2/22/2002	17:50	1.88	1751	AO21	-
2/22/2002	18:50	1.84	1851	AO21	-
2/22/2002	19:50	1.93	1951	AO21	-
2/22/2002	20:50	1.90	2051	AO22	-
2/22/2002	21:50	1.90	2151	AO22	-
2/22/2002	22:50	1.80	2251	AO22	-
2/22/2002	23:50	1.81	2351	AO22	-
2/23/2002	0:50	1.82	51	AO20	-
2/23/2002	1:50	2.00	151	AO20	-
2/23/2002	2:50	2.07	251	AO20	-
2/23/2002	3:50	2.01	351	AO20	-
2/23/2002	4:50	1.99	451	AO20	-
2/23/2002	5:50	1.92	551	AO20	-
2/23/2002	6:50	1.92	651	AO20	-
2/23/2002	7:50	1.93	751	AO20	-
2/23/2002	8:50	1.99	851	AO20	-
2/23/2002	9:50	1.93	951	AO20	-
2/23/2002	10:50	1.98	1051	AO21	-
2/23/2002	11:50	1.98	1151	AO21	-
2/23/2002	12:50	2.11	1251	AO21	-
2/23/2002	13:50	1.98	1351	AO21	-
2/23/2002	14:50	2.04	1451	AO21	-
2/23/2002	15:50	1.98	1551	AO21	-
2/23/2002	16:50	1.98	1651	AO21	-
2/23/2002	17:50	1.94	1751	AO21	-
2/23/2002	18:50	1.96	1851	AO21	-
2/23/2002	19:50	2.18	1951	AO21	-
2/23/2002	20:50	2.20	2051	AO22	-
2/23/2002	21:50	2.24	2151	AO22	-
2/23/2002	22:50	2.43	2251	AO22	-
2/23/2002	23:50	2.05	2351	AO22	-
2/24/2002	0:50	1.91	51	AO20	-
2/24/2002	1:50	1.88	151	AO20	-
2/24/2002	2:50	1.88	251	AO20	-
2/24/2002	3:50	1.87	351	AO20	-
2/24/2002	4:50	1.89	451	AO20	-
2/24/2002	5:50	1.84	551	AO20	-
2/24/2002	6:50	1.85	651	AO20	-
2/24/2002	7:50	1.97	751	AO20	-
2/24/2002	8:50	1.95	851	AO20	-
2/24/2002	9:50	1.85	951	AO20	-
2/24/2002	10:50	1.70	1051	AO21	-
2/24/2002	11:50	1.75	1151	AO21	-
2/24/2002	12:50	2.13	1251	AO21	-
2/24/2002	13:50	2.21	1351	AO21	-
2/24/2002	14:50	2.29	1451	AO21	-
2/24/2002	15:50	2.27	1551	AO21	-
2/24/2002	16:50	2.20	1651	AO21	-
2/24/2002	17:50	2.08	1751	AO21	-
2/24/2002	18:50	2.05	1851	AO21	-
2/24/2002	19:50	1.99	1951	AO21	-

2/24/2002	20:50	2.00	2051	AO22	-
2/24/2002	21:50	2.01	2151	AO22	-
2/24/2002	22:50	2.03	2251	AO22	-
2/24/2002	23:50	2.39	2351	AO22	-
2/25/2002	0:50	3.71	51	AO20	-
2/25/2002	1:50	2.33	151	AO20	-
2/25/2002	2:50	2.91	251	AO20	-
2/25/2002	3:50	3.68	351	AO20	-
2/25/2002	4:50	2.41	451	AO20	-
2/25/2002	5:50	2.44	551	AO20	-
2/25/2002	6:50	2.41	651	AO20	-
2/25/2002	7:50	2.39	751	AO20	-
2/25/2002	8:50	2.44	851	AO20	-
2/25/2002	9:50	2.40	951	AO20	-
2/25/2002	10:50	2.65	1051	AO21	-
2/25/2002	11:50	2.18	1151	AO21	-
2/25/2002	12:50	2.10	1251	AO21	-
2/25/2002	13:50	2.05	1351	AO21	-
2/28/2002	11:51	1.71	1151	AO21	-
2/28/2002	12:51	1.72	1251	AO21	-
2/28/2002	13:51	1.73	1351	AO21	-
2/28/2002	14:51	1.74	1451	AO21	-
2/28/2002	15:51	1.77	1551	AO21	-
2/28/2002	16:51	1.77	1651	AO21	-
2/28/2002	17:51	1.80	1751	AO21	-
2/28/2002	18:51	1.80	1851	AO21	-
2/28/2002	19:51	1.89			
2/28/2002	20:51	1.86			
2/28/2002	21:51	2.35			
2/28/2002	22:51	2.01	2251	AO22	-
2/28/2002	23:51	2.02	2351	AO22	-
3/1/2002	0:51	2.05	51	AO20	-
3/1/2002	1:51	2.04	151	AO20	-
3/1/2002	2:51	2.37	251	AO20	-
3/1/2002	3:51	2.00	351	AO20	-
3/1/2002	4:51	1.97	451	AO20	-
3/1/2002	5:51	1.94	551	AO20	-
3/1/2002	6:51	1.91	651	AO20	-
3/1/2002	7:51	1.93	751	AO20	-
3/1/2002	8:51	1.94	851	AO20	-
3/1/2002	9:51	2.00	951	AO20	-
3/1/2002	10:51	2.00	1051	AO21	-
3/1/2002	11:51	2.05	1151	AO21	-
3/1/2002	12:51	1.87	1251	AO21	-
3/1/2002	13:51	1.83	1351	AO21	-
3/1/2002	14:51	1.81	1451	AO21	-
3/1/2002	15:51	1.80	1551	AO21	-
3/1/2002	16:51	1.84	1651	AO21	-
3/1/2002	17:51	1.85	1751	AO21	-
3/1/2002	18:51	2.04	1851	AO21	-
3/1/2002	19:51	2.35	1951	AO21	-
3/1/2002	20:51	2.08	2051	AO22	-

3/1/2002	21:51	2.62	2151	AO22	-
3/1/2002	22:51	2.86	2251	AO22	-
3/4/2002	11:49	1.71	1151	AO21	-
3/4/2002	12:49	1.70	1251	AO21	-
3/4/2002	13:49	1.70	1351	AO21	-
3/4/2002	14:49	1.72	1451	AO21	-
3/4/2002	15:49	1.76	1551	AO21	-
3/4/2002	16:49	1.82	1651	AO21	-
3/4/2002	17:49	1.69	1751	AO21	-
3/4/2002	18:49	1.76	1851	AO21	-
3/4/2002	19:49	1.69	1951	AO21	-
3/4/2002	20:49	1.74	2051	AO22	-
3/4/2002	21:49	1.66	2151	AO22	-
3/4/2002	22:49	1.67	2251	AO22	-
3/4/2002	23:49	1.67	2351	AO22	-
3/5/2002	0:49	1.68	51	AO20	-
3/5/2002	1:49	1.72	151	AO20	-
3/5/2002	2:49	1.70	251	AO20	-
3/5/2002	3:49	1.67	351	AO20	-
3/5/2002	4:49	1.66	451	AO20	-
3/5/2002	5:49	1.69	551	AO20	-
3/5/2002	6:49	1.71	651	AO20	-
3/5/2002	7:49	1.70	751	AO20	-
3/5/2002	8:49	1.70	851	AO20	-
3/5/2002	9:49	1.71	951	AO20	-
3/5/2002	10:49	1.82	1051	AO21	-
3/5/2002	11:49	1.94	1151	AO21	-
3/5/2002	12:49	1.86	1251	AO21	-
3/5/2002	13:49	1.79	1351	AO21	-
3/5/2002	14:49	1.79	1451	AO21	-
3/5/2002	15:49	1.82	1551	AO21	-
3/5/2002	16:49	1.74	1651	AO21	-
3/5/2002	17:49	1.73	1751	AO21	-
3/5/2002	18:49	1.76	1851	AO21	-
3/5/2002	19:49	1.79	1951	AO21	-
3/5/2002	20:49	1.91	2051	AO22	-
3/5/2002	21:49	1.97	2151	AO22	-
3/5/2002	22:49	1.95	2251	AO22	-
3/5/2002	23:49	1.93	2351	AO22	-
3/6/2002	0:49	1.87	51	AO20	-
3/6/2002	1:49	1.91	151	AO20	-
3/6/2002	2:49	2.12	251	AO20	-
3/6/2002	3:49	1.97	351	AO20	-
3/6/2002	4:49	1.80	451	AO20	-
3/6/2002	5:49	1.91	551	AO20	-
3/6/2002	6:49	2.03	651	AO20	-
3/6/2002	7:49	2.07	751	AO20	-
3/6/2002	8:49	2.26	851	AO20	-
3/6/2002	9:49	2.19	951	AO20	-
3/6/2002	10:49	2.19	1051	AO21	-
3/6/2002	11:49	2.04	1151	AO21	-
3/6/2002	12:49	1.99	1251	AO21	-

3/6/2002	13:49	1.79	1351	AO21	-
3/6/2002	14:49	1.78	1451	AO21	-
3/6/2002	15:49	1.78	1551	AO21	-
3/6/2002	16:49	1.84	1651	AO21	-
3/6/2002	17:49	1.82	1751	AO21	-
3/6/2002	18:49	1.91	1851	AO21	-
3/6/2002	19:49	1.89	1951	AO21	-
3/6/2002	20:49	1.94	2051	AO22	-
3/6/2002	21:49	2.33	2151	AO22	-
3/6/2002	22:49	2.38	2251	AO22	-
3/6/2002	23:49	2.14	2351	AO22	-
3/7/2002	0:49	1.97	51	AO20	-
3/7/2002	1:49	2.56	151	AO20	-
3/7/2002	2:49	1.99	251	AO20	-
3/7/2002	3:49	2.15	351	AO20	-
3/7/2002	4:49	2.42	451	AO20	-
3/7/2002	5:49	2.74	551	AO20	-
3/7/2002	6:49	2.41	651	AO20	-
3/7/2002	7:49	2.43	751	AO20	-
3/7/2002	8:49	2.91	851	AO20	-
3/7/2002	9:49	2.61	951	AO20	-
3/7/2002	10:49	2.41	1051	AO21	-
3/7/2002	11:49	2.15	1151	AO21	-
3/7/2002	12:49	1.85	1251	AO21	-
3/7/2002	13:49	1.75	1351	AO21	-
3/7/2002	14:49	1.75	1451	AO21	-
3/7/2002	15:49	1.79	1551	AO21	-
3/7/2002	16:49	2.09	1651	AO21	-
3/7/2002	17:49	1.87	1751	AO21	-
3/7/2002	18:49	1.88	1851	AO21	-
3/7/2002	19:49	2.07	1951	AO21	-
3/7/2002	20:49	2.38	2051	AO22	-
3/7/2002	21:49	3.15	2151	AO22	-
3/7/2002	22:49	2.98	2251	AO22	-
3/7/2002	23:49	3.12	2351	AO22	-
3/8/2002	0:49	3.15	51	AO20	-
3/8/2002	1:49	2.22	151	AO20	-
3/8/2002	2:49	2.14	251	AO20	-
3/8/2002	3:49	2.13	351	AO20	-
3/8/2002	4:49	2.16	451	AO20	-
3/8/2002	5:49	2.39	551	AO20	-
3/8/2002	6:49	2.51	651	AO20	-
3/8/2002	7:49	2.57	751	AO20	-
3/8/2002	8:49	2.90	851	AO20	-
3/8/2002	9:49	3.42	951	AO20	-
3/8/2002	10:49	3.13	1051	AO21	-
3/8/2002	11:49	2.83	1151	AO21	-
3/8/2002	12:49	2.63	1251	AO21	-
3/8/2002	13:49	2.33	1351	AO21	-
3/8/2002	14:49	2.14	1451	AO21	-
3/8/2002	15:49	2.04	1551	AO21	-
3/8/2002	16:49	1.90	1651	AO21	-

3/8/2002	17:49	1.95	1751	AO21	-
3/8/2002	18:49	1.88	1851	AO21	-
3/8/2002	19:49	1.78	1951	AO21	-
3/8/2002	20:49	1.80	2051	AO22	-
3/8/2002	21:49	1.78	2151	AO22	-
3/8/2002	22:49	1.84	2251	AO22	-
3/8/2002	23:49	2.00	2351	AO22	-
3/9/2002	0:49	2.62	51	AO20	-
3/9/2002	1:49	2.70	151	AO20	-
3/9/2002	2:49	2.38	251	AO20	-
3/9/2002	3:49	2.81	351	AO20	-
3/9/2002	4:49	2.51	451	AO20	-
3/9/2002	5:49	2.67	551	AO20	-
3/9/2002	6:49	2.44	651	AO20	-
3/9/2002	7:49	2.89	751	AO20	-
3/9/2002	8:49	2.90	851	AO20	-
3/9/2002	9:49	3.22	951	AO20	-
3/9/2002	10:49	3.50	1051	AO21	-
3/9/2002	11:49	2.98	1151	AO21	-
3/9/2002	12:49	2.15	1251	AO21	-
3/9/2002	13:49	1.99	1351	AO21	-
3/9/2002	14:49	1.83	1451	AO21	-
3/9/2002	15:49	1.77	1551	AO21	-
3/9/2002	16:49	1.78	1651	AO21	-
3/9/2002	17:49	1.78	1751	AO21	-
3/9/2002	18:49	1.82	1851	AO21	-
3/9/2002	19:49	1.78	1951	AO21	-
3/9/2002	20:49	1.78	2051	AO22	-
3/9/2002	21:49	1.78	2151	AO22	-
3/9/2002	22:49	1.75	2251	AO22	-
3/9/2002	23:49	1.66	2351	AO22	-
3/10/2002	0:49	1.65	51	AO20	-
3/10/2002	1:49	1.63	151	AO20	-
3/10/2002	2:49	1.63	251	AO20	-
3/10/2002	3:49	1.61	351	AO20	-
3/10/2002	4:49	1.57	451	AO20	-
3/10/2002	5:49	1.56	551	AO20	-
3/10/2002	6:49	1.57	651	AO20	-
3/10/2002	7:49	1.57	751	AO20	-
3/10/2002	8:49	1.59	851	AO20	-
3/10/2002	9:49	1.60	951	AO20	-
3/10/2002	10:49	1.62	1051	AO21	-
3/10/2002	11:49	1.62	1151	AO21	-
3/10/2002	12:49	1.62	1251	AO21	-
3/10/2002	13:49	1.62	1351	AO21	-
3/10/2002	14:49	1.59	1451	AO21	-
3/10/2002	15:49	1.60	1551	AO21	-
3/10/2002	16:49	1.59	1651	AO21	-
3/10/2002	17:49	1.55	1751	AO21	-
3/10/2002	18:49	1.55	1851	AO21	-
3/10/2002	19:49	1.55	1951	AO21	-
3/10/2002	20:49	1.58	2051	AO22	-

3/10/2002	21:49	1.59	2151	AO22	-
3/10/2002	22:49	1.59	2251	AO22	-
3/10/2002	23:49	1.59	2351	AO22	-
3/11/2002	0:49	1.60	51	AO20	-
3/11/2002	1:49	1.59	151	AO20	-
3/11/2002	2:49	1.61	251	AO20	-
3/11/2002	3:49	1.63	351	AO20	-
3/11/2002	4:49	1.59	451	AO20	-
3/11/2002	5:49	1.61	551	AO20	-
3/11/2002	6:49	1.64	651	AO20	-
3/11/2002	7:49	1.64	751	AO20	-
3/11/2002	8:49	1.63	851	AO20	-
3/11/2002	9:49	1.64	951	AO20	-
3/11/2002	10:49	1.66	1051	AO21	-
3/11/2002	11:49	1.67	1151	AO21	-
3/11/2002	12:49	1.67	1251	AO21	-
3/11/2002	13:49	1.66	1351	AO21	-
3/18/2002	14:51	2.34	1451	AO21	-
3/18/2002	15:51	1.95	1551	AO21	-
3/18/2002	16:51	2.99	1651	AO21	-
3/18/2002	17:51	2.62	1751	AO21	-
3/18/2002	18:51	2.05	1851	AO21	-
3/18/2002	19:51	2.01	1951	AO21	-
3/18/2002	20:51	1.97	2051	AO22	-
3/18/2002	21:51	1.98	2151	AO22	-
3/18/2002	22:51	2.05	2251	AO22	-
3/18/2002	23:51	2.03	2351	AO22	-
3/19/2002	0:51	2.02	51	AO20	-
3/19/2002	1:51	2.03	151	AO20	-
3/19/2002	2:51	4.39	251	AO20	-
3/19/2002	3:51	2.36	351	AO20	-
3/19/2002	4:51	2.85	451	AO20	-
3/19/2002	5:51	2.40	551	AO20	-
3/19/2002	6:51	2.23	651	AO20	-
3/19/2002	7:51	2.27	751	AO20	-
3/19/2002	8:51	2.29	851	AO20	-
3/19/2002	9:51	2.31	951	AO20	-
3/19/2002	10:51	2.08	1051	AO21	-
3/19/2002	11:51	2.15	1151	AO21	-
3/19/2002	12:51	2.20	1251	AO21	-
3/19/2002	13:51	2.28	1351	AO21	-
3/19/2002	14:51	2.41	1451	AO21	-
3/19/2002	15:51	2.44	1551	AO21	-
3/19/2002	16:51	2.47	1651	AO21	-
3/19/2002	17:51	2.47	1751	AO21	-
3/19/2002	18:51	2.39	1851	AO21	-
3/19/2002	19:51	2.82	1951	AO21	-
3/19/2002	20:51	2.27	2051	AO22	-
3/19/2002	21:51	2.02	2151	AO22	-
3/19/2002	22:51	2.02	2251	AO22	-
3/19/2002	23:51	2.03	2351	AO22	-
3/20/2002	0:51	1.95	51	AO20	-

3/20/2002	1:51	1.89	151	AO20	-
3/20/2002	2:51	1.90	251	AO20	-
3/20/2002	3:51	1.89	351	AO20	-
3/20/2002	4:51	1.91	451	AO20	-
3/21/2002	12:49	2.36	1251	AO21	-
3/21/2002	13:49	2.40	1351	AO21	-
3/21/2002	14:49	2.26	1451	AO21	-
3/21/2002	15:49	2.25	1551	AO21	-
3/21/2002	16:49	2.23	1651	AO21	-
3/21/2002	17:49	2.28	1751	AO21	-
3/21/2002	18:49	2.22	1851	AO21	-
3/21/2002	19:49	2.26	1951	AO21	-
3/21/2002	20:49	2.43	2051	AO22	-
3/21/2002	21:49	1.81	2151	AO22	-
3/21/2002	22:49	1.71	2251	AO22	-
3/21/2002	23:49	1.70	2351	AO22	-
3/22/2002	0:49	1.72	51	AO20	-
3/22/2002	1:49	1.69	151	AO20	-
3/22/2002	2:49	1.62	251	AO20	-
3/22/2002	3:49	1.62	351	AO20	-
3/22/2002	4:49	1.66	451	AO20	-
3/22/2002	5:49	1.63	551	AO20	-
3/22/2002	6:49	1.68	651	AO20	-
3/22/2002	7:49	1.69	751	AO20	-
3/22/2002	8:49	1.65	851	AO20	-
3/22/2002	9:49	1.67	951	AO20	-
3/22/2002	10:49	1.65	1051	AO21	-
3/22/2002	11:49	1.64	1151	AO21	-
3/22/2002	12:49	1.67	1251	AO21	-
3/22/2002	13:49	1.64	1351	AO21	-
3/22/2002	14:49	1.64	1451	AO21	-
3/22/2002	15:49	1.64	1551	AO21	-
3/22/2002	16:49	1.64	1651	AO21	-
3/22/2002	17:49	1.62	1751	AO21	-
3/22/2002	18:49	1.62	1851	AO21	-
3/22/2002	19:49	1.65	1951	AO21	-
3/22/2002	20:49	1.67	2051	AO22	-
3/22/2002	21:49	1.72	2151	AO22	-
3/22/2002	22:49	1.72	2251	AO22	-
3/22/2002	23:49	1.75	2351	AO22	-
3/23/2002	0:49	1.78	51	AO20	-
3/23/2002	1:49	1.81	151	AO20	-
3/23/2002	2:49	1.85	251	AO20	-
3/23/2002	3:49	1.83	351	AO20	-
3/23/2002	4:49	1.85	451	AO20	-
3/23/2002	5:49	1.96	551	AO20	-
3/23/2002	6:49	2.10	651	AO20	-
3/23/2002	7:49	1.93	751	AO20	-
3/23/2002	8:49	1.84	851	AO20	-
3/23/2002	9:49	1.81	951	AO20	-
3/23/2002	10:49	1.81	1051	AO21	-
3/23/2002	11:49	1.82	1151	AO21	-

3/23/2002	12:49	1.80	1251	AO21	-
3/23/2002	13:49	1.77	1351	AO21	-
3/23/2002	14:49	1.77	1451	AO21	-
3/23/2002	15:49	1.77	1551	AO21	-
3/23/2002	16:49	1.76	1651	AO21	-
3/23/2002	17:49	1.76	1751	AO21	-
3/23/2002	18:49	1.91	1851	AO21	-
3/23/2002	19:49	2.09	1951	AO21	-
3/23/2002	20:49	1.81	2051	AO22	-
3/23/2002	21:49	1.82	2151	AO22	-
3/23/2002	22:49	1.91	2251	AO22	-
3/23/2002	23:49	2.00	2351	AO22	-
3/24/2002	0:49	2.06	51	AO20	-
3/24/2002	1:49	2.05	151	AO20	-
3/24/2002	2:49	2.23	251	AO20	-
3/24/2002	3:49	2.66	351	AO20	-
3/24/2002	4:49	2.25	451	AO20	-
3/24/2002	5:49	2.22	551	AO20	-
3/24/2002	6:49	2.13	651	AO20	-
3/24/2002	7:49	2.46	751	AO20	-
3/24/2002	8:49	2.46	851	AO20	-
3/24/2002	9:49	2.03	951	AO20	-
3/24/2002	10:49	2.03	1051	AO21	-
3/24/2002	11:49	1.95	1151	AO21	-
3/24/2002	12:49	1.88	1251	AO21	-
3/24/2002	13:49	1.86	1351	AO21	-
3/24/2002	14:49	1.86	1451	AO21	-
3/24/2002	15:49	1.88	1551	AO21	-
3/24/2002	16:49	1.91	1651	AO21	-
3/24/2002	17:49	1.81	1751	AO21	-
3/24/2002	18:49	1.87	1851	AO21	-
3/24/2002	19:49	1.95	1951	AO21	-
3/24/2002	20:49	2.27	2051	AO22	-
3/24/2002	21:49	2.20	2151	AO22	-
3/24/2002	22:49	1.90	2251	AO22	-
3/24/2002	23:49	2.35	2351	AO22	-
3/25/2002	0:49	2.69	51	AO20	-
3/25/2002	1:49	2.09	151	AO20	-
3/25/2002	2:49	2.00	251	AO20	-
3/25/2002	3:49	1.96	351	AO20	-
3/25/2002	4:49	1.88	451	AO20	-
3/25/2002	5:49	1.79	551	AO20	-
3/25/2002	6:49	1.80	651	AO20	-
3/25/2002	7:49	1.81	751	AO20	-
3/25/2002	8:49	1.83	851	AO20	-
3/25/2002	9:49	1.84	951	AO20	-
3/25/2002	10:49	1.83	1051	AO21	-
3/25/2002	11:49	2.22	1151	AO21	-
3/25/2002	12:49	2.17	1251	AO21	-
3/25/2002	13:49	2.08	1351	AO21	-
3/25/2002	14:49	2.07	1451	AO21	-
3/25/2002	15:49	2.01	1551	AO21	-

3/25/2002	16:49	1.92	1651	AO21	-
3/25/2002	17:49	1.95	1751	AO21	-
3/25/2002	18:49	1.91	1851	AO21	-
3/25/2002	19:49	1.93	1951	AO21	-
3/25/2002	20:49	1.98	2051	AO22	-
3/25/2002	21:49	2.01	2151	AO22	-
3/25/2002	22:49	1.97	2251	AO22	-
3/25/2002	23:49	2.05	2351	AO22	-
3/26/2002	0:49	2.19	51	AO20	-
3/26/2002	1:49	2.20	151	AO20	-
3/26/2002	2:49	2.03	251	AO20	-
3/26/2002	3:49	2.09	351	AO20	-
3/26/2002	4:49	2.00	451	AO20	-
3/26/2002	5:49	2.04	551	AO20	-
3/26/2002	6:49	2.06	651	AO20	-
3/26/2002	7:49	2.06	751	AO20	-
3/26/2002	8:49	2.15	851	AO20	-
3/26/2002	9:49	2.44	951	AO20	-
3/26/2002	10:49	2.10	1051	AO21	-
3/26/2002	11:49	2.34	1151	AO21	-
3/26/2002	12:49	2.24	1251	AO21	-
3/26/2002	13:49	2.03	1351	AO21	-
3/26/2002	14:49	1.97	1451	AO21	-
3/26/2002	15:49	1.99	1551	AO21	-
3/26/2002	16:49	3.00	1651	AO21	-
3/26/2002	17:49	2.63	1751	AO21	-
3/26/2002	18:49	2.26	1851	AO21	-
3/26/2002	19:49	2.41	1951	AO21	-
3/26/2002	20:49	2.25	2051	AO22	-
3/26/2002	21:49	2.36	2151	AO22	-
3/26/2002	22:49	2.15	2251	AO22	-
3/26/2002	23:49	2.20	2351	AO22	-
3/27/2002	0:49	2.26	51	AO20	-
3/27/2002	1:49	2.30	151	AO20	-
3/27/2002	2:49	2.20	251	AO20	-
3/27/2002	3:49	2.87	351	AO20	-
3/27/2002	4:49	2.70	451	AO20	-
3/27/2002	5:49	2.29	551	AO20	-
3/27/2002	6:49	2.20	651	AO20	-
3/27/2002	7:49	2.25	751	AO20	-
3/27/2002	8:49	2.17	851	AO20	-
3/27/2002	9:49	2.12	951	AO20	-
3/27/2002	10:49	2.14	1051	AO21	-
3/27/2002	11:49	2.10	1151	AO21	-
3/27/2002	12:49	2.07	1251	AO21	-
3/27/2002	13:49	2.03	1351	AO21	-
3/27/2002	14:49	2.01	1451	AO21	-
3/27/2002	15:49	1.94	1551	AO21	-
3/27/2002	16:49	1.89	1651	AO21	-
3/27/2002	17:49	1.88	1751	AO21	-
3/27/2002	18:49	1.85	1851	AO21	-
3/27/2002	19:49	1.85	1951	AO21	-

3/27/2002	20:49	1.83	2051	AO22	-
3/27/2002	21:49	1.82	2151	AO22	-
3/27/2002	22:49	1.82	2251	AO22	-
3/27/2002	23:49	1.82	2351	AO22	-
3/28/2002	0:49	1.90	51	AO20	-
3/28/2002	1:49	1.93	151	AO20	-
3/28/2002	2:49	1.83	251	AO20	-
3/28/2002	3:49	1.88	351	AO20	-
3/28/2002	4:49	1.91	451	AO20	-
3/28/2002	5:49	1.82	551	AO20	-
3/28/2002	6:49	1.92	651	AO20	-
3/28/2002	7:49	1.95	751	AO20	-
4/24/2002	13:50	2.42	1351	AO21	-
4/24/2002	14:50	2.38	1451	AO21	-
4/24/2002	15:50	2.28	1551	AO21	-
4/24/2002	16:50	2.29	1651	AO21	-
4/24/2002	17:50	2.25	1751	AO21	-
4/24/2002	18:50	2.15	1851	AO21	-
4/24/2002	19:50	2.12	1951	AO21	-
4/24/2002	20:50	2.10	2051	AO22	-
4/24/2002	21:50	1.98	2151	AO22	-
4/24/2002	22:50	1.88	2251	AO22	-
4/24/2002	23:50	1.88	2351	AO22	-
4/25/2002	0:50	2.69	51	AO20	-
4/25/2002	1:50	2.25	151	AO20	-
4/25/2002	2:50	1.95	251	AO20	-
4/25/2002	3:50	2.16	351	AO20	-
4/25/2002	4:50	2.17	451	AO20	-
4/25/2002	5:50	2.57	551	AO20	-
4/25/2002	6:50	2.71	651	AO20	-
4/25/2002	7:50	2.40	751	AO20	-
4/25/2002	8:50	2.05	851	AO20	-
4/25/2002	9:50	1.96	951	AO20	-
4/25/2002	10:50	1.98	1051	AO21	-
4/25/2002	11:50	1.99	1151	AO21	-
4/25/2002	12:50	1.99	1251	AO21	-
4/25/2002	13:50	1.99	1351	AO21	-
4/25/2002	14:50	2.00	1451	AO21	-
4/25/2002	15:50	2.09	1551	AO21	-
4/25/2002	16:50	2.20	1651	AO21	-
4/25/2002	17:50	2.31	1751	AO21	-
4/25/2002	18:50	2.51	1851	AO21	-
4/25/2002	19:50	2.28	1951	AO21	-
4/25/2002	20:50	1.99	2051	AO22	-
4/25/2002	21:50	1.90	2151	AO22	-
4/25/2002	22:50	1.95	2251	AO22	-
4/25/2002	23:50	2.25	2351	AO22	-
4/26/2002	0:50	2.34	51	AO20	-
4/26/2002	1:50	2.08	151	AO20	-
4/26/2002	2:50	2.25	251	AO20	-
4/26/2002	3:50	2.24	351	AO20	-
4/26/2002	4:50	2.19	451	AO20	-

4/26/2002	5:50	2.00	551	AO20	-
4/26/2002	6:50	2.08	651	AO20	-
4/26/2002	7:50	1.99	751	AO20	-
4/26/2002	8:50	1.93	851	AO20	-
4/26/2002	9:50	1.84	951	AO20	-
4/26/2002	10:50	1.77	1051	AO21	-
4/26/2002	11:50	1.78	1151	AO21	-
4/26/2002	12:50	1.77	1251	AO21	-
4/26/2002	13:50	1.79	1351	AO21	-
4/26/2002	14:50	1.78	1451	AO21	-
4/26/2002	15:50	1.79	1551	AO21	-
4/26/2002	16:50	1.76	1651	AO21	-
4/26/2002	17:50	1.75	1751	AO21	-
4/26/2002	18:50	1.75	1851	AO21	-
4/26/2002	19:50	1.77	1951	AO21	-
4/26/2002	20:50	1.89	2051	AO22	-
4/26/2002	21:50	2.43	2151	AO22	-
4/26/2002	22:50	2.38	2251	AO22	-
4/26/2002	23:50	2.72	2351	AO22	-
4/27/2002	0:50	1.85	51	AO20	-
4/27/2002	1:50	1.85	151	AO20	-
4/27/2002	2:50	1.89	251	AO20	-
4/27/2002	3:50	1.88	351	AO20	-
4/27/2002	4:50	2.22	451	AO20	-
4/27/2002	5:50	2.17	551	AO20	-
4/27/2002	6:50	2.38	651	AO20	-
4/27/2002	7:50	3.23	751	AO20	-
4/27/2002	8:50	2.12	851	AO20	-
4/27/2002	9:50	2.23	951	AO20	-
4/27/2002	10:50	2.37	1051	AO21	-
4/27/2002	11:50	2.12	1151	AO21	-
4/27/2002	12:50	2.05	1251	AO21	-
4/27/2002	13:50	2.01	1351	AO21	-
4/27/2002	14:50	2.02	1451	AO21	-
4/27/2002	15:50	2.07	1551	AO21	-
4/27/2002	16:50	2.09	1651	AO21	-
4/27/2002	17:50	2.15	1751	AO21	-
4/27/2002	18:50	2.16	1851	AO21	-
4/27/2002	19:50	2.16	1951	AO21	-
4/27/2002	20:50	2.07	2051	AO22	-
4/27/2002	21:50	2.06	2151	AO22	-
4/27/2002	22:50	2.05	2251	AO22	-
4/27/2002	23:50	1.94	2351	AO22	-
4/28/2002	0:50	1.99	51	AO20	-
4/28/2002	1:50	2.07	151	AO20	-
4/28/2002	2:50	2.05	251	AO20	-
4/28/2002	3:50	1.97	351	AO20	-
4/28/2002	4:50	1.94	451	AO20	-
4/28/2002	5:50	1.96	551	AO20	-
4/28/2002	6:50	1.98	651	AO20	-
4/28/2002	7:50	2.11	751	AO20	-
4/28/2002	8:50	2.23	851	AO20	-

4/28/2002	9:50	2.43	951	AO20	-
4/28/2002	10:50	3.15	1051	AO21	-
4/28/2002	11:50	2.73	1151	AO21	-
4/28/2002	12:50	2.72	1251	AO21	-
4/28/2002	13:50	4.69	1351	AO21	-
4/28/2002	14:50	4.25	1451	AO21	-
4/28/2002	15:50	2.72	1551	AO21	-
4/28/2002	16:50	2.73	1651	AO21	-
4/28/2002	17:50	3.29	1751	AO21	-
4/28/2002	18:50	3.60	1851	AO21	-
4/28/2002	19:50	3.97	1951	AO21	-
4/28/2002	20:50	3.36	2051	AO22	-
4/28/2002	21:50	2.63	2151	AO22	-
4/28/2002	22:50	2.61	2251	AO22	-
4/28/2002	23:50	2.89	2351	AO22	-
4/29/2002	0:50	3.17	51	AO20	-
4/29/2002	1:50	3.19	151	AO20	-
4/29/2002	2:50	2.81	251	AO20	-
4/29/2002	3:50	2.93	351	AO20	-
4/29/2002	4:50	3.17	451	AO20	-
4/29/2002	5:50	2.53	551	AO20	-
4/29/2002	6:50	2.08	651	AO20	-
4/29/2002	7:50	2.16	751	AO20	-
4/29/2002	8:50	2.08	851	AO20	-
5/4/2002	0:50	1.80	51	AO20	-
5/4/2002	1:50	1.76	151	AO20	-
5/4/2002	2:50	1.77	251	AO20	-
5/4/2002	3:50	1.74	351	AO20	-
5/4/2002	4:50	1.86	451	AO20	-
5/4/2002	5:50	1.84	551	AO20	-
5/4/2002	6:50	1.97	651	AO20	-
5/4/2002	7:50	1.85	751	AO20	-
5/4/2002	8:50	1.96	851	AO20	-
5/4/2002	9:50	2.07	951	AO20	-
5/4/2002	10:50	2.02	1051	AO21	-
5/4/2002	11:50	1.86	1151	AO21	-
5/4/2002	12:50	1.94	1251	AO21	-
5/4/2002	13:50	2.02	1351	AO21	-
5/4/2002	14:50	1.97	1451	AO21	-
5/4/2002	15:50	1.96	1551	AO21	-
5/4/2002	16:50	1.93	1651	AO21	-
5/4/2002	17:50	1.90	1751	AO21	-
5/4/2002	18:50	1.88	1851	AO21	-
5/4/2002	19:50	1.90	1951	AO21	-
5/4/2002	20:50	1.76	2051	AO22	-
5/4/2002	21:50	1.74	2151	AO22	-
5/4/2002	22:50	1.75	2251	AO22	-
5/4/2002	23:50	1.84	2351	AO22	-
5/5/2002	0:50	3.11	51	AO20	-
5/5/2002	1:50	2.70	151	AO20	-
5/5/2002	2:50	2.53	251	AO20	-
5/5/2002	3:50	2.36	351	AO20	-

5/5/2002	4:50	2.04	451	AO20	-
5/5/2002	5:50	2.44	551	AO20	-
5/5/2002	6:50	4.14	651	AO20	-
5/5/2002	7:50	4.99	751	AO20	-
5/5/2002	8:50	2.18	851	AO20	-
5/5/2002	9:50	2.12	951	AO20	-
5/5/2002	10:50	2.12	1051	AO21	-
5/5/2002	11:50	2.09	1151	AO21	-
5/5/2002	12:50	2.31	1251	AO21	-
5/5/2002	13:50	2.32	1351	AO21	-
5/5/2002	14:50	2.22	1451	AO21	-
5/5/2002	15:50	2.03	1551	AO21	-
5/5/2002	16:50	1.92	1651	AO21	-
5/5/2002	17:50	1.96	1751	AO21	-
5/5/2002	18:50	1.99	1851	AO21	-
5/5/2002	19:50	2.01	1951	AO21	-
5/5/2002	20:50	1.99	2051	AO22	-
5/5/2002	21:50	1.95	2151	AO22	-
5/5/2002	22:50	1.92	2251	AO22	-
5/5/2002	23:50	2.08	2351	AO22	-
5/6/2002	0:50	2.64	51	AO20	-
5/6/2002	1:50	2.22	151	AO20	-
5/6/2002	2:50	16.35	251	AO20	-
5/6/2002	3:50	7.81	351	AO20	-
5/6/2002	4:50	2.49	451	AO20	-
5/6/2002	5:50	2.34	551	AO20	-
5/6/2002	6:50	2.34	651	AO20	-
5/6/2002	7:50	2.55	751	AO20	-
5/6/2002	8:50	2.75	851	AO20	-
6/13/2002	10:50	4.30	1051	AO21	-
6/13/2002	11:50	4.30	1151	AO21	-
6/13/2002	12:50	3.83	1251	AO21	-
6/13/2002	13:50	3.71	1351	AO21	-
6/13/2002	14:50	4.01	1451	AO21	-
6/13/2002	15:50	4.19	1551	AO21	-
6/13/2002	16:50	3.67	1651	AO21	-
6/13/2002	17:50	3.36	1751	AO21	-
6/13/2002	18:50	3.20	1851	AO21	-
6/13/2002	19:50	3.01	1951	AO21	-
6/13/2002	20:50	2.92	2051	AO22	-
6/13/2002	21:50	2.86	2151	AO22	-
6/13/2002	22:50	2.86	2251	AO22	-
6/13/2002	23:50	2.88	2351	AO22	-
6/14/2002	0:50	2.78	51	AO20	-
6/14/2002	1:50	2.83	151	AO20	-
6/14/2002	2:50	2.78	251	AO20	-
6/14/2002	3:50	2.87	351	AO20	-
6/14/2002	4:50	3.11	451	AO20	-
6/14/2002	5:50	3.19	551	AO20	-
6/14/2002	6:50	3.14	651	AO20	-
6/14/2002	7:50	3.09	751	AO20	-
6/14/2002	8:50	2.88	851	AO20	-

6/14/2002	9:50	2.82	951	AO20	-
6/14/2002	10:50	2.88	1051	AO21	-
6/14/2002	11:50	2.83	1151	AO21	-
6/14/2002	12:50	2.93	1251	AO21	-
6/14/2002	13:50	2.75	1351	AO21	-
6/14/2002	14:50	3.12	1451	AO21	-
6/14/2002	15:50	3.33	1551	AO21	-
6/14/2002	16:50	3.11	1651	AO21	-
6/14/2002	17:50	2.87	1751	AO21	-
6/14/2002	18:50	2.91	1851	AO21	-
6/14/2002	19:50	3.00	1951	AO21	-
6/14/2002	20:50	3.00	2051	AO22	-
6/14/2002	21:50	2.81	2151	AO22	-
6/14/2002	22:50	2.64	2251	AO22	-
6/14/2002	23:50	2.58	2351	AO22	-
6/15/2002	0:50	2.55	51	AO20	-
6/15/2002	1:50	2.59	151	AO20	-
6/15/2002	2:50	2.73	251	AO20	-
6/15/2002	3:50	2.77	351	AO20	-
6/15/2002	4:50	2.67	451	AO20	-
6/15/2002	5:50	2.39	551	AO20	-
6/15/2002	6:50	2.50	651	AO20	-
6/15/2002	7:50	2.41	751	AO20	-
6/15/2002	8:50	2.38	851	AO20	-
6/15/2002	9:50	2.45	951	AO20	-
6/15/2002	10:50	2.42	1051	AO21	-
6/15/2002	11:50	2.55	1151	AO21	-
6/15/2002	12:50	2.71	1251	AO21	-
6/15/2002	13:50	3.02	1351	AO21	-
6/15/2002	14:50	3.31	1451	AO21	-
6/15/2002	15:50	3.57	1551	AO21	-
6/15/2002	16:50	3.66	1651	AO21	-
6/15/2002	17:50	3.71	1751	AO21	-
6/15/2002	18:50	3.59	1851	AO21	-
6/15/2002	19:50	4.06	1951	AO21	-
6/15/2002	20:50	4.42	2051	AO22	-
6/15/2002	21:50	3.25	2151	AO22	-
6/15/2002	22:50	2.86	2251	AO22	-
6/15/2002	23:50	2.63	2351	AO22	-
6/16/2002	0:50	2.73	51	AO20	-
6/16/2002	1:50	3.16	151	AO20	-
6/16/2002	2:50	4.13	251	AO20	-
6/16/2002	3:50	3.26	351	AO20	-
6/16/2002	4:50	2.80	451	AO20	-
6/16/2002	5:50	2.84	551	AO20	-
6/16/2002	6:50	3.50	651	AO20	-
6/16/2002	7:50	3.16	751	AO20	-
6/16/2002	8:50	5.35	851	AO20	-
6/16/2002	9:50	3.83	951	AO20	-
6/16/2002	10:50	3.51	1051	AO21	-
6/16/2002	11:50	3.21	1151	AO21	-
6/16/2002	12:50	3.52	1251	AO21	-

6/16/2002	13:50	3.67	1351	AO21	-
6/16/2002	14:50	3.33	1451	AO21	-
6/16/2002	15:50	3.18	1551	AO21	-
6/16/2002	16:50	3.05	1651	AO21	-
6/16/2002	17:50	2.55	1751	AO21	-
6/16/2002	18:50	2.71	1851	AO21	-
6/16/2002	19:50	2.34	1951	AO21	-
6/16/2002	20:50	2.31	2051	AO22	-
6/16/2002	21:50	2.72	2151	AO22	-
6/16/2002	22:50	3.27	2251	AO22	-
6/16/2002	23:50	3.30	2351	AO22	-
6/17/2002	0:50	2.94	51	AO20	-
6/17/2002	1:50	2.82	151	AO20	-
6/17/2002	2:50	2.71	251	AO20	-
6/17/2002	3:50	2.70	351	AO20	-
6/17/2002	4:50	2.72	451	AO20	-
6/17/2002	5:50	6.60	551	AO20	-
6/17/2002	6:50	5.03	651	AO20	-
6/17/2002	7:50	3.80	751	AO20	-
6/17/2002	8:50	4.73	851	AO20	-
6/17/2002	9:50	2.50	951	AO20	-
6/17/2002	10:50	2.54	1051	AO21	-
6/17/2002	11:50	2.64	1151	AO21	-
6/17/2002	12:50	2.74	1251	AO21	-
6/17/2002	13:50	2.72	1351	AO21	-
6/17/2002	14:50	2.64	1451	AO21	-
6/17/2002	15:50	2.49	1551	AO21	-
6/17/2002	16:50	2.39	1651	AO21	-
6/17/2002	17:50	2.38	1751	AO21	-
6/17/2002	18:50	2.32	1851	AO21	-
6/17/2002	19:50	2.21	1951	AO21	-
6/17/2002	20:50	2.67	2051	AO22	-
6/17/2002	21:50	2.78	2151	AO22	-
6/17/2002	22:50	2.80	2251	AO22	-
6/17/2002	23:50	2.76	2351	AO22	-
6/18/2002	0:50	4.53	51	AO20	-
6/18/2002	1:50	3.03	151	AO20	-
6/18/2002	2:50	2.33	251	AO20	-
6/18/2002	3:50	2.51	351	AO20	-
6/18/2002	4:50	2.61	451	AO20	-
6/18/2002	5:50	3.32	551	AO20	-
6/18/2002	6:50	3.98	651	AO20	-
6/18/2002	7:50	4.44	751	AO20	-
6/18/2002	8:50	4.89	851	AO20	-
6/18/2002	9:50	3.68	951	AO20	-
6/18/2002	10:50	4.41	1051	AO21	-
6/18/2002	11:50	4.71	1151	AO21	-
6/18/2002	12:50	3.94	1251	AO21	-
6/18/2002	13:50	4.26	1351	AO21	-
6/18/2002	14:50	4.53	1451	AO21	-
6/18/2002	15:50	3.88	1551	AO21	-
6/18/2002	16:50	3.35	1651	AO21	-

6/18/2002	17:50	3.04	1751	AO21	-
6/18/2002	18:50	2.96	1851	AO21	-
6/18/2002	19:50	2.72	1951	AO21	-
6/18/2002	20:50	2.56	2051	AO22	-
6/18/2002	21:50	2.69	2151	AO22	-
6/18/2002	22:50	3.16	2251	AO22	-
6/18/2002	23:50	2.59	2351	AO22	-
6/19/2002	0:50	2.67	51	AO20	-
6/19/2002	1:50	2.96	151	AO20	-
6/19/2002	2:50	4.28	251	AO20	-
6/19/2002	3:50	4.07	351	AO20	-
6/19/2002	4:50	6.83	451	AO20	-
6/19/2002	5:50	3.82	551	AO20	-
6/19/2002	6:50	3.24	651	AO20	-
6/19/2002	7:50	3.62	751	AO20	-
6/19/2002	8:50	4.54	851	AO20	-
6/19/2002	9:50	4.40	951	AO20	-
6/19/2002	10:50	7.86	1051	AO21	-
6/19/2002	11:50	6.07	1151	AO21	-
6/19/2002	12:50	4.15	1251	AO21	-
6/19/2002	13:50	4.93	1351	AO21	-
6/19/2002	14:50	4.80	1451	AO21	-
6/19/2002	15:50	3.97	1551	AO21	-
6/19/2002	16:50	4.22	1651	AO21	-
6/19/2002	17:50	4.09	1751	AO21	-
6/19/2002	18:50	3.67	1851	AO21	-
6/19/2002	19:50	3.72	1951	AO21	-
6/19/2002	20:50	4.06	2051	AO22	-
6/19/2002	21:50	3.84	2151	AO22	-
6/19/2002	22:50	4.19	2251	AO22	-
6/19/2002	23:50	4.07	2351	AO22	-
6/20/2002	0:50	4.02	51	AO20	-
6/20/2002	1:50	3.52	151	AO20	-
6/20/2002	2:50	4.44	251	AO20	-
6/20/2002	3:50	5.86	351	AO20	-
6/20/2002	4:50	7.26	451	AO20	-
6/20/2002	5:50	9.31	551	AO20	-
6/20/2002	6:50	10.39	651	AO20	-
6/20/2002	7:50	9.50	751	AO20	-
6/20/2002	8:50	6.32	851	AO20	-
6/20/2002	9:50	5.16	951	AO20	-
6/20/2002	10:50	4.95	1051	AO21	-
6/20/2002	11:50	5.14	1151	AO21	-
6/20/2002	12:50	4.89	1251	AO21	-
6/20/2002	13:50	4.86	1351	AO21	-
6/20/2002	14:50	4.98	1451	AO21	-
6/20/2002	15:50	4.73	1551	AO21	-
6/20/2002	16:50	4.26	1651	AO21	-
6/20/2002	17:50	3.73	1751	AO21	-
6/20/2002	18:50	3.38	1851	AO21	-
6/20/2002	19:50	3.06	1951	AO21	-
6/20/2002	20:50	2.97	2051	AO22	-

6/20/2002	21:50	2.79	2151	AO22	-
6/20/2002	22:50	2.70	2251	AO22	-
6/20/2002	23:50	2.83	2351	AO22	-
6/21/2002	0:50	3.20	51	AO20	-
6/21/2002	1:50	3.87	151	AO20	-
6/21/2002	2:50	4.01	251	AO20	-
6/21/2002	3:50	3.65	351	AO20	-
6/21/2002	4:50	4.33	451	AO20	-
6/21/2002	5:50	4.24	551	AO20	-
6/21/2002	6:50	8.94	651	AO20	-
6/21/2002	7:50	6.71	751	AO20	-
6/21/2002	8:50	4.36	851	AO20	-
6/21/2002	9:50	4.22	951	AO20	-
6/21/2002	12:50	3.00	1251	AO21	-
6/21/2002	13:50	3.04	1351	AO21	-
6/21/2002	14:50	2.89	1451	AO21	-
6/21/2002	15:50	2.70	1551	AO21	-
6/21/2002	16:50	2.46	1651	AO21	-
6/21/2002	17:50	2.21	1751	AO21	-
6/21/2002	18:50	2.22	1851	AO21	-
6/21/2002	19:50	2.22	1951	AO21	-
6/21/2002	20:50	1.99	2051	AO22	-
6/21/2002	21:50	1.85	2151	AO22	-
6/21/2002	22:50	1.71	2251	AO22	-
6/21/2002	23:50	1.73	2351	AO22	-
6/22/2002	0:50	2.49	51	AO20	-
6/22/2002	1:50	2.23	151	AO20	-
6/22/2002	2:50	2.30	251	AO20	-
6/22/2002	3:50	2.53	351	AO20	-
6/22/2002	4:50	3.11	451	AO20	-
6/22/2002	5:50	3.73	551	AO20	-
6/22/2002	6:50	7.99	651	AO20	-
6/22/2002	7:50	6.96	751	AO20	-
6/22/2002	8:50	7.01	851	AO20	-
6/22/2002	9:50	4.51	951	AO20	-
6/22/2002	10:50	4.37	1051	AO21	-
6/22/2002	11:50	4.49	1151	AO21	-
6/22/2002	12:50	3.59	1251	AO21	-
6/22/2002	13:50	3.18	1351	AO21	-
6/22/2002	14:50	3.20	1451	AO21	-
6/22/2002	15:50	3.16	1551	AO21	-
6/22/2002	16:50	2.99	1651	AO21	-
6/22/2002	17:50	2.78	1751	AO21	-
6/22/2002	18:50	2.74	1851	AO21	-
6/22/2002	19:50	2.52	1951	AO21	-
6/22/2002	20:50	2.46	2051	AO22	-
6/22/2002	21:50	2.24	2151	AO22	-
6/22/2002	22:50	2.15	2251	AO22	-
6/22/2002	23:50	2.33	2351	AO22	-
6/23/2002	0:50	2.47	51	AO20	-
6/23/2002	1:50	2.31	151	AO20	-
6/23/2002	2:50	2.40	251	AO20	-

6/23/2002	3:50	1.95	351	AO20	-
6/23/2002	4:50	2.20	451	AO20	-
6/23/2002	5:50	6.00	551	AO20	-
6/23/2002	6:50	5.04	651	AO20	-
6/23/2002	7:50	4.75	751	AO20	-
6/23/2002	8:50	4.69	851	AO20	-
6/23/2002	9:50	2.71	951	AO20	-
6/23/2002	10:50	2.65	1051	AO21	-
6/23/2002	11:50	3.01	1151	AO21	-
6/23/2002	12:50	2.87	1251	AO21	-
6/23/2002	13:50	2.70	1351	AO21	-
6/23/2002	14:50	2.73	1451	AO21	-
6/23/2002	15:50	2.63	1551	AO21	-
6/23/2002	16:50	2.44	1651	AO21	-
6/23/2002	17:50	2.24	1751	AO21	-
6/23/2002	18:50	2.10	1851	AO21	-
6/23/2002	19:50	2.06	1951	AO21	-
6/23/2002	20:50	1.94	2051	AO22	-
6/23/2002	21:50	3.10	2151	AO22	-
6/23/2002	22:50	3.32	2251	AO22	-
6/23/2002	23:50	6.41	2351	AO22	-
6/24/2002	0:50	4.78	51	AO20	-
6/24/2002	1:50	3.88	151	AO20	-
6/24/2002	2:50	2.35	251	AO20	-
6/24/2002	3:50	1.96	351	AO20	-
6/24/2002	4:50	2.14	451	AO20	-
6/24/2002	5:50	2.50	551	AO20	-
6/24/2002	6:50	2.80	651	AO20	-
6/24/2002	7:50	2.68	751	AO20	-
6/24/2002	8:50	2.38	851	AO20	-
6/24/2002	9:50	2.53	951	AO20	-
6/24/2002	10:50	2.76	1051	AO21	-
6/24/2002	11:50	2.71	1151	AO21	-
6/24/2002	12:50	2.62	1251	AO21	-
6/24/2002	13:50	2.65	1351	AO21	-
6/24/2002	14:50	2.59	1451	AO21	-
6/24/2002	15:50	2.55	1551	AO21	-
6/24/2002	16:50	2.58	1651	AO21	-
6/24/2002	17:50	2.45	1751	AO21	-
6/24/2002	18:50	2.55	1851	AO21	-
6/24/2002	19:50	2.31	1951	AO21	-
6/24/2002	20:50	2.43	2051	AO22	-
6/24/2002	21:50	3.02	2151	AO22	-
6/24/2002	22:50	3.61	2251	AO22	-
6/24/2002	23:50	3.61	2351	AO22	-
6/25/2002	0:50	4.97	51	AO20	-
6/25/2002	1:50	4.46	151	AO20	-
6/25/2002	2:50	4.55	251	AO20	-
6/25/2002	3:50	3.32	351	AO20	-
6/25/2002	4:50	4.12	451	AO20	-
6/25/2002	5:50	3.76	551	AO20	-
6/25/2002	6:50	4.02	651	AO20	-

6/25/2002	7:50	3.98	751	AO20	-
6/25/2002	8:50	3.26	851	AO20	-
6/25/2002	11:50	2.55	1151	AO21	-
6/25/2002	12:50	2.42	1251	AO21	-
6/25/2002	13:50	2.47	1351	AO21	-
6/25/2002	14:50	2.47	1451	AO21	-
6/25/2002	15:50	2.60	1551	AO21	-
6/25/2002	16:50	2.81	1651	AO21	-
6/25/2002	17:50	2.57	1751	AO21	-
6/25/2002	18:50	2.30	1851	AO21	-
6/25/2002	19:50	2.21	1951	AO21	-
6/25/2002	20:50	2.14	2051	AO22	-
6/25/2002	21:50	2.07	2151	AO22	-
6/25/2002	22:50	2.48	2251	AO22	-
6/25/2002	23:50	2.72	2351	AO22	-
6/26/2002	0:50	2.95	51	AO20	-
6/26/2002	1:50	2.76	151	AO20	-
6/26/2002	2:50	3.39	251	AO20	-
6/26/2002	3:50	4.11	351	AO20	-
6/26/2002	4:50	4.17	451	AO20	-
6/26/2002	5:50	4.11	551	AO20	-
6/26/2002	6:50	4.32	651	AO20	-
6/26/2002	7:50	4.39	751	AO20	-
6/26/2002	8:50	5.71	851	AO20	-
6/26/2002	9:50	4.16	951	AO20	-
6/26/2002	10:50	3.97	1051	AO21	-
6/26/2002	11:50	4.01	1151	AO21	-
6/26/2002	12:50	3.25	1251	AO21	-
6/26/2002	13:50	3.30	1351	AO21	-
6/26/2002	14:50	3.02	1451	AO21	-
6/26/2002	15:50	2.50	1551	AO21	-
6/26/2002	16:50	2.39	1651	AO21	-
6/26/2002	17:50	2.58	1751	AO21	-
6/26/2002	18:50	2.94	1851	AO21	-
6/26/2002	19:50	2.96	1951	AO21	-
6/26/2002	20:50	4.26	2051	AO22	-
6/26/2002	21:50	4.64	2151	AO22	-
6/26/2002	22:50	3.55	2251	AO22	-
6/26/2002	23:50	1.65	2351	AO22	-
6/27/2002	0:50	3.39	51	AO20	-
6/27/2002	1:50	3.53	151	AO20	-
6/27/2002	2:50	2.14	251	AO20	-
6/27/2002	3:50	2.37	351	AO20	-
6/27/2002	4:50	2.35	451	AO20	-
6/27/2002	5:50	1.77	551	AO20	-
6/27/2002	6:50	1.97	651	AO20	-
6/27/2002	7:50	1.98	751	AO20	-
6/27/2002	8:50	1.95	851	AO20	-
6/27/2002	9:50	1.81	951	AO20	-
6/27/2002	10:50	1.86	1051	AO21	-
6/27/2002	11:50	1.89	1151	AO21	-
6/27/2002	12:50	2.06	1251	AO21	-

6/27/2002	13:50	2.10	1351	AO21	-
6/27/2002	14:50	2.59	1451	AO21	-
6/27/2002	15:50	2.27	1551	AO21	-
6/27/2002	16:50	2.41	1651	AO21	-
6/27/2002	17:50	4.24	1751	AO21	-
6/27/2002	18:50	2.46	1851	AO21	-
6/27/2002	19:50	3.67	1951	AO21	-
6/27/2002	20:50	3.04	2051	AO22	-
6/27/2002	21:50	2.39	2151	AO22	-
6/27/2002	22:50	3.86	2251	AO22	-
6/27/2002	23:50	3.13	2351	AO22	-
6/28/2002	0:50	4.74	51	AO20	-
6/28/2002	1:50	3.44	151	AO20	-
6/28/2002	2:50	2.85	251	AO20	-
6/28/2002	3:50	2.73	351	AO20	-
6/28/2002	4:50	3.09	451	AO20	-
6/28/2002	5:50	2.96	551	AO20	-
6/28/2002	6:50	3.17	651	AO20	-
6/28/2002	7:50	3.18	751	AO20	-
6/28/2002	8:50	3.38	851	AO20	-
6/28/2002	9:50	3.34	951	AO20	-
6/28/2002	10:50	3.29	1051	AO21	-
6/28/2002	11:50	2.84	1151	AO21	-
6/28/2002	12:50	2.69	1251	AO21	-
6/28/2002	13:50	2.58	1351	AO21	-
6/28/2002	14:50	2.40	1451	AO21	-
6/28/2002	15:50	2.51	1551	AO21	-
6/28/2002	16:50	2.38	1651	AO21	-
6/28/2002	17:50	2.14	1751	AO21	-
6/28/2002	18:50	1.91	1851	AO21	-
6/28/2002	19:50	1.76	1951	AO21	-
6/28/2002	20:50	1.87	2051	AO22	-
6/28/2002	21:50	2.01	2151	AO22	-
6/28/2002	22:50	2.22	2251	AO22	-
6/28/2002	23:50	2.46	2351	AO22	-
6/29/2002	0:50	2.92	51	AO20	-
6/29/2002	1:50	2.98	151	AO20	-
6/29/2002	2:50	3.61	251	AO20	-
6/29/2002	3:50	2.96	351	AO20	-
6/29/2002	4:50	2.93	451	AO20	-
6/29/2002	5:50	2.45	551	AO20	-
6/29/2002	6:50	2.82	651	AO20	-
6/29/2002	7:50	2.77	751	AO20	-
6/29/2002	8:50	2.81	851	AO20	-
6/29/2002	9:50	2.41	951	AO20	-
6/29/2002	10:50	1.97	1051	AO21	-
6/29/2002	11:50	2.12	1151	AO21	-
6/29/2002	12:50	2.16	1251	AO21	-
6/29/2002	13:50	2.37	1351	AO21	-
6/29/2002	14:50	2.49	1451	AO21	-
6/29/2002	15:50	2.74	1551	AO21	-
6/29/2002	16:50	2.69	1651	AO21	-

6/29/2002	17:50	2.51	1751	AO21	-
6/29/2002	18:50	2.36	1851	AO21	-
6/29/2002	19:50	2.44	1951	AO21	-
6/29/2002	20:50	2.79	2051	AO22	-
6/29/2002	21:50	2.43	2151	AO22	-
6/29/2002	22:50	2.28	2251	AO22	-
6/29/2002	23:50	2.30	2351	AO22	-
6/30/2002	0:50	2.40	51	AO20	-
6/30/2002	1:50	3.88	151	AO20	-
6/30/2002	2:50	25.64	251	AO20	-
6/30/2002	3:50	14.58	351	AO20	-
6/30/2002	4:50	6.11	451	AO20	-
6/30/2002	5:50	4.21	551	AO20	-
6/30/2002	6:50	4.11	651	AO20	-
6/30/2002	7:50	3.58	751	AO20	-
6/30/2002	8:50	2.53	851	AO20	-
6/30/2002	9:50	2.39	951	AO20	-
6/30/2002	10:50	2.70	1051	AO21	-
6/30/2002	11:50	3.74	1151	AO21	-
6/30/2002	12:50	3.14	1251	AO21	-
6/30/2002	13:50	3.17	1351	AO21	-
6/30/2002	14:50	2.75	1451	AO21	-
6/30/2002	15:50	2.69	1551	AO21	-
6/30/2002	16:50	2.30	1651	AO21	-
6/30/2002	17:50	2.26	1751	AO21	-
6/30/2002	18:50	2.21	1851	AO21	-
6/30/2002	19:50	2.10	1951	AO21	-
6/30/2002	20:50	1.94	2051	AO22	-
6/30/2002	21:50	1.75	2151	AO22	-
6/30/2002	22:50	1.71	2251	AO22	-
6/30/2002	23:50	1.59	2351	AO22	-
7/1/2002	0:50	2.11	51	AO20	-
7/1/2002	1:50	2.34	151	AO20	-
7/1/2002	2:50	2.12	251	AO20	-
7/1/2002	3:50	2.07	351	AO20	-
7/1/2002	4:50	2.02	451	AO20	-
7/1/2002	5:50	2.05	551	AO20	-
7/1/2002	6:50	2.70	651	AO20	-
7/1/2002	7:50	2.73	751	AO20	-
7/1/2002	8:50	2.27	851	AO20	-
7/1/2002	9:50	2.20	951	AO20	-
7/1/2002	10:50	2.24	1051	AO21	-
7/1/2002	11:50	2.19	1151	AO21	-
7/1/2002	12:50	2.29	1251	AO21	-
7/1/2002	13:50	2.04	1351	AO21	-
7/1/2002	14:50	1.96	1451	AO21	-
7/1/2002	15:50	1.83	1551	AO21	-
7/1/2002	16:50	1.92	1651	AO21	-
7/1/2002	17:50	1.88	1751	AO21	-
7/1/2002	18:50	1.85	1851	AO21	-
7/1/2002	19:50	2.00	1951	AO21	-
7/1/2002	20:50	2.64	2051	AO22	-

7/1/2002	21:50	4.67	2151	AO22	-
7/1/2002	22:50	2.48	2251	AO22	-
7/1/2002	23:50	2.06	2351	AO22	-
7/2/2002	0:50	1.93	51	AO20	-
7/2/2002	1:50	2.20	151	AO20	-
7/2/2002	2:50	3.18	251	AO20	-
7/2/2002	3:50	3.15	351	AO20	-
7/2/2002	4:50	4.74	451	AO20	-
7/2/2002	5:50	2.70	551	AO20	-
7/2/2002	6:50	2.94	651	AO20	-
7/2/2002	7:50	3.14	751	AO20	-
7/2/2002	8:50	3.39	851	AO20	-
7/2/2002	9:50	3.34	951	AO20	-
7/2/2002	10:50	2.89	1051	AO21	-
7/2/2002	11:50	2.77	1151	AO21	-
7/2/2002	12:50	3.27	1251	AO21	-
7/2/2002	13:50	3.14	1351	AO21	-
7/2/2002	14:50	3.00	1451	AO21	-
7/2/2002	15:50	2.67	1551	AO21	-
7/2/2002	16:50	2.38	1651	AO21	-
7/2/2002	17:50	2.16	1751	AO21	-
7/2/2002	18:50	2.16	1851	AO21	-
7/2/2002	19:50	2.13	1951	AO21	-
7/2/2002	20:50	2.25	2051	AO22	-
7/2/2002	21:50	2.14	2151	AO22	-
7/2/2002	22:50	2.17	2251	AO22	-
7/2/2002	23:50	2.35	2351	AO22	-
7/3/2002	0:50	2.87	51	AO20	-
7/3/2002	1:50	2.21	151	AO20	-
7/3/2002	2:50	2.48	251	AO20	-
7/3/2002	3:50	2.74	351	AO20	-
7/3/2002	4:50	3.26	451	AO20	-
7/3/2002	5:50	3.68	551	AO20	-
7/3/2002	6:50	3.82	651	AO20	-
7/3/2002	7:50	3.54	751	AO20	-
7/3/2002	8:50	2.82	851	AO20	-
7/3/2002	11:50	3.08	1151	AO21	-
7/3/2002	12:50	3.02	1251	AO21	-
7/3/2002	13:50	2.85	1351	AO21	-
7/3/2002	14:50	2.55	1451	AO21	-
7/3/2002	15:50	2.50	1551	AO21	-
7/3/2002	16:50	2.21	1651	AO21	-
7/3/2002	17:50	1.96	1751	AO21	-
7/3/2002	18:50	1.80	1851	AO21	-
7/3/2002	19:50	1.87	1951	AO21	-
7/3/2002	20:50	1.94	2051	AO22	-
7/3/2002	21:50	1.82	2151	AO22	-
7/3/2002	22:50	2.03	2251	AO22	-
7/3/2002	23:50	2.23	2351	AO22	-
7/4/2002	0:50	2.43	51	AO20	-
7/4/2002	1:50	2.31	151	AO20	-
7/4/2002	2:50	3.97	251	AO20	-

7/4/2002	3:50	5.81	351	AO20	-
7/4/2002	4:50	3.43	451	AO20	-
7/4/2002	5:50	2.61	551	AO20	-
7/4/2002	6:50	2.43	651	AO20	-
7/4/2002	7:50	2.36	751	AO20	-
7/4/2002	8:50	2.42	851	AO20	-
7/4/2002	9:50	2.40	951	AO20	-
7/4/2002	10:50	2.42	1051	AO21	-
7/4/2002	11:50	2.30	1151	AO21	-
7/4/2002	12:50	2.23	1251	AO21	-
7/4/2002	13:50	2.13	1351	AO21	-
7/4/2002	14:50	2.20	1451	AO21	-
7/4/2002	15:50	2.10	1551	AO21	-
7/4/2002	16:50	1.90	1651	AO21	-
7/4/2002	17:50	1.86	1751	AO21	-
7/4/2002	18:50	1.84	1851	AO21	-
7/4/2002	19:50	1.86	1951	AO21	-
7/4/2002	20:50	1.87	2051	AO22	-
7/4/2002	21:50	1.71	2151	AO22	-
7/4/2002	22:50	1.75	2251	AO22	-
7/4/2002	23:50	1.86	2351	AO22	-
7/5/2002	0:50	1.96	51	AO20	-
7/5/2002	1:50	2.17	151	AO20	-
7/5/2002	2:50	2.35	251	AO20	-
7/5/2002	3:50	2.74	351	AO20	-
7/5/2002	4:50	2.38	451	AO20	-
7/5/2002	5:50	2.37	551	AO20	-
7/5/2002	6:50	2.17	651	AO20	-
7/5/2002	7:50	2.00	751	AO20	-
7/5/2002	8:50	2.11	851	AO20	-
7/5/2002	9:50	2.06	951	AO20	-
7/5/2002	10:50	2.03	1051	AO21	-
7/5/2002	11:50	1.96	1151	AO21	-
7/5/2002	12:50	1.93	1251	AO21	-
7/5/2002	13:50	2.05	1351	AO21	-
7/5/2002	14:50	2.15	1451	AO21	-
7/5/2002	15:50	2.14	1551	AO21	-
7/5/2002	16:50	2.07	1651	AO21	-
7/5/2002	17:50	1.84	1751	AO21	-
7/5/2002	18:50	1.90	1851	AO21	-
7/5/2002	19:50	1.75	1951	AO21	-
7/5/2002	20:50	1.81	2051	AO22	-
7/5/2002	21:50	1.78	2151	AO22	-
7/5/2002	22:50	1.83	2251	AO22	-
7/5/2002	23:50	1.93	2351	AO22	-
7/6/2002	0:50	2.13	51	AO20	-
7/6/2002	1:50	2.06	151	AO20	-
7/6/2002	2:50	2.05	251	AO20	-
7/6/2002	3:50	1.96	351	AO20	-
7/6/2002	4:50	2.00	451	AO20	-
7/6/2002	5:50	2.15	551	AO20	-
7/6/2002	6:50	2.14	651	AO20	-

7/6/2002	7:50	2.20	751	AO20	-
7/6/2002	8:50	2.22	851	AO20	-
7/6/2002	9:50	2.27	951	AO20	-
7/6/2002	10:50	2.25	1051	AO21	-
7/6/2002	11:50	2.34	1151	AO21	-
7/6/2002	12:50	2.24	1251	AO21	-
7/6/2002	13:50	2.24	1351	AO21	-
7/6/2002	14:50	2.12	1451	AO21	-
7/6/2002	15:50	2.04	1551	AO21	-
7/6/2002	16:50	2.05	1651	AO21	-
7/6/2002	17:50	1.99	1751	AO21	-
7/6/2002	18:50	1.92	1851	AO21	-
7/6/2002	19:50	1.95	1951	AO21	-
7/6/2002	20:50	1.93	2051	AO22	-
7/6/2002	21:50	1.75	2151	AO22	-
7/6/2002	22:50	1.81	2251	AO22	-
7/6/2002	23:50	1.78	2351	AO22	-
7/7/2002	0:50	1.88	51	AO20	-
7/7/2002	1:50	1.87	151	AO20	-
7/7/2002	2:50	1.88	251	AO20	-
7/7/2002	3:50	1.82	351	AO20	-
7/7/2002	4:50	1.84	451	AO20	-
7/7/2002	5:50	1.87	551	AO20	-
7/7/2002	6:50	1.93	651	AO20	-
7/7/2002	7:50	1.94	751	AO20	-
7/7/2002	8:50	1.97	851	AO20	-
7/7/2002	9:50	1.98	951	AO20	-
7/7/2002	10:50	2.15	1051	AO21	-
7/7/2002	11:50	2.21	1151	AO21	-
7/7/2002	12:50	2.35	1251	AO21	-
7/7/2002	13:50	2.45	1351	AO21	-
7/7/2002	14:50	2.42	1451	AO21	-
7/7/2002	15:50	2.27	1551	AO21	-
7/7/2002	16:50	2.19	1651	AO21	-
7/7/2002	17:50	2.09	1751	AO21	-
7/7/2002	18:50	2.02	1851	AO21	-
7/7/2002	19:50	1.91	1951	AO21	-
7/7/2002	20:50	1.91	2051	AO22	-
7/7/2002	21:50	1.89	2151	AO22	-
7/7/2002	22:50	1.87	2251	AO22	-
7/7/2002	23:50	1.87	2351	AO22	-
7/8/2002	0:50	2.98	51	AO20	-
7/8/2002	1:50	8.66	151	AO20	-
7/8/2002	2:50	10.38	251	AO20	-
7/8/2002	3:50	12.66	351	AO20	-
7/8/2002	4:50	8.09	451	AO20	-
7/8/2002	5:50	5.40	551	AO20	-
7/8/2002	6:50	10.50	651	AO20	-
7/8/2002	7:50	5.67	751	AO20	-
7/8/2002	8:50	4.39	851	AO20	-
7/8/2002	9:50	2.89	951	AO20	-
7/8/2002	10:50	1.68	1051	AO21	-

7/8/2002	11:50	2.00	1151	AO21	-
7/8/2002	12:50	2.25	1251	AO21	-
7/8/2002	13:50	2.19	1351	AO21	-
7/8/2002	14:50	2.22	1451	AO21	-
7/8/2002	15:50	2.17	1551	AO21	-
7/8/2002	16:50	2.09	1651	AO21	-
7/8/2002	17:50	1.98	1751	AO21	-
7/8/2002	18:50	1.89	1851	AO21	-
7/8/2002	19:50	1.80	1951	AO21	-
7/8/2002	20:50	2.15	2051	AO22	-
7/8/2002	21:50	8.58	2151	AO22	-
7/8/2002	22:50	2.57	2251	AO22	-
7/8/2002	23:50	2.46	2351	AO22	-
7/9/2002	0:50	2.43	51	AO20	-
7/9/2002	1:50	2.45	151	AO20	-
7/9/2002	2:50	2.76	251	AO20	-
7/9/2002	3:50	4.24	351	AO20	-
7/9/2002	4:50	4.59	451	AO20	-
7/9/2002	5:50	2.19	551	AO20	-
7/9/2002	6:50	5.13	651	AO20	-
7/9/2002	7:50	7.94	751	AO20	-
7/9/2002	8:50	3.30	851	AO20	-
7/9/2002	9:50	2.08	951	AO20	-
7/9/2002	10:50	2.19	1051	AO21	-
7/9/2002	11:50	2.23	1151	AO21	-
7/9/2002	12:50	2.34	1251	AO21	-
7/9/2002	13:50	2.39	1351	AO21	-
7/9/2002	14:50	2.23	1451	AO21	-
7/9/2002	15:50	2.13	1551	AO21	-
7/9/2002	16:50	2.02	1651	AO21	-
7/9/2002	17:50	2.06	1751	AO21	-
7/9/2002	18:50	2.95	1851	AO21	-
7/9/2002	19:50	2.17	1951	AO21	-
7/9/2002	20:50	2.39	2051	AO22	-
7/9/2002	21:50	2.59	2151	AO22	-
7/9/2002	22:50	3.26	2251	AO22	-
7/9/2002	23:50	3.91	2351	AO22	-
7/10/2002	0:50	3.19	51	AO20	-
7/10/2002	1:50	7.48	151	AO20	-
7/10/2002	2:50	4.77	251	AO20	-
7/10/2002	3:50	3.65	351	AO20	-
7/10/2002	4:50	4.56	451	AO20	-
7/10/2002	5:50	3.96	551	AO20	-
7/10/2002	6:50	4.50	651	AO20	-
7/10/2002	7:50	3.53	751	AO20	-
7/10/2002	8:50	2.88	851	AO20	-
7/10/2002	9:50	2.51	951	AO20	-
7/10/2002	10:50	2.59	1051	AO21	-
10/7/2002	12:50	1.89	1251	AO21	-
10/7/2002	13:50	1.83	1351	AO21	-
10/7/2002	14:50	1.86	1451	AO21	-
10/7/2002	15:50	2.33	1551	AO21	-

10/7/2002	16:50	2.27	1651	AO21	-
10/7/2002	17:50	2.10	1751	AO21	-
10/7/2002	18:50	2.14	1851	AO21	-
10/7/2002	19:50	1.99	1951	AO21	-
10/7/2002	20:50	2.04	2051	AO22	-
10/7/2002	21:50	2.03	2151	AO22	-
10/7/2002	22:50	2.06	2251	AO22	-
10/7/2002	23:50	2.02	2351	AO22	-
10/8/2002	0:50	2.11	0051	AO20	-
10/8/2002	1:50	2.10	0151	AO20	-
10/8/2002	2:50	1.94	0251	AO20	-
10/8/2002	3:50	2.00	0351	AO20	-
10/8/2002	4:50	2.16	0451	AO20	-
10/8/2002	5:50	2.12	0551	AO20	-
10/8/2002	6:50	1.97	0651	AO20	-
10/8/2002	7:50	2.16	0751	AO20	-
10/8/2002	12:50	1.39	1251	AO21	-
10/8/2002	13:50	1.91	1351	AO21	-
10/8/2002	14:50	2.09	1451	AO21	-
10/8/2002	15:50	2.19	1551	AO21	-
10/8/2002	16:50	2.17	1651	AO21	-
10/8/2002	17:50	2.21	1751	AO21	-
10/8/2002	18:50	2.29	1851	AO21	-
10/8/2002	19:50	2.22	1951	AO21	-
10/8/2002	20:50	2.17	2051	AO22	-
10/8/2002	21:50	2.13	2151	AO22	-
10/8/2002	22:50	2.15	2251	AO22	-
10/8/2002	23:50	1.94	2351	AO22	-
10/9/2002	0:50	4.19	0051	AO20	-
10/9/2002	1:50	3.92	0151	AO20	-
10/9/2002	2:50	2.83	0251	AO20	-
10/9/2002	3:50	2.27	0351	AO20	-
10/9/2002	4:50	2.38	0451	AO20	-
10/9/2002	5:50	2.39	0551	AO20	-
10/9/2002	6:50	2.52	0651	AO20	-
10/9/2002	7:50	3.56	0751	AO20	-
10/9/2002	8:50	2.32	0851	AO20	-
10/9/2002	9:50	2.09	0951	AO20	-
10/9/2002	10:50	2.24	1051	AO21	-
10/9/2002	11:50	1.71	1151	AO21	-
10/9/2002	12:50	1.55	1251	AO21	-
10/9/2002	13:50	1.62	1351	AO21	-
10/9/2002	14:50	1.68	1451	AO21	-
10/9/2002	15:50	1.70	1551	AO21	-
10/9/2002	16:50	1.71	1651	AO21	-
10/9/2002	17:50	1.68	1751	AO21	-
10/9/2002	18:50	1.63	1851	AO21	-
10/9/2002	19:50	1.52	1951	AO21	-
10/9/2002	20:50	1.53	2051	AO22	-
10/9/2002	21:50	1.53	2151	AO22	-
10/9/2002	22:50	1.53	2251	AO22	-
10/9/2002	23:50	1.55	2351	AO22	-

10/10/2002	0:50	1.64	0051	AO20	-
10/10/2002	1:50	1.70	0151	AO20	-
10/10/2002	2:50	1.77	0251	AO20	-
10/10/2002	3:50	1.83	0351	AO20	-
10/10/2002	4:50	1.86	0451	AO20	-
10/10/2002	5:50	1.80	0551	AO20	-
10/10/2002	6:50	1.81	0651	AO20	-
10/10/2002	7:50	1.94	0751	AO20	-
10/10/2002	8:50	1.93	0851	AO20	-
10/10/2002	9:50	1.66	0951	AO20	-
10/10/2002	10:50	1.66	1051	AO21	-
10/10/2002	11:50	1.71	1151	AO21	-
10/10/2002	12:50	1.78	1251	AO21	-
10/10/2002	13:50	1.76	1351	AO21	-
10/10/2002	14:50	1.71	1451	AO21	-
10/10/2002	15:50	1.68	1551	AO21	-
10/10/2002	16:50	1.68	1651	AO21	-
10/10/2002	17:50	1.67	1751	AO21	-
10/10/2002	18:50	1.66	1851	AO21	-
10/10/2002	19:50	1.68	1951	AO21	-
10/10/2002	20:50	1.63	2051	AO22	-
10/10/2002	21:50	1.76	2151	AO22	-
10/10/2002	22:50	1.86	2251	AO22	-
10/10/2002	23:50	2.30	2351	AO22	-
10/11/2002	0:50	2.06	0051	AO20	-
10/11/2002	1:50	1.92	0151	AO20	-
10/11/2002	2:50	2.08	0251	AO20	-
10/11/2002	3:50	2.09	0351	AO20	-
10/11/2002	4:50	1.87	0451	AO20	-
10/11/2002	5:50	1.77	0551	AO20	-
10/11/2002	6:50	1.69	0651	AO20	-
10/11/2002	7:50	1.83	0751	AO20	-
10/11/2002	8:50	2.15	0851	AO20	-
10/11/2002	9:50	2.04	0951	AO20	-
10/11/2002	10:50	2.03	1051	AO21	-
10/11/2002	11:50	2.22	1151	AO21	-
10/11/2002	12:50	1.97	1251	AO21	-
10/11/2002	13:50	1.78	1351	AO21	-
10/11/2002	14:50	1.96	1451	AO21	-
10/11/2002	15:50	1.86	1551	AO21	-
10/11/2002	16:50	2.53	1651	AO21	-
10/11/2002	17:50	2.13	1751	AO21	-
10/11/2002	18:50	1.98	1851	AO21	-
10/11/2002	19:50	1.85	1951	AO21	-
10/11/2002	20:50	1.95	2051	AO22	-
10/11/2002	21:50	1.96	2151	AO22	-
10/11/2002	22:50	2.09	2251	AO22	-
10/11/2002	23:50	1.90	2351	AO22	-
10/12/2002	0:50	2.25	0051	AO20	-
10/12/2002	1:50	2.33	0151	AO20	-
10/12/2002	2:50	2.64	0251	AO20	-
10/12/2002	3:50	2.91	0351	AO20	-

10/12/2002	4:50	3.05	0451	AO20	-
10/12/2002	5:50	2.85	0551	AO20	-
10/12/2002	6:50	2.64	0651	AO20	-
10/12/2002	7:50	2.49	0751	AO20	-
10/12/2002	8:50	2.38	0851	AO20	-
10/12/2002	9:50	2.27	0951	AO20	-
10/12/2002	10:50	2.12	1051	AO21	-
10/12/2002	11:50	1.96	1151	AO21	-
10/12/2002	12:50	2.06	1251	AO21	-
10/12/2002	13:50	2.15	1351	AO21	-
10/12/2002	14:50	2.05	1451	AO21	-
10/12/2002	15:50	2.06	1551	AO21	-
10/12/2002	16:50	2.05	1651	AO21	-
10/12/2002	17:50	2.05	1751	AO21	-
10/12/2002	18:50	1.91	1851	AO21	-
10/12/2002	19:50	1.76	1951	AO21	-
10/12/2002	20:50	1.62	2051	AO22	-
10/12/2002	21:50	1.59	2151	AO22	-
10/12/2002	22:50	1.74	2251	AO22	-
10/12/2002	23:50	1.87	2351	AO22	-
10/13/2002	0:50	1.80	0051	AO20	-
10/13/2002	1:50	1.88	0151	AO20	-
10/13/2002	2:50	1.92	0251	AO20	-
10/13/2002	3:50	1.94	0351	AO20	-
10/13/2002	4:50	1.99	0451	AO20	-
10/13/2002	5:50	1.94	0551	AO20	-
10/13/2002	6:50	1.92	0651	AO20	-
10/13/2002	7:50	1.96	0751	AO20	-
10/13/2002	8:50	2.02	0851	AO20	-
10/13/2002	9:50	2.07	0951	AO20	-
10/13/2002	10:50	3.22	1051	AO21	-
10/13/2002	11:50	2.97	1151	AO21	-
10/13/2002	12:50	2.14	1251	AO21	-
10/13/2002	13:50	2.27	1351	AO21	-
10/13/2002	14:50	2.74	1451	AO21	-
10/13/2002	15:50	2.58	1551	AO21	-
10/13/2002	16:50	3.00	1651	AO21	-
10/13/2002	17:50	2.85	1751	AO21	-
10/13/2002	18:50	2.51	1851	AO21	-
10/13/2002	19:50	2.52	1951	AO21	-
10/13/2002	20:50	2.44	2051	AO22	-
10/13/2002	21:50	2.50	2151	AO22	-
10/13/2002	22:50	1.86	2251	AO22	-
10/13/2002	23:50	1.65	2351	AO22	-
10/14/2002	0:50	1.70	0051	AO20	-
10/14/2002	1:50	1.72	0151	AO20	-
10/14/2002	2:50	1.83	0251	AO20	-
10/14/2002	3:50	1.65	0351	AO20	-
10/14/2002	4:50	1.65	0451	AO20	-
10/14/2002	5:50	1.55	0551	AO20	-
10/14/2002	6:50	1.50	0651	AO20	-
10/15/2002	10:50	1.76	1051	AO21	-

10/15/2002	12:25	1.36	1251	AO21	-
10/15/2002	13:25	1.44	1351	AO21	-
10/15/2002	14:25	1.47	1451	AO21	-
10/15/2002	15:25	1.46	1551	AO21	-
10/15/2002	16:25	1.51	1651	AO21	-
10/15/2002	17:25	1.53	1751	AO21	-
10/15/2002	18:25	1.53	1851	AO21	-
10/15/2002	19:25	1.52	1951	AO21	-
10/15/2002	20:25	1.77	2051	AO22	-
10/15/2002	21:25	1.81	2151	AO22	-
10/15/2002	22:25	2.01	2251	AO22	-
10/15/2002	23:25	2.04	2351	AO22	-
10/16/2002	0:25	1.74	0051	AO20	-
10/16/2002	1:25	1.58	0151	AO20	-
10/16/2002	2:25	1.77	0251	AO20	-
10/16/2002	3:25	1.69	0351	AO20	-
10/16/2002	4:25	1.61	0451	AO20	-
10/16/2002	5:25	1.56	0551	AO20	-
10/16/2002	6:25	1.63	0651	AO20	-
10/16/2002	7:25	1.75	0751	AO20	-
10/16/2002	8:25	1.70	0851	AO20	-
10/16/2002	9:25	1.63	0951	AO20	-
10/16/2002	10:25	1.47	1051	AO21	-
10/16/2002	12:00	1.45	1151	AO21	-
10/16/2002	13:00	1.53	1251	AO21	-
10/16/2002	14:00	1.55	1351	AO21	-
10/16/2002	15:00	1.50	1451	AO21	-
10/16/2002	16:00	1.71	1551	AO21	-
10/16/2002	17:00	1.64	1651	AO21	-
10/16/2002	18:00	1.45	1751	AO21	-
10/16/2002	19:00	1.27	1851	AO21	-
10/16/2002	20:00	1.31	1951	AO21	-
10/16/2002	21:00	1.39	2051	AO22	-
10/16/2002	22:00	1.26	2151	AO22	-
10/16/2002	23:00	1.29	2251	AO22	-
10/17/2002	0:00	1.29	2351	AO22	-
10/17/2002	1:00	1.38	0051	AO20	-
10/17/2002	2:00	1.59	0151	AO20	-
10/17/2002	3:00	1.48	0251	AO20	-
10/17/2002	4:00	1.52	0351	AO20	-
10/17/2002	5:00	1.46	0451	AO20	-
10/17/2002	6:00	1.61	0551	AO20	-
10/17/2002	7:00	1.66	0651	AO20	-
10/17/2002	8:00	2.03	0751	AO20	-
10/17/2002	9:00	1.89	0851	AO20	-
10/17/2002	10:00	1.70	0951	AO20	-
10/17/2002	11:00	1.73	1051	AO21	-
10/17/2002	12:35	1.76	1251	AO21	-
10/17/2002	13:35	2.03	1351	AO21	-
10/17/2002	14:35	2.22	1451	AO21	-
10/17/2002	15:35	2.35	1551	AO21	-
10/17/2002	16:35	2.16	1651	AO21	-

10/17/2002	17:35	2.11	1751	AO21	-
10/17/2002	18:35	2.15	1851	AO21	-
10/17/2002	19:35	2.29	1951	AO21	-
10/17/2002	20:35	1.82	2051	AO22	-
10/17/2002	21:35	1.45	2151	AO22	-
10/17/2002	22:35	1.89	2251	AO22	-
10/17/2002	23:35	1.85	2351	AO22	-
10/18/2002	0:35	1.88	0051	AO20	-
10/18/2002	1:35	1.86	0151	AO20	-
10/18/2002	2:35	1.76	0251	AO20	-
10/18/2002	3:35	2.11	0351	AO20	-
10/18/2002	4:35	1.59	0451	AO20	-
10/18/2002	5:35	1.51	0551	AO20	-
10/18/2002	6:35	1.59	0651	AO20	-
10/18/2002	7:35	1.72	0751	AO20	-
10/18/2002	8:35	1.71	0851	AO20	-
10/18/2002	9:35	1.61	0951	AO20	-
10/18/2002	10:35	1.63	1051	AO21	-
10/18/2002	12:10	1.62	1151	AO21	-
10/18/2002	13:10	1.77	1251	AO21	-
10/18/2002	14:10	1.77	1351	AO21	-
10/18/2002	15:10	1.81	1451	AO21	-
10/18/2002	16:10	1.74	1551	AO21	-
10/18/2002	17:10	1.71	1651	AO21	-
10/18/2002	18:10	1.91	1751	AO21	-
10/18/2002	19:10	1.81	1851	AO21	-
10/18/2002	20:10	1.81	1951	AO21	-
10/18/2002	21:10	2.17	2051	AO22	-
10/18/2002	22:10	1.90	2151	AO22	-
10/18/2002	23:10	2.42	2251	AO22	-
10/19/2002	0:10	2.73	2351	AO22	-
10/19/2002	1:10	2.39	0051	AO20	-
10/19/2002	2:10	2.27	0151	AO20	-
10/19/2002	3:10	1.85	0251	AO20	-
10/19/2002	4:10	1.79	0351	AO20	-
10/19/2002	5:10	1.71	0451	AO20	-
10/19/2002	6:10	2.22	0551	AO20	-
10/19/2002	7:10	1.60	0651	AO20	-
10/19/2002	8:10	1.58	0751	AO20	-
10/19/2002	9:10	1.48	0851	AO20	-
10/19/2002	10:10	1.52	0951	AO20	-
10/19/2002	11:45	1.51	1151	AO21	-
10/19/2002	12:45	1.49	1251	AO21	-
10/19/2002	13:45	1.54	1351	AO21	-
10/19/2002	14:45	1.58	1451	AO21	-
10/19/2002	15:45	1.79	1551	AO21	-
10/19/2002	16:45	1.89	1651	AO21	-
10/19/2002	17:45	1.68	1751	AO21	-
10/19/2002	18:45	1.52	1851	AO21	-
10/19/2002	19:45	1.44	1951	AO21	-
10/19/2002	20:45	1.41	2051	AO22	-
10/19/2002	21:45	1.42	2151	AO22	-

10/19/2002	22:45	2.12	2251	AO22	-
10/19/2002	23:45	1.56	2351	AO22	-
10/20/2002	0:45	1.58	0051	AO20	-
10/20/2002	1:45	1.57	0151	AO20	-
10/20/2002	2:45	1.59	0251	AO20	-
10/20/2002	3:45	1.51	0351	AO20	-
10/20/2002	4:45	1.56	0451	AO20	-
10/20/2002	5:45	1.57	0551	AO20	-
10/20/2002	6:45	1.59	0651	AO20	-
10/20/2002	7:45	1.58	0751	AO20	-
10/20/2002	8:45	1.59	0851	AO20	-
10/20/2002	9:45	1.51	0951	AO20	-
10/20/2002	10:45	1.58	1051	AO21	-
10/20/2002	12:20	1.60	1251	AO21	-
10/20/2002	13:20	1.66	1351	AO21	-
10/20/2002	14:20	1.73	1451	AO21	-
10/20/2002	15:20	1.80	1551	AO21	-
10/20/2002	16:20	1.85	1651	AO21	-
10/20/2002	17:20	1.76	1751	AO21	-
10/20/2002	18:20	1.89	1851	AO21	-
10/20/2002	19:20	2.00	1951	AO21	-
10/20/2002	20:20	2.39	2051	AO22	-
10/20/2002	21:20	2.11	2151	AO22	-
10/20/2002	22:20	1.50	2251	AO22	-
10/20/2002	23:20	1.71	2351	AO22	-
10/21/2002	0:20	1.77	0051	AO20	-
10/21/2002	1:20	2.07	0151	AO20	-
10/21/2002	2:20	2.78	0251	AO20	-
10/21/2002	3:20	2.80	0351	AO20	-
10/21/2002	4:20	2.83	0451	AO20	-
10/21/2002	5:20	3.09	0551	AO20	-
10/21/2002	6:20	4.53	0651	AO20	-
10/21/2002	7:20	1.51	0751	AO20	-
10/21/2002	8:20	1.44	0851	AO20	-
10/21/2002	9:20	1.38	0951	AO20	-
10/21/2002	10:20	1.51	1051	AO21	-
10/21/2002	11:55	1.54	1151	AO21	-
10/21/2002	12:55	1.63	1251	AO21	-
10/21/2002	13:55	1.67	1351	AO21	-
10/21/2002	14:55	1.71	1451	AO21	-
10/21/2002	15:55	1.59	1551	AO21	-
10/21/2002	16:55	1.62	1651	AO21	-
10/21/2002	17:55	1.65	1751	AO21	-
10/21/2002	18:55	1.53	1851	AO21	-
10/21/2002	19:55	1.62	1951	AO21	-
10/21/2002	20:55	1.80	2051	AO22	-
10/21/2002	21:55	1.88	2151	AO22	-
10/21/2002	22:55	1.69	2251	AO22	-
10/21/2002	23:55	2.75	2351	AO22	-
10/22/2002	0:55	1.63	0051	AO20	-
10/22/2002	1:55	1.49	0151	AO20	-
10/22/2002	2:55	1.62	0251	AO20	-

10/22/2002	3:55	1.66	0351	AO20	-
10/22/2002	4:55	1.72	0451	AO20	-
10/22/2002	5:55	1.68	0551	AO20	-
10/22/2002	6:55	1.56	0651	AO20	-
10/22/2002	7:55	1.77	0751	AO20	-
10/23/2002	11:00	1.51	1051	AO21	-
10/23/2002	12:35	1.16	1251	AO21	-
10/23/2002	13:35	1.07	1351	AO21	-
10/23/2002	14:35	1.03	1451	AO21	-
10/23/2002	15:35	1.01	1551	AO21	-
10/23/2002	16:35	1.06	1651	AO21	-
10/23/2002	17:35	1.30	1751	AO21	-
10/23/2002	18:35	1.18	1851	AO21	-
10/23/2002	19:35	0.86	1951	AO21	-
10/23/2002	20:35	0.91	2051	AO22	-
10/23/2002	21:35	1.13	2151	AO22	-
10/23/2002	22:35	1.17	2251	AO22	-
10/23/2002	23:35	1.02	2351	AO22	-
10/24/2002	0:35	1.08	0051	AO20	-
10/24/2002	1:35	1.15	0151	AO20	-
10/24/2002	2:35	1.36	0251	AO20	-
10/24/2002	3:35	1.03	0351	AO20	-
10/24/2002	4:35	3.24	0451	AO20	-
10/24/2002	5:35	2.58	0551	AO20	-
10/24/2002	6:35	1.53	0651	AO20	-
10/24/2002	7:35	1.64	0751	AO20	-
10/24/2002	8:35	1.58	0851	AO20	-
10/24/2002	9:35	1.48	0951	AO20	-
10/24/2002	10:35	1.08	1051	AO21	-
10/24/2002	11:35	0.98	1151	AO21	-
10/24/2002	12:35	1.04	1251	AO21	-
10/24/2002	13:35	1.08	1351	AO21	-
10/24/2002	14:35	1.17	1451	AO21	-
10/24/2002	15:35	1.21	1551	AO21	-
10/24/2002	16:35	1.24	1651	AO21	-
10/24/2002	17:35	1.39	1751	AO21	-
10/24/2002	18:35	1.55	1851	AO21	-
10/24/2002	19:35	1.52	1951	AO21	-
10/24/2002	20:35	1.43	2051	AO22	-
10/24/2002	21:35	1.38	2151	AO22	-
10/24/2002	22:35	1.45	2251	AO22	-
10/24/2002	23:35	1.23	2351	AO22	-
10/25/2002	0:35	1.22	0051	AO20	-
10/25/2002	1:35	1.67	0151	AO20	-
10/25/2002	2:35	1.51	0251	AO20	-
10/25/2002	3:35	1.60	0351	AO20	-
10/25/2002	4:35	1.82	0451	AO20	-
10/25/2002	5:35	1.73	0551	AO20	-
10/25/2002	6:35	1.48	0651	AO20	-
10/25/2002	7:35	1.39	0751	AO20	-
10/25/2002	8:35	1.42	0851	AO20	-
10/25/2002	9:35	1.42	0951	AO20	-

10/25/2002	10:35	1.50	1051	AO21	-
10/25/2002	11:35	1.60	1151	AO21	-
10/25/2002	12:35	1.80	1251	AO21	-
10/25/2002	13:35	1.59	1351	AO21	-
10/25/2002	14:35	1.62	1451	AO21	-
10/25/2002	15:35	1.77	1551	AO21	-
10/25/2002	16:35	1.82	1651	AO21	-
10/25/2002	17:35	1.87	1751	AO21	-
10/25/2002	18:35	1.57	1851	AO21	-
10/25/2002	19:35	1.42	1951	AO21	-
10/25/2002	20:35	1.50	2051	AO22	-
10/25/2002	21:35	1.59	2151	AO22	-
10/25/2002	22:35	1.66	2251	AO22	-
10/25/2002	23:35	1.54	2351	AO22	-
10/26/2002	0:35	1.81	0051	AO20	-
10/26/2002	1:35	1.54	0151	AO20	-
10/26/2002	2:35	1.66	0251	AO20	-
10/26/2002	3:35	1.59	0351	AO20	-
10/26/2002	4:35	1.93	0451	AO20	-
10/26/2002	5:35	1.56	0551	AO20	-
10/26/2002	6:35	1.85	0651	AO20	-
10/26/2002	7:35	1.89	0751	AO20	-
10/26/2002	8:35	2.17	0851	AO20	-
10/26/2002	9:35	1.97	0951	AO20	-
10/26/2002	10:35	1.74	1051	AO21	-
10/26/2002	11:35	1.70	1151	AO21	-
10/26/2002	12:35	1.76	1251	AO21	-
10/26/2002	13:35	1.84	1351	AO21	-
10/26/2002	14:35	1.78	1451	AO21	-
10/26/2002	15:35	1.83	1551	AO21	-
10/26/2002	16:35	1.81	1651	AO21	-
10/26/2002	17:35	1.74	1751	AO21	-
10/26/2002	18:35	1.60	1851	AO21	-
10/26/2002	19:35	1.52	1951	AO21	-
10/26/2002	20:35	1.61	2051	AO22	-
10/26/2002	21:35	1.71	2151	AO22	-
10/26/2002	22:35	1.74	2251	AO22	-
10/26/2002	23:35	1.73	2351	AO22	-
10/27/2002	0:35	1.73	0051	AO20	-
10/27/2002	1:35	1.69	0151	AO20	-
10/27/2002	2:35	1.45	0251	AO20	-
10/27/2002	3:35	1.49	0351	AO20	-
10/27/2002	4:35	1.61	0451	AO20	-
10/27/2002	5:35	1.61	0551	AO20	-
10/27/2002	6:35	1.69	0651	AO20	-
10/27/2002	7:35	1.77	0751	AO20	-
10/27/2002	8:35	1.80	0851	AO20	-
10/27/2002	9:35	1.63	0951	AO20	-
10/27/2002	10:35	1.60	1051	AO21	-
10/27/2002	11:35	1.54	1151	AO21	-
10/27/2002	12:35	1.52	1251	AO21	-
10/27/2002	13:35	1.52	1351	AO21	-

10/27/2002	14:35	1.55	1451	AO21	-
10/27/2002	15:35	1.65	1551	AO21	-
10/27/2002	16:35	1.62	1651	AO21	-
10/27/2002	17:35	1.67	1751	AO21	-
10/27/2002	18:35	1.68	1851	AO21	-
10/27/2002	19:35	1.69	1951	AO21	-
10/27/2002	20:35	1.34	2051	AO22	-
10/27/2002	21:35	1.34	2151	AO22	-
10/27/2002	22:35	1.43	2251	AO22	-
10/27/2002	23:35	1.40	2351	AO22	-
10/28/2002	0:35	1.39	0051	AO20	-
10/28/2002	1:35	1.55	0151	AO20	-
10/28/2002	2:35	1.60	0251	AO20	-
10/28/2002	3:35	1.75	0351	AO20	-
10/28/2002	4:35	1.67	0451	AO20	-
10/28/2002	5:35	1.51	0551	AO20	-
10/28/2002	6:35	1.58	0651	AO20	-
10/28/2002	7:35	1.66	0751	AO20	-
10/28/2002	8:35	1.65	0851	AO20	-
10/28/2002	9:35	1.53	0951	AO20	-
10/28/2002	10:50	1.444	1051	AO21	-
10/28/2002	11:50	1.393	1151	AO21	-
10/28/2002	12:50	1.379	1251	AO21	-
10/28/2002	13:50	1.416	1351	AO21	-
10/28/2002	14:50	1.475	1451	AO21	-
10/28/2002	15:50	1.496	1551	AO21	-
10/28/2002	16:50	1.541	1651	AO21	-
10/28/2002	17:50	1.468	1751	AO21	-
10/28/2002	18:50	1.491	1851	AO21	-
10/28/2002	19:50	1.416	1951	AO21	-
10/28/2002	20:50	1.284	2051	AO22	-
10/28/2002	21:50	1.421	2151	AO22	-
10/28/2002	22:50	1.371	2251	AO22	-
10/28/2002	23:50	1.582	2351	AO22	-
10/29/2002	0:50	1.630	0051	AO20	-
10/29/2002	1:50	1.687	0151	AO20	-
10/29/2002	2:50	1.967	0251	AO20	-
10/29/2002	3:50	1.787	0351	AO20	-
10/29/2002	4:50	1.664	0451	AO20	-
10/29/2002	5:50	1.490	0551	AO20	-
10/29/2002	6:50	1.465	0651	AO20	-
10/29/2002	7:50	1.408	0751	AO20	-
10/29/2002	8:50	1.322	0851	AO20	-
10/29/2002	9:50	1.192	0951	AO20	-
10/29/2002	10:50	1.201	1051	AO21	-
10/29/2002	12:50	1.283	1251	AO21	-
10/29/2002	13:50	1.311	1351	AO21	-
10/29/2002	14:50	1.511	1451	AO21	-
10/29/2002	15:50	1.418	1551	AO21	-
10/29/2002	16:50	1.335	1651	AO21	-
10/29/2002	17:50	1.238	1751	AO21	-
10/29/2002	18:50	1.180	1851	AO21	-

10/29/2002	19:50	1.217	1951	AO21	-
10/29/2002	20:50	1.098	2051	AO22	-
10/29/2002	21:50	1.218	2151	AO22	-
10/29/2002	22:50	1.267	2251	AO22	-
10/29/2002	23:50	1.254	2351	AO22	-
10/30/2002	0:50	1.348	0051	AO20	-
10/30/2002	1:50	1.390	0151	AO20	-
10/30/2002	2:50	1.417	0251	AO20	-
10/30/2002	3:50	1.340	0351	AO20	-
10/30/2002	4:50	1.399	0451	AO20	-
10/30/2002	5:50	1.271	0551	AO20	-
10/30/2002	6:50	1.314	0651	AO20	-
10/30/2002	7:50	1.364	0751	AO20	-
10/30/2002	8:50	1.311	0851	AO20	-
10/30/2002	9:50	1.315	0951	AO20	-
10/30/2002	10:50	1.381	1051	AO21	-
10/30/2002	11:50	1.324	1151	AO21	-
10/30/2002	12:50	1.334	1251	AO21	-
10/30/2002	13:50	1.328	1351	AO21	-
10/30/2002	14:50	1.357	1451	AO21	-
10/30/2002	15:50	1.329	1551	AO21	-
10/30/2002	16:50	1.384	1651	AO21	-
10/30/2002	17:50	1.345	1751	AO21	-
10/30/2002	18:50	1.305	1851	AO21	-
10/30/2002	19:50	1.397	1951	AO21	-
10/30/2002	20:50	1.227	2051	AO22	-
10/30/2002	21:50	1.342	2151	AO22	-
10/30/2002	22:50	1.287	2251	AO22	-
10/30/2002	23:50	1.321	2351	AO22	-
10/31/2002	0:50	1.246	0051	AO20	-
10/31/2002	1:50	1.385	0151	AO20	-
10/31/2002	2:50	1.288	0251	AO20	-
10/31/2002	3:50	1.300	0351	AO20	-
10/31/2002	4:50	1.226	0451	AO20	-
10/31/2002	5:50	1.238	0551	AO20	-
10/31/2002	6:50	1.330	0651	AO20	-
10/31/2002	7:50	1.338	0751	AO20	-
10/31/2002	8:50	1.295	0851	AO20	-
10/31/2002	9:50	1.367	0951	AO20	-
10/31/2002	10:50	1.404	1051	AO21	-
10/31/2002	11:50	1.495	1151	AO21	-
10/31/2002	12:50	1.659	1251	AO21	-
10/31/2002	13:50	1.541	1351	AO21	-
10/31/2002	14:50	1.511	1451	AO21	-
10/31/2002	15:50	1.488	1551	AO21	-
10/31/2002	16:50	1.454	1651	AO21	-
10/31/2002	17:50	1.428	1751	AO21	-
10/31/2002	18:50	1.447	1851	AO21	-
10/31/2002	19:50	2.475	1951	AO21	-
11/8/2002	12:50	1.231	1251	AO21	-
11/8/2002	13:50	1.187	1351	AO21	-
11/8/2002	14:50	1.084	1451	AO21	-

11/8/2002	15:50	1.049	1551	AO21	-
11/8/2002	16:50	1.181	1651	AO21	-
11/8/2002	17:50	1.059	1751	AO21	-
11/8/2002	18:50	1.101	1851	AO21	-
11/8/2002	19:50	1.276	1951	AO21	-
11/8/2002	20:50	1.505	2051	AO22	-
11/8/2002	21:50	1.617	2151	AO22	-
11/8/2002	22:50	1.835	2251	AO22	-
11/8/2002	23:50	1.708	2351	AO22	-
11/9/2002	0:50	1.584	0051	AO20	-
11/9/2002	1:50	1.389	0151	AO20	-
11/9/2002	2:50	1.360	0251	AO20	-
11/9/2002	3:50	1.549	0351	AO20	-
11/9/2002	4:50	1.465	0451	AO20	-
11/9/2002	5:50	1.530	0551	AO20	-
11/9/2002	6:50	1.519	0651	AO20	-
11/9/2002	7:50	1.435	0751	AO20	-
11/9/2002	8:50	1.287	0851	AO20	-
11/9/2002	9:50	1.202	0951	AO20	-
11/9/2002	10:50	1.232	1051	AO21	-
11/9/2002	12:50	1.119	1251	AO21	-
11/9/2002	13:50	1.358	1351	AO21	-
11/9/2002	14:50	1.479	1451	AO21	-
11/9/2002	15:50	1.561	1551	AO21	-
11/9/2002	16:50	1.669	1651	AO21	-
11/9/2002	17:50	1.694	1751	AO21	-
11/9/2002	18:50	1.293	1851	AO21	-
11/9/2002	19:50	1.149	1951	AO21	-
11/9/2002	20:50	1.065	2051	AO22	-
11/9/2002	21:50	1.140	2151	AO22	-
11/9/2002	22:50	1.099	2251	AO22	-
11/9/2002	23:50	1.193	2351	AO22	-
11/10/2002	0:50	1.247	0051	AO20	-
11/10/2002	1:50	1.354	0151	AO20	-
11/10/2002	2:50	1.708	0251	AO20	-
11/10/2002	3:50	1.724	0351	AO20	-
11/10/2002	4:50	1.561	0451	AO20	-
11/10/2002	5:50	1.480	0551	AO20	-
11/10/2002	6:50	1.442	0651	AO20	-
11/10/2002	7:50	1.468	0751	AO20	-
11/10/2002	8:50	1.449	0851	AO20	-
11/10/2002	9:50	1.387	0951	AO20	-
11/10/2002	10:50	1.398	1051	AO21	-
11/10/2002	12:50	1.409	1251	AO21	-
11/10/2002	13:50	1.464	1351	AO21	-
11/10/2002	14:50	1.646	1451	AO21	-
11/10/2002	15:50	1.756	1551	AO21	-
11/10/2002	16:50	1.709	1651	AO21	-
11/10/2002	17:50	1.669	1751	AO21	-
11/10/2002	18:50	1.492	1851	AO21	-
11/10/2002	19:50	1.503	1951	AO21	-
11/10/2002	20:50	1.470	2051	AO22	-

11/10/2002	21:50	1.399	2151	AO22	-
11/10/2002	22:50	1.376	2251	AO22	-
11/10/2002	23:50	1.495	2351	AO22	-
11/11/2002	0:50	1.559	0051	AO20	-
11/11/2002	1:50	1.791	0151	AO20	-
11/11/2002	2:50	1.651	0251	AO20	-
11/11/2002	3:50	1.632	0351	AO20	-
11/11/2002	4:50	1.606	0451	AO20	-
11/11/2002	5:50	1.620	0551	AO20	-
11/11/2002	6:50	2.116	0651	AO20	-
11/11/2002	7:50	1.604	0751	AO20	-
11/15/2002	17:50	2.042	1751	AO21	-
11/15/2002	18:50	2.181	1851	AO21	-
11/15/2002	19:50	2.370	1951	AO21	-
11/15/2002	20:50	2.416	2051	AO22	-
11/15/2002	21:50	2.834	2151	AO22	-
11/15/2002	22:50	2.782	2251	AO22	-
11/15/2002	23:50	3.083	2351	AO22	-
11/16/2002	0:50	2.693	0051	AO20	-
11/16/2002	1:50	2.638	0151	AO20	-
11/16/2002	2:50	2.502	0251	AO20	-
11/16/2002	3:50	1.603	0351	AO20	-
11/16/2002	4:50	1.152	0451	AO20	-
11/16/2002	5:50	1.062	0551	AO20	-
11/16/2002	6:50	1.131	0651	AO20	-
11/16/2002	7:50	1.260	0751	AO20	-
11/16/2002	8:50	1.246	0851	AO20	-
11/16/2002	9:50	1.284	0951	AO20	-
11/16/2002	10:50	1.227	1051	AO21	-
11/16/2002	11:50	1.201	1151	AO21	-
11/16/2002	12:50	1.227	1251	AO21	-
11/16/2002	13:50	1.225	1351	AO21	-
11/16/2002	14:50	1.150	1451	AO21	-
11/16/2002	15:50	1.167	1551	AO21	-
11/16/2002	16:50	0.986	1651	AO21	-
11/16/2002	17:50	1.235	1751	AO21	-
11/16/2002	18:50	1.221	1851	AO21	-
11/16/2002	19:50	1.037	1951	AO21	-
11/16/2002	20:50	1.047	2051	AO22	-
11/16/2002	21:50	1.136	2151	AO22	-
11/16/2002	22:50	1.079	2251	AO22	-
11/16/2002	23:50	1.033	2351	AO22	-
11/17/2002	0:50	1.006	0051	AO20	-
11/17/2002	1:50	1.010	0151	AO20	-
11/17/2002	2:50	1.045	0251	AO20	-
11/17/2002	3:50	1.050	0351	AO20	-
11/17/2002	4:50	1.085	0451	AO20	-
11/17/2002	5:50	1.218	0551	AO20	-
11/17/2002	6:50	1.235	0651	AO20	-
11/17/2002	7:50	1.288	0751	AO20	-
11/17/2002	8:50	1.369	0851	AO20	-
11/17/2002	9:50	1.300	0951	AO20	-

11/17/2002	10:50	1.322	1051	AO21	-
11/17/2002	11:50	1.270	1151	AO21	-
11/17/2002	12:50	1.200	1251	AO21	-
11/17/2002	13:50	1.208	1351	AO21	-
11/17/2002	14:50	1.292	1451	AO21	-
11/17/2002	15:50	1.294	1551	AO21	-
11/17/2002	16:50	1.307	1651	AO21	-
11/17/2002	17:50	1.139	1751	AO21	-
11/17/2002	18:50	1.080	1851	AO21	-
11/17/2002	19:50	1.120	1951	AO21	-
11/17/2002	20:50	1.487	2051	AO22	-
11/17/2002	21:50	1.370	2151	AO22	-
11/17/2002	22:50	1.217	2251	AO22	-
11/17/2002	23:50	1.245	2351	AO22	-
11/18/2002	0:50	1.169	0051	AO20	-
11/18/2002	1:50	1.426	0151	AO20	-
11/18/2002	12:50	1.354	1251	AO21	-
11/18/2002	13:50	1.382	1351	AO21	-
11/18/2002	14:50	1.414	1451	AO21	-
11/18/2002	15:50	1.443	1551	AO21	-
11/18/2002	16:50	1.454	1651	AO21	-
11/18/2002	17:50	1.405	1751	AO21	-
11/18/2002	18:50	1.461	1851	AO21	-
11/18/2002	19:50	1.457	1951	AO21	-
11/18/2002	20:50	1.572	2051	AO22	-
11/18/2002	21:50	1.520	2151	AO22	-
11/18/2002	22:50	1.554	2251	AO22	-
11/18/2002	23:50	1.547	2351	AO22	-
11/19/2002	0:50	1.517	0051	AO20	-
11/19/2002	1:50	1.711	0151	AO20	-
11/19/2002	2:50	1.648	0251	AO20	-
11/19/2002	3:50	1.583	0351	AO20	-
11/19/2002	4:50	1.691	0451	AO20	-
11/19/2002	5:50	1.755	0551	AO20	-
11/19/2002	6:50	1.873	0651	AO20	-
11/19/2002	7:50	2.347	0751	AO20	-
11/19/2002	8:50	2.266	0851	AO20	-
11/19/2002	9:50	1.905	0951	AO20	-
11/19/2002	10:50	1.798	1051	AO21	-
11/19/2002	11:50	1.883	1151	AO21	-
11/19/2002	12:50	1.631	1251	AO21	-
11/19/2002	13:50	1.613	1351	AO21	-
11/19/2002	14:50	1.636	1451	AO21	-
11/19/2002	15:50	1.587	1551	AO21	-
11/19/2002	16:50	1.534	1651	AO21	-
11/19/2002	17:50	1.556	1751	AO21	-
11/19/2002	18:50	1.472	1851	AO21	-
11/19/2002	19:50	1.515	1951	AO21	-
11/19/2002	20:50	1.596	2051	AO22	-
11/19/2002	21:50	1.513	2151	AO22	-
11/19/2002	22:50	1.646	2251	AO22	-
11/19/2002	23:50	1.826	2351	AO22	-

11/20/2002	0:50	1.804	0051	AO20	-
11/20/2002	1:50	1.773	0151	AO20	-
11/20/2002	2:50	1.777	0251	AO20	-
11/20/2002	3:50	2.174	0351	AO20	-
11/20/2002	4:50	2.197	0451	AO20	-
11/20/2002	5:50	2.263	0551	AO20	-
11/20/2002	6:50	2.037	0651	AO20	-
11/20/2002	7:50	1.956	0751	AO20	-
11/20/2002	8:50	1.963	0851	AO20	-
11/20/2002	9:50	2.001	0951	AO20	-
11/20/2002	10:50	2.043	1051	AO21	-
11/20/2002	11:50	2.030	1151	AO21	-
11/20/2002	12:50	2.058	1251	AO21	-
11/20/2002	13:50	2.050	1351	AO21	-
11/20/2002	14:50	2.148	1451	AO21	-
11/20/2002	15:50	2.112	1551	AO21	-
11/20/2002	16:50	1.960	1651	AO21	-
11/20/2002	17:50	1.875	1751	AO21	-
11/20/2002	18:50	1.995	1851	AO21	-
11/20/2002	19:50	2.090	1951	AO21	-
11/20/2002	20:50	2.025	2051	AO22	-
11/20/2002	21:50	2.182	2151	AO22	-
11/20/2002	22:50	2.173	2251	AO22	-
11/20/2002	23:50	2.117	2351	AO22	-
11/21/2002	0:50	2.282	0051	AO20	-
11/21/2002	1:50	2.560	0152	AO20	-
11/21/2002	2:50	13.170	0251	AO20	-
11/21/2002	3:50	20.359	0351	AO20	-
11/21/2002	4:50	4.894	0451	AO20	-
11/21/2002	5:50	4.026	0551	AO20	-
11/21/2002	6:50	4.188	0651	AO20	-
11/21/2002	7:50	4.323	0751	AO20	-
11/21/2002	8:50	4.911	0851	AO20	-
11/21/2002	9:50	4.091	0951	AO20	-
11/21/2002	10:50	3.862	1051	AO21	-
11/21/2002	11:50	3.710	1151	AO21	-
11/21/2002	12:50	3.091	1251	AO21	-
11/21/2002	13:50	2.061	1351	AO21	-
11/21/2002	14:50	1.827	1451	AO21	-
11/21/2002	15:50	1.924	1551	AO21	-
11/21/2002	16:50	2.067	1651	AO21	-
11/21/2002	17:50	2.010	1751	AO21	-
11/21/2002	18:50	2.087	1851	AO21	-
11/21/2002	19:50	2.281	1951	AO21	-
11/21/2002	20:50	2.437	2051	AO22	-
11/21/2002	21:50	2.293	2151	AO22	-
11/21/2002	22:50	2.133	2251	AO22	-
11/21/2002	23:50	2.288	2351	AO22	-
11/22/2002	0:50	2.082	0051	AO20	-
11/22/2002	1:50	2.101	0151	AO20	-
11/22/2002	2:50	2.110	0251	AO20	-
11/22/2002	3:50	1.997	0351	AO20	-

11/22/2002	4:50	1.840	0451	AO20	-
11/22/2002	5:50	1.898	0551	AO20	-
11/22/2002	6:50	1.877	0651	AO20	-
11/22/2002	7:50	1.779	0751	AO20	-
11/22/2002	8:50	1.859	0851	AO20	-
11/22/2002	12:50	2.447	1251	AO21	-
11/22/2002	13:50	2.748	1351	AO21	-
11/22/2002	14:50	2.248	1451	AO21	-
11/22/2002	15:50	1.976	1551	AO21	-
11/22/2002	16:50	1.842	1651	AO21	-
11/22/2002	17:50	1.860	1751	AO21	-
11/22/2002	18:50	1.651	1851	AO21	-
11/22/2002	19:50	1.701	1951	AO21	-
11/22/2002	20:50	1.660	2051	AO22	-
11/22/2002	21:50	1.778	2151	AO22	-
11/22/2002	22:50	1.850	2251	AO22	-
11/22/2002	23:50	1.902	2351	AO22	-
11/23/2002	0:50	1.863	0051	AO20	-
11/23/2002	1:50	1.779	0151	AO20	-
11/23/2002	2:50	1.473	0251	AO20	-
11/23/2002	3:50	1.373	0351	AO20	-
11/23/2002	4:50	1.430	0451	AO20	-
11/23/2002	5:50	1.439	0551	AO20	-
11/23/2002	6:50	1.490	0651	AO20	-
11/23/2002	7:50	1.496	0751	AO20	-
11/23/2002	8:50	1.471	0851	AO20	-
11/23/2002	9:50	1.467	0951	AO20	-
11/23/2002	10:50	1.472	1051	AO21	-
11/23/2002	11:50	1.457	1151	AO21	-
11/23/2002	12:50	1.471	1251	AO21	-
11/23/2002	13:50	1.495	1351	AO21	-
11/23/2002	14:50	1.487	1451	AO21	-
11/23/2002	15:50	1.474	1551	AO21	-
11/23/2002	16:50	1.467	1651	AO21	-
11/23/2002	17:50	1.420	1751	AO21	-
11/23/2002	18:50	1.389	1851	AO21	-
11/23/2002	19:50	1.384	1951	AO21	-
11/23/2002	20:50	1.398	2051	AO22	-
11/23/2002	21:50	1.410	2151	AO22	-
11/23/2002	22:50	1.406	2251	AO22	-
11/23/2002	23:50	1.431	2351	AO22	-
11/24/2002	0:50	1.460	0051	AO20	-
11/24/2002	1:50	1.652	0151	AO20	-
11/24/2002	2:50	1.684	0251	AO20	-
11/24/2002	3:50	1.620	0351	AO20	-
11/24/2002	4:50	1.498	0451	AO20	-
11/24/2002	5:50	1.597	0551	AO20	-
11/24/2002	6:50	1.754	0651	AO20	-
1/20/2003	13:50	1.171	1351	AO2	-
1/20/2003	14:50	1.189	1451	AO2	-
1/20/2003	15:50	1.230	1551	AO2	-
1/20/2003	16:50	1.236	1651	AO2	-

1/20/2003	17:50	1.197	1751	AO2	-
1/20/2003	18:50	1.175	1851	AO2	-
1/20/2003	19:50	1.175	1951	AO2	-
1/20/2003	20:50	1.192	2051	AO2	-
1/20/2003	21:50	1.244	2151	AO2	-
1/20/2003	22:50	1.248	2251	AO2	-
1/20/2003	23:50	1.231	2351	AO2	-
1/21/2003	0:50	1.202	0051	AO2	-
1/21/2003	1:50	1.260	0151	AO2	-
1/21/2003	2:50	1.272	0251	AO2	-
1/21/2003	3:50	1.263	0351	AO2	-
1/21/2003	4:50	1.269	0451	AO2	-
1/21/2003	5:50	1.314	0551	AO2	-
1/21/2003	6:50	1.401	0651	AO2	-
1/21/2003	7:50	1.445	0751	AO2	-
1/21/2003	8:50	1.380	0851	AO2	-
1/21/2003	9:50	1.345	0951	AO2	-
1/21/2003	10:50	1.345	1051	AO2	-
1/21/2003	11:50	1.347	1151	AO2	-
1/21/2003	12:50	1.314	1251	AO2	-
1/21/2003	13:50	1.358	1351	AO2	-
1/21/2003	14:50	1.408	1451	AO2	-
1/21/2003	15:50	1.339	1551	AO2	-
1/21/2003	16:50	1.351	1651	AO2	-
1/21/2003	17:50	1.356	1751	AO2	-
1/21/2003	18:50	1.337	1851	AO2	-
1/21/2003	19:50	1.352	1951	AO2	-
1/21/2003	20:50	1.318	2051	AO2	-
1/21/2003	21:50	1.309	2151	AO2	-
1/21/2003	22:50	1.335	2251	AO2	-
1/21/2003	23:50	1.341	2351	AO2	-
1/22/2003	0:50	1.336	0051	AO2	-
1/22/2003	1:50	1.291	0151	AO2	-
1/22/2003	2:50	1.280	0251	AO2	-
1/22/2003	3:50	1.310	0351	AO2	-
1/22/2003	4:50	1.352	0451	AO2	-
1/22/2003	5:50	1.307	0551	AO2	-
1/22/2003	6:50	1.343	0651	AO2	-
1/22/2003	7:50	1.401	0751	AO2	-
1/22/2003	8:50	1.411	0851	AO2	-
1/22/2003	9:50	1.336	0951	AO2	-
1/22/2003	10:50	1.353	1051	AO2	-
1/22/2003	11:50	1.372	1151	AO2	-
1/22/2003	12:50	1.346	1251	AO2	-
1/22/2003	13:50	1.303	1351	AO2	-
1/22/2003	14:50	1.340	1451	AO2	-
1/22/2003	15:50	1.305	1551	AO2	-
1/22/2003	16:50	1.310	1651	AO2	-
1/22/2003	17:50	1.320	1751	AO2	-
1/22/2003	18:50	1.284	1851	AO2	-
1/22/2003	19:50	1.260	1951	AO2	-
1/22/2003	20:50	1.258	2051	AO2	-

1/22/2003	21:50	1.269	2151	AO2	-
1/22/2003	22:50	1.279	2251	AO2	-
1/22/2003	23:50	1.277	2351	AO2	-
1/23/2003	0:50	1.255	0051	AO2	-
1/23/2003	1:50	1.227	0151	AO2	-
1/23/2003	2:50	1.236	0251	AO2	-
1/23/2003	3:50	1.743	0351	AO2	-
1/23/2003	4:50	1.283	0451	AO2	-
1/23/2003	5:50	1.292	0551	AO2	-
1/23/2003	6:50	1.315	0651	AO2	-
1/23/2003	7:50	1.345	0751	AO2	-
1/23/2003	10:50	1.339	1051	AO2	-
1/23/2003	11:50	1.358	1151	AO2	-
1/23/2003	12:50	1.369	1251	AO2	-
1/23/2003	13:50	1.336	1351	AO2	-
1/23/2003	14:50	1.433	1451	AO2	-
1/23/2003	15:50	1.389	1551	AO2	-
1/23/2003	16:50	1.358	1651	AO2	-
1/23/2003	17:50	1.300	1751	AO2	-
1/23/2003	18:50	1.270	1851	AO2	-
1/23/2003	19:50	1.288	1951	AO2	-
1/23/2003	20:50	1.235	2051	AO2	-
1/23/2003	21:50	1.200	2151	AO2	-
1/23/2003	22:50	1.209	2251	AO2	-
1/23/2003	23:50	1.216	2351	AO2	-
1/24/2003	0:50	1.305	0051	AO2	-
1/24/2003	1:50	1.316	0151	AO2	-
1/24/2003	2:50	1.301	0251	AO2	-
1/24/2003	3:50	1.289	0351	AO2	-
1/24/2003	4:50	1.285	0451	AO2	-
1/24/2003	5:50	1.283	0551	AO2	-
1/24/2003	6:50	2.776	0651	AO2	-
1/24/2003	7:50	5.044	0751	AO2	-
1/24/2003	8:50	1.362	0851	AO2	-
1/24/2003	9:50	1.374	0951	AO2	-
1/24/2003	10:50	1.354	1051	AO2	-
1/24/2003	12:50	1.547	1251	AO2	-
1/24/2003	13:50	1.509	1351	AO2	-
1/24/2003	14:50	1.443	1451	AO2	-
1/24/2003	15:50	1.441	1551	AO2	-
1/24/2003	16:50	1.408	1651	AO2	-
1/24/2003	17:50	1.406	1751	AO2	-
1/24/2003	18:50	1.390	1851	AO2	-
1/24/2003	19:50	1.383	1951	AO2	-
1/24/2003	20:50	1.381	2051	AO2	-
1/24/2003	21:50	1.377	2151	AO2	-
1/24/2003	22:50	1.449	2251	AO2	-
1/24/2003	23:50	1.468	2351	AO2	-
1/25/2003	0:50	1.451	0051	AO2	-
1/25/2003	1:50	1.411	0151	AO2	-
1/25/2003	2:50	1.412	0251	AO2	-
1/25/2003	3:50	1.400	0351	AO2	-

1/25/2003	4:50	1.504	0451	AO2	-
1/25/2003	5:50	1.524	0551	AO2	-
1/25/2003	6:50	1.538	0651	AO2	-
1/25/2003	7:50	1.572	0751	AO2	-
1/25/2003	8:50	1.731	0851	AO2	-
1/25/2003	9:50	1.744	0951	AO2	-
1/25/2003	10:50	1.755	1051	AO2	-
1/25/2003	11:50	1.811	1151	AO2	-
1/25/2003	12:50	1.785	1251	AO2	-
1/25/2003	13:50	1.742	1351	AO2	-
1/25/2003	14:50	1.590	1451	AO2	-
1/25/2003	15:50	1.574	1551	AO2	-
1/25/2003	16:50	1.578	1651	AO2	-
1/25/2003	17:50	1.580	1751	AO2	-
1/25/2003	18:50	1.615	1851	AO2	-
1/25/2003	19:50	1.663	1951	AO2	-
1/25/2003	20:50	1.714	2051	AO2	-
1/25/2003	21:50	1.736	2151	AO2	-
1/25/2003	22:50	1.641	2251	AO2	-
1/26/2003	0:50	2.272	0051	AO2	-
1/26/2003	1:50	1.937	0151	AO2	-
1/26/2003	2:50	1.821	0251	AO2	-
1/26/2003	3:50	1.828	0351	AO2	-
1/26/2003	4:50	1.841	0451	AO2	-
1/26/2003	5:50	1.851	0551	AO2	-
1/26/2003	6:50	2.173	0651	AO2	-
1/26/2003	7:50	2.320	0751	AO2	-
1/26/2003	8:50	2.133	0851	AO2	-
1/26/2003	9:50	2.555	0951	AO2	-
1/26/2003	10:50	3.236	1051	AO2	-
1/26/2003	11:50	2.651	1151	AO2	-
1/26/2003	12:50	2.456	1251	AO2	-
1/26/2003	13:50	2.336	1351	AO2	-
1/26/2003	14:50	2.588	1451	AO2	-
1/26/2003	15:50	2.450	1551	AO2	-
1/26/2003	16:50	2.058	1651	AO2	-
1/26/2003	17:50	1.811	1751	AO2	-
1/26/2003	18:50	1.907	1851	AO2	-
1/26/2003	19:50	1.905	1951	AO2	-
1/26/2003	20:50	1.771	2051	AO2	-
1/26/2003	21:50	1.696	2151	AO2	-
1/26/2003	22:50	1.696	2251	AO2	-
1/26/2003	23:50	1.729	2351	AO2	-
1/27/2003	0:50	1.678	0051	AO2	-
1/27/2003	1:50	1.513	0151	AO2	-
1/27/2003	2:50	1.466	0251	AO2	-
1/27/2003	3:50	1.455	0351	AO2	-
1/27/2003	4:50	1.474	0451	AO2	-
1/27/2003	5:50	1.428	0551	AO2	-
1/27/2003	6:50	1.451	0651	AO2	-
1/27/2003	7:50	1.496	0751	AO2	-
1/27/2003	8:50	1.515	0851	AO2	-

1/27/2003	9:50	1.550	0951	AO2	-
1/27/2003	10:50	1.575	1051	AO2	-
1/27/2003	12:50	1.553	1251	AO2	-
1/27/2003	13:50	1.576	1351	AO2	-
1/27/2003	14:50	1.541	1451	AO2	-
1/27/2003	15:50	1.539	1551	AO2	-
1/27/2003	16:50	1.492	1651	AO2	-
1/27/2003	17:50	1.532	1751	AO2	-
1/27/2003	18:50	1.518	1851	AO2	-
1/27/2003	19:50	1.495	1951	AO2	-
1/27/2003	20:50	1.503	2051	AO2	-
1/27/2003	21:50	1.496	2151	AO2	-
1/27/2003	22:50	1.481	2251	AO2	-
1/27/2003	23:50	1.481	2351	AO2	-
1/28/2003	0:50	1.521	0051	AO2	-
1/28/2003	1:50	1.533	0151	AO2	-
1/28/2003	2:50	1.540	0251	AO2	-
1/28/2003	3:50	1.535	0351	AO2	-
1/28/2003	4:50	1.517	0451	AO2	-
1/28/2003	5:50	1.542	0551	AO2	-
1/28/2003	6:50	1.524	0651	AO2	-
1/28/2003	7:50	1.622	0751	AO2	-
1/28/2003	8:50	1.583	0851	AO2	-
1/28/2003	9:50	1.584	0951	AO2	-
1/28/2003	10:50	1.582	1051	AO2	-
1/28/2003	11:50	1.531	1151	AO2	-
1/28/2003	12:50	1.543	1251	AO2	-
1/28/2003	13:50	1.553	1351	AO2	-
1/28/2003	14:50	1.569	1451	AO2	-
1/28/2003	15:50	1.568	1551	AO2	-
1/28/2003	16:50	1.616	1651	AO2	-
1/28/2003	17:50	1.594	1751	AO2	-
1/28/2003	18:50	1.500	1851	AO2	-
1/28/2003	19:50	1.504	1951	AO2	-
1/28/2003	20:50	1.582	2051	AO2	-
1/28/2003	21:50	1.700	2151	AO2	-
1/28/2003	22:50	1.709	2251	AO2	-
1/29/2003	0:50	2.005	0051	AO2	-
1/29/2003	1:50	2.184	0151	AO2	-
1/29/2003	2:50	2.177	0251	AO2	-
1/29/2003	3:50	2.026	0351	AO2	-
1/29/2003	4:50	2.028	0451	AO2	-
1/29/2003	5:50	2.024	0551	AO2	-
1/29/2003	6:50	2.011	0651	AO2	-
1/29/2003	7:50	2.164	0751	AO2	-
1/29/2003	8:50	2.077	0851	AO2	-
1/29/2003	9:50	1.973	0951	AO2	-
1/29/2003	10:50	1.933	1051	AO2	-
1/29/2003	11:50	2.098	1151	AO2	-
1/29/2003	12:50	2.782	1251	AO2	-
1/29/2003	13:50	2.230	1351	AO2	-
1/29/2003	14:50	2.342	1451	AO2	-

1/29/2003	15:50	2.289	1551	AO2	-
1/29/2003	16:50	2.232	1651	AO2	-
1/29/2003	17:50	2.388	1751	AO2	-
1/29/2003	18:50	2.221	1851	AO2	-
1/29/2003	19:50	2.260	1951	AO2	-
1/29/2003	20:50	2.125	2051	AO2	-
1/29/2003	21:50	2.398	2151	AO2	-
1/29/2003	22:50	2.469	2251	AO2	-
1/29/2003	23:50	2.388	2351	AO2	-
1/30/2003	0:50	2.434	0051	AO2	-
1/30/2003	1:50	2.269	0151	AO2	-
1/30/2003	2:50	2.283	0251	AO2	-
1/30/2003	3:50	2.111	0351	AO2	-
1/30/2003	4:50	1.978	0451	AO2	-
1/30/2003	5:50	1.914	0551	AO2	-
1/30/2003	6:50	1.944	0651	AO2	-
1/30/2003	7:50	1.929	0751	AO2	-
1/30/2003	8:50	1.868	0851	AO2	-
1/30/2003	9:50	1.960	0951	AO2	-
1/30/2003	10:50	2.007	1051	AO2	-
1/30/2003	12:50	2.493	1251	AO2	-
1/30/2003	13:50	2.343	1351	AO2	-
1/30/2003	14:50	2.417	1451	AO2	-
1/30/2003	15:50	2.337	1551	AO2	-
1/30/2003	16:50	2.494	1651	AO2	-
1/30/2003	17:50	2.377	1751	AO2	-
1/30/2003	18:50	2.263	1851	AO2	-
1/30/2003	19:50	2.220	1951	AO2	-
1/30/2003	20:50	2.213	2051	AO2	-
1/30/2003	21:50	2.086	2151	AO2	-
1/30/2003	22:50	2.135	2251	AO2	-
1/30/2003	23:50	2.850	2351	AO2	-
1/31/2003	0:50	2.151	0051	AO2	-
1/31/2003	1:50	2.040	0151	AO2	-
1/31/2003	2:50	2.039	0251	AO2	-
1/31/2003	3:50	2.042	0351	AO2	-
1/31/2003	4:50	2.006	0451	AO2	-
1/31/2003	5:50	2.007	0551	AO2	-
1/31/2003	6:50	1.858	0651	AO2	-
1/31/2003	7:50	1.866	0751	AO2	-
1/31/2003	8:50	1.954	0851	AO2	-
1/31/2003	9:50	1.993	0951	AO2	-
1/31/2003	10:50	1.972	1051	AO2	-
1/31/2003	11:50	2.014	1151	AO2	-
1/31/2003	12:50	2.054	1251	AO2	-
1/31/2003	13:50	2.097	1351	AO2	-
1/31/2003	14:50	2.044	1451	AO2	-
1/31/2003	15:50	2.042	1551	AO2	-
1/31/2003	16:50	2.016	1651	AO2	-
1/31/2003	17:50	1.986	1751	AO2	-
1/31/2003	18:50	1.964	1851	AO2	-
1/31/2003	19:50	2.019	1951	AO2	-

1/31/2003	20:50	2.001	2051	AO2	-
1/31/2003	21:50	2.050	2151	AO2	-
1/31/2003	22:50	2.129	2251	AO2	-
2/1/2003	0:50	2.045	51	AO2	-
2/1/2003	1:50	1.947	151	AO2	-
2/1/2003	2:50	1.914	251	AO2	-
2/1/2003	3:50	1.896	351	AO2	-
2/1/2003	4:50	1.836	451	AO2	-
2/1/2003	5:50	1.915	551	AO2	-
2/1/2003	6:50	1.898	651	AO2	-
2/1/2003	7:50	1.859	751	AO2	-
2/1/2003	8:50	1.999	851	AO2	-
2/1/2003	9:50	1.932	951	AO2	-
2/1/2003	10:50	1.966	1051	AO2	-
2/1/2003	11:50	1.952	1151	AO2	-
2/1/2003	12:50	1.927	1251	AO2	-
2/1/2003	13:50	1.962	1351	AO2	-
2/1/2003	14:50	1.793	1451	AO2	-
2/1/2003	15:50	1.747	1551	AO2	-
2/1/2003	16:50	1.733	1651	AO2	-
2/1/2003	17:50	2.990	1751	AO2	-
2/1/2003	18:50	2.303	1851	AO2	-
2/1/2003	19:50	1.968	1951	AO2	-
2/1/2003	20:50	2.136	2051	AO2	-
2/1/2003	21:50	2.076	2151	AO2	-
2/1/2003	22:50	2.273	2251	AO2	-
2/1/2003	23:50	2.125	2351	AO2	-
2/2/2003	0:50	1.871	51	AO2	-
2/2/2003	1:50	1.797	151	AO2	-
2/2/2003	2:50	1.876	251	AO2	-
2/2/2003	3:50	1.813	351	AO2	-
2/2/2003	4:50	1.896	451	AO2	-
2/2/2003	5:50	1.934	551	AO2	-
2/2/2003	6:50	1.852	651	AO2	-
2/2/2003	7:50	1.779	751	AO2	-
2/2/2003	8:50	1.760	851	AO2	-
2/2/2003	9:50	1.692	951	AO2	-
2/2/2003	10:50	1.775	1051	AO2	-
2/2/2003	12:50	2.059	1251	AO2	-
2/2/2003	13:50	2.037	1351	AO2	-
2/2/2003	14:50	1.935	1451	AO2	-
2/2/2003	15:50	1.863	1551	AO2	-
2/2/2003	16:50	1.813	1651	AO2	-
2/2/2003	17:50	1.772	1751	AO2	-
2/2/2003	18:50	1.659	1851	AO2	-
2/2/2003	19:50	1.627	1951	AO2	-
2/2/2003	20:50	1.643	2051	AO2	-
2/2/2003	21:50	1.732	2151	AO2	-
2/2/2003	22:50	1.732	2251	AO2	-
2/2/2003	23:50	1.739	2351	AO2	-
2/3/2003	0:50	1.748	51	AO2	-
2/3/2003	1:50	1.676	151	AO2	-

2/3/2003	2:50	1.652	251	AO2	-
2/3/2003	3:50	1.761	351	AO2	-
2/3/2003	4:50	1.760	451	AO2	-
2/3/2003	5:50	1.902	551	AO2	-
2/3/2003	6:50	1.923	651	AO2	-
2/3/2003	7:50	2.116	751	AO2	-
2/3/2003	8:50	1.976	851	AO2	-
2/3/2003	9:50	1.777	951	AO2	-
2/3/2003	10:50	1.903	1051	AO2	-
2/3/2003	11:50	2.089	1151	AO2	-
2/3/2003	12:50	2.068	1251	AO2	-
2/3/2003	13:50	2.173	1351	AO2	-
2/3/2003	14:50	2.245	1451	AO2	-
2/3/2003	15:50	2.286	1551	AO2	-
2/3/2003	16:50	2.311	1651	AO2	-
2/3/2003	17:50	2.063	1751	AO2	-
2/3/2003	18:50	2.100	1851	AO2	-
2/3/2003	19:50	2.269	1951	AO2	-
2/3/2003	20:50	2.245	2051	AO2	-
2/3/2003	21:50	2.065	2151	AO2	-
2/3/2003	22:50	2.003	2251	AO2	-
2/4/2003	0:50	1.867	51	AO2	-
2/4/2003	1:50	1.980	151	AO2	-
2/4/2003	2:50	2.127	251	AO2	-
2/4/2003	3:50	2.242	351	AO2	-
2/4/2003	4:50	2.074	451	AO2	-
2/4/2003	5:50	1.963	551	AO2	-
2/4/2003	6:50	1.856	651	AO2	-
2/4/2003	7:50	1.977	751	AO2	-
2/4/2003	8:50	2.355	851	AO2	-
2/4/2003	9:50	2.347	951	AO2	-

Sky Conditions	Visibility	Weather Type	Dry Bulb Temp (F)	Dew Point Temp (F)	Wet Bulb Temp (F)	% Relative Humidity
FEW095 OVC140	9SM	-	51	45	48	81
FEW055 BKN140 OVC250	9SM	-	53	43	48	70
FEW055 BKN140 OVC250	10SM	-	54	44	49	70
BKN140 OVC250	10SM	-	53	44	49	72
FEW055 BKN140 OVC250	10SM	-	52	44	48	75
SCT060 BKN140 OVC250	10SM	-	52	44	48	75
SCT048 BKN070 OVC095	10SM	-	54	50	52	88
BKN055 BKN070 OVC080	10SM	-	56	50	53	82
SCT021 BKN045 OVC055	8SM	-RA	56	52	54	86
BKN019 OVC060	10SM	-	-	-	-	-
BKN015 BKN030 BKN120	10SM	-	55	50	52	83
OVC016	10SM	-	56	50	53	81
OVC015	9SM	-	55	49	52	80
SCT015	9SM	-	55	48	51	78
FEW013 BKN029 BKN037	8SM	-	54	48	51	81
SCT007 SCT022 OVC028	6SM	BR	54	53	54	97
FEW020 SCT200	4SM	BR	53	52	53	97
SCT050 BKN120 BKN250	4SM	BR	53	52	53	97
BKN070	5SM	BR	56	54	55	94
FEW015 SCT090	6SM	BR	59	56	57	90
FEW015 SCT030 BKN080	10SM	-	62	54	57	74
FEW023 BKN070 BKN250	10SM	-	61	44	52	54
FEW035 BKN070 BKN250	10SM	-	61	39	50	44
FEW050 SCT080 BKN250	10SM	-	64	36	50	35
SCT065	10SM	-	63	36	50	37
FEW060 SCT075	10SM	-	62	34	49	35
FEW060 SCT080	10SM	-	59	33	47	38
FEW065	10SM	-	57	31	45	37
FEW065	10SM	-	55	32	45	42
FEW070	10SM	-	53	32	44	45
CLR	10SM	-	52	32	43	47
SCT085	10SM	-	50	31	42	48
OVC095	10SM	-	50	31	42	48
OVC100	10SM	-	49	32	42	52
BKN100 OVC120	10SM	-	49	32	42	52
BKN100	10SM	-	47	32	40	56
BKN100	10SM	-	46	32	40	58
SCT055 BKN100	10SM	-	45	32	40	61
SCT055	10SM	-	41	32	37	70
FEW060 BKN090	10SM	-	43	32	38	65
FEW060 BKN110	10SM	-	43	32	38	65
FEW050 OVC065	10SM	-	45	31	39	58
FEW040 SCT100 SCT250	10SM	-	46	26	38	46
FEW045 BKN110 BKN230	10SM	-	48	25	39	41
FEW045 BKN110 BKN230	10SM	-	50	25	40	38
SCT050	10SM	-	50	27	40	41
SCT050	10SM	-	50	26	40	39
BKN050	10SM	-	49	27	40	43
BKN050	10SM	-	49	27	40	43
SCT050	10SM	-	49	27	40	43

BKN048	10SM	-	48	28	40	46
OVC048	10SM	-	46	27	38	47
OVC050	10SM	-	46	26	38	46
OVC050	10SM	-	45	27	38	49
OVC050	10SM	-	45	27	38	49
OVC050	10SM	-	44	28	38	53
OVC050	10SM	-	44	28	38	53
OVC050	10SM	-	43	28	37	56
OVC050	10SM	-	42	28	37	58
OVC050	10SM	-	41	30	37	65
OVC050	10SM	-	40	27	35	60
OVC046	10SM	-	39	26	34	60
OVC042	10SM	-	38	25	33	60
OVC040	10SM	-	37	22	32	54
BKN040	10SM	-	36	20	30	52
SCT040	10SM	-	35	19	30	52
FEW040	10SM	-	37	18	31	46
FEW250	10SM	-	38	16	31	41
FEW250	10SM	-	39	16	31	39
FEW250	10SM	-	42	17	33	36
FEW250	10SM	-	43	14	33	31
FEW250	10SM	-	44	14	34	30
FEW250	10SM	-	46	13	35	26
FEW250	10SM	-	46	11	34	24
FEW250	10SM	-	46	11	34	24
FEW250	10SM	-	44	10	33	25
SCT250	10SM	-	43	10	32	26
CLR	10SM	-	42	11	32	28
CLR	10SM	-	40	12	31	32
CLR	10SM	-	39	14	31	36
CLR	10SM	-	37	15	30	41
CLR	10SM	-	35	18	29	50
CLR	10SM	-	33	18	28	54
CLR	10SM	-	32	18	27	56
CLR	10SM	-	32	17	27	54
CLR	10SM	-	30	18	26	61
CLR	10SM	-	29	18	25	64
CLR	10SM	-	29	18	25	64
CLR	10SM	-	30	18	26	61
CLR	10SM	-	32	20	28	61
CLR	10SM	-	35	21	30	57
CLR	10SM	-	38	20	32	48
CLR	10SM	-	41	20	33	43
CLR	10SM	-	43	20	35	40
CLR	10SM	-	45	20	36	37
CLR	10SM	-	46	19	36	34
CLR	10SM	-	47	19	37	33
FEW250	10SM	-	48	17	37	29
FEW250	10SM	-	47	20	37	34
FEW250	10SM	-	42	30	37	62
SCT250	10SM	-	41	31	37	67
SCT250	10SM	-	41	32	37	70

FEW250	10SM	-	40	32	37	73
FEW250	10SM	-	39	33	37	79
FEW250	10SM	-	38	34	36	86
CLR	10SM	-	37	32	35	82
CLR	10SM	-	37	30	34	76
SCT250	10SM	-	36	30	34	79
SCT250	10SM	-	36	29	33	76
SCT250	10SM	-	36	31	34	82
BKN250	10SM	-	35	30	33	82
BKN250	10SM	-	35	29	33	78
BKN250	8SM	-	35	31	33	85
BKN250	7SM	-	37	32	35	82
BKN250	9SM	-	41	33	38	74
BKN250	10SM	-	44	35	40	71
FEW140 BKN250	10SM	-	47	33	41	59
FEW140 BKN250	10SM	-	49	33	42	55
FEW140 BKN250	10SM	-	50	35	43	57
FEW140 BKN250	10SM	-	49	39	44	69
FEW060	10SM	-	39	8	29	28
FEW060	10SM	-	40	9	30	28
FEW070	10SM	-	41	9	31	27
FEW075	10SM	-	42	9	31	25
FEW075	10SM	-	41	9	31	27
FEW075	10SM	-	40	8	30	27
FEW075	10SM	-	38	9	29	30
FEW070	10SM	-	37	10	29	33

BKN250	10SM	-	34	12	27	40
SCT250	10SM	-	33	11	26	40
SCT250	10SM	-	32	11	26	41
CLR	10SM	-	30	12	25	47
CLR	10SM	-	28	13	24	53
BKN250	10SM	-	28	13	24	53
BKN250	10SM	-	28	12	23	51
CLR	10SM	-	27	12	23	53
FEW080	10SM	-	27	13	23	55
SCT250	10SM	-	29	13	24	51
SCT250	10SM	-	32	14	26	47
FEW250	10SM	-	36	15	29	42
CLR	10SM	-	38	17	31	43
FEW050	10SM	-	42	17	33	36
FEW050 BKN250	10SM	-	45	18	35	34
FEW050 SCT250	10SM	-	47	17	36	30
FEW050 BKN250	10SM	-	48	15	36	27
FEW250	10SM	-	48	17	37	29
FEW250	10SM	-	46	18	36	33
FEW250	10SM	-	46	17	36	31
SCT250	10SM	-	44	15	34	31
SCT250	10SM	-	43	18	34	37
SCT250	10SM	-	42	19	34	40

SCT250	10SM	-	42	19	34	40
SCT250	10SM	-	41	20	33	43
BKN045 BKN250	10SM	-	38	15	30	39
BKN045 BKN250	10SM	-	37	12	29	36
BKN050 BKN250	10SM	-	39	12	30	33
BKN055 BKN250	10SM	-	36	14	29	40
FEW040 BKN055 BKN250	10SM	-	35	13	28	40
FEW040 BKN060 BKN075	10SM	-	32	17	27	54
FEW040 SCT060 BKN075	10SM	-	31	13	25	47
FEW030 SCT045 BKN060	7SM	-SN	29	18	25	64
FEW040 SCT055 BKN075	9SM	-	27	18	24	69
SCT042 BKN055	10SM	-	27	13	23	55
FEW050 SCT085	10SM	-	26	11	22	53
FEW080	10SM	-	25	8	20	48
FEW050 SCT085	10SM	-	25	7	20	46
FEW050 SCT085	10SM	-	24	6	19	46
FEW039 BKN050	10SM	-	23	13	20	65
SCT032 BKN042	10SM	-	23	12	20	63
FEW042	10SM	-	21	6	17	52
CLR	10SM	-	20	3	16	48
CLR	10SM	-	19	2	15	47
SCT200 BKN250	10SM	-	19	1	15	45
SCT150 BKN250	10SM	-	20	-1	15	40
BKN250	10SM	-	23	-1	18	35
FEW095 OVC250	10SM	-	24	-1	18	33
SCT250	10SM	-	27	-1	20	30
FEW055 SCT250	10SM	-	30	3	23	31
FEW065 SCT250	10SM	-	32	7	25	35
BKN060	10SM	-	32	6	25	33
SCT060	10SM	-	35	8	27	32
OVC066	10SM	-	35	10	27	35
BKN065 BKN250	10SM	-	34	11	27	38
SCT065	10SM	-	34	11	27	38
CLR	10SM	-	33	12	27	42
CLR	10SM	-	31	13	26	47
CLR	10SM	-	32	15	27	50
CLR	10SM	-	32	18	27	56
CLR	10SM	-	31	19	27	61
CLR	10SM	-	31	19	27	61
FEW100	10SM	-	31	20	27	64
FEW100	10SM	-	30	20	27	66
BKN080	10SM	-	31	21	27	67
BKN080	10SM	-	31	22	28	69
BKN090	10SM	-	32	23	29	69
BKN100	10SM	-	30	24	28	79
SCT095 BKN250	10SM	-	31	25	29	79
BKN110 OVC250	10SM	-	36	27	33	70
FEW110 BKN150 OVC250	10SM	-	39	28	35	65
FEW110 BKN150 OVC250	10SM	-	43	28	37	56
FEW110 BKN150 OVC250	10SM	-	45	28	38	52
FEW110 BKN150 OVC250	10SM	-	49	29	41	46
FEW110 BKN150 OVC250	10SM	-	55	29	44	37

FEW090 SCT150 BKN250	10SM	-	56	29	44	36
FEW110 SCT150 OVC250	10SM	-	58	30	46	35
FEW090 OVC250	10SM	-	59	30	46	33
SCT250	10SM	-	58	30	46	35
CLR	10SM	-	56	30	45	37
FEW250	10SM	-	55	31	44	40
CLR	10SM	-	53	33	44	47
CLR	10SM	-	52	34	44	50
CLR	10SM	-	50	34	43	54
CLR	10SM	-	48	34	42	58
CLR	10SM	-	48	33	42	56
CLR	10SM	-	46	33	40	61
CLR	10SM	-	45	33	40	63
CLR	10SM	-	43	33	39	68
CLR	10SM	-	43	33	39	68
SCT250	10SM	-	41	33	38	74
SCT250	10SM	-	39	33	37	79
BKN250	10SM	-	41	34	38	76
BKN250	10SM	-	46	35	41	66
BKN250	10SM	-	51	35	44	54
BKN250	10SM	-	55	36	46	49
BKN250	10SM	-	61	33	48	35
BKN250	10SM	-	65	30	49	27
OVC250	10SM	-	65	31	49	28
OVC250	10SM	-	66	32	50	28
FEW110 BKN250	10SM	-	66	33	50	29
FEW110 SCT150 BKN250	10SM	-	66	34	51	31
FEW120 BKN150 OVC250	10SM	-	64	34	50	33
BKN085 BKN250	10SM	-	64	35	50	34
BKN100 OVC120	10SM	-	62	38	50	41
BKN090 BKN120	10SM	-	60	40	50	48
SCT090	10SM	-	59	41	50	51
OVC100	10SM	-	57	41	49	55
SCT100	10SM	-	56	40	48	55
FEW100	10SM	-	51	40	46	66
CLR	10SM	-	47	38	43	71
CLR	10SM	-	46	37	42	71
CLR	10SM	-	42	37	40	82
CLR	10SM	-	42	37	40	82
CLR	8SM	-	41	40	40	96
CLR	6SM	BR	40	40	40	100
BKN250	5SM	BR	41	41	41	100
OVC250	4SM	BR	44	43	44	96
OVC250	4SM	BR	45	44	45	97
SCT004 OVC250	4SM	BR	47	44	46	90
SCT018 OVC250	3SM	BR	48	44	46	86
BKN250	4SM	HZ	50	44	47	80
FEW012 BKN250	5SM	BR	50	46	48	86
FEW012 BKN250	6SM	HZ	53	47	50	80
BKN250	5SM	BR	52	48	50	86
FEW014 BKN250	5SM	BR	50	49	49	96
SCT012 BKN250	5SM	BR	49	49	49	100

FEW012 BKN250	5SM	BR	48	48	48	100
OVC005	5SM	BR	46	46	46	100
OVC003	1/2SM	BR	45	45	45	100
OVC001	1/2SM	BR	45	45	45	100
VV001	1/2SM	FG	45	45	45	100
OVC001	1/2SM	BR	45	45	45	100
OVC001	3/4SM	BR	46	46	46	100
OVC003	1 1/2SM	BR	46	46	46	100
OVC004	1 1/2SM	BR	46	46	46	100
OVC004	1 1/2SM	BR	46	46	46	100
OVC004	1 1/2SM	BR	46	46	46	100
OVC002	1/4SM	FG	45	45	45	100
VV001	1/4SM	FG	45	45	45	100
VV001	1/4SM	BR	45	45	45	100
OVC003	1SM	BR	46	46	46	100
OVC005	2 1/2SM	BR	49	49	49	100
FEW030 BKN250	4SM	BR	52	50	51	93
FEW046 SCT150 SCT250	4SM	HZ	57	51	54	81
FEW049 SCT250	7SM	-	62	53	57	73
FEW043 BKN070 BKN250	10SM	-	62	53	57	73
FEW050 BKN065 BKN080 BK	10SM	-	65	55	59	70
BKN055 BKN080 BKN250	10SM	-	64	55	59	73
FEW060 BKN090 BKN130 OV	10SM	-	64	55	59	73
FEW055 SCT095 BKN130 BK	10SM	-	64	56	59	75
SCT036 BKN100 BKN250	10SM	-	61	56	58	84
SCT035 BKN075 BKN095	10SM	-	60	57	58	90
FEW038 BKN085 BKN110	10SM	-	61	59	60	93
SCT050 BKN070 OVC120	9SM	-RA	60	60	60	100
SCT024 BKN075 OVC110	10SM	-	61	60	60	97
SCT023 OVC080	10SM	-	62	60	61	93
SCT023CB BKN060 OVC080	10SM	TS	62	60	61	93
SCT028 BKN100	10SM	-	62	60	61	93
SCT029 BKN033 OVC100	10SM	-	63	60	61	90
FEW033 SCT049 OVC080	5SM	RA BR	53	51	52	93
OVC060	10SM	-	48	36	43	63
FEW055 SCT080	10SM	-	44	24	36	45
FEW065	10SM	-	41	19	33	41
FEW065	10SM	-	38	18	31	44
FEW065	10SM	-	39	17	31	41
FEW060	10SM	-	41	13	32	32
FEW060	10SM	-	41	14	32	33
SCT070	10SM	-	44	14	34	30
SCT075	10SM	-	44	11	33	26
SCT080	10SM	-	44	9	33	24
SCT075	10SM	-	42	10	32	27
SCT075	10SM	-	43	7	32	23
SCT090	10SM	-	41	5	30	22
SCT090	10SM	-	41	5	30	22
FEW090	10SM	-	38	7	29	27
FEW080	10SM	-	36	7	27	30
FEW080	10SM	-	34	7	26	32
FEW070	10SM	-	33	8	26	35

SCT070	10SM	-	32	8	25	36
FEW070	10SM	-	31	7	24	36
FEW060	10SM	-	30	8	24	39
FEW050	10SM	-	29	8	23	41
FEW050	10SM	-	29	8	23	41
FEW055	10SM	-	28	9	23	45
FEW055	10SM	-	27	12	23	53
CLR	10SM	-	27	10	22	49
FEW040	10SM	-	27	11	22	51
FEW050	10SM	-	27	8	22	45
FEW250	10SM	-	29	7	23	39
FEW250	10SM	-	31	7	24	36
FEW250	10SM	-	34	8	26	34
BKN250	10SM	-	35	8	27	32
BKN250	10SM	-	38	8	29	29
OVC250	10SM	-	39	8	29	28
BKN250	10SM	-	39	8	29	28
BKN008 OVC011	5SM	-RA BR	40	38	39	93
BKN008 OVC013	3SM	BR	40	39	40	97
BKN006 OVC015	2SM	-RA BR	40	40	40	100
OVC004	1 1/2SM	BR	39	39	39	100
SCT005 OVC010	2SM	-DZ BR	38	38	38	100
OVC005	2SM	-DZ BR	38	38	38	100
OVC005	2SM	BR	39	38	38	96
OVC007	4SM	BR	39	38	38	96
OVC007	7SM	-	38	37	38	97
OVC006	9SM	-	38	37	38	97
OVC008	10SM	-	38	37	38	97
OVC006	7SM	-	38	37	38	97
OVC006	8SM	-	38	37	38	97
OVC008	10SM	-	38	36	37	93
OVC009	10SM	-	37	35	36	93
FEW009 OVC042	10SM	-	38	36	37	93
FEW010 SCT035 BKN250	10SM	-	39	36	38	89
FEW010 SCT035 BKN250	10SM	-	41	35	38	79
FEW016 BKN250	10SM	-	43	34	39	71
BKN028 BKN035	10SM	-	44	34	40	68
BKN030 BKN037 OVC250	10SM	-	44	33	39	65
BKN030 OVC037	10SM	-	45	34	40	66
OVC033	10SM	-	45	33	40	63
BKN032 OVC041	10SM	-	44	35	40	71
BKN036 OVC044	10SM	-	45	34	40	66
BKN037 OVC055	10SM	-	46	33	40	61
BKN036 OVC050	10SM	-	46	33	40	61
OVC044	10SM	-	46	34	41	63
BKN038 OVC050	10SM	-	44	36	40	73
SCT035 BKN140 BKN250	10SM	-	43	35	40	74
BKN036 OVC140	10SM	-	42	35	39	76
BKN038 OVC055	10SM	-	42	33	38	71
FEW040 OVC140	10SM	-	42	32	38	68
BKN025 BKN130 OVC250	10SM	-	42	34	39	73
BKN020 BKN030 OVC040	10SM	-	42	34	39	73

FEW020 OVC040	10SM	-	42	35	39	76
FEW020 BKN030 OVC045	10SM	-	42	35	39	76
SCT018 SCT022 OVC031	10SM	-RA	41	37	39	86
SCT021 BKN026 OVC055	10SM	-	42	35	39	76
SCT250	10SM	-	53	32	44	45
FEW250	10SM	-	55	30	44	39
FEW250	10SM	-	56	32	45	40
FEW250	10SM	-	51	37	45	59
FEW250	10SM	-	56	29	44	36
FEW250	10SM	-	54	30	44	40
FEW250	10SM	-	50	37	44	61
FEW070 SCT110 BKN250	10SM	-	51	32	43	48
SCT042 BKN049 OVC060	7SM	-RA	40	35	38	83
OVC046	6SM	-SN	36	29	33	76
FEW014 BKN023 OVC035	3SM	-SN	32	26	30	79
FEW023 BKN040 OVC080	6SM	HZ	29	14	24	54
OVC095	10SM	-	28	6	22	39
OVC110	10SM	-	27	1	20	32
SCT050 BKN120	10SM	-	25	1	19	35
BKN045	10SM	-	24	6	19	46
SCT042 SCT050	10SM	-	23	3	18	42
FEW042	10SM	-	22	3	17	44
FEW043	10SM	-	23	2	18	40
SCT048	10SM	-	24	3	19	40
SCT055	10SM	-	27	2	21	34
SCT060	10SM	-	28	1	21	31
SCT060	10SM	-	30	2	23	30
SCT065	10SM	-	34	1	25	24
BKN060	10SM	-	34	0	25	23
BKN050	10SM	-	34	1	25	24
SCT050 BKN060	10SM	-	33	3	25	28
SCT050 BKN065	10SM	-	32	2	24	28
SCT050 BKN065	10SM	-	32	3	24	29
FEW050 BKN070	10SM	-	31	2	23	29
FEW050 BKN070	10SM	-	31	3	23	30
FEW050 SCT070	10SM	-	30	4	23	33
FEW070	10SM	-	29	6	23	38
CLR	10SM	-	29	7	23	39
FEW060	10SM	-	28	7	22	41
CLR	10SM	-	27	7	22	43
CLR	10SM	-	27	8	22	45
CLR	10SM	-	26	9	21	48
CLR	10SM	-	26	9	21	48
CLR	10SM	-	25	11	21	55
CLR	10SM	-	25	12	21	58
CLR	10SM	-	25	12	21	58
CLR	10SM	-	27	12	23	53
CLR	10SM	-	31	11	25	43
CLR	10SM	-	34	11	27	38
FEW050	10SM	-	37	12	29	36
FEW060	10SM	-	41	14	32	33
FEW060	10SM	-	43	12	33	28

FEW060	10SM	-	45	12	34	26
FEW070	10SM	-	46	11	34	24
CLR	10SM	-	48	11	35	22
CLR	10SM	-	49	12	36	23
CLR	10SM	-	49	12	36	23
CLR	10SM	-	47	12	35	24
CLR	10SM	-	44	17	34	34
CLR	10SM	-	44	17	34	34
CLR	10SM	-	43	17	34	35
CLR	10SM	-	42	18	33	38
CLR	10SM	-	41	18	33	39
CLR	10SM	-	40	18	32	41
CLR	10SM	-	40	17	32	40
CLR	10SM	-	37	18	31	46
CLR	10SM	-	38	14	30	37
CLR	10SM	-	38	16	31	41
CLR	10SM	-	36	18	30	48
CLR	10SM	-	34	17	28	50
SCT250	10SM	-	37	20	31	50
SCT250	10SM	-	41	18	33	39
BKN250	10SM	-	46	18	36	33
BKN250	10SM	-	50	19	38	29
SCT200 BKN250	10SM	-	54	21	41	28
FEW050 BKN200 OVC250	10SM	-	53	21	40	29
FEW050 SCT140 OVC200	10SM	-	55	21	41	27
SCT110 BKN180 OVC220	10SM	-	55	21	41	27
SCT100 BKN150 OVC200	10SM	-	55	19	41	24
SCT100 BKN140 OVC200	10SM	-	54	20	41	26
FEW075 SCT120 OVC200	10SM	-	54	20	41	26
FEW090 SCT120 BKN200	10SM	-	53	19	40	26
FEW090 BKN120 OVC200	10SM	-	51	21	39	31
BKN090 BKN120 OVC200	10SM	-	51	22	40	32
OVC085	10SM	-	50	24	40	36
OVC080	10SM	-	50	24	40	36
BKN075 OVC095	10SM	-	49	25	39	39
OVC065	10SM	-	49	24	39	38
BKN075 OVC150	10SM	-	48	24	38	39
OVC100	10SM	-	48	33	42	56
OVC110	10SM	-	47	33	41	59
OVC110	10SM	-	46	33	40	61
OVC100	10SM	-	39	28	35	65
BKN090 OVC200	10SM	-	37	25	33	62
OVC027	10SM	-	37	23	32	57
BKN030 OVC130	10SM	-	37	19	31	48
FEW035 BKN100 OVC140	10SM	-	40	18	32	41
FEW080 BKN100 OVC140	10SM	-	41	15	32	35
FEW075 BKN130 OVC200	10SM	-	43	18	34	37
FEW100 BKN130	10SM	-	44	18	35	35
SCT095 BKN140 OVC200	10SM	-	45	19	35	35
BKN100 OVC140	10SM	-	45	18	35	34
BKN100 OVC140	10SM	-	45	18	35	34
FEW037 BKN100 OVC150	10SM	-	45	19	35	35

FEW040 SCT110 BKN130	10SM	-	43	31	38	63
SCT030 BKN110 OVC140	10SM	-	43	29	37	58
FEW040 BKN100 OVC140	10SM	-	41	29	36	62
OVC120	10SM	-	41	27	36	57
OVC110	10SM	-	42	26	36	53
BKN080 OVC095	10SM	-PLRA	39	30	35	70
SCT055 OVC075	6SM	-PLRA	38	33	36	83
FEW055 OVC080	10SM	-PLRA	39	30	35	70
FEW018 BKN070 OVC090	10SM	-RA	39	32	36	76
BKN023 OVC045	10SM	-RA	39	33	37	79
OVC031	10SM	-	39	33	37	79
SCT029 BKN042 OVC140	10SM	-	39	32	36	76
SCT020 OVC040	10SM	-	40	32	37	73
SCT021 OVC036	10SM	-	40	31	36	70
FEW022 OVC036	10SM	-	40	30	36	68
FEW028 OVC034	10SM	-	40	29	36	65
BKN028 OVC032	10SM	-	40	30	36	68
BKN025 OVC032	10SM	-	40	31	36	70
BKN019 OVC028	8SM	-	40	34	37	79
OVC013	8SM	-	40	36	38	86
BKN008 OVC012	3SM	BR	40	38	39	93
BKN006 OVC012	2SM	-DZ BR	40	38	39	93
BKN005 OVC010	1 3/4SM	-DZ BR	41	39	40	93
BKN004 OVC009	1 1/2SM	-DZ BR	41	40	40	96
BKN004 OVC009	1SM	-DZ BR	42	41	42	96
BKN003 OVC007	1SM	-DZ BR	42	41	42	96
OVC002	1SM	-DZ BR	41	40	40	96
OVC002	1 1/2SM	-DZ BR	42	41	42	96
OVC002	1 1/2SM	BR	42	42	42	100
BKN002 BKN009 OVC016	2SM	+RA BR SQ	44	42	43	93
FEW012 OVC050	8SM	-RA	44	43	44	96
FEW037 BKN070 OVC080	5SM	RA BR	44	42	43	93
SCT030 OVC070	4SM	-RA BR	44	43	44	96
OVC006	5SM	-RA BR	45	44	45	97
OVC004	8SM	-	46	45	46	96
BKN004 BKN009 OVC020	4SM	-RA BR	46	45	46	96
FEW004 SCT017 OVC028	10SM	-	46	44	45	93
FEW012 SCT024 OVC047	10SM	-	46	43	45	89
FEW020 BKN030 BKN150	10SM	-	46	41	44	83
BKN030 BKN150 BKN200	10SM	-	46	38	42	73
FEW028 BKN150 BKN200	10SM	-	47	35	42	63
SCT033 SCT150 BKN250	10SM	-	48	34	42	58
SCT033 SCT250	10SM	-	52	33	44	49
SCT040 SCT250	10SM	-	53	34	44	49
FEW045 SCT250	10SM	-	54	34	45	47
FEW045 SCT250	10SM	-	54	33	45	45
FEW045 SCT250	10SM	-	52	31	43	45
FEW045 SCT250	10SM	-	51	30	42	45
FEW045 SCT250	10SM	-	48	29	40	48
FEW045 SCT250	10SM	-	44	27	37	51
FEW045	10SM	-	42	26	36	53
BKN045	10SM	-	42	26	36	53

BKN045	10SM	-	41	25	35	53	
SCT045	10SM	-	40	25	34	55	
FEW045	10SM	-	39	24	33	55	
SCT035	10SM	-	39	25	34	57	
FEW035	10SM	-	38	23	33	55	
FEW035	10SM	-	38	23	33	55	
CLR	10SM	-	37	23	32	57	
CLR	10SM	-	36	24	32	62	
CLR	10SM	-	35	24	31	64	
CLR	10SM	-	35	24	31	64	
CLR	10SM	-	37	24	32	60	
CLR	10SM	-	41	24	35	51	
FEW050	10SM	-	60	21	44	22	
CLR	10SM	-	59	22	44	24	
CLR	10SM	-	59	29	46	32	
CLR	10SM	-	57	27	44	32	
CLR	10SM	-	56	27	44	33	
FEW250	10SM	-	53	28	42	38	
FEW250	10SM	-	52	27	42	38	
FEW250	10SM	-	50	27	40	41	
CLR	10SM	-	48	27	39	44	
CLR	10SM	-	47	29	40	50	
CLR	10SM	-	46	31	40	56	
CLR	10SM	-	46	32	40	58	
CLR	10SM	-	45	35	41	68	
FEW250	10SM	-	46	35	41	66	
BKN250	10SM	-	44	36	40	73	
BKN250	10SM	-	44	35	40	71	
OVC070	10SM	-	45	37	42	74	
OVC070	10SM	-	50	39	45	66	
FEW030 OVC065	10SM	-	51	42	47	71	
FEW020 OVC055	10SM	-	51	42	47	71	
FEW021 OVC050	10SM	-	50	43	47	77	
FEW022 OVC046	8SM	-RA	50	42	46	74	
FEW020 BKN037 OVC044	2SM	-RA BR	48	44	46	86	
SCT008 OVC011	2 1/2SM	RA BR	47	45	46	93	
FEW005 BKN007 OVC011	2SM	-RA BR	48	46	47	93	
BKN006 OVC012	5SM	-RA BR	49	47	48	93	
FEW004 BKN006 OVC012	1 1/2SM	-RA BR	49	48	48	97	
FEW003 BKN005 OVC012	3SM	BR	50	48	49	93	
SCT007 BKN024 BKN037	10SM	-	50	46	48	86	
FEW007 SCT040	10SM	-	50	41	46	71	
FEW030	10SM	-	49	38	44	66	
CLR	10SM	-	48	37	43	66	
CLR	10SM	-	46	36	42	68	
CLR	10SM	-	45	36	41	71	
CLR	10SM	-	44	34	40	68	
SCT095	10SM	-	41	36	39	82	
SCT100	10SM	-	40	36	38	86	
CLR	10SM	-	41	34	38	76	
FEW100	10SM	-	41	32	37	70	
CLR	10SM	-	40	32	37	73	

CLR	10SM	-	41	32	37	70
CLR	10SM	-	45	30	39	56
FEW034	10SM	-	48	27	39	44
FEW045	10SM	-	50	23	39	35
SCT052	10SM	-	52	22	40	31
SCT070	10SM	-	54	24	42	31
SCT070	10SM	-	56	23	42	28
SCT080	10SM	-	55	21	41	27
BKN080 BKN250	10SM	-	59	25	45	27
BKN080 BKN250	10SM	-	57	24	43	28
SCT085	10SM	-	60	24	45	25
SCT090	10SM	-	59	23	44	25
FEW090	10SM	-	59	22	44	24
FEW090	10SM	-	57	22	43	26
CLR	10SM	-	56	24	43	29
CLR	10SM	-	53	29	43	40
CLR	10SM	-	49	30	41	48
CLR	10SM	-	50	25	40	38
CLR	10SM	-	46	30	39	54
CLR	10SM	-	44	31	39	60
CLR	10SM	-	43	30	38	60
CLR	10SM	-	42	28	37	58
CLR	10SM	-	42	27	36	55
CLR	10SM	-	40	25	34	55
CLR	10SM	-	42	26	36	53
CLR	10SM	-	45	25	37	46
CLR	10SM	-	48	24	39	39
CLR	10SM	-	49	23	39	36
CLR	10SM	-	51	22	40	32
FEW250	10SM	-	54	25	42	33
FEW250	10SM	-	58	25	44	28
FEW250	10SM	-	61	27	46	27
SCT250	10SM	-	63	27	47	26
FEW250	10SM	-	64	30	49	28
SCT250	10SM	-	64	27	48	25
CLR	10SM	-	64	28	48	26
OVC250	10SM	-	57	39	48	51
OVC250	10SM	-	55	40	48	57
FEW100 OVC250	10SM	-	53	40	47	61
SCT120 BKN250	10SM	-	53	40	47	61
BKN095 OVC250	10SM	-	52	39	46	61
FEW080 OVC100	10SM	-	51	41	46	69
OVC060	6SM	-RA	50	43	47	77
BKN045 OVC065	4SM	-RA BR	49	46	47	90
BKN033 BKN050 OVC070	5SM	-RA BR	49	46	47	90
SCT009 BKN028 OVC055	5SM	-RA BR	49	47	48	93
SCT009 BKN018 OVC024	4SM	RA BR	49	47	48	93
OVC005	2 1/2SM	RA BR	49	47	48	93
OVC006	2SM	RA BR	49	47	48	93
OVC005	2SM	RA BR	50	49	49	96
OVC005	2SM	RA BR	52	51	51	97
OVC005	1 1/2SM	-RA BR	53	52	53	96

OVC005	1 3/4SM	RA BR	52	51	51	97
OVC003	1 1/2SM	-RA BR	53	53	53	100
OVC003	2SM	-RA BR	54	53	53	97
OVC003	2SM	BR	55	53	54	93
OVC003	1 3/4SM	BR	55	53	54	93
OVC003	1SM	BR	54	53	53	97
OVC003	3/4SM	BR	55	54	55	96
OVC003	3/4SM	BR	57	55	56	93
OVC004	3/4SM	BR	56	55	55	97
OVC004	1 3/4SM	BR	56	55	55	97
BKN002 BKN011CB OVC039	2 1/2SM	TSRA BR	55	53	54	93
SCT019CB BKN036 OVC080	7SM	-TSRA	54	53	53	97
SCT023 SCT040CB OVC140	10SM	-	54	52	53	93
FEW040 BKN140	10SM	-	53	51	52	93
OVC006	10SM	-	53	51	52	93
SCT006 OVC090	8SM	-	52	50	51	93
FEW005 BKN055 OVC090	5SM	BR	51	50	51	96
FEW030 BKN039 OVC047	5SM	BR	52	50	51	93
SCT045 BKN060 OVC140	10SM	-	54	51	52	90
FEW045 SCT065 OVC090	10SM	-	54	49	51	83
SCT041 BKN050 OVC085	10SM	-	54	48	51	80
BKN048 BKN090	10SM	-	54	46	50	75
BKN026 BKN038 BKN053	10SM	-	51	44	48	77
FEW025 SCT034 BKN044	10SM	-	52	38	46	59
CLR	10SM	-	47	29	40	50
CLR	10SM	-	45	30	39	56
CLR	10SM	-	45	30	39	56
CLR	10SM	-	44	31	39	60
CLR	10SM	-	43	31	38	63
CLR	10SM	-	44	32	39	63
CLR	10SM	-	48	33	42	56
CLR	10SM	-	52	33	44	49
CLR	10SM	-	57	34	46	42
CLR	10SM	-	59	30	46	33
CLR	10SM	-	60	25	45	26
CLR	10SM	-	62	30	47	30
FEW250	10SM	-	65	28	48	25
FEW250	10SM	-	66	28	49	24
SCT250	10SM	-	65	28	48	25
BKN250	10SM	-	64	34	50	33
BKN250	10SM	-	63	34	49	34
SCT100 BKN250	10SM	-	60	37	49	42
SCT100 BKN250	10SM	-	60	34	48	38
BKN150 BKN250	10SM	-	58	35	47	42
BKN150 OVC250	10SM	-	58	36	48	44
SCT150 BKN250	10SM	-	56	35	46	46
FEW120 SCT150 BKN250	10SM	-	56	34	46	44
SCT150 BKN250	10SM	-	53	34	44	49
BKN150 OVC250	10SM	-	53	33	44	47
BKN150 OVC250	10SM	-	52	34	44	50
BKN130 BKN250	10SM	-	52	36	45	55
BKN130 BKN250	10SM	-	51	36	44	56

FEW130 SCT250	10SM	-	48	38	44	68	
FEW130	10SM	-	49	40	45	71	
FEW090	10SM	-	54	39	47	57	
FEW090	10SM	-	58	37	48	46	
FEW090 SCT130	10SM	-	62	38	50	41	
FEW130 SCT250	10SM	-	64	37	51	37	
FEW250	10SM	-	67	34	51	30	
FEW040 SCT250	10SM	-	67	38	53	35	
FEW040 SCT250	10SM	-	68	40	54	36	
FEW050 SCT250	10SM	-	68	40	54	36	
FEW060 FEW250	10SM	-	68	40	54	36	
FEW250	10SM	-	67	43	55	42	
CLR	10SM	-	66	45	55	47	
CLR	10SM	-	65	48	56	54	
CLR	10SM	-	63	48	55	58	
CLR	10SM	-	61	48	54	63	
CLR	10SM	-	60	49	54	67	
CLR	10SM	-	58	48	53	70	
CLR	10SM	-	56	48	52	75	
CLR	10SM	-	56	47	51	72	
CLR	10SM	-	54	48	51	80	
CLR	10SM	-	53	47	50	80	
CLR	10SM	-	52	48	50	86	
CLR	8SM	-	52	48	50	86	
CLR	6SM	BR	51	48	49	89	
SCT250	6SM	BR	52	49	50	89	
FEW250	5SM	HZ	55	50	52	83	
FEW250	6SM	HZ	59	50	54	72	
CLR	7SM	-	64	51	57	63	
SCT017 OVC025	7SM	-	64	54	58	70	
SCT017 OVC023	9SM	-	64	55	59	73	
BKN027 BKN035 OVC095	9SM	-	66	55	60	68	
SCT027 SCT035 BKN095 OV	8SM	-	67	56	61	68	
BKN025 OVC035	10SM	-	65	56	60	73	
BKN025 OVC035	9SM	-	63	56	59	78	
FEW015 OVC025	9SM	-	62	56	59	81	
BKN015 OVC025	7SM	-	62	55	58	78	
OVC015	7SM	-	62	55	58	78	
OVC013	10SM	-	61	55	58	81	
OVC013	9SM	-	61	55	58	81	
BKN015 OVC023	10SM	-	61	55	58	81	
OVC015	10SM	-	61	55	58	81	
OVC015	10SM	-	61	55	58	81	
OVC013	10SM	-	61	56	58	84	
BKN015 OVC020	10SM	-	60	55	57	84	
OVC016	10SM	-RA	60	56	58	86	
FEW013 OVC100	9SM	-RA	60	56	58	86	
FEW010 OVC017	4SM	-RA BR	59	57	58	93	
SCT009 OVC014	2 1/2SM	-RA BR	59	56	57	90	
BKN009 BKN015 OVC020	5SM	BR	59	57	58	93	
BKN009 BKN013 OVC018	10SM	-	60	55	57	84	
BKN007 OVC013	6SM	-RA BR	59	56	57	90	

BKN007 OVC015	4SM	-RA BR	59	56	57	90
BKN007 OVC015	10SM	-RA	60	56	58	86
BKN007 OVC013	9SM	-RA	59	56	57	90
SCT005 BKN009 OVC028	4SM	-RA BR	59	57	58	93
BKN007 BKN017 OVC032	4SM	RA BR	59	57	58	93
BKN008 BKN012 OVC019	4SM	-RA BR	60	58	59	93
BKN008 BKN013 OVC017	2SM	RA BR	60	58	59	93
BKN008 OVC015	4SM	BR	61	58	59	90
SCT003 BKN005 OVC012	1 1/4SM	-RA BR	60	59	60	96
BKN005 OVC013	1 1/2SM	-RA BR	60	59	60	96
BKN004 OVC010	1 1/2SM	-RA BR	60	58	59	93
SCT005 OVC010	6SM	-RA BR	59	57	58	93
BKN010 OVC014	9SM	-	60	57	58	90
BKN005 OVC015	1 3/4SM	BR	57	56	56	96
BKN005 OVC011	2SM	BR	57	56	56	96
SCT005 OVC011	1 1/2SM	-RA BR	57	56	56	96
BKN007 BKN012 OVC017	1 1/2SM	BR	57	55	56	93
BKN007 OVC010	1 1/2SM	-RA BR	56	55	55	97
SCT007 OVC010	3SM	-RA BR	56	54	55	93
FEW004 OVC014	2 1/2SM	-RA BR	55	54	55	96
BKN005 OVC012	5SM	BR	56	54	55	93
BKN005 OVC010	5SM	-DZ BR	56	54	55	93
BKN007 OVC012	6SM	-DZ BR	57	54	55	90
BKN009 OVC012	10SM	-	57	54	55	90
OVC012	10SM	-	58	54	56	87
OVC014	10SM	-	59	53	56	81
OVC014	8SM	-	60	53	56	78
OVC016	8SM	-	61	54	57	78
OVC018	7SM	-	63	54	58	73
OVC020	8SM	-	63	54	58	73
BKN022 OVC045	7SM	-	63	55	58	76
OVC022	7SM	-	64	55	59	73
BKN024 OVC048	7SM	-	64	56	59	75
BKN027 BKN050 OVC095	6SM	HZ	63	57	60	81
FEW027 SCT050 BKN110	6SM	HZ	63	57	60	81
FEW018 OVC024	7SM	-	62	57	59	84
BKN012 OVC041	7SM	-RA	61	57	59	87
BKN010 OVC090	9SM	-	61	58	59	90
BKN010 OVC075	7SM	-	61	58	59	90
FEW049	7SM	-	60	58	59	93
BKN055	6SM	BR	60	58	59	93
FEW055	8SM	-	60	56	58	86
FEW055 SCT110	9SM	-	59	55	57	87
SCT110	7SM	-	58	55	56	90
FEW060 BKN120	8SM	-	60	55	57	84
FEW050 BKN100 OVC250	7SM	-	61	56	58	84
OVC090	9SM	-	61	55	58	81
BKN090	10SM	-	63	56	59	78
FEW035 SCT090	10SM	-	70	56	62	61
SCT065 SCT090 BKN250	10SM	-	74	57	64	56
SCT060 SCT150 BKN250	10SM	-	77	57	65	50
SCT050 BKN250	10SM	-	77	57	65	50

FEW035 BKN075 BKN250	10SM	-DZ	76	53	62	45
SCT065CB BKN250	10SM	-	79	54	64	42
SCT055CB BKN100 BKN250	10SM	-	79	53	64	41
FEW055CB SCT085 BKN250	10SM	-	75	57	64	54
FEW050 SCT100 BKN250	10SM	-	76	56	64	50
FEW050CB SCT100 BKN250	10SM	-	76	54	63	47
SCT090 BKN250	10SM	-	74	55	63	52
SCT110 BKN250	10SM	-	70	58	63	66
SCT070 BKN100 BKN250	10SM	-	70	54	61	57
BKN095 BKN250	10SM	-	68	53	60	59
BKN100	10SM	-	66	53	59	63
FEW090 BKN110	10SM	-	65	53	58	66
FEW075	10SM	-	64	52	57	65
SCT070	10SM	-	62	53	57	73
FEW100	10SM	-	61	53	57	75
FEW110 SCT250	10SM	-	60	53	56	78
FEW110 SCT250	9SM	-	63	54	58	73
FEW110 SCT250	10SM	-	67	54	60	63
FEW250	10SM	-	70	53	60	55
FEW045 SCT250	10SM	-	73	52	61	48
FEW045	10SM	-	75	52	62	45
SCT050	10SM	-	75	53	62	46
FEW055 SCT065 SCT250	10SM	-	76	50	61	40
SCT055	10SM	-	76	52	62	43
SCT065	10SM	-	80	49	62	34
SCT065	10SM	-	80	48	62	33
SCT065	10SM	-	80	47	61	31
FEW065 SCT100	10SM	-	80	48	62	33
FEW065CB BKN110	10SM	-	78	48	61	35
FEW060CB SCT100 BKN250	10SM	-	77	48	61	36
SCT060CB BKN090 BKN120	10SM	-TSRA	74	52	61	46
FEW060CB SCT090 SCT120	10SM	-	67	53	59	61
FEW070 SCT120 SCT250	10SM	-	67	52	58	59
FEW090	10SM	-	64	53	58	68
FEW090	10SM	-	63	53	57	70
FEW090	10SM	-	62	52	56	70
CLR	10SM	-	61	51	56	70
CLR	10SM	-	62	50	56	65
FEW250	10SM	-	60	50	55	70
FEW250	10SM	-	61	50	55	67
SCT250	10SM	-	63	52	57	68
BKN250	10SM	-	67	51	58	57
BKN250	10SM	-	69	49	58	49
BKN250	10SM	-	72	49	59	44
BKN250	10SM	-	73	49	60	43
FEW045 SCT250	10SM	-	76	48	60	37
FEW050 SCT250	10SM	-	78	48	61	35
FEW060 SCT090 BKN250	10SM	-	79	49	62	35
FEW070 SCT090 BKN250	10SM	-	80	47	61	31
BKN075 BKN150 OVC250	10SM	-	77	52	62	42
SCT085 BKN250	10SM	-	76	53	63	45
FEW075 SCT090 BKN250	10SM	-	76	53	63	45

FEW090 SCT150 BKN250	10SM	-	75	54	63	48
SCT065 SCT090 BKN150 BK	10SM	-	74	52	61	46
FEW070 BKN110 BKN250	10SM	-	70	56	62	61
FEW070 SCT080 BKN110	10SM	-	67	58	62	73
BKN100	10SM	-	67	57	61	71
SCT090	10SM	-	67	57	61	71
CLR	10SM	-	66	56	60	70
CLR	10SM	-	67	54	60	63
CLR	10SM	-	66	55	60	68
OVC090	9SM	-RA	64	56	59	75
SCT055 OVC100	7SM	-RA	63	58	60	84
SCT060 OVC100	9SM	-	63	58	60	84
SCT045 OVC095	6SM	-RA	63	58	60	84
SCT100 BKN110	8SM	-	65	59	62	81
FEW055 SCT100	9SM	-	70	59	63	68
FEW100 SCT250	9SM	-	72	57	63	60
FEW050 SCT100 SCT250	10SM	-	74	58	64	57
FEW030 SCT045 BKN110 BK	10SM	-	75	59	65	58
FEW030 SCT120 SCT250	10SM	-	76	56	64	50
FEW035 SCT120 SCT250	10SM	-	77	58	65	52
FEW040 SCT110 BKN250	10SM	-	77	60	67	56
FEW040 SCT110 BKN250	10SM	-	77	61	67	58
FEW045CB SCT110 BKN150	10SM	-	78	60	67	54
SCT045CB BKN070 BKN250	7SM	TSRA	77	58	65	52
SCT026 BKN045CB BKN075	9SM	-TSRA	64	55	59	73
FEW045 FEW120 SCT220	9SM	-	68	58	62	70
FEW045 FEW120 SCT220	8SM	-	66	60	62	81
FEW120	9SM	-	68	61	64	78
FEW120	8SM	-	65	59	62	81
CLR	10SM	-	67	58	62	73
CLR	9SM	-	66	59	62	78
CLR	7SM	-	65	59	62	81
CLR	7SM	-	63	58	60	84
CLR	5SM	BR	62	59	60	90
CLR	6SM	HZ	63	58	60	84
CLR	4SM	HZ	64	58	60	81
CLR	3SM	HZ	66	61	63	84
CLR	4SM	HZ	69	61	64	76
CLR	4SM	HZ	71	62	65	73
FEW090	4SM	HZ	73	61	66	66
FEW080	5SM	HZ	76	61	67	60
SCT055	6SM	HZ	77	62	68	60
SCT050	7SM	-	78	61	67	56
SCT045	9SM	-	79	58	66	49
SCT045	10SM	-	79	57	66	47
FEW065	10SM	-	79	56	65	45
FEW065	10SM	-	76	58	65	54
FEW065	10SM	-	75	58	65	55
FEW250	10SM	-	73	56	63	55
FEW250	10SM	-	72	56	63	57
FEW250	10SM	-	69	61	64	76
FEW250	10SM	-	68	62	64	81

FEW250	10SM	-	68	62	64	81
FEW250	10SM	-	67	61	63	81
CLR	10SM	-	67	61	63	81
CLR	10SM	-	66	61	63	84
CLR	10SM	-	65	61	63	87
CLR	9SM	-	64	60	62	87
CLR	8SM	-	63	59	61	87
FEW250	7SM	-	63	59	61	87
CLR	6SM	BR	65	61	63	87
CLR	8SM	-	68	61	64	78
CLR	10SM	-	71	61	65	71
CLR	10SM	-	74	60	65	62
CLR	10SM	-	76	60	66	58
SCT055	10SM	-	82	61	69	49
SCT060	10SM	-	82	59	68	46
SCT060	10SM	-	82	59	68	46
FEW060	10SM	-	82	59	68	46
FEW060	10SM	-	81	58	67	46
CLR	10SM	-	79	58	66	49
FEW250	10SM	-	77	58	65	52
FEW180 SCT250	10SM	-	75	57	64	54
CLR	10SM	-	74	57	64	56
FEW250	10SM	-	73	57	64	57
CLR	10SM	-	70	57	62	64
CLR	10SM	-	70	57	62	64
CLR	10SM	-	69	56	61	63
CLR	10SM	-	68	56	61	66
CLR	10SM	-	66	57	61	73
SCT250	10SM	-	66	57	61	73
FEW250	10SM	-	64	57	60	78
FEW250	10SM	-	66	58	61	75
FEW120 SCT250	10SM	-	69	59	63	70
SCT075 SCT250	10SM	-	73	59	65	62
FEW250	10SM	-	76	60	66	58
FEW250	10SM	-	81	61	68	51
FEW250	10SM	-	85	62	70	46
SCT060 SCT250	9SM	-	88	62	71	42
FEW065 SCT250	9SM	-	88	61	71	40
FEW065 SCT250	9SM	-	87	61	70	42
FEW060 SCT250	10SM	-	88	59	70	38
SCT050 SCT250	10SM	-	87	60	70	40
FEW050 SCT250	10SM	-	87	59	69	39
FEW050 SCT250	10SM	-	86	58	68	39
FEW120 SCT250	10SM	-	84	59	68	43
SCT250	10SM	-	80	62	69	54
CLR	10SM	-	78	62	68	58
CLR	10SM	-	76	61	67	60
FEW250	10SM	-	76	60	66	58
CLR	10SM	-	75	59	65	58
CLR	10SM	-	73	55	62	53
CLR	10SM	-	72	54	62	53
CLR	10SM	-	70	55	61	59

SCT100	10SM	-	69	56	61	63
FEW100 BKN250	10SM	-	69	57	62	66
CLR	10SM	-	70	58	63	66
FEW090 SCT250	10SM	-	72	59	64	64
FEW090 SCT250	10SM	-	75	60	66	60
FEW150 SCT250	10SM	-	80	62	69	54
FEW150 BKN250	10SM	-	82	62	69	51
BKN250	10SM	-	83	63	70	51
BKN250	10SM	-	87	64	72	46
SCT250	9SM	-	88	63	72	43
BKN250	9SM	-	87	64	72	46
CLR	8SM	-	88	65	73	46
CLR	8SM	-	87	64	72	46
FEW250	8SM	-	87	65	73	48
FEW100 SCT250	8SM	-	86	65	72	50
FEW250	8SM	-	85	64	71	50
FEW140 SCT250	9SM	-	84	64	71	51
FEW140 SCT250	9SM	-	82	65	71	56
FEW140 BKN250	10SM	-	81	66	71	61
SCT120 BKN250	10SM	-	80	65	70	60
FEW120 BKN250	10SM	-	78	65	70	64
FEW140 BKN250	9SM	-	77	65	69	66
FEW140 BKN250	9SM	-	76	66	69	72
FEW140 BKN250	9SM	-	75	66	69	74
SCT250	9SM	-	74	65	68	74
SCT250	8SM	-	74	64	68	71
SCT250	8SM	-	76	64	68	67
SCT250	6SM	HZ	80	65	70	60
SCT250	5SM	HZ	83	66	72	57
BKN250	6SM	HZ	85	67	73	55
BKN250	6SM	HZ	87	68	74	53
FEW048 SCT150 BKN250	8SM	-	87	67	74	51
SCT050 BKN130 BKN250	9SM	-	89	67	74	48
FEW050 BKN140	10SM	-	90	66	74	45
FEW055 BKN140	10SM	-	90	64	73	42
FEW055 SCT140 BKN250	10SM	-	90	65	73	44
SCT055 BKN250	10SM	-	89	66	74	47
SCT050 BKN250	10SM	-	90	68	75	49
BKN050 BKN250	10SM	-	87	67	74	51
SCT055TCU SCT150 BKN250	10SM	-	87	66	73	50
SCT060 BKN140 BKN250	10SM	-	86	64	72	48
FEW060 BKN140	10SM	-	85	64	71	50
SCT140	10SM	-	83	65	71	55
SCT140	10SM	-	82	64	70	55
BKN120	9SM	-	80	65	70	60
SCT120 BKN250	7SM	-	78	66	70	67
OVC120	6SM	HZ	77	67	70	71
OVC090	6SM	HZ	77	67	70	71
OVC070	9SM	-	77	65	69	66
BKN090 OVC110	6SM	HZ	77	66	70	69
FEW090 BKN130	6SM	HZ	77	67	70	71
FEW090 SCT150 BKN250	5SM	HZ	80	66	71	62

SCT065 BKN140 OVC250	9SM	-	81	60	68	49
FEW065 BKN130 BKN250	10SM	-	81	53	64	38
FEW080 SCT140 SCT250	10SM	-	82	45	61	27
FEW140 SCT250	10SM	-	81	52	64	37
FEW250	10SM	-	82	55	66	40
FEW140	10SM	-	83	59	68	44
FEW140	10SM	-	83	58	67	43
SCT140 BKN250	10SM	-	81	55	65	41
BKN140 BKN250	10SM	-	78	56	65	47
FEW140 SCT250	10SM	-	75	59	65	58
FEW140 BKN250	10SM	-	75	62	67	64
SCT250	9SM	-	74	65	68	74
SCT250	8SM	-	74	66	69	76
SCT250	6SM	HZ	74	67	69	79
SCT250	6SM	HZ	75	68	71	79
SCT250	5SM	HZ	75	68	71	79
SCT250	4SM	HZ	76	69	71	79
FEW250	4SM	HZ	75	69	71	82
FEW250	4SM	BR	73	69	71	87
FEW250	3SM	HZ	75	70	72	84
FEW250	3SM	HZ	76	70	72	82
FEW250	3SM	HZ	79	70	73	74
CLR	3SM	HZ	83	71	75	67
CLR	4SM	HZ	87	71	76	59
FEW035	4SM	HZ	89	72	77	57
FEW035	4SM	HZ	92	72	78	52
SCT045TCU	5SM	HZ	92	72	78	52
SCT045CB BKN075	5SM	TS HZ	91	73	78	56
SCT050CB SCT080 BKN250	8SM	-	92	70	77	49
FEW050CB SCT150 OVC250	10SM	-	94	67	75	41
FEW060 BKN150 BKN250	10SM	-	91	69	76	49
SCT060 BKN100 BKN250	10SM	-	92	67	75	44
BKN070 BKN100 OVC150	7SM	-	82	69	73	65
SCT065 BKN130 OVC150	6SM	HZ	83	71	75	67
BKN150	6SM	HZ	81	73	76	77
BKN250	7SM	-	82	72	75	72
SCT150 BKN250	10SM	-	82	72	75	72
SCT250	10SM	-	82	72	75	72
SCT130 BKN250	10SM	-	82	72	75	72
BKN130	10SM	-	81	72	75	74
BKN130	10SM	-	81	72	75	74
BKN130	10SM	-	80	72	74	76
BKN130	10SM	-	79	71	74	77
SCT130 OVC250	9SM	-	79	71	74	77
FEW130 BKN250	9SM	-	79	71	74	77
BKN250	10SM	-	81	70	74	69
BKN250	9SM	-	83	70	74	65
BKN250	8SM	-	85	70	75	61
FEW045 SCT120 BKN250	8SM	-	87	69	75	55
FEW045 SCT120 BKN250	7SM	-	88	70	76	55
SCT041 BKN130 BKN250	8SM	-	90	70	76	52
FEW042 BKN250	8SM	-	91	69	76	49

SCT045 BKN250	8SM	-	90	69	76	50
SCT055	8SM	-	92	68	75	46
SCT050TCU BKN150 BKN250	9SM	-	90	66	74	45
FEW030 OVC055CB	2SM	TSRA	82	71	74	69
BKN035 BKN050CB OVC100	6SM	-TSRA	75	70	72	84
SCT050CB BKN070 OVC100	9SM	TS	76	70	72	82
SCT006 SCT020 OVC045CB	6SM	-TSRA BR	72	69	70	91
OVC035CB	4SM	TSRA BR	71	69	70	94
SCT045 OVC150	9SM	-	72	69	70	91
FEW015 SCT040 BKN150	8SM	-	72	69	70	91
FEW015 SCT050 BKN150	9SM	-	71	68	69	90
OVC150	10SM	-	71	67	68	87
OVC100	8SM	-	70	67	68	90
SCT100	7SM	-	70	65	67	84
SCT008 BKN100 BKN250	7SM	-	70	67	68	90
FEW008 BKN120 OVC250	5SM	BR	70	67	68	90
FEW048 BKN070 OVC250	5SM	BR	70	68	69	93
FEW050 SCT070 BKN140	6SM	BR	72	68	69	87
FEW035 SCT140 BKN250	7SM	-	75	68	70	79
FEW018 SCT025 BKN140	8SM	-	77	67	70	71
BKN030 BKN140	10SM	-	79	65	70	62
SCT033 SCT049 BKN140	10SM	-	81	64	70	57
SCT038 BKN055 BKN140	10SM	-	82	65	71	56
FEW040TCU BKN140 OVC25	10SM	-	85	66	72	53
FEW047 BKN150 BKN250	10SM	-	85	64	71	50
FEW050 SCT140 BKN250	10SM	-	86	63	71	46
SCT050CB BKN080 BKN140	10SM	-	84	63	70	49
FEW050 SCT140 BKN250	10SM	-	84	63	70	49
FEW050TCU SCT140 SCT25	10SM	-	84	64	71	51
FEW060CB SCT140 SCT250	10SM	-	82	64	70	55
FEW060CB SCT150 SCT250	10SM	-	81	63	69	54
FEW060 SCT250	10SM	-	79	61	68	54
SCT250	10SM	-	78	61	67	56
CLR	10SM	-	78	57	65	48
CLR	10SM	-	76	55	64	48
CLR	10SM	-	74	54	62	50
CLR	10SM	-	73	54	62	51
CLR	10SM	-	72	55	62	55
FEW120	10SM	-	72	55	62	55
FEW120	10SM	-	70	56	62	61
FEW100 SCT250	10SM	-	72	57	63	60
FEW100 SCT250	10SM	-	75	57	64	54
SCT250	10SM	-	78	58	66	50
SCT250	10SM	-	80	58	66	47
FEW060 SCT250	10SM	-	82	58	67	44
FEW060 SCT250	10SM	-	83	56	66	40
SCT070 SCT250	10SM	-	85	55	67	36
SCT070 SCT250	10SM	-	84	54	66	36
SCT075 BKN250	10SM	-	84	54	66	36
SCT070 BKN250	10SM	-	85	56	67	37
FEW070 BKN250	10SM	-	84	53	65	35
FEW070 BKN250	10SM	-	85	54	66	35

OVC250	10SM	-	85	52	65	32
FEW075 OVC250	10SM	-	84	54	66	36
BKN250	10SM	-	82	53	65	37
BKN250	10SM	-	78	62	68	58
BKN250	10SM	-	76	61	67	60
BKN250	10SM	-	74	60	65	62
BKN250	10SM	-	74	59	65	60
SCT150 BKN250	10SM	-	73	60	65	64
SCT150 BKN250	10SM	-	72	61	65	69
SCT150 BKN250	10SM	-	70	61	65	73
FEW250	10SM	-	70	61	65	73
FEW065	10SM	-	70	62	65	76
FEW065	9SM	-	71	63	66	76
FEW065	7SM	-	71	64	67	79
FEW065	9SM	-	74	64	68	71
FEW065 SCT250	10SM	-	77	65	69	66
FEW250	9SM	-	81	65	71	58
FEW050 SCT250	10SM	-	84	64	71	51
SCT055 BKN250	10SM	-	84	63	70	49
SCT060	10SM	-	84	61	69	46
SCT065 BKN130 BKN250	10SM	-	86	62	71	45
SCT070 BKN090	10SM	-	86	63	71	46
BKN060 BKN090	10SM	-	85	62	70	46
SCT060 BKN090	10SM	-	83	62	70	49
SCT060 BKN075 BKN100	10SM	-	83	61	69	48
FEW060 SCT080 SCT250	10SM	-	82	61	69	49
SCT080 BKN250	10SM	-	80	60	68	51
SCT100 BKN250	10SM	-	78	59	66	52
SCT250	10SM	-	76	59	65	56
FEW250	10SM	-	75	57	64	54
FEW100	10SM	-	75	56	64	52
FEW100	10SM	-	72	57	63	60
FEW100	10SM	-	72	58	64	61
SCT110	10SM	-	72	59	64	64
BKN100 OVC130	10SM	-	71	60	64	68
BKN110	10SM	-	71	61	65	71
SCT110 BKN250	10SM	-	72	61	65	69
FEW110 BKN250	10SM	-	74	62	67	67
BKN250	10SM	-	77	64	69	64
BKN250	10SM	-	82	65	71	56
BKN250	9SM	-	85	64	71	50
OVC250	9SM	-	86	65	72	50
OVC250	10SM	-	87	64	72	46
FEW055 OVC250	9SM	-	88	65	73	46
FEW060 SCT140 OVC250	9SM	-	88	64	72	45
FEW060 BKN140 OVC250	9SM	-	87	63	71	45
FEW060 BKN140 OVC250	9SM	-	89	65	73	45
FEW060 SCT140 BKN250	9SM	-	88	64	72	45
FEW140 SCT250	8SM	-	87	64	72	46
FEW250	8SM	-	86	64	72	48
CLR	7SM	-	85	65	72	51
SCT250	8SM	-	84	65	71	53

FEW250	8SM	-	82	66	71	58
FEW250	7SM	-	80	67	71	64
CLR	9SM	-	78	64	69	62
CLR	10SM	-	77	63	68	62
CLR	10SM	-	76	61	67	60
CLR	10SM	-	75	62	67	64
FEW250	10SM	-	75	63	67	66
FEW140 SCT250	8SM	-	74	64	68	71
FEW250	7SM	-	75	62	67	64
CLR	6SM	HZ	77	67	70	71
CLR	6SM	HZ	81	68	72	65
CLR	5SM	HZ	85	70	75	61
CLR	4SM	HZ	88	71	76	57
SCT250	5SM	HZ	92	72	78	52
FEW050 SCT250	5SM	HZ	94	73	79	51
SCT055TCU	5SM	HZ	95	72	79	47
SCT060TCU	6SM	HZ	96	72	79	46
FEW060TCU BKN250	6SM	HZ	97	70	78	42
FEW060 SCT250	6SM	HZ	96	71	78	44
FEW050TCU SCT250	6SM	HZ	95	73	79	49
FEW055 BKN250	5SM	HZ	94	73	79	51
FEW060 BKN250	5SM	HZ	92	73	78	54
BKN250	5SM	HZ	91	72	78	54
BKN250	6SM	HZ	90	72	77	56
SCT250	6SM	HZ	89	73	78	59
SCT250	6SM	HZ	88	74	78	63
FEW250	5SM	HZ	85	73	77	68
FEW250	5SM	HZ	84	74	77	72
FEW250	5SM	HZ	84	74	77	72
FEW015 SCT250	4SM	HZ	83	74	77	74
FEW060 SCT250	5SM	HZ	82	74	76	77
BKN250	4SM	HZ	83	73	76	72
SCT250	4SM	HZ	83	73	76	72
SCT250	5SM	HZ	85	72	76	65
BKN250	7SM	-	88	71	76	57
BKN250	8SM	-	89	72	77	57
FEW055 BKN250	10SM	-	95	69	77	43
SCT055 BKN250	10SM	-	97	68	77	39
SCT060 BKN250	10SM	-	98	69	78	39
SCT065 BKN250	10SM	-	98	70	78	40
SCT065 BKN250	10SM	-	97	70	78	42
SCT065 BKN250	10SM	-	96	69	77	42
FEW065 SCT250	10SM	-	96	69	77	42
FEW045 SCT140 SCT250	10SM	-	94	69	77	44
FEW060 SCT250	10SM	-	93	69	76	46
BKN250	10SM	-	92	70	77	49
SCT250	10SM	-	90	71	77	54
SCT250	10SM	-	88	72	77	59
FEW250	10SM	-	88	72	77	59
FEW250	10SM	-	86	70	75	59
CLR	10SM	-	86	71	76	61
CLR	10SM	-	85	70	75	61

FEW250	10SM	-	83	69	74	63
SCT250	10SM	-	81	72	75	74
SCT250	10SM	-	84	71	75	65
SCT250	10SM	-	87	72	76	61
SCT250	10SM	-	89	72	77	57
FEW250	10SM	-	91	72	78	54
FEW040 SCT250	10SM	-	94	71	78	48
FEW050 SCT250	10SM	-	96	68	77	40
FEW055 SCT250	10SM	-	96	68	77	40
SCT055	10SM	-	97	69	77	40
SCT060	10SM	-	98	70	78	40
FEW065	10SM	-	99	68	77	37
FEW065	10SM	-	99	67	77	35
FEW070	10SM	-	98	66	76	35
FEW070	10SM	-	96	67	76	39
FEW045 BKN250	10SM	-	93	68	76	44
SCT150 SCT250	10SM	-	91	70	76	50
FEW045 SCT130 BKN250	9SM	-	90	70	76	52
SCT100 BKN250	9SM	-	89	70	76	53
BKN070 BKN250	10SM	-	88	70	76	55
BKN060 BKN075	10SM	-	86	70	75	59
BKN065	10SM	-	84	68	73	59
SCT090 BKN250	10SM	-	83	67	72	59
SCT060 BKN090 BKN250	10SM	-	81	67	72	62
FEW250	10SM	-	80	56	65	44
FEW250	10SM	-	78	52	63	40
FEW250	10SM	-	77	51	62	40
FEW250	10SM	-	77	53	63	44
FEW250	10SM	-	78	55	64	45
FEW150 SCT250	10SM	-	81	54	65	39
FEW150 SCT250	10SM	-	82	51	64	34
FEW050 FEW150 SCT250	10SM	-	83	50	64	32
FEW050 FEW120 SCT250	10SM	-	84	50	64	31
FEW050 FEW120 SCT250	10SM	-	85	50	64	30
FEW050 FEW120 SCT250	10SM	-	84	50	64	31
FEW060 BKN250	10SM	-	84	50	64	31
FEW060 SCT250	10SM	-	83	50	64	32
FEW060 SCT250	10SM	-	82	50	63	33
FEW070 BKN250	10SM	-	80	50	63	35
FEW065 BKN250	10SM	-	77	49	61	37
FEW065 BKN250	10SM	-	76	50	61	40
BKN250	10SM	-	74	49	60	41
BKN250	9SM	-	72	52	60	50
SCT250	10SM	-	71	52	60	51
SCT250	10SM	-	70	52	60	53
SCT250	10SM	-	69	47	57	45
SCT250	10SM	-	67	53	59	61
SCT250	10SM	-	66	53	59	63
SCT250	10SM	-	66	52	58	61
CLR	9SM	-	66	49	57	54
CLR	10SM	-	67	44	55	44
CLR	10SM	-	70	54	61	57

CLR	10SM	-	72	53	61	52
CLR	10SM	-	75	55	63	50
FEW050 SCT250	10SM	-	78	54	64	43
FEW050 BKN250	10SM	-	80	53	64	39
FEW050 BKN250	10SM	-	81	53	64	38
FEW055 OVC250	10SM	-	81	53	64	38
FEW060 OVC250	10SM	-	81	54	65	39
FEW070 BKN250	10SM	-	82	51	64	34
OVC230	5SM	HZ	81	50	63	34
OVC230	4SM	HZ	80	51	63	37
OVC230	4SM	HZ	78	49	62	36
OVC230	4SM	HZ	77	50	62	39
SCT230	4SM	HZ	75	50	61	42
BKN230	5SM	HZ	74	49	60	41
BKN230	5SM	HZ	73	50	60	44
BKN230	5SM	HZ	72	50	60	46
BKN230	5SM	HZ	71	48	58	44
BKN230	5SM	HZ	69	51	59	53
CLR	5SM	HZ	68	51	58	55
SCT230	5SM	HZ	67	51	58	57
BKN230	4SM	HZ	68	51	58	55
FEW250	3SM	HZ	68	51	58	55
CLR	3SM	HZ	69	52	59	55
CLR	3SM	HZ	70	53	60	55
CLR	3SM	HZ	72	54	62	53
CLR	2 1/2SM	HZ	75	55	63	50
CLR	2SM	HZ	78	55	64	45
FEW060 SCT250	2SM	HZ	82	55	66	40
FEW060 SCT250	2SM	HZ	84	53	65	35
FEW065 SCT250	3SM	HZ	87	56	68	35
FEW120 SCT250	3SM	HZ	88	53	67	30
CLR	5SM	FU	89	52	67	28
CLR	5SM	FU	89	52	67	28
CLR	4SM	FU	87	54	67	32
CLR	4SM	FU	86	53	66	32
CLR	4SM	FU	84	54	66	36
CLR	4SM	FU	82	56	66	41
CLR	4SM	HZ FU	80	57	66	45
CLR	5SM	HZ FU	78	56	65	47
CLR	5SM	HZ FU	76	56	64	50
CLR	5SM	HZ FU	74	56	63	54
CLR	5SM	HZ FU	71	56	62	59
CLR	5SM	HZ FU	69	56	61	63
SCT250	5SM	HZ	68	57	62	68
FEW250	5SM	HZ	68	58	62	70
SCT250	4SM	HZ	65	55	59	70
SCT250	4SM	HZ	68	55	60	63
SCT250	5SM	HZ	72	58	64	61
SCT250	7SM	-	78	58	66	50
SCT250	10SM	-	85	56	67	37
BKN250	10SM	-	87	53	66	31
BKN250	8SM	-	88	57	69	35

BKN250	3SM	HZ	90	53	67	28
BKN250	3SM	HZ	91	54	68	28
OVC250	3SM	HZ	92	54	68	28
OVC250	3SM	HZ	91	53	68	28
BKN250	3SM	HZ	91	55	69	30
FEW090 BKN250	6SM	HZ	92	57	70	31
FEW095 BKN250	6SM	HZ	90	57	69	33
BKN250	6SM	HZ	89	57	69	34
BKN250	6SM	HZ	86	60	69	42
BKN250	6SM	HZ	86	59	69	40
SCT250	5SM	HZ	84	62	70	48
BKN250	4SM	HZ	79	63	69	58
SCT250	4SM	HZ	78	63	69	60
SCT250	4SM	HZ	77	61	67	58
OVC250	4SM	HZ	76	62	67	62
OVC250	4SM	HZ	75	63	67	66
BKN250	4SM	HZ	74	65	68	74
FEW140 BKN250	4SM	HZ	74	65	68	74
SCT140 BKN250	3SM	HZ	75	66	69	74
BKN150 OVC250	4SM	HZ	77	66	70	69
SCT150 OVC250	4SM	HZ	78	65	70	64
FEW150 BKN250	4SM	HZ	82	65	71	56
BKN150 BKN250	5SM	HZ	86	66	73	51
BKN130 OVC250	4SM	HZ	88	67	74	50
BKN140 BKN250	5SM	HZ	89	66	74	47
BKN140 BKN250	6SM	HZ	92	67	75	44
FEW060 BKN140 BKN250	7SM	-	94	67	75	41
FEW060 BKN140 BKN250	6SM	HZ	94	69	77	44
SCT065 SCT090 BKN150 OV	6SM	HZ	92	69	76	47
BKN060CB BKN070 OVC150	2SM	TS BR	77	75	76	94
FEW090 BKN150	5SM	HZ	81	75	77	82
FEW080 BKN110	5SM	BR	78	74	75	87
FEW070 BKN120	7SM	-	78	73	75	85
SCT080 BKN130	7SM	-	78	72	74	82
BKN085 OVC110	7SM	-	78	72	74	82
FEW080 BKN150 OVC250	6SM	HZ	77	72	74	85
SCT075 BKN120	5SM	BR	76	73	74	91
BKN027 OVC065	5SM	BR	75	72	73	90
BKN027 OVC075	4SM	BR	74	72	73	94
FEW070 OVC095	6SM	HZ	75	70	72	84
FEW031 OVC100	6SM	HZ	74	69	71	85
BKN055 BKN090 OVC110	6SM	HZ	73	68	70	84
SCT055 BKN070	6SM	HZ	73	67	69	81
FEW022 SCT060 BKN110 BK	6SM	HZ	74	65	68	74
FEW060 SCT130 BKN250	4SM	HZ	76	64	68	67
SCT029 SCT060 BKN250	4SM	HZ	78	65	70	64
SCT029 BKN250	5SM	HZ	78	65	70	64
SCT038	7SM	-	81	64	70	57
SCT042 SCT060 BKN140 BK	10SM	-	77	55	64	47
FEW044 SCT140 BKN200	10SM	-	78	54	64	43
FEW045 SCT065 OVC130	10SM	-	75	54	63	48
FEW050 SCT130 BKN200	10SM	-	74	54	62	50

FEW055 SCT130 BKN250	10SM	-	72	50	60	46
FEW055 SCT130 BKN250	10SM	-	69	48	58	47
FEW100 SCT250	10SM	-	66	45	55	47
CLR	10SM	-	64	42	53	45
CLR	10SM	-	62	40	51	44
CLR	10SM	-	60	38	49	44
CLR	10SM	-	59	37	49	44
CLR	10SM	-	57	38	48	49
CLR	10SM	-	56	38	47	51
CLR	10SM	-	54	39	47	57
CLR	10SM	-	53	39	46	59
CLR	10SM	-	51	39	46	64
CLR	10SM	-	51	39	46	64
CLR	10SM	-	50	39	45	66
FEW025	10SM	-	51	39	46	64
FEW025	10SM	-	53	40	47	61
SCT049 BKN250	10SM	-	60	37	49	42
SCT049 BKN250	10SM	-	61	37	49	41
FEW055 BKN250	10SM	-	61	37	49	41
FEW055 BKN250	10SM	-	61	37	49	41
BKN250	10SM	-	61	37	49	41
BKN250	10SM	-	58	38	48	48
SCT250	10SM	-	58	39	49	50
SCT250	10SM	-	58	39	49	50
BKN250	10SM	-	58	40	49	51
BKN250	10SM	-	58	40	49	51
SCT250	10SM	-	55	41	48	59
SCT250	9SM	-	54	42	48	64
BKN250	10SM	-	51	43	47	74
BKN250	10SM	-	50	44	47	80
BKN250	10SM	-	50	44	47	80
BKN250	10SM	-	49	44	47	83
SCT250	10SM	-	48	45	47	89
BKN130 BKN250	10SM	-	48	45	47	89
FEW100 BKN130 BKN250	10SM	-	50	46	48	86
FEW090 BKN130 OVC200	10SM	-	52	46	49	80
FEW027 SCT090 BKN130 OV	10SM	-	55	48	51	77
FEW035 BKN130 OVC200	10SM	-	60	50	55	70
BKN039 OVC130	10SM	-	63	47	55	56
BKN037 OVC130	10SM	-	63	48	55	58
FEW036 BKN046 BKN130	10SM	-	64	49	56	58
SCT038 BKN047 BKN130	10SM	-	64	49	56	58
BKN033 OVC060	10SM	-	63	50	56	63
SCT032 BKN047 OVC060	10SM	-	63	50	56	63
BKN035 OVC043	10SM	-	62	49	55	62
BKN030 OVC040	10SM	-	62	50	56	65
OVC030	10SM	-	62	50	56	65
OVC030	10SM	-	62	50	56	65
OVC032	10SM	-	62	50	56	65
OVC032	10SM	-	62	50	56	65
BKN028 OVC035	10SM	-	62	53	57	73
OVC028	10SM	-	63	53	57	70

OVC028	10SM	-	63	52	57	68
OVC032	10SM	-	63	53	57	70
OVC028	10SM	-	63	53	57	70
OVC025	10SM	-	63	54	58	73
BKN027 OVC037	10SM	-	63	54	58	73
BKN028 OVC034	10SM	-	64	55	59	73
BKN030 OVC041	10SM	-	64	56	59	75
FEW015 OVC023	10SM	-RA	63	56	59	78
SCT015 BKN021 OVC028	9SM	-	62	58	60	86
FEW015 BKN025 OVC036	10SM	-	63	57	60	81
FEW007 BKN010 OVC017	2 1/2SM	-RA BR	62	59	60	90
BKN010 BKN021 OVC027	10SM	-	63	58	60	84
BKN018 OVC023	10SM	-RA	64	56	59	75
BKN025 OVC031	10SM	-RA	64	55	59	73
SCT025 OVC045	10SM	-	63	54	58	73
FEW025 OVC045	10SM	-	63	55	58	76
SCT050 BKN080 OVC100	10SM	-	62	53	57	73
SCT027 BKN049 OVC070	9SM	-RA	61	54	57	78
FEW025 SCT044 OVC090	8SM	-RA	59	54	56	83
SCT024 OVC085	7SM	-RA	58	54	56	87
SCT024 OVC090	6SM	-RA BR	57	54	55	90
FEW014 BKN023 OVC028	5SM	-RA BR	58	55	56	90
SCT008 BKN014 OVC028	5SM	-RA BR	58	56	57	93
BKN008 BKN013 OVC019	5SM	-RA BR	57	55	56	93
OVC013	5SM	-RA BR	57	54	55	90
FEW011 OVC019	5SM	-RA BR	57	54	55	90
BKN044 OVC070	4SM	RA BR	56	54	55	93
SCT010 BKN024 OVC044	4SM	RA BR	57	55	56	93
FEW011 BKN035 OVC049	6SM	-RA BR	56	55	55	97
SCT012 BKN030 OVC045	7SM	-RA	56	53	54	90
BKN009 OVC020	2 1/2SM	RA BR	56	55	55	97
BKN005 OVC012	2 1/2SM	-RA BR	57	55	56	93
BKN006 OVC020	2 1/2SM	RA BR	58	56	57	93
BKN006 BKN022 OVC028	2 1/2SM	-RA BR	59	56	57	90
BKN005 OVC028	2SM	+RA BR	60	58	59	93
BKN005 BKN013 OVC018	2 1/2SM	RA BR	59	58	58	96
BKN005 OVC013	2 1/2SM	RA BR	60	59	60	96
BKN007 OVC013	2 1/2SM	-RA BR	60	59	60	96
OVC005	2 1/2SM	-RA BR	61	59	60	93
OVC005	2 1/2SM	RA BR	62	60	61	93
BKN008 BKN014 OVC020	2 1/2SM	RA BR	62	61	61	96
BKN008 OVC018	2 1/2SM	RA BR	62	60	61	93
BKN014 OVC019	2 1/2SM	-RA BR	62	60	61	93
FEW004 OVC009	2 1/2SM	-RA BR	62	61	61	96
SCT006 OVC009	2 1/2SM	-RA BR	62	61	61	96
BKN007 OVC012	2 1/2SM	RA BR	62	61	61	96
FEW004 BKN010 OVC020	2 1/2SM	-RA BR	62	61	61	96
BKN004 OVC016	1 1/2SM	RA BR	62	61	61	96
BKN004 OVC009	1 3/4SM	RA BR	63	62	62	97
OVC004	1 3/4SM	+RA BR	63	62	62	97
OVC008	1 3/4SM	RA BR	62	60	61	93
BKN008 OVC013	1 3/4SM	BR	61	60	60	97

BKN008 OVC014	6SM	DZ BR	61	60	60	97
SCT008 OVC011	6SM	-RA BR	61	60	60	97
BKN010 OVC016	2 1/2SM	-RA BR	62	60	61	93
BKN005 BKN010 OVC016	1 1/2SM	-RA BR	61	60	60	97
BKN009 OVC015	2 1/2SM	-RA BR	61	59	60	93
BKN009 OVC016	2SM	-RA BR	61	59	60	93
FEW004 BKN012 OVC018	2SM	-RA BR	61	59	60	93
SCT007 BKN010 OVC015	3SM	-RA BR	61	59	60	93
SCT007 BKN015 OVC021	3SM	DZ BR	61	59	60	93
SCT007 BKN012 OVC019	3SM	-DZ BR	61	59	60	93
BKN006 BKN012 OVC019	3SM	-DZ BR	61	59	60	93
BKN008 OVC014	3SM	-DZ BR	60	58	59	93
BKN008 BKN016 OVC022	3SM	-RA BR	59	58	58	96
BKN008 BKN016 OVC022	3SM	-RA	59	57	58	93
BKN007 OVC013	3SM	-RA BR	58	57	57	97
BKN007 OVC015	3SM	BR	58	57	57	97
BKN008 OVC012	3SM	BR	58	57	57	97
BKN008 OVC013	3SM	-DZ BR	57	57	57	100
BKN008 OVC013	3SM	-DZ BR	57	56	56	96
BKN007 OVC011	2SM	-DZ BR	57	56	56	96
BKN006 OVC013	2SM	-DZ BR	57	56	56	96
BKN006 OVC011	2SM	-DZ BR	56	56	56	100
BKN004 OVC009	2SM	-DZ BR	56	56	56	100
OVC007	2SM	BR	56	56	56	100
BKN004 OVC007	2 1/2SM	BR	56	56	56	100
OVC004	2 1/2SM	BR	56	56	56	100
OVC004	2SM	BR	56	56	56	100
OVC004	1 1/2SM	BR	57	56	56	96
OVC006	2SM	BR	57	56	56	96
OVC006	2SM	BR	58	57	57	97
OVC006	2SM	BR	59	57	58	93
OVC008	2SM	BR	60	58	59	93
OVC008	3SM	BR	61	58	59	90
BKN008 OVC012	3SM	BR	62	58	60	86
BKN010 OVC015	3SM	BR	62	58	60	86
SCT010 OVC020	5SM	HZ	63	58	60	84
OVC014	7SM	-	62	58	60	86
BKN016 OVC055	7SM	-	62	58	60	86
FEW010 SCT035 OVC045	7SM	-	62	58	60	86
OVC012	7SM	-	62	59	60	90
FEW013 BKN019 OVC049	6SM	-RA BR	62	59	60	90
FEW023 OVC070	10SM	-	59	48	53	67
OVC080	10SM	-	58	46	52	65
FEW050	10SM	-	56	46	51	70
SCT050	10SM	-	55	46	51	72
FEW029 SCT035	10SM	-	54	44	49	69
FEW035	10SM	-	52	34	44	50
CLR	10SM	-	50	33	43	52
CLR	10SM	-	49	34	42	57
FEW040 SCT250	10SM	-	48	34	42	58
FEW040 SCT250	10SM	-	48	33	42	56
FEW035 SCT140 BKN250	10SM	-	55	32	45	42

FEW040 SCT150 BKN250	10SM	-	56	38	47	51
SCT040 BKN140 OVC250	10SM	-	57	39	48	51
SCT036 BKN140 OVC200	10SM	-	57	43	50	60
BKN036	10SM	-	56	41	49	57
BKN040 OVC200	10SM	-	56	42	49	60
BKN040 BKN150 OVC250	10SM	-	56	43	49	62
BKN032 BKN150 OVC250	10SM	-	56	44	50	65
FEW035 BKN110 BKN250	10SM	-	56	45	50	67
BKN031 OVC110	10SM	-	56	45	50	67
FEW035 OVC140	10SM	-	56	47	51	72
BKN033 OVC120	10SM	-	56	48	52	75
BKN021 BKN034 OVC070	10SM	-	56	48	52	75
BKN021 OVC038	10SM	-RA	55	50	52	83
BKN017 OVC030	10SM	-RA	56	51	53	84
FEW019 BKN030 OVC044	10SM	-RA	56	52	54	87
OVC016	6SM	-RA BR	54	52	53	93
BKN013 OVC022	5SM	-RA BR	53	52	53	96
BKN007 OVC013	3SM	-RA BR	52	51	51	97
BKN005 OVC011	2SM	-RA BR	52	50	51	93
BKN006 OVC011	2SM	-RA BR	51	50	51	96
BKN007 OVC011	3SM	-RA BR	51	49	50	92
BKN006 OVC011	1 1/2SM	-RA BR	52	50	51	93
BKN006 OVC015	1 1/2SM	-RA BR	53	51	52	93
BKN004 OVC011	1 1/2SM	-RA BR	53	52	53	96
BKN004 OVC014	1 1/4SM	-RA BR	54	53	53	97
BKN003 OVC010	1 1/4SM	RA BR	54	53	53	97
BKN005 OVC010	1 1/4SM	-RA BR	54	52	53	93
BKN005 OVC010	1 1/4SM	-RA BR	52	50	51	93
SCT008 OVC012	4SM	-RA BR	51	48	49	89
SCT018 BKN030	10SM	-	51	46	49	83
SCT030 BKN060	10SM	-	52	45	49	77
CLR	10SM	-	51	46	49	83
FEW030	10SM	-	51	46	49	83
FEW027	10SM	-	50	44	47	80
SCT028	10SM	-	50	44	47	80
SCT028	10SM	-	49	44	47	83
CLR	10SM	-	48	43	46	83
CLR	10SM	-	46	44	45	93
FEW027	10SM	-	47	44	46	90
CLR	10SM	-	45	43	44	93
CLR	10SM	-	46	43	45	89
FEW120	10SM	-	44	42	43	93
FEW050	10SM	-	47	44	46	90
FEW050	10SM	-	50	44	47	80
FEW040	10SM	-	54	45	49	72
FEW035	10SM	-	59	45	52	60
SCT032	10SM	-	61	45	53	56
FEW035 SCT042 BKN060	10SM	-	61	44	52	54
SCT045 BKN070	10SM	-	60	45	52	58
BKN050 BKN070	10SM	-	61	44	52	54
BKN070	10SM	-	59	45	52	60
FEW040 OVC080	10SM	-	60	46	53	60

BKN045 BKN075	10SM	-	59	47	53	64
BKN040 OVC090	10SM	-RA	59	48	53	67
SCT045 BKN055 OVC075	8SM	-RA	53	47	50	80
BKN040 OVC055	10SM	-RA	52	46	49	80
OVC060	10SM	-	51	45	48	80
SCT070 OVC085	10SM	-	51	45	48	80
FEW065 SCT080 BKN200	10SM	-	49	45	47	86
FEW080 BKN130 OVC200	10SM	-	49	43	46	80
OVC130	10SM	-	48	42	45	80
SCT055 BKN130	10SM	-	46	42	44	86
BKN055	10SM	-	46	41	44	83
FEW050 SCT130	10SM	-	45	40	43	83
FEW050 SCT130	10SM	-	45	39	42	80
CLR	10SM	-	45	39	42	80
FEW018	10SM	-	48	40	44	74
FEW028	10SM	-	49	38	44	66
FEW032	10SM	-	51	36	44	56
FEW040	10SM	-	53	35	45	51
FEW040	10SM	-	56	35	46	46
FEW050	10SM	-	57	34	46	42
SCT055	10SM	-	58	34	47	41
SCT055	10SM	-	58	33	47	39
FEW060	10SM	-	58	34	47	41
FEW060	10SM	-	56	33	46	42
CLR	10SM	-	54	34	45	47
CLR	10SM	-	52	35	44	53
CLR	10SM	-	52	36	45	55
CLR	10SM	-	50	37	44	61
CLR	10SM	-	47	38	43	71
CLR	10SM	-	46	38	42	73
CLR	10SM	-	47	38	43	71
CLR	10SM	-	45	38	42	77
CLR	10SM	-	45	38	42	77
SCT120	10SM	-	46	38	42	73
SCT140	10SM	-	45	38	42	77
FEW250	10SM	-	45	39	42	80
FEW150 SCT250	10SM	-	45	39	42	80
SCT150 SCT250	9SM	-	48	41	45	77
BKN120 BKN250	10SM	-	52	43	48	72
BKN120	10SM	-	54	43	49	67
OVC110	10SM	-	56	44	50	65
BKN080 OVC120	10SM	-RA	59	47	53	64
OVC080	10SM	-	60	45	52	58
SCT070 BKN100 BKN200	10SM	-	62	47	54	58
BKN060 OVC100	10SM	-	63	47	55	56
OVC060	10SM	-	62	47	54	58
OVC055	10SM	-	61	48	54	63
BKN050 OVC060	10SM	-	60	48	54	65
FEW060 BKN090	10SM	-	59	49	54	69
FEW055 SCT090 BKN250	10SM	-	58	49	53	72
FEW055 SCT095 BKN150	10SM	-	57	49	53	75
SCT090 BKN150	10SM	-	57	49	53	75

FEW060 SCT100 BKN150 OV	10SM	-	56	49	52	77
FEW050 BKN140 OVC250	10SM	-	56	48	52	75
FEW045 OVC150	10SM	-	55	46	51	72
FEW047 OVC250	10SM	-	53	41	47	64
CLR	10SM	-	52	38	46	59
FEW045 BKN150 OVC250	10SM	-	51	37	45	59
FEW045 SCT075 SCT250	10SM	-	49	37	44	64
FEW070 SCT150 SCT250	10SM	-	48	37	43	66
SCT075 OVC250	10SM	-	49	37	44	64
FEW075 OVC250	10SM	-	51	37	45	59
FEW070 BKN250	10SM	-	54	38	46	55
FEW045 BKN250	10SM	-	56	37	47	49
FEW045 OVC250	10SM	-	58	37	48	46
FEW055 BKN250	10SM	-	60	36	49	41
FEW055 BKN250	10SM	-	60	36	49	41
FEW090 BKN250	10SM	-	60	35	48	39
BKN250	10SM	-	60	35	48	39
FEW150 BKN250	10SM	-	58	34	47	41
BKN250	10SM	-	57	34	46	42
BKN250	10SM	-	57	35	47	44
BKN250	10SM	-	55	34	46	45
FEW150 BKN200	10SM	-	53	36	45	52
SCT150 BKN250	10SM	-	50	37	44	61
SCT150 BKN250	10SM	-	50	38	44	63
BKN150 BKN250	10SM	-	51	37	45	59
BKN055 BKN140	10SM	-	50	40	45	68
FEW060 BKN140 OVC250	10SM	-	48	38	44	68
FEW060 OVC140	10SM	-	47	38	43	71
FEW060 SCT140 OVC250	10SM	-	46	39	43	77
BKN140 OVC250	10SM	-	48	36	43	63
BKN140 OVC250	10SM	-	48	33	42	56
BKN140 BKN250	10SM	-	48	32	41	54
BKN140 BKN250	10SM	-	49	31	41	50
SCT140 BKN250	10SM	-	50	31	42	48
SCT140 BKN250	10SM	-	53	30	43	41
SCT140 BKN250	10SM	-	54	31	44	42
FEW055 SCT150 BKN250	10SM	-	56	31	45	39
FEW050 SCT150 SCT250	10SM	-	56	31	45	39
FEW050 SCT250	10SM	-	56	32	45	40
FEW050 SCT250	10SM	-	56	31	45	39
FEW050 SCT200	10SM	-	56	32	45	40
FEW200	10SM	-	54	32	44	43
SCT150 SCT250	10SM	-	52	32	43	47
FEW150	10SM	-	52	31	43	45
FEW150	10SM	-	51	31	42	46
FEW150	10SM	-	48	32	41	54
CLR	10SM	-	46	33	40	61
CLR	10SM	-	46	32	40	58
CLR	10SM	-	44	32	39	63
CLR	10SM	-	44	32	39	63
SCT250	10SM	-	42	32	38	68
SCT250	10SM	-	41	32	37	70

SCT250	10SM	-	40	31	36	70
FEW250	10SM	-	41	30	37	65
FEW250	10SM	-	40	31	36	70
FEW130 SCT250	10SM	-	40	32	37	73
FEW250	10SM	-	43	33	39	68
OVC021	10SM	-	47	38	43	71
FEW030 SCT130 SCT250	10SM	-	52	35	44	53
FEW030 SCT130 SCT250	10SM	-	54	33	45	45
FEW048 SCT250	10SM	-	55	32	45	42
FEW048 SCT130 BKN250	10SM	-	54	32	44	43
SCT045 SCT140 BKN250	10SM	-	54	30	44	40
SCT140 SCT250	10SM	-	51	29	42	43
FEW130 SCT250	10SM	-	49	28	40	45
SCT130	10SM	-	48	29	40	48
SCT130	10SM	-	47	28	39	48
SCT250	10SM	-	45	28	38	52
SCT250	10SM	-	44	28	38	53
FEW150 SCT250	10SM	-	43	29	37	58
FEW250	10SM	-	41	30	37	65
FEW250	10SM	-	38	31	35	76
CLR	10SM	-	37	30	34	76
CLR	10SM	-	38	28	34	68
CLR	10SM	-	38	28	34	68
FEW250	10SM	-	37	27	33	67
FEW150 SCT250	10SM	-	37	26	33	65
FEW150 SCT250	10SM	-	39	26	34	60
FEW100 BKN250	10SM	-	42	23	35	47
FEW100 BKN250	10SM	-	45	23	37	42
FEW120 SCT250	10SM	-	47	22	37	37
SCT110 BKN250	10SM	-	48	21	38	34
FEW090 BKN110 BKN250	10SM	-	49	22	38	35
BKN100 BKN120 BKN250	10SM	-	48	22	38	36
SCT070 BKN095 BKN250	10SM	-	49	25	39	39
SCT075 BKN100 BKN250	10SM	-	49	24	39	38
BKN065 BKN100 OVC250	10SM	-	49	26	40	41
BKN060 OVC100	10SM	-	49	25	39	39
BKN060 OVC100	10SM	-	49	27	40	43
OVC060	10SM	-	48	29	40	48
OVC060	10SM	-	48	29	40	48
OVC055	10SM	-	47	29	40	50
OVC055	10SM	-	47	29	40	50
OVC045	10SM	-	47	32	41	56
OVC055	10SM	-	46	30	39	54
OVC050	10SM	-	46	31	40	56
BKN042 OVC049	10SM	-	46	31	40	56
BKN042 OVC050	10SM	-	45	31	39	58
OVC047	10SM	-	45	36	41	71
OVC044	10SM	-	45	36	41	71
OVC044	10SM	-	45	36	41	71
OVC040	10SM	-	47	34	41	61
OVC040	10SM	-	47	34	42	60
OVC038	10SM	-	50	33	43	52

OVC036	10SM	-	50	33	43	52
OVC041	10SM	-	49	31	41	50
OVC032	10SM	-	49	30	41	48
OVC036	10SM	-	50	32	42	50
OVC040	10SM	-	51	31	42	46
OVC060	10SM	-	51	31	42	46
OVC060	10SM	-	51	31	42	46
FEW042 OVC055	10SM	-	51	31	42	46
FEW043 OVC055	10SM	-	51	36	44	56
FEW060 OVC090	10SM	-	52	37	45	57
FEW032 OVC080	10SM	-RA	52	42	47	68
FEW028 BKN070 OVC085	10SM	-RA	52	44	48	74
SCT024 BKN031 OVC055	8SM	-RA	51	47	49	86
SCT014 BKN018 OVC023	3SM	RA BR	51	48	49	89
SCT009 BKN013 OVC025	3SM	RA BR	51	49	50	92
BKN009 OVC017	3SM	RA BR	51	49	50	92
OVC007	3SM	RA BR	51	49	50	92
OVC007	5SM	-RA BR	53	52	53	96
SCT009 BKN015 OVC021	3SM	+RA BR	54	53	53	97
BKN005 BKN009 OVC031	3SM	-RA BR	52	51	51	97
BKN005 OVC022	3SM	BR	53	52	53	96
SCT005 BKN023 OVC027	4SM	-DZ BR	54	53	53	97
SCT005 BKN010 BKN080	9SM	-	56	54	55	93
BKN008 OVC016	9SM	-	57	55	56	93
OVC006	8SM	-	57	55	56	93
OVC008	10SM	-	58	54	56	87
OVC008	10SM	-	57	53	55	87
BKN010 BKN014	10SM	-	58	51	54	78
BKN017 BKN035	9SM	-	57	51	54	81
SCT017 BKN024 BKN035	10SM	-	57	49	53	75
FEW022 SCT035	10SM	-	57	48	52	72
FEW024	10SM	-	56	47	51	72
CLR	10SM	-	54	47	50	77
CLR	10SM	-	53	48	51	83
CLR	10SM	-	52	47	49	83
CLR	10SM	-	51	47	49	86
BKN038	10SM	-	49	46	47	90
BKN036	10SM	-	51	47	49	86
OVC034	10SM	-	53	43	48	69
BKN038	10SM	-	52	41	47	66
FEW036	10SM	-	51	39	46	64
CLR	10SM	-	49	36	43	61
CLR	10SM	-	48	36	43	63
CLR	10SM	-	47	36	42	66
CLR	10SM	-	46	37	42	71
FEW250	10SM	-	49	38	44	66
CLR	10SM	-	53	40	47	61
CLR	10SM	-	54	40	47	59
SCT040 SCT250	10SM	-	58	42	50	56
SCT045 BKN250	10SM	-	58	42	50	56
BKN050 BKN250	10SM	-	59	42	51	54
BKN060 BKN250	10SM	-	60	43	51	53

BKN046 OVC055	10SM	-	59	43	51	56
FEW042 BKN055	10SM	-	59	42	51	54
BKN060	10SM	-	59	42	51	54
BKN065	10SM	-	59	42	51	54
BKN060	10SM	-	57	39	48	51
SCT050 BKN065	10SM	-	54	36	46	51
BKN050	10SM	-	53	32	44	45
BKN060	10SM	-	52	33	44	49
BKN065	10SM	-	51	34	44	52
SCT065	10SM	-	49	35	43	59
BKN065	10SM	-	48	36	43	63
BKN065	10SM	-	48	36	43	63
FEW065 BKN140	10SM	-	48	34	42	58
FEW065 BKN140	10SM	-	48	35	42	61
BKN120	10SM	-	48	34	42	58
BKN130	10SM	-	47	35	42	63
BKN130 BKN250	10SM	-	46	36	42	68
FEW060 BKN100	10SM	-	48	34	42	58
OVC110	10SM	-	48	34	42	58
SCT110 BKN250	10SM	-	49	34	42	57
FEW055 SCT130 BKN250	10SM	-	50	34	43	54
FEW040 SCT130 BKN250	10SM	-	52	31	43	45
FEW045 SCT110 BKN250	10SM	-	52	31	43	45
FEW045 BKN130 BKN250	10SM	-	52	31	43	45
FEW045 BKN120 BKN250	10SM	-	53	30	43	41
FEW045 BKN100 BKN250	10SM	-	52	30	42	43
FEW045 BKN100 BKN250	10SM	-	51	31	42	46
FEW045 SCT110 SCT250	10SM	-	50	29	41	44
FEW110 SCT250	10SM	-	49	30	41	48
FEW250	10SM	-	47	28	39	48
CLR	10SM	-	46	28	39	50
FEW150	10SM	-	45	27	38	49
CLR	10SM	-	44	28	38	53
CLR	10SM	-	41	30	37	65
CLR	10SM	-	40	30	36	68
CLR	10SM	-	40	31	36	70
CLR	10SM	-	40	31	36	70
CLR	10SM	-	39	31	36	73
CLR	10SM	-	38	31	35	76
CLR	10SM	-	37	31	35	79
FEW150 SCT250	10SM	-	38	31	35	76
FEW012 SCT150 SCT250	10SM	-	40	30	36	68
FEW020 SCT250	10SM	-	43	28	37	56
FEW020 BKN250	10SM	-	44	27	37	51
FEW028 SCT150 OVC250	10SM	-	44	25	37	47
FEW055 BKN130 OVC200	10SM	-	45	24	37	44
FEW045 BKN130 OVC200	10SM	-	45	23	37	42
FEW065 BKN130 OVC200	10SM	-	45	24	37	44
SCT065 BKN130 OVC200	10SM	-	44	25	37	47
BKN055 OVC130	10SM	-	44	26	37	49
SCT050 OVC080	10SM	-	43	27	37	53
OVC028	5SM	-PLRA	40	31	36	70

OVC023	9SM	-RA	41	30	37	65
OVC023	6SM	-RASN	39	28	35	65
SCT025 OVC055	10SM	-RA	39	31	36	73
BKN055 BKN070 OVC095	10SM	-PLRA	39	31	36	73
SCT048 BKN060 OVC085	10SM	-RA	37	32	35	82
SCT050 OVC080	10SM	-	38	37	37	95
FEW050 OVC090	10SM	-	39	29	35	67
OVC046	10SM	-	40	26	35	58
FEW037 OVC046	10SM	-	41	24	35	51
SCT035 BKN045 OVC080	10SM	-PLRA	39	26	34	60
BKN055 OVC075	10SM	-	39	27	34	62
OVC039	10SM	-	40	26	35	58
OVC046	10SM	-	40	26	35	58
OVC048	10SM	-	41	26	35	55
OVC048	10SM	-	42	27	36	55
BKN048 OVC060	10SM	-	42	27	36	55
OVC048	10SM	-	43	28	37	56
BKN047 OVC070	10SM	-	44	29	38	55
OVC049	10SM	-	44	28	38	53
BKN045 OVC070	10SM	-	44	30	38	58
BKN045 OVC065	10SM	-	43	30	38	60
SCT070 OVC100	10SM	-DZ	43	30	38	60
BKN047 OVC080	10SM	-RA	41	34	38	76
FEW041 OVC070	8SM	-RA	38	34	36	86
OVC055	10SM	-RA	38	32	36	79
OVC050	10SM	-RA	37	31	35	79
FEW045 OVC055	10SM	-RA	38	31	35	76
BKN041 OVC049	10SM	-	38	30	35	73
SCT042 OVC090	10SM	-	39	28	35	65
FEW034 OVC090	10SM	-	38	27	34	65
FEW060 OVC090	10SM	-	39	27	34	62
SCT055 OVC100	10SM	-	39	27	34	62
OVC100	10SM	-	38	25	33	60
BKN100	10SM	-	38	24	33	57
OVC100	10SM	-	38	22	32	53
FEW085 BKN110 BKN150	10SM	-	38	21	32	51
FEW080 BKN110 BKN150	10SM	-	38	20	32	48
SCT100 BKN150	10SM	-	40	21	33	47
FEW110 SCT150 SCT250	10SM	-	42	20	34	41
FEW130	10SM	-	45	19	35	35
FEW130	10SM	-	47	19	37	33
FEW130 SCT250	10SM	-	50	17	38	27
FEW140 SCT250	10SM	-	50	17	38	27
FEW150 SCT250	10SM	-	51	12	37	21
FEW150 SCT250	10SM	-	51	16	38	25
SCT150 BKN250	10SM	-	49	17	37	28
FEW150 SCT250	10SM	-	49	16	37	27
SCT100 BKN250	10SM	-	48	18	37	30
BKN110 OVC250	10SM	-	45	25	37	46
FEW250	10SM	-	59	35	48	41
FEW250	10SM	-	61	35	49	38
FEW250	10SM	-	61	35	49	38

BKN250	10SM	-	60	35	48	39
BKN250	10SM	-	57	36	47	45
BKN250	10SM	-	56	38	47	51
BKN250	10SM	-	54	38	46	55
BKN250	10SM	-	53	39	46	59
SCT250	10SM	-	51	40	46	66
SCT250	10SM	-	50	40	45	68
SCT250	10SM	-	49	40	45	71
SCT250	9SM	-	48	41	45	77
SCT250	8SM	-	48	41	45	77
SCT250	8SM	-	46	41	44	83
FEW250	8SM	-	47	42	45	83
FEW250	7SM	-	46	42	44	86
BKN250	7SM	-	46	42	44	86
FEW250	6SM	BR	45	41	43	86
FEW150 BKN250	5SM	BR	44	41	43	89
FEW150 BKN250	4SM	BR	46	43	45	89
FEW150 BKN250	6SM	HZ	49	43	46	80
FEW150 BKN250	7SM	-	53	44	49	72
BKN250	8SM	-	55	44	50	67
FEW150 SCT200 BKN250	10SM	-	59	44	51	58
SCT150 SCT200 BKN250	10SM	-	61	44	52	54
SCT150 BKN250	10SM	-	64	44	54	48
SCT150 BKN250	10SM	-	62	45	53	54
BKN150 BKN250	10SM	-	60	45	52	58
SCT150 BKN250	10SM	-	60	45	52	58
SCT150 BKN250	10SM	-	58	46	52	65
SCT150 BKN250	10SM	-	59	46	52	62
BKN150 BKN250	10SM	-	58	46	52	65
SCT150 BKN250	10SM	-	56	46	51	70
SCT150 BKN250	10SM	-	56	47	51	72
BKN150 BKN250	9SM	-	55	48	51	77
BKN150 BKN250	9SM	-	55	49	52	80
BKN150 BKN250	8SM	-	54	49	51	83
SCT055 BKN150	8SM	-	54	50	52	87
BKN055 OVC150	8SM	-	54	50	52	87
SCT060 BKN150	10SM	-	54	50	52	87
SCT060 BKN150	10SM	-	55	50	52	83
BKN065 OVC140	10SM	-	56	51	53	84
FEW060 OVC070	10SM	-	59	53	56	81
FEW050 BKN070 BKN150	10SM	-	62	53	57	73
BKN070 BKN100	10SM	-	64	53	58	68
BKN080	10SM	-	66	54	59	65
BKN036 BKN043 OVC065	10SM	-	70	58	63	66
SCT040 BKN065 BKN150 OV	10SM	-	72	59	64	64
FEW036 SCT085 BKN120 OV	10SM	-	71	59	64	66
BKN039 BKN060 BKN090 OV	10SM	-RA	69	60	64	73
BKN039 BKN048 BKN140	10SM	-	66	59	62	78
BKN060	10SM	-	66	59	62	78
SCT060 BKN120	10SM	-	66	59	62	78
BKN045 BKN055 BKN080	10SM	-	65	58	61	78
BKN045	10SM	-	63	58	60	84

SCT047 OVC065	10SM	-	63	58	60	84
OVC070	10SM	-	65	60	62	84
BKN065 BKN080	10SM	-	65	61	63	87
SCT075	10SM	-	65	60	62	84
SCT021 BKN080	10SM	-	64	60	62	87
FEW008 BKN017 BKN110	10SM	-	65	61	63	87
FEW008 OVC015	10SM	-	66	62	64	87
OVC017	10SM	-	66	62	64	87
OVC017	10SM	-	67	62	64	84
OVC015	10SM	-	67	63	64	87
OVC014	9SM	-	68	63	65	84
FEW180 BKN250	10SM	-	56	35	46	46
FEW150 BKN250	10SM	-	54	36	46	51
BKN250	10SM	-	54	36	46	51
BKN150 BKN250	10SM	-	54	36	46	51
SCT120 BKN150 BKN250	10SM	-	51	36	44	56
FEW120	10SM	-	52	37	45	57
SCT150 BKN250	10SM	-	49	38	44	66
SCT130 BKN250	10SM	-	50	37	44	61
BKN130 OVC250	10SM	-	48	39	44	71
BKN110 OVC250	10SM	-	47	38	43	71
OVC110	10SM	-	47	38	43	71
OVC080	10SM	-	46	38	42	73
OVC070	10SM	-	46	37	42	71
OVC065	10SM	-	45	36	41	71
BKN023 OVC070	10SM	-RA	45	37	42	74
OVC023	10SM	-RA	44	38	41	79
OVC021	8SM	-RA	47	41	44	80
OVC019	8SM	-RA	46	41	44	83
OVC016	7SM	-RA	45	41	43	86
OVC016	10SM	-DZ	45	40	43	83
OVC012	7SM	-RA	45	42	44	90
OVC012	6SM	-RA BR	46	43	45	89
OVC010	2 1/2SM	RA BR	44	42	43	93
BKN010 OVC021	3SM	-RA BR	43	41	42	93
BKN010 OVC014	3SM	-RA BR	42	40	41	92
BKN010 OVC014	6SM	-RA BR	42	39	41	89
BKN010 OVC014	5SM	-RA BR	40	38	39	93
OVC012	8SM	-RA	40	38	39	93
OVC012	6SM	-RA BR	39	37	38	93
OVC014	7SM	-RA	39	36	38	89
OVC012	4SM	RA BR	39	36	38	89
OVC014	5SM	-RA BR	39	37	38	93
SCT010 OVC017	4SM	RA BR	40	38	39	93
FEW007 BKN014 OVC019	5SM	-RA BR	38	37	38	97
BKN009 OVC015	6SM	-RA BR	39	37	38	93
SCT010 OVC017	6SM	-RA BR	39	37	38	93
BKN010 BKN014 OVC020	6SM	-RA BR	39	37	38	93
BKN010 OVC015	6SM	BR	39	37	38	93
BKN010 OVC023	10SM	-	39	37	38	93
BKN010 OVC013	10SM	-	41	37	39	86
OVC011	10SM	-	41	38	40	89

BKN004 OVC011	2 1/2SM	BR	41	39	40	93
BKN007 OVC012	6SM	BR	41	40	40	96
BKN007 OVC012	10SM	-	42	40	41	92
OVC009	10SM	-	43	40	42	89
OVC009	5SM	-RA BR	42	40	41	92
OVC011	5SM	-RA BR	42	40	41	92
FEW009 BKN018 OVC024	6SM	-RA BR	42	40	41	92
SCT007 BKN013 OVC020	6SM	-RA BR	42	40	41	92
FEW007 BKN023 OVC033	5SM	RA BR	41	39	40	93
FEW007 SCT013 OVC020	7SM	-RA	41	38	40	89
SCT009 BKN017 OVC021	7SM	-RA	41	37	39	86
SCT009 OVC026	10SM	-RA	40	37	39	89
SCT029 BKN065 OVC080	8SM	-RA	40	37	39	89
FEW010 SCT017 OVC040	8SM	-RA	39	37	38	93
SCT009 BKN025 OVC035	9SM	-RA	39	37	38	93
SCT014 OVC070	10SM	-	39	36	38	89
SCT046	10SM	-	47	28	39	48
SCT048	10SM	-	48	29	40	48
FEW049	10SM	-	49	28	40	45
FEW049 SCT250	10SM	-	47	28	39	48
FEW049 SCT250	10SM	-	46	27	38	47
FEW046	10SM	-	45	27	38	49
FEW046	10SM	-	44	27	37	51
FEW050	10SM	-	42	27	36	55
FEW050	10SM	-	41	26	35	55
FEW050	10SM	-	40	26	35	58
FEW040 SCT250	10SM	-	39	26	34	60
FEW040 SCT250	10SM	-	38	27	34	65
FEW250	10SM	-	37	27	33	67
FEW250	10SM	-	36	27	33	70
BKN250	10SM	-	35	28	32	76
CLR	10SM	-	35	27	32	72
SCT250	10SM	-	35	27	32	72
BKN250	10SM	-	35	28	32	76
FEW150 BKN250	10SM	-	37	28	34	70
OVC220	10SM	-	35	30	33	82
OVC220	10SM	-	38	29	35	70
OVC220	10SM	-	41	29	36	62
OVC220	10SM	-	43	32	38	65
FEW040 SCT150 OVC220	10SM	-	45	32	40	61
FEW035 BKN140 OVC220	10SM	-	46	31	40	56
FEW035 BKN140 OVC200	10SM	-	47	31	40	54
BKN130 OVC200	10SM	-	48	35	42	61
FEW075 BKN130 OVC200	10SM	-	49	35	43	59
BKN075 BKN130 OVC200	10SM	-	49	36	43	61
BKN044 BKN060 OVC120	10SM	-	49	39	44	69
BKN047 OVC075	10SM	-	49	40	45	71
BKN080 BKN200	10SM	-	48	40	44	74
BKN100 BKN150	10SM	-	47	40	44	77
SCT050 BKN070 BKN140	10SM	-	47	40	44	77
SCT041 BKN065 BKN140	10SM	-	45	40	43	83
CLR	10SM	-	44	38	41	79

CLR	10SM	-	44	36	40	73
CLR	10SM	-	43	35	40	74
CLR	9SM	-	43	36	40	76
CLR	9SM	-	40	35	38	83
CLR	9SM	-	41	36	39	82
CLR	8SM	-	39	35	37	86
CLR	6SM	BR	38	35	37	89
CLR	6SM	BR	40	36	38	86
FEW250	7SM	-	44	37	41	76
FEW250	7SM	-	46	37	42	71
FEW250	9SM	-	51	37	45	59
SCT250	10SM	-	54	36	46	51
SCT250	10SM	-	57	36	47	45
SCT250	10SM	-	57	37	48	47
SCT250	10SM	-	58	37	48	46
FEW250	10SM	-	57	36	47	45
FEW250	8SM	-	52	40	46	64
FEW250	9SM	-	50	41	46	71
FEW250	10SM	-	51	41	46	69
FEW250	9SM	-	49	40	45	71
FEW250	10SM	-	47	40	44	77
FEW250	9SM	-	47	39	43	74
CLR	9SM	-	44	38	41	79
CLR	9SM	-	42	37	40	82
SCT250	8SM	-	42	37	40	82
SCT250	8SM	-	41	37	39	86
CLR	8SM	-	40	36	38	86
SCT250	8SM	-	40	36	38	86
BKN250	7SM	-	40	36	38	86
OVC250	5SM	BR	39	37	38	93
BKN085 BKN150 OVC250	4SM	BR	40	38	39	93
SCT065 BKN150 BKN250	4SM	BR	42	38	40	85
FEW090 BKN130 OVC250	3SM	HZ	45	39	42	80
FEW090 BKN130 OVC200	4SM	HZ	46	40	43	79
FEW090 SCT130 OVC200	5SM	HZ	50	40	45	68
FEW110 OVC130	5SM	HZ	52	43	48	72
FEW080 BKN100 OVC130	10SM	-	53	42	48	66
BKN095 BKN140 OVC200	10SM	-	54	40	47	59
BKN090 OVC130	9SM	-	54	42	48	64
SCT090 OVC130	7SM	-	54	44	49	69
OVC065	7SM	-	54	45	49	72
BKN065 OVC085	9SM	-RA	53	44	49	72
BKN030 OVC060	7SM	-RA	52	45	49	77
SCT028 OVC060	5SM	-RA BR	50	47	48	89
SCT021 BKN038 OVC070	4SM	-RA BR	49	48	48	97
BKN005 OVC023	2SM	-RA BR	50	48	49	93
FEW008 SCT025 OVC080	2SM	-RA BR	49	48	48	97
BKN005 BKN025 OVC080	2SM	-RA BR	49	48	48	97
OVC006	2SM	-RA BR	49	47	48	93
OVC006	2SM	-RA BR	49	47	48	93
BKN006 OVC009	2SM	-RA BR	48	47	47	96
OVC007	3SM	-RA BR	48	47	47	96

SCT005 BKN008 OVC080	3SM	BR	48	46	47	93
OVC007	3SM	-RA BR	48	46	47	93
OVC005	3SM	BR	48	46	47	93
OVC005	3SM	BR	48	46	47	93
OVC005	3SM	BR	48	46	47	93
OVC003	1 1/4SM	BR	50	49	49	96
OVC003	1/2SM	FG	51	50	51	96
SCT003 BKN005 OVC010	2 1/2SM	BR	53	51	52	93
OVC007	2 1/2SM	-RA BR	53	51	52	93
SCT014 BKN030CB OVC046	5SM	TSRA BR	50	47	48	89
FEW011 SCT021 OVC033	10SM	-	49	43	46	80
OVC055	10SM	-RA	48	42	45	80
SCT023 BKN090 OVC150	10SM	-	47	41	44	80
SCT110	10SM	-	44	40	42	85
BKN035 BKN110	10SM	-	42	39	41	89
FEW035	10SM	-	42	37	40	82
BKN080	10SM	-	42	36	39	79
SCT049 SCT055 OVC075	10SM	-	42	35	39	76
FEW025 BKN030 OVC090	10SM	-	42	35	39	76
SCT039 BKN075 OVC100	10SM	-	41	32	37	70
FEW023 OVC044	10SM	-RA	38	32	36	79
SCT025 BKN035 OVC110	10SM	-	39	31	36	73
BKN037 OVC044	10SM	-	38	26	33	62
BKN041	10SM	-	38	24	33	57
BKN043	10SM	-	37	23	32	57
SCT045	10SM	-	38	21	32	51
FEW047 SCT100	10SM	-	40	21	33	47
FEW045 SCT110	10SM	-	41	21	34	45
FEW050 SCT110	10SM	-	43	21	35	42
FEW050	10SM	-	44	21	35	40
FEW050	10SM	-	45	20	36	37
FEW060	10SM	-	45	19	35	35
FEW060	10SM	-	43	20	35	40
FEW060	10SM	-	42	20	34	41
FEW070	10SM	-	42	20	34	41
CLR	10SM	-	41	22	34	47
CLR	10SM	-	39	24	33	55
CLR	10SM	-	39	23	33	53
CLR	10SM	-	38	24	33	57
BKN080	10SM	-	38	24	33	57
OVC085	10SM	-	38	25	33	60
BKN080	10SM	-	37	25	33	62
FEW250	10SM	-	36	25	32	64
SCT120	10SM	-	36	25	32	64
CLR	10SM	-	35	26	32	70
OVC050	10SM	-	37	27	33	67
BKN055	10SM	-	37	27	33	67
BKN055	10SM	-	37	26	33	65
FEW045 SCT250	10SM	-	32	-2	23	23
FEW045 SCT250	10SM	-	30	0	22	27
FEW050 SCT250	10SM	-	29	2	22	31
FEW050 SCT250	10SM	-	27	4	21	37

FEW050 SCT200	10SM	-	26	2	20	35
FEW060 SCT200	10SM	-	24	3	19	40
FEW060 SCT250	10SM	-	24	4	19	42
FEW060	10SM	-	22	5	18	48
FEW055	10SM	-	21	5	17	50
FEW055	10SM	-	20	9	17	62
SCT044	10SM	-	19	8	16	62
SCT047	10SM	-	18	6	15	60
CLR	10SM	-	18	6	15	60
CLR	10SM	-	17	-1	13	45
BKN200	10SM	-	17	-1	13	45
SCT250	10SM	-	16	-3	12	43
FEW050 SCT250	10SM	-	16	-3	12	43
FEW150 SCT250	10SM	-	15	-3	11	44
FEW140 BKN250	10SM	-	16	-1	12	47
FEW120 SCT250	10SM	-	18	0	14	45
FEW035 SCT120 SCT250	10SM	-	20	0	15	41
FEW046 SCT250	10SM	-	23	2	18	40
FEW049 SCT250	10SM	-	26	0	20	32
SCT049 SCT250	10SM	-	26	-2	19	29
FEW050 SCT250	10SM	-	27	-2	20	28
FEW050 SCT250	10SM	-	27	-4	20	26
FEW065	10SM	-	26	-4	19	26
FEW045	10SM	-	24	-5	18	27
CLR	10SM	-	23	-4	17	30
CLR	10SM	-	22	-2	17	35
CLR	10SM	-	21	-2	16	36
CLR	10SM	-	20	-2	15	38
FEW050	10SM	-	19	-3	14	37
FEW050	10SM	-	18	-2	14	41
FEW050	10SM	-	16	-2	12	45
CLR	10SM	-	15	-4	11	42
FEW050	10SM	-	14	-5	10	42
CLR	10SM	-	13	-5	9	44
CLR	10SM	-	13	-5	9	44
CLR	10SM	-	12	-5	9	46
FEW120 BKN250	10SM	-	12	-4	9	48
SCT110 BKN250	10SM	-	12	-4	9	48
FEW120 SCT250	10SM	-	13	-3	10	49
FEW130 SCT250	10SM	-	16	-2	12	45
FEW037 SCT250	10SM	-	19	-1	15	41
FEW037 SCT250	10SM	-	21	-2	16	36
FEW040	10SM	-	23	-3	17	32
FEW050	10SM	-	23	-5	17	29
FEW050 SCT250	10SM	-	23	-6	17	27
SCT060	10SM	-	24	-5	18	27
SCT060 SCT250	10SM	-	22	-5	16	30
FEW060	10SM	-	20	-5	15	33
FEW065	10SM	-	19	-3	14	37
FEW065 SCT250	10SM	-	18	-4	13	37
FEW065	10SM	-	16	-5	12	39
FEW060	10SM	-	15	-5	11	40

FEW060	10SM	-	13	-8	9	38
CLR	10SM	-	12	-10	8	36
CLR	10SM	-	11	-10	8	38
CLR	10SM	-	10	-10	7	39
CLR	10SM	-	10	-10	7	39
CLR	10SM	-	9	-9	6	43
CLR	10SM	-	9	-9	6	43
CLR	10SM	-	9	-8	6	46
CLR	10SM	-	8	-8	6	47
SCT250	10SM	-	8	-7	6	50
FEW055 SCT250	10SM	-	8	-7	6	50
FEW040 FEW250	10SM	-	18	-4	13	37
FEW045 SCT250	10SM	-	19	-4	14	36
FEW050 SCT250	10SM	-	20	-4	15	34
BKN050 BKN250	10SM	-	21	-4	16	33
FEW035 BKN050 BKN250	10SM	-	21	-3	16	34
FEW038 BKN055	10SM	-	19	-2	15	39
FEW035 SCT060 SCT250	10SM	-	18	-1	14	43
SCT050 SCT250	10SM	-	17	-2	13	43
BKN040 BKN250	10SM	-	15	-1	12	49
BKN045 BKN065 OVC250	10SM	-	13	-5	9	44
BKN050 OVC250	10SM	-	11	-6	8	46
OVC046	10SM	-	10	-7	7	45
OVC050	9SM	-SN	10	-4	8	53
OVC045	10SM	-	9	-5	6	52
OVC045	10SM	-	9	-7	6	48
BKN049	10SM	-	8	-9	5	45
CLR	10SM	-	8	-9	5	45
CLR	10SM	-	8	-9	5	45
CLR	10SM	-	8	-8	6	47
CLR	10SM	-	8	-7	6	50
CLR	10SM	-	9	-7	6	48
CLR	10SM	-	11	-6	8	46
CLR	10SM	-	14	-6	10	40
CLR	10SM	-	18	-6	13	34
CLR	10SM	-	21	-6	15	30
CLR	10SM	-	27	-8	19	21
FEW250	10SM	-	29	-6	21	21
SCT250	10SM	-	29	-7	21	20
BKN250	10SM	-	27	-6	20	23
BKN250	10SM	-	26	-5	19	25
BKN250	10SM	-	25	-5	18	26
BKN250	10SM	-	24	-5	18	27
BKN250	10SM	-	24	-8	17	24
BKN250	10SM	-	23	-7	17	26
BKN250	10SM	-	23	-5	17	29
BKN250	10SM	-	23	-4	17	30
BKN250	10SM	-	22	-1	17	36
BKN250	10SM	-	22	1	17	40
BKN250	10SM	-	21	3	17	45
BKN250	10SM	-	20	3	16	48
BKN250	10SM	-	19	4	15	52

BKN250	10SM	-	19	4	15	52
BKN120 OVC150	10SM	-	20	4	16	50
OVC110	10SM	-	20	4	16	50
OVC100	10SM	-	20	6	17	55
FEW080 OVC100	10SM	-	21	7	17	54
FEW080 OVC100	10SM	-	22	7	18	52
BKN080 BKN100	10SM	-	26	8	21	46
FEW085 SCT150 SCT250	10SM	-	28	7	22	41
FEW150	10SM	-	30	6	23	36
FEW150	10SM	-	32	3	24	29
FEW150 SCT250	10SM	-	32	5	24	32
FEW200	10SM	-	31	6	24	35
FEW060 SCT150 SCT250	10SM	-	29	5	22	36
FEW060 SCT150	10SM	-	29	6	23	38
BKN050	10SM	-	29	7	23	39
OVC050	10SM	-	29	7	23	39
OVC044	10SM	-	29	8	23	41
BKN046 OVC140	10SM	-	29	8	23	41
FEW050 BKN250	10SM	-	28	10	23	47
FEW050 SCT140	10SM	-	26	9	21	48
CLR	10SM	-	27	9	22	47
CLR	10SM	-	26	9	21	48
CLR	10SM	-	25	11	21	55
CLR	10SM	-	23	10	19	57
FEW065 SCT200	10SM	-	23	12	20	63
SCT045 BKN250	10SM	-	24	12	21	60
BKN055 BKN090	10SM	-	24	14	21	65
OVC050	9SM	-	26	15	23	63
BKN090 OVC150	10SM	-	27	15	23	61
OVC050	9SM	-	29	16	25	58
OVC055	10SM	-	30	17	26	59
OVC055	10SM	-	31	16	26	54
OVC055	10SM	-	32	16	27	52
OVC055	10SM	-	32	17	27	54
OVC060	10SM	-	32	18	27	56
OVC050	10SM	-	31	20	27	64
OVC050	8SM	-SN	31	21	27	67
OVC046	7SM	-SN	30	23	28	75
SCT035 BKN060 OVC090	4SM	-SN BR	30	26	29	85
SCT040 BKN055 OVC090	4SM	-SN BR	30	26	29	85
BKN038 OVC047	2 1/2SM	-SN BR	29	27	28	92
BKN019 OVC034	2SM	-SN BR	29	27	28	92
BKN070 OVC095	10SM	-	29	22	27	75
FEW023 BKN070 OVC100	9SM	-	26	18	24	71
BKN043 BKN055 OVC120	10SM	-	24	14	21	65
OVC045	10SM	-	22	6	18	50
OVC055	10SM	-	20	6	17	55
OVC070	10SM	-	17	4	14	56
FEW070 SCT080	10SM	-	14	-1	11	51
FEW075	10SM	-	12	-4	9	48
FEW033 SCT075	10SM	-	12	-4	9	48
CLR	10SM	-	12	-5	9	46

FEW035	10SM	-	13	-5	10	44
CLR	10SM	-	15	-5	11	40
CLR	10SM	-	17	-8	12	32
CLR	10SM	-	18	-10	13	28
CLR	10SM	-	17	-12	12	26
CLR	10SM	-	16	-13	11	26
CLR	10SM	-	15	-13	11	27
CLR	10SM	-	13	-11	9	33
CLR	10SM	-	13	-12	9	31
CLR	10SM	-	12	-11	8	34
CLR	10SM	-	11	-10	8	38
CLR	10SM	-	10	-9	7	41
CLR	10SM	-	9	-9	6	43
CLR	10SM	-	9	-8	6	46
CLR	10SM	-	8	-8	6	47
CLR	10SM	-	8	-7	6	50
BKN150	10SM	-	8	-7	6	50
BKN120	10SM	-	9	-6	6	50
OVC110	10SM	-	10	-5	7	50
BKN085 OVC110	10SM	-	11	-4	8	51
FEW080 BKN100 OVC110	10SM	-	11	-4	8	51
OVC100	10SM	-	12	-2	9	53
OVC085	10SM	-	13	-2	10	51
FEW065 OVC080	10SM	-	15	-2	12	46
OVC080	10SM	-	18	-1	14	43
OVC065	10SM	-	19	-1	15	41
OVC060	10SM	-	20	0	15	41
OVC055	10SM	-	21	1	16	42
OVC050	10SM	-	22	1	17	40
OVC055	10SM	-	22	2	17	42
OVC050	10SM	-	22	2	17	42
OVC046	10SM	-	23	2	18	40
OVC044	10SM	-	23	3	18	42
OVC040	10SM	-	23	4	18	44
OVC040	10SM	-	24	5	19	44
BKN040 OVC055	10SM	-	24	5	19	44
FEW055 OVC110	10SM	-	24	6	19	46
OVC044	10SM	-	25	6	20	44
BKN034 OVC085	10SM	-	26	8	21	46
FEW025 BKN045 OVC060	10SM	-	25	12	21	58
BKN045 OVC080	9SM	-	26	13	22	57
OVC049	10SM	-	26	14	22	60
BKN049 BKN070 OVC085	10SM	-	26	15	23	63
SCT025 OVC039	5SM	-SN	26	16	23	66
FEW009 BKN019 OVC029	2SM	-SN BR	25	21	24	85
SCT015 BKN035 OVC048	3SM	-SN BR	26	22	25	84
SCT006 BKN009 OVC021	2SM	-SN BR	27	24	26	89
SCT008 BKN015 OVC021	2SM	-SN BR	28	25	27	88
FEW008 BKN014 OVC025	2SM	-SN BR	29	25	27	85
FEW010 SCT014 OVC026	3SM	-SN	30	25	28	82
FEW007 BKN010 OVC024	3SM	-SN	31	25	29	79
SCT011 OVC024	5SM	-SN	32	26	30	79

BKN015 BKN026 OVC060	6SM	-SN	32	26	30	79
FEW007 BKN015 OVC020	1 1/2SM	-SN	32	27	30	82
SCT009 BKN029 OVC060	2 1/2SM	-SN	32	28	31	85
FEW010 BKN030 OVC050	5SM	-SN	32	27	30	82
OVC055	7SM	-	33	27	31	78
SCT050	6SM	HZ	31	26	29	82
SCT050	7SM	-	31	25	29	79
FEW055 SCT150	5SM	HZ	30	25	28	82
FEW055	5SM	BR	28	24	27	85
CLR	4SM	BR	26	24	25	92
CLR	4SM	BR	24	23	24	96
CLR	6SM	BR	22	19	21	89
CLR	7SM	-	23	19	22	85
CLR	9SM	-	23	18	22	81
SCT250	8SM	-	22	17	20	82
BKN250	8SM	-	19	15	18	85
SCT250	9SM	-	22	16	20	78
BKN250	10SM	-	26	18	24	71
BKN250	10SM	-	28	19	25	69
FEW150 BKN250	10SM	-	29	19	26	66
SCT150 BKN250	10SM	-	32	18	27	56
SCT150 BKN250	10SM	-	33	19	28	56
FEW030 SCT150 SCT250	10SM	-	35	20	30	54
FEW030 SCT150 SCT250	10SM	-	34	19	29	54
FEW150 BKN250	8SM	-	32	21	28	64
SCT150 BKN250	9SM	-	31	22	28	69
OVC250	10SM	-	30	21	27	69
SCT150 OVC250	10SM	-	28	20	25	72
OVC250	9SM	-	29	21	26	72
BKN120 OVC200	9SM	-	30	22	27	72
BKN120 OVC200	9SM	-	30	21	27	69
OVC110	9SM	-	31	22	28	69
BKN021 OVC110	10SM	-	31	20	27	64
OVC013	10SM	-	31	20	27	64
OVC013	10SM	-	31	22	28	69
OVC013	10SM	-	32	22	29	66
OVC015	10SM	-	32	24	29	73
OVC014	9SM	-SN	32	25	29	75
SCT019 OVC036	8SM	-	32	25	29	75
BKN028 OVC033	8SM	-	33	25	30	72
OVC023	8SM	-	34	25	31	70
OVC012	2 1/2SM	-DZ	34	29	32	82
BKN008 OVC014	2SM	-DZ BR	34	32	33	92
OVC005	2SM	-DZ BR	34	33	34	97
OVC004	1 3/4SM	-DZ BR	35	33	34	93
OVC005	1 3/4SM	-DZ BR	35	34	35	96
OVC004	1 3/4SM	-DZ BR	35	34	35	96
OVC007	2 1/2SM	-DZ BR	35	33	34	93
FEW008 OVC012	3SM	-DZ BR	35	33	34	93
FEW009 OVC014	5SM	BR	35	32	34	89
OVC017	4SM	BR	36	32	34	86
OVC014	2 1/2SM	BR	36	33	35	89

OVC014	5SM	BR	35	33	34	93
OVC014	6SM	BR	36	33	35	89
OVC012	4SM	BR	35	33	34	93
FEW120 BKN250	7SM	-	46	38	42	73
FEW120 BKN250	7SM	-	46	38	42	73
BKN120 BKN250	7SM	-	46	38	42	73
OVC085	7SM	-RA	46	38	42	73
OVC090	7SM	-	47	40	44	77
BKN090	6SM	BR	45	41	43	86
BKN060 OVC095	5SM	-RA BR	45	42	44	90
BKN060 OVC095	3SM	-RA BR	45	42	44	90
BKN060 OVC080	3SM	-RA BR	45	43	44	93
BKN036 OVC090	3SM	-RA BR	46	43	45	89
BKN042 BKN050 OVC080	2SM	-RA BR	45	43	44	93
SCT007 BKN034 OVC050	1 3/4SM	-RA BR	43	42	43	97
OVC007	4SM	-RA BR	41	39	40	93
OVC005	1 1/2SM	RA BR	40	39	40	97
BKN009 OVC020	1 3/4SM	RA BR	41	39	40	93
OVC009	2SM	-RA BR	39	38	39	96
OVC009	4SM	RA BR	39	37	38	93
OVC013	5SM	RA BR	39	36	38	89
OVC011	7SM	-RA	38	36	37	93
BKN010 OVC015	2 1/2SM	RA BR	38	37	38	97
BKN010 OVC014	2 1/2SM	+RA BR	38	37	38	97
OVC006	5SM	-RA BR	38	36	37	93
OVC012	4SM	-RA BR	37	36	37	96
BKN012 OVC019	7SM	-RA	37	35	36	93
SCT012 BKN021 OVC030	6SM	RA BR	37	35	36	93
SCT012 BKN028 OVC045	8SM	-RA	37	34	36	89
SCT016 BKN022 OVC042	10SM	-	37	34	36	89
SCT018 OVC044	10SM	-	38	34	36	86
OVC018	10SM	-	37	32	35	82
BKN020 OVC043	10SM	-	36	31	34	82
OVC032	10SM	-	35	29	33	78
FEW030 BKN048 BKN250	10SM	-	34	26	31	73
FEW030 OVC044	10SM	-	33	27	31	78
SCT030 OVC040	10SM	-	33	27	31	78
FEW025 OVC034	10SM	-	34	25	31	70
OVC042	10SM	-	35	24	31	64
OVC045	10SM	-	32	23	29	69
BKN045 OVC150	10SM	-	32	22	29	66
BKN045 OVC100	10SM	-	32	23	29	69
BKN030 OVC045	10SM	-	31	21	28	67
OVC032	10SM	-	30	22	27	72
OVC025	10SM	-FZDZ	30	24	28	79
BKN008 OVC020	3SM	-FZDZ BR	28	25	27	88
SCT008 OVC013	3SM	-FZDZ BR	28	26	27	92
FEW008 OVC015	3SM	-FZDZ BR	29	28	29	96
OVC015	10SM	-FZDZ	31	26	29	82
BKN015 BKN021 OVC046	2SM	-SN BR	30	28	29	92
BKN015 BKN038 OVC046	2SM	-SN BR	30	28	29	92
BKN011 OVC019	2SM	-SN BR	30	28	29	92

OVC015	2SM	-SN BR	29	27	28	92
OVC013	6SM	-SN BR	30	27	29	88
OVC015	6SM	-FZDZ BR	31	28	30	89
OVC011	6SM	-FZDZ BR	32	28	31	85
OVC011	4SM	-SN BR	32	30	31	92
OVC012	6SM	BR	33	30	32	89
BKN009 OVC012	4SM	-RA BR	33	32	33	96
OVC008	4SM	-DZ BR	34	32	33	92
OVC005	2SM	-RA BR	34	33	34	97
OVC006	3SM	-PLRA BR	34	33	34	97
OVC007	3SM	-RA BR	34	32	33	92
OVC006	3SM	-RA BR	34	32	33	92
BKN008 OVC013	3SM	-RA BR	34	32	33	92
OVC005	2SM	-RA BR	34	33	34	97
OVC010	2SM	-RA BR	34	33	34	97
FEW006 OVC010	2 1/2SM	-RA BR	33	32	33	96
BKN009 OVC012	2 1/2SM	-RA BR	33	32	33	96
OVC007	4SM	-RA BR	33	32	33	96
BKN010 BKN016 OVC021	4SM	-RA BR	33	32	33	96
FEW008 BKN010 OVC015	5SM	-RA BR	33	32	33	96
BKN010 OVC014	10SM	-RA	33	32	33	96
FEW008 OVC012	10SM	-RA	34	32	33	92
FEW009 BKN012 OVC016	6SM	-RA BR	34	32	33	92
FEW009 BKN012 OVC017	6SM	-RA BR	33	31	32	92
SCT014 BKN020 OVC027	2SM	-SN BR	32	31	32	96
FEW022 OVC033	8SM	-SN	33	29	31	85
FEW014 BKN035 OVC042	6SM	-SN BR	33	30	32	89
FEW016 OVC035	9SM	-SN	33	30	32	89
BKN039 BKN047 OVC100	9SM	-SN	34	29	32	82
FEW025 OVC037	9SM	-SN	34	29	32	82
FEW025 OVC035	10SM	-	35	29	33	78

Wind Speed (KT)	Wind Dir	Wind Char. Gusts(KT)	Val. For Wind Char.	Station Pressure	Pressure Tendency	Sea Level Pressure
6	100	-	0	29.93	-	146
6	130	-	0	29.92	6	142
6	160	-	0	29.90	-	135
10	150	-	0	29.87	-	123
7	170	-	0	29.85	6	118
8	180	-	0	29.84	-	115
11	190	G	18	29.83	-	110
9	190	-	0	29.80	8	100
10	190	-	0	29.76	-	088
10	200	-	0	-	-	-
7	190	-	0	29.75	6	084
8	200	-	0	29.74	-	079
8	210	-	0	29.72	-	074
6	250	-	0	29.71	6	071
4	250	-	0	29.72	-	072
5	270	-	0	29.72	-	075
6	160	-	0	29.74	3	081
4	250	-	0	29.74	-	080
7	260	-	0	29.75	-	083
7	260	-	0	29.74	4	081
10	300	-	0	29.74	-	081
11	280	-	0	29.73	-	079
16	270	-	0	29.73	8	076
17	270	G	20	29.71	-	069
11	300	-	0	29.70	-	068
15	290	-	0	29.71	5	071
18	280	G	23	29.74	-	082
13	280	-	0	29.77	-	089
8	270	-	0	29.79	1	096
8	260	-	0	29.79	-	098
7	280	-	0	29.81	-	104
6	280	-	0	29.81	0	103
6	280	-	0	29.80	-	102
6	280	-	0	29.81	-	105
8	280	-	0	29.81	3	105
9	290	-	0	29.82	-	107
9	270	-	0	29.82	-	107
5	270	-	0	29.82	1	108
5	230	-	0	29.82	-	108
8	230	-	0	29.83	-	111
7	240	-	0	29.84	3	113
13	260	G	18	29.86	-	122
15	270	G	20	29.87	-	123
18	270	G	23	29.87	1	125
16	290	G	20	29.87	-	123
13	300	-	0	29.87	-	123
13	280	G	20	29.85	8	118
13	310	G	22	29.84	-	116
13	280	G	18	29.85	-	119
13	280	G	18	29.88	3	128

13	290	-	0	29.90	-	133
15	310	-	0	29.92	-	141
8	310	-	0	29.93	1	145
8	270	-	0	29.96	-	153
10	260	-	0	29.97	-	158
10	290	-	0	29.98	1	162
10	290	-	0	29.97	-	159
11	290	-	0	29.97	-	159
8	310	-	0	29.99	3	164
12	350	-	0	29.99	-	165
12	360	-	0	30.00	-	169
10	340	-	0	30.01	3	173
8	330	-	0	30.02	-	176
9	340	G	21	30.04	-	183
11	330	G	19	30.06	3	189
10	340	-	0	30.09	-	198
14	340	-	0	30.09	-	200
8	360	-	0	30.08	0	196
8	350	-	0	30.07	-	191
8	360	G	16	30.06	-	190
9	360	-	0	30.04	8	181
6	VRB	-	0	30.04	-	180
9	330	-	0	30.03	-	178
9	340	-	0	30.03	6	177
9	340	G	17	30.04	-	183
7	320	-	0	30.06	-	190
9	340	-	0	30.08	3	197
9	360	-	0	30.10	-	202
11	350	-	0	30.11	-	204
11	360	-	0	30.12	2	210
10	010	-	0	30.13	-	212
12	030	-	0	30.14	-	216
11	030	-	0	30.15	3	220
8	030	-	0	30.17	-	225
12	020	-	0	30.16	-	221
10	040	-	0	30.17	3	227
10	030	-	0	30.19	-	234
10	020	-	0	30.21	-	238
12	020	-	0	30.23	3	246
13	020	-	0	30.25	-	254
7	060	-	0	30.25	-	253
7	050	-	0	30.26	1	255
3	VRB	-	0	30.27	-	259
4	VRB	-	0	30.26	-	257
4	VRB	-	0	30.24	8	251
3	VRB	-	0	30.23	-	246
4	VRB	-	0	30.23	-	245
4	100	-	0	30.22	6	243
7	100	-	0	30.22	-	242
8	140	-	0	30.23	-	245
6	150	-	0	30.24	3	249
5	150	-	0	30.25	-	253

4	190	-	0	30.27	-	259
3	200	-	0	30.26	0	255
4	210	-	0	30.26	-	255
6	270	-	0	30.26	-	257
4	260	-	0	30.26	0	256
0	000	-	0	30.26	-	255
3	160	-	0	30.23	-	248
0	000	-	0	30.23	8	246
0	000	-	0	30.23	-	247
0	000	-	0	30.24	-	248
3	230	-	0	30.23	8	246
3	180	-	0	30.24	-	248
5	250	-	0	30.23	-	246
9	210	-	0	30.22	8	242
10	190	-	0	30.21	-	241
9	210	-	0	30.19	-	232
10	150	-	0	30.14	8	216
11	120	-	0	30.12	-	209
16	300	G	22	30.01	-	171
19	290	-	0	30.00	0	167
15	280	G	23	30.00	-	168
12	290	G	19	30.00	-	169
12	340	G	19	30.01	3	172
8	330	-	0	30.03	-	178
8	010	-	0	30.06	-	187
5	VRB	-	0	30.10	3	202

8	270	-	0	30.19	-	232
6	280	-	0	30.21	-	238
6	260	-	0	30.22	3	244
4	210	-	0	30.24	-	249
6	240	-	0	30.26	-	255
6	240	-	0	30.27	1	259
7	260	-	0	30.30	-	268
7	260	-	0	30.34	-	281
6	260	-	0	30.36	1	289
7	260	-	0	30.38	-	297
12	250	-	0	30.39	-	301
10	280	-	0	30.40	1	305
7	230	-	0	30.40	-	304
12	240	-	0	30.38	-	297
15	230	G	24	30.36	8	290
13	240	-	0	30.35	-	286
16	270	G	25	30.36	-	290
14	270	-	0	30.37	3	292
12	240	-	0	30.39	-	299
10	260	-	0	30.42	-	309
6	280	-	0	30.44	3	319
6	250	-	0	30.47	-	326
5	270	-	0	30.50	-	339

6	250	-	0	30.53	3	347
0	000	-	0	30.53	-	346
13	270	G	18	29.90	-	134
11	280	-	0	29.88	8	127
13	300	G	19	29.87	-	124
10	330	G	18	29.87	-	126
17	320	G	23	29.90	3	133
19	330	G	25	29.94	-	147
15	330	G	23	29.98	-	161
13	340	G	20	30.03	3	179
12	340	-	0	30.07	-	190
13	300	G	19	30.10	-	203
13	310	-	0	30.13	1	211
11	300	G	19	30.15	-	219
11	300	-	0	30.18	-	229
10	320	-	0	30.20	1	235
7	300	-	0	30.22	-	241
10	290	-	0	30.23	-	245
11	280	-	0	30.25	3	253
12	280	-	0	30.27	-	260
11	290	-	0	30.29	-	266
10	280	-	0	30.31	3	274
12	280	-	0	30.33	-	281
10	290	-	0	30.34	-	284
6	270	-	0	30.34	0	282
13	250	G	16	30.33	-	279
14	270	G	23	30.31	-	273
15	260	-	0	30.28	8	262
13	280	G	20	30.27	-	259
21	250	G	24	30.27	-	259
20	280	G	24	30.27	6	258
17	280	-	0	30.28	-	263
13	280	-	0	30.29	-	267
7	270	-	0	30.31	1	272
4	230	-	0	30.31	-	272
5	220	-	0	30.32	-	276
6	200	-	0	30.33	3	280
5	200	-	0	30.32	-	278
6	200	-	0	30.31	-	274
10	210	-	0	30.31	6	274
9	230	-	0	30.30	-	270
8	240	-	0	30.29	-	265
6	250	-	0	30.29	5	265
7	240	-	0	30.30	-	269
4	230	-	0	30.29	-	267
6	230	-	0	30.28	8	264
11	230	-	0	30.27	-	261
14	230	-	0	30.25	-	253
9	240	-	0	30.25	6	251
13	230	-	0	30.23	-	247
11	250	-	0	30.21	-	240
16	240	-	0	30.17	8	224

19	230	G	26	30.14	-	215
20	240	G	27	30.13	-	211
22	240	G	26	30.11	6	207
19	240	G	23	30.11	-	205
15	220	-	0	30.11	-	205
10	210	-	0	30.12	3	210
16	220	-	0	30.13	-	213
18	230	G	22	30.15	-	219
13	240	-	0	30.17	3	225
11	240	-	0	30.17	-	226
11	230	-	0	30.17	-	226
9	240	-	0	30.17	2	226
7	240	-	0	30.16	-	223
8	240	-	0	30.16	-	221
7	240	-	0	30.16	5	222
5	240	-	0	30.17	-	227
6	220	-	0	30.19	-	231
7	230	-	0	30.20	1	235
9	230	-	0	30.22	-	243
6	240	-	0	30.23	-	246
6	240	-	0	30.23	1	246
8	260	-	0	30.23	-	245
10	250	-	0	30.21	-	239
12	250	-	0	30.19	8	232
12	220	G	20	30.17	-	225
11	260	-	0	30.17	-	225
11	230	-	0	30.17	6	225
12	240	-	0	30.18	-	229
9	270	-	0	30.21	-	239
7	300	-	0	30.24	3	250
6	340	-	0	30.26	-	257
3	320	-	0	30.28	-	264
6	190	-	0	30.32	3	276
0	000	-	0	30.33	-	278
5	070	-	0	30.33	-	281
7	020	-	0	30.34	2	283
9	040	-	0	30.35	-	288
6	040	-	0	30.36	-	291
9	040	-	0	30.38	1	295
8	040	-	0	30.40	-	302
8	040	-	0	30.42	-	311
7	040	-	0	30.43	1	314
9	040	-	0	30.46	-	324
6	100	-	0	30.48	-	330
6	100	-	0	30.48	1	332
4	100	-	0	30.48	-	331
7	100	-	0	30.46	-	325
5	190	-	0	30.46	8	322
6	130	-	0	30.44	-	316
7	160	-	0	30.44	-	316
8	160	-	0	30.44	5	317
6	130	-	0	30.45	-	322

8	150	-	0	30.45	-	322
7	120	-	0	30.45	1	322
6	120	-	0	30.44	-	318
5	100	-	0	30.45	-	320
7	100	-	0	30.45	5	321
4	090	-	0	30.47	-	327
3	070	-	0	30.47	-	327
7	030	-	0	30.46	0	324
7	030	-	0	30.45	-	319
7	040	-	0	30.43	-	312
6	020	-	0	30.43	5	314
6	050	-	0	30.43	-	313
4	090	-	0	30.42	-	310
0	000	-	0	30.42	6	309
5	040	-	0	30.42	-	311
3	VRB	-	0	30.42	-	310
5	070	-	0	30.39	8	300
4	050	-	0	30.36	-	289
6	090	-	0	30.32	-	278
5	090	-	0	30.27	8	261
11	160	-	0	30.23	-	246
15	160	G	20	30.20	-	235
12	160	-	0	30.18	6	228
13	170	G	20	30.15	-	220
12	150	-	0	30.13	-	212
8	170	-	0	30.09	8	200
13	180	G	21	30.06	-	189
12	170	-	0	30.02	-	175
15	180	G	20	29.97	8	158
16	190	G	24	29.93	-	144
16	190	G	24	29.87	-	123
19	200	G	24	29.81	8	105
21	210	G	26	29.77	-	090
22	290	G	31	29.81	-	105
19	290	G	23	29.85	3	117
25	280	G	31	29.89	-	130
30	280	G	38	29.93	-	143
18	290	G	28	29.96	1	154
28	280	G	33	29.98	-	163
20	280	G	34	29.99	-	165
27	280	G	34	29.98	0	161
23	290	G	35	29.97	-	157
29	280	G	36	29.97	-	157
30	270	G	37	29.96	6	154
21	290	G	34	29.96	-	154
25	270	G	34	29.96	-	154
23	270	G	33	29.98	3	160
24	280	G	32	30.01	-	171
25	280	G	33	30.05	-	184
18	280	G	27	30.10	3	202
19	300	G	28	30.14	-	214
14	300	G	20	30.17	-	227

13	310	G	21	30.20	1	235
10	310	G	18	30.21	-	239
15	290	G	20	30.24	-	248
9	300	G	16	30.25	3	254
10	300	-	0	30.26	-	257
12	330	-	0	30.28	-	264
14	310	-	0	30.29	2	267
11	280	G	18	30.32	-	277
8	290	-	0	30.36	-	291
8	270	-	0	30.40	3	303
12	280	G	17	30.42	-	308
10	320	G	17	30.41	-	308
11	300	G	15	30.40	0	303
11	330	-	0	30.39	-	300
8	320	-	0	30.37	-	295
12	280	G	19	30.37	6	293
9	260	G	19	30.35	-	285
7	090	-	0	30.20	-	235
6	080	-	0	30.20	5	237
5	040	-	0	30.21	-	239
10	010	-	0	30.22	-	243
9	040	-	0	30.22	0	243
9	030	-	0	30.24	-	248
9	030	-	0	30.24	-	248
10	050	-	0	30.23	0	244
8	030	-	0	30.23	-	246
6	040	-	0	30.22	-	244
5	040	-	0	30.24	3	249
7	030	-	0	30.24	-	249
6	020	-	0	30.24	-	248
6	030	-	0	30.24	3	250
5	010	-	0	30.26	-	255
5	340	-	0	30.27	-	260
5	310	-	0	30.29	3	266
7	350	-	0	30.31	-	271
12	360	-	0	30.31	-	275
7	020	-	0	30.33	1	279
5	VRB	-	0	30.32	-	276
6	050	-	0	30.33	-	280
3	VRB	-	0	30.30	8	270
6	190	-	0	30.31	-	273
4	230	-	0	30.33	-	279
0	000	-	0	30.32	0	277
3	110	-	0	30.34	-	283
4	110	-	0	30.35	-	285
7	130	-	0	30.36	1	288
6	140	-	0	30.38	-	296
8	130	-	0	30.37	-	294
9	120	-	0	30.38	1	296
5	120	-	0	30.37	-	295
6	120	-	0	30.36	-	291
8	140	-	0	30.37	5	293

6	140	-	0	30.36	-	291
12	130	G	15	30.33	-	280
11	120	-	0	30.31	8	272
12	120	G	17	30.28	-	263
8	210	-	0	29.84	8	114
13	230	-	0	29.80	-	100
14	210	-	0	29.76	-	088
10	150	-	0	29.73	6	077
10	230	G	16	29.68	-	059
9	200	-	0	29.64	-	045
8	170	-	0	29.62	6	040
12	230	G	19	29.61	-	038
28	330	G	37	29.69	-	062
19	330	G	36	29.73	3	078
23	340	G	31	29.79	-	096
23	340	G	34	29.81	-	105
16	330	G	26	29.86	1	119
24	330	G	30	29.87	-	125
21	330	G	29	29.90	-	133
17	330	G	22	29.92	3	140
21	320	G	27	29.95	-	152
14	320	G	25	29.99	-	164
17	310	G	23	30.00	1	166
17	300	G	25	30.01	-	172
21	310	G	27	30.02	-	175
15	310	G	25	30.02	1	176
18	320	G	25	30.01	-	172
11	310	G	26	29.98	-	162
16	280	G	24	29.97	8	158
18	280	G	23	29.95	-	152
14	290	G	19	29.95	-	152
18	320	G	22	29.95	5	153
14	300	-	0	29.97	-	156
17	270	G	24	29.99	-	164
13	280	G	20	30.01	3	172
15	280	-	0	30.04	-	183
13	280	-	0	30.07	-	193
13	270	G	21	30.08	1	196
13	280	-	0	30.08	-	196
13	260	-	0	30.08	-	196
12	270	-	0	30.09	3	199
13	270	-	0	30.09	-	200
12	250	-	0	30.09	-	197
11	240	-	0	30.09	3	200
11	240	-	0	30.10	-	201
10	240	-	0	30.10	-	202
10	240	-	0	30.10	3	203
17	250	G	23	30.10	-	201
16	250	G	26	30.08	-	196
18	230	G	25	30.05	8	187
24	240	G	29	30.01	-	172
19	240	G	29	29.98	-	162

23	240	G	31	29.95	6	150
24	250	G	31	29.90	-	134
25	250	G	30	29.87	-	123
23	270	G	34	29.85	6	116
23	250	G	30	29.83	-	112
22	240	G	27	29.85	-	116
16	220	-	0	29.86	3	121
17	230	G	23	29.89	-	130
13	230	-	0	29.91	-	137
11	240	-	0	29.94	3	146
12	230	-	0	29.95	-	153
11	230	-	0	29.96	-	156
10	230	-	0	29.98	1	160
9	240	-	0	29.98	-	162
8	250	-	0	29.99	-	165
8	250	-	0	30.01	3	173
4	220	-	0	30.04	-	183
5	230	-	0	30.06	-	190
5	220	-	0	30.09	1	199
3	190	-	0	30.10	-	202
5	230	-	0	30.10	-	203
12	220	-	0	30.09	0	200
15	230	G	18	30.07	-	192
14	230	-	0	30.06	-	189
13	240	-	0	30.04	6	183
16	250	G	22	30.02	-	176
17	240	-	0	30.01	-	173
14	220	-	0	30.00	6	169
11	250	-	0	30.00	-	167
11	270	-	0	30.02	-	173
6	240	-	0	30.02	3	175
5	240	-	0	30.04	-	181
5	230	-	0	30.05	-	185
6	200	-	0	30.05	0	184
7	210	-	0	30.06	-	189
6	270	-	0	30.06	-	189
7	360	-	0	30.07	1	190
10	010	-	0	30.08	-	197
8	010	-	0	30.10	-	201
9	010	-	0	30.10	0	201
20	040	G	25	30.14	-	216
19	030	-	0	30.20	-	237
12	050	-	0	30.24	1	249
18	030	-	0	30.27	-	258
18	030	G	21	30.29	-	265
16	020	-	0	30.30	1	270
14	030	-	0	30.30	-	271
9	030	G	18	30.30	-	268
12	030	-	0	30.29	8	267
9	070	-	0	30.29	-	265
8	070	-	0	30.29	-	265
11	030	-	0	30.30	3	269

8	150	-	0	30.32	-	275
7	110	-	0	30.31	-	271
9	130	-	0	30.30	0	270
9	120	-	0	30.32	-	277
4	VRB	-	0	30.37	-	292
8	050	-	0	30.37	1	294
6	080	-	0	30.37	-	293
6	070	-	0	30.37	-	293
7	070	-	0	30.37	6	293
8	090	-	0	30.38	-	297
8	080	-	0	30.37	-	292
9	090	-	0	30.35	8	286
10	080	-	0	30.37	-	293
9	090	-	0	30.36	-	291
10	080	G	17	30.36	0	291
12	080	G	19	30.36	-	288
9	070	-	0	30.34	-	282
10	090	-	0	30.32	8	277
10	080	G	16	30.30	-	271
10	080	-	0	30.25	-	253
12	090	G	16	30.22	8	243
11	100	-	0	30.18	-	229
8	090	-	0	30.13	-	212
13	080	G	17	30.09	6	199
6	080	-	0	30.05	-	187
7	050	-	0	30.01	-	172
10	040	-	0	29.97	8	157
5	VRB	-	0	29.91	-	138
8	050	-	0	29.85	-	119
16	290	G	33	29.91	5	137
4	100	-	0	29.86	-	121
3	110	-	0	29.85	-	118
4	140	-	0	29.86	5	119
0	000	-	0	29.82	-	108
9	330	G	16	29.84	-	114
5	290	-	0	29.84	6	114
5	260	-	0	29.86	-	120
9	280	-	0	29.88	-	128
10	310	-	0	29.88	0	127
9	310	-	0	29.90	-	133
17	320	G	22	29.91	-	139
19	330	G	23	29.91	0	137
15	330	G	20	29.90	-	135
13	330	G	17	29.91	-	137
13	310	G	20	29.90	7	136
13	330	-	0	29.90	-	135
17	340	G	21	29.91	-	136
15	330	G	21	29.92	3	141
19	320	G	27	29.95	-	150
19	330	-	0	29.97	-	159
16	330	G	24	29.99	1	165
13	340	G	21	30.01	-	171

14	340	-	0	30.02	-	174
11	340	-	0	30.04	3	180
13	340	G	18	30.05	-	184
11	340	-	0	30.05	-	186
10	340	-	0	30.06	2	189
8	350	-	0	30.06	-	188
8	320	-	0	30.06	-	188
8	320	-	0	30.06	5	189
7	330	-	0	30.07	-	192
9	320	-	0	30.09	-	199
9	330	-	0	30.11	3	205
8	350	-	0	30.12	-	209
4	60	-	0	30.17	-	227
3	VRB	-	0	30.15	-	220
13	160	-	0	30.15	-	218
13	180	G	18	30.15	-	220
12	180	-	0	30.16	-	222
11	180	-	0	30.17	3	227
9	190	-	0	30.19	-	231
9	190	-	0	30.19	-	234
10	220	-	0	30.21	3	239
8	220	-	0	30.22	-	242
9	210	-	0	30.2	-	235
5	170	-	0	30.18	8	230
4	180	-	0	30.18	-	228
0	0	-	0	30.14	-	217
5	290	-	0	30.15	5	219
0	0	-	0	30.13	-	213
3	260	-	0	30.14	-	215
7	150	-	0	30.09	8	200
11	160	G	18	30.07	-	191
13	160	G	20	30.06	-	188
12	160	G	17	30.04	6	182
12	160	-	0	30.01	-	171
11	150	G	19	29.97	-	157
13	140	G	18	29.93	8	145
10	140	G	16	29.89	-	130
6	140	-	0	29.86	-	119
3	120	-	0	29.84	6	114
7	320	-	0	29.85	-	116
11	330	-	0	29.87	-	123
13	330	-	0	29.9	3	136
14	330	-	0	29.96	-	156
10	350	-	0	29.99	-	166
8	360	-	0	30	1	170
5	340	-	0	30.01	-	171
3	310	-	0	30.02	-	174
4	290	-	0	30.02	0	174
8	300	-	0	30.02	-	176
5	350	-	0	30.04	-	182
7	280	-	0	30.06	3	187
7	280	-	0	30.09	-	198

4	270	-	0	30.11	-		204
6	260	-	0	30.12		1	208
16	280	G	21	30.12	-		207
17	310	G	22	30.13	-		211
10	320	G	19	30.13		3	211
12	300	G	20	30.12	-		210
10	290	-	0	30.12	-		208
7	290	-	0	30.11		8	206
16	290	G	22	30.1	-		203
13	260	G	21	30.1	-		203
15	270	G	22	30.11		5	204
15	280	G	21	30.11	-		206
12	300	G	20	30.12	-		209
7	280	-	0	30.14		3	215
6	320	-	0	30.17	-		224
5	40	-	0	30.2	-		237
7	40	-	0	30.22		1	244
15	20	-	0	30.26	-		257
12	40	-	0	30.28	-		262
6	40	-	0	30.29		1	267
9	40	-	0	30.31	-		271
5	10	-	0	30.32	-		276
8	30	-	0	30.33		3	280
6	20	-	0	30.35	-		287
4	30	-	0	30.37	-		294
5	330	-	0	30.39		2	301
9	360	-	0	30.39	-		302
6	VRB	-	0	30.39	-		299
0	0	-	0	30.35		8	287
6	240	-	0	30.35	-		288
7	310	-	0	30.33	-		280
8	270	G	22	30.31		8	273
14	270	G	20	30.27	-		260
15	230	-	0	30.26	-		257
14	260	G	21	30.23		6	248
10	270	-	0	30.23	-		245
8	170	-	0	30.23	-		245
8	160	-	0	30.22		6	243
7	200	-	0	30.23	-		246
6	190	-	0	30.24	-		249
7	190	-	0	30.22		0	244
6	200	-	0	30.22	-		242
3	VRB	-	0	30.2	-		236
0	0	-	0	30.17		8	226
6	110	-	0	30.13	-		212
8	140	-	0	30.09	-		200
7	100	-	0	30.04		8	182
11	100	G	15	30	-		169
12	100	G	18	29.96	-		156
9	50	-	0	29.93		6	143
10	80	-	0	29.88	-		127
9	50	-	0	29.83	-		111

10	30	-	0	29.79	6	97	
9	30	-	0	29.74	-	80	
8	360	-	0	29.7	-	68	
4	360	-	0	29.66	6	52	
9	20	-	0	29.62	-	39	
7	30	-	0	29.57	-	23	
6	30	-	0	29.54	6	13	
6	60	-	0	29.48	-	993	
5	40	-	0	29.49	-	994	
4	20	-	0	29.5	5	1	
5	60	-	0	29.49	-	997	
6	60	-	0	29.46	-	984	
5	20	-	0	29.45	6	981	
0	0	-	0	29.45	-	983	
5	30	-	0	29.47	-	987	
5	40	-	0	29.46	0	987	
7	40	-	0	29.47	-	987	
0	0	-	0	29.48	-	993	
7	260	-	0	29.49	3	997	
9	270	-	0	29.5	-	0	
8	280	-	0	29.52	-	5	
15	280	G	20	29.53	3	10	
14	330	-	0	29.56	-	20	
15	330	G	21	29.58	-	28	
5	270	-	0	30.17	1	227	
6	250	-	0	30.19	-	232	
7	250	-	0	30.22	-	241	
7	280	-	0	30.23	3	248	
6	280	-	0	30.25	-	253	
7	240	-	0	30.26	-	256	
6	270	-	0	30.29	3	267	
5	340	-	0	30.3	-	270	
6	290	-	0	30.32	-	276	
0	0	-	0	30.31	0	273	
0	0	-	0	30.29	-	265	
4	VRB	-	0	30.26	-	257	
9	270	G	17	30.23	8	245	
5	VRB	-	0	30.21	-	239	
13	210	G	19	30.19	-	231	
11	170	-	0	30.16	8	224	
10	160	-	0	30.16	-	223	
10	180	-	0	30.17	-	226	
10	180	-	0	30.17	3	227	
12	210	-	0	30.2	-	236	
10	210	-	0	30.19	-	234	
10	200	-	0	30.2	1	234	
10	230	-	0	30.2	-	235	
6	220	-	0	30.21	-	238	
8	240	-	0	30.21	2	238	
7	230	-	0	30.2	-	237	
6	230	-	0	30.2	-	236	
4	270	-	0	30.2	6	235	

6		230	-			0		30.22	-			241							
5		230	-			0		30.23	-			246							
6		280	-			0		30.24		1		251							
5		270	-			0		30.24	-			251							
3	VRB		-			0		30.25	-			252							
0		0	-			0		30.24		0		251							
3	VRB		-			0		30.24	-			248							
0		0	-			0		30.22	-			244							
5		210	-			0		30.21		8		241							
11		170	G			17		30.2	-			236							
12		170	-			0		30.2	-			235							
10		160	-			0		30.2		5		235							
11		170	-			0		30.19	-			233							
9		170	-			0		30.2	-			236							
9		190	-			0		30.21		3		239							
9		190	-			0		30.23	-			247							
7		190	-			0		30.25	-			253							
9		220	-			0		30.26		1		255							
7		230	-			0		30.26	-			256							
11		230	-			0		30.26	-			256							
8		230	-			0		30.26		0		256							
8		230	-			0		30.26	-			256							
7		230	-			0		30.26	-			257							
8		240	-			0		30.28		3		261							
8		230	-			0		30.28	-			262							
4		210	-			0		30.27	-			259							
6		230	-			0		30.28		3		265							
5		230	-			0		30.28	-			264							
6		180	-			0		30.28	-			263							
6		130	-	0		29.85		-		119									
5		170	-	0		29.87		-		125									
5		150	-	0		29.86		0		120									
4		VRB	-	0		29.85		-		117									
9		180	-	0		29.85		-		116									
9		160	-	0		29.85		6		116									
8		140	-	0		29.85		-		119									
6		150	-	0		29.85		-		118									
7		160	-	0		29.86		1		120									
7		160	-	0		29.86		-		122									
5		140	-	0		29.86		-		120									
4		150	-	0		29.86		0		120									
7		150	-	0		29.86		-		120									
4		140	-	0		29.86		-		120									
4		180	-	0		29.85		8		119									
5		110	-	0		29.82		-		108									
3		VRB	-	0		29.80		-		102									
7		100	-	0		29.79		6		096									
4		110	-	0		29.79		-		096									
8		090	-	0		29.78		-		094									
8		080	-	0		29.78		8		092									
8		110	-	0		29.77		-		092									
8		100	-	0		29.75		-		085									

9	090	-	0	29.74	8	081
7	090	-	0	29.74	-	080
7	090	-	0	29.73	-	076
7	100	-	0	29.72	8	073
6	060	-	0	29.73	-	076
7	060	-	0	29.71	-	071
8	070	-	0	29.69	8	063
6	060	-	0	29.69	-	063
8	060	-	0	29.68	-	061
6	070	-	0	29.71	3	071
8	040	-	0	29.71	-	070
10	070	-	0	29.71	-	069
9	070	-	0	29.72	3	074
10	050	-	0	29.71	-	072
8	030	-	0	29.70	-	068
8	050	-	0	29.68	8	060
11	040	-	0	29.66	-	055
12	040	-	0	29.65	-	049
8	040	-	0	29.67	5	057
9	040	-	0	29.67	-	056
10	040	-	0	29.66	-	052
9	030	-	0	29.66	5	053
11	050	-	0	29.65	-	050
8	040	-	0	29.66	-	052
7	040	-	0	29.66	3	053
4	050	-	0	29.66	-	054
4	350	-	0	29.66	-	054
0	000	-	0	29.65	8	049
0	000	-	0	29.65	-	049
4	130	-	0	29.64	-	048
4	240	-	0	29.65	5	049
0	000	-	0	29.64	-	047
3	200	-	0	29.65	-	051
3	240	-	0	29.67	3	056
5	180	-	0	29.68	-	060
8	170	-	0	29.69	-	064
9	200	-	0	29.69	0	064
6	190	-	0	29.69	-	063
5	210	-	0	29.69	-	062
8	240	-	0	29.68	8	060
6	230	-	0	29.68	-	060
9	230	-	0	29.68	-	061
6	270	-	0	29.69	3	063
4	240	-	0	29.70	-	066
5	240	-	0	29.69	-	064
5	210	-	0	29.70	1	067
7	240	-	0	29.72	-	072
5	220	-	0	29.70	-	067
11	240	-	0	29.69	8	064
10	250	G	16	29.68	-	061
11	250	-	0	29.67	-	058
11	240	G	22	29.66	8	054

13	230	-	0	29.65	-	051
14	230	-	0	29.64	-	045
16	250	-	0	29.64	5	047
11	270	-	0	29.66	-	053
12	270	G	17	29.67	-	056
11	270	-	0	29.69	3	065
8	270	-	0	29.72	-	074
10	360	-	0	29.76	-	086
7	340	-	0	29.77	1	091
6	VRB	-	0	29.77	-	092
4	310	-	0	29.77	-	090
3	310	-	0	29.78	3	093
0	000	-	0	29.78	-	093
4	270	-	0	29.79	-	097
4	240	-	0	29.80	3	100
4	250	-	0	29.82	-	106
5	240	-	0	29.83	-	110
6	240	-	0	29.84	1	115
7	280	-	0	29.85	-	117
8	280	-	0	29.85	-	116
11	280	-	0	29.84	8	114
8	220	-	0	29.84	-	115
10	270	G	18	29.83	-	111
10	250	G	17	29.83	8	110
14	240	G	18	29.82	-	106
15	250	G	18	29.82	-	106
14	260	-	0	29.81	6	105
11	270	-	0	29.81	-	103
12	260	-	0	29.83	-	110
9	270	-	0	29.84	3	115
11	260	-	0	29.87	-	126
7	350	-	0	29.91	-	138
3	360	-	0	29.93	1	144
7	220	-	0	29.94	-	149
6	290	-	0	29.95	-	153
5	290	-	0	29.96	1	156
3	280	-	0	29.97	-	158
7	340	-	0	29.98	-	162
0	000	-	0	30.01	3	171
0	000	-	0	30.03	-	178
0	000	-	0	30.05	-	184
4	330	-	0	30.06	1	190
3	VRB	-	0	30.09	-	197
0	000	-	0	30.09	-	199
4	210	-	0	30.09	1	200
4	260	-	0	30.10	-	202
5	VRB	-	0	30.10	-	204
9	250	-	0	30.10	0	203
4	VRB	-	0	30.09	-	200
13	160	-	0	30.09	-	200
11	160	-	0	30.09	6	199
11	180	-	0	30.09	-	200

7	190	-	0	30.12	-	210
8	200	-	0	30.14	3	214
13	230	-	0	30.16	-	221
11	250	-	0	30.18	-	228
6	280	-	0	30.19	1	232
5	300	-	0	30.21	-	239
5	320	-	0	30.22	-	242
3	350	-	0	30.21	0	240
0	000	-	0	30.21	-	240
6	260	-	0	30.23	-	247
5	160	-	0	30.25	3	253
3	280	-	0	30.27	-	260
4	200	-	0	30.29	-	265
7	010	-	0	30.29	1	266
4	VRB	-	0	30.30	-	270
0	000	-	0	30.30	-	269
5	200	-	0	30.31	3	275
7	220	-	0	30.32	-	276
4	170	-	0	30.31	-	274
6	190	-	0	30.31	8	274
13	220	-	0	30.31	-	274
7	190	-	0	30.30	-	270
6	150	-	0	30.31	5	272
9	150	-	0	30.31	-	274
10	230	-	0	30.33	-	279
0	000	-	0	30.34	3	283
5	220	-	0	30.35	-	288
9	240	-	0	30.37	-	293
4	210	-	0	30.37	1	294
0	000	-	0	30.38	-	297
6	270	-	0	30.38	-	298
0	000	-	0	30.38	0	296
0	000	-	0	30.38	-	295
0	000	-	0	30.39	-	299
0	000	-	0	30.39	3	300
0	000	-	0	30.40	-	305
0	000	-	0	30.42	-	311
0	000	-	0	30.44	3	318
4	VRB	-	0	30.45	-	320
5	090	-	0	30.45	-	320
4	100	-	0	30.45	1	320
5	210	-	0	30.45	-	321
9	190	-	0	30.44	-	317
8	140	-	0	30.43	8	315
8	170	-	0	30.43	-	313
9	150	-	0	30.42	-	312
9	150	-	0	30.42	6	311
10	150	-	0	30.42	-	311
7	150	-	0	30.42	-	310
8	160	-	0	30.42	5	311
9	140	-	0	30.42	-	311
5	140	-	0	30.45	-	320

4	180	-	0	30.45	0	319
0	000	-	0	30.45	-	319
0	000	-	0	30.44	-	318
3	180	-	0	30.44	8	317
0	000	-	0	30.43	-	313
0	000	-	0	30.41	-	309
0	000	-	0	30.42	5	312
4	280	-	0	30.43	-	314
0	000	-	0	30.43	-	314
6	250	-	0	30.44	3	317
6	230	-	0	30.45	-	320
4	260	-	0	30.44	-	317
5	VRB	-	0	30.43	8	314
10	180	-	0	30.39	8	300
11	180	-	0	30.37	-	292
8	160	-	0	30.35	-	286
8	160	-	0	30.33	6	279
9	170	-	0	30.32	-	275
9	180	-	0	30.31	-	275
8	180	-	0	30.32	5	276
6	190	-	0	30.34	-	283
6	210	-	0	30.35	-	286
9	200	-	0	30.33	0	281
8	220	-	0	30.32	-	276
9	230	-	0	30.31	-	273
8	240	-	0	30.30	6	270
9	240	-	0	30.29	-	265
7	230	-	0	30.28	-	263
6	230	-	0	30.29	5	265
7	220	-	0	30.30	-	269
8	220	-	0	30.30	-	271
7	220	-	0	30.31	1	274
6	230	-	0	30.31	-	274
7	240	-	0	30.30	-	271
7	260	-	0	30.29	8	268
7	270	-	0	30.29	-	265
10	270	G	17	30.27	-	260
9	250	-	0	30.25	8	252
9	270	G	14	30.23	-	246
8	250	-	0	30.21	-	239
12	230	-	0	30.19	6	233
7	230	-	0	30.18	-	230
9	250	-	0	30.18	-	229
9	230	-	0	30.18	6	230
10	200	-	0	30.19	-	232
9	210	-	0	30.21	-	238
7	210	-	0	30.22	3	243
10	230	-	0	30.23	-	246
11	240	-	0	30.22	-	243
11	240	-	0	30.22	8	242
8	230	-	0	30.21	-	240
6	240	-	0	30.21	-	239

8	230	-	0	30.20	8	236
8	230	-	0	30.19	-	233
7	240	-	0	30.20	-	237
6	240	-	0	30.20	3	236
8	240	-	0	30.20	-	238
9	250	-	0	30.19	-	233
8	250	-	0	30.19	8	233
4	210	-	0	30.17	-	227
10	240	-	0	30.14	-	216
11	260	-	0	30.11	8	206
11	220	-	0	30.09	-	200
8	240	G	16	30.08	-	194
15	240	G	19	30.06	8	188
14	250	-	0	30.04	-	182
13	230	-	0	30.04	-	181
14	240	-	0	30.04	6	180
12	240	-	0	30.04	-	183
12	240	-	0	30.06	-	188
12	240	-	0	30.05	0	185
14	240	-	0	30.04	-	182
12	240	-	0	30.03	-	179
13	250	-	0	30.01	8	173
12	250	-	0	30.00	-	167
12	260	-	0	29.98	-	163
10	250	-	0	29.98	6	162
8	270	-	0	29.98	-	163
9	280	-	0	29.99	-	166
9	310	-	0	30.01	3	170
8	340	-	0	30.01	-	171
13	340	-	0	30.01	-	171
10	350	G	19	30.01	3	174
14	360	G	19	30.02	-	175
11	300	G	18	30.01	-	171
12	330	-	0	30.00	8	169
11	350	G	19	30.00	-	168
8	280	G	17	29.99	-	165
8	360	-	0	29.98	8	162
8	300	-	0	29.98	-	160
8	350	-	0	29.99	-	163
7	310	-	0	29.99	3	165
8	330	-	0	29.99	-	166
6	VRB	-	0	30.01	-	173
6	360	-	0	30.02	2	174
5	VRB	-	0	30.01	-	173
6	030	-	0	30.02	-	174
7	030	-	0	30.02	3	175
6	040	-	0	30.02	-	174
7	030	-	0	30.02	-	175
6	040	-	0	30.03	3	179
5	040	-	0	30.04	-	182
5	020	-	0	30.06	-	188
4	080	-	0	30.07	3	192

7	080	-	0	30.08	-	197
5	VRB	-	0	30.08	-	195
9	160	-	0	30.09	-	199
7	180	-	0	30.07	8	194
8	170	-	0	30.06	-	187
8	180	-	0	30.04	-	181
7	150	-	0	30.03	6	179
8	140	-	0	30.01	-	172
7	150	-	0	30.02	-	174
7	180	-	0	30.01	6	172
3	VRB	-	0	30.01	-	173
4	150	-	0	30.02	-	175
0	000	-	0	30.03	3	177
0	000	-	0	30.02	-	176
3	190	-	0	30.01	-	172
4	180	-	0	30.00	8	167
0	000	-	0	29.98	-	161
0	000	-	0	29.97	-	158
4	230	-	0	29.97	6	157
3	250	-	0	29.98	-	160
4	230	-	0	29.98	-	162
5	250	-	0	29.98	1	163
3	VRB	-	0	29.98	-	161
0	000	-	0	29.96	-	155
6	170	-	0	29.95	8	152
8	190	-	0	29.93	-	146
11	180	-	0	29.91	-	138
12	160	-	0	29.88	8	126
13	210	G	17	29.87	-	123
11	240	-	0	29.84	-	114
10	230	-	0	29.82	8	109
15	260	-	0	29.83	-	110
13	020	-	0	29.85	-	118
5	040	-	0	29.85	0	116
3	070	-	0	29.83	-	112
3	200	-	0	29.83	-	110
11	210	-	0	29.81	8	104
13	220	-	0	29.80	-	102
10	230	-	0	29.79	-	099
12	230	-	0	29.79	8	096
11	240	-	0	29.77	-	092
10	240	-	0	29.77	-	091
11	240	-	0	29.77	5	092
11	250	-	0	29.77	-	092
13	250	G	19	29.78	-	093
13	260	G	19	29.79	3	096
17	260	G	20	29.78	-	095
15	250	-	0	29.78	-	093
14	280	-	0	29.77	8	090
14	260	-	0	29.76	-	088
8	250	G	20	29.75	-	084
15	270	G	19	29.73	8	078

15	220	-	0	29.70	-	068
17	230	G	22	29.68	-	060
13	240	G	21	29.67	6	057
11	300	G	28	29.67	-	057
6	310	-	0	29.69	-	064
7	010	-	0	29.68	0	059
13	260	-	0	29.72	-	074
9	230	-	0	29.76	-	086
7	190	-	0	29.72	0	075
8	240	-	0	29.71	-	072
10	240	-	0	29.71	-	069
12	240	-	0	29.71	5	070
12	240	-	0	29.70	-	067
6	240	-	0	29.70	-	067
10	240	-	0	29.71	3	071
9	240	-	0	29.73	-	076
6	230	-	0	29.74	-	081
9	250	-	0	29.76	3	086
6	VRB	-	0	29.76	-	087
6	290	-	0	29.77	-	092
9	320	-	0	29.79	3	096
12	290	-	0	29.78	-	095
10	280	G	16	29.79	-	096
11	280	-	0	29.78	8	093
12	290	G	18	29.78	-	093
12	300	-	0	29.77	-	091
15	300	G	19	29.77	5	092
11	310	-	0	29.78	-	096
12	310	-	0	29.80	-	101
10	300	-	0	29.81	2	104
10	320	-	0	29.84	-	114
11	330	-	0	29.87	-	126
7	330	-	0	29.90	1	134
8	350	-	0	29.92	-	142
9	350	-	0	29.94	-	147
8	360	-	0	29.95	1	151
10	360	-	0	29.96	-	155
7	360	-	0	29.97	-	158
8	360	-	0	29.99	3	164
7	020	-	0	30.00	-	169
5	020	-	0	30.02	-	177
8	360	-	0	30.04	3	183
12	360	-	0	30.06	-	189
12	350	-	0	30.07	-	193
11	340	-	0	30.08	1	197
9	360	-	0	30.09	-	200
9	330	G	15	30.10	-	201
10	040	-	0	30.09	0	199
7	040	G	15	30.08	-	195
5	040	-	0	30.07	-	193
6	020	-	0	30.06	6	189
5	030	-	0	30.06	-	188

8	060	-	0	30.07	-	191
3	160	-	0	30.08	3	197
0	000	-	0	30.09	-	198
5	180	-	0	30.11	-	204
5	210	-	0	30.12	3	210
5	220	-	0	30.13	-	214
5	220	-	0	30.14	-	215
6	240	-	0	30.14	1	216
5	240	-	0	30.13	-	212
4	230	-	0	30.13	-	214
3	230	-	0	30.14	3	216
0	000	-	0	30.16	-	221
4	190	-	0	30.18	-	229
4	200	-	0	30.19	2	233
5	210	-	0	30.19	-	233
7	210	-	0	30.18	-	231
7	200	-	0	30.18	8	229
6	190	-	0	30.16	-	224
5	200	-	0	30.15	-	219
8	190	-	0	30.14	6	214
7	180	-	0	30.13	-	211
9	160	-	0	30.11	-	206
10	170	-	0	30.10	8	202
6	170	-	0	30.10	-	202
9	190	-	0	30.10	-	203
9	190	-	0	30.10	3	204
10	190	-	0	30.12	-	207
12	200	-	0	30.12	-	210
8	210	-	0	30.12	0	209
9	220	-	0	30.13	-	212
9	220	G	17	30.13	-	211
7	220	-	0	30.11	8	206
8	240	-	0	30.11	-	206
10	230	-	0	30.11	-	206
8	230	-	0	30.12	3	207
8	230	-	0	30.12	-	210
8	240	-	0	30.12	-	208
12	250	-	0	30.13	3	212
9	260	-	0	30.12	-	208
7	260	-	0	30.11	-	205
12	280	-	0	30.10	6	202
11	280	-	0	30.09	-	199
11	270	-	0	30.08	-	196
10	250	-	0	30.07	8	192
9	270	G	15	30.05	-	184
9	250	-	0	30.02	-	177
11	290	-	0	30.02	6	175
10	260	-	0	30.01	-	173
8	250	-	0	30.01	-	173
9	250	-	0	30.01	6	172
8	230	-	0	30.02	-	175
10	230	-	0	30.03	-	178

9	240	-	0	30.03	1	178
11	230	-	0	30.03	-	178
9	230	-	0	30.02	-	175
11	240	G	21	30.01	8	170
12	240	-	0	30.00	-	169
9	230	-	0	29.99	-	166
9	240	-	0	29.99	7	164
7	230	-	0	29.99	-	167
6	230	-	0	30.00	-	167
8	230	-	0	30.00	0	167
7	260	-	0	29.99	-	165
5	240	-	0	29.99	-	165
4	250	-	0	29.98	8	162
6	280	-	0	29.96	-	155
4	VRB	-	0	29.96	-	155
7	240	-	0	29.94	8	147
7	310	-	0	29.91	-	139
9	310	G	18	29.89	-	132
11	270	-	0	29.88	6	127
12	280	G	20	29.86	-	122
10	270	-	0	29.87	-	124
10	270	-	0	29.86	6	123
9	270	-	0	29.87	-	124
10	270	-	0	29.88	-	126
9	270	-	0	29.87	0	125
9	270	-	0	29.87	-	124
7	250	-	0	29.88	-	127
8	250	-	0	29.88	3	128
6	270	-	0	29.87	-	123
5	290	-	0	29.87	-	123
5	320	-	0	29.87	5	124
5	VRB	-	0	29.87	-	125
5	310	-	0	29.87	-	126
8	330	-	0	29.88	3	128
7	340	-	0	29.88	-	129
7	320	-	0	29.87	-	124
7	290	-	0	29.84	-	114
5	VRB	G	16	29.83	8	110
10	320	-	0	29.82	-	108
12	280	-	0	29.81	-	103
9	280	-	0	29.80	8	099
8	320	G	15	29.79	-	096
11	320	-	0	29.79	-	097
8	280	-	0	29.80	3	100
6	290	-	0	29.80	-	101
7	280	-	0	29.81	-	103
6	290	-	0	29.81	3	105
7	300	-	0	29.82	-	107
7	330	-	0	29.82	-	107
8	340	-	0	29.82	1	109
5	330	-	0	29.82	-	108
7	330	-	0	29.83	-	110

7	300	-	0	29.84	3	116
5	300	-	0	29.85	-	119
0	000	-	0	29.86	-	123
10	320	-	0	29.88	3	126
10	330	-	0	29.88	-	129
5	VRB	-	0	29.88	-	126
7	300	-	0	29.86	8	123
10	330	G	19	29.85	-	119
11	290	G	18	29.84	-	116
6	VRB	G	17	29.83	8	112
13	270	G	17	29.82	-	106
15	280	G	20	29.80	-	102
17	300	G	20	29.79	6	097
14	280	-	0	29.78	-	095
14	280	G	18	29.78	-	095
8	290	-	0	29.78	6	095
9	290	-	0	29.79	-	098
9	270	-	0	29.81	-	104
7	290	-	0	29.82	3	107
6	300	-	0	29.82	-	107
10	320	-	0	29.83	-	110
12	360	-	0	29.83	3	112
9	350	-	0	29.83	-	112
12	340	-	0	29.84	-	115
11	330	-	0	29.86	3	120
9	340	-	0	29.86	-	123
14	340	G	21	29.88	-	127
12	320	G	19	29.89	3	132
12	350	-	0	29.90	-	136
12	010	G	24	29.91	-	137
16	330	G	22	29.91	1	137
18	320	G	22	29.92	-	140
15	330	G	22	29.91	-	137
16	340	G	24	29.91	1	138
16	320	G	26	29.91	-	139
19	330	G	23	29.92	-	143
19	320	G	24	29.93	3	144
16	330	G	22	29.94	-	149
16	350	G	20	29.96	-	156
17	360	G	22	29.97	1	159
12	340	-	0	29.99	-	165
15	330	G	19	30.00	-	170
11	350	-	0	30.01	1	173
11	340	-	0	30.04	-	180
12	340	-	0	30.04	-	181
8	330	-	0	30.03	0	178
3	VRB	-	0	30.01	-	172
4	290	-	0	30.00	-	169
4	270	-	0	29.99	6	167
5	310	-	0	29.99	-	166
8	340	-	0	30.00	-	169
9	340	-	0	30.02	3	174

8	350	-	0	30.02	-	175
8	020	-	0	30.02	-	176
12	010	-	0	30.02	0	175
12	350	-	0	30.01	-	172
15	350	G	21	29.99	-	166
13	330	-	0	29.98	8	162
8	310	-	0	29.98	-	161
15	310	G	18	29.98	-	161
11	340	G	21	29.97	8	158
14	310	G	19	29.97	-	159
11	330	-	0	29.98	-	162
10	310	-	0	29.99	3	166
11	300	-	0	30.00	-	169
10	310	G	17	30.02	-	174
12	320	-	0	30.02	1	176
11	320	-	0	30.03	-	178
6	300	-	0	30.03	-	178
6	260	-	0	30.03	1	178
6	250	-	0	30.03	-	179
4	300	-	0	30.02	-	176
5	310	-	0	30.04	3	180
7	310	-	0	30.05	-	185
10	310	-	0	30.07	-	191
6	VRB	-	0	30.08	1	196
6	310	-	0	30.08	-	195
7	300	-	0	30.08	-	194
10	310	-	0	30.08	3	197
8	310	-	0	30.08	-	194
6	VRB	-	0	30.06	-	188
10	290	-	0	30.05	8	185
12	310	-	0	30.04	-	182
12	310	G	19	30.03	-	179
13	300	-	0	30.02	8	175
9	300	-	0	30.02	-	176
11	280	-	0	30.04	-	182
10	280	-	0	30.06	3	187
8	280	-	0	30.07	-	194
6	VRB	-	0	30.09	-	199
5	VRB	-	0	30.10	1	203
6	270	-	0	30.11	-	205
5	230	-	0	30.10	-	203
3	250	-	0	30.11	2	206
5	240	-	0	30.11	-	206
3	230	-	0	30.12	-	209
3	230	-	0	30.12	3	210
5	240	-	0	30.13	-	212
7	240	-	0	30.15	-	220
3	240	-	0	30.17	3	224
4	VRB	-	0	30.16	-	223
8	300	-	0	30.15	-	220
12	270	-	0	30.14	8	214
8	310	G	16	30.11	-	207

12	240	-	0	30.10	-	204
8	260	G	16	30.07	8	193
11	280	-	0	30.06	-	190
13	270	G	17	30.05	-	185
10	270	-	0	30.03	8	179
9	270	G	14	30.02	-	175
10	290	-	0	30.02	-	175
7	250	-	0	30.02	5	176
9	240	-	0	30.02	-	176
10	230	-	0	30.02	-	176
10	240	-	0	30.01	8	174
8	210	-	0	30.00	-	169
9	230	-	0	30.00	-	168
12	240	G	19	29.99	6	166
10	240	-	0	29.98	-	161
11	240	-	0	29.97	-	158
9	240	-	0	29.96	6	155
11	240	-	0	29.95	-	151
10	240	-	0	29.94	-	149
11	240	-	0	29.94	5	150
15	250	-	0	29.94	-	147
12	250	-	0	29.93	-	145
11	260	-	0	29.92	8	141
11	260	G	15	29.90	-	135
11	260	-	0	29.88	-	130
9	240	-	0	29.86	8	121
13	240	-	0	29.84	-	116
15	260	G	19	29.82	-	107
14	250	-	0	29.80	8	100
14	270	-	0	29.84	-	113
12	300	-	0	29.84	-	114
9	310	-	0	29.86	1	120
8	310	-	0	29.87	-	123
7	330	-	0	29.85	-	119
4	270	-	0	29.86	1	120
8	250	-	0	29.87	-	124
7	250	-	0	29.86	-	122
9	260	G	16	29.86	1	122
7	290	-	0	29.83	-	112
10	360	-	0	29.82	-	106
8	350	G	17	29.84	5	115
8	010	-	0	29.87	-	124
9	360	-	0	29.89	-	130
15	020	-	0	29.91	1	137
12	040	-	0	29.91	-	139
12	040	-	0	29.92	-	142
9	010	-	0	29.92	0	141
11	340	G	15	29.91	-	140
14	260	G	19	29.88	8	127
13	280	-	0	29.87	-	126
12	270	-	0	29.87	-	126
14	290	-	0	29.89	3	131

12	290	-	0	29.92	-	142
14	340	G	19	29.95	-	152
11	340	-	0	29.98	2	163
16	360	-	0	30.00	-	169
12	360	-	0	30.03	-	178
14	360	-	0	30.05	2	184
13	350	-	0	30.06	-	188
12	360	-	0	30.09	-	198
8	340	G	18	30.11	3	206
9	330	-	0	30.12	-	209
7	340	-	0	30.13	-	211
6	010	-	0	30.15	3	218
6	350	-	0	30.18	-	228
7	360	-	0	30.21	-	238
8	010	-	0	30.24	1	248
9	030	-	0	30.25	-	253
5	030	-	0	30.25	8	253
6	340	-	0	30.24	-	248
0	000	-	0	30.23	-	246
4	080	-	0	30.22	6	244
5	100	-	0	30.23	-	245
5	050	-	0	30.23	-	246
3	050	-	0	30.24	3	249
0	000	-	0	30.25	-	253
0	000	-	0	30.26	-	258
0	000	-	0	30.26	1	258
3	320	-	0	30.27	-	261
3	030	-	0	30.28	-	262
5	030	-	0	30.28	1	262
7	040	-	0	30.28	-	262
8	030	-	0	30.27	-	260
7	040	-	0	30.27	5	261
8	040	-	0	30.28	-	264
6	030	-	0	30.30	-	269
7	030	-	0	30.31	3	275
8	040	-	0	30.32	-	276
9	040	-	0	30.31	-	274
6	040	-	0	30.31	8	272
7	140	-	0	30.30	-	269
8	150	-	0	30.29	-	265
9	160	-	0	30.27	8	260
8	150	G	16	30.26	-	258
11	150	-	0	30.26	-	257
7	140	-	0	30.26	5	258
9	150	-	0	30.27	-	258
6	VRB	-	0	30.27	-	258
6	150	-	0	30.27	2	259
6	160	-	0	30.27	-	261
4	150	-	0	30.28	-	262
6	140	-	0	30.27	8	259
9	170	-	0	30.26	-	255
3	140	-	0	30.26	-	257

7	160	-	0	30.26	5	258
3	120	-	0	30.26	-	257
0	000	-	0	30.25	-	254
6	140	-	0	30.26	5	256
3	VRB	-	0	30.27	-	259
3	VRB	-	0	30.27	-	261
0	000	-	0	30.28	3	264
6	180	-	0	30.30	-	268
5	170	-	0	30.31	-	272
7	160	-	0	30.31	1	273
7	180	-	0	30.30	-	270
7	170	-	0	30.30	-	269
7	140	-	0	30.29	8	265
6	120	-	0	30.28	-	264
9	120	-	0	30.28	-	264
10	120	-	0	30.29	5	265
9	120	-	0	30.28	-	262
7	140	-	0	30.30	-	268
7	130	-	0	30.31	3	271
6	120	-	0	30.31	-	273
5	090	-	0	30.31	-	273
5	080	-	0	30.31	0	272
7	080	-	0	30.30	-	268
9	080	-	0	30.28	-	264
7	070	-	0	30.28	5	265
7	060	-	0	30.28	-	263
8	070	-	0	30.25	-	254
7	050	-	0	30.26	5	255
11	050	-	0	30.25	-	253
9	060	-	0	30.25	-	252
6	060	-	0	30.25	5	254
11	070	-	0	30.26	-	257
11	080	-	0	30.25	-	254
8	060	-	0	30.24	8	251
9	060	-	0	30.24	-	250
8	040	-	0	30.22	-	244
10	040	-	0	30.19	8	234
11	050	-	0	30.17	-	226
8	060	-	0	30.16	-	223
10	050	-	0	30.16	6	221
10	060	-	0	30.16	-	221
9	080	-	0	30.15	-	220
9	080	-	0	30.15	8	217
7	060	-	0	30.15	-	218
6	060	-	0	30.14	-	216
10	050	-	0	30.13	8	212
13	050	-	0	30.11	-	207
9	050	-	0	30.10	-	203
7	070	-	0	30.09	6	199
9	060	-	0	30.08	-	197
9	050	-	0	30.09	-	198
9	050	-	0	30.08	6	196

10	040	-	0	30.09	-	200
11	040	-	0	30.10	-	201
13	050	-	0	30.10	1	202
15	030	-	0	30.12	-	208
11	050	-	0	30.12	-	209
13	040	-	0	30.13	1	212
14	040	-	0	30.13	-	211
12	050	-	0	30.12	-	208
16	050	-	0	30.11	8	205
14	050	-	0	30.11	-	205
12	050	-	0	30.11	-	206
12	040	-	0	30.12	3	210
13	050	-	0	30.12	-	211
11	040	-	0	30.13	-	213
12	040	-	0	30.15	3	217
10	040	-	0	30.14	-	217
11	030	-	0	30.14	-	217
11	040	-	0	30.13	8	213
11	040	-	0	30.13	-	211
10	030	-	0	30.12	-	208
9	040	-	0	30.12	6	208
8	030	-	0	30.10	-	203
8	030	-	0	30.10	-	203
8	030	-	0	30.11	5	204
7	030	-	0	30.11	-	206
8	030	-	0	30.11	-	205
9	030	-	0	30.11	8	204
7	030	-	0	30.11	-	205
7	020	-	0	30.11	-	206
8	010	-	0	30.10	8	203
7	040	-	0	30.09	-	198
4	060	-	0	30.06	-	189
0	000	-	0	30.05	6	186
0	000	-	0	30.04	-	182
0	000	-	0	30.04	-	183
0	000	-	0	30.04	6	181
4	VRB	-	0	30.04	-	181
3	VRB	-	0	30.04	-	183
4	280	-	0	30.05	3	186
5	270	-	0	30.05	-	186
15	300	G	26	30.07	-	191
15	340	G	23	30.09	3	197
14	350	-	0	30.10	-	200
12	350	-	0	30.12	-	209
7	330	-	0	30.13	3	213
18	350	G	21	30.14	-	217
17	340	G	22	30.16	-	222
11	340	-	0	30.18	3	230
14	340	-	0	30.20	-	236
16	340	G	21	30.21	-	239
11	340	G	18	30.25	3	252
5	100	-	0	30.19	-	234

7	110	-	0	30.14	8	216
7	150	-	0	30.12	-	209
9	110	-	0	30.11	-	206
7	120	-	0	30.10	6	201
8	090	-	0	30.08	-	197
10	110	-	0	30.07	-	193
7	070	-	0	30.06	7	188
6	080	-	0	30.05	-	185
9	060	-	0	30.02	-	174
7	070	-	0	30.00	8	168
10	090	G	18	29.98	-	161
9	080	-	0	29.95	-	151
9	060	-	0	29.92	8	142
13	070	-	0	29.88	-	129
10	050	-	0	29.86	-	120
14	040	-	0	29.82	6	108
15	040	-	0	29.80	-	100
19	040	-	0	29.77	-	089
18	050	G	27	29.72	8	074
21	050	G	28	29.70	-	065
21	040	G	30	29.63	-	044
20	050	G	29	29.56	8	019
17	040	G	28	29.50	-	999
20	040	G	25	29.45	-	981
17	030	-	0	29.37	8	956
19	010	-	0	29.30	-	932
21	360	G	26	29.27	-	920
16	300	G	22	29.27	6	920
23	310	G	29	29.33	-	942
21	320	G	28	29.39	-	960
14	320	G	21	29.43	1	976
10	270	-	0	29.50	-	999
9	280	-	0	29.54	-	013
10	290	-	0	29.59	1	028
9	280	-	0	29.63	-	043
5	270	-	0	29.63	-	044
6	240	-	0	29.66	1	052
7	220	-	0	29.70	-	068
9	250	-	0	29.72	-	073
5	240	-	0	29.73	1	078
8	250	-	0	29.78	-	093
6	230	-	0	29.81	-	105
6	240	-	0	29.84	1	114
7	270	-	0	29.86	-	122
6	320	-	0	29.87	-	124
10	340	-	0	29.86	0	122
7	340	-	0	29.87	-	126
4	350	-	0	29.86	8	121
5	090	-	0	29.85	-	117
8	260	-	0	29.85	-	116
10	210	-	0	29.84	6	116
5	180	-	0	29.85	-	119

6	250	-	0	29.87	-	123
11	260	-	0	29.89	3	130
8	290	-	0	29.90	-	134
7	270	-	0	29.92	-	141
5	VRB	-	0	29.91	0	137
6	280	-	0	29.91	-	137
7	280	-	0	29.91	-	136
8	280	-	0	29.93	3	143
6	290	-	0	29.95	-	150
9	280	-	0	29.95	-	152
11	300	-	0	29.97	3	159
8	290	-	0	30.00	-	168
7	340	-	0	30.02	-	175
7	320	-	0	30.04	1	182
9	330	G	15	30.07	-	192
10	350	-	0	30.09	-	199
7	350	-	0	30.10	1	204
4	VRB	G	14	30.11	-	205
5	300	-	0	30.10	-	201
8	260	-	0	30.08	8	196
7	300	-	0	30.08	-	195
9	280	-	0	30.09	-	198
10	280	-	0	30.09	3	199
9	250	-	0	30.09	-	199
9	250	-	0	30.12	-	207
8	250	-	0	30.14	3	214
8	240	-	0	30.15	-	218
6	250	-	0	30.16	-	221
6	230	-	0	30.15	0	220
5	240	-	0	30.14	-	217
7	240	-	0	30.14	-	215
6	230	-	0	30.13	7	211
4	240	-	0	30.11	-	204
3	230	-	0	30.08	-	196
4	220	-	0	30.08	6	196
8	210	-	0	30.07	-	193
5	230	-	0	30.06	-	188
7	200	-	0	30.03	8	180
14	220	-	0	30.03	-	178
15	210	-	0	30.01	-	171
10	210	-	0	29.99	8	165
15	200	G	20	29.89	-	132
17	220	G	27	29.85	8	117
15	230	G	22	29.81	-	105
17	230	G	23	29.80	-	099
11	250	-	0	29.81	5	103
8	260	-	0	29.83	-	109
9	250	-	0	29.83	-	112
10	230	-	0	29.83	0	111
8	240	-	0	29.84	-	115
11	230	G	18	29.85	-	116
10	240	-	0	29.84	0	115

7	270	-	0	29.86	-	120
9	260	-	0	29.86	-	122
6	260	-	0	29.87	1	124
10	290	-	0	29.88	-	127
6	270	-	0	29.89	-	130
5	270	-	0	29.90	1	133
3	260	-	0	29.91	-	137
6	270	-	0	29.93	-	145
7	280	-	0	29.93	1	146
9	280	-	0	29.96	-	154
8	330	-	0	29.97	-	157
13	310	-	0	29.96	0	156
8	300	-	0	29.96	-	153
9	310	-	0	29.93	8	143
3	VRB	-	0	29.92	-	142
0	000	-	0	29.92	-	140
8	330	-	0	29.92	5	142
8	330	-	0	29.94	-	149
6	330	-	0	29.96	-	156
6	330	-	0	29.98	1	161
8	020	-	0	29.99	-	165
7	020	-	0	30.00	-	168
5	030	-	0	30.02	3	175
4	020	-	0	30.01	-	173
0	000	-	0	30.01	-	173
3	280	-	0	30.02	5	174
3	230	-	0	30.02	-	175
4	260	-	0	30.01	-	173
0	000	-	0	30.01	8	172
6	340	-	0	30.04	-	180
8	010	-	0	30.04	-	183
8	010	-	0	30.08	3	194
13	350	-	0	30.10	-	202
11	020	-	0	30.11	-	206
11	350	-	0	30.12	1	207
5	020	-	0	30.10	-	203
12	360	G	16	30.08	-	195
15	010	-	0	30.07	6	191
10	360	-	0	30.06	-	187
6	010	-	0	30.06	-	188
5	VRB	-	0	30.07	5	191
10	010	-	0	30.08	-	196
9	030	-	0	30.10	-	200
8	010	-	0	30.11	3	206
7	350	-	0	30.12	-	208
12	020	-	0	30.14	-	216
9	020	-	0	30.16	3	222
9	020	-	0	30.17	-	224
7	030	-	0	30.18	-	227
9	020	-	0	30.18	2	229
9	030	-	0	30.18	-	230
9	030	-	0	30.17	-	226

8	030	-	0	30.17	5	227
9	020	-	0	30.20	-	235
9	030	-	0	30.21	-	239
9	040	-	0	30.22	1	242
8	030	-	0	30.23	-	244
11	050	-	0	30.24	-	251
14	040	-	0	30.23	0	245
8	010	-	0	30.23	-	244
11	360	-	0	30.22	-	244
11	360	-	0	30.23	3	247
14	350	-	0	30.24	-	249
16	350	-	0	30.28	-	263
7	360	-	0	30.30	3	269
7	010	-	0	30.32	-	276
7	340	-	0	30.34	-	283
7	010	-	0	30.35	1	285
8	020	-	0	30.35	-	288
10	010	-	0	30.36	-	288
10	020	-	0	30.36	1	290
9	030	-	0	30.38	-	296
7	030	-	0	30.38	-	298
6	020	-	0	30.39	1	301
7	010	-	0	30.40	-	302
6	360	-	0	30.40	-	304
7	360	-	0	30.42	3	310
9	010	-	0	30.43	-	314
8	040	-	0	30.43	-	314
7	030	-	0	30.42	0	311
7	020	-	0	30.40	-	305
5	VRB	-	0	30.38	-	298
3	050	-	0	30.37	6	294
0	000	-	0	30.36	-	290
4	230	-	0	30.35	-	288
0	000	-	0	30.34	7	283
5	210	-	0	30.34	-	283
0	000	-	0	30.34	-	283
7	290	-	0	30.34	3	284
6	300	-	0	30.34	-	283
5	330	-	0	30.36	-	290
4	360	-	0	30.37	3	292
0	000	-	0	30.36	-	289
3	320	-	0	30.35	-	288
9	350	-	0	30.34	8	285
6	340	-	0	30.35	-	288
6	350	-	0	30.36	-	290
6	040	-	0	30.37	1	292
9	020	-	0	30.37	-	293
10	040	-	0	30.37	-	292
10	040	-	0	30.37	3	294
11	030	-	0	30.38	-	299
9	040	-	0	30.40	-	304
7	040	-	0	30.40	1	304

9	030	-	0	30.39	-	301
7	060	-	0	30.37	-	295
4	100	-	0	30.35	8	285
5	080	-	0	30.33	-	281
7	120	-	0	30.31	-	275
8	090	-	0	30.29	8	266
7	120	-	0	30.28	-	264
6	110	-	0	30.28	-	262
8	090	-	0	30.25	8	254
6	090	-	0	30.21	-	239
7	080	-	0	30.18	-	228
7	090	-	0	30.15	6	219
8	060	-	0	30.11	-	206
10	060	-	0	30.10	-	202
10	080	-	0	30.06	8	188
10	080	-	0	30.02	-	174
9	080	-	0	29.96	-	153
8	080	-	0	29.93	6	144
7	050	-	0	29.93	-	144
9	020	-	0	29.91	-	137
8	040	-	0	29.89	8	132
8	040	-	0	29.87	-	125
10	040	-	0	29.85	-	119
10	020	-	0	29.82	8	108
9	350	-	0	29.81	-	104
12	350	-	0	29.80	-	099
10	340	G	17	29.79	6	096
10	340	-	0	29.78	-	094
7	330	-	0	29.80	-	102
13	330	G	21	29.81	3	105
13	330	-	0	29.83	-	109
10	320	G	18	29.85	-	119
6	300	-	0	29.86	1	122
7	240	-	0	29.87	-	125
5	260	-	0	29.90	-	134
6	270	-	0	29.92	3	141
4	240	-	0	29.93	-	146
4	250	-	0	29.95	-	150
10	320	-	0	29.97	3	158
6	320	-	0	30.00	-	168
11	360	-	0	30.01	-	170
11	360	-	0	30.01	1	170
9	330	-	0	30.01	-	172
3	300	-	0	30.02	-	175
7	300	-	0	30.04	3	182
8	280	-	0	30.06	-	188
9	300	-	0	30.06	-	187
7	290	-	0	30.05	0	186
10	280	-	0	30.04	-	182
6	290	-	0	30.02	-	176
9	310	-	0	30.01	8	171
7	250	-	0	29.99	-	164

9	260	-	0	29.98	-	162
7	270	-	0	29.98	6	161
4	310	-	0	29.98	-	163
7	270	-	0	30.02	-	175
13	010	-	0	30.05	3	186
12	350	-	0	30.06	-	188
11	340	-	0	30.07	-	191
6	310	-	0	30.07	2	193
7	300	-	0	30.08	-	196
6	310	-	0	30.09	-	198
5	320	-	0	30.09	1	199
5	290	-	0	30.09	-	199
8	320	-	0	30.08	-	195
4	320	-	0	30.07	8	192
6	320	-	0	30.08	-	195
4	300	-	0	30.09	-	198
4	280	-	0	30.10	3	200
9	320	-	0	30.12	-	208
9	320	-	0	30.12	-	207
9	330	G	14	30.10	0	202
6	300	-	0	30.09	-	197
9	330	-	0	30.07	-	191
9	340	-	0	30.05	8	185
8	300	-	0	30.04	-	182
12	310	-	0	30.04	-	182
6	340	-	0	30.04	6	180
10	360	-	0	30.04	-	180
11	350	-	0	30.06	-	187
10	350	-	0	30.08	3	194
10	340	-	0	30.09	-	198
10	340	-	0	30.10	-	201
10	360	-	0	30.11	3	205
11	360	-	0	30.11	-	205
7	030	-	0	30.11	-	206
4	010	-	0	30.12	3	210
7	030	-	0	30.14	-	214
5	040	-	0	30.14	-	217
9	030	-	0	30.15	1	218
10	030	-	0	30.15	-	218
11	030	-	0	30.16	-	223
9	030	-	0	30.17	3	227
14	030	-	0	30.19	-	234
17	030	-	0	30.18	-	228
16	030	-	0	30.17	8	224
9	050	-	0	30.15	-	218
11	020	-	0	30.10	6	200
8	010	-	0	30.09	-	200
9	010	-	0	30.11	-	204
9	020	-	0	30.07	8	193
11	040	-	0	30.03	-	177
10	020	-	0	30.06	-	188
12	020	G	19	30.07	5	191

9	040	-	0	30.06	-	188
12	050	G	20	30.04	-	181
8	030	-	0	30.04	6	181
7	010	-	0	30.05	-	185
14	040	-	0	30.05	-	185
11	050	-	0	30.02	8	175
11	050	-	0	29.98	-	163
14	040	-	0	29.97	-	158
10	040	-	0	29.96	6	156
10	030	-	0	29.98	-	160
10	030	-	0	29.97	-	159
12	040	-	0	29.97	0	158
13	030	-	0	30.00	-	168
14	050	-	0	29.99	-	164
16	030	-	0	29.98	0	163
14	040	-	0	29.96	-	154
10	060	-	0	29.94	-	148
11	040	-	0	29.92	6	142
13	020	-	0	29.91	-	139
11	050	-	0	29.91	-	138
13	030	-	0	29.90	8	136
12	030	-	0	29.89	-	131
12	030	-	0	29.92	-	140
14	030	-	0	29.93	3	144
15	030	-	0	29.93	-	143
10	020	-	0	29.94	-	147
10	010	-	0	29.94	3	149
8	020	-	0	29.94	-	148
10	020	-	0	29.94	-	146
11	020	-	0	29.93	8	143
8	020	-	0	29.92	-	140
10	030	-	0	29.91	-	138
11	030	-	0	29.93	3	145
12	010	-	0	29.95	-	151
12	020	-	0	29.97	-	157
9	010	-	0	29.99	3	166
10	030	-	0	30.01	-	171
10	030	-	0	30.01	-	173
11	010	-	0	30.01	0	172
6	360	-	0	30.00	-	168
6	030	-	0	29.97	-	160
7	340	-	0	29.97	6	157
5	330	-	0	29.97	-	157
7	010	-	0	29.96	-	156
8	010	-	0	29.96	6	156
7	010	-	0	29.96	-	156
0	000	-	0	29.98	-	161
0	000	-	0	29.99	3	166
4	270	-	0	30.00	-	169
19	230	-	0	30.00	8	169
18	240	G	23	29.98	-	161
17	240	G	21	29.98	-	160

15	230	-	0	29.98	5	161
12	230	-	0	29.97	-	158
10	220	-	0	29.98	-	161
10	220	-	0	29.99	3	166
8	220	-	0	30.01	-	171
10	210	-	0	30.01	-	171
10	220	-	0	30.01	1	172
9	220	-	0	30.01	-	172
9	210	-	0	30.01	-	172
9	230	-	0	30.01	8	171
8	220	-	0	30.02	-	174
9	230	-	0	30.02	-	176
6	240	-	0	30.02	0	175
4	260	-	0	30.03	-	178
0	000	-	0	30.02	-	176
3	220	-	0	30.04	3	182
4	220	-	0	30.05	-	185
8	200	-	0	30.05	-	186
9	230	-	0	30.05	0	186
9	210	-	0	30.03	-	177
9	200	-	0	29.97	8	159
7	200	-	0	29.95	-	150
8	190	-	0	29.94	-	147
6	180	-	0	29.94	6	148
5	210	-	0	29.95	-	152
4	180	-	0	29.94	-	149
7	220	-	0	29.97	3	158
6	180	-	0	29.96	-	154
6	190	-	0	29.97	-	158
3	160	-	0	29.97	3	158
5	190	-	0	29.96	-	155
5	190	-	0	29.96	-	155
4	180	-	0	29.95	8	152
0	000	-	0	29.94	-	149
0	000	-	0	29.93	-	146
0	000	-	0	29.92	8	140
3	210	-	0	29.92	-	140
4	170	-	0	29.91	-	137
5	190	-	0	29.91	5	138
8	200	-	0	29.91	-	139
7	200	-	0	29.91	-	136
10	200	-	0	29.89	8	131
14	190	-	0	29.86	-	122
11	200	G	21	29.80	8	099
15	200	-	0	29.76	-	087
10	180	-	0	29.75	-	085
11	180	-	0	29.76	5	089
6	170	-	0	29.77	-	091
4	150	-	0	29.78	-	094
4	180	-	0	29.79	1	096
5	160	-	0	29.76	-	088
4	120	-	0	29.75	-	083

0	000	-	0	29.76	5	087
8	190	-	0	29.75	-	083
8	190	-	0	29.73	-	076
8	180	-	0	29.71	8	069
6	170	-	0	29.69	-	063
7	170	-	0	29.68	-	061
10	200	-	0	29.71	3	069
8	190	-	0	29.72	-	072
6	180	-	0	29.71	-	071
10	190	-	0	29.74	3	079
10	190	-	0	29.74	-	080
9	240	-	0	29.99	-	165
6	210	-	0	30.01	3	171
8	240	-	0	30.02	-	176
7	260	-	0	30.03	-	178
4	240	-	0	30.03	1	178
0	000	-	0	30.04	-	181
5	220	-	0	30.06	-	188
0	000	-	0	30.05	0	186
4	020	-	0	30.04	-	183
11	030	-	0	30.05	-	184
12	030	-	0	30.06	3	189
12	040	-	0	30.08	-	194
13	020	-	0	30.10	-	202
11	030	-	0	30.12	3	210
13	030	-	0	30.14	-	217
13	040	-	0	30.14	-	216
14	050	G	18	30.15	1	218
10	050	-	0	30.14	-	215
13	040	G	19	30.12	-	207
16	060	G	20	30.09	8	198
16	060	G	20	30.08	-	194
14	060	-	0	30.08	-	197
12	050	G	21	30.10	3	201
13	050	-	0	30.09	-	199
17	040	G	23	30.07	-	190
16	050	G	23	30.07	5	192
16	040	G	21	30.05	-	186
17	050	G	23	30.03	-	177
19	040	-	0	30.00	8	169
20	050	G	24	29.94	-	147
18	050	G	25	29.89	-	132
20	050	G	25	29.83	6	110
15	040	G	24	29.78	-	095
16	030	-	0	29.75	-	082
19	030	-	0	29.70	8	067
15	020	-	0	29.71	-	071
16	020	-	0	29.70	-	066
17	040	-	0	29.68	8	059
16	040	G	23	29.64	-	047
16	040	G	21	29.62	-	041
10	020	-	0	29.65	5	048

11	020	-	0	29.67	-	057
17	040	-	0	29.61	-	037
10	030	-	0	29.61	8	037
11	050	-	0	29.62	-	038
8	040	-	0	29.60	-	034
8	020	-	0	29.60	8	033
9	010	-	0	29.58	-	027
9	020	-	0	29.60	-	033
8	040	-	0	29.59	6	030
12	020	-	0	29.58	-	027
9	010	-	0	29.60	-	033
7	010	-	0	29.57	8	022
8	360	-	0	29.52	-	007
10	270	-	0	29.58	-	025
8	290	-	0	29.57	3	022
12	280	-	0	29.57	-	022
19	300	G	27	29.97	1	159
18	290	G	26	30.00	-	169
16	290	G	26	30.03	-	179
19	280	G	25	30.06	2	189
14	270	-	0	30.11	-	206
11	280	-	0	30.16	-	222
6	270	-	0	30.20	1	235
7	270	-	0	30.21	-	241
7	270	-	0	30.25	-	251
9	270	-	0	30.27	3	258
8	280	-	0	30.28	-	263
5	310	-	0	30.29	-	265
5	330	-	0	30.28	0	264
4	300	-	0	30.29	-	268
6	230	-	0	30.31	-	273
5	260	-	0	30.30	0	269
4	270	-	0	30.32	-	275
3	360	-	0	30.31	-	273
3	170	-	0	30.30	0	271
4	230	-	0	30.31	-	273
5	290	-	0	30.32	-	275
3	VRB	-	0	30.30	8	268
5	220	-	0	30.30	-	269
5	210	-	0	30.28	-	263
6	200	-	0	30.24	8	251
5	180	-	0	30.20	-	236
7	150	-	0	30.18	-	228
8	150	G	14	30.16	6	221
7	170	-	0	30.16	-	222
4	VRB	-	0	30.16	-	223
4	190	-	0	30.16	0	222
5	190	-	0	30.15	-	220
3	210	-	0	30.17	-	224
6	260	-	0	30.16	3	223
4	250	-	0	30.16	-	223
7	250	-	0	30.16	-	223

7	280	-	0	30.16	8	222
4	270	-	0	30.17	-	226
4	190	-	0	30.17	-	227
6	220	-	0	30.19	1	231
6	230	-	0	30.19	-	233
0	000	-	0	30.20	-	236
5	270	-	0	30.21	3	238
7	260	-	0	30.23	-	245
4	270	-	0	30.23	-	247
0	000	-	0	30.23	1	247
4	310	-	0	30.23	-	245
3	VRB	-	0	30.19	-	233
4	290	-	0	30.18	8	228
6	200	-	0	30.16	-	221
6	190	-	0	30.16	-	222
7	190	-	0	30.16	5	222
5	180	-	0	30.17	-	225
4	200	-	0	30.17	-	226
4	190	-	0	30.17	0	225
4	230	-	0	30.16	-	223
5	200	-	0	30.15	-	218
0	000	-	0	30.14	6	217
3	220	-	0	30.13	-	212
5	240	-	0	30.13	-	213
0	000	-	0	30.12	8	208
0	000	-	0	30.12	-	207
0	000	-	0	30.11	-	204
0	000	-	0	30.08	8	196
0	000	-	0	30.07	-	192
3	040	-	0	30.06	-	188
0	000	-	0	30.04	8	183
0	000	-	0	30.04	-	181
0	000	-	0	30.03	-	177
4	030	-	0	30.02	6	176
0	000	-	0	30.01	-	171
4	140	-	0	29.97	-	158
3	150	-	0	29.92	8	142
5	160	-	0	29.92	-	140
6	110	-	0	29.89	-	130
5	120	-	0	29.87	8	125
4	090	-	0	29.86	-	121
3	100	-	0	29.86	-	120
5	050	-	0	29.84	8	114
7	040	-	0	29.83	-	110
7	050	-	0	29.80	-	100
6	040	-	0	29.77	8	089
6	050	-	0	29.74	-	081
6	040	-	0	29.72	-	072
7	030	-	0	29.69	6	064
7	040	-	0	29.66	-	053
7	020	-	0	29.64	-	045
7	030	-	0	29.63	6	043

8	030	-	0	29.60	-	033
5	030	-	0	29.58	-	026
7	010	-	0	29.58	6	025
7	030	-	0	29.57	-	023
7	020	-	0	29.55	-	017
4	080	-	0	29.46	7	985
3	080	-	0	29.43	-	977
6	140	-	0	29.41	-	970
5	140	-	0	29.38	8	959
6	200	-	0	29.39	-	963
14	310	G	18	29.41	-	967
6	280	-	0	29.41	1	969
11	270	-	0	29.41	-	970
12	260	-	0	29.42	-	972
10	250	-	0	29.43	3	975
11	260	-	0	29.42	-	971
15	250	-	0	29.41	-	968
17	260	G	22	29.41	6	967
17	270	-	0	29.42	-	970
19	280	G	23	29.45	-	982
17	280	G	24	29.48	3	993
15	280	-	0	29.50	-	000
22	300	G	31	29.54	-	012
16	280	G	21	29.57	3	021
16	280	G	21	29.61	-	036
18	290	G	28	29.65	-	049
26	300	G	31	29.68	1	058
19	300	G	34	29.69	-	063
23	310	G	30	29.69	-	064
20	290	G	29	29.71	3	070
19	300	G	28	29.74	-	080
19	300	G	26	29.78	-	094
17	310	G	23	29.81	1	103
14	300	-	0	29.83	-	112
10	280	-	0	29.87	-	123
13	260	-	0	29.90	3	134
15	270	G	21	29.90	-	135
18	270	-	0	29.91	-	137
12	270	G	20	29.93	3	143
14	270	-	0	29.93	-	143
11	270	-	0	29.92	-	140
9	240	-	0	29.93	5	143
8	240	-	0	29.93	-	144
9	230	-	0	29.94	-	148
10	240	-	0	29.94	1	148
5	230	-	0	29.95	-	151
12	230	-	0	29.94	-	149
11	240	-	0	29.96	3	156
24	300	G	33	29.67	-	056
22	310	G	28	29.70	-	065
14	310	G	25	29.73	3	077
14	290	G	27	29.77	-	092

19	310	G	26	29.83	-	111
16	300	G	22	29.86	1	121
13	310	G	18	29.89	-	130
17	300	G	21	29.91	-	138
5	290	-	0	29.94	3	148
14	330	G	21	29.95	-	150
12	280	G	17	29.97	-	157
9	300	-	0	29.98	3	160
7	270	-	0	30.00	-	168
7	300	-	0	30.01	-	172
7	270	-	0	30.02	1	173
7	250	-	0	30.00	-	169
8	270	-	0	30.01	-	170
8	280	-	0	30.01	5	171
7	300	-	0	30.00	-	169
9	300	G	15	30.02	-	174
11	280	-	0	30.02	3	173
11	260	-	0	30.00	-	168
16	320	G	20	29.96	-	155
15	310	G	22	29.93	8	146
15	320	G	21	29.92	-	140
17	320	G	21	29.91	-	139
14	280	-	0	29.92	5	141
12	310	-	0	29.94	-	146
12	320	-	0	29.96	-	155
8	310	G	14	29.97	1	157
10	300	-	0	29.97	-	159
13	310	G	22	29.98	-	162
15	310	G	21	29.99	3	165
18	330	G	32	30.00	-	169
16	340	G	21	30.01	-	171
11	330	-	0	30.00	0	168
13	320	G	17	30.01	-	171
10	310	-	0	30.02	-	175
9	320	G	16	30.01	0	170
9	290	-	0	30.00	-	167
9	270	-	0	29.98	-	163
8	270	-	0	30.00	5	168
9	270	-	0	29.99	-	163
11	290	G	18	29.98	-	162
17	280	G	24	29.98	6	160
19	320	G	25	29.97	-	158
18	300	G	32	29.94	-	148
20	330	G	29	29.93	8	143
17	320	G	28	29.93	-	143
16	300	G	23	29.93	-	145
17	310	-	0	29.95	3	152
21	310	G	26	29.97	-	157
13	310	G	19	29.98	-	162
16	310	G	22	29.99	1	163
13	310	G	29	30.00	-	167
13	330	G	20	30.00	-	168

14	340	-	0	30.01	1	171
15	330	G	23	30.01	-	171
16	310	G	22	30.02	-	175
12	300	-	0	30.00	8	167
14	300	-	0	30.00	-	168
9	300	-	0	29.99	-	165
11	280	-	0	29.95	8	152
8	290	-	0	29.95	-	151
10	270	-	0	29.95	-	150
12	270	-	0	29.94	8	146
9	290	-	0	29.92	-	142
18	310	G	25	29.84	-	114
17	310	G	21	29.80	-	100
15	330	G	21	29.77	7	089
14	300	G	24	29.76	-	087
19	310	G	24	29.76	-	086
21	340	G	26	29.74	8	080
19	330	G	24	29.73	-	075
17	320	G	22	29.74	-	080
17	340	G	22	29.76	3	088
18	330	G	24	29.79	-	096
16	330	G	23	29.79	-	098
18	340	G	26	29.81	1	103
18	350	-	0	29.82	-	108
14	330	-	0	29.84	-	115
17	340	-	0	29.87	3	125
12	340	G	18	29.91	-	137
16	350	-	0	29.93	-	146
17	340	-	0	29.95	1	150
11	330	G	18	29.98	-	160
17	330	G	24	30.00	-	168
14	340	-	0	30.04	3	180
13	330	-	0	30.07	-	193
14	340	G	25	30.09	-	198
15	340	-	0	30.11	1	205
18	340	-	0	30.11	-	204
18	330	G	22	30.10	8	202
15	310	G	24	30.11	-	204
15	310	G	23	30.14	-	214
14	310	G	21	30.17	3	224
14	320	G	18	30.19	-	232
11	300	G	17	30.20	-	237
10	310	-	0	30.23	3	245
13	310	-	0	30.24	-	248
8	300	-	0	30.24	-	250
10	330	-	0	30.24	0	250
11	330	-	0	30.25	-	251
11	310	G	18	30.25	-	253
8	320	-	0	30.25	3	254
7	310	-	0	30.26	-	256
7	300	-	0	30.26	-	257
4	270	-	0	30.26	0	255

5	270	-	0	30.25	-	251
6	260	-	0	30.25	-	251
6	240	-	0	30.27	3	260
9	240	-	0	30.27	-	259
11	250	-	0	30.28	-	262
10	270	-	0	30.27	8	259
9	280	-	0	30.26	-	256
11	270	-	0	30.23	-	246
8	270	-	0	30.19	8	233
9	290	-	0	30.18	-	228
11	290	-	0	30.17	-	224
13	250	-	0	30.17	5	226
9	240	-	0	30.18	-	228
12	250	-	0	30.19	-	233
9	230	-	0	30.20	1	234
10	250	-	0	30.19	-	234
6	230	-	0	30.18	-	229
10	240	-	0	30.17	8	227
6	200	-	0	30.17	-	227
6	220	-	0	30.15	8	218
9	240	-	0	30.15	-	220
5	240	-	0	30.15	-	217
5	190	-	0	30.14	8	215
5	210	-	0	30.14	-	217
4	180	-	0	30.13	-	210
5	170	-	0	30.12	8	210
3	250	-	0	30.12	-	209
0	000	-	0	30.12	-	208
0	000	-	0	30.11	8	204
0	000	-	0	30.08	-	196
0	000	-	0	30.05	-	184
0	000	-	0	30.01	8	172
3	230	-	0	29.99	-	164
3	170	-	0	29.98	-	160
3	230	-	0	29.97	6	158
4	260	-	0	29.96	-	155
5	260	-	0	29.97	-	158
6	250	-	0	29.98	3	160
7	270	-	0	29.98	-	161
6	270	-	0	29.98	-	160
6	300	-	0	29.98	2	161
5	VRB	-	0	29.98	-	162
10	330	-	0	29.99	-	166
17	330	G	24	30.02	3	173
12	340	G	20	30.05	-	184
15	340	G	24	30.08	-	194
21	320	G	24	30.10	1	202
17	320	G	25	30.14	-	215
11	320	-	0	30.18	-	229
15	320	G	23	30.22	3	243
16	330	G	22	30.26	-	255
15	340	G	23	30.29	-	267

19	330	G	24	30.31	1	271
19	330	-	0	30.31	-	273
17	320	G	24	30.28	8	263
18	340	G	28	30.29	-	265
17	330	G	25	30.30	-	268
21	340	G	24	30.30	1	268
17	320	G	26	30.33	-	280
12	320	-	0	30.36	-	289
13	330	G	21	30.39	1	300
14	320	G	19	30.39	-	300
12	320	-	0	30.40	-	302
14	330	G	21	30.40	3	304
5	VRB	-	0	30.39	-	299
9	320	G	16	30.37	-	293
9	330	-	0	30.38	5	295
7	350	-	0	30.37	-	294
9	320	-	0	30.36	-	288
6	320	-	0	30.35	8	285
3	VRB	-	0	30.35	-	286
7	300	-	0	30.35	-	287
6	270	-	0	30.34	8	282
4	260	-	0	30.32	-	277
7	270	-	0	30.31	-	274
7	280	-	0	30.31	6	272
9	250	-	0	30.28	-	264
12	250	-	0	30.26	-	255
10	270	-	0	30.22	8	244
10	240	-	0	30.19	-	233
9	250	-	0	30.18	-	229
11	240	-	0	30.18	6	228
14	250	-	0	30.19	-	232
11	250	-	0	30.19	-	232
10	250	-	0	30.20	1	234
9	250	-	0	30.19	-	232
7	280	-	0	30.18	-	231
7	240	-	0	30.18	8	227
7	250	-	0	30.17	-	225
7	240	-	0	30.15	6	217
0	000	-	0	30.13	-	212
3	260	-	0	30.13	-	213
0	000	-	0	30.11	8	204
3	270	-	0	30.10	-	201
4	210	-	0	30.09	-	198
6	200	-	0	30.09	5	199
3	VRB	-	0	30.09	-	198
0	000	-	0	30.10	-	202
0	000	-	0	30.11	3	206
0	000	-	0	30.11	-	205
3	320	-	0	30.10	-	200
3	280	-	0	30.08	8	196
0	000	-	0	30.06	-	187
0	000	-	0	30.07	-	193

3	220	-	0	30.09	3	200
3	300	-	0	30.12	-	207
6	310	-	0	30.14	-	215
5	360	-	0	30.17	3	225
5	330	-	0	30.20	-	236
5	030	-	0	30.23	-	246
6	010	-	0	30.25	1	252
3	070	-	0	30.27	-	258
0	000	-	0	30.28	-	262
3	070	-	0	30.30	3	268
5	040	-	0	30.32	-	277
7	040	-	0	30.34	-	283
7	040	-	0	30.36	1	288
6	040	-	0	30.37	-	293
7	030	-	0	30.39	-	300
7	030	-	0	30.42	3	309
8	030	-	0	30.43	-	313
8	040	-	0	30.45	-	320
8	030	-	0	30.45	1	320
7	020	-	0	30.45	-	320
0	000	-	0	30.43	8	314
0	000	-	0	30.41	-	307
3	VRB	-	0	30.40	-	304
4	050	-	0	30.40	6	303
9	030	-	0	30.38	-	295
8	030	-	0	30.38	-	296
8	040	-	0	30.38	5	296
6	040	-	0	30.38	-	298
3	040	-	0	30.38	-	296
8	040	-	0	30.37	8	292
7	030	-	0	30.36	-	290
8	020	-	0	30.36	-	288
9	030	-	0	30.35	8	286
9	030	-	0	30.33	-	280
9	030	-	0	30.32	-	275
8	030	-	0	30.30	7	270
9	020	-	0	30.30	-	270
11	030	-	0	30.30	-	269
11	040	-	0	30.28	8	264
8	030	-	0	30.29	-	265
8	030	-	0	30.29	-	266
8	030	-	0	30.30	3	268
10	030	-	0	30.28	-	262
9	030	-	0	30.25	-	253
11	040	-	0	30.21	8	240
10	030	-	0	30.18	-	231
10	030	-	0	30.16	-	223
8	030	-	0	30.15	6	219
7	030	-	0	30.15	-	217
8	030	-	0	30.14	-	214
7	040	-	0	30.14	6	214
6	040	-	0	30.12	-	209

7	040	-	0	30.11	-	207
7	030	-	0	30.10	8	201
7	040	-	0	30.08	-	196
7	220	-	0	29.94	3	148
5	260	-	0	29.96	-	155
7	260	-	0	29.98	-	162
3	270	-	0	29.97	0	157
0	000	-	0	29.96	-	154
3	170	-	0	29.96	-	154
3	250	-	0	29.98	3	161
0	000	-	0	30.00	-	167
8	010	-	0	30.02	-	173
7	040	-	0	29.99	0	164
11	040	-	0	29.97	-	156
12	050	-	0	29.90	-	136
13	040	-	0	29.88	8	127
9	040	-	0	29.85	-	118
11	060	-	0	29.82	-	106
13	040	-	0	29.81	6	102
13	050	-	0	29.78	-	092
18	050	-	0	29.76	-	086
17	040	-	0	29.70	8	066
15	040	-	0	29.67	-	057
14	030	-	0	29.64	-	048
19	030	G	24	29.63	6	042
14	020	-	0	29.65	-	050
16	030	-	0	29.65	-	050
18	030	-	0	29.66	1	052
18	030	G	24	29.66	-	052
14	010	-	0	29.69	-	063
11	010	-	0	29.72	3	074
15	010	-	0	29.76	-	087
15	020	-	0	29.81	-	104
13	010	G	21	29.87	3	123
18	010	-	0	29.91	-	139
16	020	-	0	29.97	-	159
13	020	-	0	30.00	1	169
13	030	-	0	30.00	-	169
14	050	-	0	29.99	8	166
16	030	-	0	30.02	-	173
13	030	-	0	30.05	-	186
8	030	-	0	30.09	3	199
11	040	-	0	30.11	-	206
11	030	-	0	30.13	-	213
12	040	-	0	30.15	1	219
12	030	-	0	30.17	-	225
9	030	-	0	30.17	-	227
7	050	-	0	30.16	0	222
11	080	-	0	30.16	-	222
11	070	-	0	30.15	-	220
10	060	-	0	30.15	8	218
11	050	-	0	30.15	-	218

10	050	-	0	30.13	-	212
11	050	-	0	30.10	8	201
13	050	-	0	30.09	-	197
12	060	-	0	30.09	-	197
12	060	-	0	30.07	8	190
13	070	-	0	30.05	-	186
13	050	-	0	30.04	-	182
13	050	-	0	30.01	8	173
12	050	-	0	29.97	-	158
12	050	-	0	29.94	-	147
13	040	-	0	29.89	8	132
15	050	G	22	29.87	-	123
18	050	-	0	29.83	-	110
16	050	G	22	29.80	6	101
17	050	G	23	29.79	-	097
17	040	G	23	29.77	-	090
16	030	-	0	29.76	6	087
17	020	-	0	29.73	-	078
19	020	G	24	29.70	-	066
19	040	-	0	29.66	8	052
17	030	-	0	29.64	-	047
13	010	G	19	29.60	6	032
13	010	-	0	29.62	-	038
12	360	-	0	29.62	-	041
10	360	-	0	29.63	1	042
11	360	-	0	29.63	-	044
13	350	G	20	29.64	-	047
13	350	-	0	29.66	3	054
12	350	-	0	29.69	-	063
14	350	-	0	29.72	-	074
10	340	-	0	29.74	1	081

Report Type	Precip. Total (in)
AA	-
AA	-
AA	-
AA	-
AA	-
AA	-
AA	-
AA	T
AA	T
SP	-
AA	.01
AA	-
AA	-
AA	-
AA	-
AA	-
AA	-
AA	-
AA	-
AA	-
AA	-
AA	-
AA	-
AA	-
AA	-
AA	-
AA	-
AA	-
AA	-
AA	-
AA	-
AA	-
AA	-
AA	-
AA	-
AA	-
AA	-
AA	-
AA	-
AA	-
AA	-
AA	-
AA	-
AA	-
AA	-
AA	-
AA	-
AA	-
AA	-
AA	-

AA	-	
AA	-	
AA	-	
AA	-	
AA	-	
AA	-	
AA	-	
AA	-	
AA	-	
AA	-	
AA	-	
AA	-	
AA	-	
AA	-	
AA	-	
AA	-	
AA	-	
AA	-	
AA	-	
AA	-	
AA	-	
AA	-	
AA	-	
AA	-	
AA	-	
AA	-	
AA	-	
AA	-	
AA	-	
AA	-	
AA	-	
AA	-	
AA	-	
AA	-	
AA	-	
AA	-	
AA	-	
AA	-	
AA	-	
AA	-	
AA	-	
AA	-	
AA	-	
AA	-	
AA	-	
AA	-	
AA	-	
AA	-	
AA	-	
AA	-	
AA	-	
AA	-	

AA	-
AA	-
AA	-
AA	-
AA	-
AA	-
AA	-
AA	-
AA	-
AA	-
AA	-
AA	-
AA	-
AA	-
AA	-
AA	-
AA	-
AA	-
AA	-
AA	-
AA	-
AA	-
AA	-
AA	-
AA	-
AA	-
AA	-
AA	-
AA	-

AA	-
AA	-
AA	-
AA	-
AA	-
AA	-
AA	-
AA	-
AA	-
AA	-
AA	-
AA	-
AA	-
AA	-
AA	-
AA	-
AA	-
AA	-
AA	-
AA	-
AA	-
AA	-
AA	-
AA	-
AA	-
AA	-
AA	-
AA	-
AA	-

AA	-	
AA	-	
AA	-	
AA	-	
AA	-	
AA	-	
AA	-	
AA	-	
AA	-	
AA	T	
AA	T	
AA	-	
AA	-	
AA	-	
AA	-	
AA	-	
AA	-	
AA	-	
AA	-	
AA	-	
AA	-	
AA	-	
AA	-	
AA	-	
AA	-	
AA	-	
AA	-	
AA	-	
AA	-	
AA	-	
AA	-	
AA	-	
AA	-	
AA	-	
AA	-	
AA	-	
AA	-	
AA	-	
AA	-	
AA	-	
AA	-	
AA	-	
AA	-	
AA	-	
AA	-	
AA	-	
AA	-	
AA	-	
AA	-	
AA	-	
AA	-	
AA	-	

AA	-
AA	-
AA	-
AA	-
AA	-
AA	-
AA	-
AA	-
AA	-
AA	-
AA	-
AA	-
AA	-
AA	-
AA	-
AA	-
AA	-
AA	-
AA	-
AA	-
AA	-
AA	-
AA	-
AA	-
AA	-
AA	-
AA	-
AA	-
AA	-
AA	-
AA	-
AA	-
AA	-
AA	-
AA	-
AA	-
AA	-
AA	-
AA	-
AA	-
AA	-
AA	-
AA	-
AA	-
AA	-
AA	-
AA	-
AA	-
AA	-
AA	-
AA	-
AA	-

AA	-
AA	-
AA	-
AA	-
AA	-
AA	-
AA	-
AA	-
AA	-
AA	-
AA	-
AA	-
AA	-
AA	-
AA	-
AA	-
AA	-
AA	-
AA	-
AA	-
AA	-
AA	-
AA	-
AA	-
AA	-
AA	-
AA	-
AA	-
AA	-
AA	.01
AA	T
AA	.01
AA	T
AA	T
AA	-
AA	.04
AA	.03
AA	-
AA	-
AA	-
AA	-
AA	-
AA	-
AA	-
AA	-
AA	-
AA	-
AA	-
AA	-
AA	-
AA	-
AA	-
AA	-
AA	-
AA	-

AA	-
AA	-
AA	-
AA	-
AA	-
AA	-
AA	-
AA	-
AA	-
AA	-
AA	-
AA	-
AA	-
AA	-
AA	-
AA	-
AA	-
AA	-
AA	T
AA	T
AA	.01
AA	.01
AA	T
AA	T
AA	T
AA	-
AA	-
AA	-
AA	-
AA	-
AA	-
AA	-
AA	-
AA	-
AA	-
AA	-
AA	-
AA	-
AA	-
AA	-
AA	-
AA	-
AA	-
AA	-
AA	-
AA	-
AA	-
AA	-
AA	-
AA	-
AA	-
AA	-
AA	-
AA	-

AA	-	
AA	-	
AA	T	
AA	-	
AA	-	
AA	-	
AA	-	
AA	-	
AA	-	
AA	-	
AA	-	
AA	-	
AA	T	
AA	T	
AA	.01	
AA	T	
AA	-	
AA	-	
AA	-	
AA	-	
AA	-	
AA	-	
AA	-	
AA	-	
AA	-	
AA	-	
AA	-	
AA	-	
AA	-	
AA	-	
AA	-	
AA	-	
AA	-	
AA	-	
AA	-	
AA	-	
AA	-	
AA	-	
AA	-	
AA	-	
AA	-	
AA	-	
AA	-	
AA	-	
AA	-	
AA	-	
AA	-	
AA	-	
AA	-	
AA	-	
AA	-	
AA	-	

AA	-	
AA	-	
AA	-	
AA	-	
AA	-	
AA	-	
AA	-	
AA	-	
AA	-	
AA	-	
AA	-	
AA	-	
AA	-	
AA	-	
AA	-	
AA	-	
AA	-	
AA	-	
AA	-	
AA	-	
AA	-	
AA	-	
AA	-	
AA	-	
AA	-	
AA	-	
AA	-	
AA	-	
AA	-	
AA	-	
AA	-	
AA	-	
AA	-	
AA	-	
AA	-	
AA	-	
AA	-	
AA	-	
AA	-	
AA	-	
AA	-	
AA	-	
AA	-	
AA	-	
AA	-	
AA	-	
AA	-	
AA	-	
AA	-	
AA	-	
AA	-	
AA	-	

AA	-
AA	-
AA	-
AA	-
AA	-
AA	T
AA	.02
AA	.01
AA	.01
AA	T
AA	T
AA	-
AA	-
AA	-
AA	-
AA	-
AA	-
AA	-
AA	-
AA	-
AA	.01
AA	T
AA	T
AA	T
AA	.01
AA	.01
AA	T
AA	.01
AA	T
AA	.02
AA	.09
AA	.07
AA	.12
AA	.08
AA	.04
AA	T
AA	.01
AA	-
AA	-
AA	-
AA	-
AA	-
AA	-
AA	-
AA	-
AA	-
AA	-
AA	-
AA	-
AA	-
AA	-

AA	-	
AA	-	
AA	-	
AA	-	
AA	-	
AA	-	
AA	-	
AA	-	
AA	-	
AA	-	
AA	-	
AA	-	
AA	-	
AA	-	
AA	-	
AA	-	
AA	-	
AA	-	
AA	-	
AA	-	
AA	-	
AA	-	
AA	-	
AA	-	
AA	-	
AA	-	
AA	-	
AA	-	
AA	-	
AA	-	
AA	-	
AA	-	
AA	T	
AA		0.01
AA		0.05
AA		0.1
AA		0.1
AA		0.16
AA		0.05
AA		0.02
AA		0.01
AA	-	
AA	-	
AA	-	
AA	-	
AA	-	
AA	-	
AA	-	
AA	-	
AA	-	
AA	-	
AA	-	

AA	-	
AA	-	
AA	-	
AA	-	
AA	-	
AA	-	
AA	-	
AA	-	
AA	-	
AA	-	
AA	-	
AA	-	
AA	-	
AA	-	
AA	-	
AA	-	
AA	-	
AA	-	
AA	-	
AA	-	
AA	-	
AA	-	
AA	-	
AA	-	
AA	-	
AA	-	
AA	-	
AA	-	
AA	-	
AA	-	
AA	-	
AA	-	
AA	-	
AA	-	
AA	-	
AA	-	
AA	-	
AA	-	
AA	-	
AA	-	
AA	-	
AA	-	
AA		0.02
AA		0.04
AA		0.07
AA		0.02
AA		0.1
AA		0.21
AA		0.26
AA		0.2
AA		0.19
AA		0.12

AA		0.08
AA		0.04
AA	T	
AA		0.01
AA	-	
AA	-	
AA	-	
AA	-	
AA	-	
AA	-	
AA		0.16
AA		0.05
AA	T	
AA	-	
AA	-	
AA	-	
AA	-	
AA	-	
AA	-	
AA	-	
AA	-	
AA	-	
AA	T	
AA	-	
AA	-	
AA	-	
AA	-	
AA	-	
AA	-	
AA	-	
AA	-	
AA	-	
AA	-	
AA	-	
AA	-	
AA	-	
AA	-	
AA	-	
AA	-	
AA	-	
AA	-	
AA	-	
AA	-	
AA	-	
AA	-	
AA	-	
AA	-	
AA	-	
AA	-	
AA	-	

AA	-
AA	-
AA	-
AA	-
AA	-
AA	-
AA	-
AA	-
AA	-
AA	-
AA	-
AA	-
AA	-
AA	-
AA	-
AA	-
AA	-
AA	-
AA	-
AA	-
AA	-
AA	-
AA	-
AA	-
AA	-
AA	-
AA	-
AA	-
AA	-
AA	-
AA	-
AA	-
AA	-
AA	-
AA	-
AA	-
AA	-
AA	-
AA	-
AA	-
AA	T
AA	-
AA	T
AA	-
AA	-
AA	.01
AA	.01
AA	.03
AA	.03
AA	.02
AA	-
AA	.02

AA	.04
AA	.02
AA	T
AA	.14
AA	.23
AA	.08
AA	.05
AA	.02
AA	.01
AA	.02
AA	.02
AA	T
AA	T
AA	.01
AA	-
AA	.02
AA	.02
AA	T
AA	.01
AA	.01
AA	.01
AA	T
AA	T
AA	T
AA	-
AA	-
AA	-
AA	-
AA	-
AA	-
AA	-
AA	-
AA	-
AA	-
AA	-
AA	-
AA	T
AA	T
AA	-
AA	-
AA	-
AA	-
AA	-
AA	-
AA	-
AA	-
AA	T
AA	-
AA	-
AA	-
AA	-

AA	T
AA	T
AA	-
AA	-
AA	-
AA	-
AA	-
AA	-
AA	-
AA	-
AA	-
AA	-
AA	-
AA	-
AA	-
AA	-
AA	-
AA	-
AA	-
AA	-
AA	-
AA	-
AA	-
AA	-
AA	-
AA	-
AA	-
AA	-
AA	-
AA	-
AA	-
AA	T
AA	T
AA	-
AA	-
AA	-
AA	-
AA	-
AA	-
AA	-
AA	-
AA	-
AA	-
AA	-
AA	-
AA	-
AA	-
AA	-
AA	-
AA	-
AA	-
AA	-
AA	-
AA	-
AA	-
AA	-
AA	-
AA	-

AA	-	
AA	-	
AA	-	
AA	T	
AA	T	
AA	-	
AA	-	
AA	-	
AA	-	
AA	T	
AA	.03	
AA	T	
AA	.02	
AA	T	
AA	-	
AA	-	
AA	-	
AA	-	
AA	T	
AA	-	
AA	-	
AA	-	
AA	-	
AA	T	
AA	1.71	
AA	T	
AA	-	
AA	-	
AA	-	
AA	-	
AA	-	
AA	-	
AA	-	
AA	-	
AA	-	
AA	-	
AA	-	
AA	-	
AA	-	
AA	-	
AA	-	
AA	-	
AA	-	
AA	-	
AA	-	
AA	-	
AA	-	
AA	-	
AA	-	
AA	-	
AA	-	
AA	-	

AA	-	
AA	-	
AA	-	
AA	-	
AA	-	
AA	-	
AA	-	
AA	-	
AA	-	
AA	-	
AA	-	
AA	-	
AA	-	
AA	-	
AA	-	
AA	-	
AA	-	
AA	-	
AA	-	
AA	-	
AA	-	
AA	-	
AA	-	
AA	-	
AA	-	
AA	-	
AA	-	
AA	-	
AA	-	
AA	-	
AA	-	
AA	-	
AA	-	
AA	-	
AA	-	
AA	-	
AA	-	
AA	-	
AA	-	
AA	-	
AA	-	
AA	-	
AA	-	
AA	-	
AA	-	
AA	-	
AA	-	
AA	-	
AA	-	
AA	-	
AA	-	
AA	-	

AA	-	
AA	-	
AA	-	
AA	-	
AA	-	
AA	-	
AA	-	
AA	-	
AA	-	
AA	-	
AA	-	
AA	-	
AA	-	
AA	-	
AA	-	
AA	-	
AA	-	
AA	-	
AA	-	
AA	-	
AA	-	
AA	-	
AA	-	
AA	-	
AA	-	
AA	-	
AA	-	
AA	-	
AA	-	
AA	-	
AA	-	
AA	-	
AA	-	
AA	-	
AA	-	
AA	-	
AA	-	
AA	-	
AA	-	
AA	-	
AA	-	
AA	-	
AA	-	
AA	-	
AA	-	
AA	-	
AA	-	
AA	-	
AA	-	
AA	-	
AA	-	
AA	-	

AA	-
AA	-
AA	-
AA	-
AA	-
AA	-
AA	-
AA	-
AA	-
AA	-
AA	-
AA	-
AA	-
AA	-
AA	-
AA	-
AA	-
AA	-
AA	-
AA	-
AA	-
AA	-
AA	-
AA	-
AA	-
AA	-
AA	-
AA	-
AA	-
AA	-
AA	-
AA	-
AA	-
AA	T
AA	-
AA	-
AA	T
AA	-
AA	-
AA	-
AA	-
AA	-
AA	-
AA	-
AA	-
AA	-
AA	-
AA	-
AA	-
AA	-
AA	-
AA	-
AA	-
AA	-
AA	-
AA	-
AA	-
AA	-
AA	-
AA	-
AA	-
AA	-

AA	-
AA	-
AA	-
AA	.07
AA	.2
AA	.03
AA	.42
AA	.13
AA	.07
AA	T
AA	T
AA	-
AA	-
AA	-
AA	-
AA	-
AA	-
AA	-
AA	-
AA	-
AA	-
AA	.01
AA	-
AA	-
AA	-
AA	-
AA	-
AA	T
AA	-
AA	-
AA	-
AA	-
AA	-
AA	-
AA	-
AA	-
AA	-
AA	-
AA	-
AA	-
AA	-
AA	-
AA	-
AA	-
AA	-
AA	-
AA	-
AA	-
AA	-
AA	-
AA	-
AA	-

AA	-
AA	-
AA	-
AA	-
AA	-
AA	-
AA	-
AA	-
AA	-
AA	-
AA	-
AA	-
AA	-
AA	-
AA	-
AA	-
AA	-
AA	-
AA	-
AA	-
AA	-
AA	-
AA	-
AA	-
AA	-
AA	-
AA	-
AA	-
AA	-
AA	-
AA	-
AA	-
AA	-
AA	-
AA	-
AA	-
AA	-
AA	-
AA	-
AA	-
AA	-
AA	-
AA	-
AA	-
AA	-
AA	-
AA	-
AA	-
AA	-
AA	-
AA	-
AA	-

AA	-
AA	-
AA	-
AA	-
AA	-
AA	-
AA	-
AA	-
AA	-
AA	-
AA	-
AA	-
AA	-
AA	-
AA	-
AA	-
AA	-
AA	-
AA	-
AA	-
AA	-
AA	-
AA	-
AA	-
AA	-
AA	-
AA	-
AA	-
AA	-
AA	-
AA	-
AA	-
AA	-
AA	-
AA	-
AA	-
AA	-
AA	-
AA	-
AA	-
AA	-
AA	-
AA	-
AA	-
AA	-
AA	-
AA	-
AA	-
AA	-
AA	-
AA	-
AA	-

AA	-	
AA	-	
AA	-	
AA	-	
AA	-	
AA	-	
AA	-	
AA	-	
AA	-	
AA	-	
AA	-	
AA	-	
AA	-	
AA	-	
AA	-	
AA	-	
AA	-	
AA	-	
AA	-	
AA	-	
AA	-	
AA	-	
AA	-	
AA	-	
AA	-	
AA	-	
AA	-	
AA	-	
AA	-	
AA	-	
AA	-	
AA	-	
AA	-	
AA	-	
AA	-	
AA	-	
AA	-	
AA	-	
AA	-	
AA	-	
AA	-	
AA	-	
AA	-	
AA	-	
AA	-	
AA	-	
AA	-	
AA	-	
AA	-	
AA	-	
AA	-	
AA	-	

AA	-
AA	-
AA	-
AA	-
AA	-
AA	-
AA	-
AA	-
AA	-
AA	-
AA	-
AA	-
AA	-
AA	-
AA	-
AA	-
AA	-
AA	-
AA	-
AA	-
AA	-
AA	-
AA	-
AA	-
AA	-
AA	-
AA	-
AA	-
AA	-
AA	-
AA	-
AA	-
AA	-
AA	-
AA	-
AA	-
AA	-
AA	-
AA	-
AA	-
AA	-
AA	-
AA	-
AA	-
AA	-
AA	-
AA	-
AA	-
AA	-
AA	-
AA	-
AA	-

AA	-
AA	-
AA	-
AA	-
AA	-
AA	-
AA	-
AA	-
AA	-
AA	-
AA	-
AA	-
AA	-
AA	-
AA	-
AA	-
AA	-
AA	-
AA	-
AA	-
AA	-
AA	-
AA	-
AA	-
AA	-
AA	-
AA	-
AA	-
AA	-
AA	-
AA	-
AA	-
AA	-
AA	-
AA	-
AA	-
AA	T
AA	-
AA	T
AA	-
AA	-
AA	-
AA	-
AA	-
AA	-
AA	-
AA	-
AA	-
AA	-
AA	-
AA	-
AA	-

AA	-
AA	-
AA	-
AA	-
AA	-
AA	-
AA	-
AA	-
AA	-
AA	-
AA	-
AA	-
AA	-
AA	-
AA	-
AA	-
AA	-
AA	-
AA	-
AA	-
AA	-
AA	-
AA	-
AA	-
AA	-
AA	-
AA	-
AA	-
AA	-
AA	-
AA	-
AA	-
AA	-
AA	-
AA	-
AA	-
AA	-
AA	-
AA	-
AA	-
AA	-
AA	-
AA	-
AA	-
AA	-
AA	-
AA	-
AA	-
AA	-
AA	-
AA	-
AA	-

AA	-
AA	-
AA	-
AA	-
AA	-
AA	-
AA	-
AA	T
AA	T
AA	-
AA	.01
AA	.01
AA	T
AA	T
AA	T
AA	-
AA	T
AA	.01
AA	.02
AA	.04
AA	.06
AA	.06
AA	.06
AA	.07
AA	.09
AA	.07
AA	.12
AA	.11
AA	.1
AA	.04
AA	.08
AA	.21
AA	.12
AA	.06
AA	.16
AA	.14
AA	.11
AA	.07
AA	.05
AA	.08
AA	.21
AA	.18
AA	.07
AA	.09
AA	.09
AA	.13
AA	.13
AA	.16
AA	.22
AA	.26
AA	.17
AA	.05

AA	T
AA	.01
AA	.01
AA	.08
AA	.03
AA	.05
AA	.06
AA	.01
AA	.01
AA	T
AA	T
AA	T
AA	.02
AA	T
AA	.02
AA	.02
AA	.01
AA	.01
AA	.01
AA	.01
AA	.01
AA	.01
AA	.01
AA	T
AA	-
AA	.01
AA	-
AA	.01
AA	.01
AA	-
AA	-
AA	-
AA	-
AA	-
AA	-
AA	-
AA	-
AA	-
AA	-
AA	-
AA	T
AA	.01
AA	-
AA	-
AA	-
AA	-
AA	-
AA	-
AA	-
AA	-
AA	-
AA	-

AA	-
AA	-
AA	-
AA	-
AA	-
AA	-
AA	-
AA	-
AA	-
AA	-
AA	-
AA	-
AA	T
AA	T
AA	T
AA	.02
AA	.06
AA	.09
AA	.06
AA	.03
AA	.02
AA	.07
AA	.07
AA	.08
AA	.1
AA	.29
AA	.24
AA	.03
AA	.01
AA	T
AA	-
AA	-
AA	-
AA	-
AA	-
AA	-
AA	-
AA	-
AA	-
AA	-
AA	-
AA	-
AA	-
AA	-
AA	-
AA	-
AA	-
AA	-
AA	-
AA	-
AA	-
AA	-

AA	-
AA	T
AA	.02
AA	T
AA	.01
AA	-
AA	-
AA	-
AA	-
AA	-
AA	-
AA	-
AA	-
AA	-
AA	-
AA	-
AA	-
AA	-
AA	-
AA	-
AA	-
AA	-
AA	-
AA	-
AA	-
AA	-
AA	-
AA	-
AA	-
AA	-
AA	-
AA	-
AA	-
AA	-
AA	-
AA	-
AA	-
AA	-
AA	-
AA	-
AA	-
AA	T
AA	T
AA	T
AA	-
AA	-
AA	-
AA	-
AA	-
AA	-
AA	-
AA	-

AA	-
AA	-
AA	-
AA	-
AA	-
AA	-
AA	-
AA	-
AA	-
AA	-
AA	-
AA	-
AA	-
AA	-
AA	-
AA	-
AA	-
AA	-
AA	-
AA	-
AA	-
AA	-
AA	-
AA	-
AA	-
AA	-
AA	-
AA	-
AA	-
AA	-
AA	-
AA	-
AA	-
AA	-
AA	-
AA	-
AA	-
AA	-
AA	-
AA	-
AA	-
AA	-
AA	-
AA	-
AA	-
AA	-
AA	-
AA	-
AA	-
AA	-
AA	-
AA	-

AA	-
AA	-
AA	-
AA	-
AA	-
AA	-
AA	-
AA	-
AA	-
AA	-
AA	-
AA	-
AA	-
AA	-
AA	-
AA	-
AA	-
AA	-
AA	-
AA	-
AA	-
AA	-
AA	-
AA	-
AA	-
AA	-
AA	-
AA	-
AA	-
AA	-
AA	-
AA	-
AA	-
AA	-
AA	-
AA	-
AA	-
AA	-
AA	-
AA	-
AA	-
AA	-
AA	-
AA	-
AA	-
AA	-
AA	-
AA	-
AA	-
AA	-
AA	-
AA	-

AA	-
AA	-
AA	-
AA	-
AA	-
AA	-
AA	-
AA	-
AA	-
AA	-
AA	T
AA	T
AA	.03
AA	.17
AA	.18
AA	.22
AA	.09
AA	.08
AA	.27
AA	.09
AA	.05
AA	.02
AA	T
AA	-
AA	-
AA	-
AA	-
AA	-
AA	-
AA	-
AA	-
AA	-
AA	-
AA	-
AA	-
AA	-
AA	-
AA	-
AA	-
AA	-
AA	-
AA	-
AA	-
AA	-
AA	-
AA	-
AA	-
AA	-
AA	-
AA	-
AA	-
AA	-

AA	-
AA	-
AA	-
AA	-
AA	-
AA	-
AA	-
AA	-
AA	-
AA	-
AA	-
AA	-
AA	-
AA	-
AA	-
AA	-
AA	-
AA	-
AA	-
AA	-
AA	-
AA	-
AA	-
AA	-
AA	-
AA	-
AA	-
AA	-
AA	-
AA	-
AA	-
AA	-
AA	-
AA	-
AA	-
AA	-
AA	-
AA	-
AA	-
AA	-
AA	-
AA	-
AA	-
AA	-
AA	-
AA	-
AA	-
AA	-
AA	-
AA	-
AA	-
AA	.01

AA	T
AA	.03
AA	.02
AA	.01
AA	.02
AA	T
AA	T
AA	-
AA	-
AA	T
AA	T
AA	T
AA	-
AA	-
AA	-
AA	-
AA	-
AA	-
AA	T
AA	-
AA	-
AA	T
AA	T
AA	.02
AA	.01
AA	.03
AA	T
AA	T
AA	-
AA	-
AA	-
AA	-
AA	-
AA	-
AA	-
AA	-
AA	-
AA	-
AA	-
AA	-
AA	-
AA	-
AA	-
AA	-
AA	-
AA	-
AA	-
AA	-
AA	-
AA	-

AA	-	
AA	-	
AA	-	
AA	-	
AA	-	
AA	-	
AA	-	
AA	-	
AA	-	
AA	-	
AA	-	
AA	-	
AA	-	
AA	-	
AA	-	
AA	-	
AA	-	
AA	-	
AA	-	
AA	-	
AA	-	
AA	-	
AA	-	
AA	-	
AA	-	
AA	-	
AA	-	
AA	-	
AA	-	
AA	-	
AA	-	
AA	-	
AA	-	
AA	-	
AA	-	
AA	-	
AA	-	
AA	-	
AA	-	
AA	-	
AA	-	
AA	-	
AA	-	
AA	-	
AA	-	
AA	-	
AA	T	
AA	T	
AA	-	
AA	-	
AA	-	
AA	-	

AA	-
AA	T
AA	-
AA	-
AA	-
AA	-
AA	-
AA	-
AA	-
AA	-
AA	-
AA	-
AA	-
AA	-
AA	-
AA	-
AA	-
AA	-
AA	-
AA	-
AA	-
AA	-
AA	-
AA	-
AA	T
AA	T
AA	.01
AA	.02
AA	T
AA	T
AA	.01
AA	.01
AA	.04
AA	.07
AA	.05
AA	T
AA	.03
AA	.05
AA	.07
AA	.07
AA	.08
AA	.09
AA	.17
AA	.14
AA	.06
AA	.08
AA	.05
AA	.01
AA	-
AA	-
AA	-

AA	-
AA	-
AA	-
AA	-
AA	T
AA	.06
AA	.1
AA	.07
AA	.14
AA	.09
AA	.05
AA	.07
AA	.03
AA	.1
AA	-
AA	.06
AA	-
AA	-
AA	-
AA	-
AA	-
AA	-
AA	-
AA	-
AA	-
AA	-
AA	-
AA	-
AA	-
AA	-
AA	-
AA	-
AA	-
AA	-
AA	-
AA	-
AA	-
AA	-
AA	-
AA	-
AA	-
AA	-
AA	-
AA	-
AA	-
AA	-
AA	T
AA	-
AA	-
AA	-
AA	-
AA	-

AA	-
AA	-
AA	-
AA	-
AA	-
AA	-
AA	-
AA	-
AA	-
AA	-
AA	-
AA	-
AA	-
AA	-
AA	-
AA	-
AA	-
AA	-
AA	-
AA	-
AA	-
AA	-
AA	-
AA	-
AA	-
AA	-
AA	-
AA	-
AA	-
AA	-
AA	-
AA	-
AA	-
AA	-
AA	-
AA	-
AA	-
AA	-
AA	-
AA	-
AA	-
AA	-
AA	T
AA	-
AA	.01
AA	-
AA	-
AA	-
AA	.07
AA	.02
AA	-
AA	-

AA	.02
AA	.02
AA	T
AA	T
AA	-
AA	-
AA	-
AA	T
AA	T
AA	-
AA	-
AA	T
AA	T
AA	.01
AA	-
AA	-
AA	-
AA	-
AA	-
AA	-
AA	T
AA	T
AA	-
AA	-
AA	-
AA	-
AA	-
AA	-
AA	-
AA	-
AA	-
AA	-
AA	-
AA	-
AA	-
AA	-
AA	-
AA	-
AA	-
AA	-
AA	-
AA	-
AA	-
AA	-
AA	-
AA	-
AA	-
AA	-
AA	-
AA	-
AA	-
AA	-

AA	-
AA	-
AA	-
AA	-
AA	-
AA	-
AA	-
AA	-
AA	-
AA	-
AA	-
AA	-
AA	-
AA	-
AA	-
AA	-
AA	-
AA	-
AA	-
AA	-
AA	-
AA	-
AA	-
AA	-
AA	-
AA	-
AA	-
AA	-
AA	-
AA	-
AA	-
AA	-
AA	-
AA	-
AA	-
AA	-
AA	-
AA	-
AA	-
AA	-
AA	-
AA	-
AA	-
AA	-
AA	-
AA	-
AA	-
AA	-
AA	-
AA	-
AA	-
AA	-

AA	-
AA	-
AA	-
AA	-
AA	-
AA	-
AA	-
AA	-
AA	-
AA	-
AA	-
AA	-
AA	-
AA	-
AA	-
AA	-
AA	-
AA	-
AA	-
AA	-
AA	-
AA	-
AA	-
AA	-
AA	T
AA	T
AA	-
AA	-
AA	-
AA	-
AA	-
AA	-
AA	-
AA	-
AA	-
AA	-
AA	-
AA	-
AA	-
AA	-
AA	-
AA	-
AA	-
AA	-
AA	-
AA	-
AA	-
AA	-
AA	-
AA	-
AA	-
AA	-
AA	-
AA	-

AA	-
AA	-
AA	-
AA	-
AA	-
AA	-
AA	-
AA	-
AA	-
AA	-
AA	-
AA	-
AA	-
AA	-
AA	-
AA	-
AA	-
AA	-
AA	-
AA	-
AA	-
AA	-
AA	-
AA	-
AA	-
AA	-
AA	-
AA	-
AA	-
AA	-
AA	-
AA	-
AA	-
AA	-
AA	-
AA	-
AA	-
AA	-
AA	-
AA	-
AA	T
AA	T
AA	T
AA	T
AA	T
AA	T
AA	-
AA	T
AA	T
AA	-
AA	-
AA	-
AA	-
AA	-
AA	-
AA	-
AA	-
AA	-

AA	-	
AA	-	
AA	-	
AA	-	
AA	-	
AA	-	
AA	-	
AA	-	
AA	-	
AA	-	
AA	-	
AA	-	
AA	-	
AA	-	
AA	-	
AA	-	
AA	-	
AA	-	
AA	-	
AA	-	
AA	-	
AA	-	
AA	-	
AA	-	
AA	-	
AA	-	
AA	-	
AA	-	
AA	-	
AA	-	
AA	-	
AA	-	
AA	-	
AA	-	
AA	-	
AA	-	
AA	-	
AA	-	
AA	-	
AA	T	
AA	T	
AA	-	
AA	-	
AA	T	
AA	T	
AA	T	
AA	.01	
AA	T	
AA	.01	
AA	-	
AA	T	
AA	T	

AA	T	
AA	T	
AA	T	
AA	-	
AA	T	
AA	-	
AA	-	
AA	-	
AA	-	
AA	-	
AA	-	
AA	-	
AA	-	
AA	-	
AA	-	
AA	-	
AA	-	
AA	-	
AA	-	
AA	-	
AA	-	
AA	-	
AA	-	
AA	-	
AA	-	
AA	-	
AA	-	
AA	-	
AA	-	
AA	-	
AA	-	
AA	-	
AA	-	
AA	-	
AA	-	
AA	-	
AA	-	
AA	T	
AA	T	
AA	-	
AA	-	
AA	T	
AA	T	
AA	T	
AA	T	
AA	T	
AA	T	
AA	T	
AA	T	
AA	T	
AA	-	
AA	-	

AA	-
AA	-
AA	-
AA	-
AA	-
AA	-
AA	T
AA	T
AA	-
AA	.01
AA	T
AA	.01
AA	.03
AA	.04
AA	.04
AA	.07
AA	.08
AA	.13
AA	.17
AA	.09
AA	.03
AA	.06
AA	.22
AA	.26
AA	.27
AA	.18
AA	.03
AA	.09
AA	.15
AA	.01
AA	-
AA	-
AA	-
AA	-
AA	-
AA	-
AA	-
AA	-
AA	-
AA	-
AA	-
AA	-
AA	-
AA	-
AA	T
AA	T
AA	T
AA	T
AA	T
AA	T
AA	T
AA	T

AA	T
AA	-
AA	.01
AA	T
AA	.02
AA	T
AA	.02
AA	.03
AA	.03
AA	.01
AA	.07
AA	T
AA	T
AA	.01
AA	.02
AA	.01
AA	.04
AA	.04
AA	.17
AA	.13
AA	-
AA	-
AA	.03
AA	.01
AA	T
AA	.01
AA	T
AA	T
AA	T
AA	T
AA	T

Appendix 5: Total gaseous mercury concentrations above SDM at the Bayonne landfill.

Date	Time	Lower (ng m^{-3})	Upper (ng m^{-3})	Height (m)
8/30/2001	11:35:01	8.317		0.7874
8/30/2001	11:40:01	4.311		0.7874
8/30/2001	11:45:01	4.613		0.7874
8/30/2001	11:50:01	3.892		0.7874
8/30/2001	11:55:01	5.035		0.7874
8/30/2001	12:00:01	3.443		0.7874
8/30/2001	12:40:01	7.039		0.7874
8/30/2001	12:45:01	5.087		0.7874
8/30/2001	12:50:01	4.904		0.7874
8/30/2001	12:55:01	3.975		0.7874
8/30/2001	13:00:01	4.870		0.7874
8/30/2001	13:05:01	4.396		0.7874
8/30/2001	13:10:01	4.416		0.7874
8/30/2001	13:26:28		3.820	2.9972
8/30/2001	13:31:28		3.710	2.9972
8/30/2001	13:36:28		3.286	2.9972
8/30/2001	13:41:28		3.508	2.9972
8/30/2001	13:46:28		3.370	2.9972
8/30/2001	13:51:28		3.277	2.9972
8/30/2001	13:56:28	3.465		0.7874
8/30/2001	14:01:28	3.436		0.7874
8/30/2001	14:06:28	3.049		0.7874
8/30/2001	14:11:28	2.925		0.7874
8/30/2001	14:16:28	3.296		0.7874
8/30/2001	14:21:28		2.611	2.9972
8/30/2001	14:26:28		2.302	2.9972
8/30/2001	14:31:28	2.679		0.7874
8/30/2001	14:36:28	2.725		0.7874
8/30/2001	14:41:28		4.400	2.9972
8/30/2001	14:46:28		2.374	2.9972
8/30/2001	14:51:28		3.591	2.9972
10/23/2001	10:40:01	3.135		0.15
10/23/2001	10:45:01	3.81		0.15
10/23/2001	10:50:01	3.132		0.15
10/23/2001	10:55:01	3.242		0.15
10/23/2001	11:00:01	2.95		0.15
10/23/2001	11:05:01		3.18	1.5
10/23/2001	11:10:01		2.752	1.5
10/23/2001	11:15:01		2.826	1.5
10/23/2001	11:20:01		2.667	1.5
10/23/2001	11:25:01		2.796	1.5
10/23/2001	11:30:01	2.546		0.15
10/23/2001	11:35:01	3.16		0.15
10/23/2001	11:40:01	2.659		0.15
10/23/2001	11:45:01	3.203		0.15

10/23/2001	11:50:01	2.844		0.15
10/23/2001	11:55:01		2.763	1.5
10/23/2001	12:00:01		2.408	1.5
10/23/2001	12:05:01		2.963	1.5
10/23/2001	12:10:01		2.82	1.5
10/23/2001	12:15:01		2.963	1.5
10/23/2001	13:00:01	1.204		0.15
10/23/2001	13:05:01	1.201		0.15
10/23/2001	13:10:01	1.076		0.15
10/23/2001	13:15:01	1.173		0.15
10/23/2001	13:20:01	1.049		0.15
10/23/2001	13:25:01		0.987	1.5
10/23/2001	13:30:01		0.898	1.5
10/23/2001	13:35:01		0.933	1.5
10/24/2001	12:05:01	4.742		0.2
10/24/2001	12:10:01	4.513		0.2
10/24/2001	12:15:01	4.600		0.2
10/24/2001	12:20:01	4.089		0.2
10/24/2001	12:25:01	5.751		0.2
10/24/2001	12:30:01	5.656		0.2
10/24/2001	12:35:01	5.020		0.2
10/24/2001	12:40:01		4.087	1.2
10/24/2001	12:45:01		4.748	1.2
10/24/2001	12:50:01		4.180	1.2
10/24/2001	12:55:01		3.050	1.2
10/24/2001	13:00:01		2.897	1.2
10/24/2001	13:05:01		2.811	1.2
10/24/2001	13:10:01		3.177	1.2
10/24/2001	13:15:01	3.880		0.2
10/24/2001	13:20:01	3.317		0.2
10/24/2001	13:25:01	4.315		0.2
10/24/2001	13:30:01	5.650		0.2
10/24/2001	14:00:01	6.199		0.2
10/24/2001	14:05:01	4.635		0.2
10/24/2001	14:10:01	4.663		0.2
10/24/2001	14:15:01	4.132		0.2
10/24/2001	14:20:01	4.391		0.2
10/24/2001	14:40:01		4.362	1.2
10/24/2001	14:45:01		3.407	1.2
10/24/2001	14:50:01		3.759	1.2
10/24/2001	14:55:01		3.209	1.2
10/24/2001	15:00:01		4.237	1.2
10/24/2001	15:05:01		4.335	1.2
10/24/2001	15:10:01		3.924	1.2
10/24/2001	15:15:01		3.270	1.2
10/24/2001	15:20:01	5.357		0.2
10/24/2001	15:25:01	5.243		0.2
10/24/2001	15:30:01	5.707		0.2
10/24/2001	15:35:01	4.925		0.2

10/24/2001	15:40:01	3.353		0.2
10/24/2001	15:45:01	3.112		0.2
10/24/2001	15:50:01		3.053	1.2
10/24/2001	15:55:01		2.796	1.2
10/24/2001	16:00:01		3.345	1.2
10/24/2001	16:05:01		2.640	1.2
10/24/2001	16:10:01	3.207		0.2
10/25/2001	10:10:01		4.595	1.2
10/25/2001	10:15:01		3.271	1.2
10/25/2001	10:20:01		3.685	1.2
10/25/2001	10:25:01		3.569	1.2
10/25/2001	10:30:01		3.955	1.2
10/25/2001	10:35:01		3.680	1.2
10/25/2001	10:40:01		4.209	1.2
10/25/2001	10:45:01		3.455	1.2
10/25/2001	10:50:01		4.502	1.2
10/25/2001	10:55:01		3.469	1.2
10/25/2001	11:00:01		4.240	1.2
10/25/2001	11:05:01		3.931	1.2
10/25/2001	11:10:01		4.925	1.2
10/25/2001	11:15:01	4.740		0.2
10/25/2001	11:25:01	5.342		0.2
10/25/2001	11:30:01	6.876		0.2
10/25/2001	11:35:01	5.269		0.2
10/25/2001	11:40:01	6.113		0.2
10/25/2001	11:45:01	4.403		0.2
10/25/2001	11:50:01	5.050		0.2
10/25/2001	11:55:01	3.666		0.2
10/25/2001	12:00:01	3.726		0.2
10/25/2001	12:05:01	3.729		0.2
10/25/2001	12:10:01	5.290		0.2
10/25/2001	12:15:01		5.283	1.2
10/25/2001	12:20:01		3.604	1.2
10/25/2001	12:25:01		2.605	1.2
10/25/2001	12:30:01		2.543	1.2
10/25/2001	12:35:01		2.247	1.2
10/25/2001	12:40:01		3.376	1.2
10/25/2001	12:45:01		2.921	1.2
10/25/2001	12:50:01		5.454	1.2
10/25/2001	12:55:01		7.049	1.2
10/25/2001	13:00:01		6.612	1.2
10/25/2001	13:05:01		3.193	1.2
10/25/2001	13:10:01		3.474	1.2
10/25/2001	13:15:01		3.133	1.2
10/25/2001	13:20:01		3.054	1.2
10/25/2001	13:25:01		5.535	1.2
10/25/2001	13:30:01		8.946	1.2
10/25/2001	13:35:01		7.586	1.2
10/25/2001	13:40:01		7.012	1.2

10/25/2001	13:45:01		3.919	1.2
10/25/2001	13:50:01	4.961		0.2
10/25/2001	13:55:01	4.366		0.2
10/25/2001	14:00:01	5.270		0.2
10/25/2001	14:05:01	5.889		0.2
10/25/2001	14:10:01	7.005		0.2
10/25/2001	14:15:01	6.479		0.2
10/25/2001	14:20:01	7.565		0.2
10/25/2001	14:25:01	7.874		0.2
10/25/2001	14:30:01	8.263		0.2
10/25/2001	14:35:01	9.878		0.2
10/25/2001	14:40:01	11.046		0.2
10/25/2001	14:45:01	9.442		0.2
10/25/2001	14:50:01		10.694	1.2
10/25/2001	14:55:01		8.114	1.2
10/25/2001	15:00:01		6.085	1.2
10/25/2001	15:05:01		4.647	1.2
10/25/2001	15:10:01		8.370	1.2
10/25/2001	15:15:01		7.182	1.2
10/25/2001	15:20:01		7.983	1.2
10/25/2001	15:25:01		6.521	1.2
5/7/2002	10:45:01		3.288	2.9972
5/7/2002	10:50:01		3.473	2.9972
5/7/2002	10:55:01	4.14		0.7874
5/7/2002	11:00:01	3.689		0.7874
5/7/2002	11:05:01		3.401	2.9972
5/7/2002	11:10:01		3.309	2.9972
5/7/2002	11:15:01	4.141		0.7874
5/7/2002	11:20:01	3.934		0.7874
5/7/2002	11:25:01		3.308	2.9972
5/7/2002	11:30:01		3.544	2.9972
5/7/2002	11:35:01	4.677		0.7874
5/7/2002	11:40:01	4.555		0.7874
5/7/2002	11:45:01		3.384	2.9972
5/7/2002	11:50:01		3.915	2.9972
5/7/2002	11:55:01	4.935		0.7874
5/7/2002	12:00:01	4.806		0.7874
5/7/2002	12:05:01		4.146	2.9972
5/7/2002	12:10:01		4.068	2.9972
5/7/2002	12:15:01	4.707		0.7874
5/7/2002	12:20:01	4.921		0.7874
5/7/2002	12:25:01		4.065	2.9972
5/7/2002	12:30:01		3.823	2.9972
5/7/2002	12:35:01	4.269		0.7874
5/7/2002	12:40:01	4.163		0.7874
5/7/2002	12:45:01		3.424	2.9972
5/7/2002	12:50:01		3.036	2.9972
5/7/2002	12:55:01	3.506		0.7874
5/7/2002	13:00:01	3.613		0.7874

5/7/2002	13:05:01		3.148	2.9972
5/7/2002	13:10:01		3.265	2.9972
5/7/2002	13:15:01	3.557		0.7874
5/7/2002	13:20:01	3.448		0.7874
5/7/2002	13:25:01		2.902	2.9972
5/7/2002	13:30:01		2.99	2.9972
5/7/2002	13:35:01	3.025		0.7874
5/7/2002	13:40:01	2.771		0.7874
5/7/2002	13:45:01		2.461	2.9972
5/7/2002	13:50:01		2.573	2.9972
5/7/2002	13:55:01	3.073		0.7874
5/7/2002	14:00:01	2.937		0.7874
5/7/2002	14:05:01		2.737	2.9972
5/7/2002	14:10:01		2.6	2.9972
5/7/2002	14:15:01	3.019		0.7874
5/7/2002	14:20:01	3.179		0.7874
5/7/2002	14:25:01		2.679	2.9972
5/7/2002	14:30:01		2.553	2.9972
5/7/2002	14:35:01	2.79		0.7874
5/7/2002	14:40:01	2.679		0.7874
5/7/2002	14:45:01		2.389	2.9972
5/7/2002	14:55:01	2.771		0.7874
5/7/2002	20:30:01		2.918	2.9972
5/7/2002	20:35:01		2.964	2.9972
5/7/2002	20:40:01	4.268		0.7874
5/7/2002	20:45:01	2.735		0.7874
5/7/2002	20:50:01		3.201	2.9972
5/7/2002	20:55:01		2.911	2.9972
5/7/2002	21:00:01	2.618		0.7874
5/7/2002	21:05:01	2.643		0.7874
5/7/2002	21:10:01		2.557	2.9972
5/7/2002	21:15:01		2.646	2.9972
5/7/2002	21:20:01	3.595		0.7874
5/7/2002	21:25:01	3.382		0.7874
5/7/2002	21:30:01		2.81	2.9972
5/7/2002	21:35:01		3.301	2.9972
5/7/2002	21:40:01	3.667		0.7874
5/7/2002	21:45:01	3.848		0.7874
5/7/2002	21:50:01		3.555	2.9972
5/7/2002	21:55:01		4.049	2.9972
5/7/2002	22:00:01	3.505		0.7874
5/7/2002	22:05:01	3.203		0.7874
5/7/2002	22:10:01		3.162	2.9972
5/7/2002	22:15:01		3.235	2.9972
5/7/2002	22:20:01	3.315		0.7874
5/7/2002	22:25:01	3.383		0.7874
5/7/2002	22:30:01		3.1	2.9972
5/7/2002	22:35:01		3.235	2.9972
5/7/2002	22:40:01	4.27		0.7874

5/7/2002	22:45:01	4.447		0.7874
5/7/2002	22:50:01		3.925	2.9972
5/7/2002	22:55:01		3.692	2.9972
5/7/2002	23:00:01	3.56		0.7874
5/7/2002	23:05:01	3.468		0.7874
5/7/2002	23:10:01		3.861	2.9972
5/7/2002	23:15:01		3.695	2.9972
5/8/2002	9:55	3.533		0.7874
5/8/2002	10:00	3.153		0.7874
5/8/2002	10:05		4.003	2.9972
5/8/2002	10:10		3.645	2.9972
5/8/2002	10:15	3.109		0.7874
5/8/2002	10:20	3.043		0.7874
5/8/2002	10:25		3.678	2.9972
5/8/2002	10:30		3.269	2.9972
5/8/2002	10:35	2.995		0.7874
5/8/2002	10:40	3.107		0.7874
5/8/2002	10:45		3.532	2.9972
5/8/2002	10:50		3.446	2.9972
5/8/2002	10:55	3.099		0.7874
5/8/2002	11:00	3.041		0.7874
5/8/2002	11:05		3.637	2.9972
5/8/2002	11:10		3.65	2.9972
5/8/2002	11:15	3.126		0.7874
5/8/2002	11:20	3.149		0.7874
5/8/2002	11:25		3.583	2.9972
5/8/2002	11:30		3.398	2.9972
5/8/2002	11:35	2.907		0.7874
5/8/2002	11:40	3.035		0.7874
5/8/2002	11:45		3.33	2.9972
5/8/2002	11:50		3.27	2.9972
5/8/2002	11:55	2.775		0.7874
5/8/2002	12:00	2.816		0.7874
5/8/2002	12:05		3.407	2.9972
5/8/2002	12:10		3.286	2.9972
5/8/2002	12:15	3.142		0.7874
5/8/2002	12:20	3.074		0.7874
5/8/2002	13:30	3.139		0.7874
5/8/2002	13:35	2.858		0.7874
5/8/2002	13:40		3.303	2.9972
5/8/2002	13:45		3.224	2.9972
5/8/2002	13:50	2.893		0.7874
5/8/2002	13:55	2.809		0.7874
5/8/2002	14:00		3.353	2.9972
5/8/2002	14:05		3.21	2.9972
5/8/2002	14:10	3.138		0.7874
5/8/2002	14:15	3.522		0.7874
5/8/2002	14:20		3.689	2.9972

5/8/2002	14:25		3.471	2.9972
5/8/2002	14:30	3.301		0.7874
5/8/2002	14:35	2.901		0.7874
5/8/2002	14:40		3.182	2.9972
5/8/2002	14:45		3.111	2.9972
5/8/2002	14:50	3.139		0.7874
5/8/2002	14:55	3.052		0.7874
5/8/2002	15:00		3.3	2.9972
5/8/2002	15:05		3.361	2.9972
5/8/2002	15:10	3.136		0.7874
5/8/2002	15:15	3.107		0.7874
5/8/2002	15:20		3.515	2.9972
5/8/2002	15:25		3.192	2.9972
5/8/2002	15:30	2.858		0.7874
5/8/2002	15:35	3.001		0.7874
5/8/2002	15:40		3.344	2.9972
5/8/2002	15:45		3.225	2.9972
5/8/2002	15:50	3.075		0.7874
5/8/2002	15:55	3.019		0.7874
5/8/2002	16:00		3.338	2.9972
11/14/2002	10:00:01	2.656		0.7874
11/14/2002	10:10:01		2.341	2.9972
11/14/2002	10:20:01	2.316		0.7874
11/14/2002	10:30:01		2.282	2.9972
11/14/2002	10:40:01	2.019		0.7874
11/14/2002	10:50:01		1.917	2.9972
11/14/2002	11:00:01	1.885		0.7874
11/14/2002	11:10:01		1.911	2.9972
11/14/2002	11:20:01	1.744		0.7874
11/14/2002	11:30:01		1.727	2.9972
11/14/2002	11:40:01	1.772		0.7874
11/14/2002	11:50:01		1.886	2.9972
11/14/2002	12:00:01	1.683		0.7874
11/14/2002	12:10:01		1.719	2.9972
11/14/2002	12:20:01	1.847		0.7874
11/14/2002	13:20:01		1.88	2.9972
11/14/2002	13:30:01	2.073		0.7874
11/14/2002	13:40:01		1.842	2.9972
11/14/2002	13:50:01	1.832		0.7874
11/14/2002	14:00:01		2.026	2.9972
11/14/2002	14:10:01	2.061		0.7874
11/14/2002	14:20:01		2.083	2.9972
11/14/2002	14:30:01	2.063		0.7874
11/14/2002	15:05:01		2.003	2.9972
11/14/2002	15:15:01	1.908		0.7874
11/14/2002	15:25:01		1.92	2.9972
11/14/2002	15:35:01	1.893		0.7874
11/14/2002	15:45:01		1.832	2.9972
11/14/2002	15:55:01	1.846		0.7874

11/14/2002	16:05:01		1.62	2.9972
11/14/2002	16:15:01	1.668		0.7874
11/14/2002	16:25:01		1.68	2.9972
11/14/2002	16:35:01	1.666		0.7874
11/14/2002	16:45:01		1.752	2.9972
11/15/2002	9:20:01		2.586	2.9972
11/15/2002	9:30:01	2.657		0.7874
11/15/2002	9:40:01		2.727	2.9972
11/15/2002	9:50:01	2.735		0.7874
11/15/2002	10:00:01		2.815	2.9972
11/15/2002	10:10:01	2.741		0.7874
11/15/2002	11:00:01		2.702	2.9972
11/15/2002	11:10:01	2.492		0.7874
11/15/2002	11:20:01		2.57	2.9972
11/15/2002	11:30:01	2.623		0.7874
11/15/2002	11:40:01		2.764	2.9972
11/15/2002	11:50:01	2.707		0.7874
11/15/2002	12:00:01		2.854	2.9972
11/15/2002	12:10:01	3.125		0.7874
11/15/2002	12:20:01		2.979	2.9972
11/15/2002	12:30:01	2.855		0.7874
11/15/2002	12:40:01		2.715	2.9972
11/15/2002	12:50:01	2.841		0.7874
11/15/2002	13:00:01		2.691	2.9972
11/15/2002	13:10:01	2.576		0.7874
11/15/2002	13:20:01		2.462	2.9972
11/15/2002	13:30:01	2.541		0.7874
11/15/2002	13:40:01		2.41	2.9972
11/15/2002	13:50:01	2.427		0.7874
11/15/2002	14:00:01		2.412	2.9972

Total gaseous mercury (TGM) concentrations used to estimate vertic fluxes above SDM at the Bayonne landfill.

[1]Percent gradient = $|TGM_{lower} - TGM_{upper}|/TGM_{lower} * 100$. Samples with percent grac uncertainty) are assigned vertical fluxes of zero.
[2]Vertical fluxes were estimated as Flux = $\kappa u^*(TGM_{lower} - TGM_{upper})/[\phi_C \ln(Z_2/Z_1)]$ whe is the friction velocity.

Date	time	TGM (lower) (ng m^{-3})	time	TGM (upper) (ng m^{-3})	Percent gradient[1]	u* (m s^{-1})	ϕ_C
30-Aug-01	13:10	4.41	13:31	3.77	14.5	0.49	1.19
	14:01	3.45	13:51	3.32	3.8	0.49	1.19
	14:16	3.11	14:26	2.46	20.9	0.49	1.19
	14:36	2.70	14:26	2.46	8.9	0.49	1.19
23-Oct-01	11:00	3.10	11:10	2.97	4.1	0.21	1.00
	11:35	2.85	11:25	2.73	4.3	0.21	1.00
	11:50	3.02	12:00	2.59	14.3	0.21	1.00
23-Oct-01	13:20	3.06	13:30	2.60	15.0	0.24	0.50
24-Oct-01	12:35	5.34	12:45	4.42	17.2	0.22	0.91
	13:20	3.60	13:10	2.99	16.9	0.22	0.91
	14:20	4.26	14:45	3.88	8.9	0.22	0.91
	15:25	5.30	15:15	3.60	32.1	0.22	0.91
	15:45	3.23	15:55	2.92	9.6	0.22	0.91
25-Oct-01	11:20	6.54	11:10	4.43	32.3	0.32	1.00
25-Oct-01	14:45	10.24	14:55	9.40	8.2	0.45	1.00
7-May-02	10:55	4.14	10:45	3.29	20.6	0.19	0.18
	11:00	3.69	10:50	3.47	5.9	0.19	0.18
	11:15	4.14	11:05	3.40	17.9	0.19	0.18
	11:20	3.93	11:10	3.31	15.9	0.19	0.18
	11:35	4.68	11:25	3.31	29.3	0.19	0.18
	11:40	4.56	11:30	3.54	22.2	0.19	0.18
	11:55	4.94	11:45	3.38	31.4	0.19	0.18
	12:00	4.81	11:50	3.92	18.5	0.19	0.18
	12:15	4.71	12:05	4.15	11.9	0.29	0.33
	12:20	4.92	12:10	4.07	17.3	0.29	0.33
	12:35	4.27	12:25	4.07	4.8	0.29	0.33

	12:40	4.16	12:30	3.82	8.2	0.29	0.33
	12:55	3.51	12:45	3.42	**2.3**	0.29	0.33
	13:00	3.61	12:50	3.04	16.0	0.29	0.33
	13:15	3.56	13:05	3.15	11.5	0.29	0.33
	13:20	3.45	13:10	3.27	5.3	0.29	0.33
	13:35	3.03	13:25	2.90	4.1	0.29	0.33
	13:40	2.77	13:30	2.99	7.9	0.29	0.33
	13:55	3.07	13:45	2.46	19.9	0.29	0.33
	14:00	2.94	13:50	2.57	12.4	0.29	0.33
	14:15	3.02	14:05	2.74	9.3	0.29	0.33
	14:20	3.18	14:10	2.60	18.2	0.29	0.33
	14:35	2.79	14:25	2.68	4.0	0.29	0.33
	14:40	2.68	14:30	2.55	4.7	0.29	0.33
	14:55	2.77	14:45	2.39	13.8	0.29	0.33
7-May-02	20:40	4.27	20:30	2.92	31.6	0.10	1.73
	20:45	2.74	20:35	2.96	8.4	0.10	1.73
	21:00	2.62	20:50	3.20	22.3	0.10	1.73
	21:05	2.64	20:55	2.91	10.1	0.10	1.73
	21:20	3.60	21:10	2.56	28.9	0.10	1.73
	21:25	3.38	21:15	2.65	21.8	0.10	1.73
	21:40	3.67	21:30	2.81	23.4	0.10	1.73
	21:45	3.85	21:35	3.30	14.2	0.10	1.73
	22:00	3.51	21:50	3.56	**1.4**	0.10	1.73
	22:05	3.20	21:55	4.05	26.4	0.10	1.73
	22:20	3.32	22:10	3.16	4.6	0.10	1.73
	22:25	3.38	22:15	3.24	4.4	0.10	1.73
	22:40	4.27	22:30	3.10	27.4	0.10	1.73
	22:45	4.45	22:35	3.24	27.3	0.10	1.73
	23:00	3.56	22:50	3.93	10.3	0.10	1.73
	23:05	3.47	22:55	3.69	6.5	0.10	1.73
8-May-02	10:05	4.00	9:55	3.53	11.7	0.67	0.34
	10:10	3.65	10:00	3.15	13.5	0.67	0.34
	10:25	3.68	10:15	3.11	15.5	0.67	0.34
	10:30	3.27	10:20	3.04	6.9	0.67	0.34
	10:45	3.53	10:35	3.00	15.2	0.67	0.34
	10:50	3.45	10:40	3.11	9.8	0.67	0.34
	11:05	3.64	10:55	3.10	14.8	0.67	0.34
	11:10	3.65	11:00	3.04	16.7	0.67	0.34
	11:25	3.58	11:15	3.13	12.8	0.67	0.34
	11:30	3.40	11:20	3.15	7.3	0.67	0.34
	11:45	3.33	11:35	2.91	12.7	0.67	0.34
	11:50	3.27	11:40	3.04	7.2	0.67	0.34
	12:05	3.41	11:55	2.78	18.6	0.67	0.34
	12:10	3.29	12:00	2.82	14.3	0.67	0.34
	13:40	3.30	13:30	3.14	5.0	0.69	0.36

	13:45	3.22	13:35	2.86	11.4	0.69	0.36
	14:00	3.35	13:50	2.89	13.7	0.69	0.36
	14:05	3.21	13:55	2.81	12.5	0.69	0.36
	14:20	3.69	14:10	3.14	14.9	0.69	0.36
	14:25	3.47	14:15	3.52	**1.5**	0.69	0.36
	14:40	3.18	14:30	3.30	3.7	0.69	0.36
	14:45	3.11	14:35	2.90	6.8	0.69	0.36
	15:00	3.30	14:50	3.14	4.9	0.69	0.36
	15:05	3.36	14:55	3.05	9.2	0.69	0.36
	15:20	3.52	15:10	3.14	10.8	0.69	0.36
	15:25	3.19	15:15	3.11	2.7	0.69	0.36
	15:40	3.34	15:30	2.86	14.5	0.69	0.36
	15:45	3.23	15:35	3.00	6.9	0.69	0.36
	16:00	3.34	15:50	3.08	7.9	0.69	0.36
14-Nov-02	10:00	2.66	10:10	2.34	11.9	0.18	0.30
	10:20	2.32	10:30	2.28	**1.5**	0.18	0.30
	10:40	2.02	10:50	1.92	5.1	0.18	0.30
	11:00	1.89	11:10	1.91	**1.4**	0.18	0.30
	11:20	1.74	11:30	1.73	**1.0**	0.18	0.30
	11:40	1.77	11:50	1.89	6.4	0.18	0.30
	12:20	1.85	12:10	1.72	6.9	0.23	0.41
	13:30	2.07	13:20	1.88	9.3	0.23	0.41
	13:50	1.83	13:40	1.84	**0.5**	0.23	0.41
	14:10	2.06	14:00	2.03	**1.7**	0.23	0.41
	14:30	2.06	14:20	2.08	**1.0**	0.23	0.41
	15:15	1.91	15:05	2.00	5.0	0.23	0.41
	15:35	1.89	15:25	1.92	**1.4**	0.23	0.41
	15:55	1.85	15:45	1.83	**0.8**	0.23	0.41
	16:15	1.67	16:05	1.62	2.9	0.23	0.41
	16:35	1.67	16:25	1.68	**0.8**	0.23	0.41
15-Nov-02	9:30	2.66	9:20	2.59	2.7	0.24	0.73
	9:50	2.74	9:40	2.73	**0.3**	0.24	0.73
	10:10	2.74	10:00	2.82	2.7	0.24	0.73
	11:10	2.49	11:00	2.70	8.4	0.24	0.73
	11:30	2.62	11:20	2.57	**2.0**	0.24	0.73
	11:50	2.71	11:40	2.76	**2.1**	0.24	0.73
	12:10	3.13	12:20	2.98	4.7	0.26	0.81
	12:30	2.86	12:40	2.72	4.9	0.26	0.81
	12:50	2.84	13:00	2.69	5.3	0.26	0.81
	13:10	2.58	13:20	2.46	4.4	0.26	0.81
	13:30	2.54	13:40	2.41	5.2	0.26	0.81
	13:50	2.43	14:00	2.41	**0.6**	0.26	0.81

ical concentration gradients and

dients < 2.6% (twice the analytical

ere κ is the von Karmon constant (0.41) and u*

Lower Height (Z_1; m)	Upper Height (Z_2; m)	Vertical Gradient (ng m^{-3})	Flux[2] (ng m^{-2} h^{-1})
0.79	3.00	0.64	289
0.79	3.00	0.13	59
0.79	3.00	0.65	293
0.79	3.00	0.24	108
	Averages:	**0.42**	**187**
0.15	1.50	0.13	17
0.15	1.50	0.12	16
0.15	1.50	0.43	58
	Averages:	**0.23**	**30**
0.15	1.50	**0.46**	**139**
0.20	1.20	0.92	183
0.20	1.20	0.61	121
0.20	1.20	0.38	76
0.20	1.20	1.70	339
0.20	1.20	0.31	62
	Averages:	**0.78**	**156**
0.20	1.20	**2.11**	**559**
0.20	1.20	**0.84**	**310**
0.79	3.00	0.85	980
0.79	3.00	0.22	248
0.79	3.00	0.74	851
0.79	3.00	0.63	719
0.79	3.00	1.37	1574
0.79	3.00	1.01	1163
0.79	3.00	1.55	1783
0.79	3.00	0.89	1025
	Averages:	**0.91**	**1043**
0.79	3.00	0.56	546
0.79	3.00	0.85	831
0.79	3.00	0.20	199

0.79	3.00	0.34	331
0.79	3.00	0.00	0
0.79	3.00	0.58	562
0.79	3.00	0.41	398
0.79	3.00	0.18	178
0.79	3.00	0.12	120
0.79	3.00	-0.22	-213
0.79	3.00	0.61	596
0.79	3.00	0.36	355
0.79	3.00	0.28	275
0.79	3.00	0.58	564
0.79	3.00	0.11	108
0.79	3.00	0.13	123
0.79	3.00	0.38	372
Averages:		**0.32**	**314**
0.79	3.00	1.35	86
0.79	3.00	-0.23	-15
0.79	3.00	-0.58	-37
0.79	3.00	-0.27	-17
0.79	3.00	1.04	66
0.79	3.00	0.74	47
0.79	3.00	0.86	55
0.79	3.00	0.55	35
0.79	3.00	0.00	0
0.79	3.00	-0.85	-54
0.79	3.00	0.15	10
0.79	3.00	0.15	9
0.79	3.00	1.17	75
0.79	3.00	1.21	78
0.79	3.00	-0.37	-23
0.79	3.00	-0.22	-14
Averages:		**0.29**	**19**
0.79	3.00	0.47	1017
0.79	3.00	0.49	1065
0.79	3.00	0.57	1231
0.79	3.00	0.23	489
0.79	3.00	0.54	1162
0.79	3.00	0.34	734
0.79	3.00	0.54	1164
0.79	3.00	0.61	1318
0.79	3.00	0.46	989
0.79	3.00	0.25	539
0.79	3.00	0.42	915
0.79	3.00	0.24	509
0.79	3.00	0.63	1368
0.79	3.00	0.47	1017
Averages:		**0.45**	**966**
0.79	3.00	0.16	345

0.79	3.00	0.37	769
0.79	3.00	0.46	967
0.79	3.00	0.40	843
0.79	3.00	0.55	1158
0.79	3.00	0.00	0
0.79	3.00	-0.12	-250
0.79	3.00	0.21	442
0.79	3.00	0.16	338
0.79	3.00	0.31	650
0.79	3.00	0.38	797
0.79	3.00	0.09	179
0.79	3.00	0.49	1022
0.79	3.00	0.22	471
0.79	3.00	0.26	553
	Averages:	**0.26**	**552**
0.79	3.00	0.32	212
0.79	3.00	0.00	0
0.79	3.00	0.10	68
0.79	3.00	0.00	0
0.79	3.00	0.00	0
0.79	3.00	-0.11	-77
	Averages:	**0.05**	**34**
0.79	3.00	0.13	79
0.79	3.00	0.19	119
0.79	3.00	0.00	0
0.79	3.00	0.00	0
0.79	3.00	0.00	0
0.79	3.00	-0.10	-58
0.79	3.00	0.00	0
0.79	3.00	0.00	0
0.79	3.00	0.05	30
0.79	3.00	0.00	0
	Averages:	**0.03**	**17**
0.79	3.00	0.07	25
0.79	3.00	0.00	0
0.79	3.00	-0.07	-26
0.79	3.00	-0.21	-75
0.79	3.00	0.00	0
0.79	3.00	0.00	0
	Averages:	**-0.04**	**-13**
0.79	3.00	0.15	52
0.79	3.00	0.14	50
0.79	3.00	0.15	54
0.79	3.00	0.11	41
0.79	3.00	0.13	47
0.79	3.00	0.00	0
	Averages:	**0.11**	**41**

Day	T (upper)	T (lower)	dT (upper - lower)	e (lower)	e (upper)	LE
8/1/01 9:20 AM	23.074	23.536	-0.46	3.3251	3.3264	125.78
8/1/01 9:40 AM	23.661	24.256	-0.59	3.3841	3.373	146.33
8/1/01 10:00 AM	24.48	25.018	-0.54	3.5268	3.5113	160.1
8/1/01 10:20 AM	24.482	25.883	-1.40	3.6995	3.6808	205.31
8/1/01 10:40 AM	24.896	27.088	-2.19	3.8551	3.8426	240.74
8/1/01 11:00 AM	26.018	27.82	-1.80	3.9961	3.9787	257.34
8/1/01 11:20 AM	27.039	28.248	-1.21	4.1789	4.1625	250.21
8/1/01 11:40 AM	27.638	28.775	-1.14	4.3284	4.3135	262.44
8/1/01 12:00 PM	28.476	29.573	-1.10	4.4677	4.4545	230.9
8/1/01 12:20 PM	29.013	29.185	-0.17	4.5756	4.569	221.64
8/1/01 12:40 PM	29.384	29.555	-0.17	4.643	4.6381	220.1733
8/1/01 1:00 PM	29.663	28.357	1.31	4.6438	4.6463	493.83
8/1/01 1:20 PM	29.51	28.624	0.89	4.573	4.58	365.85
8/1/01 1:40 PM	29.877	29.648	0.23	4.6242	4.6117	463.45
8/1/01 2:00 PM	29.404	28.636	0.77	4.6736	4.6791	321.21
8/1/01 2:20 PM	29.25	28.481	0.77	4.584	4.5949	279.98
8/1/01 2:40 PM	29.468	29.26	0.21	4.4652	4.4733	139.75

Day	T (lower)	T (upper)	dT (upper - lower)	e (lower)	e (upper)	LE
8/29/01 21:40	24.50	25.09	0.59	1.57	1.52	39.08
8/29/01 22:00	24.44	24.85	0.42	1.56	1.51	64.47
8/29/01 22:20	24.19	24.59	0.41	1.55	1.50	35.20
8/29/01 22:40	23.76	24.07	0.31	1.55	1.50	11.08
8/29/01 23:00	23.48	24.11	0.63	1.56	1.51	39.61
8/29/01 23:20	23.03	23.47	0.43	1.50	1.45	11.87
8/29/01 23:40	22.75	23.12	0.38	1.52	1.49	2.79
8/30/01 0:00	22.60	23.02	0.42	1.55	1.50	35.27
8/30/01 0:20	22.16	23.12	0.96	1.54	1.50	9.81
8/30/01 0:40	22.10	22.72	0.61	1.50	1.46	43.13
8/30/01 1:00	21.87	22.06	0.19	1.53	1.49	42.67
8/30/01 1:20	21.56	21.64	0.08	1.55	1.51	38.84
8/30/01 1:40	21.25	21.38	0.13	1.56	1.53	54.00
8/30/01 2:00	20.96	21.08	0.12	1.58	1.55	43.40

	T (lower)	T (upper)	dT (upper - lower)	e (lower)	e (upper)	LE
8/29/01 12:20	25.37	25.98	0.61	1.85	1.78	212.25
8/29/01 12:40	26.02	26.25	0.23	1.84	1.79	224.77
8/29/01 13:00	26.01	26.70	0.69	1.77	1.72	213.68
8/29/01 13:20	28.39	26.97	-1.42	1.68	1.64	215.92
8/29/01 13:40	28.60	26.71	-1.88	1.53	1.53	169.40
8/29/01 14:00	28.57	26.80	-1.77	1.68	1.65	225.56
8/29/01 14:20	28.93	27.21	-1.72	1.68	1.65	206.17
8/29/01 14:40	29.19	27.32	-1.87	1.74	1.70	191.35
8/29/01 15:00	29.58	27.63	-1.95	1.70	1.67	183.35
8/29/01 15:20	30.03	28.05	-1.99	1.70	1.67	217.89
8/29/01 15:40	30.07	28.03	-2.04	1.75	1.72	205.89
8/29/01 16:00	29.86	27.92	-1.94	1.89	1.83	205.73
8/29/01 16:20	29.17	27.15	-2.01	1.94	1.92	201.32
8/29/01 16:40	28.41	26.57	-1.85	1.91	1.89	154.79
8/30/01 11:00	23.73	23.45	-0.29	1.93	1.86	69.67

8/30/01 11:20	24.03	23.68	-0.35	2.10	2.05	103.86
8/30/01 11:40	24.82	24.24	-0.59	2.14	2.09	147.17
8/30/01 12:00	25.37	24.58	-0.79	2.19	2.13	137.03
8/30/01 12:20	25.55	25.10	-0.45	2.33	2.26	145.20
8/30/01 12:40	26.09	25.98	-0.12	2.35	2.31	131.53
8/30/01 13:00	26.18	25.67	-0.50	2.38	2.34	121.02
8/30/01 13:20	26.22	25.76	-0.46	2.41	2.38	122.75
8/30/01 13:40	26.03	25.65	-0.38	2.42	2.39	97.05
8/30/01 14:00	25.44	25.11	-0.33	2.44	2.42	87.32
8/30/01 14:20	25.01	24.79	-0.22	2.46	2.44	44.03
8/30/01 14:40	24.80	24.71	-0.09	2.48	2.46	30.40

Date/Time	Temp Lower	Temp Upper	dT (upper - lower)	e Lower	e Upper	LE
10/23/01 11:20	19.01	18.37	-0.63	1.70	1.67	31.02
10/23/01 11:40	18.81	18.29	-0.52	1.66	1.66	30.53
10/23/01 12:00	18.49	18.02	-0.47	1.65	1.65	28.03
10/23/01 12:20	18.32	17.82	-0.50	1.64	1.64	34.64
10/23/01 12:40	18.59	18.13	-0.47	1.64	1.64	23.30
10/23/01 13:00	18.69	18.15	-0.54	1.68	1.68	32.23
10/23/01 13:20	18.82	18.26	-0.57	1.69	1.69	41.06
10/23/01 13:40	19.24	18.68	-0.56	1.69	1.68	28.70
10/23/01 14:00	19.18	18.52	-0.66	1.70	1.69	49.48
10/23/01 14:20	19.59	18.98	-0.61	1.72	1.70	46.09
10/23/01 14:40	19.77	19.17	-0.60	1.72	1.70	43.48
10/23/01 15:00	19.71	19.13	-0.58	1.72	1.70	33.01
10/23/01 15:20	19.69	19.10	-0.59	1.72	1.71	32.82
10/23/01 15:40	19.83	19.26	-0.57	1.72	1.70	24.89
10/23/01 16:00	19.74	19.19	-0.55	1.73	1.71	23.05
10/23/01 16:20	19.49	19.02	-0.47	1.72	1.71	23.64
10/23/01 16:40	19.37	18.56	-0.81	1.74	1.73	23.57
10/23/01 17:00	19.67	19.08	-0.60	1.73	1.72	11.21
10/23/01 17:20	19.31	18.87	-0.44	1.71	1.70	7.82
10/23/01 17:40	18.82	18.45	-0.37	1.71	1.70	4.54
10/23/01 18:00	18.56	18.48	-0.08	1.69	1.69	-4.67
10/23/01 18:20	17.91	18.26	0.35	1.68	1.68	-2.61
10/23/01 18:40	17.59	18.06	0.48	1.69	1.69	-4.16
10/23/01 19:00	17.93	18.28	0.35	1.79	1.78	-8.67
10/23/01 19:20	18.06	18.33	0.27	1.77	1.77	-9.65
10/23/01 19:40	17.94	18.15	0.21	1.73	1.73	-6.01
10/23/01 20:00	17.04	17.56	0.52	1.72	1.72	-11.49
10/23/01 20:20	16.92	17.48	0.56	1.73	1.73	-10.85
10/23/01 20:40	16.81	17.37	0.57	1.75	1.76	-16.56
10/23/01 21:00	16.92	17.43	0.51	1.77	1.79	-8.41
10/23/01 21:20	17.40	17.74	0.35	1.79	1.81	-3.48
10/23/01 21:40	17.72	17.95	0.24	1.79	1.80	-5.92
10/23/01 22:00	17.59	17.92	0.32	1.79	1.80	-4.49
10/23/01 22:20	17.74	17.93	0.18	1.80	1.81	-7.19
10/23/01 22:40	17.86	17.87	0.01	1.80	1.81	-4.55
10/23/01 23:00	17.94	18.00	0.06	1.80	1.82	-5.12
10/23/01 23:20	17.99	18.04	0.05	1.81	1.82	-5.86
10/23/01 23:40	17.87	17.91	0.04	1.81	1.82	-9.54

10/24/01 0:00	17.96	18.05	0.09	1.82	1.83	-6.20
10/24/01 0:20	18.49	18.43	-0.06	1.83	1.83	-3.95
10/24/01 0:40	19.08	18.76	-0.32	1.79	1.80	-5.93
10/24/01 1:00	18.47	18.35	-0.12	1.76	1.76	17.59
10/24/01 1:20	17.86	17.90	0.04	1.76	1.76	-8.88
10/24/01 1:40	16.89	17.46	0.57	1.78	1.78	0.00
10/24/01 2:00	17.09	17.50	0.41	1.83	1.82	-4.42
10/24/01 2:20	17.73	17.97	0.23	1.87	1.86	-3.82
10/24/01 2:40	18.11	18.26	0.15	1.87	1.88	-6.48
10/24/01 3:00	18.35	18.40	0.05	1.86	1.88	-4.93
10/24/01 3:20	18.45	18.50	0.05	1.85	1.87	-6.60
10/24/01 3:40	18.61	18.49	-0.11	1.85	1.86	-6.94
10/24/01 4:00	18.41	18.33	-0.08	1.83	1.83	-10.63
10/24/01 4:20	18.09	18.05	-0.04	1.82	1.83	-7.49
10/24/01 4:40	18.06	18.00	-0.05	1.81	1.82	-11.12
10/24/01 5:00	18.22	18.01	-0.22	1.80	1.81	-5.62
10/24/01 5:20	17.75	17.73	-0.03	1.79	1.79	-11.44
10/24/01 5:40	17.66	17.87	0.21	1.78	1.79	-3.32
10/24/01 6:00	17.40	17.60	0.20	1.77	1.78	-6.75
10/24/01 6:20	17.31	17.47	0.17	1.77	1.78	-7.38
10/24/01 6:40	17.14	17.31	0.16	1.76	1.78	-10.13
10/24/01 7:00	17.19	17.29	0.10	1.76	1.77	-10.91
10/24/01 7:20	17.56	17.63	0.07	1.74	1.75	-6.46
10/24/01 7:40	17.20	17.38	0.18	1.71	1.72	9.37
10/24/01 8:00	16.12	16.53	0.41	1.71	1.70	15.72
10/24/01 8:20	16.02	16.41	0.39	1.76	1.75	-0.13
10/24/01 8:40	16.56	16.84	0.27	1.81	1.79	11.03
10/24/01 9:00	17.44	17.59	0.15	1.85	1.83	14.29
10/24/01 9:20	17.89	18.14	0.25	1.91	1.89	37.13
10/24/01 9:40	19.08	19.18	0.10	1.98	1.99	53.23
10/24/01 10:00	20.41	20.10	-0.31	2.06	2.07	85.40
10/24/01 10:20	21.72	20.95	-0.77	2.13	2.13	94.69
10/24/01 10:40	23.03	22.61	-0.42	2.19	2.20	113.72
10/24/01 11:00	23.98	23.66	-0.32	2.23	2.25	113.90
10/24/01 11:20	24.97	24.67	-0.29	2.19	2.21	92.61
10/24/01 11:40	24.90	24.24	-0.66	2.14	2.14	115.24
10/24/01 12:00	25.45	24.70	-0.75	2.20	2.21	114.80
10/24/01 12:20	26.64	25.78	-0.86	2.26	2.28	176.53
10/24/01 12:40	27.89	27.17	-0.73	2.30	2.33	147.34
10/24/01 13:00	29.97	28.07	-1.90	2.32	2.34	101.65
10/24/01 13:20	31.95	26.42	-5.53	2.33	2.34	165.17
10/24/01 13:40	29.64	27.68	-1.96	2.32	2.32	182.07
10/24/01 14:00	28.53	28.18	-0.35	2.30	2.32	122.51
10/24/01 14:20	29.44	29.05	-0.38	2.28	2.28	143.58
10/24/01 14:40	32.31	29.99	-2.32	2.32	2.26	197.28
10/24/01 15:00	31.01	28.82	-2.19	2.17	2.14	117.13
10/24/01 15:20	29.85	28.08	-1.77	2.11	2.08	105.78
10/24/01 15:40	28.84	27.86	-0.98	2.13	2.11	148.47
10/24/01 16:00	29.23	28.30	-0.92	2.14	2.12	101.28
10/24/01 16:20	29.96	28.90	-1.06	2.11	2.11	65.00
10/24/01 16:40	28.98	28.18	-0.80	2.07	2.07	70.59
10/24/01 17:00	27.99	27.26	-0.73	2.03	2.03	48.53

10/24/01 17:20	26.66	26.24	-0.42	1.99	1.99	40.79
10/24/01 17:40	25.68	25.24	-0.44	1.94	1.93	34.09
10/24/01 18:00	24.91	24.51	-0.41	1.90	1.89	26.19
10/24/01 18:20	23.53	23.29	-0.24	1.86	1.85	24.78
10/24/01 18:40	22.74	22.55	-0.20	1.83	1.82	19.34
10/24/01 19:00	21.84	21.71	-0.13	1.80	1.79	13.90
10/24/01 19:20	22.33	21.98	-0.35	1.77	1.77	9.99
10/24/01 19:40	20.96	20.82	-0.13	1.73	1.72	8.07
10/24/01 20:00	17.49	18.02	0.52	1.74	1.74	16.90
10/24/01 20:20	18.78	18.87	0.10	1.85	99999.00	31.05
10/24/01 20:40	19.57	19.28	-0.29	1.89	1.89	30.13
10/24/01 21:00	20.74	20.50	-0.23	1.91	1.90	44.07
10/24/01 21:20	21.67	21.69	0.02	1.91	1.91	37.90
10/24/01 21:40	22.40	22.10	-0.31	1.90	1.90	19.68
10/24/01 22:00	22.29	21.92	-0.37	1.89	1.89	17.68
10/24/01 22:20	22.14	21.81	-0.33	1.87	1.87	19.93
10/24/01 22:40	21.86	21.60	-0.27	1.85	1.86	23.86
10/24/01 23:00	21.80	21.49	-0.31	1.84	1.84	17.29
10/24/01 23:20	21.50	21.26	-0.24	1.82	1.83	14.52
10/24/01 23:40	21.36	21.15	-0.21	1.81	1.81	8.35
10/25/01 0:00	21.14	21.04	-0.10	1.81	1.81	9.06
10/25/01 0:20	20.79	20.72	-0.06	1.83	1.83	7.28
10/25/01 0:40	20.95	20.76	-0.19	1.80	1.81	8.47
10/25/01 1:00	21.61	21.35	-0.26	1.75	1.74	5.06
10/25/01 1:20	20.25	20.15	-0.10	1.70	1.69	6.03
10/25/01 1:40	18.94	19.04	0.10	1.66	1.65	-0.50
10/25/01 2:00	17.94	18.17	0.23	1.65	1.63	-1.94
10/25/01 2:20	17.23	17.55	0.32	1.65	1.64	-4.95
10/25/01 2:40	17.31	17.57	0.26	1.64	1.63	-3.62
10/25/01 3:00	17.11	17.38	0.27	1.64	1.62	-4.95
10/25/01 3:20	16.85	17.14	0.29	1.65	1.63	-6.71
10/25/01 3:40	17.03	17.24	0.21	1.65	1.63	-5.04
10/25/01 4:00	16.98	17.16	0.18	1.64	1.63	-2.51
10/25/01 4:20	16.73	16.94	0.21	1.64	1.62	-7.81
10/25/01 4:40	16.67	16.87	0.20	1.65	1.63	-5.14
10/25/01 5:00	17.00	17.08	0.08	1.66	1.64	15.36
10/25/01 5:20	16.89	17.01	0.12	1.65	1.63	-3.36
10/25/01 5:40	16.65	16.83	0.17	1.65	1.63	-4.26
10/25/01 6:00	16.18	16.54	0.37	1.66	1.65	-10.11
10/25/01 6:20	16.48	16.77	0.29	1.68	1.67	-1.64
10/25/01 6:40	16.78	16.98	0.19	1.67	1.67	0.20
10/25/01 7:00	16.90	17.00	0.10	1.66	1.65	-1.34
10/25/01 7:20	16.64	16.80	0.16	1.65	1.64	-1.69
10/25/01 7:40	16.38	16.60	0.22	1.65	1.64	-0.03
10/25/01 8:00	16.21	16.49	0.29	1.66	1.65	0.67
10/25/01 8:20	15.70	16.29	0.59	1.70	1.68	-1.28
10/25/01 8:40	14.89	15.87	0.98	1.82	1.78	32.17
10/25/01 9:00	17.41	18.10	0.68	1.97	1.94	51.69
10/25/01 9:20	19.85	20.26	0.41	2.04	2.06	70.46
10/25/01 9:40	21.54	21.80	0.26	2.10	2.10	66.61
10/25/01 10:00	22.55	22.74	0.18	2.15	2.14	64.96
10/25/01 10:20	23.37	23.55	0.19	2.19	2.18	78.50

10/25/01 10:40	24.36	24.56	0.20	2.20	2.18	79.03
10/25/01 11:00	25.25	25.50	0.25	2.19	2.17	91.32
10/25/01 11:20	25.89	26.19	0.30	2.18	2.16	100.42
10/25/01 11:40	26.98	27.34	0.36	2.16	2.18	83.64
10/25/01 12:00	28.03	28.33	0.30	2.10	2.11	75.94
10/25/01 12:20	28.68	28.66	-0.02	2.01	2.01	53.81
10/25/01 12:40	27.48	27.01	-0.47	1.82	1.89	48.31
10/25/01 13:00	25.50	25.07	-0.43	1.55	1.66	44.89
10/25/01 13:20	25.95	25.79	-0.15	1.41	1.53	66.86
10/25/01 13:40	26.09	25.88	-0.20	1.39	1.45	59.78
10/25/01 14:00	25.18	25.32	0.15	1.39	1.45	77.17
10/25/01 14:20	25.18	25.10	-0.07	1.32	1.42	104.95
10/25/01 14:40	26.45	26.05	-0.40	1.24	1.32	128.56

	Temp (lower))	Temp (upper)	dT (lower - upper)	e (lower)	e (upper)	LE
5/6/02 11:40	21.94	22.21	-0.26	1.15	1.13	284.16
5/6/02 12:00	22.85	22.71	0.14	1.18	1.15	251.48
5/6/02 12:20	21.58	21.41	0.17	1.33	1.31	337.26
5/6/02 12:40	21.43	21.22	0.21	1.41	1.40	445.69
5/6/02 13:00	20.52	20.35	0.18	1.42	1.42	554.62
5/6/02 13:20	20.64	20.27	0.37	1.43	1.44	550.04
5/6/02 13:40	20.96	20.53	0.43	1.47	1.47	577.06
5/6/02 14:00	21.51	21.05	0.46	1.47	1.48	382.10
5/6/02 14:20	20.67	20.29	0.39	1.45	1.45	408.58
5/6/02 14:40	20.76	20.33	0.44	1.41	1.41	298.08
5/6/02 15:00	21.17	20.77	0.40	1.38	1.38	364.60
5/6/02 15:20	21.63	21.29	0.34	1.35	1.34	362.57
5/6/02 15:40	22.66	22.41	0.25	1.26	1.24	379.73
5/6/02 16:00	22.43	22.27	0.16	1.16	1.14	275.11
5/6/02 16:20	22.21	22.09	0.12	1.11	1.10	319.31
5/6/02 16:40	21.53	21.49	0.04	1.07	1.05	249.62
5/6/02 17:00	21.32	21.29	0.03	1.04	1.02	201.42
5/6/02 17:20	20.65	20.64	0.01	1.02	1.01	205.64
5/6/02 17:40	20.44	20.46	-0.02	1.01	1.00	155.46
5/6/02 18:00	20.03	20.06	-0.03	1.00	0.99	133.03
5/6/02 18:20	19.51	19.55	-0.04	1.00	1.00	102.60
5/6/02 18:40	18.97	19.03	-0.06	1.02	1.02	77.69
5/7/02 9:20	18.25	18.02	0.23	2.06	2.11	113.99
5/7/02 9:40	18.66	18.54	0.11	2.32	2.30	92.85
5/7/02 10:00	19.59	19.37	0.23	1.62	1.76	119.71
5/7/02 10:20	20.25	20.05	0.20	1.57	1.55	160.76
5/7/02 10:40	20.39	20.05	0.34	1.65	1.64	155.51
5/7/02 11:00	21.53	21.21	0.33	1.70	1.68	221.24
5/7/02 11:20	21.93	21.60	0.32	1.71	1.69	231.54
5/7/02 11:40	22.37	21.91	0.45	1.72	1.70	182.87
5/7/02 12:00	23.02	22.56	0.46	1.75	1.73	202.61
5/7/02 12:20	23.31	22.59	0.72	1.77	1.75	166.65
5/7/02 12:40	23.59	23.08	0.51	1.77	1.75	218.04
5/7/02 13:00	24.42	24.18	0.24	1.78	1.76	211.44
5/7/02 13:20	25.42	25.14	0.28	1.79	1.76	306.96
5/7/02 13:40	25.68	25.41	0.26	1.78	1.74	297.17

5/7/02 14:00	25.60	25.39	0.22	1.75	1.72	220.99
5/7/02 14:20	25.73	25.55	0.19	1.75	1.72	231.04
5/7/02 14:40	25.87	25.71	0.17	1.75	1.73	221.83
5/7/02 15:00	25.88	25.77	0.11	1.73	1.71	216.13
5/7/02 15:20	25.76	25.67	0.09	1.72	1.69	175.32
5/7/02 15:40	25.87	25.80	0.07	1.71	1.68	178.85
5/7/02 16:00	26.21	26.12	0.10	1.72	1.70	214.85
5/7/02 19:40	25.01	25.35	-0.34	2.35		47.63
5/7/02 20:00	24.70	25.03	-0.33	3.12	3.12	31.19
5/7/02 20:20	24.54	24.89	-0.34	3.07	3.08	16.16
5/7/02 20:40	21.16	21.80	-0.64	3.01	3.02	8.39
5/7/02 21:00	21.74	22.24	-0.49	2.84	2.86	25.06
5/7/02 21:20	23.50	23.99	-0.49	2.73	2.73	26.61
5/7/02 21:40	22.82	23.44	-0.62	2.71	2.71	23.18
5/7/02 22:00	22.86	23.40	-0.54	2.70	2.70	8.30
5/7/02 22:20	22.26	22.80	-0.54	2.66	2.67	8.78
5/7/02 22:40	22.07	22.71	-0.64	2.59	2.60	4.71
5/7/02 23:00	21.70	22.39	-0.69	2.54	2.54	1.54
5/7/02 23:20	21.68	22.34	-0.66	2.49	2.49	-5.98
5/7/02 23:40	20.44	21.67	-1.23	2.14	2.13	3.78
5/8/02 0:00	20.32	21.15	-0.83	1.64	1.63	0.00
5/8/02 0:20	20.68	21.27	-0.59	1.60	1.60	0.56
5/8/02 0:40	19.75	20.46	-0.72	1.58	1.59	1.99
5/8/02 1:00	19.65	20.27	-0.61	1.58	1.59	7.69
5/8/02 1:20	20.04	20.58	-0.54	1.57	1.58	21.64
5/8/02 1:40	20.61	20.94	-0.33	1.57	1.57	15.95
5/8/02 2:00	20.53	20.81	-0.28	1.55	1.56	14.01
5/8/02 2:20	20.07	20.34	-0.27	1.54	1.55	16.64
5/8/02 2:40	19.93	20.22	-0.29	1.54	1.54	49.03
5/8/02 3:00	19.93	20.15	-0.22	1.54	1.54	18.25
5/8/02 3:20	19.65	19.85	-0.20	1.54	1.54	23.10
5/8/02 3:40	19.41	19.58	-0.17	1.52	1.53	25.56
5/8/02 4:00	19.17	19.32	-0.16	1.50	1.51	36.73
5/8/02 4:20	18.91	19.04	-0.12	1.47	1.48	21.18
5/8/02 4:40	18.70	18.83	-0.13	1.41	1.42	32.91
5/8/02 5:00	18.21	18.37	-0.16	1.36	1.36	35.71
5/8/02 5:20	17.77	17.93	-0.16	1.31	1.31	37.37
5/8/02 5:40	17.31	17.43	-0.12	1.27	1.27	32.80
5/8/02 6:00	16.80	16.95	-0.15	1.25	1.24	28.59
5/8/02 6:20	16.63	16.73	-0.10	1.23	1.23	21.07
5/8/02 6:40	16.59	16.68	-0.09	1.22	1.22	30.83
5/8/02 7:00	16.52	16.64	-0.12	1.22	1.21	43.37
5/8/02 7:20	16.82	16.91	-0.09	1.23	1.22	35.80
5/8/02 7:40	16.82	16.85	-0.03	1.24	1.24	58.44
5/8/02 8:00	17.25	17.18	0.08	1.25	1.25	115.97
5/8/02 8:20	17.76	17.63	0.13	1.27	1.27	138.80
5/8/02 8:40	17.94	17.76	0.18	1.29	1.28	134.98
5/8/02 9:00	18.38	18.16	0.22	1.30	1.30	145.06
5/8/02 9:20	18.68	18.32	0.36	1.32	1.32	184.38
5/8/02 9:40	19.27	18.72	0.55	1.33	1.33	161.69
5/8/02 10:00	19.47	19.05	0.42	1.35	1.34	197.70

5/8/02 10:20	19.70	19.33	0.37	1.36	1.36	185.20
5/8/02 10:40	19.87	19.57	0.30	1.31	1.31	219.97
5/8/02 11:00	19.78	19.73	0.05	1.23	1.22	255.31
5/8/02 11:20	20.52	20.32	0.20	1.25	1.23	296.33
5/8/02 11:40	20.59	20.50	0.09	1.24	1.22	314.59
5/8/02 12:00	20.72	20.70	0.02	1.15	1.15	221.40
5/8/02 12:20	20.50	20.53	-0.03	1.14	1.11	154.49
5/8/02 12:40	20.74	20.67	0.07	1.15	1.13	157.69
5/8/02 13:00	21.06	21.00	0.06	1.15	1.13	327.76
5/8/02 13:20	21.89	21.81	0.08	1.17	1.15	164.65
5/8/02 13:40	22.01	22.04	-0.03	1.19	1.17	234.79
5/8/02 14:00	21.98	21.99	0.00	1.18	1.16	295.83
5/8/02 14:20	21.63	21.70	-0.07	1.19	1.17	356.90
5/8/02 14:40	18.62	19.13	-0.51	1.25	1.23	287.47
5/8/02 15:00	17.65	18.03	-0.39	1.24	1.24	313.92
5/8/02 15:20	17.34	17.49	-0.15	1.23	1.23	226.84
5/8/02 15:40	16.36	16.61	-0.25	1.21	1.21	223.27
5/8/02 16:00	15.93	16.10	-0.17	1.21	1.20	234.89
5/10/02 8:20	16.97	16.57	0.40	1.84	1.89	
5/10/02 8:40	17.04	16.90	0.14	2.03	2.01	48.50
5/10/02 9:00	17.55	17.64	-0.09	2.08	2.17	182.57
5/10/02 9:20	18.16	18.21	-0.04	2.31	2.30	186.71
5/10/02 9:40	19.13	18.98	0.16	2.44	2.43	244.30
5/10/02 10:00	19.88	19.63	0.25	2.56	2.54	263.24
5/10/02 10:20	20.48	20.27	0.21	2.68	2.67	243.58
5/10/02 10:40	20.86	20.62	0.24	2.75	2.74	321.43
5/10/02 11:00	20.99	20.77	0.22	2.76	2.76	296.54
5/10/02 11:20	21.19	20.98	0.21	2.75	2.75	378.09

Day	T (lower)	T (upper)	dT (lower - upper)	L_e	U_e	LE
11/13/02 14:20	9.72	9.8391	-0.12	0.94	0.94	45.96
11/13/02 14:40	9.71	9.8668	-0.16	0.92	0.92	60.22
11/13/02 15:00	9.71	9.8799	-0.17	0.92	0.91	57.03
11/13/02 15:20	9.53	9.707	-0.18	0.90	0.88	70.06
11/13/02 15:40	9.69	9.7125	-0.02	0.88	0.87	63.89
11/13/02 16:00	9.59	9.6094	-0.02	0.86	0.85	72.48
11/13/02 16:20	9.55	9.5913	-0.04	0.85	0.84	35.44
11/13/02 16:40	9.49	9.5448	-0.06	0.84	0.83	60.84
11/13/02 17:00	9.49	9.5558	-0.07	0.83	0.82	67.92
11/13/02 17:20	9.25	9.3359	-0.08	0.82	0.81	73.47
11/13/02 17:40	9.05	9.1412	-0.09	0.80	0.79	81.81
11/13/02 18:00	8.73	8.8359	-0.10	0.78	0.77	56.12
11/13/02 18:20	8.48	8.6052	-0.13	0.76	0.76	55.25
11/13/02 18:40	8.17	8.3242	-0.16	0.75	0.75	48.58
11/13/02 19:00	7.88	8.0438	-0.16	0.74	0.74	57.72
11/13/02 19:20	7.63	7.8028	-0.18	0.72	0.73	47.70
11/13/02 19:40	7.41	7.5821	-0.17	0.72	0.72	41.51
11/13/02 20:00	7.18	7.4016	-0.22	0.71	0.71	39.05
11/13/02 20:20	6.99	7.2095	-0.22	0.70	0.71	45.58
11/13/02 20:40	6.84	7.031	-0.19	0.69	0.69	41.74

11/13/02 21:00	6.84	6.9623	-0.12	0.68	0.68	41.72
11/13/02 21:20	6.63	6.7771	-0.14	0.67	0.68	34.14
11/13/02 21:40	6.52	6.6456	-0.12	0.66	0.67	42.47
11/13/02 22:00	6.48	6.5674	-0.09	0.66	0.66	30.83
11/13/02 22:20	6.37	6.4548	-0.08	0.65	0.66	31.09
11/13/02 22:40	6.17	6.2693	-0.10	0.65	0.65	23.62
11/13/02 23:00	6.07	6.1422	-0.08	0.64	0.64	33.58
11/13/02 23:20	5.96	6.0149	-0.05	0.63	0.64	37.68
11/14/02 10:00	7.60	7.4717	0.13	0.75	0.75	55.32
11/14/02 10:20	8.48	8.2478	0.23	0.77	0.77	61.50
11/14/02 10:40	8.87	8.8213	0.05	0.79	0.79	90.86
11/14/02 11:00	9.83	9.7066	0.12	0.81	0.81	74.28
11/14/02 11:20	10.55	10.418	0.13	0.83	0.82	98.55
11/14/02 11:40	10.97	10.919	0.05	0.85	0.84	97.89
11/14/02 12:00	11.68	11.452	0.23	0.87	0.86	102.88
11/14/02 12:20	11.95	11.773	0.18	0.90	0.89	133.33
11/14/02 12:40	12.46	12.185	0.28	0.91	0.91	123.57
11/14/02 13:00	12.80	12.497	0.31	0.93	0.93	104.73
11/14/02 13:20	12.66	12.485	0.18	0.91	0.91	124.95
11/14/02 13:40	13.41	13.111	0.30	0.92	0.92	114.14
11/14/02 14:00	13.85	13.501	0.34	0.93	0.93	124.66
11/14/02 14:20	13.72	13.475	0.25	0.94	0.94	107.99
11/14/02 15:40	13.85	13.686	0.16	0.90	0.90	46.51
11/14/02 16:00	13.79	13.691	0.10	0.89	0.88	68.07
11/14/02 16:20	12.95	13.139	-0.19	0.85	0.85	61.90
11/14/02 16:40	12.78	12.918	-0.14	0.84	0.84	41.46
11/14/02 17:00	12.26	12.479	-0.22	0.82	0.82	34.03
11/14/02 17:20	11.88	12.098	-0.22	0.82	0.82	24.58
11/14/02 17:40	11.52	11.754	-0.24	0.82	0.82	29.62
11/14/02 18:00	11.43	11.744	-0.31	0.81	0.81	24.72
11/14/02 18:20	11.16	11.483	-0.33	0.82	0.82	32.53
11/14/02 18:40	11.08	11.401	-0.32	0.83	0.83	28.02
11/14/02 19:00	10.94	11.265	-0.33	0.83	0.83	23.44
11/14/02 19:20	10.94	11.228	-0.29	0.83	0.83	31.69
11/14/02 19:40	10.93	11.11	-0.18	0.82	0.82	27.14
11/14/02 20:00	10.62	10.877	-0.26	0.81	0.82	20.33
11/14/02 20:20	10.53	10.773	-0.24	0.81	0.81	29.68
11/14/02 20:40	10.66	10.855	-0.20	0.81	0.82	28.41
11/14/02 21:00	10.81	10.97	-0.16	0.81	0.82	38.94
11/14/02 21:20	10.64	10.854	-0.21	0.82	0.82	34.92
11/14/02 21:40	10.42	10.659	-0.24	0.81	0.82	24.30
11/14/02 22:00	10.36	10.585	-0.23	0.81	0.81	21.39
11/14/02 22:20	10.20	10.459	-0.26	0.81	0.81	15.25
11/14/02 22:40	10.20	10.455	-0.26	0.80	0.81	11.05
11/14/02 23:00	10.46	10.644	-0.19	0.80	0.81	16.67
11/14/02 23:20	10.64	10.801	-0.16	0.81	0.81	26.04
11/14/02 23:40	10.66	10.849	-0.19	0.81	0.82	26.54
11/15/02 0:00	10.55	10.77	-0.22	0.82	0.82	25.47
11/15/02 0:20	10.55	10.765	-0.21	0.82	0.82	27.01
11/15/02 0:40	10.60	10.803	-0.20	0.82	0.82	25.91

11/15/02 1:00	10.48	10.705	-0.22	0.82	0.82	31.04
11/15/02 1:20	10.48	10.685	-0.20	0.82	0.82	29.99
11/15/02 1:40	10.40	10.62	-0.22	0.82	0.82	24.93
11/15/02 2:00	10.36	10.591	-0.24	0.82	0.82	28.10
11/15/02 2:20	10.20	10.456	-0.25	0.81	0.81	21.42
11/15/02 2:40	9.98	10.238	-0.25	0.80	0.81	19.60
11/15/02 3:00	9.85	10.087	-0.23	0.80	0.80	18.80
11/15/02 3:20	9.49	9.7671	-0.28	0.79	0.80	19.70
11/15/02 3:40	9.33	9.5841	-0.26	0.78	0.79	21.41
11/15/02 4:00	9.07	9.3487	-0.28	0.78	0.78	14.25
11/15/02 4:20	8.92	9.1712	-0.25	0.77	0.78	14.44
11/15/02 4:40	8.83	9.0369	-0.20	0.76	0.78	17.90
11/15/02 5:00	8.74	8.9167	-0.18	0.76	0.78	16.43
11/15/02 5:20	8.52	8.702	-0.19	0.76	0.78	16.09
11/15/02 5:40	8.38	8.5633	-0.18	0.76	0.78	13.93
11/15/02 6:00	8.42	8.5636	-0.15	0.76	0.78	18.60
11/15/02 6:20	8.25	8.4195	-0.17	0.77	0.78	20.98
11/15/02 6:40	8.10	8.2861	-0.19	0.77	0.78	15.90
11/15/02 7:00	8.07	8.2434	-0.18	0.76	0.78	15.60
11/15/02 7:20	7.91	8.0698	-0.16	0.76	0.78	15.45
11/15/02 7:40	7.97	8.0903	-0.12	0.76	0.78	18.50
11/15/02 8:00	8.23	8.3229	-0.10	0.78	0.80	17.35
11/15/02 8:20	8.37	8.4761	-0.11	0.80	0.82	18.93
11/15/02 8:40	8.68	8.7748	-0.09	0.82	0.84	26.92
11/15/02 9:00	9.31	9.2858	0.03	0.85	0.86	38.56
11/15/02 9:20	9.78	9.7228	0.06	0.87	0.88	61.60
11/15/02 9:40	10.26	10.157	0.10	0.89	0.89	50.48
11/15/02 10:00	11.00	10.832	0.17	0.91	0.91	65.75
11/15/02 10:20	11.81	11.537	0.27	0.93	0.93	72.46
11/15/02 10:40	12.36	12.099	0.26	0.95	0.95	84.15
11/15/02 11:00	12.55	12.396	0.16	0.97	0.97	66.81
11/15/02 11:20	12.91	12.721	0.19	0.97	0.98	78.53
11/15/02 11:40	12.54	12.447	0.09	0.96	0.97	62.39
11/15/02 12:00	13.23	12.98	0.25	0.96	0.96	95.17
11/15/02 12:20	13.95	13.642	0.31	0.98	0.98	95.65
11/15/02 12:40	14.46	14.081	0.38	1.00	1.00	133.16
11/15/02 13:00	15.42	14.781	0.64	1.01	1.01	148.69
11/15/02 13:20	15.55	15.028	0.52	1.01	1.01	117.39
11/15/02 13:40	15.41	15.228	0.18	1.00	0.98	121.82
11/15/02 14:00	15.12	15.058	0.06	0.96	0.96	79.81

H	U (upper)	U (lower)	dU	u_star	z1 [inches]	z2 [inches	Ri
38.427	2.5519	2.1788	0.3731	0.12661	2.019201463	1.08783	-0.221533
44.101	1.9531	1.6913	0.2618	0.1078	2.019201463	1.08783	-0.578187
46.798	1.8406	1.5588	0.2818	0.17376	2.019201463	1.08783	-0.450025
71.61	1.745	1.3338	0.4112	0.17634	2.019201463	1.08783	-0.549588
101.73	2.0013	1.6219	0.3794	0.16003	2.019201463	1.08783	-1.007336
98.711	1.9444	1.5444	0.4	0.15343	2.019201463	1.08783	-0.742710
126.62	2.105	1.7513	0.3537	0.18708	2.019201463	1.08783	-0.635760
140.72	1.7994	1.4938	0.3056	0.21418	2.019201463	1.08783	-0.799427
149.3	1.6319	1.395	0.2369	0.22713	2.019201463	1.08783	-1.280043
103.67	2.04	1.7425	0.2975	0.16113	2.019201463	1.08783	-0.127232
167	1.354133	1.255827	0.098307	0.18284	2.019201463	1.08783	-1.157015
110.56	2.2713	2.0625	0.2088	0.14348	2.019201463	1.08783	1.961783
98.976	2.1231	1.9656	0.1575	0.10122	2.019201463	1.08783	2.338619
154.6	2.1944	1.95	0.2444	0.14466	2.019201463	1.08783	0.250450
82.167	2.3056	2.2375	0.0681	0.19145	2.019201463	1.08783	10.844796
21.031	2.3831	2.15	0.2331	0.21016	2.019201463	1.08783	0.927296
23.625	1.8619	1.3969	0.465	0.14214	2.019201463	1.08783	0.062924

H	U (upper)	U (lower)	dU	u_star	dz	ln(z1/z2)	Ri
-13.74	1.84	1.07	0.77	0.11	2.08	1.27	0.068528
-26.82	2.83	2.09	0.74	0.18	2.08	1.27	0.052716
-10.74	2.12	1.60	0.51	0.11	2.08	1.27	0.105517
-6.79	1.64	1.17	0.47	0.08	2.08	1.27	0.096401
0.13	1.60	1.08	0.52	0.10	2.08	1.27	0.158875
-7.06	0.96	0.48	0.48	0.06	2.08	1.27	0.131043
-1.72	0.84	0.77	0.07	0.06	2.08	1.27	6.149480
-10.59	0.99	0.60	0.38	0.08	2.08	1.27	0.196059
-1.13	0.58	0.41	0.17	0.08	2.08	1.27	2.319066
-16.12	1.90	1.45	0.45	0.10	2.08	1.27	0.212314
-16.01	2.33	1.84	0.49	0.14	2.08	1.27	0.053763
-15.18	2.32	1.86	0.46	0.13	2.08	1.27	0.026469
-18.79	2.86	2.27	0.59	0.21	2.08	1.27	0.025753
-20.04	2.71	2.30	0.41	0.18	2.08	1.27	0.049220

H	U (upper)	U (lower)		u_star	dz	ln(z1/z2)	Ri
124.36	2.91	2.52	0.38	0.22	2.08	1.27	0.282085
142.09	3.18	2.80	0.38	0.24	2.08	1.27	0.109667
121.50	2.53	2.01	0.52	0.17	2.08	1.27	0.174260
126.23	2.66	2.11	0.55	0.14	2.08	1.27	-0.316988
93.95	2.47	2.14	0.33	0.18	2.08	1.27	-1.147435
135.20	3.16	2.74	0.42	0.27	2.08	1.27	-0.680425
113.04	2.67	1.96	0.71	0.18	2.08	1.27	-0.227969
144.02	3.13	2.64	0.49	0.24	2.08	1.27	-0.526717
115.65	2.56	2.14	0.42	0.19	2.08	1.27	-0.737972
142.56	2.13	1.53	0.59	0.21	2.08	1.27	-0.380382
142.86	3.28	2.78	0.50	0.29	2.08	1.27	-0.550345
145.72	3.88	3.10	0.78	0.36	2.08	1.27	-0.216265
178.46	4.81	4.17	0.64	0.43	2.08	1.27	-0.330628
112.65	4.26	3.46	0.81	0.39	2.08	1.27	-0.193068
37.86	1.54	1.27	0.27	0.12	2.08	1.27	-0.260360

57.99	1.28	1.06	0.22	0.10	2.08	1.27	-0.493983
88.03	1.57	1.35	0.21	0.15	2.08	1.27	-0.902355
103.71	2.62	2.29	0.33	0.17	2.08	1.27	-0.495203
130.38	3.51	3.18	0.33	0.25	2.08	1.27	-0.273734
172.97	4.43	3.88	0.55	0.42	2.08	1.27	-0.025702
167.91	3.97	3.21	0.76	0.41	2.08	1.27	-0.059504
183.74	5.13	4.52	0.61	0.48	2.08	1.27	-0.083311
156.31	4.86	4.21	0.65	0.48	2.08	1.27	-0.062019
146.89	5.45	4.39	1.06	0.54	2.08	1.27	-0.019895
88.29	4.94	4.17	0.77	0.49	2.08	1.27	-0.025653
59.58	4.18	3.37	0.81	0.40	2.08	1.27	-0.009562

H	U upper	U lower	dU	u_star			
13.96	4.00	3.20	0.81	0.23	2.21	1.34	-0.072430
14.25	3.82	2.90	0.92	0.22	2.21	1.34	-0.045255
11.82	3.59	2.73	0.86	0.19	2.21	1.34	-0.047116
14.20	3.86	2.89	0.97	0.22	2.21	1.34	-0.039768
11.92	4.01	2.92	1.08	0.18	2.21	1.34	-0.029521
16.68	4.27	3.68	0.59	0.23	2.21	1.34	-0.116436
24.95	4.62	4.02	0.60	0.25	2.21	1.34	-0.117257
18.77	5.32	4.70	0.62	0.23	2.21	1.34	-0.110056
31.39	5.45	4.79	0.65	0.30	2.21	1.34	-0.114734
32.13	6.78	5.44	1.34	0.34	2.21	1.34	-0.025326
26.05	7.78	5.95	1.83	0.40	2.21	1.34	-0.013276
27.70	7.00	5.85	1.16	0.33	2.21	1.34	-0.032102
11.60	6.88	5.83	1.05	0.30	2.21	1.34	-0.039709
19.24	7.14	6.04	1.10	0.32	2.21	1.34	-0.034887
21.54	8.04	6.75	1.29	0.34	2.21	1.34	-0.024621
19.89	7.58	6.50	1.09	0.35	2.21	1.34	-0.029445
27.26	6.85	5.95	0.90	0.36	2.21	1.34	-0.074909
9.31	7.32	6.31	1.02	0.32	2.21	1.34	-0.042586
8.50	6.60	5.73	0.87	0.33	2.21	1.34	-0.042430
5.41	6.15	5.31	0.84	0.34	2.21	1.34	-0.038755
-6.40	5.64	4.88	0.76	0.30	2.21	1.34	-0.010292
-9.64	4.98	4.18	0.80	0.32	2.21	1.34	0.040524
-11.56	4.27	3.50	0.77	0.27	2.21	1.34	0.060254
-10.35	3.60	3.17	0.43	0.25	2.21	1.34	0.139421
-8.23	2.98	2.67	0.31	0.21	2.21	1.34	0.208944
-7.78	2.70	2.41	0.29	0.18	2.21	1.34	0.186331
-10.83	3.51	3.16	0.35	0.25	2.21	1.34	0.310593
-9.16	2.36	2.12	0.24	0.15	2.21	1.34	0.747664
-11.33	2.26	2.00	0.25	0.21	2.21	1.34	0.665399
-7.09	1.84	1.25	0.60	0.16	2.21	1.34	0.106479
-6.02	1.56	0.76	0.80	0.10	2.21	1.34	0.040543
-7.26	1.64	0.59	1.05	0.11	2.21	1.34	0.015920
-7.52	2.03	1.11	0.92	0.17	2.21	1.34	0.028138
-6.61	1.52	0.46	1.06	0.08	2.21	1.34	0.012169
-4.47	1.40	0.36	1.03	0.07	2.21	1.34	0.001041
-4.59	1.13	0.25	0.88	0.07	2.21	1.34	0.005809
-3.97	0.99	0.26	0.73	0.07	2.21	1.34	0.006695
-5.79	1.21	0.28	0.93	0.08	2.21	1.34	0.003267

-4.21	0.96	0.25	0.71	0.08	2.21	1.34	0.013664
-3.01	0.82	0.59	0.22	0.04	2.21	1.34	-0.096479
-1.91	1.32	1.01	0.31	0.08	2.21	1.34	-0.242851
-0.10	0.29	0.23	0.06	0.05	2.21	1.34	-2.095735
-3.51	0.90	0.59	0.31	0.05	2.21	1.34	0.030296
-4.72	0.88	0.64	0.24	0.11	2.21	1.34	0.740230
-8.42	1.69	0.41	1.28	0.11	2.21	1.34	0.018672
-6.97	1.59	0.52	1.07	0.11	2.21	1.34	0.015352
-8.28	1.93	0.42	1.51	0.10	2.21	1.34	0.004894
-7.66	2.06	0.58	1.48	0.10	2.21	1.34	0.001560
-7.99	1.87	0.45	1.42	0.10	2.21	1.34	0.001850
-8.04	2.11	0.79	1.32	0.08	2.21	1.34	-0.004802
-12.13	2.15	1.06	1.09	0.11	2.21	1.34	-0.005129
-9.32	2.32	1.17	1.15	0.10	2.21	1.34	-0.002133
-10.81	2.08	0.94	1.14	0.08	2.21	1.34	-0.002974
-4.29	1.47	0.51	0.96	0.07	2.21	1.34	-0.017446
-9.39	1.71	0.71	1.00	0.09	2.21	1.34	-0.002021
-6.22	1.32	0.58	0.74	0.09	2.21	1.34	0.028019
-7.24	1.38	0.24	1.14	0.08	2.21	1.34	0.011361
-6.65	1.24	0.22	1.02	0.09	2.21	1.34	0.011896
-9.74	1.75	0.54	1.22	0.10	2.21	1.34	0.008295
-8.13	1.25	0.34	0.91	0.08	2.21	1.34	0.008579
-7.29	0.30	0.22	0.08	0.08	2.21	1.34	0.842635
1.51	0.21	0.20	0.01	0.07	2.21	1.34	86.645290
-3.04	1.21	0.34	0.87	0.08	2.21	1.34	0.040102
-4.29	1.70	0.46	1.25	0.12	2.21	1.34	0.018481
0.25	1.82	0.62	1.20	0.11	2.21	1.34	0.014331
2.67	2.04	0.84	1.21	0.08	2.21	1.34	0.007718
13.55	2.15	0.72	1.43	0.11	2.21	1.34	0.009248
23.66	2.38	0.78	1.60	0.15	2.21	1.34	0.002834
38.79	3.27	2.59	0.68	0.24	2.21	1.34	-0.049196
56.12	3.81	2.86	0.95	0.27	2.21	1.34	-0.062358
69.17	3.88	3.22	0.66	0.28	2.21	1.34	-0.070464
71.98	3.63	3.06	0.57	0.23	2.21	1.34	-0.071876
49.42	2.96	2.50	0.45	0.27	2.21	1.34	-0.103100
73.17	2.68	2.24	0.44	0.23	2.21	1.34	-0.244544
76.32	2.45	2.03	0.42	0.23	2.21	1.34	-0.303653
80.46	2.80	2.40	0.40	0.25	2.21	1.34	-0.397869
70.53	3.21	2.77	0.44	0.26	2.21	1.34	-0.273728
78.80	1.19	0.88	0.31	0.14	2.21	1.34	-1.402091
26.51	1.08	0.88	0.20	0.14	2.21	1.34	-9.539495
48.85	2.28	1.91	0.37	0.22	2.21	1.34	-1.048695
76.90	3.37	2.86	0.50	0.18	2.21	1.34	-0.098734
43.66	3.17	2.70	0.47	0.27	2.21	1.34	-0.124383
-29.14	2.46	2.02	0.44	0.35	2.21	1.34	-0.837997
36.89	2.80	2.72	0.08	0.19	2.21	1.34	-24.477583
22.74	2.91	2.40	0.50	0.20	2.21	1.34	-0.498594
27.67	3.04	2.01	1.04	0.27	2.21	1.34	-0.065795
21.17	3.16	2.17	0.98	0.21	2.21	1.34	-0.068195
17.10	2.93	2.61	0.32	0.18	2.21	1.34	-0.732747
20.47	3.18	2.43	0.75	0.25	2.21	1.34	-0.101743
7.74	2.90	2.34	0.56	0.21	2.21	1.34	-0.165636

-5.71	3.69	2.55	1.14	0.22	2.21	1.34	-0.023390
-4.76	3.84	3.01	0.83	0.24	2.21	1.34	-0.045941
-6.43	3.70	3.16	0.55	0.22	2.21	1.34	-0.099320
-11.19	4.02	2.71	1.32	0.26	2.21	1.34	-0.010234
-11.35	3.47	2.11	1.36	0.25	2.21	1.34	-0.007827
-10.37	2.35	1.47	0.88	0.16	2.21	1.34	-0.012786
-5.35	1.97	2.03	-0.05	0.17	2.21	1.34	-9.699864
-10.34	1.70	1.53	0.17	0.14	2.21	1.34	-0.354349
-14.01	2.28	1.41	0.87	0.17	2.21	1.34	0.051416
-34.43	3.19	2.14	1.06	0.23	2.21	1.34	0.006495
-30.82	3.08	2.37	0.71	0.23	2.21	1.34	-0.042251
-44.97	3.42	2.16	1.26	0.27	2.21	1.34	-0.010802
-36.93	3.29	1.96	1.33	0.26	2.21	1.34	0.000916
-23.16	2.33	0.84	1.50	0.18	2.21	1.34	-0.010054
-23.68	2.34	0.77	1.57	0.17	2.21	1.34	-0.011120
-21.78	2.44	1.37	1.07	0.16	2.21	1.34	-0.020985
-26.76	2.69	1.23	1.46	0.18	2.21	1.34	-0.009137
-21.83	2.41	1.83	0.58	0.16	2.21	1.34	-0.067487
-23.39	2.95	2.47	0.48	0.17	2.21	1.34	-0.075576
-16.01	3.03	2.17	0.86	0.09	2.21	1.34	-0.021257
-19.35	2.60	1.64	0.96	0.13	2.21	1.34	-0.007752
-17.97	2.39	1.84	0.56	0.12	2.21	1.34	-0.014482
-14.03	1.49	1.20	0.29	0.13	2.21	1.34	-0.162788
-4.06	1.76	1.23	0.53	0.10	2.21	1.34	-0.069049
-4.06	2.03	1.49	0.54	0.15	2.21	1.34	-0.025550
-5.12	1.98	1.44	0.54	0.13	2.21	1.34	0.026586
-7.81	2.64	2.04	0.61	0.16	2.21	1.34	0.045701
-8.67	2.35	1.74	0.61	0.15	2.21	1.34	0.062983
-6.64	1.75	1.22	0.53	0.10	2.21	1.34	0.068482
-5.78	2.21	1.62	0.59	0.12	2.21	1.34	0.057901
-5.81	3.00	2.28	0.71	0.14	2.21	1.34	0.041865
-5.59	2.28	1.71	0.57	0.13	2.21	1.34	0.048480
-4.42	2.07	1.47	0.59	0.11	2.21	1.34	0.038198
-6.48	2.92	2.18	0.74	0.17	2.21	1.34	0.029271
-2.81	3.51	2.78	0.73	0.18	2.21	1.34	0.028192
-1.53	4.26	3.35	0.91	0.21	2.21	1.34	0.007215
-1.22	4.02	3.18	0.84	0.22	2.21	1.34	0.012225
-3.52	3.47	2.63	0.84	0.18	2.21	1.34	0.018382
-11.65	3.19	2.55	0.64	0.20	2.21	1.34	0.067463
-5.27	2.30	1.76	0.53	0.14	2.21	1.34	0.075940
-6.74	1.30	0.87	0.42	0.08	2.21	1.34	0.079535
-4.06	2.06	1.45	0.60	0.11	2.21	1.34	0.019807
-4.82	1.99	1.44	0.56	0.13	2.21	1.34	0.036977
-2.58	1.85	1.29	0.56	0.13	2.21	1.34	0.051003
-2.40	1.57	1.06	0.51	0.09	2.21	1.34	0.081712
-4.34	1.18	0.79	0.40	0.12	2.21	1.34	0.283030
-9.72	3.37	2.58	0.79	0.19	2.21	1.34	0.117146
-1.49	4.83	3.69	1.14	0.19	2.21	1.34	0.039209
3.96	6.20	4.84	1.36	0.24	2.21	1.34	0.016240
14.39	6.74	5.19	1.55	0.25	2.21	1.34	0.007990
24.98	6.95	5.23	1.72	0.29	2.21	1.34	0.004547
30.69	7.86	5.95	1.91	0.29	2.21	1.34	0.003715

40.00	7.83	5.98	1.85	0.25	2.21	1.34	0.004140
56.63	7.35	5.81	1.54	0.23	2.21	1.34	0.007561
69.14	6.48	4.90	1.57	0.26	2.21	1.34	0.008694
66.44	8.32	5.36	2.96	0.47	2.21	1.34	0.002967
57.12	8.02	6.07	1.96	0.34	2.21	1.34	0.005626
12.08	7.25	4.19	3.06	0.45	2.21	1.34	-0.000161
-2.84	6.90	5.10	1.80	0.33	2.21	1.34	-0.010406
53.79	7.65	5.99	1.66	0.46	2.21	1.34	-0.011331
59.67	8.06	6.66	1.40	0.47	2.21	1.34	-0.005622
33.13	7.24	6.02	1.22	0.50	2.21	1.34	-0.009844
55.58	7.75	6.75	1.00	0.43	2.21	1.34	0.010679
92.98	7.13	6.32	0.81	0.46	2.21	1.34	-0.008022
69.13	8.00	7.18	0.82	0.48	2.21	1.34	-0.042736

H	U (upper)	U (lower)	dU	u_star	dz	ln(z1/z2)	Ri
99.36	4.24	3.70	0.55	0.33	2.11	1.24	0.061791
104.27	3.70	3.02	0.68	0.37	2.11	1.24	-0.020635
193.75	4.32	3.26	1.06	0.59	2.11	1.24	-0.010496
210.08	4.24	3.41	0.82	0.60	2.11	1.24	-0.021697
229.07	4.56	3.73	0.83	0.64	2.11	1.24	-0.017909
230.81	4.69	3.74	0.95	0.62	2.11	1.24	-0.028950
200.32	4.59	3.80	0.79	0.67	2.11	1.24	-0.047869
186.61	4.04	3.35	0.70	0.54	2.11	1.24	-0.067143
166.91	4.24	3.37	0.87	0.54	2.11	1.24	-0.035613
163.34	3.82	3.09	0.73	0.51	2.11	1.24	-0.058636
118.13	4.19	3.39	0.79	0.52	2.11	1.24	-0.044983
117.21	3.91	3.13	0.78	0.53	2.11	1.24	-0.038606
120.50	4.86	3.52	1.33	0.69	2.11	1.24	-0.009929
98.40	4.56	3.43	1.12	0.62	2.11	1.24	-0.008841
83.05	5.10	3.83	1.27	0.64	2.11	1.24	-0.005374
61.53	5.03	3.88	1.15	0.62	2.11	1.24	-0.002244
54.41	4.99	3.83	1.16	0.54	2.11	1.24	-0.001623
45.65	4.90	3.71	1.20	0.56	2.11	1.24	-0.000706
24.26	4.92	3.86	1.06	0.55	2.11	1.24	0.001275
14.65	4.92	3.89	1.04	0.49	2.11	1.24	0.002190
9.91	4.83	3.74	1.09	0.49	2.11	1.24	0.002626
2.96	4.64	3.68	0.96	0.45	2.11	1.24	0.004286
41.48	1.00	0.73	0.27	0.19	2.11	1.24	-0.224691
42.66	1.42	1.13	0.29	0.18	2.11	1.24	-0.094053
54.15	2.58	2.12	0.46	0.24	2.11	1.24	-0.073842
61.86	1.94	1.55	0.39	0.23	2.11	1.24	-0.090766
67.34	1.08	0.72	0.36	0.17	2.11	1.24	-0.186414
126.75	2.05	1.67	0.39	0.20	2.11	1.24	-0.152193
87.39	2.39	1.99	0.40	0.21	2.11	1.24	-0.142293
89.25	1.76	1.35	0.41	0.18	2.11	1.24	-0.190543
89.97	2.13	1.54	0.59	0.18	2.11	1.24	-0.090934
122.37	1.98	1.64	0.34	0.26	2.11	1.24	-0.434416
140.76	2.05	1.73	0.32	0.41	2.11	1.24	-0.346305
84.46	2.86	2.39	0.47	0.22	2.11	1.24	-0.076310
122.81	3.43	2.86	0.57	0.31	2.11	1.24	-0.059420
121.34	4.53	3.84	0.68	0.33	2.11	1.24	-0.038737

64.16	5.40	4.71	0.69	0.27	2.11	1.24	-0.031029
70.44	4.17	3.66	0.52	0.28	2.11	1.24	-0.049062
69.40	3.88	3.36	0.53	0.27	2.11	1.24	-0.041624
50.59	4.31	3.72	0.59	0.28	2.11	1.24	-0.021872
33.67	4.06	3.46	0.60	0.25	2.11	1.24	-0.017422
30.62	4.22	3.66	0.56	0.29	2.11	1.24	-0.015453
40.52	3.82	3.38	0.44	0.28	2.11	1.24	-0.033583
-20.84	2.92	2.56	0.36	0.15	2.11	1.24	0.183533
-18.88	1.23	0.75	0.48	0.15	2.11	1.24	0.101165
7.49	2.35	1.93	0.42	0.13	2.11	1.24	0.133435
107.40	0.83	0.73	0.10	0.18	2.11	1.24	4.812467
-17.48	1.15	0.79	0.37	0.11	2.11	1.24	0.257744
-17.44	1.35	1.02	0.33	0.17	2.11	1.24	0.318563
-20.20	2.34	1.85	0.49	0.13	2.11	1.24	0.181308
-8.70	1.85	1.45	0.39	0.08	2.11	1.24	0.241605
-10.02	0.99	0.53	0.46	0.08	2.11	1.24	0.181182
-5.26	1.35	1.02	0.33	0.05	2.11	1.24	0.417305
-2.98	1.02	0.63	0.39	0.06	2.11	1.24	0.309134
3.06	0.91	0.56	0.34	0.05	2.11	1.24	0.394942
-5.78	0.42	0.12	0.30	0.07	2.11	1.24	0.949326
-1.39	0.43	0.12	0.31	0.02	2.11	1.24	0.598721
-2.26	0.91	0.61	0.30	0.04	2.11	1.24	0.459099
-3.76	1.44	1.14	0.30	0.04	2.11	1.24	0.555396
-9.40	1.45	1.11	0.34	0.08	2.11	1.24	0.373688
-24.07	1.54	1.17	0.38	0.19	2.11	1.24	0.268461
-23.82	2.31	1.69	0.61	0.21	2.11	1.24	0.061118
-21.44	2.10	1.37	0.74	0.23	2.11	1.24	0.036394
-23.63	2.36	1.48	0.88	0.24	2.11	1.24	0.024831
-50.41	3.18	2.20	0.98	0.40	2.11	1.24	0.021012
-26.16	3.77	2.87	0.91	0.31	2.11	1.24	0.019017
-26.18	3.44	2.44	1.01	0.34	2.11	1.24	0.013664
-27.18	3.63	2.51	1.12	0.33	2.11	1.24	0.009351
-27.99	3.98	2.75	1.22	0.37	2.11	1.24	0.007329
-19.00	3.94	2.49	1.45	0.39	2.11	1.24	0.004164
-19.52	3.93	1.96	1.97	0.29	2.11	1.24	0.002284
-24.35	3.69	2.18	1.51	0.32	2.11	1.24	0.004872
-21.40	3.90	2.42	1.48	0.31	2.11	1.24	0.005192
-20.17	4.60	2.86	1.74	0.32	2.11	1.24	0.002901
-14.93	3.92	2.57	1.35	0.30	2.11	1.24	0.005919
-7.16	3.54	2.35	1.19	0.22	2.11	1.24	0.005051
-5.54	2.96	1.78	1.18	0.23	2.11	1.24	0.004544
9.62	3.63	2.12	1.52	0.44	2.11	1.24	0.003599
17.07	4.83	2.48	2.35	0.49	2.11	1.24	0.001113
30.42	5.30	2.54	2.77	0.58	2.11	1.24	0.000268
66.25	4.15	2.07	2.08	0.79	2.11	1.24	-0.001295
105.58	5.32	2.44	2.88	0.84	2.11	1.24	-0.001088
115.85	5.84	2.81	3.03	0.78	2.11	1.24	-0.001375
130.91	4.68	2.16	2.52	0.79	2.11	1.24	-0.002470
168.82	4.92	2.88	2.04	0.87	2.11	1.24	-0.006102
147.24	5.17	2.88	2.29	0.67	2.11	1.24	-0.007400
175.15	4.26	2.62	1.63	0.71	2.11	1.24	-0.011136

175.27	4.62	2.83	1.78	0.74	2.11	1.24	-0.008236
186.11	5.42	3.81	1.61	0.73	2.11	1.24	-0.008145
221.75	4.85	3.28	1.57	0.70	2.11	1.24	-0.001506
229.05	4.60	2.63	1.97	0.76	2.11	1.24	-0.003668
224.62	4.78	2.67	2.12	0.78	2.11	1.24	-0.001428
164.33	4.80	2.84	1.96	0.58	2.11	1.24	-0.000311
118.56	3.57	2.11	1.45	0.33	2.11	1.24	0.000981
115.92	2.89	2.07	0.82	0.26	2.11	1.24	-0.007033
228.61	2.55	1.66	0.89	0.51	2.11	1.24	-0.005188
135.22	2.98	1.65	1.33	0.28	2.11	1.24	-0.003302
159.53	3.50	2.47	1.04	0.36	2.11	1.24	0.001647
223.82	3.22	2.02	1.20	0.61	2.11	1.24	0.000162
371.27	4.26	3.09	1.17	0.95	2.11	1.24	0.003455
347.88	6.28	4.75	1.53	1.03	2.11	1.24	0.015442
330.15	6.57	4.96	1.61	0.99	2.11	1.24	0.010518
237.24	5.86	4.54	1.31	0.88	2.11	1.24	0.006270
242.45	5.59	4.29	1.30	0.85	2.11	1.24	0.010649
229.05	5.73	4.35	1.38	0.82	2.11	1.24	0.006569
14.53	2.46	2.21	0.25	0.08	2.11	1.24	-0.160753
55.00	1.78	1.67	0.11	0.22	2.11	1.24	0.559929
65.51	3.36	2.94	0.42	0.28	2.11	1.24	0.017930
80.77	3.11	2.74	0.37	0.30	2.11	1.24	-0.082225
91.69	2.51	2.18	0.32	0.30	2.11	1.24	-0.166376
84.66	3.20	2.81	0.39	0.22	2.11	1.24	-0.098068
97.24	4.32	3.85	0.48	0.33	2.11	1.24	-0.075367
91.10	5.41	4.82	0.59	0.33	2.11	1.24	-0.044932
126.46	4.95	4.46	0.49	0.39	2.11	1.24	-0.060911

H	U (upper)	U (lower)	dU	u_star	dz	ln(z1/z2)	Ri
1.71	4.52	3.73	0.79	0.22	2.11	1.33	0.014378
3.58	4.47	3.62	0.84	0.32	2.11	1.33	0.016087
0.97	6.51	5.29	1.22	0.30	2.11	1.33	0.008526
-1.65	4.73	3.91	0.82	0.36	2.11	1.33	0.019678
-0.88	5.86	4.89	0.97	0.28	2.11	1.33	0.001694
-0.10	4.69	3.86	0.83	0.37	2.11	1.33	0.002278
-3.44	5.00	4.17	0.83	0.34	2.11	1.33	0.004543
-3.43	4.82	3.96	0.86	0.29	2.11	1.33	0.005654
-5.84	5.56	4.64	0.91	0.30	2.11	1.33	0.006172
-9.56	6.27	5.23	1.04	0.34	2.11	1.33	0.005578
-14.71	5.88	4.82	1.06	0.38	2.11	1.33	0.005741
-12.17	6.30	5.11	1.19	0.30	2.11	1.33	0.005209
-15.22	5.54	4.51	1.03	0.33	2.11	1.33	0.008665
-15.03	5.99	4.86	1.13	0.28	2.11	1.33	0.008912
-20.74	6.10	4.91	1.19	0.33	2.11	1.33	0.008381
-19.55	5.85	4.65	1.19	0.29	2.11	1.33	0.009119
-18.86	6.26	4.96	1.30	0.29	2.11	1.33	0.007455
-18.37	5.82	4.67	1.15	0.23	2.11	1.33	0.012297
-21.59	6.03	4.82	1.21	0.32	2.11	1.33	0.010935
-21.26	6.09	4.94	1.15	0.30	2.11	1.33	0.010464

-21.49	5.25	4.27	0.98	0.31	2.11	1.33	0.009656
-18.12	4.68	3.78	0.90	0.26	2.11	1.33	0.013010
-24.34	4.98	4.06	0.92	0.27	2.11	1.33	0.010604
-18.09	4.31	3.47	0.84	0.23	2.11	1.33	0.009114
-16.99	3.93	3.13	0.80	0.21	2.11	1.33	0.009808
-13.47	4.15	3.33	0.82	0.22	2.11	1.33	0.011161
-19.98	4.35	3.51	0.83	0.22	2.11	1.33	0.008129
-23.79	4.42	3.55	0.87	0.24	2.11	1.33	0.005116
16.99	3.20	2.70	0.51	0.13	2.11	1.33	-0.038017
23.97	3.52	2.85	0.67	0.15	2.11	1.33	-0.036825
32.80	4.25	3.39	0.85	0.24	2.11	1.33	-0.005383
29.14	4.17	3.28	0.89	0.21	2.11	1.33	-0.011161
34.46	4.35	3.46	0.89	0.24	2.11	1.33	-0.012343
38.98	3.35	2.70	0.65	0.13	2.11	1.33	-0.008039
38.82	3.29	2.65	0.64	0.18	2.11	1.33	-0.040859
55.02	2.92	2.31	0.61	0.16	2.11	1.33	-0.034213
51.93	2.44	1.96	0.47	0.27	2.11	1.33	-0.089227
41.41	2.44	2.08	0.36	0.19	2.11	1.33	-0.167171
47.67	2.73	2.24	0.49	0.23	2.11	1.33	-0.052074
47.87	2.91	2.53	0.38	0.16	2.11	1.33	-0.148394
44.79	3.25	2.72	0.53	0.22	2.11	1.33	-0.087078
38.57	4.21	3.78	0.43	0.19	2.11	1.33	-0.097935
-1.25	3.76	3.42	0.34	0.27	2.11	1.33	-0.101557
-2.24	4.14	3.61	0.53	0.24	2.11	1.33	-0.024382
-4.08	3.43	3.00	0.42	0.30	2.11	1.33	0.076370
-7.32	2.68	2.35	0.33	0.29	2.11	1.33	0.094869
-15.13	2.55	2.20	0.35	0.16	2.11	1.33	0.135525
-13.61	2.50	2.17	0.33	0.12	2.11	1.33	0.147491
-15.54	2.93	2.64	0.29	0.18	2.11	1.33	0.212528
-18.65	3.23	2.91	0.32	0.19	2.11	1.33	0.213089
-23.05	3.15	2.86	0.29	0.24	2.11	1.33	0.287837
-24.50	3.33	3.03	0.30	0.20	2.11	1.33	0.263996
-19.97	4.44	3.98	0.46	0.20	2.11	1.33	0.111264
-29.40	4.93	4.39	0.54	0.26	2.11	1.33	0.072078
-24.75	4.42	3.94	0.48	0.25	2.11	1.33	0.055896
-20.28	4.17	3.75	0.42	0.19	2.11	1.33	0.106658
-28.68	4.14	3.56	0.58	0.23	2.11	1.33	0.051641
-25.10	4.70	4.07	0.62	0.22	2.11	1.33	0.037024
-29.10	4.90	4.20	0.70	0.26	2.11	1.33	0.024758
-28.95	4.53	4.00	0.53	0.28	2.11	1.33	0.055311
-20.62	3.56	3.16	0.40	0.19	2.11	1.33	0.108006
-17.66	2.71	2.45	0.26	0.19	2.11	1.33	0.236737
-12.83	2.46	2.28	0.18	0.13	2.11	1.33	0.618898
-10.18	2.49	2.25	0.24	0.13	2.11	1.33	0.321701
-12.84	3.13	2.81	0.31	0.17	2.11	1.33	0.140649
-18.65	3.41	3.04	0.37	0.19	2.11	1.33	0.085852
-18.70	2.84	2.55	0.28	0.19	2.11	1.33	0.172184
-16.24	3.07	2.73	0.34	0.16	2.11	1.33	0.140464
-16.49	3.29	2.99	0.30	0.19	2.11	1.33	0.168439
-15.36	3.42	2.94	0.48	0.20	2.11	1.33	0.063035

-19.31	3.67	3.24	0.43	0.21	2.11	1.33	0.088652
-18.50	3.62	3.21	0.41	0.19	2.11	1.33	0.088497
-15.73	3.52	3.11	0.41	0.18	2.11	1.33	0.097996
-16.73	3.37	3.01	0.36	0.20	2.11	1.33	0.135334
-16.81	3.34	2.97	0.37	0.18	2.11	1.33	0.137266
-16.32	3.28	2.95	0.33	0.20	2.11	1.33	0.174968
-16.35	3.39	3.02	0.37	0.20	2.11	1.33	0.124065
-18.35	3.69	3.24	0.45	0.19	2.11	1.33	0.099468
-22.99	3.27	2.81	0.47	0.19	2.11	1.33	0.086837
-17.63	3.65	3.16	0.49	0.16	2.11	1.33	0.085342
-20.16	4.09	3.61	0.48	0.20	2.11	1.33	0.079683
-21.74	4.58	4.04	0.54	0.20	2.11	1.33	0.050578
-21.30	5.02	4.43	0.59	0.23	2.11	1.33	0.038058
-19.47	4.76	4.21	0.55	0.21	2.11	1.33	0.045884
-17.83	4.59	4.03	0.56	0.23	2.11	1.33	0.043668
-19.32	4.51	3.95	0.56	0.23	2.11	1.33	0.034643
-22.53	4.25	3.76	0.49	0.28	2.11	1.33	0.051976
-21.06	4.46	3.88	0.58	0.22	2.11	1.33	0.040932
-24.08	4.55	3.99	0.56	0.26	2.11	1.33	0.040960
-18.41	4.80	4.21	0.59	0.23	2.11	1.33	0.034486
-18.81	4.96	4.30	0.67	0.26	2.11	1.33	0.020667
-11.83	4.39	3.73	0.66	0.23	2.11	1.33	0.016192
-12.16	5.07	4.13	0.93	0.22	2.11	1.33	0.008933
-8.87	4.90	4.00	0.90	0.25	2.11	1.33	0.008371
1.72	5.86	4.81	1.05	0.25	2.11	1.33	-0.001916
8.61	5.42	4.49	0.93	0.31	2.11	1.33	-0.004914
12.44	4.65	3.86	0.79	0.27	2.11	1.33	-0.012073
12.49	4.43	3.61	0.82	0.24	2.11	1.33	-0.018376
22.78	3.49	2.87	0.62	0.24	2.11	1.33	-0.051480
25.83	3.22	2.65	0.57	0.25	2.11	1.33	-0.058440
18.65	2.66	2.17	0.50	0.18	2.11	1.33	-0.046062
28.46	3.43	2.85	0.58	0.20	2.11	1.33	-0.039891
20.38	3.91	3.19	0.71	0.20	2.11	1.33	-0.013427
37.43	4.08	3.32	0.76	0.23	2.11	1.33	-0.031403
38.78	3.91	3.25	0.66	0.24	2.11	1.33	-0.051245
53.58	3.86	3.23	0.64	0.28	2.11	1.33	-0.066625
63.85	3.69	3.08	0.61	0.28	2.11	1.33	-0.123294
47.26	3.93	3.24	0.69	0.25	2.11	1.33	-0.077662
19.15	3.68	3.10	0.58	0.28	2.11	1.33	-0.038358
10.00	3.75	3.10	0.65	0.25	2.11	1.33	-0.009768

	abs(Ri)	L	z/L	abs(z/L)	phi M	phi H	phi W
0.342604	0.22	-3.80	-0.53	0.53	1.08	0.67	-0.01
0.415718	0.58	-2.05	-0.98	0.98	0.89	0.64	0.09
0.622527	0.45	-8.05	-0.25	0.25	0.60	0.88	0.18
0.432960	0.55	-5.68	-0.35	0.35	0.86	1.52	0.17
0.425847	1.01	-3.09	-0.65	0.65	0.87	1.52	0.09
0.387258	0.74	-2.77	-0.72	0.72	0.96	1.24	0.11
0.534001	0.64	-4.08	-0.49	0.49	0.70	0.79	0.13
0.707579	0.80	-5.56	-0.36	0.36	0.52	0.76	0.13
0.967964	1.28	-6.39	-0.31	0.31	0.38	0.74	0.14
0.546813	0.13	-3.17	-0.63	0.63	0.68	0.12	0.05
1.877751	1.16	-3.03	-0.66	0.66	0.20	0.08	0.04
0.693762	1.96	-1.84	-1.09	1.09	0.54	-0.75	-0.01
0.648837	2.34	-0.75	-2.66	2.66	0.57	-0.40	-0.02
0.597581	0.25	-1.46	-1.37	1.37	0.62	-0.09	0.04
2.838298	10.84	-6.05	-0.33	0.33	0.13	-0.79	-0.03
0.910243	0.93	-20.61	-0.10	0.10	0.41	-3.39	-0.09
0.308612	0.06	-7.77	-0.26	0.26	1.20	-0.55	-0.09

	abs(Ri)	L	z/L	abs(z/L)	phi M	phi H	phi W
0.143127	0.07	9.56	0.21	0.21	2.29	1.72	1.39
0.249917	0.05	22.15	0.09	0.09	1.31	1.05	1.14
0.216034	0.11	13.05	0.15	0.15	1.52	1.53	1.28
0.177280	0.10	7.52	0.27	0.27	1.85	1.37	3.31
0.202620	0.16	-32.14	-0.06	0.06	1.62	-191.03	1.14
0.135915	0.13	3.45	0.58	0.58	2.41	1.45	2.16
0.902837	6.15	10.38	0.19	0.19	0.36	4.67	7.17
0.209949	0.20	5.07	0.39	0.39	1.56	1.16	1.06
0.495800	2.32	104.08	0.02	0.02	0.66	25.78	2.72
0.231560	0.21	6.61	0.30	0.30	1.42	1.43	0.91
0.292494	0.05	18.12	0.11	0.11	1.12	0.62	1.31
0.305706	0.03	17.12	0.12	0.12	1.07	0.27	1.10
0.360317	0.03	50.82	0.04	0.04	0.91	0.54	1.06
0.455984	0.05	30.19	0.07	0.07	0.72	0.41	0.99

					phi M	phi H	phi W
0.592435	0.28	-6.67	-0.30	0.30	0.55	-0.40	0.62
0.666558	0.11	-8.03	-0.25	0.25	0.49	-0.15	0.52
0.334365	0.17	-3.06	-0.65	0.65	0.98	-0.36	0.39
0.272625	0.32	-1.92	-1.04	1.04	1.20	0.62	0.21
0.573692	1.15	-5.27	-0.38	0.38	0.57	1.39	0.04
0.664415	0.68	-11.45	-0.17	0.17	0.49	1.32	0.42
0.257858	0.23	-3.91	-0.51	0.51	1.27	1.02	0.26
0.500620	0.53	-7.50	-0.27	0.27	0.65	1.16	0.39
0.464016	0.74	-4.70	-0.43	0.43	0.71	1.20	0.32
0.361009	0.38	-4.99	-0.40	0.40	0.91	1.08	0.26
0.602888	0.55	-13.92	-0.14	0.14	0.54	1.56	0.46
0.481097	0.22	-26.30	-0.08	0.08	0.68	1.81	0.88
0.702731	0.33	-37.98	-0.05	0.05	0.47	1.84	0.54
0.508719	0.19	-44.33	-0.05	0.05	0.64	2.44	0.42
0.445708	0.26	-3.36	-0.60	0.60	0.74	0.33	1.05

0.488424	0.49	-1.48	-1.35	1.35	0.67	0.23	0.48
0.733419	0.90	-2.98	-0.67	0.67	0.45	0.37	0.49
0.530967	0.50	-3.77	-0.53	0.53	0.62	0.49	0.78
0.789413	0.27	-10.28	-0.19	0.19	0.42	0.33	1.19
0.795669	0.03	-36.89	-0.05	0.05	0.41	0.11	1.09
0.565140	0.06	-35.36	-0.06	0.06	0.58	0.47	1.20
0.821019	0.08	-52.12	-0.04	0.04	0.40	0.45	1.19
0.769993	0.06	-60.58	-0.03	0.03	0.43	0.44	1.17
0.529008	0.02	-91.43	-0.02	0.02	0.62	0.46	1.20
0.661231	0.03	-113.00	-0.02	0.02	0.50	0.46	2.12
0.519489	0.01	-94.23	-0.02	0.02	0.63	0.23	2.35
0.312552	0.07	-63.96	-0.03	0.03	1.06	3.71	1.83
0.261528	0.05	-55.15	-0.04	0.04	1.26	2.84	-0.03
0.246542	0.05	-45.11	-0.04	0.04	1.34	2.76	-0.15
0.250369	0.04	-54.93	-0.04	0.04	1.32	2.76	-0.12
0.184279	0.03	-37.91	-0.05	0.05	1.79	2.54	-0.32
0.430670	0.12	-54.83	-0.04	0.04	0.77	2.65	0.34
0.460651	0.12	-49.12	-0.04	0.04	0.72	2.05	0.13
0.413933	0.11	-51.62	-0.04	0.04	0.80	2.49	0.63
0.502209	0.11	-65.99	-0.03	0.03	0.66	2.26	0.55
0.278076	0.03	-94.84	-0.02	0.02	1.19	2.32	0.99
0.238730	0.01	-185.54	-0.01	0.01	1.38	3.27	1.84
0.319078	0.03	-108.30	-0.02	0.02	1.04	2.51	1.80
0.311444	0.04	-164.21	-0.01	0.01	1.06	5.45	1.29
0.316831	0.03	-130.39	-0.02	0.02	1.04	3.35	2.08
0.291692	0.02	-149.01	-0.01	0.01	1.13	3.14	2.33
0.358339	0.03	-177.37	-0.01	0.01	0.92	2.98	2.29
0.447015	0.07	-143.60	-0.01	0.01	0.74	3.87	1.23
0.347733	0.04	-284.70	-0.01	0.01	0.95	7.36	2.41
0.415333	0.04	-343.32	-0.01	0.01	0.80	6.09	4.24
0.451980	0.04	-612.40	0.00	0.00	0.73	8.33	3.47
0.431840	0.01	339.56	0.01	0.01	0.77	-1.33	-2.48
0.439993	0.04	285.64	0.01	0.01	0.75	4.13	0.32
0.385465	0.06	141.38	0.01	0.01	0.86	3.98	3.19
0.636313	0.14	120.29	0.02	0.02	0.52	2.97	-2.11
0.756937	0.21	91.53	0.02	0.02	0.44	2.45	0.21
0.679909	0.19	60.02	0.03	0.03	0.49	1.73	-0.70
0.785434	0.31	117.62	0.02	0.02	0.42	4.31	-0.61
0.714214	0.75	31.47	0.06	0.06	0.46	3.38	0.23
0.904718	0.67	61.46	0.03	0.03	0.37	3.73	1.56
0.298863	0.11	47.76	0.04	0.04	1.11	4.18	2.32
0.144590	0.04	15.83	0.13	0.13	2.28	2.16	5.48
0.114605	0.02	14.66	0.14	0.14	2.88	1.27	3.05
0.198352	0.03	50.27	0.04	0.04	1.67	2.54	5.03
0.086508	0.01	6.95	0.29	0.29	3.82	0.82	1.76
0.079175	0.00	7.41	0.27	0.27	4.17	0.09	2.09
0.083298	0.01	5.08	0.39	0.39	3.97	0.31	1.55
0.108925	0.01	7.42	0.27	0.27	3.03	0.31	1.37
0.096694	0.00	7.27	0.27	0.27	3.42	0.19	0.73

0.117741	0.01	8.17	0.24	0.24	2.81	0.60	0.62
0.208203	0.10	1.94	1.03	1.03	1.59	-0.32	0.80
0.279527	0.24	18.94	0.11	0.11	1.18	-4.85	0.76
0.919336	2.10	-11.87	-0.17	0.17	0.36	-22.24	0.02
0.188852	0.03	3.12	0.64	0.64	1.75	0.21	-0.02
0.499814	0.74	23.74	0.08	0.08	0.66	4.76	844.48
0.098782	0.02	14.83	0.13	0.13	3.34	1.99	-1.42
0.115920	0.02	16.88	0.12	0.12	2.85	1.36	-1.17
0.069810	0.00	8.65	0.23	0.23	4.73	0.62	1.42
0.071360	0.00	9.51	0.21	0.21	4.63	0.21	3.37
0.077082	0.00	9.97	0.20	0.20	4.29	0.22	2.37
0.068002	0.00	5.51	0.36	0.36	4.86	-0.41	1.10
0.107264	0.01	8.02	0.25	0.25	3.08	-0.26	0.44
0.095562	0.00	8.73	0.23	0.23	3.46	-0.15	0.68
0.079686	0.00	4.18	0.48	0.48	4.15	-0.14	0.61
0.081968	0.02	6.65	0.30	0.30	4.03	-1.28	1.02
0.095316	0.00	5.43	0.37	0.37	3.47	-0.09	0.31
0.133673	0.03	9.81	0.20	0.20	2.47	1.08	1.62
0.082478	0.01	6.88	0.29	0.29	4.01	0.83	0.95
0.099258	0.01	9.40	0.21	0.21	3.33	0.83	1.23
0.087469	0.01	7.45	0.27	0.27	3.78	0.59	1.03
0.092663	0.01	4.39	0.46	0.46	3.57	0.33	0.52
1.081980	0.84	4.91	0.41	0.41	0.31	0.25	0.98
6.290764	86.65	-14.48	-0.14	0.14	0.05	-3.08	-0.32
0.098575	0.04	21.15	0.09	0.09	3.35	3.77	0.17
0.105296	0.02	33.94	0.06	0.06	3.14	3.84	-71.23
0.099455	0.01	-106.48	-0.02	0.02	3.32	-43.10	1.57
0.073119	0.01	-12.08	-0.17	0.17	4.52	-1.62	1.02
0.085489	0.01	-7.29	-0.27	0.27	3.86	-0.74	0.51
0.100453	0.00	-9.83	-0.20	0.20	3.29	-0.22	-0.06
0.384429	0.05	-25.55	-0.08	0.08	0.86	0.66	-0.21
0.310733	0.06	-26.85	-0.07	0.07	1.06	1.31	0.00
0.461339	0.07	-24.31	-0.08	0.08	0.72	0.61	-0.16
0.455218	0.07	-14.17	-0.14	0.14	0.73	0.37	-0.24
0.654368	0.10	-31.07	-0.06	0.06	0.50	0.57	-0.68
0.569819	0.24	-12.98	-0.15	0.15	0.58	0.74	-0.01
0.596245	0.30	-12.54	-0.16	0.16	0.55	0.80	-0.11
0.699192	0.40	-15.22	-0.13	0.13	0.47	0.97	-0.20
0.645882	0.27	-18.62	-0.11	0.11	0.51	0.95	-0.41
0.485312	1.40	-2.71	-0.74	0.74	0.68	1.19	-0.30
0.766747	9.54	-6.72	-0.30	0.30	0.43	10.60	-0.07
0.657393	1.05	-15.10	-0.13	0.13	0.50	3.13	0.06
0.394564	0.10	-6.17	-0.32	0.32	0.84	0.29	-0.19
0.626710	0.12	-31.69	-0.06	0.06	0.53	0.84	0.11
0.875785	0.84	258.59	0.01	0.01	0.38	-10.07	0.93
2.629321	24.48	-13.88	-0.14	0.14	0.13	4.07	0.34
0.436984	0.50	-23.81	-0.08	0.08	0.76	5.58	0.39
0.288304	0.07	-46.70	-0.04	0.04	1.15	3.44	0.35
0.235505	0.07	-29.55	-0.07	0.07	1.40	3.28	0.25
0.625417	0.73	-25.29	-0.08	0.08	0.53	4.06	0.02
0.372996	0.10	-57.70	-0.03	0.03	0.89	3.55	-0.10
0.404293	0.17	-70.73	-0.03	0.03	0.82	6.99	-0.03

0.212378	0.02	327.88	0.01	0.01	1.56	-5.76	0.05
0.323161	0.05	545.64	0.00	0.00	1.02	-8.10	0.30
0.436390	0.10	194.76	0.01	0.01	0.76	-4.92	0.57
0.218288	0.01	165.14	0.01	0.01	1.51	-2.03	0.93
0.201399	0.01	136.12	0.01	0.01	1.64	-1.57	1.13
0.203437	0.01	39.55	0.05	0.05	1.62	-0.75	0.61
-3.630463	9.70	90.49	0.02	0.02	-0.09	-3.92	0.72
0.903178	0.35	22.59	0.09	0.09	0.37	-0.63	1.98
0.213940	0.05	32.54	0.06	0.06	1.54	2.27	0.41
0.244219	0.01	34.60	0.06	0.06	1.35	0.24	-6541313.29
0.353470	0.04	36.13	0.06	0.06	0.93	-0.77	0.39
0.235557	0.01	41.01	0.05	0.05	1.40	-0.50	0.13
0.220005	0.00	47.55	0.04	0.04	1.50	0.06	0.10
0.134829	0.01	24.68	0.08	0.08	2.45	-0.87	0.02
0.116313	0.01	17.78	0.11	0.11	2.84	-0.94	-0.03
0.161106	0.02	16.63	0.12	0.12	2.05	-0.85	-0.10
0.136379	0.01	20.77	0.10	0.10	2.42	-0.65	-0.13
0.299630	0.07	16.55	0.12	0.12	1.10	-0.80	-0.21
0.387755	0.08	18.84	0.11	0.11	0.85	-0.61	-0.36
0.112696	0.02	3.83	0.52	0.52	2.93	-0.42	-0.44
0.145301	0.01	9.45	0.21	0.21	2.27	-0.23	0.59
0.247437	0.01	9.77	0.20	0.20	1.34	-0.15	0.06
0.488559	0.16	14.25	0.14	0.14	0.68	-0.63	-0.19
0.208764	0.07	23.49	0.09	0.09	1.58	-2.30	1.20
0.304087	0.03	79.27	0.03	0.03	1.09	-1.33	3.17
0.260342	0.03	34.11	0.06	0.06	1.27	0.91	-39.87
0.287562	0.05	43.09	0.05	0.05	1.15	1.64	-11.67
0.278192	0.06	35.17	0.06	0.06	1.19	2.02	-3.48
0.216672	0.07	14.22	0.14	0.14	1.52	1.46	-3.12
0.221490	0.06	23.03	0.09	0.09	1.49	1.95	-2.99
0.212491	0.04	35.80	0.06	0.06	1.55	2.43	-3.41
0.261263	0.05	35.19	0.06	0.06	1.26	1.80	-3.93
0.204374	0.04	25.12	0.08	0.08	1.62	1.62	-5.28
0.258238	0.03	63.13	0.03	0.03	1.28	2.04	-2.55
0.277442	0.03	169.49	0.01	0.01	1.19	4.74	-4.53
0.259387	0.01	1878.57	0.00	0.00	1.27	4.02	1.96
0.290090	0.01	641.26	0.00	0.00	1.14	7.52	-9.95
0.232856	0.02	126.37	0.02	0.02	1.42	3.15	-5.71
0.351486	0.07	58.31	0.03	0.03	0.94	2.29	-1.27
0.282777	0.08	40.87	0.05	0.05	1.17	2.69	-1.80
0.196098	0.08	5.52	0.36	0.36	1.68	0.77	2.30
0.199074	0.02	26.97	0.07	0.07	1.66	0.93	-3.83
0.252924	0.04	36.87	0.05	0.05	1.31	1.48	-5.40
0.247014	0.05	67.29	0.03	0.03	1.34	3.81	-284.16
0.192357	0.08	25.92	0.08	0.08	1.72	3.80	20.17
0.325707	0.28	31.01	0.06	0.06	1.01	5.72	-19.89
0.268388	0.12	82.46	0.02	0.02	1.23	6.98	1.92
0.185095	0.04	-284.94	-0.01	0.01	1.78	31.55	0.99
0.194307	0.02	-135.03	-0.01	0.01	1.70	-8.83	-0.49
0.176768	0.01	-71.22	-0.03	0.03	1.87	-1.63	0.02
0.184340	0.00	-70.93	-0.03	0.03	1.79	-0.76	0.22
0.165263	0.00	-57.33	-0.03	0.03	2.00	-0.62	0.33

0.148789	0.00	-30.29	-0.07	0.07	2.22	-0.44	0.47
0.167073	0.01	-17.86	-0.11	0.11	1.98	-0.36	0.56
0.184521	0.01	-21.27	-0.09	0.09	1.79	-0.41	0.55
0.175091	0.00	-128.48	-0.02	0.02	1.89	-0.92	-0.99
0.190581	0.01	-55.55	-0.04	0.04	1.73	-0.64	-0.32
0.161760	0.00	-512.99	0.00	0.00	2.04	0.28	-0.06
0.202094	0.01	-5944.46	0.00	0.00	1.63	-19.56	-3.70
0.308928	0.01	-156.53	-0.01	0.01	1.07	1.33	-9.26
0.370051	0.01	-143.01	-0.01	0.01	0.89	0.43	-7.59
0.450687	0.01	-298.97	-0.01	0.01	0.73	1.11	-4.20
0.472395	0.01	-115.34	-0.02	0.02	0.70	-0.41	-2.77
0.626808	0.01	-87.15	-0.02	0.02	0.53	0.13	-3.58
0.640476	0.04	-124.31	-0.02	0.02	0.52	0.99	-2.57

					phi M	phi H	phi W
0.628383	0.06	-25.78	-0.08	0.08	0.54	-0.34	0.26
0.574463	0.02	-36.75	-0.05	0.05	0.59	0.19	0.31
0.592544	0.01	-85.10	-0.02	0.02	0.57	0.20	0.39
0.765341	0.02	-78.35	-0.03	0.03	0.44	0.23	0.10
0.813489	0.02	-86.43	-0.02	0.02	0.42	0.19	-0.03
0.693171	0.03	-79.26	-0.03	0.03	0.49	0.39	-0.06
0.894028	0.05	-110.77	-0.02	0.02	0.38	0.56	-0.01
0.812174	0.07	-63.79	-0.03	0.03	0.42	0.52	-0.04
0.650943	0.04	-70.34	-0.03	0.03	0.52	0.48	0.02
0.745139	0.06	-64.27	-0.03	0.03	0.46	0.53	0.05
0.691959	0.04	-85.90	-0.02	0.02	0.49	0.68	0.06
0.717929	0.04	-94.05	-0.02	0.02	0.47	0.60	0.07
0.547923	0.01	-199.47	-0.01	0.01	0.62	0.56	0.44
0.581707	0.01	-178.75	-0.01	0.01	0.58	0.39	0.34
0.532957	0.01	-222.45	-0.01	0.01	0.64	0.37	0.27
0.567861	0.00	-266.44	-0.01	0.01	0.60	0.17	0.39
0.495197	0.00	-205.90	-0.01	0.01	0.69	0.12	0.48
0.496455	0.00	-261.16	-0.01	0.01	0.68	0.07	0.36
0.548191	0.00	-413.83	0.00	0.00	0.62	-0.18	0.32
0.498321	0.00	-431.47	0.00	0.00	0.68	-0.43	0.22
0.470363	0.00	-585.85	0.00	0.00	0.72	-0.84	0.26
0.490760	0.00	-940.69	0.00	0.00	0.69	-3.31	-0.02
0.743060	0.22	-11.72	-0.17	0.17	0.46	0.40	-0.71
0.646669	0.09	-10.04	-0.20	0.20	0.53	0.18	0.35
0.543293	0.07	-19.15	-0.10	0.10	0.63	0.39	-2.50
0.617418	0.09	-14.70	-0.14	0.14	0.55	0.29	0.34
0.510695	0.19	-5.95	-0.34	0.34	0.67	0.34	0.18
0.547058	0.15	-5.05	-0.40	0.40	0.62	0.20	0.15
0.548286	0.14	-7.63	-0.26	0.26	0.62	0.30	0.17
0.453781	0.19	-4.70	-0.43	0.43	0.75	0.35	0.20
0.315263	0.09	-4.77	-0.42	0.42	1.08	0.35	0.19
0.797849	0.43	-11.18	-0.18	0.18	0.43	0.58	0.28
1.339417	0.35	-37.92	-0.05	0.05	0.25	0.57	0.30
0.493397	0.08	-9.59	-0.21	0.21	0.69	0.25	0.24
0.568815	0.06	-18.14	-0.11	0.11	0.60	0.27	0.30
0.501825	0.04	-21.76	-0.09	0.09	0.68	0.27	0.41

0.404213	0.03	-21.15	-0.09	0.09	0.84	0.35	0.42
0.580693	0.05	-23.68	-0.08	0.08	0.59	0.30	0.38
0.545761	0.04	-21.39	-0.09	0.09	0.62	0.25	0.29
0.494404	0.02	-29.33	-0.07	0.07	0.69	0.24	0.31
0.444456	0.02	-31.75	-0.06	0.06	0.76	0.27	0.36
0.535823	0.02	-48.83	-0.04	0.04	0.63	0.26	0.38
0.660988	0.03	-34.31	-0.06	0.06	0.51	0.25	0.29
0.440404	0.18	17.10	0.12	0.12	0.77	0.95	69.23
0.340048	0.10	19.53	0.10	0.10	1.00	1.05	0.21
0.322256	0.13	-22.20	-0.09	0.09	1.05	-2.29	-0.34
1.981502	4.81	-4.90	-0.41	0.41	0.17	-0.42	-2.31
0.308972	0.26	6.92	0.29	0.29	1.10	1.17	-0.69
0.553764	0.32	28.84	0.07	0.07	0.61	1.86	-0.30
0.271097	0.18	9.55	0.21	0.21	1.25	1.51	-0.06
0.200861	0.24	4.64	0.43	0.43	1.69	1.81	-0.09
0.174331	0.18	4.09	0.49	0.49	1.95	1.60	-0.51
0.167243	0.42	2.49	0.80	0.80	2.03	2.42	-0.72
0.171660	0.31	8.17	0.24	0.24	1.98	5.75	-1.68
0.165810	0.39	-5.23	-0.38	0.38	2.05	-4.51	0.44
0.229226	0.95	4.51	0.44	0.44	1.48	5.42	1.35
0.059901	0.60	0.35	5.70	5.70	5.67	4.08	497.69
0.126651	0.46	1.87	1.07	1.07	2.68	3.66	-0.36
0.147399	0.56	1.82	1.10	1.10	2.31	3.12	-0.95
0.255624	0.37	5.55	0.36	0.36	1.33	2.08	-1.04
0.532941	0.27	26.90	0.07	0.07	0.64	1.66	-0.53
0.354680	0.06	34.15	0.06	0.06	0.96	1.10	0.01
0.323232	0.04	49.70	0.04	0.04	1.05	1.15	-1.07
0.291432	0.02	56.23	0.04	0.04	1.17	1.09	-0.84
0.424735	0.02	115.33	0.02	0.02	0.80	0.87	-0.24
0.357171	0.02	101.95	0.02	0.02	0.95	1.01	0.22
0.357090	0.01	141.64	0.01	0.01	0.95	0.99	-0.14
0.314013	0.01	127.75	0.02	0.02	1.08	0.79	-0.46
0.314906	0.01	168.45	0.01	0.01	1.08	0.79	-0.78
0.284317	0.00	296.58	0.01	0.01	1.20	0.98	-1.67
0.156849	0.00	128.04	0.02	0.02	2.17	0.73	-0.73
0.221585	0.00	127.12	0.02	0.02	1.53	0.79	-0.20
0.218065	0.01	134.01	0.01	0.01	1.56	0.89	0.07
0.195665	0.00	164.08	0.01	0.01	1.74	0.77	0.34
0.234177	0.01	182.58	0.01	0.01	1.45	1.19	0.29
0.196086	0.01	167.61	0.01	0.01	1.73	1.22	0.27
0.205232	0.00	312.78	0.01	0.01	1.66	1.43	0.11
0.306773	0.00	-591.62	0.00	0.00	1.11	-2.07	0.07
0.218245	0.00	-508.71	0.00	0.00	1.56	-0.95	0.28
0.221346	0.00	-493.32	0.00	0.00	1.54	-0.21	0.19
0.400601	0.00	-578.78	0.00	0.00	0.85	0.37	0.26
0.307686	0.00	-447.21	0.00	0.00	1.10	0.39	0.27
0.270070	0.00	-325.06	-0.01	0.01	1.26	0.46	0.23
0.329355	0.00	-302.55	-0.01	0.01	1.03	0.52	0.35
0.447144	0.01	-311.40	-0.01	0.01	0.76	0.71	0.13
0.308240	0.01	-165.94	-0.01	0.01	1.10	0.97	0.07
0.456825	0.01	-164.74	-0.01	0.01	0.74	0.66	0.14

0.437736	0.01	-189.37	-0.01	0.01	0.78	0.61	0.16
0.477607	0.01	-168.32	-0.01	0.01	0.71	0.45	-0.11
0.469871	0.00	-125.27	-0.02	0.02	0.72	0.06	0.33
0.405968	0.00	-153.27	-0.01	0.01	0.84	0.26	0.53
0.388940	0.00	-169.50	-0.01	0.01	0.87	0.12	0.41
0.311482	0.00	-94.73	-0.02	0.02	1.09	0.02	0.07
0.238335	0.00	-24.00	-0.08	0.08	1.43	-0.03	0.47
0.336118	0.01	-12.60	-0.16	0.16	1.01	0.06	0.32
0.604498	0.01	-46.78	-0.04	0.04	0.56	0.05	0.24
0.224727	0.00	-13.81	-0.14	0.14	1.51	0.07	0.30
0.366826	0.00	-23.57	-0.08	0.08	0.93	-0.02	0.38
0.536012	0.00	-81.47	-0.02	0.02	0.63	0.00	0.39
0.853710	0.00	-188.23	-0.01	0.01	0.40	-0.07	0.49
0.710756	0.02	-258.97	-0.01	0.01	0.48	-0.58	0.44
0.643787	0.01	-236.06	-0.01	0.01	0.53	-0.45	-0.02
0.703920	0.01	-231.42	-0.01	0.01	0.48	-0.22	0.00
0.685863	0.01	-203.64	-0.01	0.01	0.50	-0.34	-0.01
0.630695	0.01	-197.45	-0.01	0.01	0.54	-0.24	0.08
0.338994	0.16	-2.52	-0.79	0.79	1.00	0.30	0.21
2.109015	0.56	-13.32	-0.15	0.15	0.16	-0.14	-1.03
0.704450	0.02	-24.75	-0.08	0.08	0.48	-0.07	0.19
0.849198	0.08	-22.95	-0.09	0.09	0.40	0.22	0.13
0.969626	0.17	-21.16	-0.09	0.09	0.35	0.31	0.13
0.592847	0.10	-9.25	-0.22	0.22	0.57	0.22	0.10
0.727491	0.08	-26.10	-0.08	0.08	0.47	0.32	0.03
0.596299	0.04	-29.36	-0.07	0.07	0.57	0.32	-0.01
0.839596	0.06	-34.53	-0.06	0.06	0.40	0.25	0.01
					phi M	phi H	phi W
0.290457	0.01	-177.44	-0.01	0.01	1.09	-5.68	-0.02
0.396444	0.02	-343.97	-0.01	0.01	0.80	-4.99	0.06
0.258802	0.01	-457.66	0.00	0.00	1.23	-19.36	0.13
0.461842	0.02	-1189.39	0.00	0.00	0.69	14.11	0.64
0.308057	0.00	-537.58	0.00	0.00	1.03	2.56	0.26
0.473222	0.00	-876.20	0.00	0.00	0.67	29.33	0.34
0.429169	0.00	3447.19	0.00	0.00	0.74	1.55	0.42
0.354601	0.01	-2460.77	0.00	0.00	0.90	1.75	0.14
0.350338	0.01	2181.63	0.00	0.00	0.91	1.33	0.12
0.348820	0.01	775.37	0.00	0.00	0.91	1.07	0.27
0.377214	0.01	514.39	0.00	0.00	0.84	0.83	0.28
0.263879	0.01	273.40	0.01	0.01	1.20	0.90	0.16
0.339324	0.01	274.27	0.01	0.01	0.94	1.00	0.10
0.255926	0.01	150.59	0.01	0.01	1.24	1.03	-0.03
0.291047	0.01	178.77	0.01	0.01	1.09	0.93	-0.11
0.252294	0.01	121.12	0.02	0.02	1.26	0.94	-0.18
0.234810	0.01	128.78	0.02	0.02	1.35	0.96	-0.31
0.215363	0.01	68.83	0.03	0.03	1.48	1.01	-0.24
0.279294	0.01	149.29	0.01	0.01	1.14	1.16	-0.14
0.270249	0.01	118.30	0.02	0.02	1.18	0.95	-0.18

0.330144	0.01	128.78	0.02	0.02	0.96	0.64	-0.22
0.300379	0.01	90.78	0.02	0.02	1.06	0.74	-0.27
0.307258	0.01	76.51	0.03	0.03	1.03	0.49	-0.30
0.294046	0.01	67.61	0.03	0.03	1.08	0.41	-0.36
0.282789	0.01	55.59	0.04	0.04	1.12	0.39	-0.26
0.282520	0.01	74.10	0.03	0.03	1.12	0.59	-0.35
0.279481	0.01	51.12	0.04	0.04	1.14	0.31	-0.33
0.289512	0.01	54.72	0.04	0.04	1.10	0.19	-0.44
0.263951	0.04	-8.14	-0.25	0.25	1.20	0.36	-0.08
0.231190	0.04	-9.59	-0.21	0.21	1.37	0.51	-0.11
0.297722	0.01	-30.29	-0.07	0.07	1.07	0.14	-0.01
0.251575	0.01	-23.24	-0.09	0.09	1.26	0.31	0.09
0.289677	0.01	-29.97	-0.07	0.07	1.10	0.34	0.19
0.210319	0.01	-4.04	-0.50	0.50	1.51	0.06	0.19
0.289420	0.04	-9.99	-0.20	0.20	1.10	0.38	0.17
0.279677	0.03	-5.71	-0.35	0.35	1.14	0.19	0.13
0.602599	0.09	-27.80	-0.07	0.07	0.53	0.52	0.14
0.538622	0.17	-11.21	-0.18	0.18	0.59	0.50	0.07
0.484256	0.05	-17.69	-0.11	0.11	0.66	0.30	-0.04
0.437874	0.15	-6.01	-0.33	0.33	0.73	0.35	-0.03
0.435064	0.09	-17.15	-0.12	0.12	0.73	0.61	-0.08
0.457941	0.10	-11.82	-0.17	0.17	0.69	0.43	-0.02
0.855810	0.10	-881.36	0.00	0.00	0.37	-12.76	0.09
0.485793	0.02	-498.05	0.00	0.00	0.65	-3.77	0.14
0.747174	0.08	-8939.07	0.00	0.00	0.43	4.98	0.03
0.911922	0.09	448.42	0.00	0.00	0.35	2.01	-0.08
0.473333	0.14	25.06	0.08	0.08	0.67	0.83	-0.13
0.368727	0.15	11.04	0.18	0.18	0.86	0.68	-0.16
0.681291	0.21	39.55	0.05	0.05	0.47	1.02	-0.16
0.607350	0.21	32.89	0.06	0.06	0.52	1.12	-0.20
0.881557	0.29	56.99	0.04	0.04	0.36	1.24	-0.24
0.727177	0.26	32.23	0.06	0.06	0.44	0.96	-0.13
0.461071	0.11	38.13	0.05	0.05	0.69	1.19	-0.19
0.517335	0.07	57.06	0.04	0.04	0.61	0.93	-0.11
0.541360	0.06	55.56	0.04	0.04	0.59	0.64	-0.38
0.472467	0.11	30.20	0.07	0.07	0.67	0.87	-0.52
0.421572	0.05	40.63	0.05	0.05	0.75	0.71	-0.49
0.380930	0.04	41.61	0.05	0.05	0.83	0.64	-0.57
0.397388	0.02	58.13	0.03	0.03	0.80	0.54	-0.49
0.565940	0.06	73.10	0.03	0.03	0.56	0.75	-0.46
0.504769	0.11	32.43	0.06	0.06	0.63	0.82	-0.38
0.740357	0.24	33.63	0.06	0.06	0.43	0.87	-0.45
0.751697	0.62	14.32	0.14	0.14	0.42	0.94	-0.34
0.566180	0.32	19.79	0.10	0.10	0.56	1.20	-0.46
0.567661	0.14	34.69	0.06	0.06	0.56	0.90	-0.44
0.534241	0.09	33.81	0.06	0.06	0.59	0.60	-0.34
0.717073	0.17	35.82	0.06	0.06	0.44	0.70	-0.30
0.498411	0.14	24.01	0.08	0.08	0.64	0.79	-0.20
0.647840	0.17	37.40	0.05	0.05	0.49	0.87	-0.22
0.429621	0.06	47.53	0.04	0.04	0.74	0.93	-0.15

0.528183	0.09	48.72	0.04	0.04	0.60	0.89	-0.18
0.478301	0.09	33.05	0.06	0.06	0.66	0.74	-0.17
0.465985	0.10	35.48	0.06	0.06	0.68	0.93	-0.23
0.594809	0.14	46.46	0.04	0.04	0.53	1.02	-0.22
0.505202	0.14	29.83	0.07	0.07	0.63	0.95	-0.21
0.634276	0.17	42.68	0.05	0.05	0.50	1.11	-0.36
0.576916	0.12	46.57	0.04	0.04	0.55	1.04	-0.48
0.453429	0.10	36.62	0.05	0.05	0.70	1.07	-0.51
0.439526	0.09	28.69	0.07	0.07	0.72	0.79	-0.62
0.339103	0.09	19.61	0.10	0.10	0.94	0.89	-0.77
0.429763	0.08	32.93	0.06	0.06	0.74	0.88	-1.19
0.387066	0.05	32.70	0.06	0.06	0.82	0.68	-1.46
0.405831	0.04	49.24	0.04	0.04	0.78	0.70	-2.34
0.403951	0.05	42.17	0.05	0.05	0.79	0.73	-2.63
0.432763	0.04	59.78	0.03	0.03	0.73	0.86	-3.19
0.426466	0.03	54.05	0.04	0.04	0.74	0.63	-2.40
0.597579	0.05	83.14	0.02	0.02	0.53	0.74	-2.22
0.401669	0.04	46.63	0.04	0.04	0.79	0.73	-1.94
0.479568	0.04	60.98	0.03	0.03	0.66	0.68	-2.71
0.415572	0.03	61.69	0.03	0.03	0.76	0.76	-2.65
0.409772	0.02	83.27	0.02	0.02	0.78	0.62	-2.32
0.371715	0.02	101.16	0.02	0.02	0.85	0.69	-2.25
0.246203	0.01	80.85	0.02	0.02	1.29	0.69	-1.72
0.291961	0.01	189.00	0.01	0.01	1.09	0.95	-1.37
0.255131	0.00	-316.01	-0.01	0.01	1.25	1.55	-0.85
0.352313	0.00	-194.10	-0.01	0.01	0.90	0.75	-0.33
0.358292	0.01	-103.06	-0.02	0.02	0.89	0.81	-0.07
0.304990	0.02	-66.59	-0.03	0.03	1.04	1.17	-0.05
0.404117	0.05	-40.49	-0.05	0.05	0.79	1.02	-0.02
0.467392	0.06	-43.34	-0.05	0.05	0.68	0.93	-0.06
0.390172	0.05	-22.72	-0.09	0.09	0.81	0.56	-0.09
0.363190	0.04	-19.99	-0.10	0.10	0.87	0.47	-0.20
0.295589	0.01	-27.55	-0.07	0.07	1.07	0.33	-0.17
0.321034	0.03	-23.86	-0.08	0.08	0.99	0.56	-0.08
0.380853	0.05	-25.54	-0.08	0.08	0.83	0.69	-0.06
0.466296	0.07	-30.59	-0.07	0.07	0.68	0.72	-0.06
0.486211	0.12	-25.64	-0.08	0.08	0.65	1.01	-0.03
0.380766	0.08	-24.36	-0.08	0.08	0.83	1.00	0.01
0.502883	0.04	-65.45	-0.03	0.03	0.63	0.93	0.30
0.406439	0.01	-86.15	-0.02	0.02	0.78	0.52	0.16

U* (adiabatic)	U* (measured)	phi (M)	H (adiabatic)	H (measured)	phi (H)	Le (adiabatic)
0.14	0.13	1.11	-29.38	38.43	-0.69	-1.67
0.10	0.11	0.92	-26.55	44.10	-0.66	9.98
0.11	0.17	0.61	-25.84	46.80	-0.90	15.00
0.15	0.18	0.88	-98.20	71.61	-1.56	26.40
0.14	0.16	0.89	-141.76	101.73	-1.56	16.29
0.15	0.15	0.98	-122.87	98.71	-1.27	23.90
0.13	0.19	0.71	-72.89	126.62	-0.81	19.92
0.12	0.21	0.54	-59.23	140.72	-0.78	15.64
0.09	0.23	0.39	-44.30	149.30	-0.75	10.74
0.11	0.16	0.70	-8.72	103.67	-0.12	6.74
0.04	0.18	0.20	-2.87	167.00	-0.08	1.65
0.08	0.14	0.55	46.48	110.56	0.77	-1.79
0.06	0.10	0.59	23.79	98.98	0.41	-3.79
0.09	0.14	0.64	9.54	154.60	0.10	10.49
0.03	0.19	0.13	8.92	82.17	0.81	-1.29
0.09	0.21	0.42	30.56	21.03	3.48	-8.72
0.18	0.14	1.23	16.49	23.63	0.57	-12.93

U* (adiabatic)	U* (measured)	phi (M)	H (adiabatic)	H (measured)	phi (H)	Le (adiabatic)
0.25	0.11	2.35	-56.92	-13.74	1.76	108.65
0.24	0.18	1.34	-38.65	-26.82	1.07	84.55
0.17	0.11	1.56	-26.16	-10.74	1.57	59.96
0.15	0.08	1.90	-18.12	-6.79	1.41	59.43
0.17	0.10	1.66	-41.20	0.13	-195.80	63.93
0.15	0.06	2.47	-25.99	-7.06	1.49	54.05
0.02	0.06	0.37	-3.06	-1.72	4.79	6.35
0.12	0.08	1.60	-20.18	-10.59	1.19	50.90
0.05	0.08	0.68	-20.18	-1.13	26.43	15.42
0.14	0.10	1.45	-34.29	-16.12	1.47	48.38
0.16	0.14	1.15	-11.74	-16.01	0.64	54.77
0.15	0.13	1.10	-4.57	-15.18	0.27	39.97
0.19	0.21	0.93	-9.72	-18.79	0.55	45.45
0.13	0.18	0.74	-6.17	-20.04	0.42	27.13
0.12	0.22	0.57	-29.16	124.36	-0.41	64.24
0.12	0.24	0.50	-10.87	142.09	-0.15	50.27
0.17	0.17	1.01	-45.09	121.50	-0.37	71.56
0.18	0.14	1.23	98.15	126.23	0.63	47.94
0.11	0.18	0.59	78.53	93.95	1.43	3.02
0.14	0.27	0.51	92.85	135.20	1.36	40.71
0.23	0.18	1.30	153.30	113.04	1.04	60.07
0.16	0.24	0.67	114.78	144.02	1.19	42.86
0.14	0.19	0.72	103.27	115.65	1.23	35.79
0.19	0.21	0.93	147.28	142.56	1.11	45.59
0.16	0.29	0.56	127.29	142.86	1.60	45.44
0.25	0.36	0.70	189.36	145.72	1.86	107.92
0.21	0.43	0.48	161.33	178.46	1.89	44.44
0.26	0.39	0.66	185.88	112.65	2.50	36.51
0.09	0.12	0.75	9.77	37.86	0.34	47.32

0.07	0.10	0.69	9.49	57.99	0.24	29.11
0.07	0.15	0.46	15.49	88.03	0.38	28.07
0.11	0.17	0.63	32.69	103.71	0.50	57.45
0.11	0.25	0.43	18.61	130.38	0.34	63.03
0.18	0.42	0.42	7.94	172.97	0.11	51.61
0.24	0.41	0.59	47.61	167.91	0.48	73.55
0.20	0.48	0.41	34.94	183.74	0.46	51.14
0.21	0.48	0.44	31.08	156.31	0.46	42.50
0.34	0.54	0.64	43.53	146.89	0.47	56.94
0.25	0.49	0.51	21.21	88.29	0.47	40.61
0.26	0.40	0.65	9.18	59.58	0.24	39.44

0.25	0.23	1.08	57.53	13.96	3.80	52.54
0.28	0.22	1.29	53.73	14.25	2.91	-1.05
0.26	0.19	1.37	45.96	11.82	2.83	-4.90
0.30	0.22	1.35	54.40	14.20	2.83	-4.61
0.33	0.18	1.84	56.95	11.92	2.60	-11.57
0.18	0.23	0.79	35.57	16.68	2.71	7.46
0.18	0.25	0.74	38.54	24.95	2.10	3.27
0.19	0.23	0.82	39.13	18.77	2.55	12.60
0.20	0.30	0.67	48.98	31.39	2.31	15.78
0.41	0.34	1.22	92.85	32.13	2.37	47.22
0.56	0.40	1.42	123.84	26.05	3.35	96.88
0.35	0.33	1.06	75.50	27.70	2.57	53.85
0.32	0.30	1.09	70.54	11.60	5.59	39.23
0.34	0.32	1.07	70.54	19.24	3.43	47.20
0.40	0.34	1.16	80.46	21.54	3.22	53.35
0.33	0.35	0.95	57.49	19.89	3.06	43.70
0.27	0.36	0.76	81.84	27.26	3.96	18.73
0.31	0.32	0.97	68.46	9.31	7.55	22.45
0.27	0.33	0.82	43.23	8.50	6.24	23.07
0.26	0.34	0.75	34.58	5.41	8.54	10.09
0.23	0.30	0.78	6.86	-6.40	-1.37	7.77
0.25	0.32	0.77	-31.38	-9.64	4.23	-0.55
0.24	0.27	0.88	-41.45	-11.56	4.08	-9.96
0.13	0.25	0.53	-16.77	-10.35	3.04	8.30
0.09	0.21	0.45	-9.23	-8.23	2.51	-0.77
0.09	0.18	0.50	-6.86	-7.78	1.77	1.78
0.11	0.25	0.43	-20.61	-10.83	4.42	2.57
0.07	0.15	0.47	-15.06	-9.16	3.47	-1.02
0.08	0.21	0.37	-16.22	-11.33	3.82	-8.27
0.18	0.16	1.13	-34.40	-7.09	4.28	-18.89
0.24	0.10	2.34	-31.27	-6.02	2.22	-38.12
0.32	0.11	2.95	-27.98	-7.26	1.30	-45.61
0.28	0.17	1.71	-33.38	-7.52	2.60	-32.89
0.32	0.08	3.91	-21.85	-6.61	0.84	-42.33
0.32	0.07	4.28	-1.75	-4.47	0.09	-34.84
0.27	0.07	4.07	-5.94	-4.59	0.32	-27.50
0.22	0.07	3.11	-3.96	-3.97	0.32	-21.25
0.29	0.08	3.50	-3.99	-5.79	0.20	-20.73

0.22	0.08	2.88	-7.47	-4.21	0.62	-9.38
0.07	0.04	1.63	1.60	-3.01	-0.33	-4.39
0.10	0.08	1.21	11.50	-1.91	-4.97	-4.65
0.02	0.05	0.37	0.85	-0.10	-22.80	0.13
0.09	0.05	1.79	-1.36	-3.51	0.22	0.28
0.07	0.11	0.68	-15.62	-4.72	4.88	2.19
0.39	0.11	3.43	-58.99	-8.42	2.04	18.30
0.33	0.11	2.92	-28.31	-6.97	1.39	11.16
0.46	0.10	4.85	-25.55	-8.28	0.64	-38.09
0.45	0.10	4.75	-7.68	-7.66	0.21	-67.29
0.43	0.10	4.39	-7.99	-7.99	0.23	-58.62
0.41	0.08	4.98	16.86	-8.04	-0.42	-32.45
0.33	0.11	3.16	10.09	-12.13	-0.26	-12.64
0.35	0.10	3.54	4.94	-9.32	-0.15	-15.44
0.35	0.08	4.25	6.69	-10.81	-0.15	-24.63
0.29	0.07	4.13	23.23	-4.29	-1.31	-20.24
0.31	0.09	3.55	3.04	-9.39	-0.09	-10.66
0.23	0.09	2.53	-17.45	-6.22	1.11	-11.66
0.35	0.08	4.11	-25.27	-7.24	0.85	-22.48
0.31	0.09	3.41	-19.28	-6.65	0.85	-26.51
0.37	0.10	3.87	-22.68	-9.74	0.60	-34.61
0.28	0.08	3.65	-9.90	-8.13	0.33	-17.65
0.02	0.08	0.31	-0.59	-7.29	0.26	-1.69
0.00	0.07	0.05	-0.26	1.51	-3.15	-0.14
0.27	0.08	3.44	-40.32	-3.04	3.86	7.74
0.38	0.12	3.22	-54.25	-4.29	3.94	25.83
0.37	0.11	3.40	-37.16	0.25	-44.18	50.36
0.37	0.08	4.63	-20.57	2.67	-1.66	57.37
0.44	0.11	3.96	-40.97	13.55	-0.76	64.01
0.49	0.15	3.37	-17.70	23.66	-0.22	-9.83
0.21	0.24	0.88	23.28	38.79	0.68	-13.53
0.29	0.27	1.09	82.32	56.12	1.35	-0.43
0.20	0.28	0.73	31.64	69.17	0.62	-11.45
0.17	0.23	0.74	20.29	71.98	0.38	-17.28
0.14	0.27	0.52	15.03	49.42	0.59	-28.00
0.14	0.23	0.59	32.78	73.17	0.75	-0.60
0.13	0.23	0.57	35.63	76.32	0.82	-6.34
0.12	0.25	0.48	38.65	80.46	0.99	-14.51
0.13	0.26	0.52	35.96	70.53	0.97	-27.06
0.10	0.14	0.70	67.03	78.80	1.22	-18.44
0.06	0.14	0.44	127.27	26.51	10.87	-4.40
0.11	0.22	0.52	80.69	48.85	3.21	4.99
0.15	0.18	0.86	19.93	76.90	0.30	-17.09
0.14	0.27	0.54	20.22	43.66	0.86	7.14
0.14	0.35	0.39	116.29	-29.14	-10.32	60.86
0.02	0.19	0.13	19.82	36.89	4.17	4.42
0.15	0.20	0.77	100.85	22.74	5.72	27.53
0.32	0.27	1.17	114.75	27.67	3.53	52.02
0.30	0.21	1.44	102.47	21.17	3.37	31.57
0.10	0.18	0.54	38.55	17.10	4.16	0.59
0.23	0.25	0.91	67.57	20.47	3.64	-5.29
0.17	0.21	0.84	46.41	7.74	7.16	-1.15

0.35	0.22	1.59	53.81	-5.71	-5.91	2.59
0.26	0.24	1.05	41.38	-4.76	-8.30	9.09
0.17	0.22	0.78	25.16	-6.43	-5.04	9.82
0.40	0.26	1.55	36.11	-11.19	-2.08	30.54
0.42	0.25	1.68	30.64	-11.35	-1.61	31.33
0.27	0.16	1.66	13.27	-10.37	-0.77	11.97
-0.02	0.17	-0.09	-2.01	-5.35	-4.02	-0.57
0.05	0.14	0.37	2.50	-10.34	-0.64	5.10
0.27	0.17	1.58	-51.51	-14.01	2.32	9.31
0.32	0.23	1.39	-11.70	-34.43	0.25	-240498190.57
0.22	0.23	0.96	23.33	-30.82	-0.79	9.72
0.39	0.27	1.44	33.37	-44.97	-0.52	7.18
0.41	0.26	1.54	-3.30	-36.93	0.06	5.13
0.46	0.18	2.51	51.84	-23.16	-0.89	1.02
0.48	0.17	2.91	66.29	-23.68	-0.96	-1.43
0.33	0.16	2.10	40.01	-21.78	-0.87	-3.66
0.45	0.18	2.48	44.14	-26.76	-0.66	-6.33
0.18	0.16	1.13	20.13	-21.83	-0.82	-3.42
0.15	0.17	0.87	12.84	-23.39	-0.63	-3.93
0.26	0.09	3.00	20.64	-16.01	-0.43	-9.37
0.29	0.13	2.33	10.51	-19.35	-0.23	10.69
0.17	0.12	1.37	3.84	-17.97	-0.16	0.51
0.09	0.13	0.69	6.29	-14.03	-0.65	-0.93
0.16	0.10	1.62	15.53	-4.06	-2.36	8.39
0.17	0.15	1.11	6.16	-4.06	-1.36	18.18
0.16	0.13	1.30	-6.23	-5.12	0.94	21.93
0.19	0.16	1.18	-15.47	-7.81	1.68	22.75
0.19	0.15	1.22	-21.81	-8.67	2.07	17.93
0.16	0.10	1.56	-15.52	-6.64	1.49	15.09
0.18	0.12	1.53	-17.67	-5.78	2.00	19.33
0.22	0.14	1.59	-23.05	-5.81	2.49	31.17
0.17	0.13	1.30	-13.38	-5.59	1.84	21.92
0.18	0.11	1.66	-12.15	-4.42	1.66	18.79
0.23	0.17	1.31	-17.72	-6.48	2.09	22.29
0.22	0.18	1.22	-16.68	-2.81	4.86	24.28
0.28	0.21	1.31	-8.21	-1.53	4.12	33.50
0.26	0.22	1.17	-11.02	-1.22	7.71	33.29
0.26	0.18	1.45	-16.51	-3.52	3.23	30.21
0.20	0.20	0.96	-26.31	-11.65	2.34	10.57
0.16	0.14	1.20	-17.39	-5.27	2.75	3.03
0.13	0.08	1.73	-9.20	-6.74	0.79	0.68
0.19	0.11	1.70	-6.62	-4.06	0.96	7.42
0.17	0.13	1.34	-9.79	-4.82	1.52	10.43
0.17	0.13	1.37	-13.81	-2.58	3.91	10.39
0.16	0.09	1.76	-16.43	-2.40	3.90	20.44
0.12	0.12	1.04	-26.44	-4.34	5.86	22.68
0.24	0.19	1.26	-87.77	-9.72	7.15	66.69
0.35	0.19	1.83	-88.16	-1.49	32.34	80.11
0.42	0.24	1.74	-62.49	3.96	-9.05	-51.34
0.48	0.25	1.92	-46.15	14.39	-1.67	2.47
0.53	0.29	1.84	-35.74	24.98	-0.78	21.91
0.59	0.29	2.05	-40.13	30.69	-0.64	45.64

0.57	0.25	2.28	-40.74	40.00	-0.45	71.55
0.47	0.23	2.03	-42.91	56.63	-0.37	88.19
0.48	0.26	1.84	-52.71	69.14	-0.42	86.16
0.91	0.47	1.93	-120.69	66.44	-0.94	-137.39
0.60	0.34	1.78	-66.28	57.12	-0.65	-36.94
0.94	0.45	2.09	7.26	12.08	0.29	-5.57
0.55	0.33	1.68	95.41	-2.84	-20.05	-255.72
0.51	0.46	1.10	80.53	53.79	1.37	-388.95
0.43	0.47	0.92	24.00	59.67	0.44	-396.39
0.38	0.50	0.75	28.20	33.13	1.13	-160.95
0.31	0.43	0.72	-16.75	55.58	-0.42	-130.64
0.25	0.46	0.54	6.70	92.98	0.13	-173.51
0.25	0.48	0.53	37.14	69.13	1.02	-149.09
0.18	0.33	0.55	-19.05	99.36	-0.35	35.33
0.22	0.37	0.61	12.13	104.27	0.19	40.55
0.35	0.59	0.59	23.21	193.75	0.20	66.23
0.27	0.60	0.46	22.76	210.08	0.24	17.22
0.27	0.64	0.43	19.16	229.07	0.20	-5.93
0.31	0.62	0.50	46.16	230.81	0.40	-14.05
0.26	0.67	0.39	44.44	200.32	0.57	-1.68
0.23	0.54	0.43	42.43	186.61	0.53	-5.89
0.29	0.54	0.54	44.17	166.91	0.49	4.38
0.24	0.51	0.47	41.74	163.34	0.55	6.52
0.26	0.52	0.50	41.68	118.13	0.70	8.79
0.26	0.53	0.49	34.81	117.21	0.61	9.95
0.44	0.69	0.64	44.05	120.50	0.58	91.53
0.37	0.62	0.60	23.50	98.40	0.40	48.09
0.42	0.64	0.65	20.71	83.05	0.38	48.72
0.38	0.62	0.61	6.42	61.53	0.17	51.45
0.38	0.54	0.70	4.69	54.41	0.12	58.67
0.40	0.56	0.70	2.25	45.65	0.07	44.24
0.35	0.55	0.64	-2.80	24.26	-0.18	26.80
0.34	0.49	0.70	-4.55	14.65	-0.44	17.60
0.36	0.49	0.74	-6.29	9.91	-0.86	16.56
0.32	0.45	0.71	-7.13	2.96	-3.39	-0.76
0.09	0.19	0.47	7.90	41.48	0.41	-32.58
0.10	0.18	0.54	4.27	42.66	0.19	14.97
0.15	0.24	0.64	13.72	54.15	0.39	-163.88
0.13	0.23	0.56	10.31	61.86	0.30	26.22
0.12	0.17	0.68	16.20	67.34	0.35	16.55
0.13	0.20	0.64	16.59	126.75	0.21	17.63
0.13	0.21	0.64	16.97	87.39	0.31	21.11
0.14	0.18	0.77	24.33	89.25	0.36	24.18
0.20	0.18	1.10	35.86	89.97	0.36	36.91
0.11	0.26	0.44	31.89	122.37	0.60	17.22
0.11	0.41	0.26	21.21	140.76	0.58	14.60
0.16	0.22	0.71	15.05	84.46	0.25	30.37
0.19	0.31	0.61	21.02	122.81	0.28	47.58
0.23	0.33	0.69	23.58	121.34	0.28	72.75

0.23	0.27	0.86	19.68	64.16	0.36	68.62
0.17	0.28	0.60	12.78	70.44	0.30	45.00
0.17	0.27	0.64	11.57	69.40	0.26	35.67
0.20	0.28	0.70	8.68	50.59	0.24	40.62
0.20	0.25	0.78	7.20	33.67	0.27	42.46
0.19	0.29	0.65	5.26	30.62	0.26	37.27
0.15	0.28	0.53	5.51	40.52	0.26	28.39
0.12	0.15	0.79	-16.00	-20.84	0.97	2227.55
0.16	0.15	1.02	-20.87	-18.88	1.08	5.68
0.14	0.13	1.08	-18.98	7.49	-2.34	-5.13
0.03	0.18	0.18	-8.14	107.40	-0.43	-2.91
0.12	0.11	1.13	-23.64	-17.48	1.20	-16.63
0.11	0.17	0.63	-20.97	-17.44	1.91	-4.32
0.16	0.13	1.28	-40.16	-20.20	1.55	-1.42
0.13	0.08	1.73	-27.94	-8.70	1.85	-1.15
0.15	0.08	2.00	-32.74	-10.02	1.64	-7.63
0.11	0.05	2.08	-27.24	-5.26	2.49	-6.04
0.13	0.06	2.03	-35.72	-2.98	5.90	-4.49
0.11	0.05	2.10	-29.72	3.06	-4.63	-4.71
0.10	0.07	1.52	-48.77	-5.78	5.55	6.62
0.10	0.02	5.82	-33.84	-1.39	4.18	7.66
0.10	0.04	2.75	-23.37	-2.26	3.76	-0.48
0.10	0.04	2.36	-28.44	-3.76	3.20	-3.83
0.11	0.08	1.36	-27.35	-9.40	2.14	-9.35
0.12	0.19	0.65	-26.78	-24.07	1.70	-6.37
0.20	0.21	0.98	-26.42	-23.82	1.13	0.16
0.24	0.23	1.08	-27.26	-21.44	1.18	-13.84
0.29	0.24	1.20	-31.53	-23.63	1.12	-14.19
0.32	0.40	0.82	-36.96	-50.41	0.89	-8.30
0.30	0.31	0.98	-26.34	-26.16	1.03	3.35
0.33	0.34	0.98	-25.98	-26.18	1.02	-2.66
0.37	0.33	1.11	-24.36	-27.18	0.81	-11.24
0.40	0.37	1.11	-25.00	-27.99	0.81	-27.19
0.48	0.39	1.23	-23.41	-19.00	1.01	-37.10
0.65	0.29	2.22	-32.45	-19.52	0.75	-45.86
0.50	0.32	1.57	-30.95	-24.35	0.81	-9.57
0.49	0.31	1.60	-31.36	-21.40	0.92	3.53
0.58	0.32	1.78	-28.26	-20.17	0.79	17.03
0.45	0.30	1.49	-27.06	-14.93	1.22	10.38
0.40	0.22	1.78	-15.87	-7.16	1.25	8.53
0.39	0.23	1.70	-13.82	-5.54	1.47	5.00
0.50	0.44	1.14	-23.22	9.62	-2.13	2.81
0.78	0.49	1.60	-26.52	17.07	-0.97	13.65
0.92	0.58	1.57	-10.46	30.42	-0.22	14.63
0.69	0.79	0.87	21.57	66.25	0.37	22.02
0.95	0.84	1.13	47.91	105.58	0.40	35.75
1.00	0.78	1.29	70.75	115.85	0.47	33.64
0.83	0.79	1.06	73.39	130.91	0.53	45.34
0.67	0.87	0.78	96.09	168.82	0.73	15.64
0.76	0.67	1.13	165.38	147.24	0.99	11.51
0.54	0.71	0.76	90.47	175.15	0.68	18.59

0.59	0.74	0.80	87.08	175.27	0.62	20.29
0.53	0.73	0.73	63.08	186.11	0.46	-15.73
0.52	0.70	0.74	10.84	221.75	0.07	53.95
0.65	0.76	0.86	52.22	229.05	0.27	114.50
0.70	0.78	0.90	25.24	224.62	0.13	98.44
0.65	0.58	1.12	4.37	164.33	0.02	15.53
0.48	0.33	1.46	-5.60	118.56	-0.03	90.56
0.27	0.26	1.04	7.37	115.92	0.06	44.70
0.29	0.51	0.58	6.88	228.61	0.05	38.42
0.44	0.28	1.55	14.66	135.22	0.07	65.20
0.34	0.36	0.95	-3.44	159.53	-0.02	71.81
0.40	0.61	0.65	-0.52	223.82	0.00	63.30
0.39	0.95	0.41	-10.30	371.27	-0.07	61.43
0.50	1.03	0.49	-101.96	347.88	-0.60	52.47
0.53	0.99	0.54	-81.51	330.15	-0.46	-2.56
0.43	0.88	0.49	-26.19	237.24	-0.22	0.35
0.43	0.85	0.51	-43.15	242.45	-0.35	-1.03
0.46	0.82	0.55	-31.57	229.05	-0.25	8.38

0.08	0.08	1.03	4.63	14.53	0.31	8.99
0.04	0.22	0.17	-1.34	55.00	-0.15	-26.46
0.14	0.28	0.49	-2.48	65.51	-0.08	15.37
0.12	0.30	0.41	7.50	80.77	0.23	11.52
0.11	0.30	0.36	10.58	91.69	0.32	10.55
0.13	0.22	0.59	11.02	84.66	0.22	11.71
0.16	0.33	0.48	15.22	97.24	0.33	4.03
0.20	0.33	0.58	17.31	91.10	0.33	-0.94
0.16	0.39	0.41	13.52	126.46	0.26	0.78

0.24	0.22	1.12	-11.14	1.71	-5.82	-0.84
0.26	0.32	0.82	-15.05	3.58	-5.12	2.68
0.38	0.30	1.26	-24.30	0.97	-19.84	7.75
0.25	0.36	0.71	-16.81	-1.65	14.46	26.99
0.30	0.28	1.06	-2.43	-0.88	2.62	14.91
0.26	0.37	0.69	-2.04	-0.10	30.06	14.46
0.26	0.34	0.76	-4.14	-3.44	1.59	9.56
0.27	0.29	0.92	-5.65	-3.43	1.79	6.66
0.28	0.30	0.93	-7.41	-5.84	1.36	6.65
0.32	0.34	0.93	-9.79	-9.56	1.10	15.54
0.33	0.38	0.86	-10.74	-14.71	0.85	16.71
0.37	0.30	1.23	-13.88	-12.17	0.92	9.74
0.32	0.33	0.96	-15.01	-15.22	1.03	4.66
0.35	0.28	1.27	-20.24	-15.03	1.06	-1.83
0.37	0.33	1.12	-22.06	-20.74	0.95	-6.19
0.37	0.29	1.29	-24.24	-19.55	0.96	-9.58
0.40	0.29	1.39	-25.72	-18.86	0.98	-15.05
0.35	0.23	1.51	-28.81	-18.37	1.04	-11.94
0.37	0.32	1.17	-29.97	-21.59	1.19	-6.44
0.36	0.30	1.20	-25.01	-21.26	0.98	-7.70

0.30	0.31	0.99	-13.95	-21.49	0.66	-7.60
0.28	0.26	1.08	-14.90	-18.12	0.76	-8.45
0.29	0.27	1.06	-12.99	-24.34	0.50	-11.55
0.26	0.23	1.11	-8.39	-18.09	0.42	-10.46
0.25	0.21	1.15	-7.76	-16.99	0.40	-8.05
0.25	0.22	1.15	-9.42	-13.47	0.61	-8.11
0.26	0.22	1.17	-7.29	-19.98	0.31	-11.05
0.27	0.24	1.12	-5.30	-23.79	0.20	-15.96
						#DIV/0!
0.16	0.13	1.23	7.64	16.99	0.36	-4.63
0.21	0.15	1.41	17.57	23.97	0.52	-8.40
0.26	0.24	1.09	5.26	32.80	0.15	-0.85
0.27	0.21	1.29	12.16	29.14	0.32	7.20
0.27	0.24	1.12	13.68	34.46	0.35	18.02
0.20	0.13	1.55	3.47	38.98	0.06	24.55
0.20	0.18	1.13	16.84	38.82	0.39	16.53
0.19	0.16	1.16	12.49	55.02	0.19	16.79
0.15	0.27	0.54	14.93	51.93	0.53	7.79
0.11	0.19	0.60	12.71	41.41	0.51	4.02
0.15	0.23	0.67	9.95	47.67	0.31	-3.13
0.12	0.16	0.74	12.89	47.87	0.36	-2.31
0.17	0.22	0.75	21.10	44.79	0.63	-6.38
0.13	0.19	0.71	12.08	38.57	0.44	-1.49
0.10	0.27	0.38	6.22	-1.25	-13.08	1.37
0.16	0.24	0.67	5.81	-2.24	-3.86	5.49
0.13	0.30	0.44	-9.08	-4.08	5.11	0.65
0.10	0.29	0.36	-5.39	-7.32	2.06	-0.96
0.11	0.16	0.69	-8.88	-15.13	0.85	-2.69
0.10	0.12	0.88	-8.40	-13.61	0.70	-3.06
0.09	0.18	0.48	-7.78	-15.54	1.05	-1.96
0.10	0.19	0.54	-11.50	-18.65	1.15	-2.21
0.09	0.24	0.37	-10.81	-23.05	1.27	-2.44
0.09	0.20	0.45	-10.84	-24.50	0.99	-1.39
0.14	0.20	0.71	-17.24	-19.97	1.22	-2.67
0.17	0.26	0.63	-17.55	-29.40	0.95	-1.93
0.15	0.25	0.60	-9.72	-24.75	0.65	-5.26
0.13	0.19	0.69	-12.52	-20.28	0.90	-6.18
0.18	0.23	0.77	-16.20	-28.68	0.73	-9.68
0.19	0.22	0.85	-14.00	-25.10	0.65	-11.88
0.22	0.26	0.82	-13.15	-29.10	0.55	-13.37
0.16	0.28	0.58	-12.85	-28.95	0.77	-7.85
0.12	0.19	0.65	-11.20	-20.62	0.84	-5.07
0.08	0.19	0.44	-6.89	-17.66	0.89	-3.61
0.05	0.13	0.43	-5.34	-12.83	0.96	-1.94
0.07	0.13	0.58	-7.17	-10.18	1.22	-2.50
0.10	0.17	0.57	-6.77	-12.84	0.92	-3.60
0.11	0.19	0.61	-6.96	-18.65	0.61	-4.65
0.09	0.19	0.45	-6.12	-18.70	0.72	-3.10
0.10	0.16	0.65	-8.56	-16.24	0.81	-2.87
0.09	0.19	0.50	-7.35	-16.49	0.89	-2.54
0.15	0.20	0.76	-11.12	-15.36	0.96	-2.53

0.13	0.21	0.62	-10.92	-19.31	0.92	-2.96
0.13	0.19	0.68	-9.53	-18.50	0.76	-2.97
0.13	0.18	0.70	-10.45	-15.73	0.95	-3.46
0.11	0.20	0.55	-9.59	-16.73	1.05	-2.91
0.11	0.18	0.64	-10.57	-16.81	0.98	-2.45
0.10	0.20	0.51	-9.51	-16.32	1.13	-3.08
0.11	0.20	0.56	-9.83	-16.35	1.07	-4.36
0.14	0.19	0.72	-14.42	-18.35	1.09	-6.16
0.14	0.19	0.74	-13.71	-22.99	0.80	-8.34
0.15	0.16	0.96	-15.51	-17.63	0.92	-8.94
0.15	0.20	0.76	-13.76	-20.16	0.90	-11.16
0.17	0.20	0.84	-12.70	-21.74	0.69	-18.82
0.18	0.23	0.80	-12.28	-21.30	0.72	-26.38
0.17	0.21	0.81	-11.71	-19.47	0.75	-29.15
0.17	0.23	0.75	-11.80	-17.83	0.88	-28.55
0.17	0.23	0.76	-9.46	-19.32	0.64	-29.11
0.15	0.28	0.54	-9.27	-22.53	0.76	-21.63
0.18	0.22	0.81	-12.77	-21.06	0.75	-21.32
0.17	0.26	0.68	-11.32	-24.08	0.69	-24.48
0.18	0.23	0.78	-11.17	-18.41	0.77	-27.42
0.21	0.26	0.79	-9.52	-18.81	0.64	-29.17
0.20	0.23	0.88	-7.36	-11.83	0.71	-29.25
0.29	0.22	1.32	-11.40	-12.16	0.71	-36.87
0.28	0.25	1.12	-9.66	-8.87	0.98	-35.16
0.33	0.25	1.28	3.51	1.72	1.59	-35.84
0.29	0.31	0.92	6.13	8.61	0.77	-16.21
0.24	0.27	0.91	9.39	12.44	0.83	-2.65
0.25	0.24	1.07	16.03	12.49	1.20	-2.83
0.19	0.24	0.81	19.12	22.78	1.04	-1.14
0.18	0.25	0.70	17.10	25.83	0.95	-2.82
0.15	0.18	0.83	8.93	18.65	0.57	-4.24
0.18	0.20	0.90	12.29	28.46	0.48	-12.06
0.22	0.20	1.10	7.71	20.38	0.34	-9.84
0.23	0.23	1.01	21.71	37.43	0.57	-6.70
0.20	0.24	0.86	23.42	38.78	0.71	-4.17
0.20	0.28	0.70	27.48	53.58	0.73	-4.71
0.19	0.28	0.67	44.40	63.85	1.04	-2.81
0.21	0.25	0.86	41.33	47.26	1.02	1.28
0.18	0.28	0.65	11.88	19.15	0.96	20.12
0.20	0.25	0.80	4.25	10.00	0.53	8.57

Le (measured)	phi (w)		phi (M)	phi(H or W)	phi (M,H,W) We	phi(M) Dyer
125.78	-0.01		0.60	0.44	-1.37	0.57
146.33	0.07		0.46	0.31	-3.40	0.50
160.10	0.15		0.50	0.34	-0.12	0.67
205.31	0.15		0.47	0.32	-0.58	0.62
240.74	0.08		0.39	0.25	-1.91	0.54
257.34	0.09		0.43	0.28	-2.25	0.53
250.21	0.11		0.45	0.30	-1.21	0.58
262.44	0.11		0.42	0.27	-0.62	0.62
230.90	0.12		0.36	0.23	-0.41	0.64
221.64	0.04		0.69	0.52	-1.84	0.55
220.17	0.04		0.37	0.24	-1.97	0.54
493.83	-0.01		3.19	4.78	-3.90	0.48
365.85	-0.02		3.37	5.12	-10.98	0.39
463.45	0.04		1.71	2.18	-5.15	0.46
321.21	-0.03		5.59	9.42	-0.49	0.63
279.98	-0.07		2.51	3.56	0.56	0.79
139.75	-0.08		1.26	1.40	-0.16	0.66

Le (measured)	phi (w)		phi (M)	phi(H or W)	phi (M,H,W) We	phi(M) Dyer
39.08	1.18		1.28	1.43	2.09	stable
64.47	0.98		1.23	1.33	1.47	stable
35.20	1.10		1.39	1.63	1.80	stable
11.08	2.83		1.36	1.58	2.38	stable
39.61	0.97		1.52	1.86	0.72	0.84
11.87	1.84		1.46	1.74	4.01	stable
2.79	6.12		4.63	7.51	2.00	stable
35.27	0.90		1.61	2.00	3.05	stable
9.81	2.32		3.37	5.10	1.10	stable
43.13	0.77		1.64	2.06	2.57	stable
42.67	1.12		1.23	1.34	1.57	stable
38.84	0.94		1.12	1.14	1.61	stable
54.00	0.90		1.12	1.14	1.20	stable
43.40	0.85		1.21	1.31	1.34	stable
212.25	0.53		1.77	2.27	-0.35	0.64
224.77	0.44		1.40	1.65	-0.12	0.67
213.68	0.33		1.56	1.92	-1.94	0.54
215.92	0.18		0.55	0.39	-3.69	0.49
169.40	0.03		0.37	0.24	-0.71	0.61
225.56	0.36		0.44	0.29	0.21	0.72
206.17	0.22		0.60	0.43	-1.30	0.57
191.35	0.33		0.47	0.32	-0.20	0.66
183.35	0.27		0.43	0.28	-0.92	0.60
217.89	0.22		0.52	0.36	-0.81	0.61
205.89	0.40		0.47	0.32	0.35	0.74
205.73	0.75		0.61	0.44	0.66	0.82
201.32	0.46		0.54	0.38	0.76	0.86
154.79	0.36		0.63	0.46	0.80	0.87
69.67	0.90		0.58	0.41	-1.68	0.56

103.86	0.41	0.48	0.33	-5.08	0.46
147.17	0.42	0.40	0.26	-2.03	0.54
137.03	0.66	0.48	0.33	-1.39	0.57
145.20	1.02	0.57	0.41	0.12	0.70
131.53	0.93	0.89	0.74	0.76	0.86
121.02	1.02	0.80	0.63	0.75	0.85
122.75	1.02	0.75	0.58	0.83	0.89
97.05	1.00	0.79	0.63	0.85	0.90
87.32	1.03	0.91	0.77	0.90	0.93
44.03	1.81	0.89	0.74	0.92	0.94
30.40	2.01	0.95	0.82	0.90	0.93

31.02	1.56	0.77	0.60	0.86	0.90
30.53	-0.03	0.83	0.67	0.84	0.89
28.03	-0.13	0.83	0.67	0.80	0.87
34.64	-0.10	0.85	0.69	0.84	0.89
23.30	-0.27	0.88	0.72	0.76	0.86
32.23	0.29	0.70	0.53	0.84	0.89
41.06	0.11	0.70	0.53	0.82	0.88
28.70	0.54	0.71	0.54	0.83	0.89
49.48	0.47	0.71	0.53	0.86	0.91
46.09	0.84	0.89	0.74	0.91	0.93
43.48	1.57	0.94	0.80	0.95	0.96
33.01	1.54	0.87	0.71	0.92	0.94
32.82	1.10	0.85	0.69	0.95	0.96
24.89	1.77	0.86	0.70	0.93	0.95
23.05	1.99	0.90	0.74	0.94	0.95
23.64	1.96	0.88	0.72	0.95	0.96
23.57	1.05	0.77	0.60	0.94	0.95
11.21	2.06	0.84	0.68	0.97	0.97
7.82	3.62	0.84	0.68	0.97	0.98
4.54	2.97	0.85	0.69	0.99	0.99
-4.67	-2.12	0.95	0.82	1.03	stable
-2.61	0.27	1.18	1.25	1.04	stable
-4.16	2.72	1.25	1.38	1.07	stable
-8.67	-1.80	1.48	1.78	1.09	stable
-9.65	0.18	1.63	2.04	1.11	stable
-6.01	-0.59	1.58	1.96	1.17	stable
-11.49	-0.52	1.81	2.36	1.09	stable
-10.85	0.20	2.35	3.28	1.33	stable
-16.56	1.33	2.27	3.14	1.17	stable
-8.41	1.98	1.39	1.63	1.22	stable
-3.48	4.68	1.18	1.25	1.66	stable
-5.92	2.61	1.08	1.05	1.71	stable
-4.49	4.29	1.13	1.16	1.21	stable
-7.19	1.50	1.06	1.02	2.50	stable
-4.55	1.79	1.01	0.90	2.40	stable
-5.12	1.32	1.03	0.95	3.05	stable
-5.86	1.17	1.03	0.96	2.40	stable
-9.54	0.62	1.02	0.92	2.43	stable

-6.20	0.53	1.07	1.03	2.27	stable
-3.95	0.68	0.73	0.56	6.35	stable
-5.93	0.65	0.59	0.42	1.55	stable
17.59	0.02	0.31	0.19	0.24	0.72
-8.88	-0.02	1.14	1.17	4.34	stable
0.00	721.14	2.34	3.27	1.44	stable
-4.42	-1.21	1.09	1.08	1.70	stable
-3.82	-1.00	1.08	1.05	1.62	stable
-6.48	1.21	1.03	0.94	2.20	stable
-4.93	2.88	1.01	0.90	2.09	stable
-6.60	2.02	1.01	0.91	2.04	stable
-6.94	0.94	0.98	0.85	2.89	stable
-10.63	0.38	0.97	0.85	2.30	stable
-7.49	0.58	0.99	0.87	2.19	stable
-11.12	0.52	0.98	0.86	3.49	stable
-5.62	0.87	0.92	0.78	2.56	stable
-11.44	0.26	0.99	0.87	2.91	stable
-3.32	1.39	1.13	1.16	2.06	stable
-6.75	0.81	1.06	1.01	2.51	stable
-7.38	1.05	1.06	1.01	2.11	stable
-10.13	0.88	1.04	0.98	2.40	stable
-10.91	0.44	1.04	0.98	3.37	stable
-6.46	0.84	2.44	3.43	3.12	stable
9.37	-0.28	11.15	21.61	0.38	0.75
15.72	0.14	1.18	1.25	1.49	stable
-0.13	-60.83	1.09	1.08	1.31	stable
11.03	1.34	1.07	1.04	0.92	0.94
14.29	0.87	1.04	0.97	0.25	0.72
37.13	0.44	1.05	0.99	-0.23	0.66
53.23	-0.05	1.01	0.92	0.08	0.70
85.40	-0.18	0.82	0.66	0.65	0.82
94.69	0.00	0.79	0.63	0.66	0.82
113.72	-0.14	0.78	0.61	0.63	0.81
113.90	-0.20	0.77	0.61	0.36	0.74
92.61	-0.58	0.72	0.55	0.71	0.84
115.24	-0.01	0.59	0.42	0.31	0.73
114.80	-0.10	0.55	0.39	0.28	0.73
176.53	-0.17	0.51	0.36	0.41	0.75
147.34	-0.35	0.57	0.41	0.52	0.78
101.65	-0.26	0.35	0.22	-2.33	0.53
165.17	-0.06	0.19	0.10	-0.34	0.65
182.07	0.05	0.38	0.25	0.40	0.75
122.51	-0.16	0.73	0.56	-0.46	0.63
143.58	0.09	0.69	0.52	0.72	0.84
197.28	0.80	0.41	0.27	1.04	stable
117.13	0.29	0.14	0.07	0.35	0.74
105.78	0.34	0.48	0.33	0.62	0.81
148.47	0.30	0.79	0.62	0.81	0.88
101.28	0.22	0.78	0.61	0.70	0.83
65.00	0.02	0.43	0.28	0.64	0.82
70.59	-0.08	0.72	0.55	0.84	0.90
48.53	-0.03	0.65	0.48	0.87	0.91

40.79	0.04	0.90	0.75	1.03	stable
34.09	0.25	0.83	0.67	1.02	stable
26.19	0.48	0.73	0.56	1.05	stable
24.78	0.79	0.95	0.82	1.06	stable
19.34	0.96	0.96	0.83	1.08	stable
13.90	0.52	0.94	0.80	1.26	stable
9.99	0.61	0.19	0.10	1.11	stable
8.07	1.69	0.53	0.37	1.46	stable
16.90	0.35	1.22	1.33	1.32	stable
31.05	-5585993.53	1.03	0.96	1.30	stable
30.13	0.34	0.84	0.68	1.29	stable
44.07	0.11	0.95	0.81	1.25	stable
37.90	0.09	1.00	0.90	1.22	stable
19.68	0.02	0.95	0.82	1.42	stable
17.68	-0.03	0.95	0.81	1.58	stable
19.93	-0.09	0.91	0.76	1.63	stable
23.86	-0.11	0.96	0.82	1.50	stable
17.29	-0.18	0.78	0.61	1.63	stable
14.52	-0.31	0.77	0.60	1.55	stable
8.35	-0.37	0.91	0.76	3.71	stable
9.06	0.51	0.96	0.83	2.10	stable
7.28	0.05	0.93	0.79	2.06	stable
8.47	-0.16	0.65	0.48	1.73	stable
5.06	1.02	0.78	0.61	1.44	stable
6.03	2.70	0.89	0.74	1.13	stable
-0.50	-34.05	1.13	1.14	1.30	stable
-1.94	-9.96	1.20	1.29	1.24	stable
-4.95	-2.97	1.26	1.40	1.30	stable
-3.62	-2.67	1.28	1.43	1.73	stable
-4.95	-2.56	1.24	1.37	1.45	stable
-6.71	-2.91	1.19	1.26	1.29	stable
-5.04	-3.36	1.21	1.31	1.30	stable
-2.51	-4.51	1.17	1.23	1.41	stable
-7.81	-2.18	1.14	1.17	1.16	stable
-5.14	-3.87	1.13	1.16	1.06	stable
15.36	1.67	1.04	0.97	1.01	stable
-3.36	-8.49	1.06	1.02	1.02	stable
-4.26	-4.88	1.09	1.07	1.08	stable
-10.11	-1.08	1.28	1.43	1.18	stable
-1.64	-1.54	1.30	1.47	1.25	stable
0.20	1.97	1.31	1.49	2.88	stable
-1.34	-3.27	1.10	1.09	1.39	stable
-1.69	-4.61	1.17	1.23	1.28	stable
-0.03	-242.66	1.22	1.32	1.15	stable
0.67	17.23	1.32	1.51	1.40	stable
-1.28	-16.99	1.77	2.28	1.34	stable
32.17	1.64	1.42	1.68	1.13	stable
51.69	0.85	1.18	1.24	0.97	0.97
70.46	-0.42	1.08	1.06	0.93	0.95
66.61	0.02	1.04	0.97	0.87	0.91
64.96	0.18	1.02	0.94	0.87	0.91
78.50	0.28	1.02	0.93	0.84	0.90

79.03	0.40	1.02	0.93	0.70	0.84
91.32	0.48	1.04	0.97	0.50	0.77
100.42	0.47	1.04	0.98	0.58	0.79
83.64	-0.85	1.02	0.92	0.93	0.95
75.94	-0.27	1.03	0.95	0.84	0.89
53.81	-0.05	1.00	0.88	0.98	0.98
48.31	-3.16	0.95	0.81	1.00	1.00
44.89	-7.90	0.95	0.81	0.94	0.95
66.86	-6.48	0.97	0.84	0.94	0.95
59.78	-3.58	0.95	0.82	0.97	0.97
77.17	-2.36	1.05	1.00	0.92	0.94
104.95	-3.06	0.96	0.83	0.90	0.92
128.56	-2.19	0.84	0.68	0.93	0.94
284.16	0.22	1.26	1.39	0.65	0.82
251.48	0.27	0.91	0.76	0.76	0.86
337.26	0.33	0.95	0.81	0.89	0.92
445.69	0.08	0.91	0.76	0.89	0.92
554.62	-0.02	0.92	0.77	0.90	0.92
550.04	-0.05	0.88	0.73	0.89	0.92
577.06	-0.01	0.83	0.66	0.92	0.94
382.10	-0.04	0.78	0.62	0.86	0.90
408.58	0.02	0.86	0.70	0.87	0.91
298.08	0.05	0.80	0.64	0.86	0.90
364.60	0.05	0.83	0.67	0.90	0.92
362.57	0.06	0.85	0.69	0.90	0.93
379.73	0.38	0.95	0.82	0.95	0.96
275.11	0.29	0.96	0.82	0.95	0.96
319.31	0.23	0.97	0.85	0.96	0.97
249.62	0.34	0.99	0.87	0.97	0.97
201.42	0.41	0.99	0.87	0.96	0.96
205.64	0.31	1.00	0.88	0.97	0.97
155.46	0.27	1.01	0.90	0.98	0.98
133.03	0.19	1.01	0.91	0.98	0.98
102.60	0.22	1.01	0.92	0.98	0.99
77.69	-0.01	1.02	0.93	0.99	0.99
113.99	-0.61	0.60	0.43	0.23	0.72
92.85	0.30	0.74	0.57	0.10	0.70
119.71	-2.13	0.77	0.60	0.53	0.78
160.76	0.29	0.74	0.57	0.39	0.75
155.51	0.16	0.63	0.46	-0.51	0.63
221.24	0.13	0.66	0.49	-0.78	0.61
231.54	0.14	0.67	0.50	-0.18	0.66
182.87	0.17	0.63	0.46	-0.91	0.60
202.61	0.16	0.74	0.57	-0.89	0.60
166.65	0.24	0.50	0.34	0.20	0.71
218.04	0.26	0.53	0.37	0.76	0.86
211.44	0.20	0.77	0.60	0.06	0.69
306.96	0.25	0.80	0.63	0.50	0.78
297.17	0.35	0.85	0.69	0.59	0.80

220.99	0.36	0.87	0.72	0.57	0.79
231.04	0.32	0.82	0.66	0.62	0.81
221.83	0.25	0.84	0.68	0.58	0.80
216.13	0.27	0.90	0.76	0.69	0.83
175.32	0.31	0.92	0.78	0.72	0.84
178.85	0.32	0.93	0.79	0.82	0.88
214.85	0.25	0.87	0.71	0.74	0.85
47.63	59.12	1.58	1.95	1.61	stable
31.19	0.18	1.38	1.61	1.53	stable
16.16	-0.29	1.46	1.75	0.59	0.80
8.39	-1.97	4.27	6.82	-0.84	0.60
25.06	-0.59	1.72	2.20	2.50	stable
26.61	-0.26	1.83	2.38	1.36	stable
23.18	-0.05	1.57	1.95	2.09	stable
8.30	-0.08	1.69	2.15	3.24	stable
8.78	-0.43	1.57	1.94	3.54	stable
4.71	-0.62	1.97	2.63	5.18	stable
1.54	-1.44	1.81	2.35	2.27	stable
-5.98	0.37	1.94	2.57	-0.72	0.61
3.78	1.15	2.53	3.60	3.31	stable
0.00	425.01	2.20	3.01	30.63	stable
0.56	-0.31	2.03	2.72	6.56	stable
1.99	-0.81	2.15	2.93	6.71	stable
7.69	-0.89	1.91	2.52	2.87	stable
21.64	-0.45	1.74	2.23	1.39	stable
15.95	0.01	1.26	1.39	1.30	stable
14.01	-0.92	1.17	1.22	1.21	stable
16.64	-0.71	1.12	1.13	1.18	stable
49.03	-0.21	1.10	1.10	1.09	stable
18.25	0.19	1.09	1.08	1.10	stable
23.10	-0.12	1.07	1.03	1.07	stable
25.56	-0.40	1.05	0.99	1.08	stable
36.73	-0.67	1.04	0.97	1.06	stable
21.18	-1.43	1.02	0.93	1.04	stable
32.91	-0.63	1.01	0.91	1.08	stable
35.71	-0.17	1.03	0.94	1.08	stable
37.37	0.06	1.03	0.94	1.08	stable
32.80	0.29	1.02	0.92	1.06	stable
28.59	0.24	1.03	0.95	1.06	stable
21.07	0.23	1.03	0.94	1.06	stable
30.83	0.10	1.02	0.94	1.03	stable
43.37	0.06	1.02	0.93	0.98	0.99
35.80	0.24	1.01	0.90	0.98	0.98
58.44	0.16	1.00	0.89	0.98	0.98
115.97	0.22	0.99	0.88	0.98	0.99
138.80	0.23	0.99	0.88	0.98	0.98
134.98	0.19	0.99	0.87	0.97	0.98
145.06	0.30	0.99	0.87	0.97	0.98
184.38	0.11	0.97	0.84	0.97	0.98
161.69	0.06	0.96	0.83	0.95	0.96
197.70	0.12	0.95	0.81	0.95	0.96

185.20	0.14	0.96	0.83	0.95	0.96
219.97	-0.10	0.96	0.83	0.95	0.96
255.31	0.29	0.99	0.87	0.93	0.94
296.33	0.45	0.98	0.86	0.94	0.95
314.59	0.35	0.99	0.87	0.95	0.96
221.40	0.06	1.00	0.88	0.90	0.93
154.49	0.40	1.01	0.90	0.63	0.81
157.69	0.27	0.97	0.84	0.29	0.73
327.76	0.20	0.97	0.85	0.81	0.88
164.65	0.26	0.98	0.86	0.35	0.74
234.79	0.32	1.01	0.90	0.62	0.81
295.83	0.33	1.00	0.89	0.89	0.92
356.90	0.42	1.02	0.93	0.95	0.96
287.47	0.37	1.08	1.05	0.97	0.97
313.92	-0.02	1.05	1.00	0.96	0.97
226.84	0.00	1.03	0.96	0.96	0.97
223.27	-0.01	1.05	1.00	0.96	0.96
234.89	0.06	1.03	0.96	0.95	0.96

48.50	0.18	0.65	0.48	-2.58	0.52
182.57	-0.88	2.15	2.94	0.32	0.74
186.71	0.17	1.09	1.07	0.64	0.81
244.30	0.11	0.76	0.59	0.61	0.80
263.24	0.11	0.65	0.48	0.57	0.79
243.58	0.08	0.73	0.56	0.03	0.69
321.43	0.03	0.77	0.60	0.66	0.82
296.54	-0.01	0.83	0.67	0.69	0.83
378.09	0.00	0.80	0.63	0.74	0.85

45.96	-0.02	1.07	1.04	0.95	0.96
60.22	0.05	1.08	1.05	0.97	0.98
57.03	0.11	1.04	0.98	0.98	0.98
70.06	0.55	1.10	1.09	0.99	0.99
63.89	0.22	1.01	0.91	0.98	0.99
72.48	0.29	1.01	0.91	0.99	0.99
35.44	0.36	1.02	0.94	1.00	stable
60.84	0.12	1.03	0.95	1.00	1.00
67.92	0.11	1.03	0.96	1.00	stable
73.47	0.23	1.03	0.95	1.01	stable
81.81	0.24	1.03	0.95	1.02	stable
56.12	0.14	1.03	0.94	1.04	stable
55.25	0.09	1.04	0.98	1.04	stable
48.58	-0.03	1.05	0.98	1.07	stable
57.72	-0.10	1.04	0.98	1.06	stable
47.70	-0.16	1.05	0.99	1.09	stable
41.51	-0.26	1.04	0.97	1.08	stable
39.05	-0.20	1.06	1.02	1.15	stable
45.58	-0.12	1.06	1.00	1.07	stable
41.74	-0.15	1.05	1.00	1.09	stable

41.72	-0.18	1.05	0.99	1.08	stable
34.14	-0.23	1.07	1.02	1.11	stable
42.47	-0.26	1.05	1.00	1.14	stable
30.83	-0.31	1.05	0.99	1.15	stable
31.09	-0.22	1.05	0.99	1.19	stable
23.62	-0.30	1.06	1.01	1.14	stable
33.58	-0.28	1.04	0.98	1.20	stable
37.68	-0.38	1.03	0.94	1.19	stable
55.32	-0.07	0.85	0.69	-0.11	0.67
61.50	-0.10	0.86	0.70	0.06	0.69
90.86	-0.01	0.97	0.85	0.70	0.84
74.28	0.07	0.95	0.81	0.61	0.81
98.55	0.16	0.94	0.80	0.70	0.83
97.89	0.16	0.96	0.83	-1.23	0.58
102.88	0.14	0.85	0.68	0.10	0.70
133.33	0.11	0.86	0.71	-0.58	0.62
123.57	0.12	0.74	0.57	0.68	0.83
104.73	0.06	0.65	0.48	0.20	0.71
124.95	-0.04	0.82	0.65	0.49	0.77
114.14	-0.03	0.67	0.50	-0.50	0.63
124.66	-0.07	0.75	0.58	0.48	0.77
107.99	-0.02	0.73	0.56	0.24	0.72
46.51	0.08	0.72	0.55	0.99	0.99
68.07	0.12	0.90	0.75	0.98	0.98
61.90	0.02	1.30	1.48	1.00	1.00
41.46	-0.06	1.36	1.58	1.02	stable
34.03	-0.11	1.47	1.76	1.41	stable
24.58	-0.14	1.50	1.81	1.94	stable
29.62	-0.14	1.64	2.06	1.26	stable
24.72	-0.17	1.64	2.06	1.32	stable
32.53	-0.20	1.78	2.29	1.18	stable
28.02	-0.11	1.74	2.22	1.32	stable
23.44	-0.16	1.41	1.66	1.27	stable
31.69	-0.10	1.29	1.45	1.18	stable
27.14	-0.32	1.24	1.35	1.19	stable
20.33	-0.44	1.39	1.63	1.34	stable
29.68	-0.42	1.22	1.33	1.26	stable
28.41	-0.49	1.17	1.23	1.25	stable
38.94	-0.42	1.12	1.13	1.18	stable
34.92	-0.39	1.24	1.35	1.14	stable
24.30	-0.32	1.40	1.64	1.32	stable
21.39	-0.38	1.69	2.14	1.31	stable
15.25	-0.29	2.22	3.05	1.73	stable
11.05	-0.39	1.83	2.39	1.53	stable
16.67	-0.38	1.48	1.79	1.30	stable
26.04	-0.29	1.33	1.53	1.31	stable
26.54	-0.26	1.55	1.91	1.29	stable
25.47	-0.17	1.48	1.78	1.43	stable
27.01	-0.19	1.55	1.90	1.28	stable
25.91	-0.13	1.26	1.40	1.22	stable

31.04	-0.15	1.34	1.54	1.21	stable
29.99	-0.15	1.34	1.54	1.31	stable
24.93	-0.20	1.37	1.59	1.29	stable
28.10	-0.19	1.47	1.76	1.22	stable
21.42	-0.18	1.47	1.77	1.35	stable
19.60	-0.31	1.56	1.92	1.24	stable
18.80	-0.41	1.44	1.71	1.22	stable
19.70	-0.44	1.37	1.60	1.28	stable
21.41	-0.53	1.34	1.53	1.36	stable
14.25	-0.65	1.33	1.53	1.53	stable
14.44	-1.02	1.32	1.50	1.32	stable
17.90	-1.25	1.22	1.32	1.32	stable
16.43	-2.00	1.17	1.23	1.21	stable
16.09	-2.25	1.20	1.29	1.25	stable
13.93	-2.72	1.19	1.27	1.17	stable
18.60	-2.05	1.16	1.21	1.19	stable
20.98	-1.89	1.22	1.33	1.13	stable
15.90	-1.65	1.18	1.25	1.22	stable
15.60	-2.31	1.18	1.25	1.17	stable
15.45	-2.27	1.16	1.21	1.17	stable
18.50	-1.98	1.10	1.09	1.12	stable
17.35	-1.92	1.08	1.05	1.10	stable
18.93	-1.47	1.05	0.98	1.13	stable
26.92	-1.17	1.04	0.98	1.06	stable
38.56	-0.73	0.99	0.87	0.97	0.98
61.60	-0.28	0.98	0.85	0.95	0.96
50.48	-0.06	0.94	0.81	0.91	0.93
65.75	-0.04	0.92	0.77	0.86	0.91
72.46	-0.02	0.82	0.65	0.78	0.86
84.15	-0.05	0.80	0.64	0.79	0.87
66.81	-0.08	0.83	0.67	0.60	0.80
78.53	-0.17	0.85	0.69	0.55	0.79
62.39	-0.14	0.94	0.80	0.67	0.82
95.17	-0.07	0.87	0.72	0.62	0.81
95.65	-0.05	0.82	0.65	0.65	0.82
133.16	-0.05	0.79	0.62	0.71	0.84
148.69	-0.03	0.70	0.52	0.65	0.82
117.39	0.01	0.76	0.59	0.63	0.81
121.82	0.26	0.85	0.69	0.86	0.91
79.81	0.13	0.95	0.82	0.90	0.92

phi(M) Businger	**phi(H) Dyer**	**phi(H) Businger**
0.58	0.33	0.31
0.50	0.25	0.24
0.68	0.45	0.41
0.63	0.39	0.36
0.55	0.30	0.28
0.54	0.28	0.27
0.59	0.34	0.32
0.63	0.38	0.36
0.65	0.41	0.38
0.56	0.30	0.29
0.55	0.29	0.28
0.49	0.23	0.23
0.40	0.15	0.15
0.46	0.21	0.20
0.64	0.40	0.37
0.80	0.63	0.54
0.67	0.44	0.41

phi(M) Businger	phi(H) Dyer	phi(H) Businger
1.72	stable	1.72
1.16	stable	1.16
1.46	stable	1.46
1.99	stable	1.99
0.85	0.71	0.59
3.46	stable	3.46
1.65	stable	1.65
2.60	stable	2.60
0.83	stable	0.83
2.16	stable	2.16
1.26	stable	1.26
1.29	stable	1.29
0.92	stable	0.92
1.05	stable	1.05
0.65	0.42	0.38
0.68	0.45	0.41
0.55	0.30	0.28
0.50	0.24	0.23
0.62	0.38	0.35
0.72	0.51	0.46
0.58	0.33	0.31
0.67	0.44	0.40
0.61	0.36	0.34
0.61	0.37	0.34
0.75	0.55	0.49
0.83	0.67	0.57
0.86	0.74	0.61
0.88	0.76	0.62
0.56	0.31	0.29

0.47	0.21	0.20
0.55	0.29	0.28
0.58	0.32	0.31
0.71	0.49	0.45
0.86	0.73	0.61
0.86	0.72	0.60
0.89	0.79	0.64
0.90	0.81	0.65
0.93	0.86	0.68
0.94	0.88	0.69
0.93	0.86	0.68

0.91	0.82	0.65
0.90	0.80	0.64
0.88	0.76	0.63
0.90	0.79	0.64
0.86	0.74	0.61
0.90	0.79	0.64
0.89	0.78	0.63
0.89	0.79	0.64
0.91	0.82	0.66
0.93	0.86	0.68
0.96	0.92	0.71
0.94	0.88	0.69
0.96	0.91	0.70
0.95	0.90	0.69
0.96	0.91	0.70
0.96	0.92	0.71
0.95	0.90	0.70
0.98	0.95	0.72
0.98	0.96	0.72
0.99	0.97	0.73
0.77	stable	0.77
0.77	stable	0.77
0.81	stable	0.81
0.82	stable	0.82
0.84	stable	0.84
0.90	stable	0.90
0.82	stable	0.82
1.04	stable	1.04
0.89	stable	0.89
0.94	stable	0.94
1.33	stable	1.33
1.38	stable	1.38
0.93	stable	0.93
2.09	stable	2.09
2.01	stable	2.01
2.59	stable	2.59
2.01	stable	2.01
2.03	stable	2.03

1.89	stable	1.89
5.58	stable	5.58
1.24	stable	1.24
0.73	0.52	0.47
3.76	stable	3.76
1.14	stable	1.14
1.37	stable	1.37
1.30	stable	1.30
1.83	stable	1.83
1.73	stable	1.73
1.68	stable	1.68
2.45	stable	2.45
1.91	stable	1.91
1.82	stable	1.82
2.99	stable	2.99
2.15	stable	2.15
2.47	stable	2.47
1.70	stable	1.70
2.11	stable	2.11
1.74	stable	1.74
2.00	stable	2.00
2.88	stable	2.88
2.65	stable	2.65
0.76	0.56	0.49
1.18	stable	1.18
1.02	stable	1.02
0.94	0.88	0.68
0.73	0.52	0.47
0.66	0.43	0.40
0.70	0.48	0.44
0.82	0.67	0.57
0.83	0.68	0.57
0.82	0.66	0.56
0.75	0.55	0.49
0.84	0.70	0.59
0.74	0.54	0.48
0.74	0.53	0.47
0.76	0.57	0.50
0.79	0.61	0.53
0.54	0.28	0.27
0.65	0.42	0.39
0.76	0.57	0.50
0.64	0.40	0.37
0.85	0.71	0.59
0.78	stable	0.78
0.75	0.55	0.49
0.82	0.65	0.56
0.88	0.77	0.63
0.84	0.69	0.58
0.82	0.66	0.57
0.90	0.80	0.65
0.92	0.83	0.66

0.77	stable	0.77
0.76	stable	0.76
0.79	stable	0.79
0.80	stable	0.80
0.81	stable	0.81
0.98	stable	0.98
0.84	stable	0.84
1.16	stable	1.16
1.03	stable	1.03
1.01	stable	1.01
1.00	stable	1.00
0.97	stable	0.97
0.94	stable	0.94
1.12	stable	1.12
1.27	stable	1.27
1.31	stable	1.31
1.19	stable	1.19
1.31	stable	1.31
1.24	stable	1.24
3.19	stable	3.19
1.73	stable	1.73
1.70	stable	1.70
1.40	stable	1.40
1.14	stable	1.14
0.86	stable	0.86
1.02	stable	1.02
0.96	stable	0.96
1.01	stable	1.01
1.40	stable	1.40
1.15	stable	1.15
1.00	stable	1.00
1.01	stable	1.01
1.11	stable	1.11
0.89	stable	0.89
0.80	stable	0.80
0.75	stable	0.75
0.75	stable	0.75
0.81	stable	0.81
0.90	stable	0.90
0.97	stable	0.97
2.44	stable	2.44
1.09	stable	1.09
0.99	stable	0.99
0.88	stable	0.88
1.10	stable	1.10
1.04	stable	1.04
0.85	stable	0.85
0.98	0.95	0.72
0.95	0.90	0.70
0.92	0.83	0.66
0.92	0.83	0.66
0.90	0.80	0.65

0.84	0.70	0.59
0.78	0.60	0.52
0.80	0.63	0.54
0.95	0.89	0.69
0.90	0.80	0.64
0.99	0.97	0.73
1.00	1.00	0.74
0.96	0.91	0.70
0.95	0.90	0.70
0.98	0.95	0.72
0.94	0.88	0.69
0.93	0.86	0.67
0.95	0.89	0.69
0.82	0.67	0.57
0.86	0.73	0.61
0.93	0.85	0.67
0.92	0.84	0.67
0.93	0.85	0.67
0.92	0.84	0.67
0.94	0.88	0.69
0.91	0.82	0.65
0.92	0.83	0.66
0.91	0.82	0.65
0.93	0.85	0.67
0.93	0.86	0.68
0.97	0.93	0.71
0.96	0.92	0.71
0.97	0.94	0.71
0.97	0.94	0.72
0.97	0.93	0.71
0.97	0.94	0.72
0.98	0.96	0.72
0.98	0.96	0.73
0.99	0.97	0.73
0.99	0.98	0.73
0.73	0.52	0.46
0.71	0.49	0.44
0.79	0.61	0.53
0.76	0.56	0.50
0.64	0.40	0.37
0.62	0.37	0.35
0.67	0.44	0.40
0.61	0.36	0.34
0.61	0.36	0.34
0.72	0.51	0.46
0.86	0.74	0.61
0.70	0.48	0.44
0.78	0.60	0.52
0.81	0.64	0.55

0.80	0.63	0.54
0.81	0.65	0.56
0.80	0.63	0.55
0.84	0.69	0.58
0.85	0.71	0.59
0.89	0.78	0.63
0.85	0.72	0.60
1.29	stable	1.29
1.22	stable	1.22
0.81	0.64	0.55
0.61	0.36	0.34
2.10	stable	2.10
1.07	stable	1.07
1.72	stable	1.72
2.77	stable	2.77
3.04	stable	3.04
4.52	stable	4.52
1.89	stable	1.89
0.62	0.37	0.35
2.82	stable	2.82
27.53	stable	27.53
5.77	stable	5.77
5.90	stable	5.90
2.43	stable	2.43
1.09	stable	1.09
1.02	stable	1.02
0.93	stable	0.93
0.91	stable	0.91
0.82	stable	0.82
0.83	stable	0.83
0.81	stable	0.81
0.81	stable	0.81
0.80	stable	0.80
0.77	stable	0.77
0.81	stable	0.81
0.81	stable	0.81
0.81	stable	0.81
0.80	stable	0.80
0.79	stable	0.79
0.80	stable	0.80
0.77	stable	0.77
0.99	0.97	0.73
0.99	0.97	0.73
0.99	0.97	0.73
0.99	0.97	0.73
0.98	0.97	0.73
0.98	0.95	0.72
0.98	0.95	0.72
0.98	0.95	0.72
0.96	0.92	0.70
0.96	0.92	0.70

0.96	0.92	0.71
0.96	0.92	0.70
0.95	0.89	0.69
0.96	0.91	0.70
0.96	0.92	0.70
0.93	0.86	0.68
0.82	0.65	0.56
0.74	0.53	0.47
0.88	0.77	0.63
0.75	0.55	0.49
0.81	0.65	0.56
0.92	0.85	0.67
0.96	0.92	0.71
0.97	0.94	0.72
0.97	0.94	0.71
0.97	0.94	0.71
0.97	0.93	0.71
0.97	0.93	0.71

0.53	0.27	0.26
0.74	0.54	0.48
0.82	0.66	0.56
0.81	0.65	0.55
0.80	0.63	0.54
0.70	0.47	0.43
0.83	0.67	0.57
0.84	0.69	0.58
0.86	0.72	0.60

0.96	0.92	0.71
0.98	0.96	0.72
0.98	0.97	0.73
0.99	0.99	0.73
0.99	0.97	0.73
0.99	0.98	0.73
0.74	stable	0.74
1.00	0.99	0.74
0.74	stable	0.74
0.75	stable	0.75
0.76	stable	0.76
0.77	stable	0.77
0.77	stable	0.77
0.80	stable	0.80
0.79	stable	0.79
0.82	stable	0.82
0.81	stable	0.81
0.88	stable	0.88
0.80	stable	0.80
0.82	stable	0.82

0.81	stable	0.81
0.84	stable	0.84
0.86	stable	0.86
0.88	stable	0.88
0.91	stable	0.91
0.87	stable	0.87
0.92	stable	0.92
0.91	stable	0.91
0.68	0.45	0.41
0.70	0.48	0.44
0.84	0.70	0.59
0.81	0.65	0.56
0.84	0.70	0.58
0.59	0.33	0.32
0.71	0.49	0.44
0.63	0.39	0.36
0.83	0.68	0.58
0.72	0.51	0.46
0.78	0.60	0.52
0.64	0.40	0.37
0.78	0.59	0.52
0.73	0.52	0.47
0.99	0.98	0.73
0.99	0.97	0.73
1.00	1.00	0.74
0.76	stable	0.76
1.12	stable	1.12
1.59	stable	1.59
0.98	stable	0.98
1.03	stable	1.03
0.90	stable	0.90
1.03	stable	1.03
0.99	stable	0.99
0.90	stable	0.90
0.91	stable	0.91
1.05	stable	1.05
0.97	stable	0.97
0.97	stable	0.97
0.90	stable	0.90
0.87	stable	0.87
1.03	stable	1.03
1.02	stable	1.02
1.40	stable	1.40
1.21	stable	1.21
1.01	stable	1.01
1.02	stable	1.02
1.00	stable	1.00
1.13	stable	1.13
0.99	stable	0.99
0.94	stable	0.94

0.93	stable	0.93
1.02	stable	1.02
1.00	stable	1.00
0.94	stable	0.94
1.06	stable	1.06
0.96	stable	0.96
0.94	stable	0.94
1.00	stable	1.00
1.07	stable	1.07
1.22	stable	1.22
1.03	stable	1.03
1.03	stable	1.03
0.93	stable	0.93
0.96	stable	0.96
0.90	stable	0.90
0.91	stable	0.91
0.85	stable	0.85
0.94	stable	0.94
0.89	stable	0.89
0.89	stable	0.89
0.85	stable	0.85
0.83	stable	0.83
0.86	stable	0.86
0.79	stable	0.79
0.98	0.95	0.72
0.96	0.93	0.71
0.94	0.87	0.68
0.91	0.82	0.66
0.87	0.75	0.62
0.88	0.76	0.62
0.81	0.64	0.55
0.80	0.62	0.54
0.83	0.68	0.58
0.82	0.65	0.56
0.82	0.67	0.57
0.84	0.70	0.59
0.82	0.67	0.57
0.82	0.66	0.56
0.91	0.82	0.66
0.93	0.85	0.67

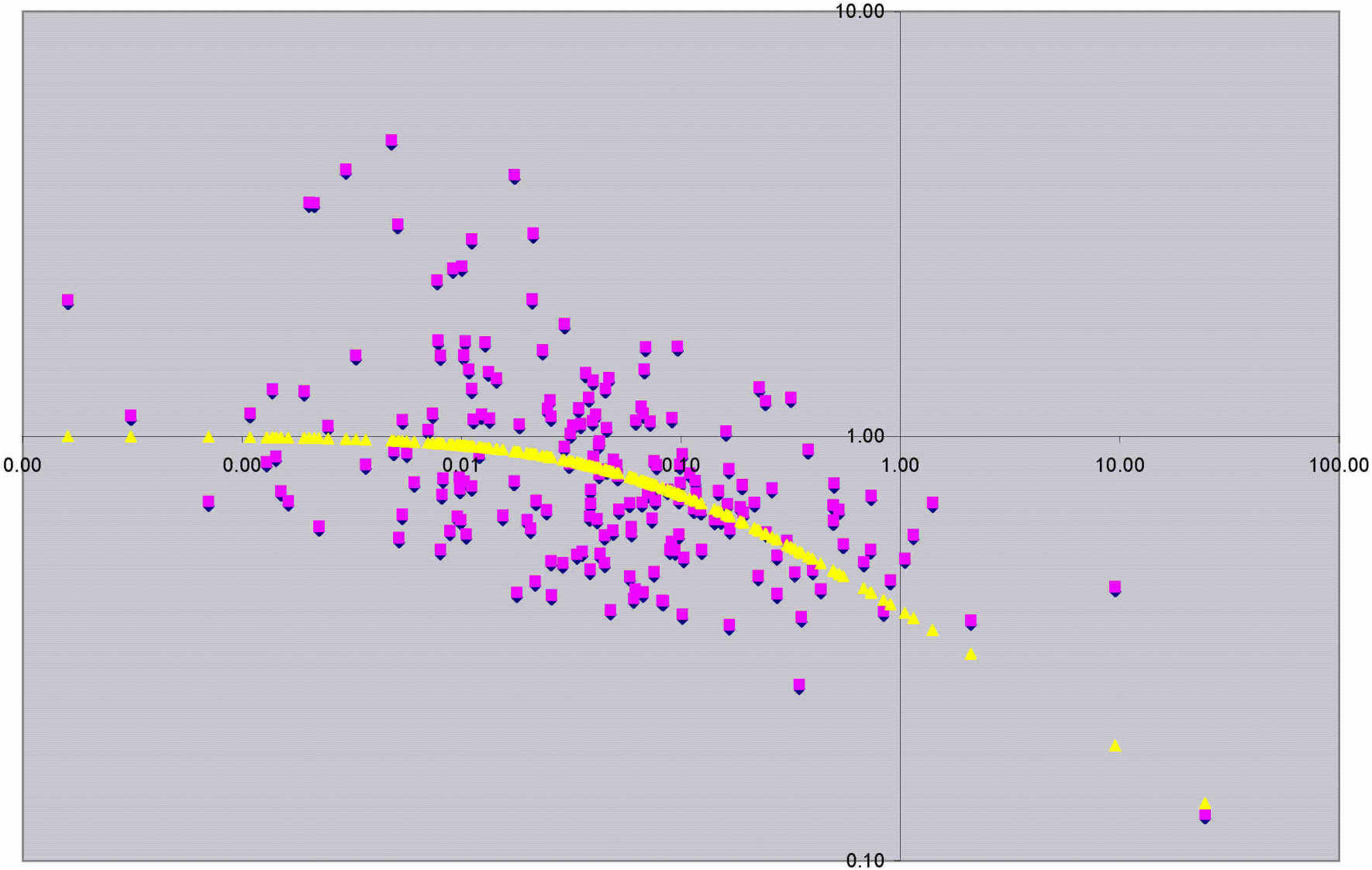
10.00
1.00
0.10
0.00
0.00
0.01
0.10
1.00
10.00
100.00

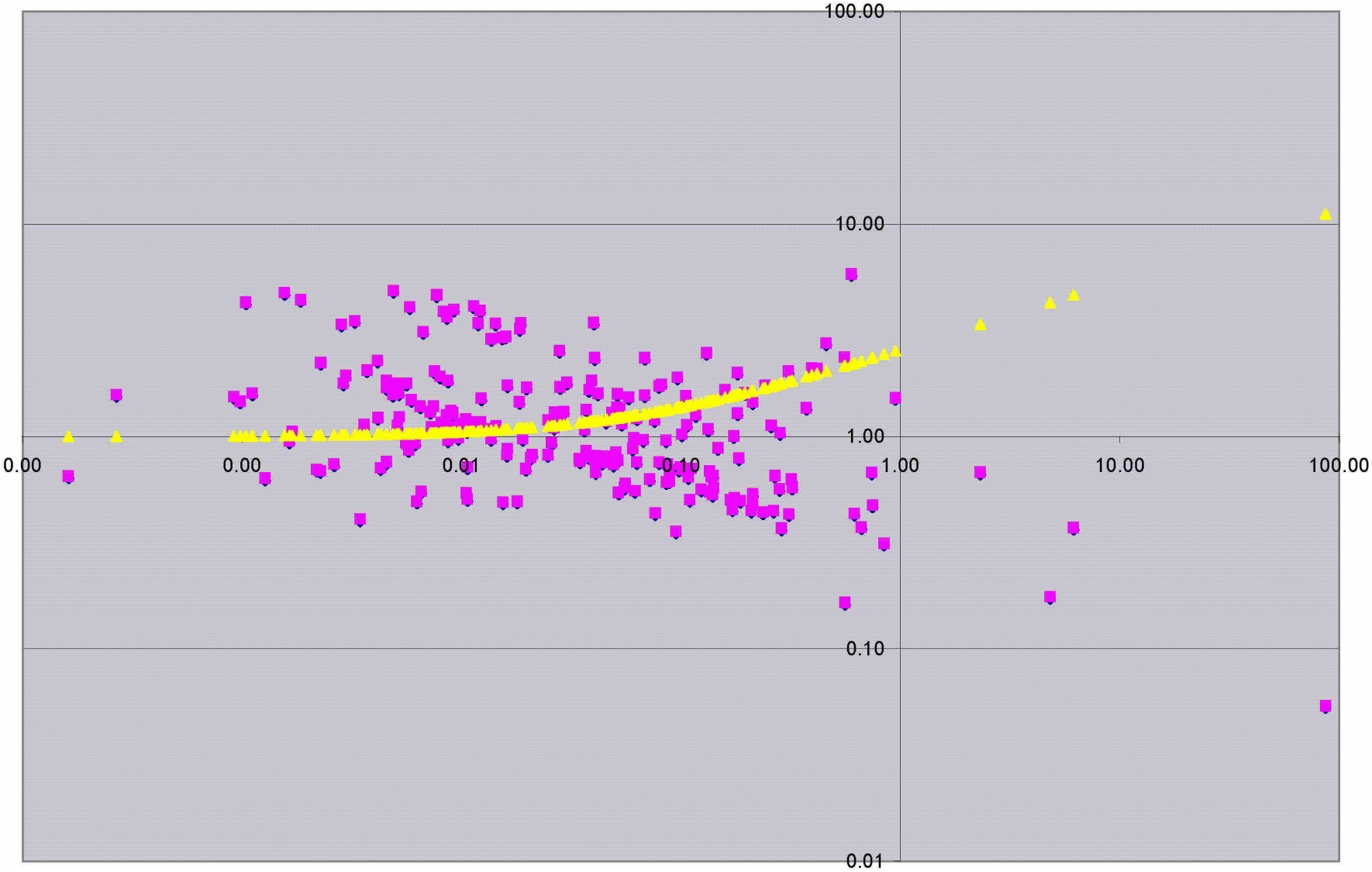
100.00
10.00
1.00
0.10
0.01
0.00
0.00
0.01
0.10
1.00
10.00
100.00

Ri		phi M	phi (M)	phi (M)
-24.477583	24.48	0.13	0.13	0.14
-9.539495	9.54	0.43	0.44	0.19
-2.095735	2.10	0.36	0.37	0.31
-1.402091	1.40	0.68	0.70	0.35
-1.147435	1.15	0.57	0.59	0.37
-1.048695	1.05	0.50	0.52	0.38
-0.902355	0.90	0.45	0.46	0.40
-0.837997	0.84	0.38	0.39	0.41
-0.737972	0.74	0.71	0.72	0.43
-0.732747	0.73	0.53	0.54	0.43
-0.680425	0.68	0.49	0.51	0.44
-0.550345	0.55	0.54	0.56	0.47
-0.526717	0.53	0.65	0.67	0.47
-0.498594	0.50	0.76	0.77	0.48
-0.495203	0.50	0.62	0.63	0.48
-0.493983	0.49	0.67	0.69	0.48
-0.434416	0.43	0.43	0.44	0.50
-0.397869	0.40	0.47	0.48	0.51
-0.380382	0.38	0.91	0.93	0.52
-0.354349	0.35	0.37	0.37	0.53
-0.346305	0.35	0.25	0.26	0.53
-0.330628	0.33	0.47	0.48	0.54
-0.316988	0.32	1.20	1.23	0.55
-0.303653	0.30	0.55	0.57	0.55
-0.273734	0.27	0.42	0.43	0.57
-0.273728	0.27	0.51	0.52	0.57
-0.260360	0.26	0.74	0.75	0.58
-0.244544	0.24	0.58	0.59	0.59
-0.242851	0.24	1.18	1.21	0.59
-0.227969	0.23	1.27	1.30	0.60
-0.224691	0.22	0.46	0.47	0.60
-0.216265	0.22	0.68	0.70	0.61
-0.193068	0.19	0.64	0.66	0.63
-0.190543	0.19	0.75	0.77	0.63
-0.186414	0.19	0.67	0.68	0.63
-0.167171	0.17	0.59	0.60	0.65
-0.166376	0.17	0.35	0.36	0.65
-0.165636	0.17	0.82	0.84	0.65
-0.162788	0.16	0.68	0.69	0.65
-0.160753	0.16	1.00	1.03	0.65
-0.152193	0.15	0.62	0.64	0.66
-0.148394	0.15	0.73	0.74	0.67
-0.142293	0.14	0.62	0.64	0.67
-0.124383	0.12	0.53	0.54	0.69
-0.123294	0.12	0.65	0.67	0.70
-0.117257	0.12	0.72	0.74	0.70
-0.116436	0.12	0.77	0.79	0.70
-0.114734	0.11	0.66	0.67	0.71
-0.110056	0.11	0.80	0.82	0.71
-0.103100	0.10	0.50	0.52	0.72
-0.101743	0.10	0.89	0.91	0.72

Ri	z/L
0.068528	0.26
0.052716	0.11
0.105517	0.19
0.096401	0.30
0.158875	-0.01
0.131043	0.65
6.149480	0.21
0.196059	0.50
2.319066	0.05
0.212314	0.37
0.053763	0.13
0.026469	0.14
0.025753	0.05
0.049220	0.08
Ri	
0.282085	-0.27
0.109667	-0.23
0.174260	-0.59
-0.316988	-0.94
-1.147435	-0.34
-0.680425	-0.16
-0.227969	-0.46
-0.526717	-0.25
-0.737972	-0.39
-0.380382	-0.37
-0.550345	-0.13
-0.216265	-0.07
-0.330628	-0.05
-0.193068	-0.04
-0.260360	-0.53
-0.493983	-1.22
-0.902355	-0.61
-0.495203	-0.49
-0.273734	-0.18
-0.025702	-0.05
-0.059504	-0.05
-0.083311	-0.04
-0.062019	-0.03
-0.019895	-0.02
-0.025653	-0.02
-0.009562	-0.02
-0.072430	-0.03
-0.045255	-0.03
-0.047116	-0.04
-0.039768	-0.03

-0.101557	0.10	0.37	0.38	0.72	-0.029521	-0.05
-0.099320	0.10	0.76	0.78	0.73	-0.116436	-0.03
-0.098734	0.10	0.84	0.86	0.73	-0.117257	-0.04
-0.098068	0.10	0.57	0.59	0.73	-0.110056	-0.04
-0.097935	0.10	0.69	0.71	0.73	-0.114734	-0.03
-0.096479	0.10	1.59	1.63	0.73	-0.025326	-0.02
-0.094053	0.09	0.53	0.54	0.74	-0.013276	-0.01
-0.090934	0.09	1.08	1.10	0.74	-0.032102	-0.02
-0.090766	0.09	0.55	0.56	0.74	-0.039709	-0.01
-0.089227	0.09	0.53	0.54	0.74	-0.034887	-0.01
-0.087078	0.09	0.73	0.75	0.75	-0.024621	-0.01
-0.083311	0.08	0.40	0.41	0.75	-0.029445	-0.01
-0.082225	0.08	0.40	0.41	0.76	-0.074909	-0.01
-0.077662	0.08	0.83	0.86	0.76	-0.042586	-0.01
-0.076310	0.08	0.69	0.71	0.77	-0.042430	-0.01
-0.075576	0.08	0.85	0.87	0.77	-0.038755	0.00
-0.075367	0.08	0.47	0.48	0.77	-0.010292	0.01
-0.074909	0.07	0.74	0.76	0.77	0.040524	0.01
-0.073842	0.07	0.63	0.64	0.77	0.060254	0.01
-0.072430	0.07	1.06	1.08	0.77	0.139421	0.02
-0.071876	0.07	0.73	0.74	0.77	0.208944	0.02
-0.070464	0.07	0.72	0.73	0.78	0.186331	0.03
-0.069049	0.07	1.58	1.62	0.78	0.310593	0.02
-0.068195	0.07	1.40	1.44	0.78	0.747664	0.06
-0.067487	0.07	1.10	1.13	0.78	0.665399	0.03
-0.067143	0.07	0.42	0.43	0.78	0.106479	0.04
-0.066625	0.07	0.68	0.70	0.79	0.040543	0.12
-0.065795	0.07	1.15	1.17	0.79	0.015920	0.13
-0.062358	0.06	1.06	1.09	0.79	0.028138	0.04
-0.062019	0.06	0.43	0.44	0.79	0.012169	0.27
-0.060911	0.06	0.40	0.41	0.80	0.001041	0.25
-0.059504	0.06	0.58	0.59	0.80	0.005809	0.37
-0.059420	0.06	0.60	0.61	0.80	0.006695	0.25
-0.058636	0.06	0.46	0.47	0.80	0.003267	0.25
-0.058440	0.06	0.68	0.70	0.80	0.013664	0.22
-0.052074	0.05	0.66	0.67	0.82	-0.096479	0.95
-0.051480	0.05	0.79	0.81	0.82	-0.242851	0.09
-0.051245	0.05	0.83	0.86	0.82	-2.095735	0.00
-0.049196	0.05	0.86	0.88	0.82	0.030296	0.55
-0.049062	0.05	0.59	0.60	0.82	0.740230	0.08
-0.047869	0.05	0.38	0.39	0.83	0.018672	0.13
-0.047116	0.05	1.34	1.37	0.83	0.015352	0.11
-0.046062	0.05	0.81	0.83	0.83	0.004894	0.22
-0.045941	0.05	1.02	1.05	0.83	0.001560	0.20
-0.045255	0.05	1.26	1.29	0.83	0.001850	0.19
-0.044983	0.04	0.49	0.50	0.83	-0.004802	0.34
-0.044932	0.04	0.57	0.58	0.83	-0.005129	0.24
-0.042736	0.04	0.52	0.53	0.84	-0.002133	0.22
-0.042586	0.04	0.95	0.97	0.84	-0.002974	0.45
-0.042430	0.04	0.80	0.82	0.84	-0.017446	0.28
-0.042251	0.04	0.93	0.96	0.84	-0.002021	0.34
-0.041624	0.04	0.62	0.64	0.84	0.028019	0.20

-0.040859	0.04	1.10	1.13	0.85	0.011361	0.27
-0.039891	0.04	0.87	0.90	0.85	0.011896	0.20
-0.039768	0.04	1.32	1.35	0.85	0.008295	0.25
-0.039709	0.04	1.06	1.09	0.85	0.008579	0.42
-0.038755	0.04	0.73	0.75	0.85	0.842635	0.39
-0.038737	0.04	0.68	0.69	0.85	86.645290	-0.10
-0.038606	0.04	0.47	0.49	0.85	0.040102	0.14
-0.038358	0.04	0.63	0.65	0.85	0.018481	0.06
-0.038017	0.04	1.20	1.23	0.85	0.014331	-0.01
-0.036825	0.04	1.37	1.41	0.86	0.007718	-0.12
-0.035613	0.04	0.52	0.54	0.86	0.009248	-0.23
-0.034887	0.03	1.04	1.07	0.86	0.002834	-0.18
-0.034213	0.03	1.14	1.16	0.86	-0.049196	-0.07
-0.033583	0.03	0.51	0.53	0.87	-0.062358	-0.07
-0.032102	0.03	1.04	1.06	0.87	-0.070464	-0.07
-0.031403	0.03	0.99	1.01	0.87	-0.071876	-0.13
-0.031029	0.03	0.84	0.86	0.87	-0.103100	-0.06
-0.029521	0.03	1.79	1.84	0.88	-0.244544	-0.14
-0.029445	0.03	0.92	0.95	0.88	-0.303653	-0.15
-0.028950	0.03	0.49	0.50	0.88	-0.397869	-0.12
-0.025702	0.03	0.41	0.42	0.89	-0.273728	-0.10
-0.025653	0.03	0.50	0.51	0.89	-1.402091	-0.68
-0.025550	0.03	1.09	1.11	0.89	-9.539495	-0.22
-0.025326	0.03	1.19	1.22	0.89	-1.048695	-0.11
-0.024621	0.02	1.13	1.16	0.90	-0.098734	-0.29
-0.024382	0.02	0.65	0.67	0.90	-0.124383	-0.05
-0.023390	0.02	1.56	1.59	0.90	-0.837997	0.01
-0.021872	0.02	0.69	0.70	0.90	-24.477583	-0.12
-0.021697	0.02	0.44	0.46	0.91	-0.498594	-0.07
-0.021257	0.02	2.93	3.00	0.91	-0.065795	-0.03
-0.020985	0.02	2.05	2.10	0.91	-0.068195	-0.05
-0.020635	0.02	0.59	0.61	0.91	-0.732747	-0.06
-0.019895	0.02	0.62	0.64	0.91	-0.101743	-0.03
-0.018376	0.02	1.04	1.07	0.92	-0.165636	-0.02
-0.017909	0.02	0.42	0.43	0.92	-0.023390	0.01
-0.017446	0.02	4.03	4.13	0.92	-0.045941	0.01
-0.017422	0.02	0.76	0.78	0.92	-0.099320	0.01
-0.015453	0.02	0.63	0.65	0.93	-0.010234	0.01
-0.014482	0.01	1.34	1.37	0.93	-0.007827	0.02
-0.013427	0.01	1.07	1.10	0.94	-0.012786	0.06
-0.013276	0.01	1.38	1.42	0.94	-9.699864	0.03
-0.012786	0.01	1.62	1.66	0.94	-0.354349	0.09
-0.012343	0.01	1.10	1.12	0.94	0.051416	0.07
-0.012073	0.01	0.89	0.91	0.94	0.006495	0.06
-0.011331	0.01	1.07	1.10	0.95	-0.042251	0.06
-0.011161	0.01	1.26	1.29	0.95	-0.010802	0.05
-0.011136	0.01	0.74	0.76	0.95	0.000916	0.04
-0.011120	0.01	2.84	2.91	0.95	-0.010054	0.09
-0.010802	0.01	1.40	1.44	0.95	-0.011120	0.12
-0.010496	0.01	0.57	0.59	0.95	-0.020985	0.13
-0.010406	0.01	1.63	1.68	0.95	-0.009137	0.10
-0.010292	0.01	0.77	0.78	0.95	-0.067487	0.13

-0.010234	0.01	1.51	1.55	0.95	-0.075576	0.11
-0.010054	0.01	2.45	2.51	0.95	-0.021257	0.54
-0.009929	0.01	0.62	0.64	0.95	-0.007752	0.22
-0.009844	0.01	0.73	0.75	0.95	-0.014482	0.21
-0.009768	0.01	0.78	0.80	0.95	-0.162788	0.15
-0.009562	0.01	0.63	0.65	0.95	-0.069049	0.09
-0.009137	0.01	2.42	2.48	0.96	-0.025550	0.03
-0.008841	0.01	0.58	0.60	0.96	0.026586	0.06
-0.008236	0.01	0.78	0.80	0.96	0.045701	0.05
-0.008145	0.01	0.71	0.73	0.96	0.062983	0.05
-0.008039	0.01	1.51	1.55	0.96	0.068482	0.14
-0.008022	0.01	0.53	0.54	0.96	0.057901	0.08
-0.007827	0.01	1.64	1.68	0.96	0.041865	0.05
-0.007752	0.01	2.27	2.33	0.96	0.048480	0.05
-0.007400	0.01	1.10	1.13	0.96	0.038198	0.08
-0.007033	0.01	1.01	1.04	0.97	0.029271	0.03
-0.006102	0.01	0.76	0.78	0.97	0.028192	0.01
-0.005622	0.01	0.89	0.92	0.97	0.007215	0.00
-0.005383	0.01	1.07	1.09	0.97	0.012225	0.00
-0.005374	0.01	0.64	0.65	0.97	0.018382	0.01
-0.005188	0.01	0.56	0.58	0.97	0.067463	0.03
-0.005129	0.01	3.08	3.16	0.97	0.075940	0.05
-0.004914	0.00	0.90	0.92	0.98	0.079535	0.36
-0.004802	0.00	4.86	4.98	0.98	0.019807	0.07
-0.003668	0.00	0.84	0.86	0.98	0.036977	0.05
-0.003302	0.00	1.51	1.55	0.98	0.051003	0.03
-0.002974	0.00	4.15	4.25	0.98	0.081712	0.08
-0.002470	0.00	1.03	1.06	0.99	0.283030	0.06
-0.002244	0.00	0.60	0.61	0.99	0.117146	0.03
-0.002133	0.00	3.46	3.54	0.99	0.039209	0.00
-0.002021	0.00	3.47	3.55	0.99	0.016240	-0.01
-0.001916	0.00	1.25	1.28	0.99	0.007990	-0.02
-0.001623	0.00	0.69	0.70	0.99	0.004547	-0.02
-0.001506	0.00	0.72	0.74	0.99	0.003715	-0.03
-0.001428	0.00	0.87	0.90	0.99	0.004140	-0.06
-0.001375	0.00	1.26	1.29	0.99	0.007561	-0.10
-0.001295	0.00	0.85	0.87	0.99	0.008694	-0.09
-0.001088	0.00	1.10	1.13	0.99	0.002967	-0.01
-0.000706	0.00	0.68	0.70	1.00	0.005626	-0.03
-0.000311	0.00	1.09	1.12	1.00	-0.000161	0.00
-0.000161	0.00	2.04	2.09	1.00	-0.010406	0.00
0.000162	0.00	0.63	0.65	1.00	-0.011331	-0.01
0.000268	0.00	1.54	1.57	1.00	-0.005622	-0.01
0.000916	0.00	1.50	1.54	1.00	-0.009844	-0.01
0.000981	0.00	1.43	1.46	1.01	0.010679	-0.02
0.001041	0.00	4.17	4.28	1.01	-0.008022	-0.02
0.001113	0.00	1.56	1.60	1.01	-0.042736	-0.01
0.001275	0.00	0.62	0.64	1.01		
0.001560	0.00	4.63	4.75	1.01	Ri	
0.001647	0.00	0.93	0.95	1.01	0.061791	-0.07
0.001694	0.00	1.03	1.06	1.01	-0.020635	-0.05
0.001850	0.00	4.29	4.39	1.01	-0.010496	-0.02

0.002190	0.00	0.68	0.70	1.01	-0.021697	-0.02
0.002278	0.00	0.67	0.69	1.01	-0.017909	-0.02
0.002284	0.00	2.17	2.22	1.01	-0.028950	-0.02
0.002626	0.00	0.72	0.74	1.01	-0.047869	-0.02
0.002834	0.00	3.29	3.37	1.01	-0.067143	-0.03
0.002901	0.00	1.74	1.78	1.02	-0.035613	-0.02
0.002967	0.00	1.89	1.93	1.02	-0.058636	-0.03
0.003267	0.00	3.42	3.50	1.02	-0.044983	-0.02
0.003455	0.00	0.40	0.41	1.02	-0.038606	-0.02
0.003599	0.00	1.11	1.14	1.02	-0.009929	-0.01
0.003715	0.00	2.00	2.05	1.02	-0.008841	-0.01
0.004140	0.00	2.22	2.28	1.02	-0.005374	-0.01
0.004164	0.00	1.20	1.23	1.02	-0.002244	-0.01
0.004286	0.00	0.69	0.71	1.02	-0.001623	-0.01
0.004543	0.00	0.74	0.76	1.02	-0.000706	-0.01
0.004544	0.00	1.66	1.70	1.02	0.001275	0.00
0.004547	0.00	1.79	1.84	1.02	0.002190	0.00
0.004872	0.00	1.53	1.57	1.03	0.002626	0.00
0.004894	0.00	4.73	4.85	1.03	0.004286	0.00
0.005051	0.01	1.73	1.78	1.03		
0.005116	0.01	1.10	1.12	1.03	-0.224691	-0.15
0.005192	0.01	1.56	1.60	1.03	-0.094053	-0.18
0.005209	0.01	1.20	1.23	1.03	-0.073842	-0.09
0.005578	0.01	0.91	0.93	1.03	-0.090766	-0.12
0.005626	0.01	1.73	1.78	1.03	-0.186414	-0.29
0.005654	0.01	0.90	0.92	1.03	-0.152193	-0.36
0.005741	0.01	0.84	0.86	1.03	-0.142293	-0.23
0.005809	0.01	3.97	4.07	1.03	-0.190543	-0.38
0.005919	0.01	1.45	1.49	1.03	-0.090934	-0.37
0.006172	0.01	0.91	0.93	1.03	-0.434416	-0.16
0.006270	0.01	0.48	0.49	1.03	-0.346305	-0.05
0.006495	0.01	1.35	1.39	1.03	-0.076310	-0.18
0.006569	0.01	0.54	0.55	1.03	-0.059420	-0.10
0.006695	0.01	3.03	3.11	1.03	-0.038737	-0.08
0.007215	0.01	1.27	1.31	1.04	-0.031029	-0.08
0.007329	0.01	1.08	1.11	1.04	-0.049062	-0.07
0.007455	0.01	1.35	1.39	1.04	-0.041624	-0.08
0.007561	0.01	1.98	2.03	1.04	-0.021872	-0.05
0.007718	0.01	4.52	4.63	1.04	-0.017422	-0.05
0.007990	0.01	1.87	1.92	1.04	-0.015453	-0.03
0.008129	0.01	1.14	1.17	1.04	-0.033583	-0.04
0.008295	0.01	3.78	3.87	1.04		
0.008371	0.01	1.09	1.12	1.04	0.183533	0.14
0.008381	0.01	1.09	1.12	1.04	0.101165	0.11
0.008526	0.01	1.23	1.26	1.04	0.133435	-0.08
0.008579	0.01	3.57	3.65	1.04	4.812467	-0.41
0.008665	0.01	0.94	0.96	1.04	0.257744	0.32
0.008694	0.01	1.79	1.84	1.04	0.318563	0.08
0.008912	0.01	1.24	1.27	1.05	0.181308	0.23
0.008933	0.01	1.29	1.32	1.05	0.241605	0.46
0.009114	0.01	1.08	1.11	1.05	0.181182	0.52
0.009119	0.01	1.26	1.29	1.05	0.417305	0.85

0.009248	0.01	3.86	3.96	1.05	0.309134	0.25
0.009351	0.01	1.08	1.11	1.05	0.394942	-0.44
0.009656	0.01	0.96	0.99	1.05	0.949326	0.46
0.009808	0.01	1.12	1.15	1.05	0.598721	5.70
0.010464	0.01	1.18	1.20	1.05	0.459099	1.09
0.010518	0.01	0.53	0.54	1.05	0.555396	1.14
0.010604	0.01	1.03	1.06	1.05	0.373688	0.38
0.010649	0.01	0.50	0.51	1.05	0.268461	0.08
0.010679	0.01	0.70	0.72	1.05	0.061118	0.06
0.010935	0.01	1.14	1.17	1.06	0.036394	0.04
0.011161	0.01	1.12	1.15	1.06	0.024831	0.04
0.011361	0.01	4.01	4.11	1.06	0.021012	0.02
0.011896	0.01	3.33	3.41	1.06	0.019017	0.02
0.012169	0.01	3.82	3.91	1.06	0.013664	0.01
0.012225	0.01	1.14	1.17	1.06	0.009351	0.02
0.012297	0.01	1.48	1.51	1.06	0.007329	0.01
0.013010	0.01	1.06	1.08	1.07	0.004164	0.01
0.013664	0.01	2.81	2.88	1.07	0.002284	0.02
0.013664	0.01	0.95	0.98	1.07	0.004872	0.02
0.014331	0.01	3.32	3.40	1.07	0.005192	0.02
0.014378	0.01	1.09	1.12	1.07	0.002901	0.01
0.015352	0.02	2.85	2.92	1.08	0.005919	0.01
0.015442	0.02	0.48	0.49	1.08	0.005051	0.01
0.015920	0.02	2.88	2.95	1.08	0.004544	0.01
0.016087	0.02	0.80	0.82	1.08	0.003599	0.00
0.016192	0.02	0.85	0.88	1.08	0.001113	0.00
0.016240	0.02	1.70	1.74	1.08	0.000268	0.00
0.017930	0.02	0.48	0.49	1.09	-0.001295	0.00
0.018382	0.02	1.42	1.45	1.09	-0.001088	0.00
0.018481	0.02	3.14	3.22	1.09	-0.001375	-0.01
0.018672	0.02	3.34	3.43	1.09	-0.002470	-0.01
0.019017	0.02	0.95	0.98	1.09	-0.006102	-0.01
0.019678	0.02	0.69	0.71	1.10	-0.007400	-0.01
0.019807	0.02	1.66	1.70	1.10	-0.011136	-0.01
0.020667	0.02	0.78	0.79	1.10	-0.008236	-0.01
0.021012	0.02	0.80	0.82	1.10	-0.008145	-0.01
0.024758	0.02	0.80	0.82	1.12	-0.001506	-0.01
0.024831	0.02	1.17	1.20	1.12	-0.003668	-0.01
0.025753	0.03	0.91	0.93	1.12	-0.001428	-0.01
0.026469	0.03	1.07	1.10	1.12	-0.000311	-0.02
0.026586	0.03	1.27	1.30	1.13	0.000981	-0.08
0.028019	0.03	2.47	2.53	1.13	-0.007033	-0.15
0.028138	0.03	1.67	1.71	1.13	-0.005188	-0.04
0.028192	0.03	1.19	1.22	1.13	-0.003302	-0.13
0.029271	0.03	1.28	1.31	1.14	0.001647	-0.08
0.030296	0.03	1.75	1.79	1.14	0.000162	-0.02
0.034486	0.03	0.76	0.78	1.16	0.003455	-0.01
0.034643	0.03	0.74	0.76	1.16	0.015442	-0.01
0.036394	0.04	1.05	1.08	1.17	0.010518	-0.01
0.036977	0.04	1.31	1.34	1.17	0.006270	-0.01
0.037024	0.04	0.83	0.85	1.17	0.010649	-0.01
0.038058	0.04	0.78	0.80	1.17	0.006569	-0.01

0.038198	0.04	1.62	1.66	1.17		
0.039209	0.04	1.78	1.83	1.18		
0.040102	0.04	3.35	3.44	1.18	-0.160753	-0.66
0.040524	0.04	0.75	0.77	1.18	0.559929	-0.12
0.040543	0.04	2.28	2.34	1.18	0.017930	-0.07
0.040932	0.04	0.79	0.81	1.18	-0.082225	-0.07
0.040960	0.04	0.66	0.68	1.18	-0.166376	-0.08
0.041865	0.04	1.55	1.59	1.19	-0.098068	-0.18
0.043668	0.04	0.73	0.75	1.19	-0.075367	-0.06
0.045701	0.05	1.15	1.18	1.20	-0.044932	-0.06
0.045884	0.05	0.79	0.81	1.20	-0.060911	-0.05
0.048480	0.05	1.26	1.30	1.21		
0.049220	0.05	0.72	0.74	1.21	Ri	
0.050578	0.05	0.82	0.84	1.22		
0.051003	0.05	1.34	1.37	1.22	0.014378	0.00
0.051416	0.05	1.54	1.58	1.22	0.016087	0.00
0.051641	0.05	0.75	0.77	1.22	0.008526	0.00
0.051976	0.05	0.53	0.54	1.22	0.019678	0.00
0.052716	0.05	1.31	1.34	1.23	0.001694	0.00
0.053763	0.05	1.12	1.15	1.23	0.002278	0.00
0.055311	0.06	0.56	0.58	1.24	0.004543	0.00
0.055896	0.06	0.59	0.60	1.24	0.005654	0.00
0.057901	0.06	1.49	1.53	1.24	0.006172	0.00
0.060254	0.06	0.86	0.88	1.25	0.005578	0.01
0.061118	0.06	0.96	0.98	1.26	0.005741	0.01
0.061791	0.06	0.54	0.55	1.26	0.005209	0.01
0.062983	0.06	1.19	1.22	1.26	0.008665	0.01
0.063035	0.06	0.74	0.76	1.26	0.008912	0.02
0.067463	0.07	0.94	0.96	1.28	0.008381	0.01
0.068482	0.07	1.52	1.56	1.28	0.009119	0.02
0.068528	0.07	2.29	2.35	1.28	0.007455	0.02
0.072078	0.07	0.61	0.63	1.29	0.012297	0.03
0.075940	0.08	1.17	1.20	1.30	0.010935	0.02
0.076370	0.08	0.43	0.44	1.30	0.010464	0.02
0.079535	0.08	1.68	1.73	1.31	0.009656	0.02
0.079683	0.08	0.74	0.76	1.32	0.013010	0.03
0.081712	0.08	1.72	1.76	1.32	0.010604	0.03
0.085342	0.09	0.94	0.96	1.33	0.009114	0.03
0.085852	0.09	0.59	0.61	1.33	0.009808	0.04
0.086837	0.09	0.72	0.74	1.34	0.011161	0.03
0.088497	0.09	0.66	0.68	1.34	0.008129	0.04
0.088652	0.09	0.60	0.62	1.34	0.005116	0.04
0.094869	0.09	0.35	0.36	1.36		
0.096401	0.10	1.85	1.90	1.36	-0.038017	-0.20
0.097996	0.10	0.68	0.70	1.37	-0.036825	-0.18
0.099468	0.10	0.70	0.72	1.37	-0.005383	-0.06
0.101165	0.10	1.00	1.02	1.38	-0.011161	-0.07
0.105517	0.11	1.52	1.56	1.39	-0.012343	-0.06
0.106479	0.11	1.11	1.13	1.39	-0.008039	-0.43
0.106658	0.11	0.67	0.69	1.39	-0.040859	-0.17
0.108006	0.11	0.63	0.65	1.40	-0.034213	-0.30
0.109667	0.11	0.49	0.50	1.40	-0.089227	-0.06

0.111264	0.11	0.69	0.71	1.41	-0.167171	-0.15
0.117146	0.12	1.23	1.26	1.42	-0.052074	-0.10
0.124065	0.12	0.55	0.56	1.44	-0.148394	-0.29
0.131043	0.13	2.41	2.47	1.46	-0.087078	-0.10
0.133435	0.13	1.05	1.08	1.46	-0.097935	-0.14
0.135334	0.14	0.53	0.55	1.47		
0.135525	0.14	0.67	0.69	1.47	-0.101557	0.00
0.137266	0.14	0.63	0.64	1.47	-0.024382	0.00
0.139421	0.14	0.52	0.53	1.48	0.076370	0.00
0.140464	0.14	0.64	0.65	1.48	0.094869	0.01
0.140649	0.14	0.56	0.57	1.48	0.135525	0.09
0.147491	0.15	0.86	0.88	1.50	0.147491	0.20
0.158875	0.16	1.62	1.66	1.52	0.212528	0.06
0.168439	0.17	0.49	0.50	1.55	0.213089	0.07
0.172184	0.17	0.44	0.45	1.55	0.287837	0.04
0.174260	0.17	0.98	1.01	1.56	0.263996	0.07
0.174968	0.17	0.50	0.51	1.56	0.111264	0.06
0.181182	0.18	1.95	2.00	1.57	0.072078	0.04
0.181308	0.18	1.25	1.28	1.57	0.055896	0.04
0.183533	0.18	0.77	0.79	1.58	0.106658	0.07
0.186331	0.19	0.49	0.50	1.58	0.051641	0.05
0.196059	0.20	1.56	1.60	1.61	0.037024	0.05
0.208944	0.21	0.44	0.45	1.63	0.024758	0.04
0.212314	0.21	1.42	1.45	1.64	0.055311	0.03
0.212528	0.21	0.47	0.48	1.64	0.108006	0.07
0.213089	0.21	0.52	0.54	1.64	0.236737	0.06
0.236737	0.24	0.43	0.44	1.69	0.618898	0.15
0.241605	0.24	1.69	1.73	1.69	0.321701	0.11
0.257744	0.26	1.10	1.13	1.72	0.140649	0.06
0.263996	0.26	0.44	0.45	1.74	0.085852	0.06
0.268461	0.27	0.64	0.65	1.74	0.172184	0.06
0.282085	0.28	0.55	0.57	1.77	0.140464	0.09
0.283030	0.28	1.01	1.04	1.77	0.168439	0.06
0.287837	0.29	0.36	0.37	1.78	0.063035	0.05
0.309134	0.31	1.98	2.03	1.81	0.088652	0.05
0.310593	0.31	0.42	0.43	1.81	0.088497	0.07
0.318563	0.32	0.61	0.63	1.83	0.097996	0.06
0.321701	0.32	0.56	0.58	1.83	0.135334	0.05
0.373688	0.37	1.33	1.36	1.91	0.137266	0.07
0.394942	0.39	2.05	2.10	1.94	0.174968	0.05
0.417305	0.42	2.03	2.08	1.97	0.124065	0.05
0.459099	0.46	2.68	2.75	2.03	0.099468	0.06
0.555396	0.56	2.31	2.36	2.15	0.086837	0.07
0.559929	0.56	0.16	0.17	2.15	0.085342	0.11
0.598721	0.60	5.67	5.82	2.20	0.079683	0.06
0.618898	0.62	0.42	0.43	2.22	0.050578	0.06
0.665399	0.67	0.37	0.37	2.27	0.038058	0.04
0.740230	0.74	0.66	0.68	2.34	0.045884	0.05
0.747664	0.75	0.46	0.47	2.35	0.043668	0.04
0.842635	0.84	0.31	0.31	2.44	0.034643	0.04
0.949326	0.95	1.48	1.52	2.53	0.051976	0.03
2.319066	2.32	0.66	0.68	3.37	0.040932	0.05

4.812467	4.81	0.17	0.18	4.27		0.040960	0.03
6.149480	6.15	0.36	0.37	4.63		0.034486	0.03
86.645290	86.65	0.05	0.05	11.15		0.020667	0.03
Ri		phi M				0.016192	0.02
Ri		phi M				0.008933	0.03
Ri		phi M				0.008371	0.01
						-0.001916	0.00
						-0.004914	-0.01
						-0.012073	-0.02
						-0.018376	-0.02
						-0.051480	-0.04
						-0.058440	-0.04
						-0.046062	-0.07
						-0.039891	-0.09
						-0.013427	-0.06
						-0.031403	-0.07
						-0.051245	-0.07
						-0.066625	-0.06
						-0.123294	-0.07
						-0.077662	-0.07
						-0.038358	-0.02
						-0.009768	-0.02

Ri	
0.068528	0.143127
0.052716	0.249917
0.105517	0.216034
0.096401	0.177280
0.158875	0.202620
0.131043	0.135915
6.149480	0.902837
0.196059	0.209949
2.319066	0.495800
0.212314	0.231560
0.053763	0.292494
0.026469	0.305706
0.025753	0.360317
0.049220	0.455984

Ri	
0.282085	0.592435
0.109667	0.666558
0.174260	0.334365
-0.316988	0.272625
-1.147435	0.573692
-0.680425	0.664415
-0.227969	0.257858
-0.526717	0.500620
-0.737972	0.464016
-0.380382	0.361009
-0.550345	0.602888
-0.216265	0.481097
-0.330628	0.702731
-0.193068	0.508719
-0.260360	0.445708
-0.493983	0.488424
-0.902355	0.733419
-0.495203	0.530967
-0.273734	0.789413
-0.025702	0.795669
-0.059504	0.565140
-0.083311	0.821019
-0.062019	0.769993
-0.019895	0.529008
-0.025653	0.661231
-0.009562	0.519489
-0.072430	0.312552
-0.045255	0.261528
-0.047116	0.246542
-0.039768	0.250369

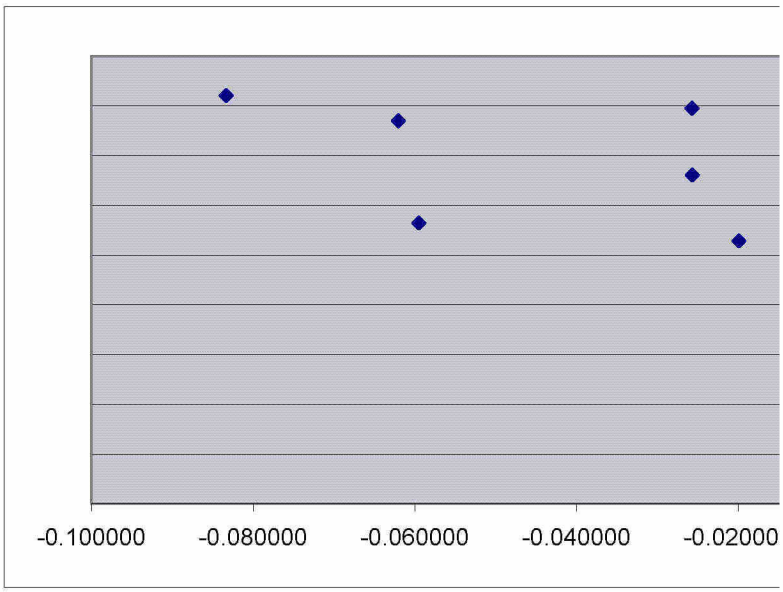

-0.029521	0.184279
-0.116436	0.430670
-0.117257	0.460651
-0.110056	0.413933
-0.114734	0.502209
-0.025326	0.278076
-0.013276	0.238730
-0.032102	0.319078
-0.039709	0.311444
-0.034887	0.316831
-0.024621	0.291692
-0.029445	0.358339
-0.074909	0.447015
-0.042586	0.347733
-0.042430	0.415333
-0.038755	0.451980
-0.010292	0.431840
0.040524	0.439993
0.060254	0.385465
0.139421	0.636313
0.208944	0.756937
0.186331	0.679909
0.310593	0.785434
0.747664	0.714214
0.665399	0.904718
0.106479	0.298863
0.040543	0.144590
0.015920	0.114605
0.028138	0.198352
0.012169	0.086508
0.001041	0.079175
0.005809	0.083298
0.006695	0.108925
0.003267	0.096694
0.013664	0.117741
-0.096479	0.208203
-0.242851	0.279527
-2.095735	0.919336
0.030296	0.188852
0.740230	0.499814
0.018672	0.098782
0.015352	0.115920
0.004894	0.069810
0.001560	0.071360
0.001850	0.077082
-0.004802	0.068002
-0.005129	0.107264
-0.002133	0.095562
-0.002974	0.079686
-0.017446	0.081968
-0.002021	0.095316
0.028019	0.133673

0.011361	0.082478
0.011896	0.099258
0.008295	0.087469
0.008579	0.092663
0.842635	1.081980
86.645290	6.290764
0.040102	0.098575
0.018481	0.105296
0.014331	0.099455
0.007718	0.073119
0.009248	0.085489
0.002834	0.100453
-0.049196	0.384429
-0.062358	0.310733
-0.070464	0.461339
-0.071876	0.455218
-0.103100	0.654368
-0.244544	0.569819
-0.303653	0.596245
-0.397869	0.699192
-0.273728	0.645882
-1.402091	0.485312
-9.539495	0.766747
-1.048695	0.657393
-0.098734	0.394564
-0.124383	0.626710
-0.837997	0.875785
-24.477583	2.629321
-0.498594	0.436984
-0.065795	0.288304
-0.068195	0.235505
-0.732747	0.625417
-0.101743	0.372996
-0.165636	0.404293
-0.023390	0.212378
-0.045941	0.323161
-0.099320	0.436390
-0.010234	0.218288
-0.007827	0.201399
-0.012786	0.203437
-9.699864	-3.630463
-0.354349	0.903178
0.051416	0.213940
0.006495	0.244219
-0.042251	0.353470
-0.010802	0.235557
0.000916	0.220005
-0.010054	0.134829
-0.011120	0.116313
-0.020985	0.161106
-0.009137	0.136379
-0.067487	0.299630

-0.075576	0.387755
-0.021257	0.112696
-0.007752	0.145301
-0.014482	0.247437
-0.162788	0.488559
-0.069049	0.208764
-0.025550	0.304087
0.026586	0.260342
0.045701	0.287562
0.062983	0.278192
0.068482	0.216672
0.057901	0.221490
0.041865	0.212491
0.048480	0.261263
0.038198	0.204374
0.029271	0.258238
0.028192	0.277442
0.007215	0.259387
0.012225	0.290090
0.018382	0.232856
0.067463	0.351486
0.075940	0.282777
0.079535	0.196098
0.019807	0.199074
0.036977	0.252924
0.051003	0.247014
0.081712	0.192357
0.283030	0.325707
0.117146	0.268388
0.039209	0.185095
0.016240	0.194307
0.007990	0.176768
0.004547	0.184340
0.003715	0.165263
0.004140	0.148789
0.007561	0.167073
0.008694	0.184521
0.002967	0.175091
0.005626	0.190581
-0.000161	0.161760
-0.010406	0.202094
-0.011331	0.308928
-0.005622	0.370051
-0.009844	0.450687
0.010679	0.472395
-0.008022	0.626808
-0.042736	0.640476

Ri	
0.061791	0.628383
-0.020635	0.574463
-0.010496	0.592544

-0.021697	0.765341
-0.017909	0.813489
-0.028950	0.693171
-0.047869	0.894028
-0.067143	0.812174
-0.035613	0.650943
-0.058636	0.745139
-0.044983	0.691959
-0.038606	0.717929
-0.009929	0.547923
-0.008841	0.581707
-0.005374	0.532957
-0.002244	0.567861
-0.001623	0.495197
-0.000706	0.496455
0.001275	0.548191
0.002190	0.498321
0.002626	0.470363
0.004286	0.490760
-0.224691	0.743060
-0.094053	0.646669
-0.073842	0.543293
-0.090766	0.617418
-0.186414	0.510695
-0.152193	0.547058
-0.142293	0.548286
-0.190543	0.453781
-0.090934	0.315263
-0.434416	0.797849
-0.346305	1.339417
-0.076310	0.493397
-0.059420	0.568815
-0.038737	0.501825
-0.031029	0.404213
-0.049062	0.580693
-0.041624	0.545761
-0.021872	0.494404
-0.017422	0.444456
-0.015453	0.535823
-0.033583	0.660988
0.183533	0.440404
0.101165	0.340048
0.133435	0.322256
4.812467	1.981502
0.257744	0.308972
0.318563	0.553764
0.181308	0.271097
0.241605	0.200861
0.181182	0.174331
0.417305	0.167243

0.309134	0.171660
0.394942	0.165810
0.949326	0.229226
0.598721	0.059901
0.459099	0.126651
0.555396	0.147399
0.373688	0.255624
0.268461	0.532941
0.061118	0.354680
0.036394	0.323232
0.024831	0.291432
0.021012	0.424735
0.019017	0.357171
0.013664	0.357090
0.009351	0.314013
0.007329	0.314906
0.004164	0.284317
0.002284	0.156849
0.004872	0.221585
0.005192	0.218065
0.002901	0.195665
0.005919	0.234177
0.005051	0.196086
0.004544	0.205232
0.003599	0.306773
0.001113	0.218245
0.000268	0.221346
-0.001295	0.400601
-0.001088	0.307686
-0.001375	0.270070
-0.002470	0.329355
-0.006102	0.447144
-0.007400	0.308240
-0.011136	0.456825
-0.008236	0.437736
-0.008145	0.477607
-0.001506	0.469871
-0.003668	0.405968
-0.001428	0.388940
-0.000311	0.311482
0.000981	0.238335
-0.007033	0.336118
-0.005188	0.604498
-0.003302	0.224727
0.001647	0.366826
0.000162	0.536012
0.003455	0.853710
0.015442	0.710756
0.010518	0.643787
0.006270	0.703920
0.010649	0.685863
0.006569	0.630695

-0.160753	0.338994
0.559929	2.109015
0.017930	0.704450
-0.082225	0.849198
-0.166376	0.969626
-0.098068	0.592847
-0.075367	0.727491
-0.044932	0.596299
-0.060911	0.839596

Ri	
0.014378	0.290457
0.016087	0.396444
0.008526	0.258802
0.019678	0.461842
0.001694	0.308057
0.002278	0.473222
0.004543	0.429169
0.005654	0.354601
0.006172	0.350338
0.005578	0.348820
0.005741	0.377214
0.005209	0.263879
0.008665	0.339324
0.008912	0.255926
0.008381	0.291047
0.009119	0.252294
0.007455	0.234810
0.012297	0.215363
0.010935	0.279294
0.010464	0.270249
0.009656	0.330144
0.013010	0.300379
0.010604	0.307258
0.009114	0.294046
0.009808	0.282789
0.011161	0.282520
0.008129	0.279481
0.005116	0.289512
-0.038017	0.263951
-0.036825	0.231190
-0.005383	0.297722
-0.011161	0.251575
-0.012343	0.289677
-0.008039	0.210319
-0.040859	0.289420
-0.034213	0.279677
-0.089227	0.602599

-0.167171	0.538622
-0.052074	0.484256
-0.148394	0.437874
-0.087078	0.435064
-0.097935	0.457941
-0.101557	0.855810
-0.024382	0.485793
0.076370	0.747174
0.094869	0.911922
0.135525	0.473333
0.147491	0.368727
0.212528	0.681291
0.213089	0.607350
0.287837	0.881557
0.263996	0.727177
0.111264	0.461071
0.072078	0.517335
0.055896	0.541360
0.106658	0.472467
0.051641	0.421572
0.037024	0.380930
0.024758	0.397388
0.055311	0.565940
0.108006	0.504769
0.236737	0.740357
0.618898	0.751697
0.321701	0.566180
0.140649	0.567661
0.085852	0.534241
0.172184	0.717073
0.140464	0.498411
0.168439	0.647840
0.063035	0.429621
0.088652	0.528183
0.088497	0.478301
0.097996	0.465985
0.135334	0.594809
0.137266	0.505202
0.174968	0.634276
0.124065	0.576916
0.099468	0.453429
0.086837	0.439526
0.085342	0.339103
0.079683	0.429763
0.050578	0.387066
0.038058	0.405831
0.045884	0.403951
0.043668	0.432763
0.034643	0.426466
0.051976	0.597579
0.040932	0.401669

0.040960	0.479568
0.034486	0.415572
0.020667	0.409772
0.016192	0.371715
0.008933	0.246203
0.008371	0.291961
-0.001916	0.255131
-0.004914	0.352313
-0.012073	0.358292
-0.018376	0.304990
-0.051480	0.404117
-0.058440	0.467392
-0.046062	0.390172
-0.039891	0.363190
-0.013427	0.295589
-0.031403	0.321034
-0.051245	0.380853
-0.066625	0.466296
-0.123294	0.486211
-0.077662	0.380766
-0.038358	0.502883
-0.009768	0.406439

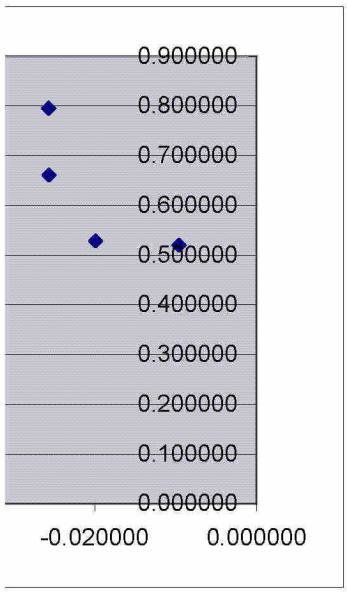
0.900000
0.800000
0.700000
0.600000
0.500000
0.400000
0.300000
0.200000
0.100000
0.000000
-0.020000
0.000000

Day	Ri		phi M	phi (M)	Theoretical phi (M)
8/29/01 21:40	0.068528	0.068528	2.290845	2.348116	1.279856
8/29/01 22:00	0.052716	0.052716	1.311962	1.344761	1.226151
8/29/01 22:20	0.105517	0.105517	1.517728	1.555671	1.390458
8/29/01 22:40	0.096401	0.096401	1.849508	1.895746	1.364842
8/29/01 23:00	0.158875	0.158875	1.618208	1.658663	1.524344
8/29/01 23:20	0.131043	0.131043	2.412406	2.472716	1.457579
8/30/01 0:00	0.196059	0.196059	1.561716	1.600758	1.605314
8/30/01 0:40	0.212314	0.212314	1.415967	1.451366	1.638274
8/30/01 1:00	0.053763	0.053763	1.120984	1.149009	1.229853
8/30/01 1:20	0.026469	0.026469	1.072539	1.099353	1.124913
8/30/01 1:40	0.025753	0.025753	0.909981	0.93273	1.121889
8/30/01 2:00	0.049220	0.04922	0.719063	0.73704	1.213624

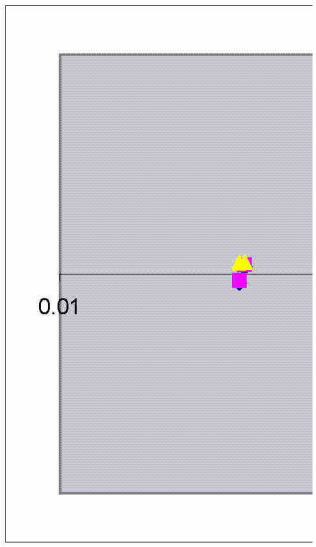

	Ri		phi M		
8/29/01 12:20	0.282085	0.282085	0.553447	0.567283	1.766603
8/29/01 12:40	0.109667	0.109667	0.491902	0.5042	1.401813
8/29/01 13:00	0.174260	0.17426	0.980609	1.005124	1.558868
8/29/01 13:20	-0.316988	0.316988	1.202682	1.232749	0.548143
8/29/01 13:40	-1.147435	1.147435	0.571529	0.585817	0.372425
8/29/01 14:00	-0.680425	0.680425	0.493489	0.505826	0.438172
8/29/01 14:20	-0.227969	0.227969	1.271558	1.303347	0.59923
8/29/01 14:40	-0.526717	0.526717	0.65495	0.671324	0.473371
8/29/01 15:00	-0.737972	0.737972	0.706616	0.724282	0.42741
8/29/01 15:20	-0.380382	0.380382	0.908236	0.930942	0.520632
8/29/01 15:40	-0.550345	0.550345	0.543851	0.557447	0.467208
8/29/01 16:00	-0.216265	0.216265	0.681528	0.698566	0.607502
8/29/01 16:20	-0.330628	0.330628	0.466581	0.478246	0.541729
8/29/01 16:40	-0.193068	0.193068	0.644523	0.660636	0.625352

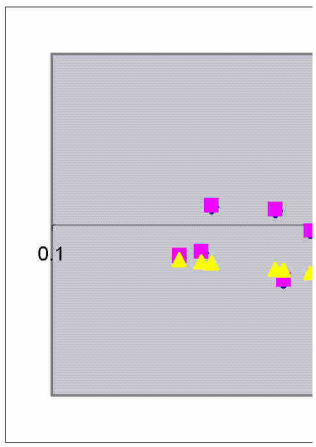

8/30/01 11:00	-0.260360	0.26036	0.735641	0.754032	0.57848
8/30/01 11:20	-0.493983	0.493983	0.671304	0.688087	0.482476
8/30/01 11:40	-0.902355	0.902355	0.447058	0.458235	0.401611
8/30/01 12:00	-0.495203	0.495203	0.617517	0.632955	0.482124
8/30/01 12:20	-0.273734	0.273734	0.415348	0.425732	0.570706
8/30/01 12:40	-0.025702	0.025702	0.412083	0.422385	0.891526
8/30/01 13:00	-0.059504	0.059504	0.580177	0.594681	0.800146
8/30/01 13:20	-0.083311	0.083311	0.399359	0.409343	0.753986
8/30/01 13:40	-0.062019	0.062019	0.425824	0.436469	0.794722
8/30/01 14:00	-0.019895	0.019895	0.619804	0.6353	0.911995
8/30/01 14:20	-0.025653	0.025653	0.495865	0.508261	0.89169
8/30/01 14:40	-0.009562	0.009562	0.631161	0.64694	0.953654

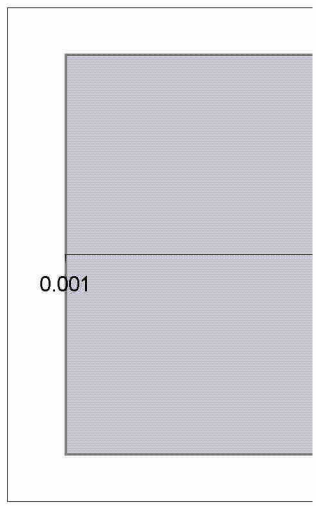

Date/Time					
10/23/01 11:20	-0.07243	0.07243	1.057055	1.083481	0.773732
10/23/01 11:40	-0.045255	0.045255	1.263287	1.294869	0.833966
10/23/01 12:00	-0.047116	0.047116	1.340077	1.373579	0.829217
10/23/01 12:20	-0.039768	0.039768	1.319592	1.352581	0.848619
10/23/01 12:40	-0.029521	0.029521	1.792853	1.837674	0.879018
10/23/01 13:00	-0.116436	0.116436	0.76714	0.786319	0.704251
10/23/01 13:20	-0.117257	0.117257	0.717213	0.735143	0.703177
10/23/01 13:40	-0.110056	0.110056	0.79816	0.818113	0.712826
10/23/01 14:00	-0.114734	0.114734	0.657862	0.674309	0.706497
10/23/01 14:20	-0.025326	0.025326	1.188109	1.217812	0.892795
10/23/01 14:40	-0.013276	0.013276	1.383926	1.418524	0.937814
10/23/01 15:00	-0.032102	0.032102	1.035434	1.06132	0.870949
10/23/01 15:20	-0.039709	0.039709	1.060816	1.087336	0.848783
10/23/01 15:40	-0.034887	0.034887	1.04278	1.06885	0.862566
10/23/01 16:00	-0.024621	0.024621	1.132649	1.160965	0.895197
10/23/01 16:20	-0.029445	0.029445	0.921988	0.945038	0.879259
10/23/01 16:40	-0.074909	0.074909	0.739091	0.757568	0.769051
10/23/01 17:00	-0.042586	0.042586	0.95011	0.973863	0.840966
10/23/01 17:20	-0.04243	0.04243	0.795469	0.815356	0.841384
10/23/01 17:40	-0.038755	0.038755	0.730971	0.749246	0.851442
10/23/01 18:00	-0.010292	0.010292	0.765063	0.78419	0.950456
10/23/01 18:20	0.040524	0.040524	0.750886	0.769658	1.18128
10/23/01 18:40	0.060254	0.060254	0.857106	0.878533	1.25233
10/23/01 19:00	0.139421	0.139421	0.519217	0.532197	1.478316
10/23/01 19:20	0.208944	0.208944	0.436476	0.447388	1.631549
10/23/01 19:40	0.186331	0.186331	0.485925	0.498073	1.584924
10/23/01 20:00	0.310593	0.310593	0.42064	0.431156	1.814036
10/23/01 20:20	0.747664	0.747664	0.462585	0.47415	2.349079
10/23/01 20:40	0.665399	0.665399	0.36518	0.374309	2.266716
10/23/01 21:00	0.106479	0.106479	1.105471	1.133108	1.393106
10/23/01 21:20	0.040543	0.040543	2.284974	2.342099	1.181352
10/23/01 21:40	0.01592	0.01592	2.882817	2.954888	1.078571
10/23/01 22:00	0.028138	0.028138	1.665646	1.707288	1.131906
10/23/01 22:20	0.012169	0.012169	3.819111	3.914589	1.061095
10/23/01 22:40	0.001041	0.001041	4.172859	4.27718	1.005523
10/23/01 23:00	0.005809	0.005809	3.96632	4.065478	1.030066
10/23/01 23:20	0.006695	0.006695	3.033128	3.108956	1.0345
10/23/01 23:40	0.003267	0.003267	3.416794	3.502213	1.017128
10/24/01 0:00	0.013664	0.013664	2.806038	2.876189	1.068126
10/24/01 0:20	-0.096479	0.096479	1.586842	1.626513	0.732566
10/24/01 0:40	-0.242851	0.242851	1.181943	1.211491	0.589333
10/24/01 1:00	-2.095735	2.095735	0.359373	0.368357	0.307086
10/24/01 1:20	0.030296	0.030296	1.749441	1.793177	1.14082
10/24/01 1:40	0.74023	0.74023	0.661015	0.67754	2.341872
10/24/01 2:00	0.018672	0.018672	3.34458	3.428194	1.091043
10/24/01 2:20	0.015352	0.015352	2.85012	2.921373	1.07596
10/24/01 2:40	0.004894	0.004894	4.732619	4.850935	1.025451
10/24/01 3:00	0.00156	0.00156	4.629816	4.745562	1.008252

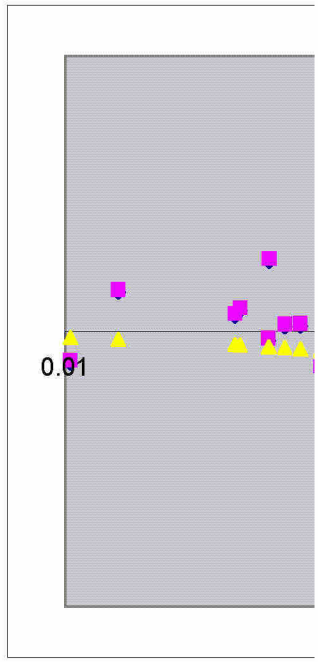

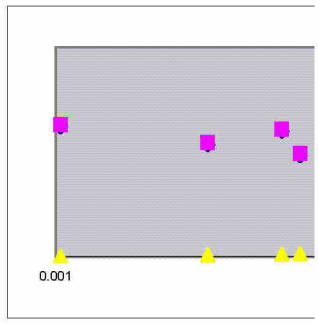

10/24/01 3:20	0.00185	0.00185	4.286122	4.393275	1.009769
10/24/01 3:40	-0.004802	0.004802	4.858484	4.979946	0.975628
10/24/01 4:00	-0.005129	0.005129	3.080097	3.1571	0.974053
10/24/01 4:20	-0.002133	0.002133	3.457288	3.54372	0.988877
10/24/01 4:40	-0.002974	0.002974	4.146078	4.24973	0.984626
10/24/01 5:00	-0.017446	0.017446	4.030667	4.131433	0.921215
10/24/01 5:20	-0.002021	0.002021	3.466214	3.552869	0.989447
10/24/01 5:40	0.028019	0.028019	2.47159	2.53338	1.131408
10/24/01 6:00	0.011361	0.011361	4.005751	4.105895	1.057252
10/24/01 6:20	0.011896	0.011896	3.328543	3.411757	1.059797
10/24/01 6:40	0.008295	0.008295	3.777169	3.871598	1.042414
10/24/01 7:00	0.008579	0.008579	3.565443	3.654579	1.043809
10/24/01 7:20	0.842635	0.842635	0.305352	0.312986	2.437499
10/24/01 7:40	86.64529	86.64529	0.052519	0.053832	11.15303
10/24/01 8:00	0.040102	0.040102	3.351613	3.435403	1.179664
10/24/01 8:20	0.018481	0.018481	3.137673	3.216115	1.090185
10/24/01 8:40	0.014331	0.014331	3.321947	3.404996	1.071237
10/24/01 9:00	0.007718	0.007718	4.518438	4.631399	1.039574
10/24/01 9:20	0.009248	0.009248	3.86465	3.961267	1.047071
10/24/01 9:40	0.002834	0.002834	3.288961	3.371185	1.014892
10/24/01 10:00	-0.049196	0.049196	0.859416	0.880901	0.824037
10/24/01 10:20	-0.062358	0.062358	1.063244	1.089825	0.794002
10/24/01 10:40	-0.070464	0.070464	0.716143	0.734046	0.777527
10/24/01 11:00	-0.071876	0.071876	0.725772	0.743916	0.774794
10/24/01 11:20	-0.1031	0.1031	0.504891	0.517513	0.72267
10/24/01 11:40	-0.244544	0.244544	0.579806	0.594301	0.588247
10/24/01 12:00	-0.303653	0.303653	0.554109	0.567962	0.554718
10/24/01 12:20	-0.397869	0.397869	0.472523	0.484337	0.513954
10/24/01 12:40	-0.273728	0.273728	0.511525	0.524313	0.57071
10/24/01 13:00	-1.402091	1.402091	0.680767	0.697786	0.349452
10/24/01 13:20	-9.539495	9.539495	0.430892	0.441664	0.186712
10/24/01 13:40	-1.048695	1.048695	0.502568	0.515132	0.383145
10/24/01 14:00	-0.098734	0.098734	0.837341	0.858275	0.729135
10/24/01 14:20	-0.124383	0.124383	0.527173	0.540352	0.694123
10/24/01 14:40	-0.837997	0.837997	0.377244	0.386675	0.41096
10/24/01 15:00	-24.47758	24.47758	0.125654	0.128795	0.136564
10/24/01 15:20	-0.498594	0.498594	0.756057	0.774958	0.481151
10/24/01 15:40	-0.065795	0.065795	1.14596	1.174609	0.786846
10/24/01 16:00	-0.068195	0.068195	1.40288	1.437952	0.782001
10/24/01 16:20	-0.732747	0.732747	0.528263	0.541469	0.428344
10/24/01 16:40	-0.101743	0.101743	0.885759	0.907903	0.724654
10/24/01 17:00	-0.165636	0.165636	0.817191	0.837621	0.649474
10/24/01 17:20	-0.02339	0.02339	1.555647	1.594538	0.899456
10/24/01 17:40	-0.045941	0.045941	1.022354	1.047913	0.832203
10/24/01 18:00	-0.09932	0.09932	0.757086	0.776013	0.728254
10/24/01 18:20	-0.010234	0.010234	1.51353	1.551368	0.95071
10/24/01 18:40	-0.007827	0.007827	1.640447	1.681458	0.961432
10/24/01 19:00	-0.012786	0.012786	1.624012	1.664613	0.939842
10/24/01 19:40	-0.354349	0.354349	0.365803	0.374948	0.531252
10/24/01 20:00	0.051416	0.051416	1.54429	1.582897	1.221521
10/24/01 20:20	0.006495	0.006495	1.35282	1.38664	1.033504
10/24/01 20:40	-0.042251	0.042251	0.93469	0.958057	0.841861

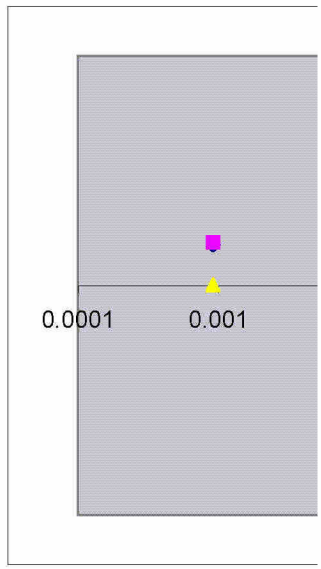

10/24/01 21:00	-0.010802	0.010802	1.402569	1.437633	0.948246
10/24/01 21:20	0.000916	0.000916	1.501711	1.539254	1.004863
10/24/01 21:40	-0.010054	0.010054	2.450401	2.511661	0.951496
10/24/01 22:00	-0.01112	0.01112	2.840475	2.911487	0.946878
10/24/01 22:20	-0.020985	0.020985	2.050732	2.102001	0.90801
10/24/01 22:40	-0.009137	0.009137	2.422546	2.48311	0.955538
10/24/01 23:00	-0.067487	0.067487	1.102642	1.130208	0.783417
10/24/01 23:20	-0.075576	0.075576	0.852044	0.873345	0.76781
10/24/01 23:40	-0.021257	0.021257	2.931644	3.004935	0.907025
10/25/01 0:00	-0.007752	0.007752	2.273788	2.330633	0.961776
10/25/01 0:20	-0.014482	0.014482	1.335226	1.368606	0.932891
10/25/01 0:40	-0.162788	0.162788	0.676243	0.693149	0.6522
10/25/01 1:00	-0.069049	0.069049	1.582577	1.622142	0.780305
10/25/01 1:20	-0.02555	0.02555	1.086481	1.113643	0.892038
10/25/01 1:40	0.026586	0.026586	1.269043	1.300769	1.125408
10/25/01 2:00	0.045701	0.045701	1.148916	1.177639	1.200743
10/25/01 2:20	0.062983	0.062983	1.187616	1.217306	1.261542
10/25/01 2:40	0.068482	0.068482	1.524813	1.562934	1.279706
10/25/01 3:00	0.057901	0.057901	1.491645	1.528936	1.244275
10/25/01 3:20	0.041865	0.041865	1.554819	1.59369	1.186382
10/25/01 3:40	0.04848	0.04848	1.264569	1.296184	1.210937
10/25/01 4:00	0.038198	0.038198	1.61657	1.656984	1.172322
10/25/01 4:20	0.029271	0.029271	1.279378	1.311363	1.136603
10/25/01 4:40	0.028192	0.028192	1.190825	1.220595	1.132131
10/25/01 5:00	0.007215	0.007215	1.273714	1.305557	1.037088
10/25/01 5:20	0.012225	0.012225	1.138904	1.167377	1.061359
10/25/01 5:40	0.018382	0.018382	1.418835	1.454306	1.089741
10/25/01 6:00	0.067463	0.067463	0.939966	0.963465	1.276379
10/25/01 6:20	0.07594	0.07594	1.168357	1.197566	1.303549
10/25/01 6:40	0.079535	0.079535	1.684791	1.726911	1.314736
10/25/01 7:00	0.019807	0.019807	1.659604	1.701094	1.096106
10/25/01 7:20	0.036977	0.036977	1.306263	1.33892	1.167566
10/25/01 7:40	0.051003	0.051003	1.337516	1.370954	1.220046
10/25/01 8:00	0.081712	0.081712	1.717564	1.760503	1.321418
10/25/01 8:20	0.28303	0.28303	1.014362	1.039721	1.768216
10/25/01 8:40	0.117146	0.117146	1.230997	1.261772	1.421823
10/25/01 9:00	0.039209	0.039209	1.784948	1.829572	1.176231
10/25/01 9:20	0.01624	0.01624	1.700327	1.742835	1.080038
10/25/01 9:40	0.00799	0.00799	1.869034	1.915759	1.040914
10/25/01 10:00	0.004547	0.004547	1.792262	1.837068	1.023685
10/25/01 10:20	0.003715	0.003715	1.999151	2.049129	1.019433
10/25/01 10:40	0.00414	0.00414	2.220491	2.276003	1.021608
10/25/01 11:00	0.007561	0.007561	1.977489	2.026927	1.038802
10/25/01 11:20	0.008694	0.008694	1.790504	1.835266	1.044369
10/25/01 11:40	0.002967	0.002967	1.886937	1.93411	1.015578
10/25/01 12:00	0.005626	0.005626	1.733562	1.776901	1.02915
10/25/01 12:20	-0.000161	0.000161	2.042436	2.093497	0.999144
10/25/01 12:40	-0.010406	0.010406	1.63481	1.675681	0.949962
10/25/01 13:00	-0.011331	0.011331	1.069455	1.096191	0.945975
10/25/01 13:20	-0.005622	0.005622	0.892808	0.915128	0.971698
10/25/01 13:40	-0.009844	0.009844	0.73307	0.751396	0.952415
10/25/01 14:00	0.010679	0.010679	0.699382	0.716867	1.053989

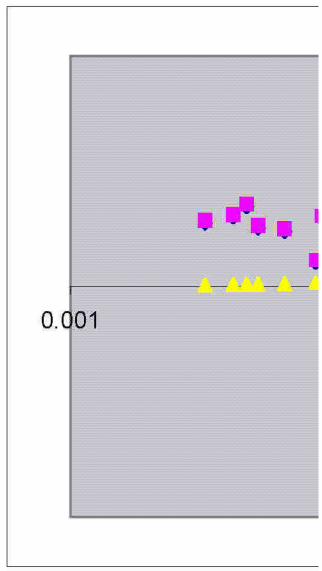

10/25/01 14:20	-0.008022	0.008022	0.527091	0.540268	0.960546
10/25/01 14:40	-0.042736	0.042736	0.515842	0.528738	0.840567
	Ri		phi M		
5/6/02 11:40	0.061791	0.061791	0.540847	0.554368	1.257535
5/6/02 12:00	-0.020635	0.020635	0.591611	0.606401	0.909283
5/6/02 12:20	-0.010496	0.010496	0.573558	0.587897	0.949568
5/6/02 12:40	-0.021697	0.021697	0.444062	0.455163	0.905443
5/6/02 13:00	-0.017909	0.017909	0.417779	0.428224	0.919442
5/6/02 13:20	-0.02895	0.02895	0.490296	0.502553	0.880843
5/6/02 13:40	-0.047869	0.047869	0.380143	0.389647	0.827328
5/6/02 14:00	-0.067143	0.067143	0.418456	0.428917	0.78411
5/6/02 14:20	-0.035613	0.035613	0.522102	0.535155	0.860435
5/6/02 14:40	-0.058636	0.058636	0.456101	0.467503	0.802052
5/6/02 15:00	-0.044983	0.044983	0.491154	0.503433	0.834668
5/6/02 15:20	-0.038606	0.038606	0.473388	0.485222	0.85186
5/6/02 15:40	-0.009929	0.009929	0.620267	0.635774	0.952041
5/6/02 16:00	-0.008841	0.008841	0.584244	0.59885	0.956856
5/6/02 16:20	-0.005374	0.005374	0.637685	0.653627	0.972881
5/6/02 16:40	-0.002244	0.002244	0.598489	0.613451	0.988308
5/6/02 17:00	-0.001623	0.001623	0.68631	0.703467	0.991493
5/6/02 17:20	-0.000706	0.000706	0.684571	0.701686	0.996265
5/6/02 17:40	0.001275	0.001275	0.619965	0.635464	1.006755
5/6/02 18:00	0.00219	0.00219	0.682007	0.699057	1.011544
5/6/02 18:20	0.002626	0.002626	0.722546	0.74061	1.013811
5/6/02 18:40	0.004286	0.004286	0.692515	0.709828	1.022355
5/7/02 9:20	-0.224691	0.224691	0.457378	0.468812	0.601501
5/7/02 9:40	-0.094053	0.094053	0.525553	0.538691	0.736331
5/7/02 10:00	-0.073842	0.073842	0.625554	0.641192	0.771051
5/7/02 10:20	-0.090766	0.090766	0.550451	0.564213	0.741558
5/7/02 10:40	-0.186414	0.186414	0.665483	0.68212	0.630875
5/7/02 11:00	-0.152193	0.152193	0.621248	0.636779	0.662757
5/7/02 11:20	-0.142293	0.142293	0.619857	0.635354	0.673269
5/7/02 11:40	-0.190543	0.190543	0.748949	0.767673	0.627425
5/7/02 12:00	-0.090934	0.090934	1.078017	1.104968	0.741286
5/7/02 12:20	-0.434416	0.434416	0.425969	0.436618	0.501032
5/7/02 12:40	-0.346305	0.346305	0.253736	0.26008	0.534713
5/7/02 13:00	-0.07631	0.07631	0.688814	0.706034	0.766455
5/7/02 13:20	-0.05942	0.05942	0.597486	0.612423	0.800328
5/7/02 13:40	-0.038737	0.038737	0.677245	0.694176	0.851492
5/7/02 14:00	-0.031029	0.031029	0.840792	0.861812	0.874267
5/7/02 14:20	-0.049062	0.049062	0.585264	0.599895	0.824369
5/7/02 14:40	-0.041624	0.041624	0.622725	0.638293	0.843549
5/7/02 15:00	-0.021872	0.021872	0.68741	0.704596	0.904817
5/7/02 15:20	-0.017422	0.017422	0.764662	0.783779	0.921308
5/7/02 15:40	-0.015453	0.015453	0.634275	0.650132	0.928999
5/7/02 16:00	-0.033583	0.033583	0.514168	0.527022	0.866452
5/7/02 19:40	0.183533	0.183533	0.771698	0.79099	1.578961
5/7/02 20:00	0.101165	0.101165	0.999443	1.02443	1.378347
5/7/02 20:20	0.133435	0.133435	1.054623	1.080988	1.463561

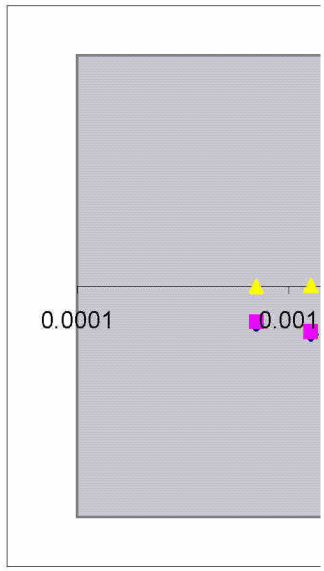

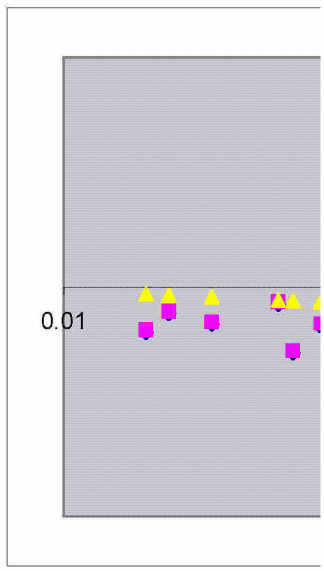

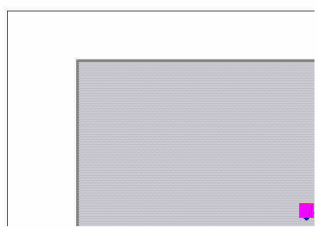

5/7/02 20:40	4.812467	4.812467	0.171516	0.175804	4.272649
5/7/02 21:00	0.257744	0.257744	1.099966	1.127465	1.723985
5/7/02 21:20	0.318563	0.318563	0.613725	0.629068	1.826862
5/7/02 21:40	0.181308	0.181308	1.253642	1.284983	1.574187
5/7/02 22:00	0.241605	0.241605	1.692008	1.734309	1.694525
5/7/02 22:20	0.181182	0.181182	1.949499	1.998237	1.573914
5/7/02 22:40	0.417305	0.417305	2.032123	2.082926	1.972702
5/7/02 23:00	0.309134	0.309134	1.97984	2.029336	1.811667
5/7/02 23:20	0.394942	0.394942	2.049688	2.100931	1.941566
5/7/02 23:40	0.949326	0.949326	1.482639	1.519705	2.529737
5/8/02 0:00	0.598721	0.598721	5.6737	5.815543	2.195275
5/8/02 0:20	0.459099	0.459099	2.68343	2.750516	2.028393
5/8/02 0:40	0.555396	0.555396	2.305705	2.363347	2.146241
5/8/02 1:00	0.373688	0.373688	1.329525	1.362763	1.911017
5/8/02 1:20	0.268461	0.268461	0.637704	0.653647	1.743005
5/8/02 1:40	0.061118	0.061118	0.958212	0.982168	1.255261
5/8/02 2:00	0.036394	0.036394	1.05144	1.077726	1.165278
5/8/02 2:20	0.024831	0.024831	1.166167	1.195321	1.117968
5/8/02 2:40	0.021012	0.021012	0.800167	0.820171	1.10143
5/8/02 3:00	0.019017	0.019017	0.951531	0.975319	1.092587
5/8/02 3:20	0.013664	0.013664	0.951744	0.975538	1.06813
5/8/02 3:40	0.009351	0.009351	1.082309	1.109366	1.047571
5/8/02 4:00	0.007329	0.007329	1.079239	1.10622	1.03765
5/8/02 4:20	0.004164	0.004164	1.195353	1.225237	1.021734
5/8/02 4:40	0.002284	0.002284	2.166795	2.220965	1.012034
5/8/02 5:00	0.004872	0.004872	1.533759	1.572103	1.025339
5/8/02 5:20	0.005192	0.005192	1.558518	1.597481	1.026959
5/8/02 5:40	0.002901	0.002901	1.736945	1.780369	1.015238
5/8/02 6:00	0.005919	0.005919	1.451289	1.487571	1.030619
5/8/02 6:20	0.005051	0.005051	1.73321	1.77654	1.026244
5/8/02 6:40	0.004544	0.004544	1.655977	1.697376	1.023671
5/8/02 7:00	0.003599	0.003599	1.107853	1.135549	1.018838
5/8/02 7:20	0.001113	0.001113	1.557235	1.596166	1.005901
5/8/02 7:40	0.000268	0.000268	1.535422	1.573807	1.001426
5/8/02 8:00	-0.001295	0.001295	0.848372	0.869582	0.993188
5/8/02 8:20	-0.001088	0.001088	1.104562	1.132176	0.994264
5/8/02 8:40	-0.001375	0.001375	1.258409	1.28987	0.99277
5/8/02 9:00	-0.00247	0.00247	1.031892	1.057689	0.987165
5/8/02 9:20	-0.006102	0.006102	0.760066	0.779068	0.969424
5/8/02 9:40	-0.0074	0.0074	1.102578	1.130143	0.963389
5/8/02 10:00	-0.011136	0.011136	0.743958	0.762557	0.946813
5/8/02 10:20	-0.008236	0.008236	0.776402	0.795812	0.959575
5/8/02 10:40	-0.008145	0.008145	0.711587	0.729377	0.959991
5/8/02 11:00	-0.001506	0.001506	0.723303	0.741385	0.992094
5/8/02 11:20	-0.003668	0.003668	0.837157	0.858086	0.981167
5/8/02 11:40	-0.001428	0.001428	0.873807	0.895653	0.992497
5/8/02 12:00	-0.000311	0.000311	1.091104	1.118381	0.998345
5/8/02 12:20	0.000981	0.000981	1.42597	1.461619	1.005204
5/8/02 12:40	-0.007033	0.007033	1.011128	1.036406	0.965078
5/8/02 13:00	-0.005188	0.005188	0.562216	0.576272	0.973767
5/8/02 13:20	-0.003302	0.003302	1.512318	1.550126	0.982984
5/8/02 13:40	0.001647	0.001647	0.926485	0.949647	1.008707

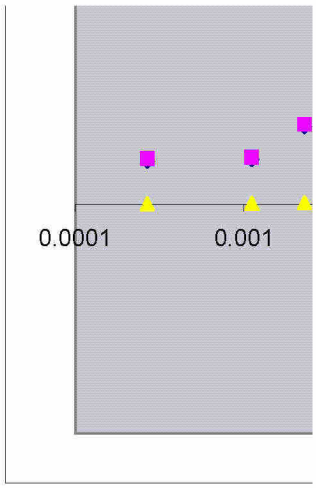

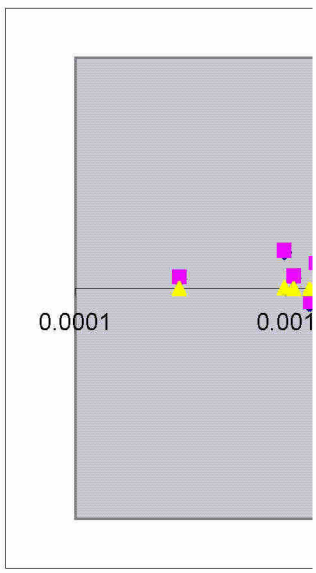

5/8/02 14:00	0.000162	0.000162	0.63405	0.649901	1.000861
5/8/02 14:20	0.003455	0.003455	0.398096	0.408048	1.018097
5/8/02 14:40	0.015442	0.015442	0.478165	0.490119	1.076375
5/8/02 15:00	0.010518	0.010518	0.527906	0.541103	1.053215
5/8/02 15:20	0.00627	0.00627	0.482809	0.494879	1.03238
5/8/02 15:40	0.010649	0.010649	0.49552	0.507908	1.053844
5/8/02 16:00	0.006569	0.006569	0.538864	0.552335	1.033875
5/10/02 8:20					
5/10/02 8:40	-0.160753	0.160753	1.002551	1.027615	0.654176
5/10/02 9:20	0.01793	0.01793	0.482445	0.494506	1.08771
5/10/02 9:40	-0.082225	0.082225	0.400212	0.410217	0.755866
5/10/02 10:00	-0.166376	0.166376	0.350505	0.359267	0.648774
5/10/02 10:20	-0.098068	0.098068	0.573265	0.587597	0.730141
5/10/02 10:40	-0.075367	0.075367	0.467166	0.478845	0.768198
5/10/02 11:00	-0.044932	0.044932	0.569947	0.584195	0.834799
5/10/02 11:20	-0.060911	0.060911	0.404788	0.414908	0.797092

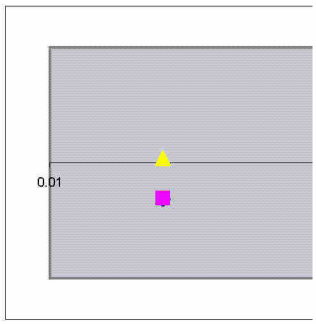

Day	Ri		phi M		
11/13/02 14:20	0.014378	0.014378	1.093764	1.121108	1.071457
11/13/02 14:40	0.016087	0.016087	0.801353	0.821386	1.079336
11/13/02 15:00	0.008526	0.008526	1.227549	1.258237	1.043549
11/13/02 15:20	0.019678	0.019678	0.68788	0.705077	1.095534
11/13/02 15:40	0.001694	0.001694	1.031275	1.057057	1.008952
11/13/02 16:00	0.002278	0.002278	0.671337	0.688121	1.012005
11/13/02 16:20	0.004543	0.004543	0.740249	0.758755	1.023664
11/13/02 16:40	0.005654	0.005654	0.895914	0.918312	1.029291
11/13/02 17:00	0.006172	0.006172	0.906816	0.929486	1.031887
11/13/02 17:20	0.005578	0.005578	0.910761	0.93353	1.028908
11/13/02 17:40	0.005741	0.005741	0.842206	0.863261	1.029725
11/13/02 18:00	0.005209	0.005209	1.203932	1.23403	1.027043
11/13/02 18:20	0.008665	0.008665	0.936249	0.959655	1.044228
11/13/02 18:40	0.008912	0.008912	1.241341	1.272375	1.045436
11/13/02 19:00	0.008381	0.008381	1.091548	1.118837	1.042835
11/13/02 19:20	0.009119	0.009119	1.259215	1.290695	1.046445
11/13/02 19:40	0.007455	0.007455	1.352977	1.386801	1.038275
11/13/02 20:00	0.012297	0.012297	1.475148	1.512026	1.061699
11/13/02 20:20	0.010935	0.010935	1.13748	1.165917	1.055213
11/13/02 20:40	0.010464	0.010464	1.17555	1.204939	1.052956
11/13/02 21:00	0.009656	0.009656	0.962284	0.986341	1.049054
11/13/02 21:20	0.01301	0.01301	1.057636	1.084077	1.065063
11/13/02 21:40	0.010604	0.010604	1.033956	1.059805	1.053628
11/13/02 22:00	0.009114	0.009114	1.080415	1.107425	1.046421
11/13/02 22:20	0.009808	0.009808	1.123425	1.15151	1.049791
11/13/02 22:40	0.011161	0.011161	1.124494	1.152606	1.056298
11/13/02 23:00	0.008129	0.008129	1.136722	1.16514	1.041599
11/13/02 23:20	0.005116	0.005116	1.097335	1.124769	1.026575

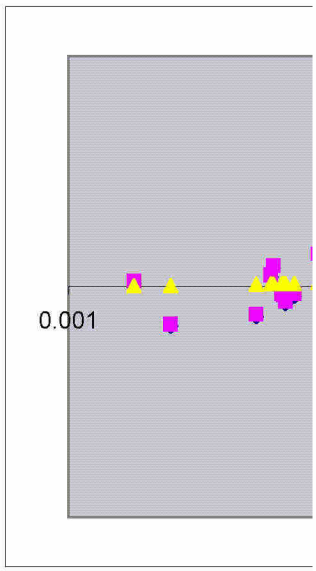

11/14/02 10:00	-0.038017	0.038017	1.203603	1.233693	0.853518
11/14/02 10:20	-0.036825	0.036825	1.374159	1.408513	0.856921
11/14/02 10:40	-0.005383	0.005383	1.067074	1.093751	0.972838

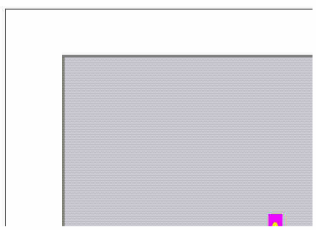

11/14/02 11:00	-0.011161	0.011161	1.262812	1.294382	0.946706
11/14/02 11:20	-0.012343	0.012343	1.096709	1.124127	0.941696
11/14/02 11:40	-0.008039	0.008039	1.510521	1.548284	0.960469
11/14/02 12:00	-0.040859	0.040859	1.097683	1.125125	0.845623
11/14/02 12:20	-0.034213	0.034213	1.135923	1.164321	0.864566
11/14/02 12:40	-0.089227	0.089227	0.527203	0.540383	0.744056
11/14/02 13:00	-0.167171	0.167171	0.589823	0.604569	0.648024
11/14/02 13:20	-0.052074	0.052074	0.65604	0.672441	0.81708
11/14/02 13:40	-0.148394	0.148394	0.725532	0.743671	0.666713
11/14/02 14:00	-0.087078	0.087078	0.730218	0.748473	0.747602
11/14/02 14:20	-0.097935	0.097935	0.693739	0.711083	0.730343
11/14/02 15:40	-0.101557	0.101557	0.371218	0.380498	0.724928
11/14/02 16:00	-0.024382	0.024382	0.653965	0.670314	0.896018
11/14/02 16:20	0.07637	0.07637	0.425191	0.435821	1.304897
11/14/02 16:40	0.094869	0.094869	0.348376	0.357086	1.360441
11/14/02 17:00	0.135525	0.135525	0.67118	0.687959	1.468746
11/14/02 17:20	0.147491	0.147491	0.861592	0.883131	1.497754
11/14/02 17:40	0.212528	0.212528	0.466309	0.477966	1.638697
11/14/02 18:00	0.213089	0.213089	0.523079	0.536156	1.639812
11/14/02 18:20	0.287837	0.287837	0.360376	0.369385	1.776377
11/14/02 18:40	0.263996	0.263996	0.436884	0.447806	1.735132
11/14/02 19:00	0.111264	0.111264	0.68903	0.706256	1.406135
11/14/02 19:20	0.072078	0.072078	0.614093	0.629446	1.291313
11/14/02 19:40	0.055896	0.055896	0.58684	0.601511	1.237332
11/14/02 20:00	0.106658	0.106658	0.672411	0.689221	1.393598
11/14/02 20:20	0.051641	0.051641	0.753588	0.772427	1.222326
11/14/02 20:40	0.037024	0.037024	0.83399	0.85484	1.167749
11/14/02 21:00	0.024758	0.024758	0.799449	0.819436	1.117657
11/14/02 21:20	0.055311	0.055311	0.561353	0.575387	1.235291
11/14/02 21:40	0.108006	0.108006	0.629381	0.645116	1.397291
11/14/02 22:00	0.236737	0.236737	0.429106	0.439834	1.685434
11/14/02 22:20	0.618898	0.618898	0.422633	0.433198	2.217381
11/14/02 22:40	0.321701	0.321701	0.561115	0.575143	1.831863
11/14/02 23:00	0.140649	0.140649	0.559651	0.573642	1.481306
11/14/02 23:20	0.085852	0.085852	0.594661	0.609527	1.333944
11/14/02 23:40	0.172184	0.172184	0.44304	0.454115	1.554298
11/15/02 0:00	0.140464	0.140464	0.637409	0.653344	1.480858
11/15/02 0:20	0.168439	0.168439	0.490386	0.502646	1.545986
11/15/02 0:40	0.063035	0.063035	0.739471	0.757957	1.261716
11/15/02 1:00	0.088652	0.088652	0.60148	0.616517	1.342286
11/15/02 1:20	0.088497	0.088497	0.664209	0.680814	1.341825
11/15/02 1:40	0.097996	0.097996	0.681764	0.698808	1.369394
11/15/02 2:00	0.135334	0.135334	0.534107	0.54746	1.468274
11/15/02 2:20	0.137266	0.137266	0.628841	0.644562	1.473037
11/15/02 2:40	0.174968	0.174968	0.500873	0.513395	1.560421
11/15/02 3:00	0.124065	0.124065	0.550673	0.564439	1.439849
11/15/02 3:20	0.099468	0.099468	0.700643	0.718159	1.373566
11/15/02 3:40	0.086837	0.086837	0.722805	0.740876	1.336891
11/15/02 4:00	0.085342	0.085342	0.936859	0.960281	1.332414
11/15/02 4:20	0.079683	0.079683	0.739226	0.757707	1.315193
11/15/02 4:40	0.050578	0.050578	0.820768	0.841287	1.21852

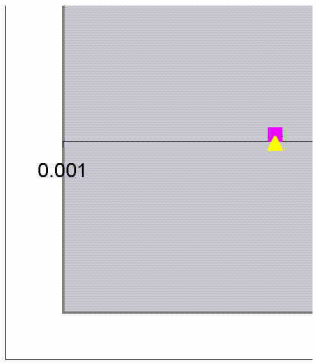

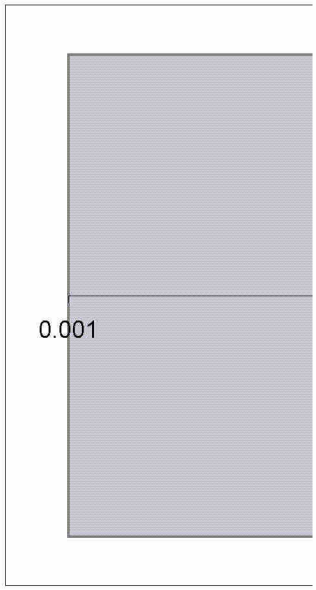

11/15/02 5:00	0.038058	0.038058	0.782817	0.802388	1.171777
11/15/02 5:20	0.045884	0.045884	0.786461	0.806122	1.201422
11/15/02 5:40	0.043668	0.043668	0.734101	0.752453	1.193177
11/15/02 6:00	0.034643	0.034643	0.74494	0.763564	1.158362
11/15/02 6:20	0.051976	0.051976	0.531631	0.544922	1.223521
11/15/02 6:40	0.040932	0.040932	0.79093	0.810703	1.182838
11/15/02 7:00	0.04096	0.04096	0.662454	0.679015	1.182944
11/15/02 7:20	0.034486	0.034486	0.764469	0.783581	1.157738
11/15/02 7:40	0.020667	0.020667	0.775289	0.794671	1.099908
11/15/02 8:00	0.016192	0.016192	0.854664	0.876031	1.079818
11/15/02 8:20	0.008933	0.008933	1.290365	1.322625	1.045537
11/15/02 8:40	0.008371	0.008371	1.088129	1.115332	1.042787
11/15/02 9:00	-0.001916	0.001916	1.24521	1.27634	0.989985
11/15/02 9:20	-0.004914	0.004914	0.901732	0.924276	0.975085
11/15/02 9:40	-0.012073	0.012073	0.886685	0.908852	0.94283
11/15/02 10:00	-0.018376	0.018376	1.041647	1.067688	0.917669
11/15/02 10:20	-0.05148	0.05148	0.786138	0.805792	0.818497
11/15/02 10:40	-0.05844	0.05844	0.679711	0.696704	0.802486
11/15/02 11:00	-0.046062	0.046062	0.814236	0.834591	0.831892
11/15/02 11:20	-0.039891	0.039891	0.874725	0.896593	0.84828
11/15/02 11:40	-0.013427	0.013427	1.074775	1.101644	0.937192
11/15/02 12:00	-0.031403	0.031403	0.98959	1.014329	0.873106
11/15/02 12:20	-0.051245	0.051245	0.834158	0.855012	0.819059
11/15/02 12:40	-0.066625	0.066625	0.681309	0.698341	0.785157
11/15/02 13:00	-0.123294	0.123294	0.653403	0.669738	0.695477
11/15/02 13:20	-0.077662	0.077662	0.834349	0.855208	0.763981
11/15/02 13:40	-0.038358	0.038358	0.631741	0.647535	0.852556
11/15/02 14:00	-0.009768	0.009768	0.781646	0.801187	0.952746

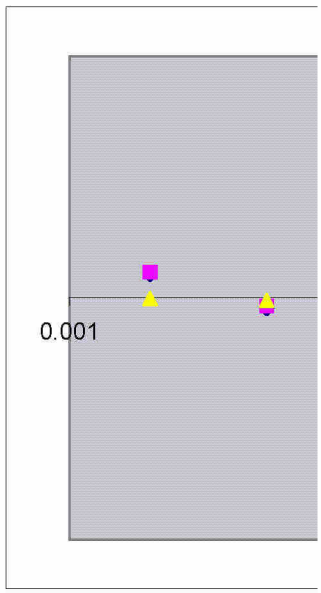

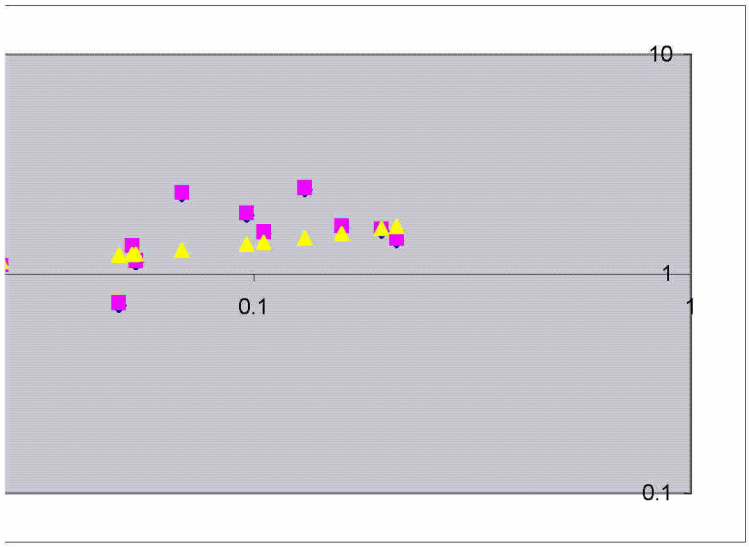
10
1
0.1
1
0.1

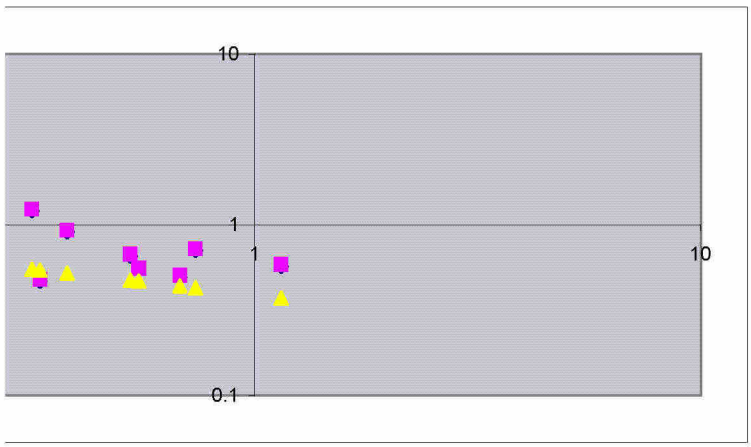
10
1
1
10
0.1

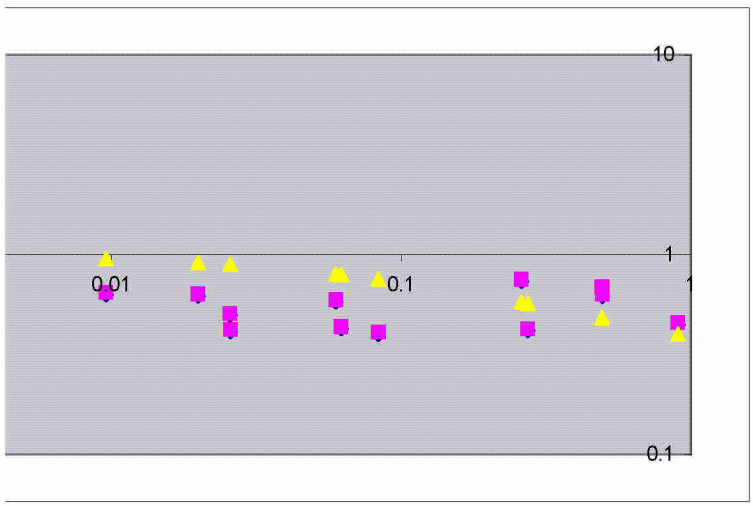
10
1
0.01
0.1
1
0.1

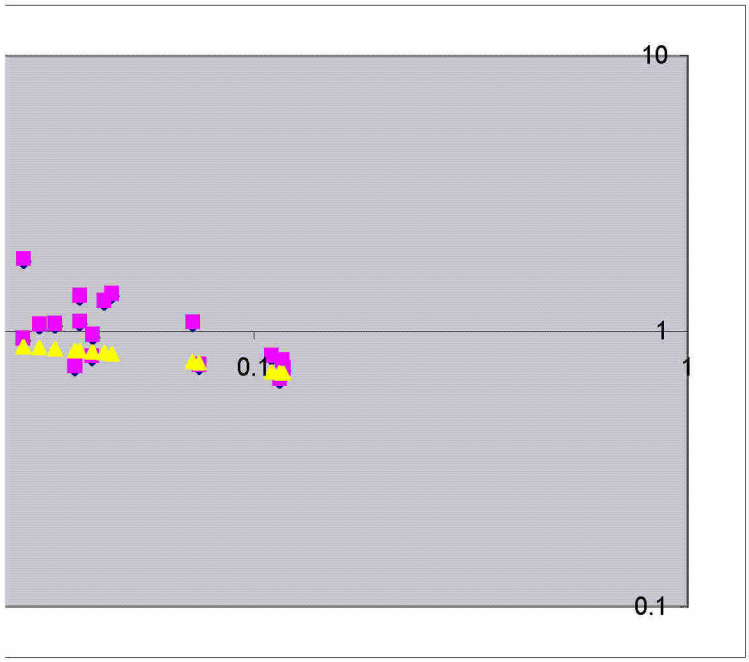
10
1
0.1
1
0.1

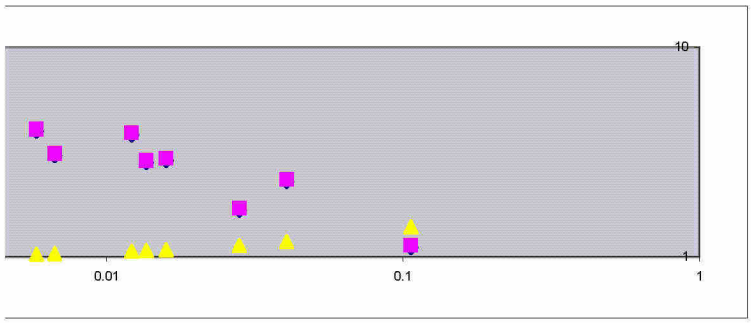
10
1
0.01
0.1
1

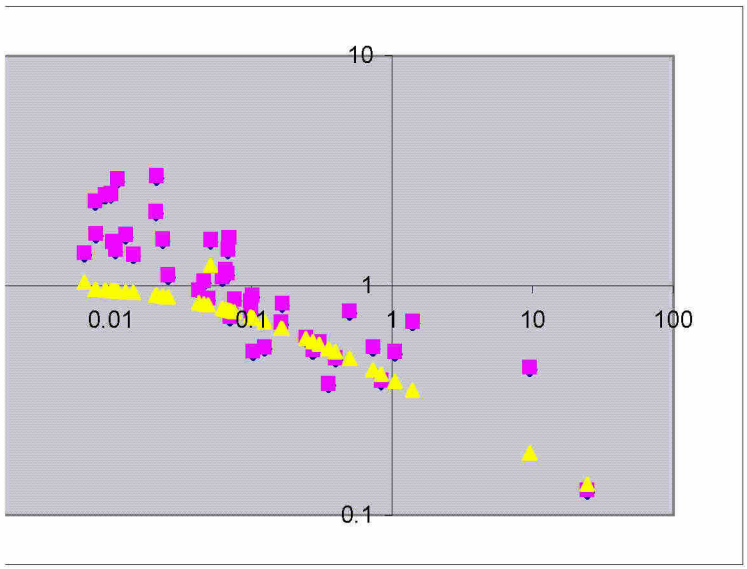
10
1
0.1
0.01
0.1
1
10
100

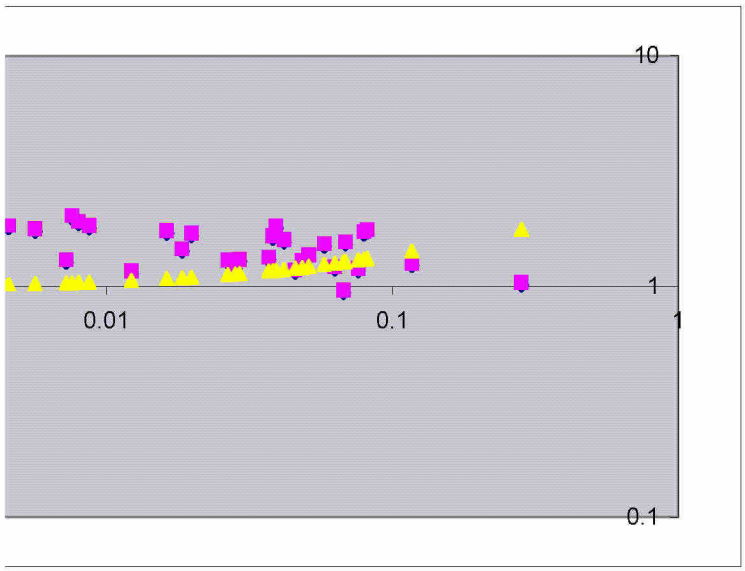
10
1
0.01
0.1
1
0.1

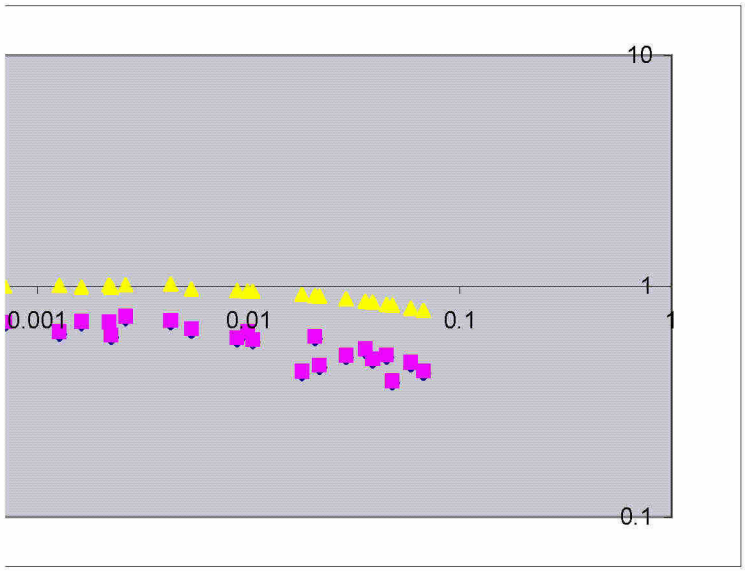
10
1
0.001
0.01
0.1
1
0.1

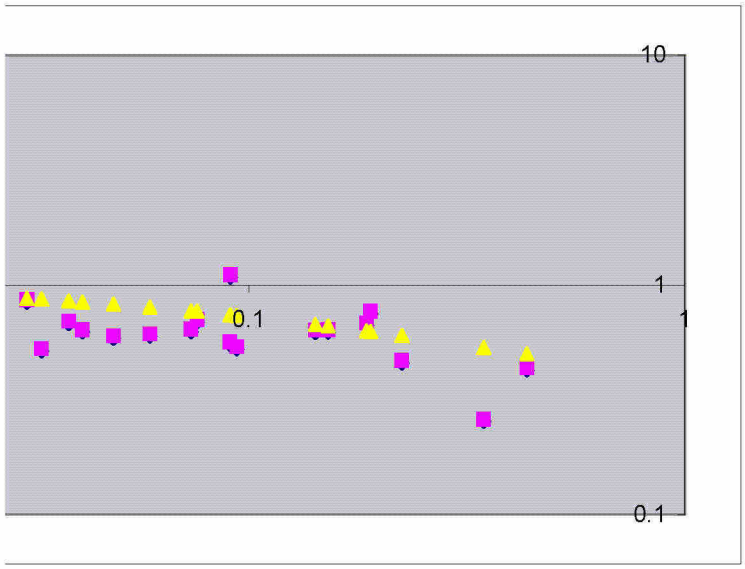
10
1
0.1
1
0.1

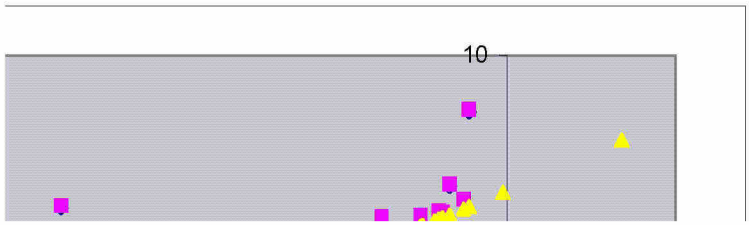
10

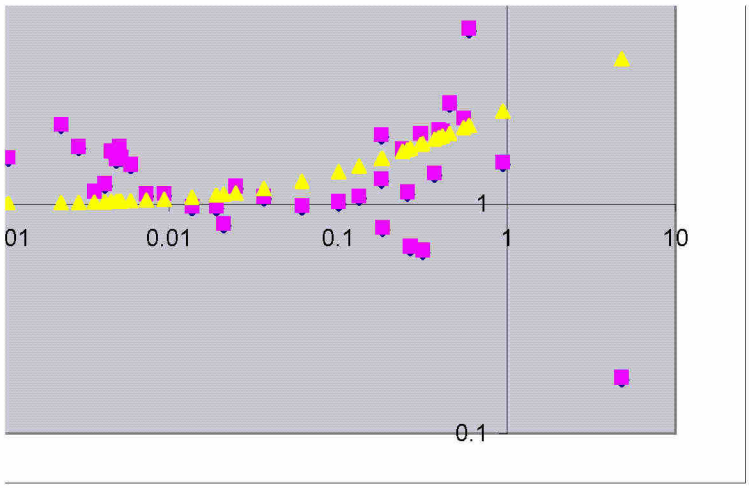
01
0.01
0.1
1
10
1
0.1

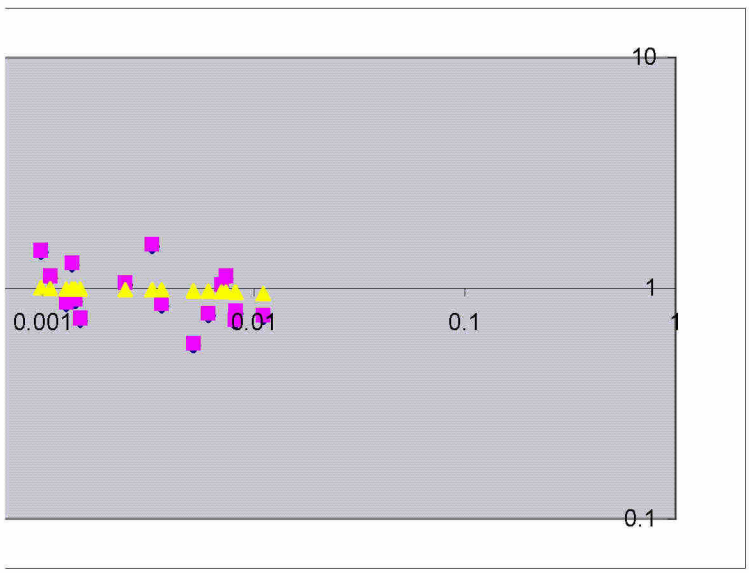
10
1
0.001
0.01
0.1
1
0.1

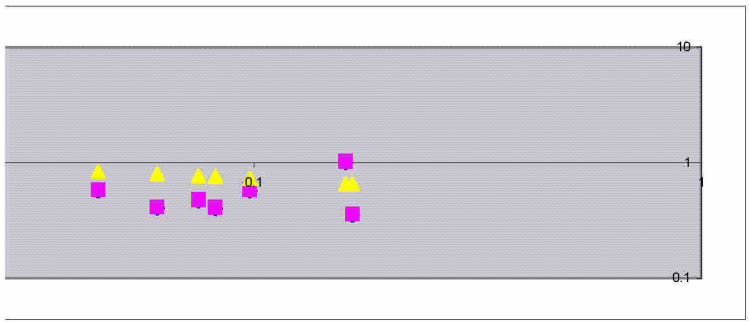
10
1
0.1
0.1

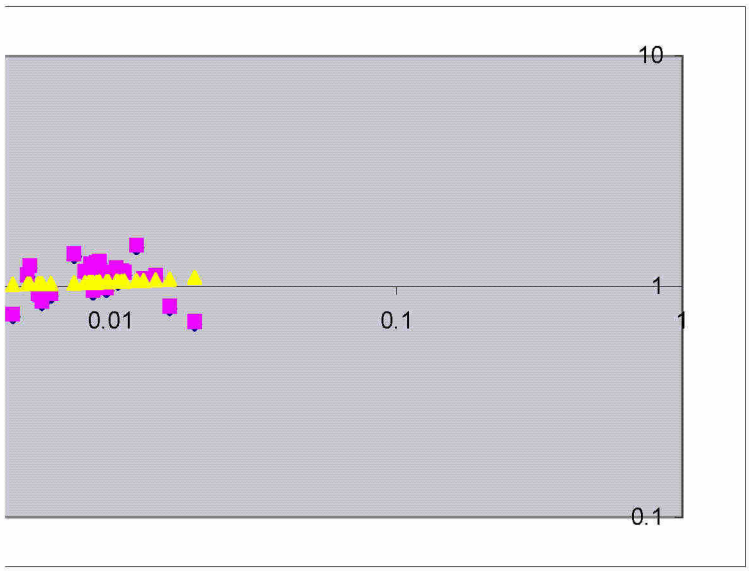
10
1
0.01
0.1
1
0.1


10

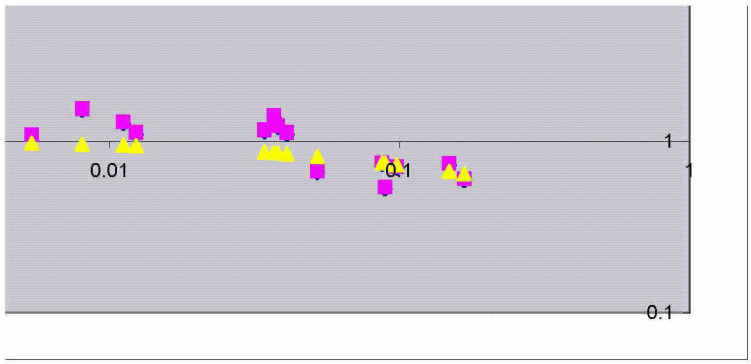
0.01
0.1
1
1
0.1

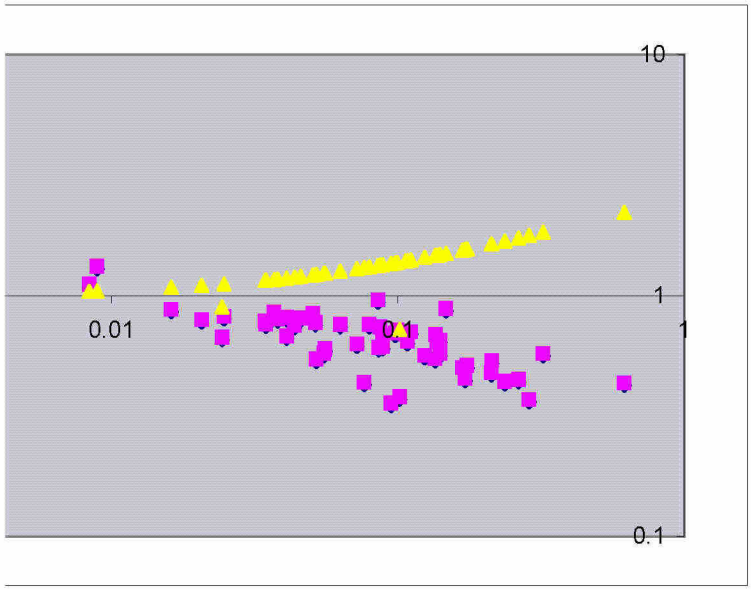
10
0.01
0.1
1
1
0.1

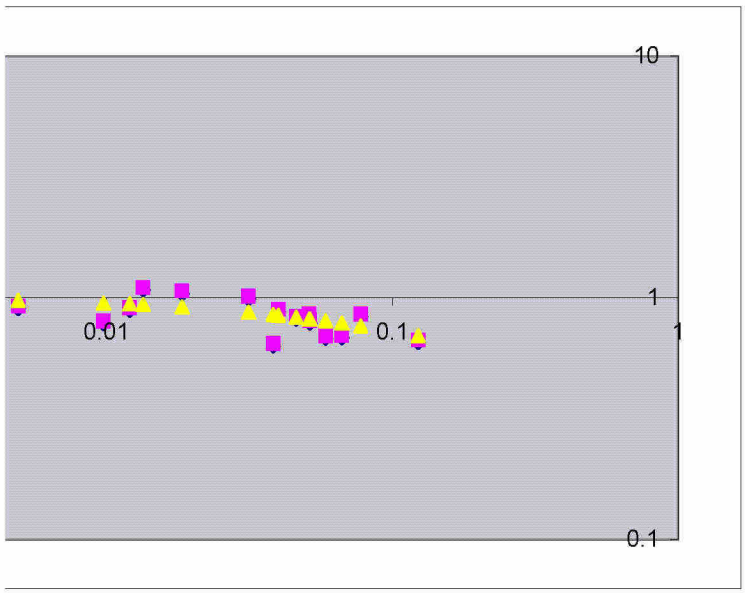
10
1
0.01
0.1
1
0.1

Appendix 8. PCB congener profiles at the SDM landfill in Bayonne.

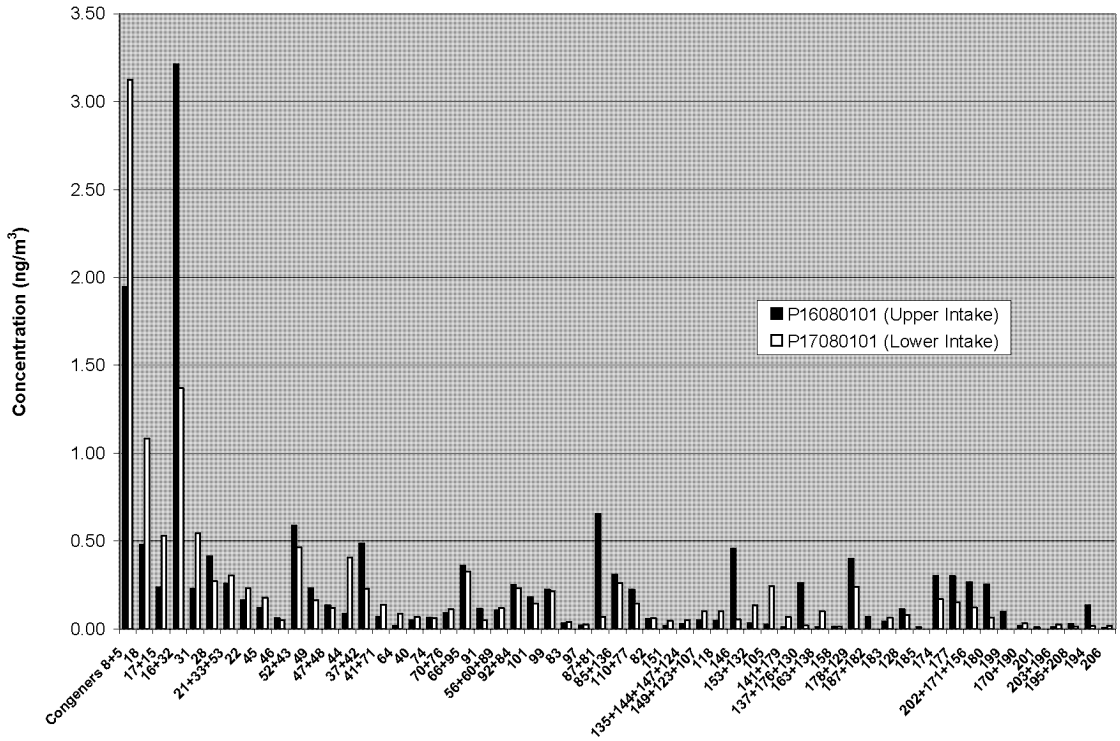

Figure 1. Gas phase PCB congener mass distribution at the Bayonne landfill, August 1, 2001.

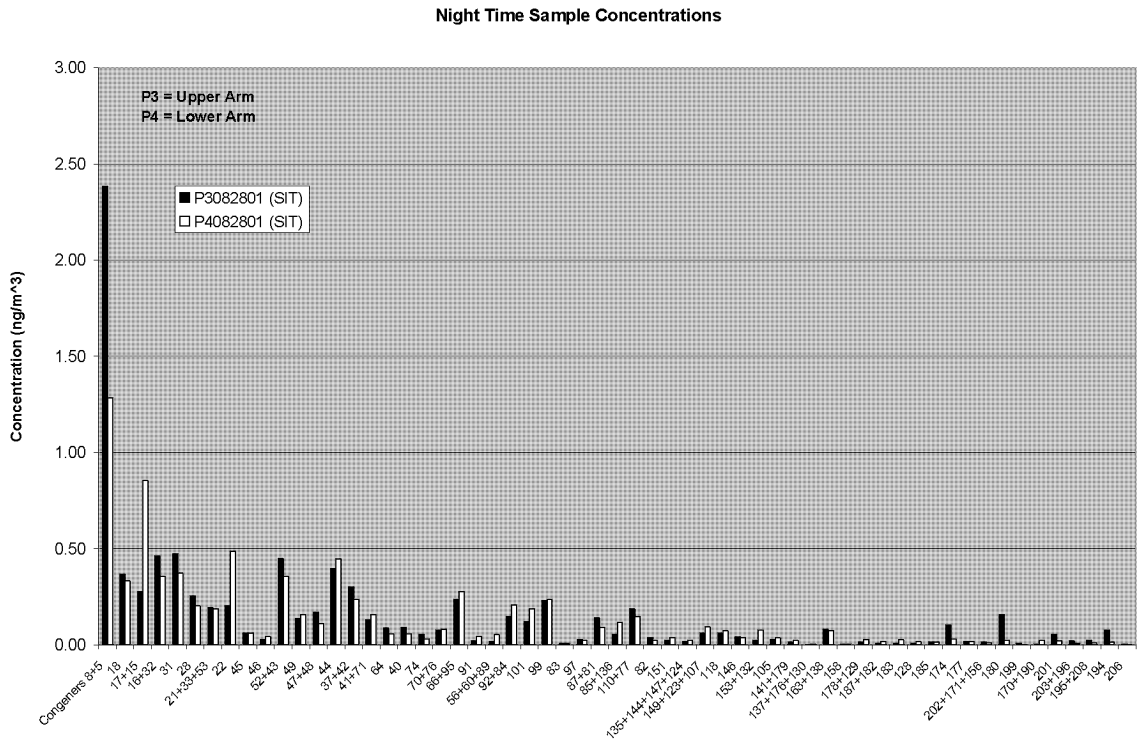

Figure 2. Nighttime PCB congener mass distributions, August 29, 2001.

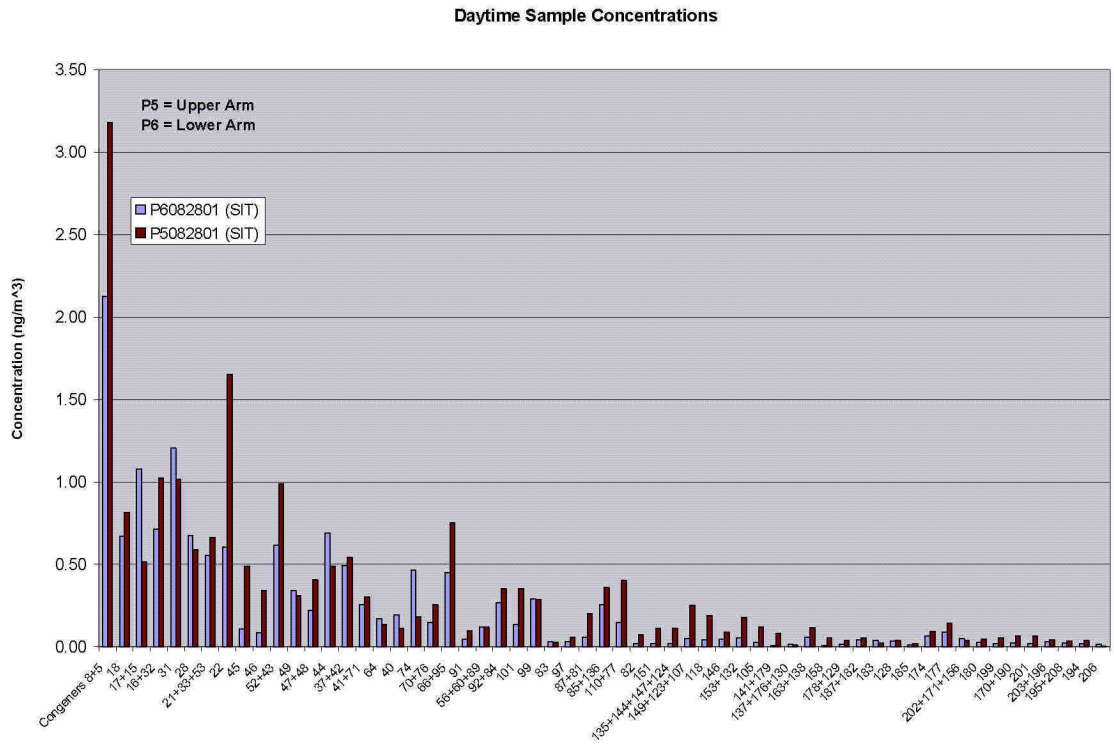

Figure 3. PCB congener mass distributions, August 30, 2001.

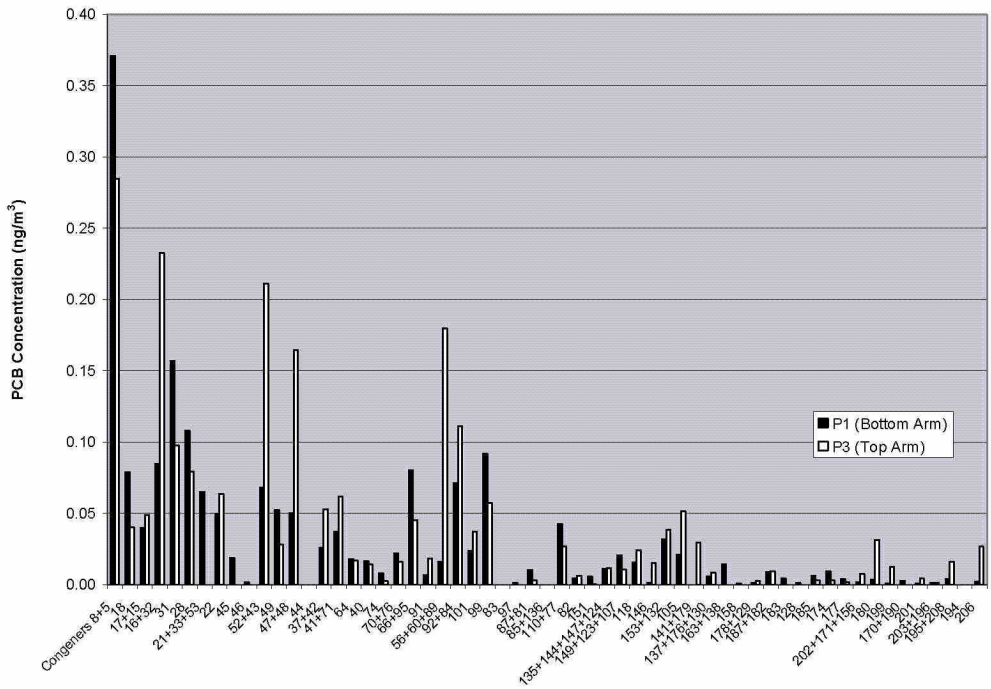

Figure 4. PCB congener mass distributions, October 23, 2001, morning.

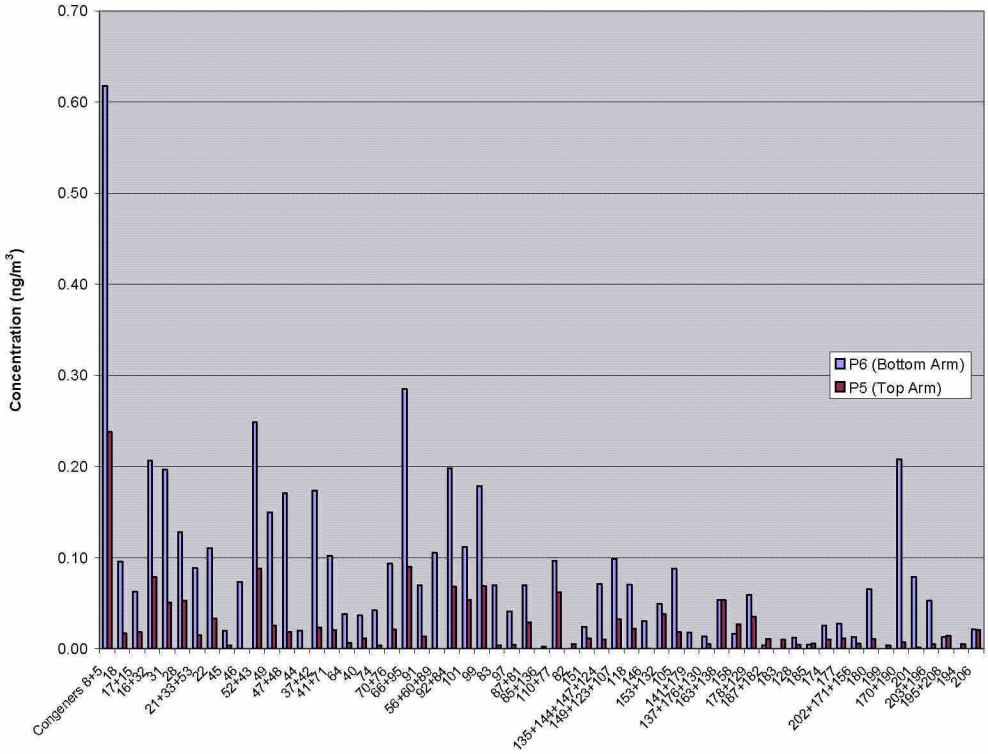

Figure 5. PCB congener mass distributions, October 23, 2001, afternoon.

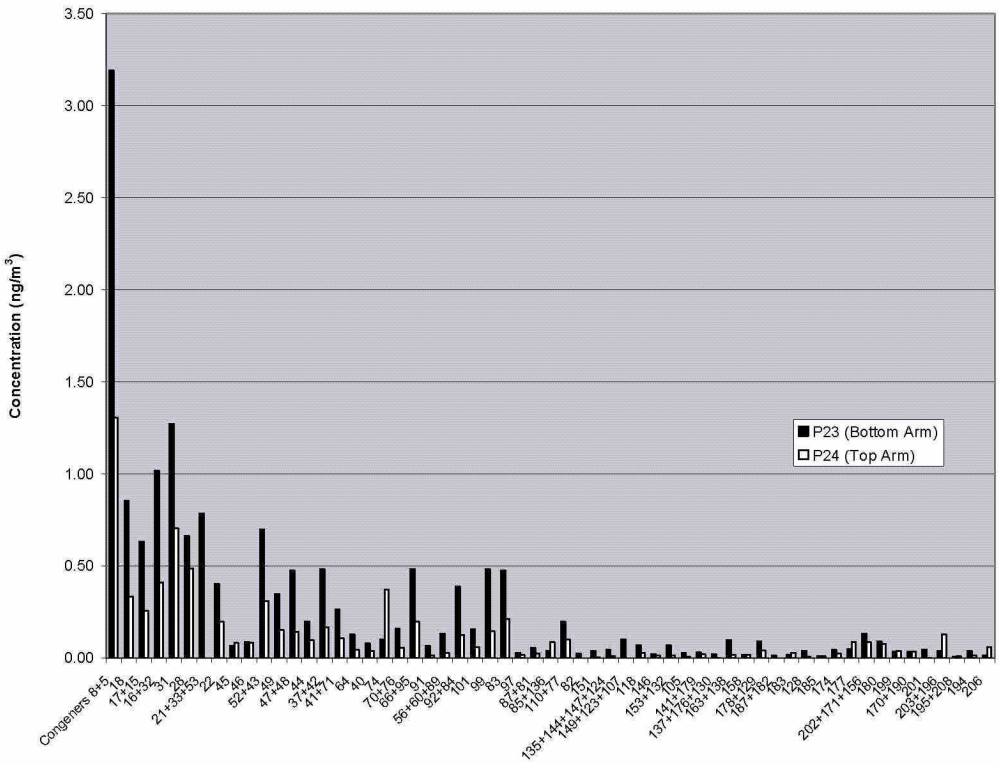

Figure 6. PCB congener mass distributions, October 24, 2001, midday.

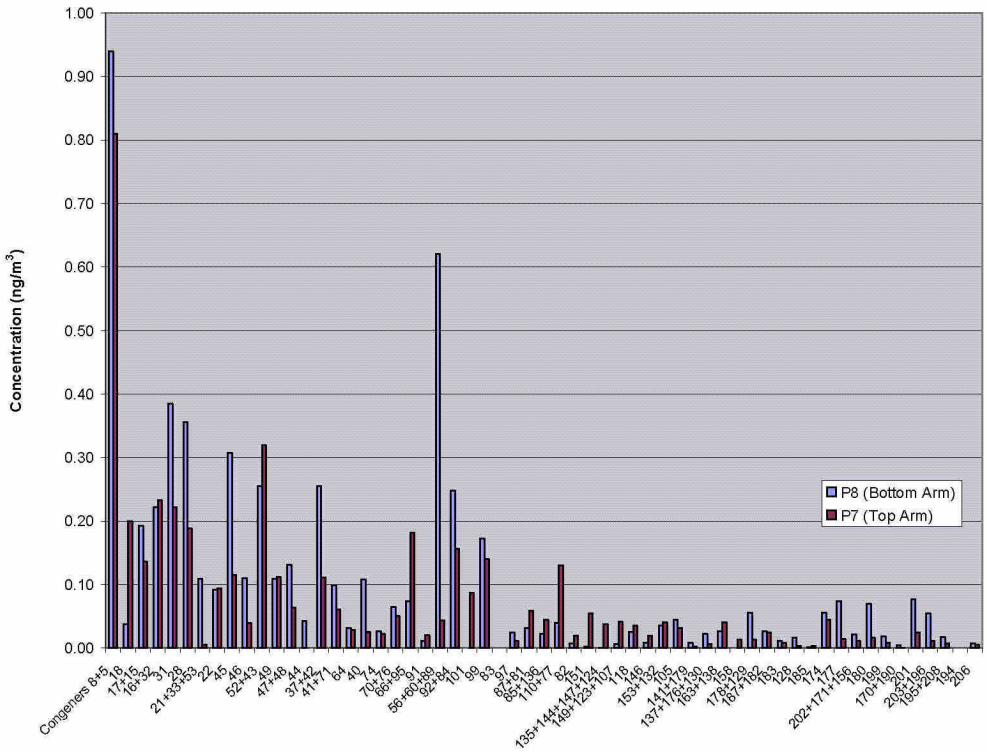

Figure 7. PCB congener mass distributions, October 24, 2001, nighttime.

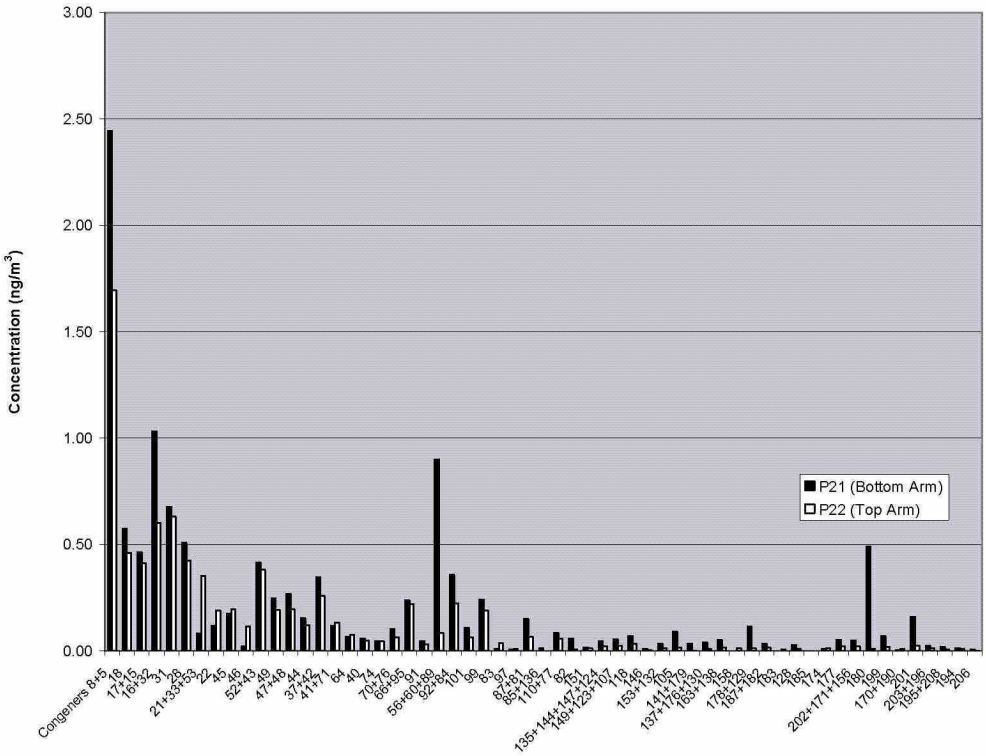

Figure 8. PCB congener mass distributions, October 25, 2001.

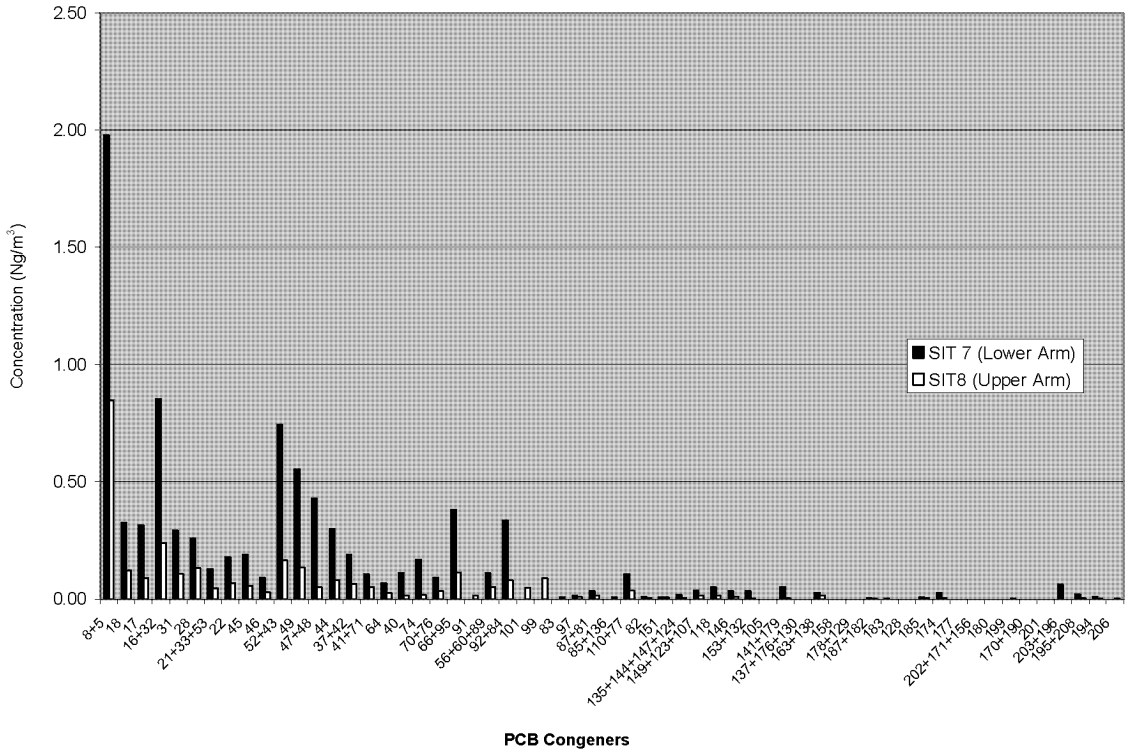

Figure 9. PCB congener mass distributions, May 6, 2002, 12:30 – 15:30.

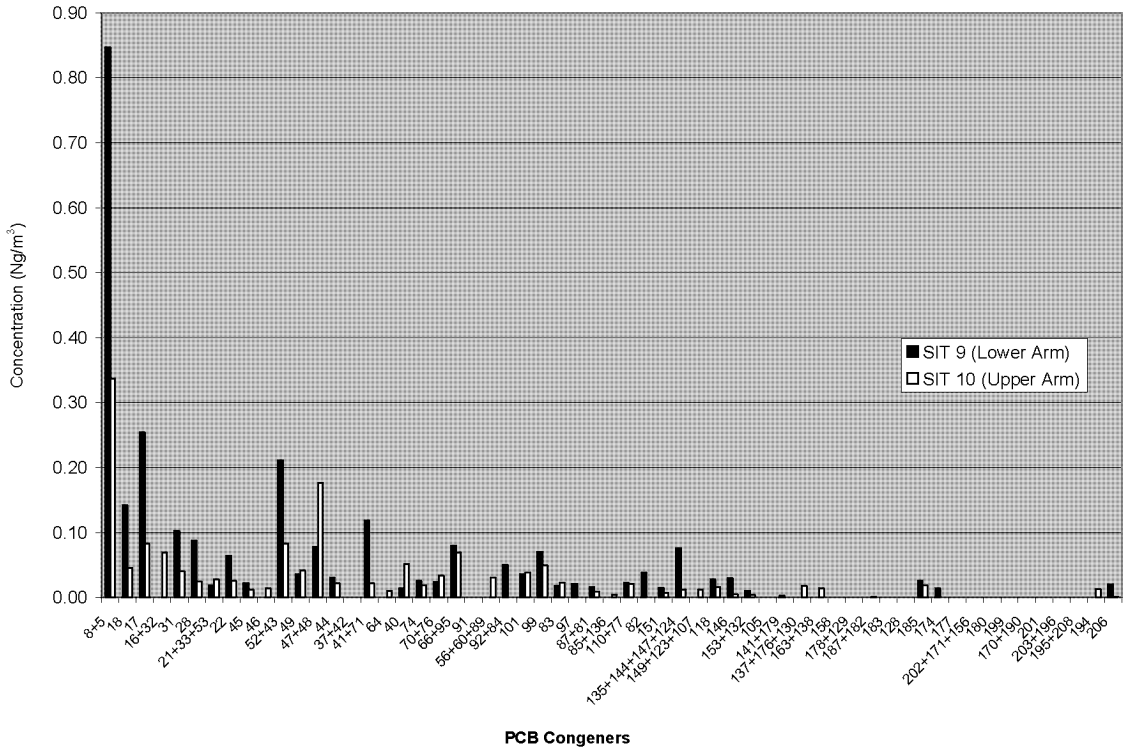

Figure 10. PCB congener mass distributions, May 6, 2002, 15:30 – 18:30.

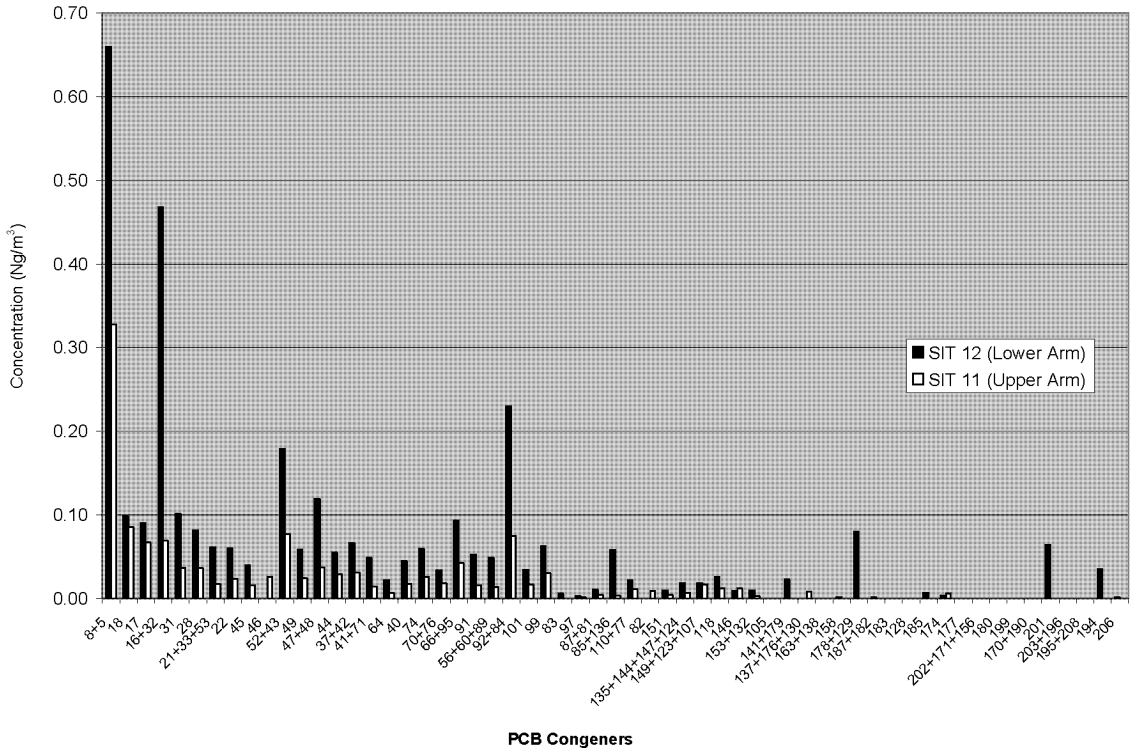

Figure 11. PCB congener mass distributions, May 7, 2002, 9:30 – 12:30.

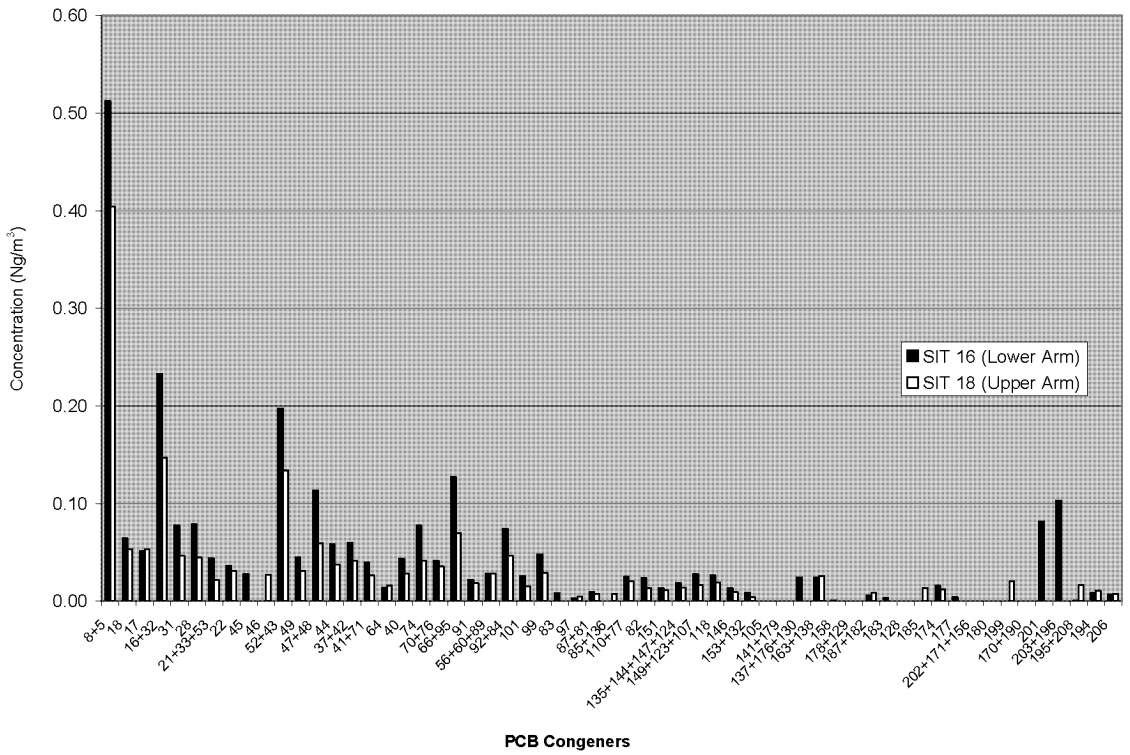

Figure 12. PCB congener mass distributions, May 7, 2002, 13:00 – 16:00.

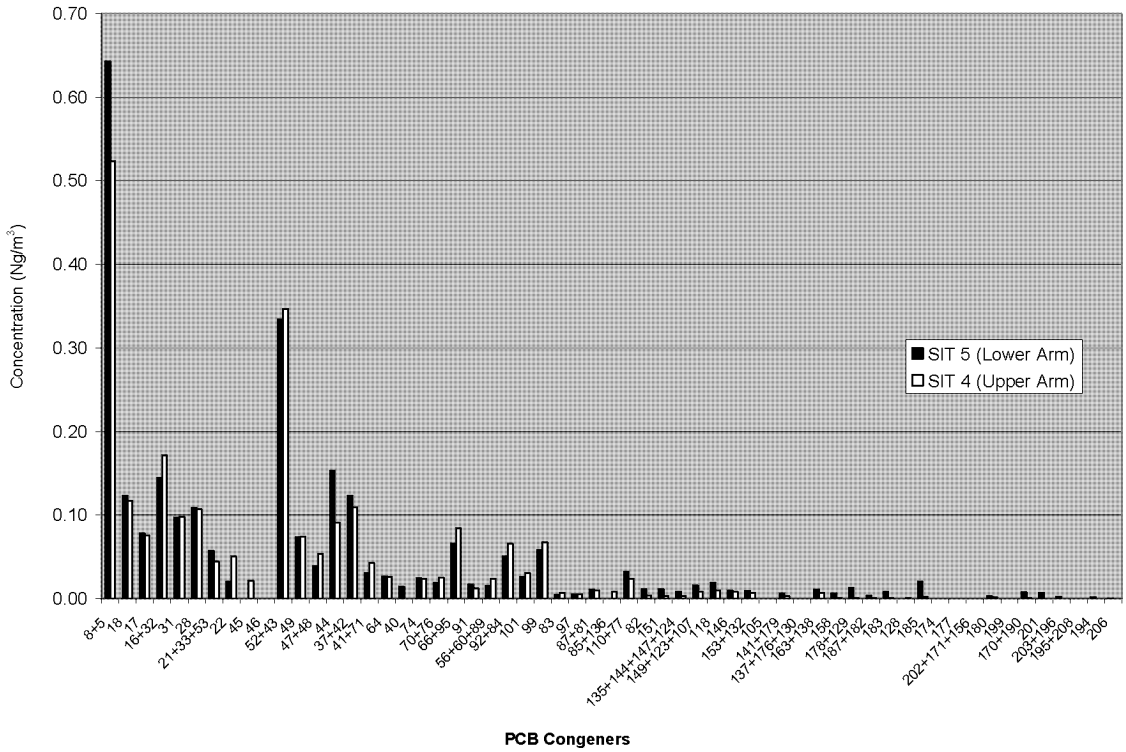

Figure 13. PCB congener mass distributions, May 7, 2002, 20:00 – 23:15.

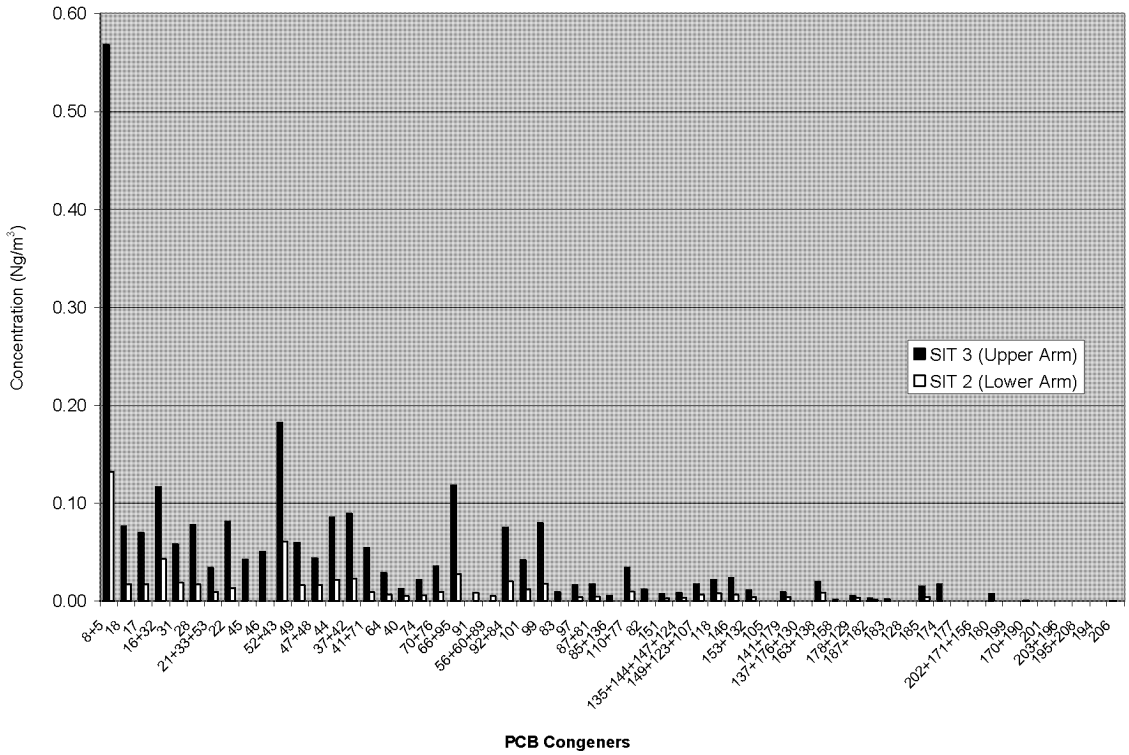

Figure 14. PCB congener mass distributions, May 8, 2002, 9:30 – 12:30.

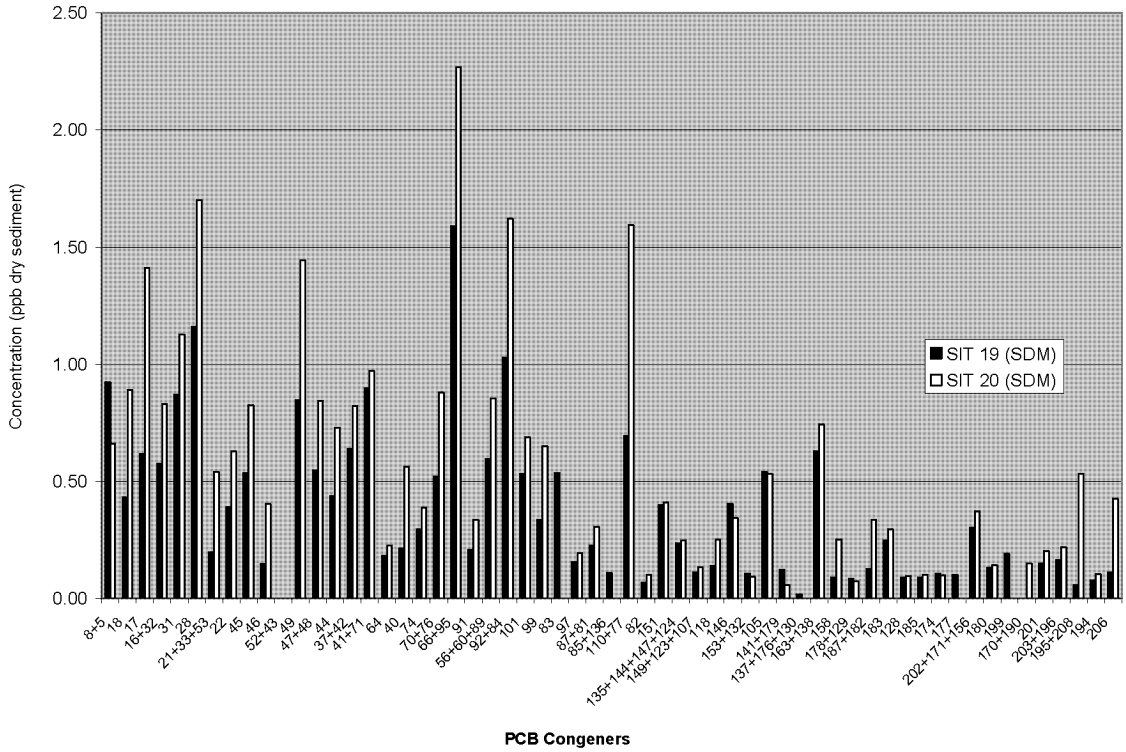

Figure 15. PCB congener mass distributions in SDM collected in May 2002.

Appendix 9. Station Information for Bergen Point West Reach, NY.

Water Level Station Information:

Station Name:	**Bergen Point West Reach, NY**
Station Identification Number:	**8519483**
Latitude:	**40° 38.4' N**
Longitude:	**74° 8.8' W**
Date Established:	**Sep 17 1981**
Maximum Water Level:	**3.60 ft. above** MHHW (03/29/1984)
Minimum Water Level:	**-3.28 ft. below** MLLW (02/08/1985)
Mean Range:	**5.00 ft.**
Diurnal Range:	**5.56 ft.**
Tidal and Geodetic Datums:	**Click HERE**
Bench Mark Data Sheet:	**Click HERE**

Click image for larger image.